

Zbornik radova Proceedings



**8. Međunarodna konferencija
o obnovljivim izvorima električne energije**
Beograd, 16. oktobar 2020

**8th International Conference
on Renewable Electrical Power Sources**
Belgrade, October 16, 2020

ZBORNİK RADOVA

Proceedings

**pisanih za 8. Međunarodnu konferenciju o
obnovljivim izvorima električne energije**

**8th International Conference on Renewable
Electrical Power Sources**

CIP - Каталогизacija y publikaciji - Narodna biblioteka Srbije, Beograd

502.171:620.9(082)(0.034.2)

MEĐUNARODNA konferencija o obnovljivim izvorima električne energije (8 ; 2020 ; Beograd)

Zbornik radova [Elektronski izvor] / 8. Međunarodna konferencija o obnovljivim izvorima električne energije, Beograd, 16. oktobar 2020 ; [urednik Zoran Stević] = Proceedings / 8th International Conference on Renewable Electrical Power Sources, Belgrade, October 16, 2020 ; [editor Zoran Stević]. - Beograd : Savez mašinskih i elektrotehničkih inženjera i tehničara Srbije - SMEITS, 2020 (Beograd : Paragon). - 1 elektronski optički disk (CD-ROM) ; 12 cm

Sistemska zahteva: Nisu navedeni. - Nasl. sa naslovne strane dokumenta. - Tiraž 150. - Abstrakti. - Bibliografija uz svaki rad.

ISBN 978-86-85535-06-2

a) Энергетски извори - Одрживи развој - Зборници

COBISS.SR-ID 25077513



2020

**ZBORNİK RADOVA
pisanih za 8. Međunarodnu konferenciju o
obnovljivim izvorima
električne energije**

Hotel „Zepter“, Beograd
16. oktobar 2020.

**PROCEEDINGS
8th International Conference
on Renewable Electrical
Power Sources**

Hotel „Zepter“, Belgrade
October 16, 2020

Izdavač

Savez mašinskih i
elektrotehničkih inženjera
i tehničara Srbije (SMEITS)
Društvo za obnovljive izvore
električne energije
Kneza Miloša 7a/II,
11000 Beograd

Publisher

Union of Mechanical and
Electrotechnical Engineers and Technicians of
Serbia (SMEITS)
Society for Renewable Electrical
Power Sources
Kneza Miloša str. 7a/II,
11000 Beograd

**Predsednik Društva za
obnovljive izvore
električne energije
pri SMEITS-u**

Dr Zoran Nikolić, dipl. inž.

**President to the Society
for Renewable Electrical
Power Sources
within the SMEITS**

Zoran Nikolić, Ph. D.

Urednik

Prof. dr Zoran Stević

Editor

Prof Zoran Stević, Ph. D.

Za izdavača

Vladan Galebović

For Publisher

Vladan Galebović

Tiraž

150 primeraka

CD umnožava

Paragon, Beograd

ISBN

978-86-85535-06-2

**Organizator
Organizer**

Savez mašinskih i elektrotehničkih
inženjera i tehničara Srbije (SMEITS),
**Društvo za obnovljive izvore
električne energije**

Union of Mechanical and Electrotechnical
Engineers and Technicians of Serbia (SMEITS),
**Society for Renewable Electrical
Power Sources**

Kneza Miloša 7a/II, 11000 Beograd
Tel. +381 (0) 11 3230-041, +381 (0) 11 3031-696, tel./faks +381 (0) 11 3231-372
office@smeits.rs • www.smeits.rs

Održavanje 8. MKOIEE finansijski je pomoglo
Ministarstvo prosvete, nauke i tehnološkog
razvoja Republike Srbije



Međunarodni programski odbor
International Programme Committee

Prof. dr Slađana Alagić	Srbija
Prof. Viorel Badescu	Rumunija
Prof. dr Pellumb Berberi	Albanija
Prof. dr Miroslav Bjekić	Srbija
Prof. dr Oleksandr Bondarenko	Ukrajina
Prof. dr Alla Denysova	Bugarska
Dr Stevan Dimitrijević	Srbija
Akademik prof. dr Zoran Đurić	Srbija
Dr Aleksandar Ivančić	Španija
Prof. dr Miroljub Jevtić	Srbija
Prof. dr Branko Kovačević	Srbija
Prof. Vladimir Krstić	Kanada
Prof. Nikolay Lopatkin	Rusija
Prof. Nikolay Mihailov	Bugarska
Prof. dr Milica Naumović	Srbija
Prof. dr Stefka Nedeltcheva	Bugarska
Dr Dušan Nikolić	Australija
Dr Zoran Nikolić	Srbija
Prof. dr Elena Ponomaryova	Ukrajina
Dr Mila Pucar	Srbija
Prof. dr Nikola Rajaković	Srbija
Prof. dr Birgit Scheppat	Nemačka
Prof. dr Valerij Sytnikov	Ukrajina
Prof. dr Velimir Stefanović	Srbija
Prof. dr Zoran Stević	Serbia (predsednik)
Prof. dr Zoran Stojiljković	Srbija
Prof. dr Volodymyr Sydorets	Ukrajina
Prof. dr Nada Štrbac	Srbija
Prof. dr Dragan Tasić	Srbija
Prof. dr Michael Todorov	Bugarska
Dr Nataša Tomić	Srbija
Dr Milica Vlahović	Srbija
Dr Zhongying Wang	Kina
Dr Wanxing Wang	Kina
Dr Xuejun Wang	Kina
Prof. dr Hengzhao Yang	SAD
Dr Ruiying Zhang	Kina

Organizacioni odbor
Organizing Committee

Mila Pucar
Rastislav Kragić
Zoran Nikolić (*predsednik*)
Ilija Radovanović
Žarko Ševaljević
Jelena Salević
Vladan Galebović

FOREWORD

Science, technology and industry accelerated development leads to improvements of human life, but also creates new risky situations. Humanity faces unprecedented risks. Global warming is an example. Although most experts in the field of climate change state that global warming is created by humans, some scientists do not agree. One of the main problems in these risky situations is – question of responsibility. The world governments should not leave all responsibility to scientists and experts. Authorities should consult experts to declare state of emergency. A strong political initiative is necessary to start dealing with serious ecological problems such as global warming or local environment pollution. Highest level political agreements achieved within the Kyoto Protocol are not enough to stop these phenomena. Clean technologies designed to provide superior performances at lower prices, with lowering losses of conventional offerings – have great chances to be the next driving force to ensure economy growth.

Science is the first to define problems of Earth and life survival. Science is trying to provide solutions, limited by political, social, economic and technology factors. Preservation of life on Earth is the common priority.

Science and technical and technology development can contribute in several fields:

- renewable power sources;*
- efficient energy usage;*
- waste reducing;*
- harmfulness of waste mitigation;*
- recycling;*
- soil, water and air purification;*
- residual waste neutralization.*

Important factor for political decisions making is the public opinion.

Therefore, it is extremely important to raise awareness and widely educate population on necessary transition to renewable, ecologically acceptable power sources, which is one of long-term goals of this Conference.

For eight time, this international event is organized by the Society of Renewable Electrical Power Sources (DOIEE) within the Union of Mechanical and Electrotechnical Engineers and Technicians of Serbia (SMETS).

*Belgrade,
October 2020.*

PREDGOVOR

Ubrzani napredak nauke, tehnologije i industrije dovodi do poboljšanja kvaliteta ljudskog života, ali i do stvaranja novih rizičnih situacija. Čovečanstvo je suočeno sa rizicima kakvih u ranijoj ljudskoj istoriji nije bilo. Globalno zagrevanje je tipičan primer. Iako većina eksperata koji proučavaju klimatske promene tvrde da globalno zagrevanje postoji i da je čovek taj koji ga uzrokuje, postoje naučnici koji dovode u sumnju takve tvrdnje. Jedan od glavnih problema vezanih za nove rizične situacije jeste – pitanje odgovornosti. Vlade država u svetu ne smeju teret odgovornosti prepustiti isključivo naučnicima i ekspertima. Vlasti treba da se konsultuju sa ekspertima i da dobro procene kada treba proglasiti opasnost od rizične situacije. Potrebna je jaka politička inicijativa da bi se počeli rešavati ozbiljni ekološki problemi kao što je globalno zagrevanje, ali i lokalno zagađenje životne sredine. Politički dogovori na svetskom nivou koji su do sada postignuti u okviru Kjoto protokola, nedovoljni su za zaustavljanje ovog fenomena. Čiste tehnologije – tehnologije koje su dizajnirane da obezbeđuju superiorne performance za nižu cenu dok istovremeno kreiraju manji gubitak od konvencionalnih ponuda – imaju velike šanse da budu sledeća motorna snaga koja će obezbediti ekonomski rast.

Nauka, naravno, pre svih uočava probleme opstanka planete i života na njoj. Ona takođe pokušava da ih reši i uspeva onoliko koliko je to realno moguće, imajući u vidu političke, socijalne, ekonomske i tehnološke faktore. Može se konstatovati da su praktično svi prioriteti posvećeni očuvanju života na Zemlji. Nauka i razvoj tehnike i tehnologije mogu tome doprineti u više segmenata:

- obnovljivi izvori energije;*
- energetska efikasnost;*
- smanjenje količine otpada;*
- smanjenje štetnosti otpada;*
- reciklaža;*
- prečišćavanje zemlje, vode i vazduha;*
- neutralizacija preostalog otpada.*

Bitan faktor za donošenje političkih odluka je i javno mnjenje. Zato je jako važno podizanje opšte svesti i što šira edukacija stanovništva o neophodnosti prelaska na obnovljive, ekološki prihvatljive izvore energije, što je jedan od dugoročnih ciljeva ove Konferencije.

Ovaj međunarodni skup po osmi put organizuje Društvo za obnovljive izvore električne energije (DOIEE) Saveza mašinskih i elektrotehničkih inženjera i tehničara Srbije (SMEITS).

*U Beogradu,
oktobra 2020.*

SADRŽAJ / CONTENTS

PREDGOVOR

Prof. dr Zoran STEVIĆ 7

1. Novi materijali i nove tehnologije u oblasti OIE

Plenarno predavanje – po pozivu

1. **“SUPERALKALNI“ KLASITERI, PROIZVODNJA, POTENCIJALNA PRIMENA KAO MATERIJAL ZA SKLADIŠTENJE ENERGIJE**
“SUPERALKALI” CLUSTERS, PRODUCTION, POTENTIAL APPLICATION LIKE ENERGY STORAGE MATERIALS
Suzana VELIČKOVIĆ, Xianglei KONG. 15

Redovna izlaganja

2. **UPOTREBA NIKLA KAO MEĐUPREVLAKE U CILJU SMANJENJA KONTAKTNE KOROZIJE NA ELEKTRIČNIM KONTAKTIMA AL-CU**
USE OF NICKEL AS AN INTERMEDIATE COATING TO REDUCE CONTACT CORROSION ON ELECTRICAL CONTACTS AL-CU
Silvana DIMITRIJEVIĆ, Zoran STEVIĆ, Aleksandra IVANOVIĆ, Stevan DIMITRIJEVIĆ, Saša MARJANOVIĆ, Nikhil DHAWAN 23
3. **SINTEZA SREBRNIH ČESTICA VELIČINE MIKROMETRA PRIMENJIVE ZA DEBELO FILMNE KONTAKTE NA SOLARNIM ČELIJAMA**
SYNTHESIS OF MICRO-SIZED SILVER PARTICLES SUITABLE FOR THICK FILM CONTACTS ON SOLAR CELLS
Stevan DIMITRIJEVIĆ, Silvana DIMITRIJEVIĆ, Michele MILICIANI, Željko KAMBEROVIĆ, Zara CHERKEZOVA-ZHELEVA. 29
4. **SINTEZA I KARAKTERIZACIJA PREMAZA EPOKSIDNE SMOLE SA POBOLJŠANOM OTPORNOŠĆU NA PLAMEN UPOTREBOM MODIFIKOVANE TANINSKE KISELINE**
SYNTHESIS AND CHARACTERIZATION OF EPOXY RESIN COATING WITH IMPROVED FIRE RESISTANCE BY THE ADDITION OF MODIFIED TANNIC ACID
Andreja ŽIVKOVIĆ, Nataša TOMIĆ, Marija VUKSANOVIĆ, Aleksandar MARINKOVIĆ 35
5. **PRIMENA KONCEPTA 3D ŠTAMPE BETONA U IZRADI VETROGENERATORA**
APPLYING CONCEPT OF 3D PRINTING CONCRETE IN WIND TOWER CONSTRUCTION
Aleksandar SAVIĆ, Miša STEVIĆ, Sanja MARTINOVIĆ, Milica VLAHOVIĆ, Tatjana VOLKOV HUSOVIĆ 43
6. **TERMOVIZIJSKI MONITORING TOPLOTE HIDRATACIJE BETONA**
THERMOVISION MONITORING OF CONCRETE HEAT OF HYDRATION
Aleksandar SAVIĆ, Zoran STEVIĆ, Sanja MARTINOVIĆ, Milica VLAHOVIĆ, Tatjana VOLKOV HUSOVIĆ 47

7.	UTICAJ MEHANOHEMIJSKE AKTIVACIJE KOMPONENTI NA SINTEZU KORDIJERITNE KERAMIKE ZA PRIMENU U ELEKTRONICI INFLUENCE OF MECHANOCHEMICAL ACTIVATION OF COMPONENTS ON SYNTHESIS OF CORDIERITE CERAMICS FOR APPLICATION IN ELECTRONICS Nataša ĐORĐEVIĆ, Milica VLAHOVIĆ, Slavica MIHAJLOVIĆ, Sanja MARTINOVIĆ	51
8.	UTICAJ VREMENA RELAKSACIJE AKTIVIRANE SMEŠE NA SINTEZU KERAMIKE ZA NAMENU U ELEKTRONICI IMPACT OF RELAXATION TIME OF ACTIVATED MIXTURE ON CERAMICS SYNTHESIS FOR ELECTRONICS PURPOSES Nataša ĐORĐEVIĆ, Milica VLAHOVIĆ, Slavica MIHAJLOVIĆ, Sanja MARTINOVIĆ	57
2. Energetski izvori i skladištenje energije		
9.	POTENCIJAL POLJOPRIVREDNE BIOMASE U SISTEMIMA PROIZVODNJE BIOGASA U REPUBLICI SRBIJI POTENTIAL OF AGRICULTURAL BIOMASS IN BIOGAS PRODUCTION SYSTEMS IN THE REPUBLIC OF SERBIA Olivera EĆIM-ĐURIĆ, Dragan KRECULJ, Danijela ŽIVOJINOVIĆ, Miloš VORKAPIĆ	63
10.	GASIFIKACIJA OSTATAKA BIOMASE ZA POTREBE PROIZVODNJE ELEKTRIČNE ENERGIJE GASIFICATION OF BIOMASS WASTES AND RESIDUES FOR ELECTRICITY PRODUCTION Marta TRNINIĆ	71
11.	POBOLJŠANJE SVOJSTAVA BETONA DODATKOM LETEĆEG PEPELA IZ TERMoeLEKTRANE ZA PRIMENU U GEOTERMALNIM SISTEMIMA ENHANCING PROPERTIES OF CONCRETE BY ADDITION OF FLY ASH FROM A THERMAL POWER PLANT FOR APPLICATION IN GEOTHERMAL SYSTEMS Milica VLAHOVIĆ, Aleksandar SAVIĆ, Sanja MARTINOVIĆ, Nataša ĐORĐEVIĆ, Zoran STEVIĆ, Tatjana VOLKOV HUSOVIĆ.	77
12.	PRIMENA OBNOVLJIVIH IZVORA ENERGIJE U ZGRADARSTVU APPLICATION OF RENEWABLE ENERGY RESOURCES IN BUILDINGS Njegoš DRAGOVIĆ, Milovan VUKOVIĆ, Igor UROŠEVIĆ	87
13.	EFIKASNA SINHRONIZACIJA DIZEL GENERATORA U USLOVIMA PROMENLJIVE FREKVENCIJE IMPROVED SYNCHRONIZATION OF DIESEL GENERATORS IN VARIABLE FREQUENCY CONDITIONS USING PREDICTIVE METHOD Zoran NIKOLIĆ, Dušan NIKOLIĆ	95
14.	KORIŠĆENJE OBNOVLJIVIH IZVORA – PRETVARANJE GEOTERMALNE ENERGIJE U ELEKTRIČNU UTILIZING RENEWABLE RESOURCES – CONVERTING GEOTHERMAL ENERGY TO ELECTRICITY Miljan VLAHOVIĆ, Milica VLAHOVIĆ, Zoran STEVIĆ	101
15.	OBNOVLJIVI IZVORI ENERGIJE, POTENCIJALI I PRIMENA U SVETSKIM OKVIRIMA I U SRBIJI RENEWABLE ENERGY SOURCES, POTENTIALS AND APPLICATIONS WORLDWIDE AND IN SERBIA Miomir MIKIĆ, Sanja PETROVIC, Zorica SOVRLIĆ, Daniela UROŠEVIĆ	111

16.	OCENA ŽIVOTNOG CIKLUSA BIOENERGETSKIH SISTEMA LIFE CYCLE ASSESSMENT OF BIOENERGY SYSTEMS Slobodan CVETKOVIĆ, Mirjana KIJEVČANIN.	119
3. Energija vetra		
17.	VETROTURBINE SNAGE PREKO 20 MW – TEHNOLOŠKA PERSPEKTIVA WIND TURBINE BEYOND 20 MW – TECHNOLOGY PERSPECTIVE Aleksandar SIMONVIĆ, Aleksandar KOVAČEVIĆ, Toni IVANOV, Miloš VORKAPIĆ	123
18.	NUMERIČKA PROCENA AERODINAMIČKIH PERFORMANSI ROTORA VETROTURBINE SA VERTIKALNOM OSOM OBRTANJA I KONCENTRATOROM NUMERICAL EVALUATION OF AERODYNAMIC PERFORMANCES OF VERTICAL-AXIS WIND TURBINE ROTOR WITH FLOW CONCENTRATOR Jelena SVORCAN, Ognjen PEKOVIĆ, TONI IVANOV, Miloš VORKAPIĆ	135
19.	UPRAVLJANJE PRETVARAČIMA U VETROTURBINAMA CONTROL OF CONVERTERS IN WIND TURBINES Stevan JOKIĆ, Zoran STEVIĆ	143
4. Solarna energija		
20.	NAPREDNI SOFTVERSKI SISTEM ZA MONITORING SOLARNOG NAPAJANJA ADVANCED SOFTWARE SYSTEM FOR MONITORING OF SOLAR PANELS Vuk JOVANOVIĆ, Ilija RADOVANOVIĆ, Zoran STEVIĆ.	155
21.	ANALIZA I POREĐENJE RAZLIČITIH METODA MPPT KOD PV SISTEMA NAPAJANJA ANALYSIS AND COMPARISON OF DIFFERENT MPPT METHODS IN PV POWER SYSTEMS Zoran STEVIĆ, Miša STEVIĆ, Ilija RADOVANOVIĆ	159
22.	SOLARNA ENERGIJA U SRBIJI SOLAR ENERGY IN SERBIA 163 Sanja PETROVIĆ, Miomir MIKIĆ, Daniela UROŠEVIĆ	163
23.	MOGUĆNOSTI IMPLEMENTACIJE FOTONAPONSKIH SOLARNIH PANELA U PODRUČJIMA NAMENJENIM VIŠEPORODIČNOM STANOVANJU POSSIBILITIES OF IMPLEMENTATION OF PHOTOVOLTAIC SOLAR PANELS IN MULTI-FAMILY HOUSING AREAS Borjan BRANKOV, Ana STANOJEVIĆ, Mila PUCAR, Marina NENKOVIĆ-RIZNIC	167
24.	PRIMENA SOLARNE ENERGIJE U FUNKCIJI ODRŽIVOG RAZVOJA U JP EPS, OGRANAK RB „KOLUBARA“- ORG. CEL. PRERADA APPLICATION OF SOLAR ENERGY IN THE FUNCTION OF SUSTAINABLE DEVELOPMENT IN PC EPS, BRANCH OF RB „KOLUBARA“ - ORG. CEL. PROCESSING Momčilo MOMČILOVIĆ, Milisav TOMIĆ.	177

5. Energetska efikasnost

25. **ENERGETSKA EFIKASNOST U SEKTORU JAVNIH ZGRADA
NA TERITORIJI GRADA KRAGUJEVCA – STUDIJA SLUČAJA
OŠ „MILUTIN I DRAGINJA TODOROVIĆ“**
ENERGY EFFICIENCY IN THE PUBLIC BUILDINGS SECTOR
IN THE TERRITORY OF THE CITY OF KRAGUJEVAC – CASE STUDY OF
“MILUTIN AND DRAGINJA TODOROVIĆ” ELEMENTARY SCHOOL
Ana RADOJEVIĆ, Aleksandar NEŠOVIĆ,
Jasmina SKERLIĆ, Dušan GORDIĆ, Danijela NIKOLIĆ 189
26. **SIMULACIJA INVERTORA ZA INDUKCIONO GREJANJE**
SIMULATION OF INVERTERS FOR INDUCTION HEATING
Biljana BAKOVIĆ, Zoran STEVIĆ. 199
27. **PRIMENA SUPERKONDENZATORA U ELEKTRIČNIM VOZILIMA**
APPLICATION OF SUPERCAPACITORS IN ELECTRIC VEHICLES
Zoran STEVIĆ, Ilija RADOVANOVIĆ, Miša STEVIĆ 207
28. **ENERGETSKI EFIKASAN SISTEM ZA STERILIZACIJU DRVETA**
ENERGY EFFICIENT SISTEM FOR WOOD STERILIZATION
Miloš MARJANOVIĆ, Miša STEVIĆ, Miloš MILEŠEVIĆ,
Žarko ŠEVALJEVIĆ, Sanja PETRONIĆ, Marta TRNINIĆ, Zoran STEVIĆ. 211

6. Aplikacije i usluge

29. **KOJE VEŠTINE SU POTREBNE U PROIZVODNJI LITIJUM-JONSKIH
BATERIJA ZA ELEKTRIČNA VOZILA**
WHAT SKILLS ARE NEEDED IN PRODUCTION OF
LITHIUM-ION BATTERIES FOR ELECTRICAL VEHICLES
Zoran KARASTOJKOVIĆ 217
30. **PRIMENA LASERA U AUTOMOBILSKOJ INDUSTRIJI**
APPLICATION OF LASERS IN AUTOMOTIVE INDUSTRY
Milesa SREĆKOVIĆ, Nenad IVANOVIĆ, Stanko OSTOJIĆ,
Aleksander KOVAČEVIĆ, Nada RATKOVIĆ KOVAČEVIĆ,
Zoran KARASTOJKOVIĆ, Sanja JEVTIĆ 223
31. **RASTVARANJE KATODNOG MATERIJALA IZ LIB
U SUMPORNOJ KISELINI U PRISUSTVU AZOTA**
DISSOLUTION OF LIBS CATHODE MATERIAL
IN SULFURIC ACID IN THE PRESENCE OF NITROGEN
Dragana V. MEDIĆ, Snežana M. MILIĆ, Slađana Č. ALAGIĆ,
Zoran M. STEVIĆ, Boban R. SPALOVIĆ, Maja M. NUJKIĆ, Ivan N. ĐORĐEVIĆ. 241
32. **INTEGRACIJA DISTRIBUIRANIH PV SISTEMA U PAMETNIM SREDINAMA
KORISTECI FOG COMPUTING ARHITEKTURU**
INTEGRATION OF DISTRIBUTED PHOTOVOLTAIC SYSTEMS IN THE SMART
ENVIRONMENT THROUGH FOG COMPUTING ARCHITECTURE 247
Ilija RADOVANOVIĆ, Ivan POPOVIĆ. 247
33. **PRIMENA METODOLOGIJE PAMETNIH MREŽA
U DISTRIBUCIJI ELEKTRIČNE ENERGIJE**
SMART GRID TECHNOLOGY IN POWER DISTRIBUTION SYSTEMS
Ivan POPOVIĆ. 251
34. **MOGUĆNOSTI PRIMENE IIOT PLATFORME
U ELEKTROENERGETSKIM SISTEMIMA**
POSSIBILITIES OF IIOT APPLICATION PLATFORMS IN THE ELECTRICAL
POWER SYSTEMS 255
Vojkan NIKOLIĆ, Zoran STEVIĆ, Stefana JANIĆIJEVIĆ, Dragan KRECULJ 255

35.	ISTRAŽIVANJE UTICAJA RELATIVNE VLAŽNOSTI I TEMPERATURE NA IOT REŠENJE ZASNOVANO NA JEFTINIM SENZORIMA ZA PRAĆENJE KVALITETA VAZDUHA INVESTIGATION OF THE INFLUENCE OF RELATIVE HUMIDITY AND TEMPERATURE ON THE IOT SOLUTION WITH LOW COST AIR QUALITY MONITORING SENSORS Ivan VAJS, Dejan DRAJIĆ, Ilija RADOVANOVIĆ.	261
36.	RAČUNARSKO UPRAVLJANJE ENERGETSKI EFIKASNIM SISTEMOM ZA STERILIZACIJU DRVETA COMPUTER CONTROL OF ENERGY EFFICIENT WOOD STERILIZATION SYSTEM Miša STEVIĆ, Miloš MARJANOVIĆ, Ilija RADOVANOVIĆ, Zoran STEVIĆ.	267
37.	VAŽNOST PRIMENE ANALIZE RIZIKA KOD OPREME POD PRITISKOM KOJA SE ISPITUJE PO POSEBNOM PROGRAMU IMPORTANCE OF APPLYING RISK ANALYSIS TO PRESSURE EQUIPMENT TESTED BY A SPECIAL PROGRAM Sanja PETRONIĆ, Marko JARIĆ, Katarina ČOLIĆ, Suzana POLIĆ, Dimitrije MALJEVIĆ	271
38.	AUTOMATIZACIJA PROCESA PROIZVODNJE BAKARNE ŽICE METODOM LIVENJA U VIS – PODSISTEM ZA INDUKCIONO ZAGREVANJE AUTOMATION OF A COPPER WIRE MANUFACTURING PROCESS USING UP-CASTING METHOD – SUBSYSTEM FOR INDUCTION HEATING Nada RATKOVIĆ KOVAČEVIĆ, Misa STEVIĆ, Milos MILEŠEVIĆ, Srđan MAKSIMOVIĆ, Đorđe DIHOVIČNI, Zoran STEVIĆ.	279
39.	POVEĆANJE TOLERANCIJE GREŠKE ADC AD7799 INCREASING FAULT TOLERANCE OF ADC AD7799 Artem BASKO, Elena PONOMARYOVA	287
40.	MOGUĆNOST KORIŠĆENJA KOŠTICA VIŠNJE KAO BIOGORIVA ZA DOBIJANJE TOPLOTNE ENERGIJE POSSIBILITY OF USING SOUR CHERRY PITS AS BIOFUEL FOR OBTAINING THERMAL ENERGY Milorad PETROVIĆ, Milan JOVANOVIĆ, Zoran ŠTIRBANOVIĆ, Jovica SOKOLOVIĆ, Vojka GARDIĆ	295

“SUPERALKALNI“ KLASITERI, PROIZVODNJA, POTENCIJALNA PRIMENA KAO MATERIJAL ZA SKLADIŠTENJE ENERGIJE

“SUPERALKALI” CLUSTERS, PRODUCTION, POTENTIAL APPLICATION LIKE ENERGY STORAGE MATERIALS

Suzana VELIČKOVIĆ¹ and Xianglei KONG²

¹Department of Physical Chemistry, VINČA Institute of Nuclear Sciences - National Institute of the Republic of Serbia, University of Belgrade, Belgrade, Serbia

²The State Key Laboratory and Institute of Elemento-Organic Chemistry, College of Chemistry, Nankai University, China

<https://doi.org/10.24094/mkoiee.020.8.1.15>

Jedan od glavnih događaja prošlog veka bilo je prepoznavanje klastera kao gradivnih blokova novih materijala. „Superalkalni“ klasteri zbog svoje energije ionizacije koja je niža od alkalnih atoma, predstavljaju odlična redukciona sredstva; stoga su prepoznati kao dobri kandidati za sintezu neobično jedinjenja. „Superalkali“, igra važnu ulogu u nauci o hemiji i materijalima zbog svog potencijala da služe kao strukturne jedinice za sastavljanje novih nanostrukturisanih funkcionalnih materijala, kao što su nelinearni optički materijali, materijali za skladištenje vodonika, kao i odličan redukциони reagens za smanjenje emisije ugljen-dioksida, azot-oksida i molekularnog azota. Jedan od načina za dobijanje klastera je korišćenje nekonvencionalnih metoda. Do danas, masena spektrometrija se pokazala ključnom metodom koja nema alternativu u oblasti proizvodnje „superalkalijskih“ klastera. Međutim, da bi se dobili ovi klasteri, potrebno je izvršiti modifikacije masenih spektrometra dostupnih na tržištu. U ovom radu će biti predstavljene mogućnosti dobijanja „superalkalnih“ klastera kombinacijom dve klasične metode masene spektrometrije, poput Knudsenove ćelije i površinske ionizacije u magnetnom masenom spektrometru. Modifikovana klasična površinska jonizacija masena spektrometrija potvrdila se kao efikasna i jeftina metoda za dobijanje ovih klastera.

Ključne reči: „Superalkalni“ klasteri; masena spektrometrija; Knudsenova ćelija

One of the major developments of the past century was the recognition of clusters as building blocks of new materials. “Superalkali” clusters because of their ionization energies which lower than alkaline atoms, present the excellent reducing agents; hence, they are recognized as good candidates for the synthesis of unusually compounds. “Superalkalis”, plays an important role in the chemistry and material science because of their potential to serve as structural units for the assembly of novel nanostructured functional materials, such as nonlinear optical materials, hydrogen storage materials, as well as an excellent reduction reagent for decreasing emissions of carbon dioxide, nitrogen oxides, and molecular nitrogen. One way to get a cluster is to use unconventional methods. To date, the mass spectrometry has proven itself a crucial method, which has no alternative, in the field of the production “superalkali” clusters. However, in order to obtain these clusters, it is necessary to make modifications of the mass spectrometers available on the market. Within this paper, the possibilities of obtaining “superalkali” clusters by combining two classical methods of mass spectrometry such as, Knudsen cell and the surface ionization within a magnetic mass spectrometer will be presented. The modified classic surface ionization mass spectrometry has confirmed to be an efficient and inexpensive method for obtaining these clusters.

Key words: “Superalkali” clusters; mass spectrometry; Knudsen cell

¹ Corresponding author, email: vsuzana@vin.bg.ac.rs

1 Introduction

The direct translation of the word cluster means group, however, in different disciplines clusters have different meanings. In physics and chemistry, a cluster means a group of atoms or molecules formed by interactions ranging from very weak van der Waals to strong ionic bonds with regular and arbitrarily scalable repetition of a basic unit. Clusters can be composed of a few to a few thousand basic units, and their size is intermediate between atoms and balks. The most important feature of clusters is that their characteristics can be changed by adding a single atom or electron. Clusters possess a large number of energetically close isomers, and the number of isomers grows huge with increasing cluster size, this is different from molecules that have a well-defined composition and structure (organic compound have only a small number of isomers). The fact that clusters can be produced from almost any element in the periodic table leads to a wide-ranging interest of researchers in the studies of clusters of various compositions. In the cluster area, another great discovery was the fact that clusters could be the basic structural unit of new materials, which are relatively easy and cheap to produce in laboratory conditions [1, 2].

“Superalkalis” are a class of heterogeneously clusters that are characterized by lower ionization energies than that of an alkali metals atom (Li, Na, K, Rb, Cs). Here, it should be highlighted, that “superhalogen” clusters that possess higher electron affinities than those of electronegative elements (such as, F, Cl, O, and so on) exist as well. The concept of “superalkal” and “superhalogen” were defined by Gutsev and Boldyrev, who are still continuously researching the design of these clusters and concept expansion of them. They described mononuclear “superalkals” like a series of molecules ML_{k+1} , where M is an electronegative atom with the maximal formal valence k, while L is an alkali metal atom (for example, OLi_4 , CLi_6 , FLi_2 , FNa_2 or Li_2F , Na_2F , Li_4O , Li_6C); while the general formula for “superhalogen” is MX_{k+1} where M can be an element of metals, k represents the valence and the number of center atom M, X represents highly electronegative ligands, for example NaF_2 , LiF_2 , Pt_2Cl_3 , (unfortunately, they used the mark M in both cases which can lead to confusion) [3-15].

The mononuclear Li_nF ($n = 2$ and 3) clusters violate stoichiometry based on the octet rule since they have nine or more valence electrons. However, theoretical calculations by Schleyer et al. indicate that stability of this cluster originates from their chemical bonding which consists of the attractive electrostatic interaction between the positively charged metal “network” (Li_n^+) and negatively charged electronegative atom (F^-) [16].

The theoretical work of several research groups has shown that in addition to mononuclear, there are other types of “superalkalis” such as, binuclear (M is two different electronegative atom, for example, $CNLi_2$ or Li_2CN cluster), polynuclear (M is CO_3 , SO_3 , PO_4 , AsO_4), bimetallic (L are “mixed” alkali atoms, for example, $LiNaCl$ cluster), and non-metallic species [17]. These clusters, their chemical bonds, which are more complex than previously described, as well as their isomers, go beyond the scope and goal of this paper and therefore are not described in detail.

The aim of this paper is to briefly present theoretical research of potential applications and to describe ways to obtain “superalkali” clusters.

2 Potential application

Castelman and Khana have recently demonstrated that “superalkali”/“superhalogen” clusters mimic the chemical behavior of elements in the periodic table, and maintain their structural and electronic integrities when assembled with other species. Hence “superalkalis/superhalogens” may be excellent candidates to combine with other atoms or clusters. For example, together “superalkali” and “superhalogen”, can form new kinds of clusters, called “superatoms”. Those “superatoms” may serve as potential building blocks for the new cluster assembled materials with unique properties [18, 19].

Li et al. have predicted a series of “superatom” clusters which exhibit extraordinarily large non-linear optical response [20]. Paduani et al. have shown that mononuclear “superalkali” Li_3O , Li_4O , and Na_8 clusters can be combined with Gd or V and form compounds with an outstanding magnetic response [21, 22].

Generally, “superalkali” clusters have a strong tendency to give up an electron and to become a cationic species, while “superhalogens” have a tendency to accept an electron and to become anionic species. For these reasons, “superalkali” and “superhalogen” clusters are recognized as strong reduction and oxidation reagents, respectively. Because “superalkalis” possess excellent reducibility they can be employed to reduce carbon dioxide (CO_2), nitrogen oxides (NO_x , $x = 1$ and 2), and nitrogen (N_2) molecules, which have extremely high stability [23, 24, 25].

It is well known that carbon dioxide emission, due to ever so quick industrialization, is a problem everywhere on our planet. Materials for capturing CO_2 need to have a high and selective absorption. There are many proposed materials for this purpose, such as monoethanolamine, porous organic polymers, carbon materials, zeolites, metal-organic frameworks [26, 27, 28, 29]. However, these materials have many weaknesses, such as low selectivity and high cost. Hence a different strategy for decreasing the concentration of CO_2 in the atmosphere is proposed. This new strategy requires suitable compounds for the complete oxidation or reduction of the thermally stable CO_2 molecule. Czapla and Skurski have calculated that the “superhalogen” series $\text{Sb}_n\text{F}_{5n+1}$ ($n = 1-3$), especially the largest cluster Sb_3F_{16} , can ionize CO_2 by accepting an electron from it [30]. However, Park and Meloni have shown that the chemical bond formed between Li_3F_2 and CO_2 is stronger than that of a “superhalogen” cluster and CO_2 . Due to the easy electron transfer from the “superalkali” Li_3F_2 clusters to the CO_2 , it is formed CO_2^- , despite the fact that CO_2 possesses no positive electron affinity. This process can be utilized for the conversion of CO_2 to useful products (methanol fuel and carboxylic acid) [23].

Nitrogen oxides (NO_n , $n = 1, 2$) are known to be major air pollutants because NO and NO_2 gases react with certain organic compounds forming smog and destroying ozone, which has a significant impact on human health (damage to lung tissue and reduction in lung function) [31, 32]. To date, urea or ammonia with or without the use of a catalyst are used for the reduction of NO_n . In this case, NO_n are converted into nitrogen molecule, water and carbon dioxide. Srivastava has found that “superalkali” FLi_2 represents the effective mean in the single-electron reduction of NO_n into NO_n^- [24].

Nitrogen (N_2) is the most abundant gas molecule on Earth, and very useful for biological systems, but not in the form of molecules. Nitrogen is an inertness gas due to its negative electron affinity of 1.8 eV, and high ionization energy (15.0 eV), which is why it is so difficult for reduction and oxidation [33]. The process of converting N_2 into a useful form is called fixation or activation. To date industrial way to activate N_2 (nitrogen fixation) is converting N_2 to ammonia (NH_3) using Haber–Bosch hydrogenation. This reaction occurs under extreme conditions - temperature range from 600 to 800 K, and pressures as high as 500 atm. Biological fixation performed by the nitrogenase enzyme, the iron (Fe) and the molybdenum iron (MoFe) proteins, is the reaction that occurs under much less extreme conditions (ca. 290 K and 0.8 atm) than the Haber–Bosch hydrogenation [34].

Many studies have been done in both practical and theoretical areas to discover more effective ways to activate N_2 , which is based on the greatest possible distancing of the nitrogen atom. Computational analysis has confirmed that in the metal complexes, such as aluminum clusters with nitrogen, $\text{Al}_{44}\text{N}_2^+$, can successfully stretch the N-N bond length up to the average value of 1.65 Å [35]. Schleyer and co-workers investigated the complexes of N_2 with various lithium “superalkali” clusters (Li_2 , Li_4 , Li_6 , and Li_8). They have shown that in the complex $\text{Li}_n\text{-N}_2$ occurs to stepwise cleavage of the N-N bond and elongated the bond length up to 3.023 Å [36]. Park and Meloni have calculated bond length between N_2 in $(\text{Li}_3\text{F}_2)_6\text{N}_2$ is 5.501 Å, such that it can be concluded that N_2 is completely separated. The activation of diatomic nitrogen can be explained in terms of the addition of electrons, from “superalkali” Li_3F_2 clusters, into the N_2 empty MOs, as a result, increases the distance between the atoms of the nitrogen [25].

“Superalkali” clusters have the potential to become effective hydrogen storage materials because their positively charged metal “network” can bond with molecular hydrogen through electrostatic interactions. Wang et al. found an improved electron transfer between H_2 and “superalkali” (Li_2F) -coated C_{60} . They have shown that 68 H_2 molecules can be stably stored by the $\text{C}_{60}(\text{Li}_2\text{F})_{12}$

cluster. This result suggests that the hydrogen storage capacities for solid sorbents can be greatly improved using “superalkalis”, which can enhance interactions between the hydrogen and host [37].

In the past few decades, there are many theoretical publications about the applications of “superalkali” clusters, but the experimental research is rare.

3 Production “superalkali” clusters

Mass spectrometry is a key method for producing clusters. It can be briefly described that three major components of mass spectrometers have following roles: ion source, for producing cluster ions with a mix of size from the appropriate sample; a mass analyzer, for separate the cluster ions to their mass-to-charge ratio; and detector system, for identification the cluster ions and recording the relative stabilities of each of the detected ionic species. To date, many ion sources have been used for obtaining mononuclear “superalkali” clusters; among them, the most significant are Knudsen cell-electron impact and laser ablation [9-12, 39]. It should be noted that the production of clusters requires significant modifications of commercial mass spectrometers.

The magnetic sector mass spectrometer, with the ionization chamber which is equipped with three classical ionization methods (the electron impact, the surface ionization, and the Knudsen cell) was constructed in the Department of Physical Chemistry (Figure 1).

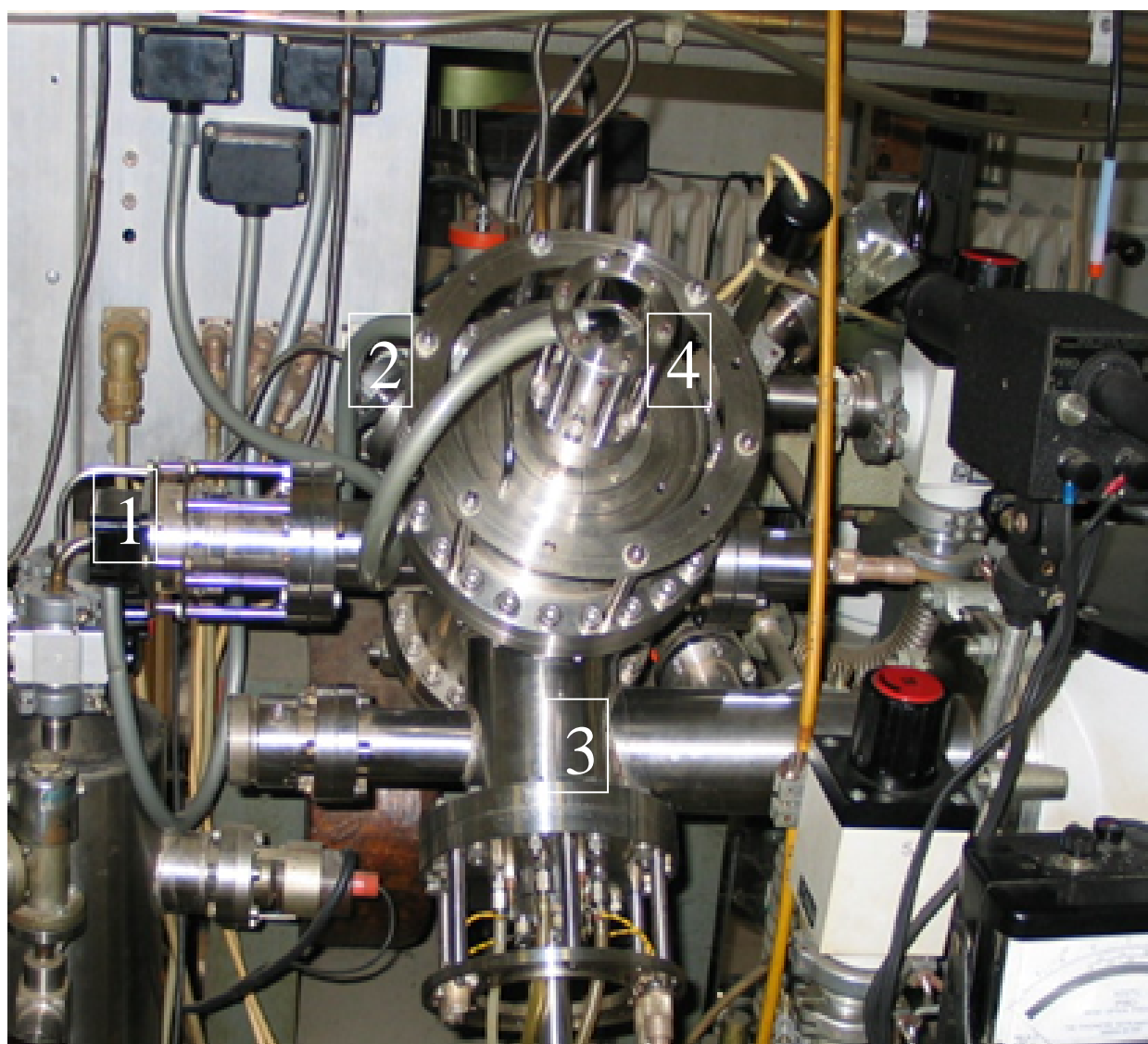


Figure 1. The ionization chamber of the magnetic sector mass spectrometer, 1 - electron source, 2 - gas inlet, 3 - standard Knudsen cell, 4 – the carrier for the surface ionization source or the Knudsen cell.

The triple filament source of surface ionization which consists of the side (evaporation) filament and central filaments and the Knudsen cell are presented in Figure 2.

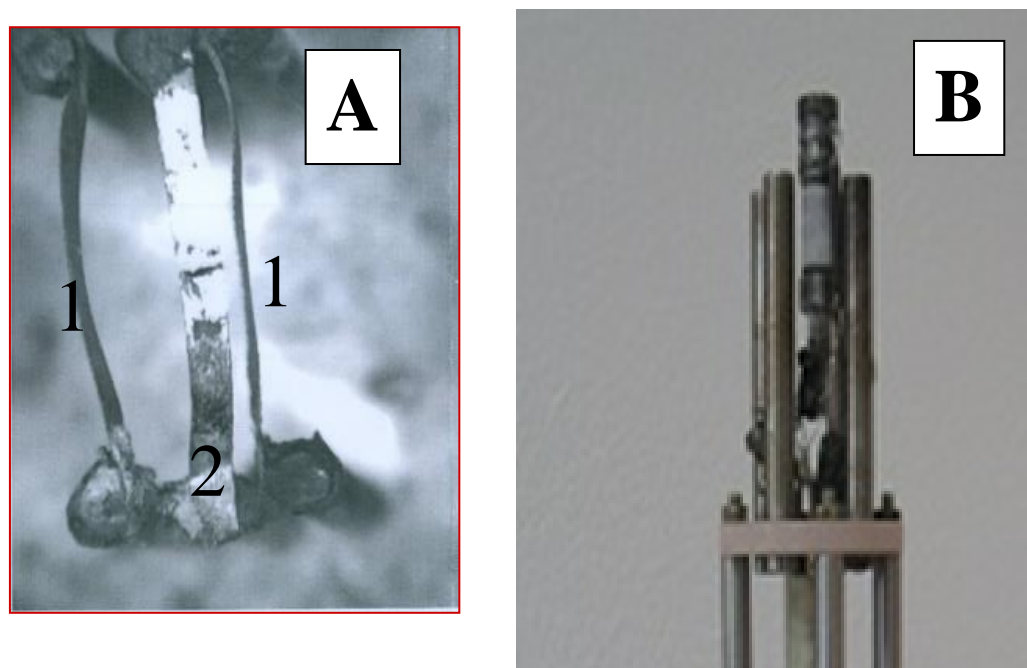


Figure 2. A) The triple filament source of surface ionization, 1 – the side filament, 2 – the central filament. B) The Knudsen cell.

There are several ways to use this mass spectrometer as the source of “superalkali” clusters.

Generally, the surface ionization is a method for generating ions at the hot metal filaments, but it has been shown that this method can be used to obtain these kinds of clusters. The triple filament source of surface ionization was used for that purpose (Figure 2A). The ion source is made of three rhenium filaments of the same dimension ($8\text{mm} \times 1\text{mm} \times 0.05\text{mm}$). The samples were the solutions of $\text{LiX/LiI/C}_2\text{H}_5\text{OH}$, ($\text{X} = \text{F}, \text{Cl}, \text{Br}$), which were deposited on the side filaments, while the C_{60} /toluene solution was deposited on the central filament. The temperature of the side evaporation filaments was in the range of (200 - 1000 K), while the temperature range of central filament was (200-2000 K). The resulting mononuclear clusters were of the type Li_nX , $n=2$ and 3, ($\text{X} = \text{F}, \text{Cl}, \text{Br}, \text{I}$) [39].

It is known that the small size “superalkali” clusters of type Li_nX , (Li_3O , Li_2F , Li_6C , Li_4O , Li_4S , Li_4P , Li_2CN) were obtained by the standard Knudsen cell mass spectrometry combined with the electron impact ionization [9-12].

The standard experimental setup places Knudsen cell outside of the ionization chamber. Neutral clusters are obtained from an appropriate mixture of inorganic salts, which heats up in the Knudsen's cell. The neutral clusters obtained from the cell were ionized used the electron impact method. However, in the experimental research that was carried out at the Department of Physical Chemistry, the Knudsen cell was placed into the ionization chamber so that the Knudsen cell orifice was closer to the electron beam than in the standard case. This enabled more efficient ionization of the neutral clusters formed in the cell. Another modification was that the Knudsen cell can be held on at + 30V with respect to the ionization chamber, it allowed direct identification of positive charge cluster ions generated in the cell. The Knudsen's cell was cylindrical in shape, was made of tantalum or nickel. The height of the cylinder was 7 mm, the outside diameter was 6mm and the orifice diameter was 0.1 mm (Figure 2B). The sample was the LiI/LiF/C_{70} mixture. Thanks to the mentioned changes and variation of the molar ratio of LiF and LiI , two series of clusters were obtained Li_nI and Li_nF ($n = 2, 3, 4, 5$, and 6), for the first time [40].

Heating the Knudsen cell is an important issue. In the standard case, the heater is tungsten wire which is uniformly wrapped around the Knudsen cell. The results showed that the Knudsen cell becomes a more efficient cluster source if the heater is placed directly in the cell. The filament of the surface ionization source can be used as a heater. This filament of rhenium is placed in the centre of the bottom of Knudsen cell. In this experimental setup, the temperature of the cell is not uniform throughout the inner cavity. The heater temperature was between 500 - 2700 K. The sample was inorganic salt such as, MX, M - Li or K, X - F, Cl, Br, I, which were loaded in this Knudsen cell. The serial of lithium and potassium mononuclear clusters such as Li_nBr , Li_nCl^+ K_nX ($n = 2 - 6$) were obtained. The binuclear clusters like as $\text{K}_n\text{Br}_{n-1}^+$ ($n = 3 - 5$) Li_nCl_2^+ ($n = 4 - 7$), and $\text{Li}_n\text{Cl}_{n-1}^+$ ($n = 3 - 5$) were detected, too [41-47].

4 Conclusion

“Superalkalis”, are excellent reducing substances, and thus, are attracting more and more attention in recent years. Theoretically, the potential for discovering new “superalkalis” is limitless, so hence their practical application remains still a challenge.

It has been shown that the combination of the Knudsen cell and surface ionization is a simple, inexpensive, and efficient method for obtaining mononuclear and binuclear “superalkali” clusters. However, the experimental works on “superalkalis” are still limited to the detection of cluster ions in the gas phase; hence more efforts should be paid to produce “superalkalis” in large quantities.

Acknowledgment

The research was funded by the Ministry of Education, Science and Technological Development of the Republic of Serbia, Contract number: 451-03-68/2020-14/200017

References

- [1] **Reinhard, P.G., Suraud, E.**, *Introduction to Clusters Dynamics*, WILEY-VCH Verlag GmbH, Weinheim, 2004.
- [2] **Castleman, A. W., S. N. Khanna, S. N.**, Clusters, Superatoms, and Building Blocks of New Materials, *J. Phys. Chem. C*, *113* (2009), pp. 2664–2675.
- [3] **Gutsev G. L., Boldyrev A. I.**, DVM-X α calculations on the ionization potentials of MX_{k+1}^- complex anions and the electron affinities of MX_{k+1} “superhalogens”, *Chem. Phys.*, *56* (1981), pp. 277-283.
- [4] **Gutsev G. L., Boldyrev A. I.**, DVM X α calculations on the electronic structure of “superalkali” cations, *Chemical Physics Letters.*, *92*, (1982), pp. 262-266.
- [5] **Rehm E., Boldyrev A. I., Schleyer P. v. R.**, Ab initio study of superalkalis. First ionization potentials and thermodynamic stability, *Inorg. Chem.*, *31* (1992), pp. 4834-4842.
- [6] **Boldyrev A. I., Wang L.-S.**, Beyond Classical Stoichiometry: Experiment and Theory, *J. Phys. Chem. A*, *105* (2001), pp. 10759-10775.
- [7] **Wang X. B., Ding C. F., Wang L. S., Boldyrev A. I., Simons J.**, First experimental photoelectron spectra of superhalogens and their theoretical interpretations, *J. Chem. Phys.*, *110*, (1999), pp. 4763-4771.
- [8] **Alexandrova A. N., Boldyrev A. I., Fu Y. J., Yang X., Wang X. B., Wang L. S.**, Structure of the $\text{Na}_x\text{Cl}_{x+1}^-$ ($x = 1-4$) clusters via *ab initio* genetic algorithm and photoelectron spectroscopy, *J. Chem. Phys.*, *121*, (2004), pp. 5709-5719.
- [9] **Kudo H.**, Observation of Hypervalent CLi_6 by Knudsen-effusion Mass Spectrometry, *Nature.*, *355*, (1992), pp. 432-434.
- [10] **Kudo H., Wu C. H., Ihle H. R.**, Mass-spectrometric study of the vaporization of $\text{Li}_2\text{O}(\text{s})$ and thermochemistry of gaseous LiO , Li_2O , Li_3O , and Li_2O_2 , *J. Nucl. Mater.*, *78*, (1978), pp. 380-389.
- [11] **Wu C. H.**, The stability of the molecules Li_4O and Li_5O , *Chem. Phys. Lett.*, *139* (1987), pp. 357-359.

- [12] **Kudo H., Zmbov K. F.**, Observation of gaseous Li_4P : A hypervalent molecule, *Chem. Phys. Lett.* 187 (1991), pp. 77-80.
- [13] **Kudo H., Yokoyama K., Wu C. H.**, The stability and structure of the hyperlithiated molecules Li_3S and Li_4S : An experimental and ab initio study, *J. Chem. Phys.*, 101, (1994), pp. 4190-4197.
- [14] **Kudo H., Yokoyama K.**, The Structures and Bonding of Hyperlithated Molecules, *Bull. Chem. Soc. Jpn.*, 69 (1996), pp. 1459-1469.
- [15] **Shi Y., Bian S., Ma Y., Wang Y., Ren J., Kong X.**, Structures and Superhalogen Properties of Pt_2Cl_n ($2 \leq n \leq 10$) Clusters, *J. Phys. Chem. A*, 123, (2019), pp. 187-193.
- [16] **Schleyer P. V. R.**, *New Horizons in Quantum Chemistry Lowdin P-O, Pullman B (eds). Reidel Dordrecht.* 1983.
- [17] **Sun W.-M., Wu D.**, Recent Progress on the Design, Characterization, and Application of Superalkalis, *Chem. Eur. J.*, 25, (2019), pp. 9568 – 9579.
- [18] **Reber A. C., Khanna S. N., Castleman A. W. J.**, Superaatom Compounds, Clusters, and Assemblies: Ultra Alkali Motifs and Architectures, *J. Am. Chem. Soc.*, 129, (2007), pp. 10189-10194.
- [19] **Claridge S. A., Castelman A.W., Khanna S. N., Murray C. B., Sen A., Weiss P. S.**, Cluster-Assembled Materials. *ACS Nano.*, 3, (2009), pp. 244-255.
- [20] **Li Y., Wu D., Li Z. R.**, Compounds of superaatom clusters: Preferred structures and significant nonlinear optical properties of the $\text{BLi}_6\text{-X}$ ($\text{X} = \text{F}, \text{LiF}_2, \text{BeF}_3, \text{BF}_4$) motifs, *Inorg. Chem.*, 47 (2008), pp. 9773-9778.
- [21] **Paduani C.**, Magnetic Hyperalkali Species of Gd-Based Clusters, *J. Phys. Chem. A*, 122 (2018), pp. 5037–5042.
- [22] **Zhang X., Wang Y., Wang H., Lim A., Gantefoer G., K. Bowen H., Reveles J. U., Khanna S. N.**, On the Existence of Designer Magnetic Superaatoms, *J. Am. Chem. Soc.*, 135, (2013), pp. 4856–4861.
- [23] **Park H., Meloni G.**, Reduction of carbon dioxide with a superalkali, *Dalton Trans.*, 46, (2017), pp. 11942–11949.
- [24] **Srivastava A. K.**, Reduction of Nitrogen Oxides (NO_x) by Superalkalis, *Chemical Physics Letters*, 695 (2018) pp. 205-210.
- [25] **Park H., Meloni G.**, Activation of Dinitrogen with a Superalkali Species, Li_3F_2 , *Chem-PhysChem.*, 19, (2018), pp. 256 – 260.
- [26] **Hansen J., Johnson D., Lacis A., Lebedeff S., Lee P., Russell G.**, Climate Impact of Increasing Atmospheric Carbon Dioxide, *Science*, 213, (1981) pp. 957–966.
- [27] **Mirzaei S., Shamiri A., Aroua M. K.**, Simulation of Aqueous Blend of Monoethanolamine and Glycerol for Carbon Dioxide Capture from Flue Gas, *Energy Fuels*, 30, (2016), pp. 9540–9553.
- [28] **McDonald T. M., Lee W. R., Mason J. A., Wiers B. M., Hong C. S., Long J. R.**, Capture of Carbon Dioxide from Air and Flue Gas in the Alkylamine-Appended Metal–Organic Framework $\text{mmen-Mg}_2(\text{dobpdc})$, *J. Am. Chem. Soc.*, 134, (2012), pp. 7056–7065.
- [29] **Plaza M. G., Garcia S., Rubiera F., Pis J. J., Pevida C.**, Post-combustion CO_2 capture with a commercial activated carbon: Comparison of different regeneration strategies, *Chem. Eng. J.*, 163, (2010), pp. 41–47.
- [30] **Czapla M., Skurski P.**, Oxidizing CO_2 with superhalogens, *Phys. Chem. Chem. Phys.*, 19, (2017), pp. 5435–5440.
- [31] **Omidvarborna H., Kumar A., Kim D. S.**, NO_x emissions from low-temperature combustion of biodiesel made of various feedstocks and blends, *Fuel Process. Technol.*, 140, (2015) pp. 113-118.
- [32] NO_x How Nitrogen Oxides Affect The Way We Live And Breathe, Available online at: <https://nepis.epa.gov/Exe/ZyPURL.cgi?Dockey=P10006ZO.txt> (Retrieved 20-12-2017).

- [33] **Shaver M. P., Fryzuk M. D.**, Activation of Molecular Nitrogen: Coordination, Cleavage and Functionalization of N₂ Mediated By Metal Complexes , *Adv. Synth. Catal.*, 345, (2003), pp. 1061–1076.
- [34] **Howard J. B., Rees D. C.**, Structural Basis of Biological Nitrogen Fixation, *Chem. Rev.*, 96, (1996), pp. 2965–2982.
- [35] **. Cao B., A. Starace K., Judd O. H., Bhattacharyya I., Jarrold M. F., Lopez J. M., Agua-do A.**, Activation of Dinitrogen by Solid and Liquid Aluminum Nanoclusters: A Combined Experimental and Theoretical Study, *J. Am. Chem. Soc.*, 132, (2010), pp. 12906–12918.
- [36] **Roy D., Vazquez A. N., Schleyer P.v. R.**, Modeling Dinitrogen Activation by Lithium: A Mechanistic Investigation of the Cleavage of N₂ by Stepwise Insertion into Small Lithium Clusters, *J. Am. Chem. Soc.*, 131, (2009), pp. 13045–13053.
- [37] **Wang K., Liu Z., Wang X., Cui X.**, Enhancement of hydrogen binding affinity with low ionization energy Li₂F coating on C₆₀ to improve hydrogen storage capacity, *Int. J. Hydrogen Energy*, 39, (2014), pp. 15639–15645.
- [38] **Yokoyama K., Haketa N., Hasimoto M., Furukawa K., Tanaka H., Kudo H.**, Production of hyperlithiated Li₂F by a laser ablation of LiF–Li₃N mixture, *Chem.Phys.Lett.*, 320, (2000), pp. 645–650.
- [39] **Veličković S., Đorđević V., Cvetičanin J., Đustebek J., Veljković., Nešković O.**, Ionization energies of Li_nX (n = 2,3; X = Cl, Br, I) molecules, *Rapid Commun. Mass Spectrom.*, 20, (2006), pp. 3151–3153.
- [40] **Djustebek J., Veličković S., Jerosimić S., Veljković.**, Mass spectrometric study of the structures and ionization potential of Li_nI (n=2, 4, 6) clusters, *J. Anal. Atom. Spectrom.*, 26, (2011), pp. 1641–1647.
- [41] **Veličković S., Djustebek J., Veljković F., Radak B., Veljković M.**, Formation and ionization energies of small chlorine-doped lithium clusters by thermal ionization mass spectrometry, *Rapid Commun. Mass Spectrom.*, 26, (2012), pp. 443–448.
- [42] **Veličković S., Djustebek J., Veljković., Veljković M.**, Formation of positive cluster ions Li_nBr (n = 2 – 7) and ionization energies studied by thermal ionization mass spectrometry, *J. Mass Spectrom.*, 47, (2012), pp. 627–631.
- [43] **Veljković F., Djustebek J., Veljković M., Veličković S., Perić-Grujić A.**, Production and ionization energies of K_nF (n=2–6) clusters by thermal ionization mass spectrometry, *Rapid Commun. Mass Spectrom.*, 26, (2012), pp. 1–6.
- [44] **Veljković F., Djustebek., Veljković M., Perić-Grujić A., Veličković S.**, Study of small chlorine-doped potassium clusters by thermal ionization mass spectrometry, *J. Mass Spectrom.*, 47, (2012), pp. 1495–1499.
- [45] **Milivanović M., Veličković S., Veljković F., Jerosimić S.**, Structure and stability of small lithium-chloride Li_nCl_m^(0,1+) (n < m, n = 1 –6, m = 1 – 3) clusters, *Physical Chemistry Chemical Physics*, 19, (2017), pp. 30481–30497.
- [46] **Milovanović B., Milovanović M., Veličković S., Veljković F., Perić-Grujić A., Jerosimić S.**, Theoretical and experimental investigation of geometry and stability of small potassium-iodide KnI (n = 2 – 6) clusters, *Int. J. Quantum Chem.*, 119, (2019), pp. 26009–26026.
- [47] **Mitić M., Milovanović M., Veljković F., Perić-Grujić A., Veličković S., Jerosimić S.**, Theoretical and experimental study of small potassium-bromide KnB^{r(0,1+)} (n =2–6) and K_nB_{m-1}^(0,1+) (n = 3 - 5) clusters, *Journal of Alloys and Compounds*, 835, (2020), pp. 155301–155301.

UPOTREBA NIKLA KAO MEĐUPREVLAKE U CILJU SMANJENJA KONTAKTNE KOROZIJE NA ELEKTRIČNIM KONTAKTIMA AL-CU

USE OF NICKEL AS AN INTERMEDIATE COATING TO REDUCE CONTACT CORROSION ON ELECTRICAL CONTACTS AL-CU

Silvana DIMITRIJEVIĆ¹¹, Zoran STEVIĆ², Aleksandra IVANOVIĆ¹,
Stevan DIMITRIJEVIĆ³, Saša MARJANOVIĆ², Nikhil DHAWAN⁴

¹Mining and Metallurgy Institute Bor, Serbia

²Technical faculty in Bor, University of Belgrade, Bor

³Innovation Centre of TMF Belgrade, University of Belgrade, Belgrade

⁴ Indian Institute of Technology, IIT-Roorkee, India

Do kontaktne ili galvanske korozije dolazi jer svaki metal ima svoj specifični električni potencijal. To je prvenstveno elektrohemijski proces koji se javlja kada je razlika potencijala elektroda veća od 0,25 V. Aluminijsko-bakarni kontakti široko se koriste u elektrotehnici (izloženi atmosferskoj koroziji) i tipičan su primer kontaktne korozije jer su vrednosti standardnih elektronskih potencijala +0,337 V (Cu) i -1,662 (Al). Iz tog razloga se nikel (potencijal elektrode -0,25 V) obično koristi kao međuprevlaka za sprečavanje kontaktne korozije. U ovom radu urađena su uporedna istraživanja korozije i mehaničkih osobina kontakta Al-Cu, Al-Ni i Al-Ni-Cu.

Ključne reči: galvanska korozija, međuprevlaka, električni kontakti

Contact or galvanic corrosion occurs because each metal has its own specific electrical potential. It is primarily an electrochemical process which occurs when the electrode potential difference is greater than 0.25V. Aluminum-copper contacts are widely used in electrical engineering (exposed to atmospheric corrosion) and are a typical example of contact corrosion since the values of standard electrode potentials are +0.337 V (Cu) and -1.662 (Al). For this reason, nickel (electrode potential -0.25 V) is usually used as an intermediate coating to prevent contact corrosion. These studies will include comparative investigations of the corrosion and mechanical properties of Al-Cu, Al-Ni, and Al-Ni-Cu contact.

Key words: galvanic corrosion, intermediate coating, electrical contacts

1 Introduction

Aluminum, the third most represented metal in the earth's crust, is widely used in the aviation and automotive industries. It is extremely resistant to corrosion and is therefore of considerable use in the construction of small and medium-sized yachts [1-2]. Copper is a very widely used material for its excellent electrical and thermal conductivities in many industrial applications [3- 4].

In electronics, contacts, Al-Cu, are used. The common corrosion forms occurring in the metallic materials include pitting corrosion, intergranular corrosion, stress corrosion, corrosion fatigue, and high-temperature corrosion. [5-7].

It is difficult to make a stable and reliable copper-aluminum joint due to these difference between Cu and Al such as large melting point differences, thermal expansion coefficient, electrode potential and mass formation of brittle intermetallic compounds. Besides, the intermetallic compounds formed in the joint are very different from both Cu and Al in these aspects. To solve these joining problems, many joining technologies were employed [8]. Flash welding was firstly utilized to join copper to aluminum, [9] and then other welding technologies were employed, such as diffusion welding, friction welding, friction stir welding, laser beam welding and ultrasonic welding [10-13]. However, the problem of Cu-Al joints corrosion is still existing and it deteriorates the properties of Cu-Al joints, which severely shorten the service life of components.

¹ Corresponding author, email: silvana.dimitrijevic@irmbor.co.rs

2 Experperimental investigatons

In this research, the influence of nickel as an intermediate coating on the mechanical and corrosion properties of the electrical contacts (contact corrosion of Al-Cu) was investigated. Figure 1 (a – d) shows the most commonly used Al-Cu contacts.

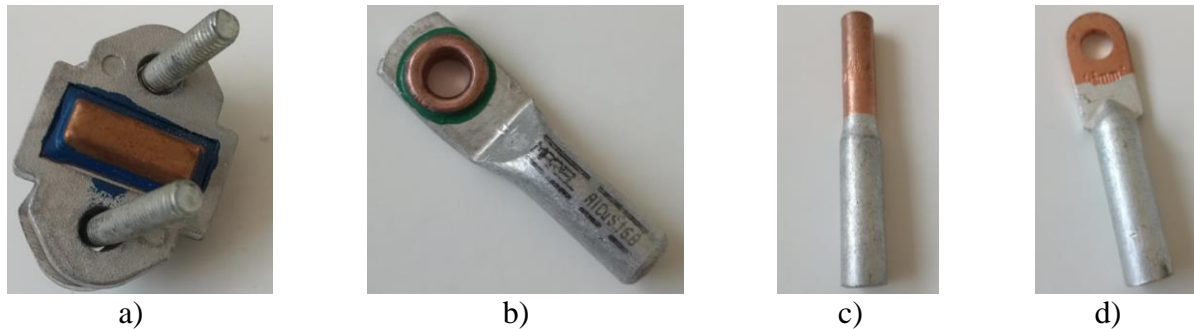


Figure 1. The most commonly used Al-Cu contacts in practice

Laboratory research was performed in four phases:

1. Deposition of copper directly on aluminum
2. Deposition of nickel directly on aluminum
3. Deposition of nickel as an intermediate coating on aluminum/copper
4. Investigation of the physico-mechanical and electrochemical properties of pure metals (Al, Cu, and Ni) and contacts (Al-Ni, Al-Cu, and Al-Ni-Cu).

Aluminum samples (sheet 3x1 cm, 0.3 mm thickness) were chemically degreased with preparation ALOKSIL HOALB (for aluminum and aluminum alloys). After chemical degreasing, the surface of aluminum samples was activated using a solution of sodium chloride. Prepared plates are chemical copper plated with the BAKROHEM preparation. For the electrochemical nickel plating process by the NISAL EXTRA preparation aluminum samples are prepared in the same way as for the chemical copper plating process. Freshly nickel plated plates were electrochemically copper coated using the BAKROCIN CBB preparation.

Figure 2 shows the samples: a) pure copper; b) pure aluminum; c) pure nickel; d) aluminium-copper; e) aluminum-nickel; f) copper- aluminum with nickel as an intermediate coating.

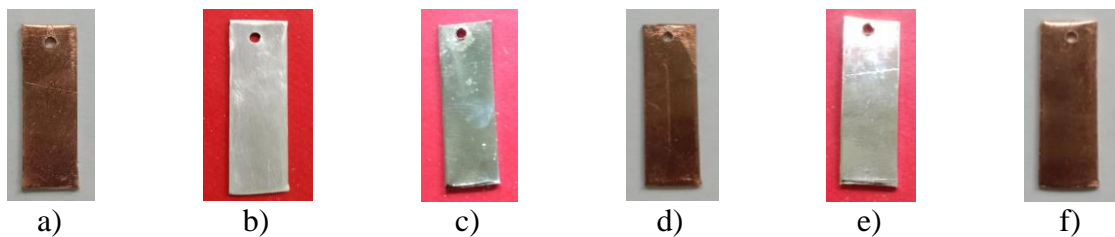


Figure 2. Aluminum samples: a) pure copper; b) pure aluminum; c) pure nickel; d) aluminium-copper; e) aluminum-nickel; f) aluminu - copper with nickel as an intermediate coating.

2.1 Measuring microhardness and electrical conductivity

The microhardness was measured by the Vickers hardness test method and the specific electrical conductivity by the 4 point method [14,15].

In Table 1 are shown the measured values of microhardness and electrical conductivity for the tested samples.

From Table 1, it can be concluded that the use of nickel as an intermediate coating in the Al-Cu electrical contacts significantly improves the mechanical properties. The microhardness of the Al-Ni-Cu (91.0 HV) sample is higher than of the Al-Cu (75 HV) contact while the electrical conductivity is almost the same.

Table 1. Microhardness and electrical conductivity of pure metals and contacts

	Microhardness (HV)	Electrical conductivity (MS/m)
Al	40	37.7
Cu	69.1	57.6
Ni	63.0	14.3
Al-Cu	75.3	36.6
Al-Ni	31.0	17.5
Al-Ni-Cu	91.0	35.1

2.2 Measuring the open circuit potential (POC)

The electrochemical properties of the contacts were examined by measuring the open circuit potential (OCP) for 60 minutes. The open circuit potential (OCP) represents the potential of an electrochemical system when the current in it is negligibly small (weighs zero). In real systems (depending on the impedance of the measuring device), these are currents (for electrodes of the order of cm² size) of the order of nanoamperes or picoamps. This makes this value very close to thermodynamically equilibrium.

The open circuit potential is measured over a period of minutes to several hours, based here on ASTM G3-89 (2010) and ISO 17474: 2012 corrosion standards for metals and alloys, which defines an OCP measurement duration of 3600 seconds (one hour).

Typically, higher OCP values mean higher corrosion resistance ("noble" metals in an electrochemical series, more resistant alloys), or slower corrosion processes. However, since corrosion itself is kinetic (non-equilibrium) and not just a thermodynamic process (especially for alloys), there are many exceptions to this rule. This is most often conditioned by passivation processes, where metals (such as aluminum) with low values of this parameter have low values of corrosion current. Simply, oxides created on the surface (can be hydrates or mixed oxides, as well as other insoluble compounds) prevent further corrosion. Here it is applied in a standard suitable form - as a comparative method for multiple alloys in the same environment.

Gamry Instruments Inc.'s Interface 1000E model potentiostat/galvanostat/equilibrium ammeter was used for electrochemical experiments with the framework software package (version 6.25). Gamry Echem Analyst software was used to analyze the results.

Two-electrode experiments performed. In a two-electrode setup, the current-carrying electrodes are also used for sense measurement. The physical setup for two-electrode mode has the current and sense leads connected together: Working (W) and Working Sense (WS) are connected to a (working) electrode, and Reference (R) and Counter (C) are connected to a second (aux, counter, or quasi-/pseudo-reference) electrode (Figure 3. - diagram of a 2-electrode cell setup).

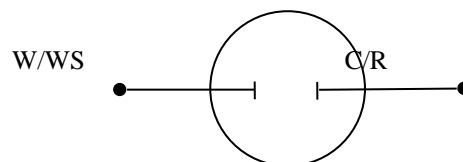


Figure 3. Two-electrode cell setup

The working electrodes were of the pure aluminum, copper and nickel and contacts: Al-Cu, Al-Ni, and Al-Ni-Cu. The counter electrodes were copper and nickel. Experiments were performed at a

temperature of 25 ± 1 ° C. Open Circuit Potential (POC) were measured for 60 minutes in three solutions: 0.5 M Na₂SO₄, NaCl, and NaNO₃.

Results of the open circuit potential measurements are shown in Tables 2,3 and 4 as the initial value (the first second of measurement), and as the final value after 1 h.

Table 2. Results of the open circuit potential measurements in 0.5M Na₂SO₄

	OCP (mV) initial value	OCP (mV) final value after 1 h
Al-Cu (pure metals)	-659,9	-486,4
Al-Ni (pure metals)	-558,0	-411,0
Ni-Cu (pure metals)	-307,8	-188,1
Al+Ni - Cu	-257,1	-210,1
Al+Cu-Cu	-133,1	-62,2
Al+Ni+Cu-Cu	-79,1	-47,56

Table 3. Results of the open circuit potential measurements in 0.5M NaCl

	OCP (mV) initial value	OCP (mV) final value after 1 h
Al-Cu (pure metals)	-580,7	-516,7
Al-Ni (pure metals)	-710,7	-732,9
Ni-Cu (pure metals)	-206,9	-177,1
Al+Ni - Cu	-269,4	-284,3
Al+Cu- Cu	-111,1	-88,3
Al+Ni+Cu-Cu	-87,2	-49,3

Table 3. Results of the open circuit potential measurements in 0.5M NaNO₃

	OCP (mV) initial value	OCP (mV) final value after 1 h
Al-Cu (pure metals)	-469,8	-420,2
Al-Ni (pure metals)	-279,7	-249,5
Ni-Cu (pure metals)	-289,39	200,1
Al+Ni - Cu	-166,0	-145,2
Al+Cu- Cu	-69,3	55,6
Al+Ni+Cu-Cu	-66,3	38,3

3 Conclusion

Tests have shown that the use of nickel as an intermediate coating on Al-Cu electrical contacts improves mechanical and electrical properties. The Al-Cu contact hardness was increased from 75.3 HV to 91.0 HV (Al-Ni-Cu). The electrical conductivity was decreased by just from 36.6 MS/m to 35.1 MS/m (for 4%), which is acceptable. The difference in potential of Al-Cu contact was reduced approximately ten times for all three test solutions. It is also lower in comparison with Al+Cu without Ni intermediate layer for 60 mV in the sulfate solution. The overall effect of the Ni coating between Al and Cu can be considered as positive.

Acknowledgment

This article is the result of the Project funded by the Innovation Fund: “The use of nickel as an intermediate coating to reduce contact corrosion at the Al-Cu electrical contacts”, (ProjecId=282) for which the authors on this occasion would like to thank.

4. References

- [1] <https://en.wikipedia.org/wiki/Aluminium>
- [2] **Vračar R., Živković Ž.**, Ekstraktivna metalurgija aluminijuma, Naučna knjiga, Beograd, 1993.
- [3] **Barouni K., Bazzi L., Salghi R., Mihit M., Hammouti B., Albourine A. and El Issami S.**, Some amino acids as corrosion inhibitors for copper in nitric acid solution, *Mater. Lett.*, 62 3325-3327., (2005)
- [4] **Musa A. Y., Mohamad A. B., Kadhun A. A. H. and Tabal Y. B. A.**, *Intern. J of electroch. Scien.*, Galvanic Corrosion of Aluminum Alloy (Al2024) and Copper in 1.0 M Nitric Acid, 6(10) 5052-5065, (2011)
- [5] **Ye Z., Yang H., Huang J., Yang J., Chen S.**, *J. Mater. Lett.* A novel Zn-Al-Si corrosion resistant filler metal for Cu/Al brazing, 206 201-204, (2017)
- [6] **Guérin M., Andrieu E., Odemer G., Alexis J., Blanc C.**, *J. Corr. Scien.*, Effect of varying conditions of exposure to an aggressive medium on the corrosion behavior of the 2050 Al-Cu-Li alloy, 85 455-470, (2014)
- [7] **Rao CV., Reddy GM., Rao KS.**, *J. Defence Technol.*, Microstructure and pitting corrosion resistance of AA2219 Al–Cu alloy friction stir welds - Effect of tool profile, 11 123-131, (2015)
- [8] **Xia C., Li Y., Puchkov UA., Gerasimov SA., Wang J.**, *J. Vacuum*, Microstructure and phase constitution near the interface of Cu/Al vacuum brazing using Al Si filler metal. 82 799-804, (2008)
- [9] **Wang XG., Li XG., Yan FJ., Wang CG.**, *J. Welding*, World Effect of heat treatment on the interfacial microstructure and properties of Cu-Al joints. 61: 187-196.1, (2016)
- [10] **Wang XG., Yan FJ., Li XG., Wang CG.**, *J. Scien. Technol. Welding and Joining*, Induction diffusion brazing of copper to aluminium., 22: 170-175. 6, (2016)
- [11] **Lee WB., Bang KS., Jung SB.**, *J. All. and Comp.*, Effects of intermetallic compound on the electrical and mechanical properties of friction welded Cu/Al bimetallic joints during annealing, 390: 212-219, (2005)
- [12] **Bisadi H., Tavakoli A., Sangsaraki MT., Sangsaraki KT.**, *J. Mater. & Design*, The influences of rotational and welding speeds on microstructures and mechanical properties of friction stir welded Al5083 and commercially pure copper sheets lap joints. 43: 80-88. 8. (2013)
- [13] **Watanabe T., Yanagisawa A., Konuma S., Yoneda A., Ohashi O.**, *J. Weld. Intern.*, Ultrasonic welding of Al-Cu and Al-SUS304. Study of ultrasonic welding of dissimilar metals (1st Report), 13: 875-886, (2010)
- [14] **Fischer-Cripps, Anthony C.**, Introduction to contact mechanics (2nd ed.). New York: Springer. 212–213, (2007)
- [15] **Osmokrović P.**, Elektrotehnički materijali, Elektrotehnički fakultet, Beograd, 2003.

SINTEZA SREBRNIH ČESTICA VELIČINE MIKROMETRA PRIMENJIVE ZA DEBELO FILMNE KONTAKTE NA SOLARNIM ČELIJAMA

SYNTHESIS OF MICRO-SIZED SILVER PARTICLES SUITABLE FOR THICK FILM CONTACTS ON SOLAR CELLS

Stevan DIMITRIJEVIĆ¹, Silvana DIMITRIJEVIĆ²,
Michele MILICIANI³, Željko KAMBEROVIĆ⁴,
Zara CHERKEZOVA-ZHELEVA⁵

¹ Innovation Centre of TMF Belgrade, University of Belgrade, Serbia,

² Mining and Metallurgy Institute Bor, Serbia

³ Chimet S.p.A., Arezzo, Italy

⁴ Faculty of Technology and Metallurgy (TMF), University of Belgrade, Serbia

⁵ Institute of Catalysis, Bulgarian Academy of Sciences, Sofia, Bulgaria

<https://doi.org/10.24094/mkoiee.020.8.1.29>

Glavni cilj studije bio je utvrditi parametre za proizvodnju srebrnog praha veličine oko jednog mikrometra, koji se može primeniti na paste koje se koriste u proizvodnji i održavanju solarnih ćelija. U svim eksperimentima korišćeni su rastvor srebro nitrata i askorbinske kiseline, kao izvor srebra, odnosno redukciono sredstvo. Polivinilpirolidon (PVP) i želatin su korišćeni kao disperzanti. Dispersant u ovom sistemu deluje kao zaštitno sredstvo na način da sprečava procese aglomeracije i agregacije. Uticaj korišćenih agenasa bio je različit, a jedan od ciljeva istraživanja bio je utvrditi njihove prednosti i nedostatke. Optimalni parametri sinteze bili su: temperatura rastvora od 45 °C, pH=7, koncentracija srebra i askorbinske kiseline od 45 g/l, odnosno 30 g/l. Iako se PVP pokazao pogodnim zaštitnim sredstvom za ciljeve studije, najbolji rezultati su dobijeni upotrebom želatina kao disperzanta u odnosu koncentracije prema srebrnim jonima od 2,5 mas. %.

Ključne reči: srebro; pasta; električni kontakti; solarne ćelije; debeli filmovi.

The main goal of the study was to determine parameters for the production of the micro-sized silver powder applicable to the pastes that are in use in solar cell production and maintenance. In all experiments, silver nitrate solution and ascorbic acid were used, as a silver source and reducing agent, respectively. Polyvinylpyrrolidone and gelatine were used as dispersants. The dispersant in this system acts as a protective agent in a way that prevents agglomeration and aggregation processes. The influence of used agents was different, and one of the aims in the research was to determine the pros and cons of them. The optimal parameters of the synthesis were the solution temperature of 45 °C, pH=7, and concentrations of silver and ascorbic acid of 45 g/l and 30 g/l, respectively. Although PVP has proved to be a suitable protecting agent for the goals of the study, the best results were obtained with the use of gelatine as a dispersant in the concentration ratio against the silver ions of 2.5 wt. %.

Key words: silver; past; electrical contacts; solar cells; thick films.

1 Introduction

Silver is used through a long history as a precious metal, mostly for the production of coins and for artistic purposes. It has extraordinary properties such as the highest electrical and thermal conductivity of all metals [1]. Silver also has excellent ductility, malleability, as well as, optical and antimicrobial properties [2, 3]. These characteristics have led to the wide use of silver in various industries, in the electronics, in the energy sector, for optics and medicine applications, in the environmental sector, like a catalyst in the chemical industry, and many others [4-6].

¹ Corresponding author, email: stevad@gmail.com

Silver nanoparticles and nanostructures have been studied intensively in the last few decades due to their exceptional physico-chemical properties that are conditional and determined by their unique interfacial effects [7]. This provides very special applications in many fields of applied science such as biotechnology (biosensors, pest & microbial control, biosynthesis, pharmaceutical industry, etc.), special catalysis processes, photonics, photovoltaic devices, biofuels, lithium batteries and similar [8-10].

In the present time, a large number of the synthesis methods, for AgNPs (silver nanoparticles) obtaining, are developed. The most important of them are chemical reduction, use of gamma-rays, laser-assisted processes, electrochemical procedures, photochemical reduction, template method, and various biosynthesis [11-14]. Chemical reduction with the support of the polymer systems is still the simplest but very effective method, with low costs and excellent control of the particle size [15]. Aggregation processes can be hindered by stabilization and protection with the interpolyelectrolyte complexes [16].

Conductive inks and pastes, with the use of AgNPs, are used for printed and flexible electronics and front contacts of the crystalline silicon solar cells [17-18]. However, nanotechnology is not exclusive for this kind of application, and the silver powder with the particle size of 500-1500 nm has been extensively used for them [19, 20]. The aim of the paper is to establish maximal concentration of the reagents for the wet chemical reduction synthesis of the micro-sized silver powder in goal to achieve the most economic process for use in small and medium industry conditions. Additional aim was to get near spheric particles with small dispersion of their sizes and use that fine powder for the thin film in the solar energy applications.

2 Experimental

The following chemicals were used in the experiments: silver nitrate (extra pure, $\geq 99\%$, Chimet S.p.A., Italy), L-Ascorbic acid (p.a. grade, Kemika, Croatia), polyvinylpyrrolidone, PVP type K30 (pharmaceutical grade; Ashland, Nederland), gelatin (pharmaceutical grade; Institute Torlak, Serbia). Auxiliary reagents were citric acid monohydrate (for analysis, Carlo Erba Reagents, Italy) and sodium hydroxide (for analysis, $\geq 99\%$, Merck, Germany) for pH regulation and absolute ethanol (pro analysis, Zorka Pharma, Serbia) in the aim of silver powder rinsing. Double distilled water, with conductivity $\leq 1 \mu\text{S}/\text{cm}$ (ISO 3696:1987, Grade 2), was used for solution preparation and the single distilled water with conductivity $\leq 5 \mu\text{S}/\text{cm}$ (the same standard, Grade 3) for rinsing of the obtained silver powders.

The procedure in the experiments consisted of the following: two solutions were made separately, solution 1 was the solution of AgNO_3 , and solution 2 was the solution of ascorbic acid (AA). The dispersant was equally divided into both solutions. Solution 1 has been added to solution 2 with continuous stirring. The temperature for the synthesis was $44\text{--}46^\circ\text{C}$. In the experiments without pH corrections for the system, the total pH of the system was $3.4\text{--}3.7$. Higher pH values were obtained by the use of 10% NaOH. Citric acid has been used only for fine-tuning of the pH. The exact pH values and concentration of reagents in the experiments are noted in the further text.

Scanning electron microscope (SEM) images and electron diffraction spectroscopy (EDS) analysis were performed on a JSM IT 300LV (JEOL, Japan) operated at 20 keV and an X-max (Oxford Instruments, UK), respectively. The particle size distribution was measured and analyzed using a Malvern Mastersizer 2000 and software Version 5.1 (Malvern Instruments, UK). The pH values of the solutions were measured by HI 991301 pH/EC/TDS meter (Hanna Instruments, Romania).

3 Results and discussion

The silver powder obtained by classical chemical reduction of Ag^+ ions with ascorbic acid in the presence of PVP polymer without pH adjustment was the referent material for comparison with the other more advanced procedures. This operation was the simplified industrial process and studied in previous research of the team [21]. Concentrations of the reagents were 45 g/L for Ag(I) ions, 30 g/L for ascorbic acid, and 10 g/L (approximately 1% wt.) for PVP. The reaction duration was 45 minutes, and the realized powder is in figure 1.

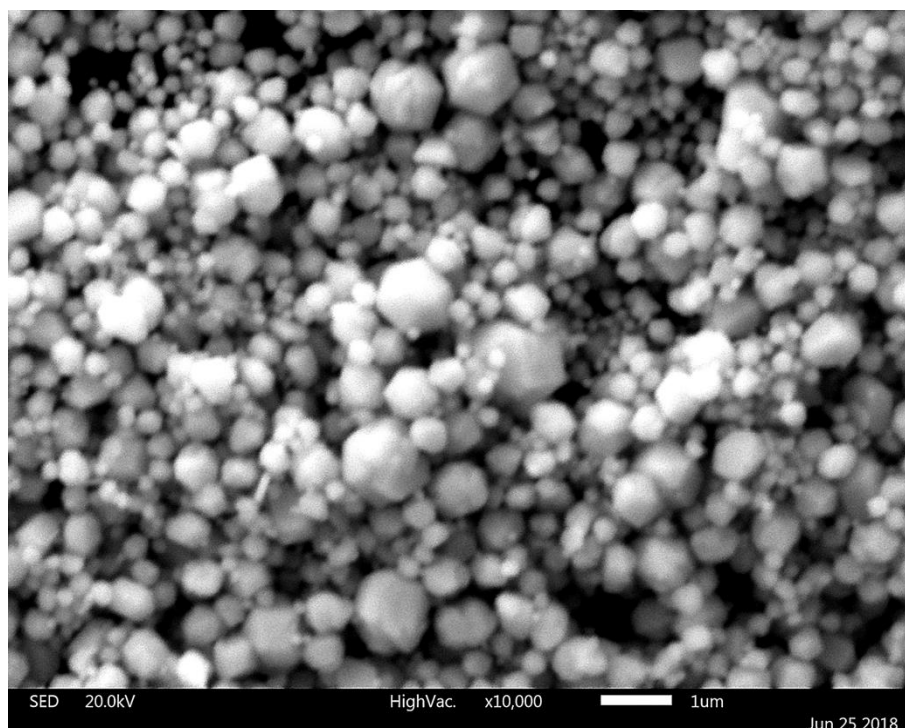


Figure 1. Silver powder after reduction of Ag^+ (45 g/L) with ascorbic acid (30 g/L); 10 g/L PVP

The benefit of the method is that it is simple, inexpensive, and good enough for fine powder with particles with a size of 1-2 μm . As can be seen in figure 1, silver powder has a wide distribution of particle size, which is the main disadvantage of the procedure. Particle size is mainly from 300 nm up to 3 μm , with the majority in the interval from 500 to 2000 nm. Although smaller particles were nearly spherical, the larger were mainly polyhedric, which was not preferable but tolerably since the large aggregates in great numbers have the hexagonal intersection with good packaging characteristics. The picture suggests two parallel mechanisms, agglomeration for smaller and near-spherical particles and aggregation for the larger.

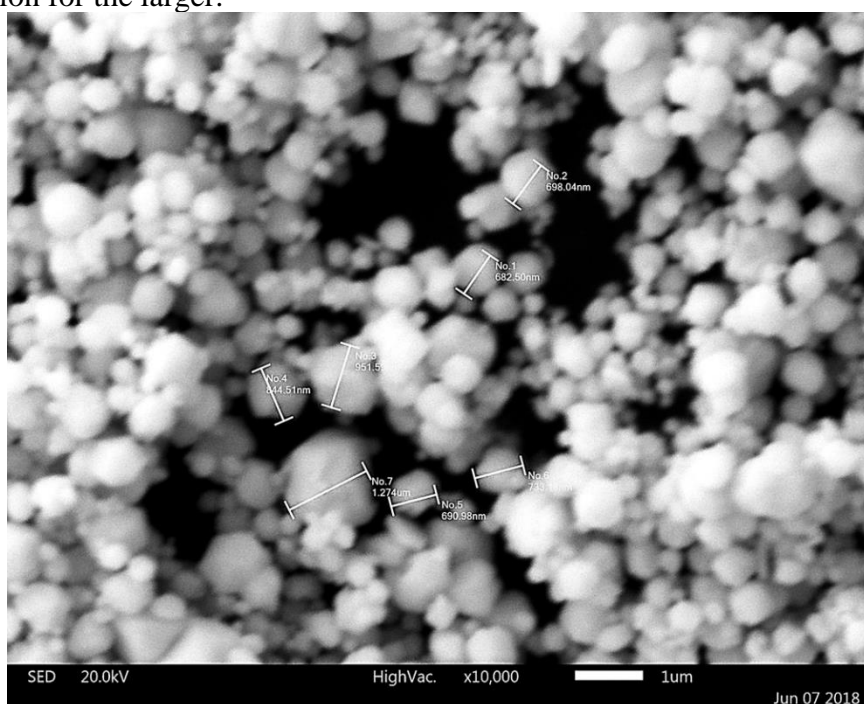


Figure 2. Silver powder after reduction of Ag^+ (30 g/L) with ascorbic acid (20 g/L); 10 g/L PVP

Optimization of the process could be performed differently. In this study, priority was to keep the yield of the process near 100% and to use concentrations as high as possible to achieve lower production costs. With this strategy, very good results are obtained by lowering the concentration of silver on 30 g/L and ascorbic acid in the same percentage (down to 20 g/L). The concentration of PVP also needs to be as low as possible, and it was kept at 10 g/L. The value of pH was raised and kept between 7 and 8. Powder obtained with these parameters is presented in figure 2.

The narrower size distribution of the particles is obvious, as shown in figure 2. Particles are about 1000 nm on average. Small rulers in the figure for particulate grains illustrate that fact. Size for the measured particles ranged from 682 to 1274 nm. Agglomeration is obvious, but agglomeration occurs in two stages, from nanoparticles (about 100 nm), also visible in the figure, to particles with size about 250-300 nm which made final particles. A small sample (not statistically important) that measured by SEM has an average size of approximately 840 nm. Particles are more spherical than in the previous experiment.

Further improvement of the technology was the change of the dispersant. The use of gelatin instead of PVP has given even better results and lower costs. The same concentrations of reaction reagents as with PVP were used for the optimal results of the experiments. The concentration of gelatin was much lower than PVP concentration and was 1:40 in mass ratio against Ag (0.75 g/L). The resulting powder with this modification is shown in figure 3.

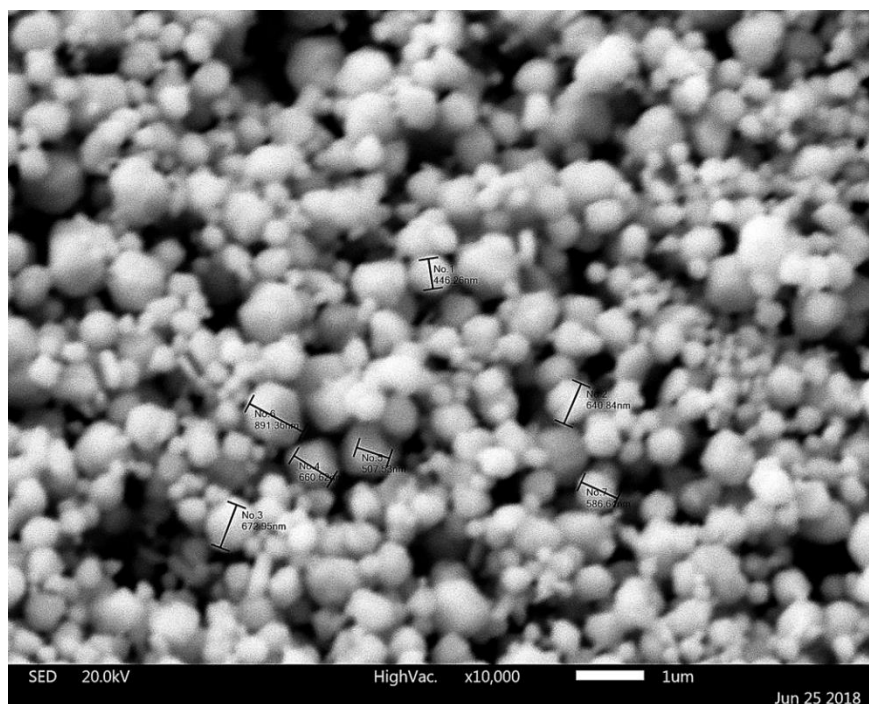


Figure 3. Silver powder after reduction of Ag^+ (30 g/L) with ascorbic acid (20 g/L); 0.75 g/L gelatin

The improvement over the use of PVP is in the more spherical particles than both experiments with PVP as a dispersant (protecting agent), smaller particles, and lower costs (not just that gelatin is less expensive than PVP, but the lower concentration is needed). From figure 3 it can be seen that most of the particles are from 200 to 1000 nm. Characteristics particles were measured and ranged from 446 to 891 nm, with an average size of nearly 630 nm. This powder was measured by laser diffraction, and the results are shown in figure 4.

As can be seen from figure 4, laser diffraction (LD) has given a higher average value for the particle size than SEM which is known from the literature. Nevertheless, the agreement between these two methods is good enough. Figure 4 also illustrates quite a narrow size distribution, LD gives values from 0.5 to 2 μm , and the average value of about 1 μm . The cumulative curve also shows that about 80% of the particles are smaller than 1.5 μm .

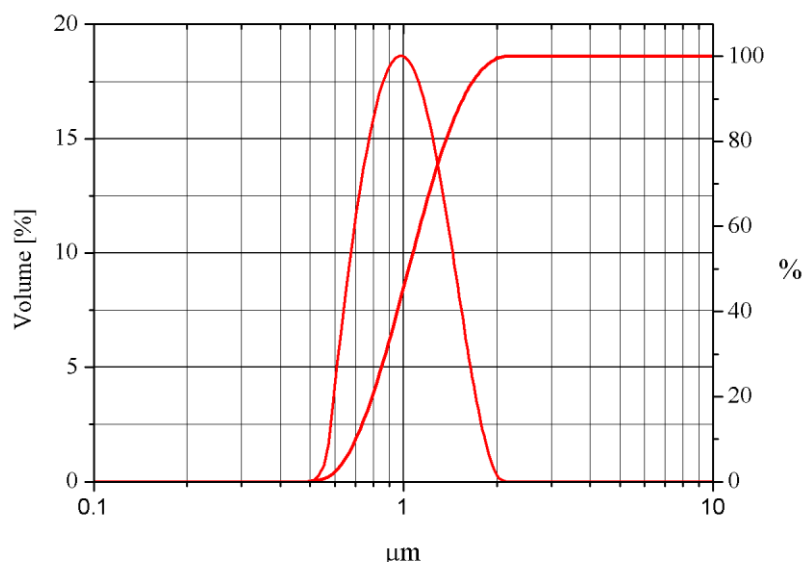


Figure 4. Granulometric composition of the powder obtained by use of gelatin, 1:40 vs silver

4 Conclusions

The study has shown that even high concentrations of reagents (silver ions and ascorbic acid) and low concentration of PVP can produce a silver powder with an average size between 1 and 2 μm . The disadvantage of that reaction parameter is the very wide size distribution of the particles.

Optimization of parameters with the same reagents gives better results, with the average size of nearly 1 μm and narrower size distribution of the particles. Further improvement was achieved by the use of gelatin instead of PVP polymer. Smaller and more spherical particles with a further decrease of the size distribution are obtained. This silver powder can be used for the thick film technology that would be applied in the solar energy industry.

Acknowledgments

This work was supported by the Ministry of Education, Science and Technological Development of the Republic of Serbia (Contract No. 451-03-68/2020-14/200135). This work has resulted from the research project between IC TMF and Chimet company and is based on the project activities of the bilateral project "Green synthesis of advanced catalytic materials for environmental protection" and also COST Action 19140.

5 References

- [1] **Wang, P. J., C. C. Lee**, Silver joints between silicon chips and copper substrates made by direct bonding at low-temperature, *IEEE Transactions on Components and Packaging Technologies*, 33 (2010), 1, pp. 10-15.
- [2] **Nitayaphat, W., T. Jintakosol**, Removal of silver(I) from aqueous solutions by chitosan/bamboo charcoal composite beads, *Journal of Cleaner Production*, 87 (2015), (15 January 2015), pp. 850–855.
- [3] **Gu, T., C. M. Gourlay, T. B. Britton**, Evaluating creep deformation in controlled microstructures of Sn-3Ag-0.5Cu solder, *Journal of Electronic Materials*, 48 (2019), 1, pp. 107–121.
- [4] **Ardestani, M.**, Thermochemical synthesis and sintering of silver-8 wt.% copper oxide nanocomposite powders, *International Journal of Material Research*, 106 (2015), 12, pp. 1294–1297.
- [5] **Pethkar, A. V., K. M. Paknikar**, Thiosulfate biodegradation–silver biosorption process for the treatment of photofilm processing wastewater, *Process Biochemistry*, 38 (2003), 6, pp. 855-860.

- [6] **Toscano, L. M., E. Long**, A new surface finish for the electronics industry: Electroless nickel/immersion silver, *Proceedings 9th International Microsystems, Packaging, Assembly and Circuits Technology Conference (IMPACT)*, IEEE, Taipei, Taiwan, 2014.
- [7] **Vivekanandhan, S., L. Christensen, M. Misra, A. K. Mohanty**, Green process for impregnation of silver nanoparticles into microcrystalline cellulose and their antimicrobial bionanocomposite film, *Journal of Biomaterials and Nanobiotechnology*, 3 (2012), 3, pp. 371–376.
- [8] **Chen, Y, W. H. Tse, L. Chen, J. Zhang**, Ag nanoparticles-decorated ZnO nanorod array on a mechanical flexible substrate with enhanced optical and antimicrobial properties, *Nanoscale Research Letters*, 10 (2015), Article number: 106.
- [9] **Razack, S. A., S. Duraiarasan, M. Vijay**, Biosynthesis of silver nanoparticle and its application in cell wall disruption to release carbohydrate and lipid from *C. vulgaris* for biofuel production, *Biotechnology Reports* 11 (2016), September 2016, pp. 70–76.
- [10] **Tanju, E., N. Atar, M L. Yola, H. Karimi-maleh, A. T. Çolak, A. Olgun**, Facile and green fabrication of silver nanoparticles on a polyoxometalate for Li-ion battery, *Ionics*, 21 (2015), 8, pp. 2193–2199.
- [11] **Iravani, S., H. Korbekandi, S. V. Mirmohammadi, B. Zolfaghari**, Synthesis of silver nanoparticles: chemical, physical and biological methods, *Research in Pharmaceutical Sciences*, 9 (2014), 6, pp. 385–406.
- [12] **Singaravelan, R., S. B. S. Alwar**, Electrochemical synthesis, characterisation and phyto-genic properties of silver nanoparticles, *Applied Nanoscience*, 5 (2015), pp. 983–991.
- [13] **Srikar, S. K., D. D. Giri, D.B. Pal, P. K. Mishra, S. N. Upadhyay**, Green synthesis of silver nanoparticles: A Review, *Green and Sustainable Chemistry*, 6 (2016), 1, pp. 34–56.
- [14] **Ovais, M., A. T. Khalil, M. Ayaz, I. Ahmad, S.K. Nethi, S. Mukherjee**, Biosynthesis of metal nanoparticles via microbial enzymes: a mechanistic approach, *International journal of molecular sciences*, 19 (2018), 12, 4100, 1–20.
- [15] **Demchenko, V., S. Riabov, S. Kobylinskyi, L. Goncharenko, N. Rybalchenko, A. Kruk, O. Moskalenko, M. Shut**, Effect of the type of reducing agents of silver ions in interpolyelectrolyte-metal complexes on the structure, morphology and properties of silver-containing nanocomposites, *Scientific Reports* 10 (2020), 7126.
- [16] **Zezin, A. A.**, Synthesis of hybrid materials in polyelectrolyte matrixes: control over sizes and spatial organization of metallic nanostructures, *Polymer Science C*, 58 (2016), 1, pp. 118–130.
- [17] **Venkata, R. K., K. V. Abhinav, P. S. Karthik, S. S. Prakash**, Conductive silver inks and their applications in printed and flexible electronics, *RSC Advances*, 5 (2015), 95, pp. 77760–77790.
- [18] **Che, Q., H. Yang, L. Lu, Y. Wang**, Nanoparticles-aided silver front contact paste for crystalline silicon solar cells, *Journal of Materials Science Materials in Electronics*, 24 (2013), 2, pp. 524–528.
- [19] **Moudir, N., N. Moulai-Mostefa, Y. Boukennous**, Silver micro- and nano-particles obtained using different glycols as reducing agents and measurement of their conductivity, *Chemical Industry & Chemical Engineering Quarterly*, 22 (2016), 2, 227–234.
- [20] **Sannohe, K., T. Ma, S. Hayase**, Synthesis of monodispersed silver particles: Synthetic techniques to control shapes, particle size distribution and lightness of silver particles, *Advanced Powder Technology*, 30 (2019), 12, pp. 3088–3098.
- [21] **Dimitrijević, S. P., Ž. Kamberović, M. Korać, Z. Andić, S. B. Dimitrijević, N. Vuković**, Influence of reducing agents and surfactants on size and shape of silver fine powder particles, *Metallurgical and Materials Engineering*, 20 (2014), 2, pp. 73–87.

SINTEZA I KARAKTERIZACIJA PREMAZA EPOKSIDNE SMOLE SA POBOLJŠANOM OTPORNOŠĆU NA PLAMEN UPOTREBOM MODIFIKOVANE TANINSKE KISELINE

SYNTHESIS AND CHARACTERIZATION OF EPOXY RESIN COATING WITH IMPROVED FIRE RESISTANCE BY THE ADDITION OF MODIFIED TANNIC ACID

Andreja ŽIVKOVIĆ¹, Nataša TOMIĆ,
Marija VUKSANOVIĆ, Aleksandar MARINKOVIĆ,
Faculty of Technology and Metallurgy, University of Belgrade, Serbia

<https://doi.org/10.24094/mkoiee.020.8.1.35>

U radu je predstavljen novi postupak za dobijanje eko-epoksidnih materijala sa smanjenom zapaljivošću ili su potpuno negorovi, a koji se sintetišu iz bio-obnovljivih sirovina, čiji se proizvodni proces sastoji od dve faze. Poseban aspekt od višestrukog značaja za životnu sredinu je upotreba bio-obnovljivih resursa i smanjenje udela toksične epoksidne komponente u proizvodnji epoksidnih materijala. Prva faza razmatra sintezu derivata komponenata epoksidne smole: epoksi funkcionalizovana taninska kiselina (TA) - ETA i sinteza fosfatnih derivata TA - glicidil ester TA modifikovan fosforom kiselinom (PGET). Drugi faza razmatra sintezu bio-epoksi smole korišćenjem ETA, i PGET koji se koriste kao zamena komponente epoksidne smole (A) – bisfenol A epoksida u odnosu 25-100% kao reaktivni razblaživač za dobijanje proizvoda koji se mogu koristiti u građevinarstvu i drugim industrijskim oblastima, a imaju smanjenu zapaljivost ili potpuno su nezapaljivi. U drugom delu prikazani su rezultati termalnih i mehaničkih ispitivanja za neke od dobijenih derivata. Dodavanje 25% TA derivata poboljšalo je žilavost i zateznu čvrstoću epoksidnog materijala. Termogravimetrija je pokazala da uzorci koji sadrže taninski epoksid pokazuju više ostatka. Delimična ili potpuna zamena epoksidna komponenta sa produktom tanina koristi ekološki prihvatljiv materijal sa značajno povećanom otpornošću na vatru (V-2 do V-0).

Ključne reči: epoksid; tanijska kiselina; retardacija plamena; mehanička svojstva; termalna svojstva

The paper presents a new process for obtaining eco-epoxide materials with reduced combustibility or completely non-combustible, which are synthesized from bio-renewable raw materials, whose production process consists of two stages. A particular aspect of multiple environmental significance is the use of bio-renewable resources and the reduction of the share of the toxic epoxy component in the production of epoxy materials. The first stage considers the synthesis epoxy resin components: epoxy functionalized tannic acid (TA) – ETA, and synthesis of phosphate derivatives of TA - glycidyl ester of TA modified by phosphoric acid (PGET). The second stage considers the synthesis of bio-epoxy resins using ETA and PGET that are used as a replacement of the epoxy resin component (A) – bisphenol A based epoxy in a ratio 25-100% as a reactive diluent to obtain products that can be used in the construction and other industrial fields and have reduced combustibility or completely non-combustible. The second part presents the results of thermal and mechanical tests for some of the obtained derivatives. The addition of 25% of TA derivate improved the toughness as well as the tensile strength of epoxy material. Thermogravimetry showed that samples containing tannin epoxide showed more residue left. Partial or full replacement of the epoxy component with a tannin component produces eco-friendly material with while significantly increased fire resistance (V-2 to V-0).

Key words: epoxy; tannic acid; flame retardant; mechanical properties; thermal properties

¹ Corresponding author, email: sd.andreja@yahoo.com

1 Introduction

The term 'epoxy resin' is used for both crosslinked and non-crosslinked resins. Only non-crosslinked resin contains epoxy - oxirane groups, after which they got their name. In the crosslinked, all reactive epoxy groups reacted. Although there are no longer any epoxy groups in crosslinked resins, they are still called epoxy resins.

Bis (4-hydroxyphenylene) -2,2-propane, also known as bisphenol A (BPA), is used as the base for most epoxides, and it is the monomer derived from fossil fuels. Aromatic compounds are widely used as materials of organic origin due to their stability, strength, toughness and especially the ability to establish intermolecular interactions by overlapping π -bonds, which allows BPA epoxides to have good thermal and mechanical properties, as well as anticorrosive and barrier properties [1,2]. Most epoxies, including BPA epoxy, are subject to hydrolysis to some extent, which can cause the release of BPA and its exposure and contact with humans and the environment [3,4].

BPA epoxide in hydrolyzed form is classified as carcinogenic, mutagenic and reprotoxic (respiratory poisoning) - CMR substance, and is also registered as a cause of endocrine problems (destroyer / hormone disruptor - impact on the sterility of human and animal species) [3-5]. With all this in mind, and the fact that fossil fuels are a non-renewable resource and will eventually deplete, it should be replaced with a naturally found monomer from renewable resources.

Tannins are a secondary biodegradable/biorenewable source of natural aromatic derivatives and the third most common component that can be extracted from wood biomass (cellulose is the most abundant, closely followed by lignin). Tannins are found in the soft tissue of wood, bark, leaves, needles, roots and fruits of many plants, it leaves a dried feeling in the mouth, and it has a bitter, basic taste [6]. It helps with cardiovascular problems, regulates blood pressure and circulation if used properly, it is mostly found in urns and teas such as black, green and white tea. In the plant, they play a protective role from external influences and regulate the growth of the plant, and also give the tissue strength.

Tannins are polyphenolic derivatives, a natural polymer of low molar mass, an undefined structure of molecules that can be divided into three main categories: Hydrolyzable tannins, condensed tannins and complex or compact tannins, complex or compact tannins are a combination of the first two [7]. Tannin can easily be converted into tannic acid (TA).

Fire hazard is a combination of factors, including ignitability, ease of extinction, flammability of the volatile products generated, amount of heat released on burning, rate of heat release, flame spread, smoke obscuration, and smoke toxicity, as well as the fire scenario. Fire fatalities are usually reported as resulting from the lethal atmosphere generated by fires. Carbon monoxide concentrations measured in real fires can reach up to 7500 ppm, which would probably result in a loss of consciousness in 4 minutes. Other components of acute toxicity found in real fires play a secondary role.

The combustion reaction involves two factors: one or more combustibles (reducing agents) and a combusting (oxidizing agent). The combusting is generally the oxygen in the air. The whole process usually starts with an increase in the temperature of the polymeric material due to a heat source, to such an extent that it induces polymer bond scissions. The volatile fraction of the resulting polymer fragments diffuses into the air and creates a combustible gaseous mixture (also called fuel) [8]. This gaseous mixture ignites when the auto-ignition temperature (defined as the temperature at which the activation energy of the combustion reaction is attained) is reached, liberating heat. Alternatively, the fuel can also ignite at a lower temperature (called the flash point) upon reaction with an external source of intense energy (spark, flame, etc.). The decomposition mechanism is highly dependent on the weakest bonds, and also on the presence or absence of oxygen in the solid and gas phases. Generally, thermal decomposition is the result of a combination of the effects of heat and oxygen. We can therefore distinguish between non-oxidizing thermal degradation and oxidizing thermal degradation [8].

Flame retardancy and inhibition of inflammation are very often spoken of as one and the same phenomena and are easily mixed up. Even though quite similar in end results there is some difference to how they prevent flame hazards. Flame inhibition refers to increasing the activation energy of inflammation reaction and therefore making the material burn on much higher temperature than

originally. Flame inhibition does not make inflammation reaction any different in its products and heat generated, it just delays the beginning temperature of the reaction, and once reaction starts it will continue spontaneously until it has finished or forcefully stopped. Therefore inhibition is not enough and it is always combined with another mechanism that will slow the reaction, stop it, adsorb the heat generated and/or isolate the burning material from the source of heat by making a protective barrier, which is collectively classified as flame retardancy. So flame retardancy includes all effects that will prevent a material from ignition.

Flame retardant systems are intended to inhibit or to stop the polymer combustion process previously described. In function of their nature, flame retardant systems can either act physically (by cooling, formation of a protective layer or fuel dilution) or chemically (reaction in the condensed or gas phase). They can interfere with the various processes involved in polymer combustion (heating, pyrolysis, ignition, propagation of thermal degradation). The main modes of action of flame retardant systems are reported and discussed below [9, 10].

Initially, halogenated epoxy materials were used, which had very good flame retardant and mechanical properties, but released very toxic halogen gases harmful to humans and the environment, which is why their use is prohibited [9, 10].

Halogenated reduced flammability materials have been replaced by materials containing additives based on phosphorus compounds that form polymerized phosphoric acid at elevated temperature and / or condensed structures that serve as an improved flame retardant and inhibition of inflammation barrier [9, 10].

Chemical modification of tannic acid yielded an epoxide with improved flame retardant properties, which were achieved by modifying tannic acid molecules with phosphorus oxychloride. Epoxidation was performed by adding glycidol to phosphorus oxychloride modified tannic acid molecules, or by modification of TA with epichlorohydrin (EPH).

The aim of this study is to investigate the thermal and mechanical properties of products obtained from TA by process of epoxidation, reduce BPA epoxy content or completely replace BPA epoxy in cured samples of obtained epoxide. Methods used for characterization are FTIR Analysis, UL94 V test, thermogravimetry analysis (TG) and tensile strength test.

2 Experimental session

2.1 Materials

Chemicals used in synthesis of modified TA: epichlorohydrin (EPH), sodium hydroxide (NaOH), Chloroform, N-methyl-2-pyrrolidone (NMP), phosphorus oxychloride (POCl_3), glycidol (G), N,N-Dimethylformamide (DMF), deionized water (MiliQ), magnesium sulphate (MgSO_4), calcium chloride (CaCl_2) were used as received and supplied from Sigma Aldrich, USA. Reference adhesive was selected to be BPA based epoxy (LG700 epoxy component and HG 700R curing agent) was supplied from GI-NI ltd. Belgrade, Serbia (epoxy value 0.62, epoxy equivalent weight is 160 g / mol, $T_g = 79.4^\circ\text{C}$).

2.2 Synthesis of glycidyl phosphate ester of TA (PGET)

In 250ml three-neck round-bottomed flask equipped with magnetic stirrer 6g of TA was added and dissolved in 40 to 50ml of 1:1 ratio mixture of chloroform and NMP at room temperature for 30 minutes. After 30 minutes had passed, temperature of the oil bath should be set to the value of 70°C , 250ml three-neck round-bottomed flask should be equipped with vacuum condenser, and if all of the tannic acid hasn't been dissolved 1 to 2ml of DMF should be added to the reaction mixture. Two vacuum dropping funnels should also be equipped to the reactor, one should contain 9.75g of POCl_3 diluted to 20ml with chloroform, and the other one should contain 9.42g of G diluted to 40ml with chloroform. As soon as reaction temperature reaches 70°C reaction should be initiated by addition of POCl_3 solution under constant stirring and low vacuum. POCl_3 should be added dropwise for duration of 1 minute, then reaction should be left to occur for 10 minutes after which G should be added also dropwise for duration of 2 minutes, reaction should be yet again be left to occur for 10 minutes. POCl_3 and G should be added the same way in ratio of 1 : 2 until all of the reactants are added, after which

temperature should be risen to the value of 80 or 85°C and vacuum should be gradually be increased, until all the chloroform had been removed. Reaction should be left to occur for at least 12 more hours after which maximum vacuum should be applied in order to remove NMP. When the reaction is finally over PGET should be left in air dryer for a few days or in vacuum desiccator with MgSO₄ and CaCl₂ drying mixture overnight. In order to purify the product following procedure is followed. To the solution was slowly added to 200 mL cold MiliQ water. Extraction of the product with toluene (3 times 70 mL) was followed by drying of organic extract with MgSO₄ overnight. After filtration toluene solution was transferred to flask equipped with short distillation column, Liebig condenser and recipient fitted well to sustain high vacuum (app. 1000 Pa). Concomitant increase of temperature (2 °C/min) was followed by pressure decrease in order to remove all volatile residual compounds in mixture. TA and segment of a modified TA (ETA and PGET) made for the purpose of this research will be presented on figure 1.

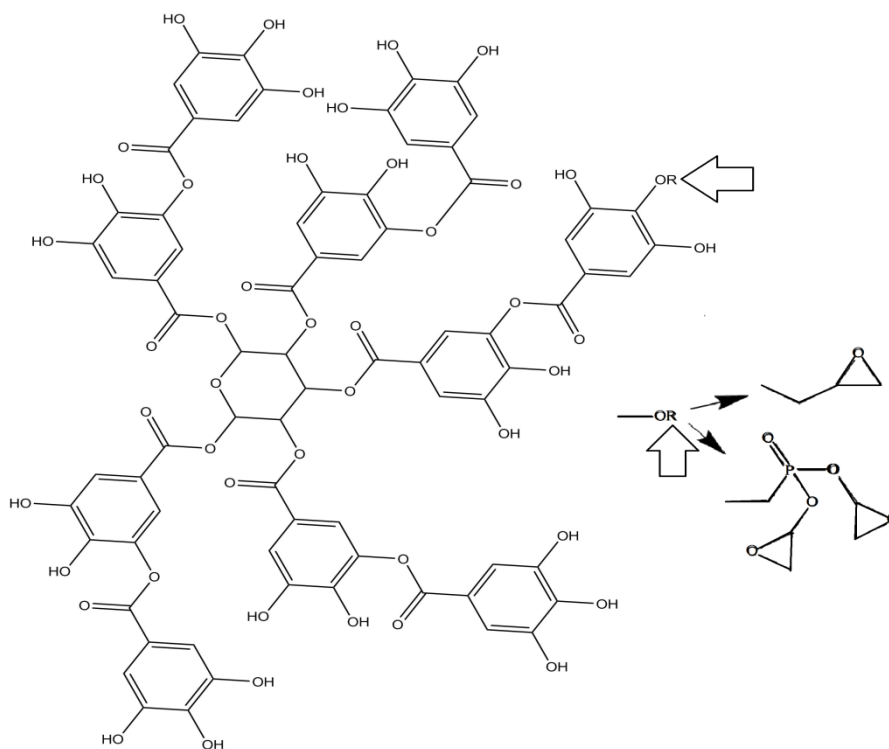


Figure 1. Tannic acid molecule and a segment of modified TA epoxy molecule

2.3 Synthesis of glycidyl ether of TA (ETA)

Epoxy functionalized tannic acid – ETA, or glycidyl ether of TA was obtained by reaction of TA with EPH at 80°C and at 1:1.5 wt. ratio of TA to 20% NaOH solution in ethanol (or alternatively saturated water solution) [11]. EPH (15 g) was mixed with 10 mL of water at room temperature under magnetic stirring for 30 min. In meanwhile, the solution was placed in a 100 mL three-neck round-bottomed flask equipped with a reflux condenser, pressure equalizing dropping funnel and nitrogen inlet tube, and followed by addition of TA (3 g) and heating to 80 °C under magnetic stirring for 1h. Afterward, 22.5 ml 20% NaOH ethanol solution (or 4.5 g NaOH in 4.5 mL of water NaOH solution) was added dropwise using a dropping funnel while continuing to stir. The reaction was heated at 80 °C for 4 h to achieve completion of reaction. After that, the solution was left to cool down, and after was purified in the same way as PGET. ETA modified segment of TA, along with PGET is also shown on figure 1.

2.4 Curing of Eco-epoxy

The crosslinking of the components of the epoxy system was performed with or without the use of solvents in order to improve homogenization (ethanol or methanol). Mixtures of epoxide based on tannic acid (PGET) and commercial epoxy - LG 700 (component A) were made in different molar

ratios so that component A was replaced with 25%, 50% and 75 % and 100% of the synthesized epoxy component of PGET to give the materials TA-epoks 25%, TA-epoks50%, TA-epoks 75% and TA-epoks 100%, respectively. TA-epoks and component A in the mixture should have total weight of 2g and curing agent - HG 700R (component B) should weight 1g. The prepared reaction mixture is homogenized by a combined mixing and ultrasound treatment. In case of using solvents, it is necessary to heat the reaction mixture to 50 °C until the solvent evaporates, it was treated in an ultrasonic bath and under reduced pressure. The epoxy mixture is then poured into molds and crosslinked at 50 and 80 °C for 12 hours, 120 and 150 °C for 6 hours, and at 180 °C for 4 hours. Epoxy functionalized tannic acid (TA) – ETA was cured in analog way.

3 Characterization methods

3.1 FTIR Analysis

Analysis was done using a Nicolet™ iS™10 6700 spectrometer (Thermo Scientific) in the attenuated total reflectance (ATR) mode with a single bounce 45 °F Golden Gate ATR accessory with a diamond crystal, and DTGS detector. FTIR spectra were obtained at 4 cm⁻¹ resolution with ATR correction. The FTIR spectrometer was equipped with OMNIC software and recorded the spectra in the wavelength range from 2.5 µm to 20 µm (i.e., 4000 –500 cm⁻¹).

3.2 UL94 V test

This test is the subject of an international standard (IEC 60695-11-10) for small flames (50 W). It is a simple test of vertical combustion that classifies materials as V-0, V-1 or V-2. The corresponding experimental device is shown in Figure 2. And test parameters are shown on table 1.

Table 1. UL94 V test parameters

Fire Classification	Experiment
V - 0	t_1 and t_2 less than 10s for each specimen $t_1 + t_2$ less than 50s for the five specimens $t_1 + t_2$ less than 30s for each specimen No afterflame or afterglow up to the holding clamp No burning drops
V - 1	t_1 and t_2 less than 30s for each specimen $t_1 + t_2$ less than 250s for the five specimens $t_1 + t_2$ less than 60s for each specimen No afterflame or afterglow up to the holding clamp No burning drops
V - 2	t_1 and t_2 less than 10s for each specimen $t_1 + t_2$ less than 50s for the five specimens $t_1 + t_2$ less than 30s for each specimen No afterflame or afterglow up to the holding clamp Burning drops allowed

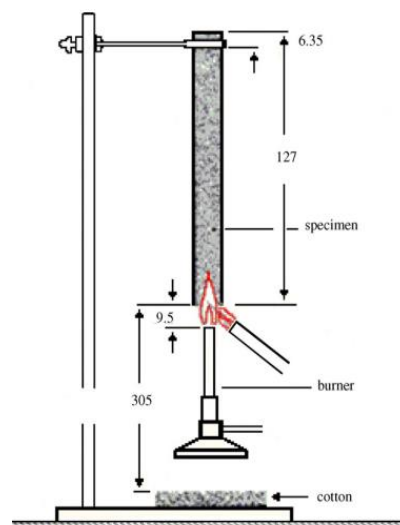


Figure 2. Experimental set-up for the UL94 V flammability test

3.3 Tensile strength test

Determination of tensile strength during axial (static) stretching of standard-sized specimens was done according to the ASTM D882 method on the AG-X plus Universal testing machine, Shimadzu. Test resin tubes, standard dimensions (80 x 10 x4 mm), All tests were performed at 25 °C with a shear rate of 0.5 mm/min.

3.4 Thermogravimetry

For thermogravimetry analysis (TG) SDT Q600 simulated TGA-DTA instrument (TA Instruments) coupled with mass spectrometer Hiden HPR-20/QIC was used. Samples were heated to 800 °C for thermal analysis.

4 Results and discussion

4.1 FTIR analysis

It can be noticed that at wave number of about 3260 cm^{-1} there was a significant decrease in -OH groups and an increase in band intensity at 2955 and 2820 cm^{-1} peaks represent C-H stretching of methylene groups due to the introduction of glycidol into the TA structure. Peaks at about 1190 and 750 occur upon reaction with POCl_3 represent P=O stretch and P-aryl stretch, respectively. The peaks at about 875 and 825 cm^{-1} represent the vibrations of the epoxy group, while the peak observed at 875 to 1150 cm^{-1} represents the conjugate spectrum caused by the shift due to the mutual influence of the phosphine group bound to the epoxy ring and their mutual interactions. This is the most significant indicator of successfully synthesized PGET. ETA doesn't show conjugate spectrum as PGET does show increase of -OH groups at about 3300 cm^{-1} (which may represent oxirane ring opening) and stretching of C-O-C ethers at about 1050 cm^{-1} wavenumbers [12]. Another characteristic change on FTIR during epoxidation is at a wave number of about 915 cm^{-1} which belongs to the oxirane group and represents the C-O vibration deformation, and the group belonging to the C-O-C stretch of the oxirane group - epoxy ring appears at a wave number of about 830 cm^{-1} [12]. FTIR spectrum that compares TA with PGET and ETA epoxy is shown on figure 3.

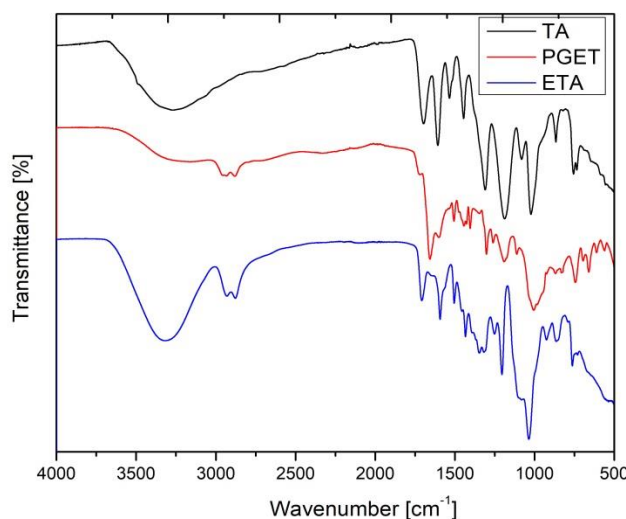


Figure 3. FTIR spectrum of TA, PGET and ETA comparison.

4.2 Tensile strength test

The results of determining the tensile properties of the obtained samples are given in Figure 4. Analysis of the tensile test results shows an increase in the toughness of the material with an increase in the amount of PGET, a decrease in the modulus of elasticity, losses on the tensile strength and an increase in relative deformation up to 4 times.

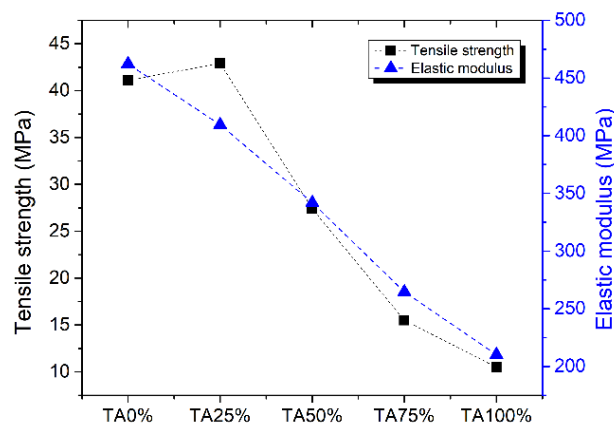


Figure 4. Mechanical properties of TA-epoxy materials obtained by replacement of epoxy component A by modified TA (PGET)

4.3 UL94 V test

Results of UL94 V test are shown in table 2. Each sample burns superficially while the interior remains undamaged, there is no burning drip and there are no burning burns in the receiving place. Sample of 25% ETA didn't show significant flame retardant effects, but it burned for about 3 minutes longer period of time than 0% samples.

Table 2. UL94 V test results

Test results category, UL94 V	Tested specimen
V - 0	Epoxy+100% PGET
V - 1	Epoxy+50% and 75% PGET / 75% and 100% ETA
V - 2	Epoxy+25% PGET / 50% ETA

4.4 Thermogravimetry

Thermogravimetry showed that the initial temperature of thermal degradation is higher for the TA-epoks 25% sample than for the Komer-c-epoks sample. The residue after heat treatment obtained for the TA-epoks 25% sample can be attributed to obtaining a more stable crosslinked sample structure at high temperatures, due to the presence of PGET. The results of thermogravimetric analysis show that improved thermal stability of epoxy material was achieved with the addition of TA component, which is presented on figure 5. Similar results were obtained for all other samples, so for better illustration only commercial bisphenol A epoxy and TA epoxy of PGET 25% sample were used. With same amounts of PGET and ETA results were quite similar, which indicates that solely TA contributes to residue/char levels.

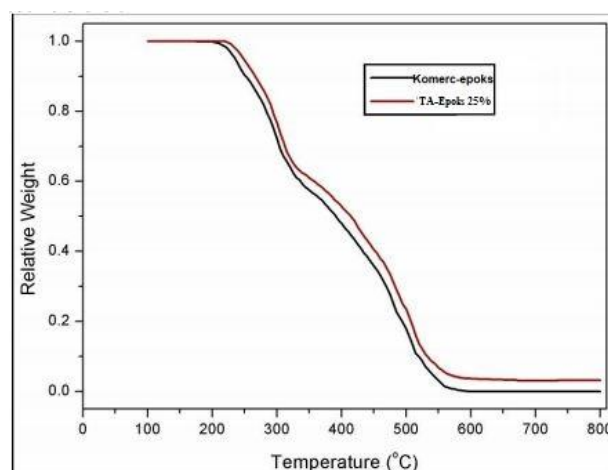


Figure 5. Thermogravimetric diagram for commercial epoxy and for 25% PGET epoxy.

5 Conclusions

Tannic acid was modified in process of epoxidation with with epichlorohydrin / POCl_3 and glycidol in order to make ETA / PGET respectively. ETA and PGET were used as a replacement of the epoxy resin component (A) – bisphenol A based epoxy in a ratio 25-100% as a reactive diluent to obtain test samples for thermal and mechanical experiments. The tensile test results indicate an increase in toughness with increase in the amount of PGET at 25% and a decrease in toughness with higher PGET amounts, a decrease in the modulus of elasticity, and an increase in relative deformation. Results of UL94 V test show an increase of flame retardant properties of PGET and ETA. PGET had shown much better thermal properties than ETA. Thermogravimetric analysis indicates that there is a slight improvement in the thermal stability of the material with an increase in PGET in the product, products with higher amounts of PGET would start degrading at higher temperatures and have more solid residue. In contrast to the above properties, a significant improvement was obtained in terms of reducing flammability: (PGET) material TA-epoks 100% has no practical significance due to poor mechanical properties. Optimal mechanical and thermal properties show TA-epoks 25% and TA-epoks 50%.

6 References

- [1] **Pascault, J.-P.; Williams, R.J.J.** Epoxy Polymers: New Materials and Innovations; Wiley-VCH Verlag GmbH & Co. KGaA: Weinheim, Germany, 2010; p. 367
- [2] **Araya-Hermosilla, R.; Fortunato, G.; Pucci, A.; Raffa, P.; Polgar, L.; Broekhuis, A.A.; Pourhossein, P.; Lima, G.M.R.; Beljaars, M.; Picchioni, F.** Thermally reversible rubber-toughened thermoset networks via Diels-Alder chemistry. *Eur. Polym. J.* 2016, 74, 229–240.
- [3] **Calafat, A.M.; Kuklennyik, Z.; Reidy, J.A.; Caudill, S.P.; Ekong, J.; Needham, L.L.** Urinary concentrations of bisphenol A and 4-nonylphenol in a human reference population. *Environ. Health Perspect.* 2005, 113, 391–395.
- [4] **Vom Saal, F.S.; Akingbemi, B.T.; Belcher, S.M.; Birnbaum, L.S.; Crain, D.A.; Eriksen, M.; Farabollini, F.; Guillette, L.J., Jr.; Hauser, R.; Heindel, J.J.; et al.** Chapel Hill bisphenol A expert panel consensus statement: Integration of mechanisms, effects in animals and potential to impact human health at current levels of exposure. *Reprod. Toxicol.* 2007, 24, 131–138.
- [5] **Okada, H.; Tokunaga, T.; Liu, X.; Takayanagi, S.; Matsushima, A.; Shimohigashi, Y.** Direct evidence revealing structural elements essential for the high binding ability of bisphenol A to human estrogen-related receptor- γ . *Environ. Health Perspect.* 2008, 116, 32–38.
- [6] **Eghbaliferiz, S.; Iranshahi, M.** Prooxidant Activity of Polyphenols, Flavonoids, Anthocyanins and Carotenoids: Updated Review of Mechanisms and Catalyzing Metals. *Phytother. Res.* 2016, 30, 1379–1391.
- [7] **Ekambaram, S.P.; Perumal, S.S.; Balakrishnan, A.** Scope of Hydrolysable Tannins as Possible Antimicrobial Agent. *Phytother. Res.* 2016, 30, 1035–1045.
- [8] **G. Pal, H. Macskasy,** *Plastics: Their behavior in fires*, Elsevier, New York, 1991.
- [9] **J. Troitzsch,** *International Plastics Flammability Handbook*, second ed., Hanser Publishers, Munich, 1990.
- [10] **A.R. Horrocks, D. Price,** *Fire Retardant Materials*, CRC Press, Boston, 2001.
- [11] **Jahanshahi S, Pizzi A, Abdulkhani A, Shakeri A.** Analysis and Testing of Bisphenol A—Free Bio-Based Tannin Epoxy-Acrylic Adhesives. *Polymers (Basel)* 2016;8:143. doi:10.3390/polym8040143.
- [12] **González MG, Cabanelas JC, Baselga J.** Applications of FTIR on Epoxy Resins - Identification, Monitoring the Curing Process, Phase Separation and Water Uptake. *Infrared Spectrosc. - Mater. Sci. Eng. Technol., InTech*; 2012. doi:10.5772/36323.

PRIMENA KONCEPTA 3D ŠTAMPE BETONA U IZRADI VETROGENERATORA

APPLYING CONCEPT OF 3D PRINTING CONCRETE IN WIND TOWER CONSTRUCTION

Aleksandar SAVIĆ, Miša STEVIĆ², Sanja MARTINOVIĆ³,
Milica VLAHOVIĆ^{1,3}, Tatjana VOLKOV HUSOVIĆ⁴,

¹ University of Belgrade, Faculty of Civil Engineering, Belgrade, Serbia

² Mikroelektronika, Belgrade, Serbia

³ University of Belgrade, Institute of Chemistry, Technology and Metallurgy, Belgrade, Serbia

⁴ University of Belgrade, Faculty of Technology and Metallurgy, Belgrade, Serbia

<https://doi.org/10.24094/mkoiee.020.8.1.43>

Iako je najčešće primenjivan materijal u savremenoj građevinskoj praksi zbog svojih očiglednih prednosti, beton poseduje izvestan broj nedostataka. Jedan od najvažnijih principa već decenijama je da se omogući masovna upotreba ovog materijala na gradilištima sa prihvatljivim svojstvima, neophodnim da bi on podneo specifične uslove. Koncept 3d štampe betona predstavlja obećavajuću osnovu za dalje poboljšanje ovog principa. Zadržavajući što veći broj preduslova i osnovnih svojstava da bi se zadovoljili konstruktivni zahtevi, ovaj materijal mora umnogome evoluirati da bi zadovoljio 3d concept, što bi, zauzvrat, popločalo put do sledećeg nivoa njegovog širokog obima primene u graditeljstvu. Cilj ovog rada je da sadrži osnovne principe 3d štampe betona, diskutujući glavne ciljeve i nedostatke koji se moraju sagledati i rešiti pre šire primene. Takođe, konstrukcija stuba vetrogeneratora, kao specifična konstrukcija biće diskutovana kao potencijalno obećavajuća osnova za ovaj stari građevinski materijal odeven u novo odelo.

Ključne reči: beton; 3d štampa; concept projektovanja; zahtevi; nedostaci; specifična primena;

Abstract: Although a most prominent material in contemporary construction practice due to its' obvious advantages, concrete incorporates a number of drawbacks. It is one of the most advantageous principles for decades to enable a large-scale on-site application of this materials with acceptable properties, needed to withstand specific conditions. A concept of 3d printing concrete presents a promising ground for further improvement of this principle. While maintaining as much as possible of the prerequisite and common properties to answer the construction demands, this material has to evolve as much as possible to fulfill the 3d concept, which would, in turn, pave a way for next level of its wide range of construction applications. This paper aims to contain main principles of 3d printing concrete, discussing the main goals and the drawbacks that have to be addressed and solved prior to wider application. Also, wind tower construction, as a specific construction will be discussed as a potentially promising ground for this old construction material dressed in a new suit.

Key words: Concrete; 3d printing; design concepts; requests; drawbacks; specific application;

1 Introduction

While the development of theory of building structures have been already highly developed, an obvious breakthrough effects of construction industry can be sought in the area of materials and technologies. Based on the never fully realized, but quite old, concept of concrete prefabrication, and provoked by the last decades achievements in many other industries (such as automotive, aerospace, food, pharmacy, biomedicine and others), additive manufacturing (AM) process is implemented in building industry. Some of the improvements that outcome from this technology are improved

¹ Corresponding author, email: mvlahovic@tmf.bg.ac.rs

efficiency, safety and environmental benefits [1,2]. There is a wide range of different AM processes, varying in the materials used, or approaches based on

Additive manufacturing process is also known as 3d printing. The main philosophy of this process is to convert an existing digital design into a real structure by adding materials in layers, one above another. In the field of concrete production, this concept is identified with manufacturing technique in which linear fragments of cementitious composites are placed on top of each other in order to form objects without the use of formwork [3]. A wide range of AM techniques and materials is implemented in construction practice, but still there are several similarities in all of them including the following aspects: robotization in placement of the material, elimination of formwork use, substantially wider range of shapes and forms which can be produced, new functionalities, and tailored fabrication [4]. The current development of this process is often characterized by the visible layers in the product appearance (Fig. 1).



Figure 1 – The appearance of 3d printed product [4]

There is a number of challenges that have to be addressed prior to the use of concrete in such a manner. Also, techniques and procedures have to be developed in order to make this process possible. The development of equipment is also expected, accompanied by the knowledge of the involved experts. All of the stated make 3d printing concrete one of the most dynamic fields in contemporary building industry. The thorough understanding of the relation between process parameters (ambient temperature, humidity, and their changes) and the mechanical properties of 3D printed concrete have to be reached.

2 Most significant advantages and disadvantages of 3d printing concrete

The main advantages of 3d printing involve the possibility to completely apply the digital design in the produced structure. The usual approach to generate a building starts with design, and then this design is realized by the contractor. This means that there is an obvious discontinuity in the process, which sometimes results in a structure which is quite different than the one that was designed. Different interpretations, errors, or personal selections of preferred materials and techniques are quite usual in the production phase of the building structure. Adding the fact that the contractor's approach is ultimately based on their experience, practice and motivations, and having in mind the occasional but omnipresent miscommunication between the designer and the contractor, the structure is never realized as designed, strictly put. The 3d printing process eliminates all the stated issues, but excluding at the same time the opportunity to rethink and optimize the structure once its' erection once started.

The possibility to fabricate a concrete element prior to its placement has been one of the development directions concerning concrete structures. There is a number of prefabrication companies in the world, as well as in the region, that produce concrete elements, such as columns, beams, plates and others, which are then transported to the building site and placed. The main advantages of this

approach include the usually high quality of the produced elements, which have been made from concrete properly produced, installed, vibrated, and cured, unlike the concrete which was transported and applied in the building site under, often harsh, environmental conditions, and sometimes with untrained personnel. Unlike on-site erected structures, and unlike steel structures also, concrete structures made of prefabricated elements incorporate a disadvantage regarding the joints between elements. Namely, these details were often identified as weak spots, being the cause of structure collapse under earthquakes. This serious drawback, which caused the limitation of concrete prefabrication, may not be an issue when 3d printing is taking place, because of the layered design, where elements are monolithized layer wise. In 3d printing, this sensitive question is transferred on the compatibility of layers. Due to the nature of cement composites such as concrete and mortar, the consecutive layers are more likely to be better connected, especially when executed one after another, and including chemical admixtures improving adhesion. Nevertheless, a statement has to be made that both prefabricated and on-site 3d printed structures are being produced, resulting with a variety of differences in equipment, material and cure of the 3d printed structures.

Several inherited drawbacks of conventional concrete can be found in 3d printed concrete. One of the main is the brittleness of concrete, and its' low performance under tensile, bending and shear loadings. Therefore, a steel reinforcement is always introduced in traditional concrete structures. In the sphere of 3d printing, introducing the reinforcement, although not uncommon, seriously compromises the whole principle, because usually the reinforcement presence makes it impossible to 3d print concrete in one phase. This is an issue which has to be addressed because divided in several phases (3d printing concrete, placing the reinforcement and then 3d printing concrete) such an enterprise often loses the intended purpose and potential [4]. On the other hand, the solution is often found in fiber reinforcement [5,6], Figure 2.

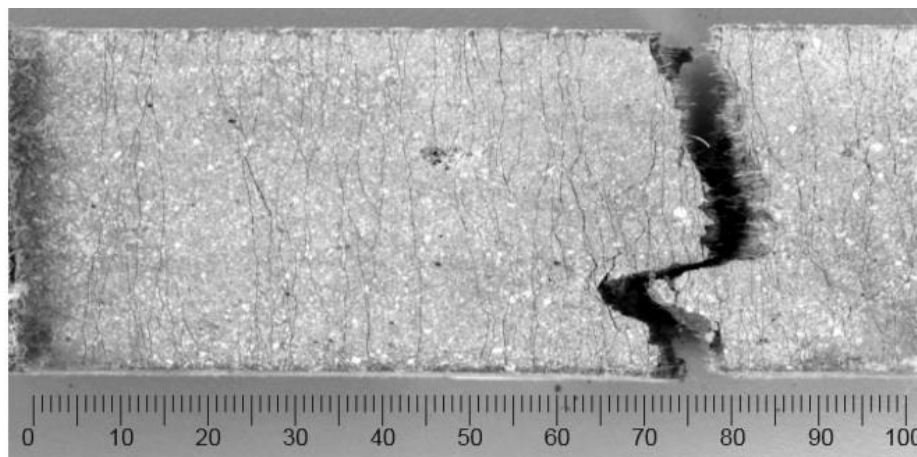


Figure 2 – The fiber reinforced specimen cut from the 3d printed concrete element [5]

3 Possibility of applying concept of 3d printing concrete in wind tower production

The 3d printing process is often thought of as one of the promising innovations, that could solve problems in many areas of industry, including onshore wind tower erections. One of the main potentials of this idea is to be able to construct higher wind towers, which is made harder due to the difficulties in transport of such elements. The transport of the 3d printing device and the component materials would be economically and environmentally (due to lower gas emissions) advanced in comparison to the transport of elements, and the dimensions of 3d printed elements could be substantially larger. This would, in turn, enable different constructions of concrete bases for steel towers of wind generators, as well as the construction of towers made entirely of concrete. Also, the amount of time and labor for building a wind tower would be also reduced.

The main challenges of this enterprise lay in the development of the material of satisfactory properties, and the on-site 3d printer with the serious requirements and high energy consumption. Also, there is little knowledge gathered regarding the behavior of such developing materials, and

structures through erection and exploitation. Finally, the stresses which can be expected to occur in such cylindrically shaped structures are expected to reach substantial tension in certain parts of the structure, based on membrane theory.

4 Conclusion

Additive manufacturing process (also known as 3d printing) presents a promising technology innovation offering the opportunity to convert an existing digital design into a real structure by adding materials in layers, one above another. Although found to be applicable in some industries, it still embeds several difficulties in the field of construction. Key challenges in this field lay in innovative materials and new procedures which have to be studied, developed and applied prior to the wider application of this process.

Onshore wind towers can be regarded as less complicated structures, from the structural engineer point of view. In the past year there have been attempts to apply 3d printing concrete technology for erection of wind towers. This concept offers several benefits if proved, environmental and economic being the main. Hopefully, the proper solutions will be reached by the involved engineers worldwide, which would pave a way to a more intense wind energy harvesting and consequently to our common better future.

5 References

- [1] **Y.W.D. Tay, B. Panda, S.C. Paul, N.A.N. Mohamed, M.J. Tan, K.F. Leong**, 3D printing trends in building and construction industry: A review, *Virtual Phys. Prototyp.* 12 (3) (2017)
- [2] **T.S. Rushing, G. Al-Chaar, B.A. Eick, J. Burroughs, J. Shannon, I. Barna, M. Case**, Investigation of concrete mixtures for additive construction, *Rapid Prototyp. J.*, 23 (1) (2017), pp. 74–80.
- [3] **R.J.M. Wolfs, F.P. Bos, T.A.M. Salet**, Hardened properties of 3D printed concrete: The influence of process parameters on interlayer adhesion, *Cem. and Concr. Res.*, 119 (2019), pp. 132–140.
- [4] **D. Asprone, C. Menna, F.P. Bos, T.A.M. Salet, J. Mata-Falcón, W. Kaufmann**, Rethinking reinforcement for digital fabrication with concrete, *Cem. and Concr. Resear.* 112 (2018), pp. 111–121
- [5] **H. Ogura, V.N. Nerella, V. Mechtcherine**, Developing and Testing of Strain-Hardening Cement-Based Composites (SHCC) in the Context of 3D-Printing, *Materials* 11 (2018), 1375 pp. 1–18
- [6] **D.G. Soltan, V.C. Li**, A self-reinforced cementitious composite for building-scale 3d printing, *Cem. and Concr. Comp.* 90 (2018) pp. 1–13

TERMOVIZIJSKI MONITORING TOPLOTE HIDRATACIJE BETONA

THERMOVISION MONITORING OF CONCRETE HEAT OF HYDRATION

Aleksandar SAVIĆ¹, Zoran STEVIĆ², Sanja MARTINOVIĆ³,
Milica VLAHOVIĆ^{1,3}, Tatjana VOLKOV HUSOVIĆ⁴

¹ University of Belgrade, Faculty of Civil Engineering, Belgrade, Serbia

² University of Belgrade, Faculty of Electrical Engineering, TF Bor, CIK, Belgrade, Serbia

³ University of Belgrade, Institute of Chemistry, Technology and Metallurgy, Belgrade, Serbia
University of Belgrade, Faculty of Technology and Metallurgy, Belgrade, Serbia

<https://doi.org/10.24094/mkoiee.020.8.1.47>

Usled hemijske reakcije Portland cementa, koja se uvek javlja u betonu prilikom očvršćavanja, izvesna količina toplote se razvija. Ova toplota mora biti kvantifikovana, obzirom da ona može oštetiti beton ili pomoći mu, zavisno od komponenata betona, elementa konstrukcije, uslova sredine i gradi-lišta. Postoji veći broj postavki za monitoring toplote hidratacije, od kojih su dve primenjene u slu-čaju prikazanom u ovom radu. Četiri vrste betona su praćene pomoću pomenute dve tehnike u traja-nju od 24 sata. Prva upotrebljena postavka koja je upotrebljena je termovizijska kamera, pomoću koje je praćena površina, a druga je termosenzor – upotrebljena za monitoring unutrašnjosti sveže betonske mase koja je očvršćavala. Potencijal primenjene postavke leži u jednostavnosti montiranja, niskoj ceni i mogućnostima za masovnu upotrebu, što može značajno doprineti monitoringu i preduprediti podbačaj betona.

Ključne reči: beton; toplota hidratacije; monitoring; termovizija; termopar.

Due to the Portland cement chemical reaction, which always takes place in a hardening concrete, a certain amount of heat is released. This heat should be quantified, as it can harm or aid the concrete itself, depending on the concrete components, structure element, ambient and building site conditions. There are number of possible setups for the monitoring of heat of hydration, two of which have been applied in the case presented in this paper. Four concretes were monitored with the use of the two stated techniques for 24 hours. First technique used is thermo-vision camera which monitored the surface, and the second is thermosensor - used for monitoring of interior of fresh concrete hard-ening mass. The potential of the applied setup lays in the ease of installation, low price, and possi-bilities of mass application, which could substantially aid the monitoring and prevent concrete fail-ure.

Key words: concrete; heat of hydration; monitoring; thermography; thermosensor

1 Introduction

Concrete presents the most prominent structural material in the building industry worldwide. Low price, the availability of components, ease of production and placement can be regarded as aspects which make it almost impossible to provide an alternative for concrete in near future. The collection of knowledges, rules and skills resulting in the production of strong and durable structural concrete are contained and explained in the technical field of concrete technology [1].

Based on the chronology and the behavior of concrete, there are two stages of concrete treated in the concrete technology, fresh and hardened concrete. The flow (kinetics) of the chemical reaction between Portland cement and water presents the basis for the chronology, dividing the first several hours of the placed concrete behavior into setting and hardening. During setting, which normally

¹ Corresponding author, email: mvlahovic@tmf.bg.ac.rs

takes up to 10 hours, a structure is formed in concrete causing it to transform from soft and almost liquid state into hardened state. After this short period, a structure is changed, providing higher strengths and other favorable properties of concrete through hardening, which takes months, and sometimes years, to finish completely.

During the setting of concrete, the exotherm chemical reaction of Portland cement with water (cement hydration) results in heat generation, referred to as heat of hydration. The chemical reaction can be divided in several phases (Table 1) [2]. In terms of the heat of hydration, the first three phases presented in this table are crucial. The generated heat increases the temperature of concrete during this sensitive phase, often resulting in occurrence of cracks in the setting and hardening concrete. Higher classes of Portland cement, larger quantities of concrete in mass elements, and unfavorable environmental condition (high ambient temperature) present the most important risk factors [3]. Therefore, timely and reliable information on the heat of hydration results in providing a proper curing regime for concrete, thus preventing strength and durability losses through crack generation.

Table 1 – Phases of the Portland cement hydration

Reaction Stage	Kinetics of Reaction	Chemical Processes
1 Initial hydrolysis	Chemical control; rapid	Dissolution of ions
2 Induction period	Nucleation control; slow	Continued dissolution of ions
3 Acceleration	Chemical control; rapid	Initial formation of hydration products
4 Deceleration	Chemical and diffusion control; slow	Continued formation of hydration products
5 Steady state	Diffusion control; slow	Slow formation of hydration products

Four mixtures of concrete were made for the experimental study, with different content. Compositions of these mixtures were different due to the differences in contents of components: water, cement, mineral addition of fly ash and chemical admixtures (accelerator and superplasticizer).

The monitoring of the heat of hydration was conducted with the aid of IR camera, and thermo-sensor beads. This experimental setup was applied on samples of all of the concrete mixtures with different expected developments of heat of hydration.

2 Experimentals

The composition of four concrete mixtures made for this study is presented in Table 2. The quantities of aggregate for the concrete production were the same for all mixtures. The content of sand (grains finer than 4 mm) was 840 kg/m³ for all the mixtures, with 543 kg/m³ and 656 kg/m³ of the II (4/8mm) and III (8/16mm) fractions of coarse aggregate. All of the mixtures were made using laboratory pan mixer Controls with the capacity of 50 dm³. After the mixing, concrete was placed in the molds and compacted on the vibrating table. The experimental procedure in the main phase of the experiment involved the placement of the monitoring equipment on five samples (four representative 15 cm cubes, each made of different concrete mixtures) and data acquisition during the period of 24 hours. The experimental setup is shown in Figure 1.

Table 2 – Composition of concrete mixtures

	Water (kg/m ³)	Cement (kg/m ³)	Fly ash (kg/m ³)	Superplasticizer (kg/m ³)	Accelerator (kg/m ³)
Mixture 1	160	400	-	-	-
Mixture 2	160	400	-	2	4
Mixture 3	160	320	80	8	4
Mixture 4	200	240	160	8	4

The experimental setup involved a number of equipment units. Thermovision camera FLIR AX8 was used to record temperature on the surface of all of the cube specimens. At the same time, each of the sample was equipped with two IC LM35 thermo sensors, one at the surface and the other placed in the middle of each fresh concrete cube sample, which were still in plastic molds. Program VLC was used to record the thermography video file, and eight canal system for measurement, display and recording of real time temperature was used for eight thermo couples. Temperature of the ambient in the laboratory was recorded with the aid of FLIR DM 93, during the total recording period of 24h. Two lap top computers were also used, one for the recording of thermography video and the other with the LabVIEW application for real time measurement of temperature in 8 spots [4].



Figure 1 – Experimental setup for the monitoring of heat of hydration of cement

The measured values of ambient temperature in the laboratory conditions were ranging between 24.3°C and 22.2°C. Heat generation from the hydration process in concrete resulted in the increase of temperature in the samples. Different quantities of heat in different samples confirmed direct relationship with the quantity of cement used for production of different concretes. The highest recorded temperature peak of 26°C corresponded with the highest quantities of cement in the first two mixtures. The third mixture exhibited similar behavior, but the generation of heat was lower, with lower recorded temperature peak of 25.5°C. For the last mixture, made with the lowest quantity of cement, temperature peak reached only 23.5°C, testifying of the lowest heat generation in this concrete mixture. This confirmed also one of the concrete technology points that, for structures with massive concrete elements, concrete mixtures with lower quantity of cement and higher quantity of pozzolanic materials (such as fly ash) present more suitable solution. The use of accelerating chemical admixture was also noticed through the recording process, providing following effect: faster temperature development was recorded both on the surface and in the middle of the samples, but the temperature of the specimen remained in the same limits, testifying of the same amount (but faster achieved) of the generated heat of hydration. The graphical interpretation of the measured temperatures with all of the 8 thermo couples is shown in Figure 2.

3 Conclusions

The experimental study presented in this paper was conducted with the aim to accentuate monitoring effects of heat of hydration generation in concrete structures, due to the fact that this heat can induce substantial cracks in concrete, resulting in strength and durability failures. The technique for prevention of such effects was offered in a form of presented experimental setup including thermography camera and thermo sensors.

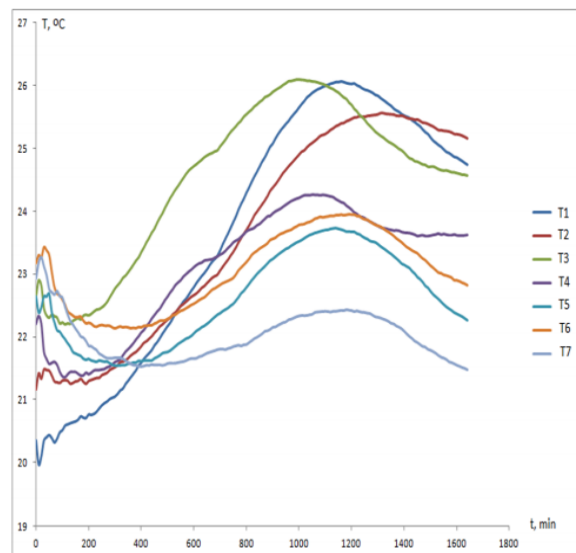


Figure 2 – The real time measured temperatures by two thermo sensors for each sample

Despite the fact that the concrete surface can emit different heat than the interior, thermography camera gave comparable and usable results for the produced concrete mixtures. Thermo sensors showed up to be part of good and simple tracking system to understand the effects of cement hydration in any concrete.

The valorization of the suggested novel experimental setup showed that this inexpensive and conditionally simple method can be applied on site, especially under harsh environmental conditions such as low and high ambient temperatures. In order to comprehend directions of development and the limitations of this method, an increase in the scope of research is expected.

4 Acknowledgement

The authors gratefully acknowledge financial support from the Ministry of Education and Science, Government of the Republic of Serbia.

5 References

- [1] **M. Muravljov**, *Osnovi teorije i tehnologije betona*, Građevinska knjiga, Beograd, Serbia, 1991.
- [2] **S. Mindess, J.F. Young, D. Darwin**. *Concrete*, Upper Saddle River, USA: Pearson Education, Inc. 2002.
- [3] **A. Patil**, Heat of Hydration in the Placement of Mass Concrete, *International Journal of Engineering and Advanced Technology (IJEAT)* 4 (3), 2015. pp. 1-4
- [4] **Z. Stević, M. Rajčić Vujasinović, A. Savić, S. Martinović, M. Vlahović, I. Radovanović, T. Volkov Husović**, Monitoring efekata toplote hidratacije betona, *17th International Symposium INFOTEH-JAHORINA*, Jahorina, BiH, 2018. Pp. 255-258.

UTICAJ MEHANOHEMIJSKE AKTIVACIJE KOMPONENTI NA SINTEZU KORDIJERITNE KERAMIKE ZA PRIMENU U ELEKTRONICI

INFLUENCE OF MECHANOCHEMICAL ACTIVATION OF COMPONENTS ON SYNTHESIS OF CORDIERITE CERAMICS FOR APPLICATION IN ELECTRONICS

Nataša ĐORĐEVIĆ¹, Milica VLAHOVIĆ^{1,2}, Slavica MIHAJLOVIĆ¹,
Sanja MARTINOVIĆ²,

¹ Institute for Technology of Nuclear and Other Mineral Raw Materials, Belgrade, Serbia

² University of Belgrade, Institute of Chemistry, Technology and Metallurgy, Belgrade, Serbia

Kordijerit, $2\text{MgO} \cdot 2\text{Al}_2\text{O}_3 \cdot 5\text{SiO}_2$, zbog svojih svojstava predstavlja izuzetno atraktivan keramički materijal koji se može primeniti u elektronici za različite namene. Kako je temperatura sinterovanja kordijerita veoma visoka (1375°C), svako sniženje temperature na kojoj se formira kordijerit donosi ekonomski benefit. Zbog toga je u ovom radu primenjena metoda mehanohemijske aktivacije smeše polaznih komponenti za sintezu kordijerita sa ciljem sniženja njegove temperature sinterovanja. Ispitivani su efekti mehanohemijske aktivacije na kordijeritnu smešu. Povećanje specifične površine aktiviranih polaznih komponenti je praćeno BET metodom. TG metoda i gubitak mase primenjeni su za praćenje promena uslovljenih temperaturom u analiziranom trokomponentnom sistemu. Na osnovu dobijenih rezultata, povećanja specifične površine i gubitka mase sa povećanjem vremena aktivacije, očekuje se sniženje temperature sinterovanja kordijerita.

Ključne reči: kordijerit; sinterovanje; mehanohemijska aktivacija; BET; TG

The properties of cordierite, $2\text{MgO} \cdot 2\text{Al}_2\text{O}_3 \cdot 5\text{SiO}_2$, makes this ceramics nowadays an attractive material, which can be used for various applications in electronics. As the sintering temperature of cordierite is very high (1375°C), any decrease in the temperature at which cordierite is formed leads to economic benefits. Therefore, in this study, the mechanochemical activation of the initial components mixture for the synthesis of cordierite was applied with the aim to lower its sintering temperature. The effects of mechanochemical activation on the cordierite mixture were investigated. Changes in the specific surface area of the activated components were determined by the BET method. The TG method and mass loss were used to monitor the temperature-induced changes in the analyzed three-component system. Based on the obtained results, increase in specific surface area and weight loss with increasing activation time, a decrease in cordierite sintering temperature is expected.

Keywords: cordierite; sintering; mechanochemical activation; BET; TG

1 Introduction

Ceramics based on cordierite ($2\text{MgO} \cdot 2\text{Al}_2\text{O}_3 \cdot 5\text{SiO}_2$) have excellent thermal shock resistance, low dielectric constant (~ 5) and low thermal expansion coefficient ($20 \cdot 10^{-7}/^\circ\text{C}$). These properties make cordierite suitable for various microelectronic components, as well as in semiconductor production, for a wide range of high-temperature applications, and applications in mechanical engineering [1-4].

However, cordierite is difficult to sinter due to its very high and narrow range of sintering temperatures ($1300\text{--}1400^\circ\text{C}$). The thermodynamic principles of the kinetics of the syntheses of cordierite ceramics are given in the literature [5].

On the other hand, during the mechanochemical activation of the powders, their free surface increases and changes in the structure of the material are induced by the mechanical energy. These

¹ Corresponding author, email: mvlahovic@tmf.bg.ac.rs

changes have a direct influence on material properties which depend on structure, mass transport and reactivity.

Mechanochemically activated samples have more accumulated energy compared to the inactivated. Bearing this in mind, it is important to analyze the possible chemical changes of the activated system after certain periods of time (relaxation period) as they can have further influence on the kinetics of the sintering process. The accumulated energy can induce surface and bulk chemisorption of components in the atmosphere. If no changes of an activated sample occur during the relaxation time, then a mechanochemically activated sample can be sintered after an unlimited period of time. FT IR spectroscopy is used to make evident changes in the samples occurring during the relaxation time [6-15].

In this work mechanochemical energy was used to activate initial cordierite mixtures containing MgO, Al₂O₃ and SiO₂ in the ratio 2:2:5 with the aim to decrease the sintering temperature of cordierite. The influence of mechanochemical activation on the initial cordierite mixture was examined and analysed.

2 Experimental

The following oxides of technical quality were used in this research: MgO (98.60 %), Al₂O₃ (99.19 %) and SiO₂ (96.10 %). A powder mixture composed of oxides MgO, Al₂O₃ and SiO₂ in the ratio 2:2:5 was prepared. The system 2MgO+2Al₂O₃+5SiO₂ was mechanochemically activated for 5, 15, 30, 60, 120 and 240 minutes (samples marked with A1-A6, respectively), in a laboratory cylindrical ceramic ball mill (VEB, model 13x10.5).

The effects of mechanochemical activation on this system were investigated by monitoring the specific surface area and mass changes during time.

The specific surface area was determined by BET method. The nitrogen adsorption isotherm was determined by a standard volumetric apparatus at a temperature of -196 °C. The samples were degasified at 110 °C for 3 hours. Specific surface area was calculated according to the Brunauer, Emmett, Teller method from the nitrogen adsorption isotherm, using values of $0.05 < p / p_0 < 0.3$.

Mass was determined by non-isothermal thermogravimetry (TG) using a NETZSCH DTA instrument with defined operating conditions: temperature range from 20 to 1500 °C, at a heating rate of 10 °C/min.

3 Results and discussion

Specific surface area values of the cordierite mixture during mechanochemical activation, obtained by the BET method, are presented in Figure 1.

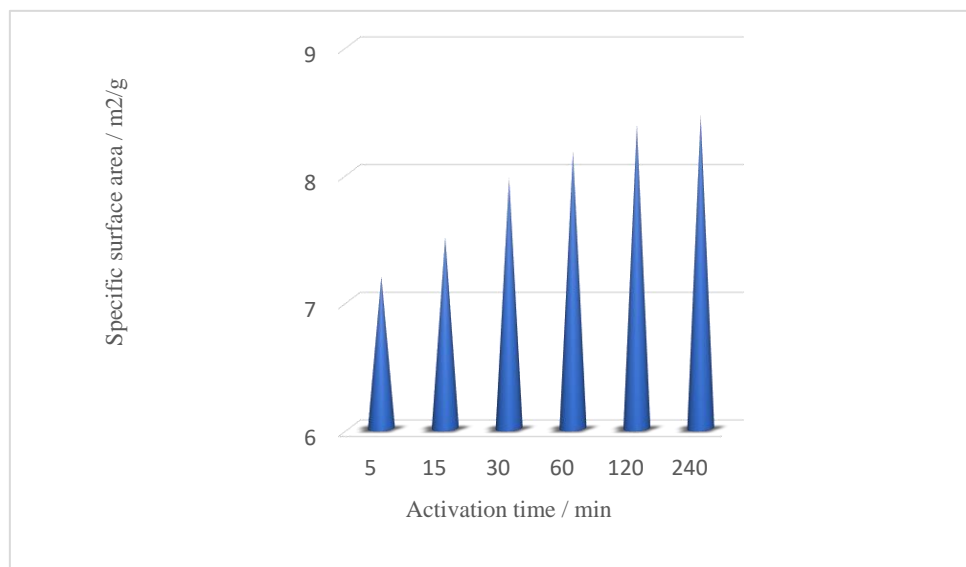


Figure 1. Specific surface changes of the cordierite mixture as a function of the time of mechanochemical activation

The results given in Figure 1 showed that the specific surface of the cordierite powder mixture ($2\text{MgO}+2\text{Al}_2\text{O}_3+\text{SiO}_2$) changed as a function of activation time in a way that longer activation time caused higher specific surface area values. The sample activated for 5 min had a specific surface area value of $7.19 \text{ m}^2/\text{g}$, while the sample activated for 240 min had a specific surface area of $8.45 \text{ m}^2/\text{g}$. This dependence is not linear but S-shaped, with a plateau from 0 to 50 minutes and another one from 120 to 240 minutes.

It can be concluded that the size of the particles decreased and therefore the specific surface of the activated powders increased with time of mechanochemical activation. These changes are especially pronounced during the first 120 minutes. Further activation resulted in only a small increase in the specific surface area.

The obtained experimental results of the changes in the specific surface area of the activated cordierite mixture can be expressed by the following kinetics equation (Eq. 1):

$$(S_{\infty}-S)/(S_{\infty}-S_0) = \exp (-kt) \quad (1)$$

where S , S_0 and S_{∞} are the specific surface areas of the powder: after time t , the starting specific surface area (before mechanochemical activation), and the final specific surface area (at the end of mechanochemical activation), respectively, and k is the rate constant of the activation process, $k = 3.1 \cdot 10^{-2} \text{ s}^{-1}$.

The chosen samples, A1, A3, A5, and A6, activated for 5, 30, 120, and 240 minutes, respectively, were allowed to relax for 24 months.

Chemical analysis of mechanochemically activated samples showed the presence of magnesium hydroxyl carbonate after 24-month relaxation. This can be explained by the reaction of hygroscopic MgO from the activated cordierite mixture with humid air. In this case, the relaxation time should be minimal and the initial cordierite mixture should be activated just before the sintering process. It can be concluded that the relaxation time of the mechanochemically activated mixture should be minimal, that is the sintering process have to be performed immediately after activation.

Non-isothermal TG analysis showed that all these samples had a rapid loss of mass at a temperature of about 400°C and that the mass loss increased with increasing the activation time, Figure 2.

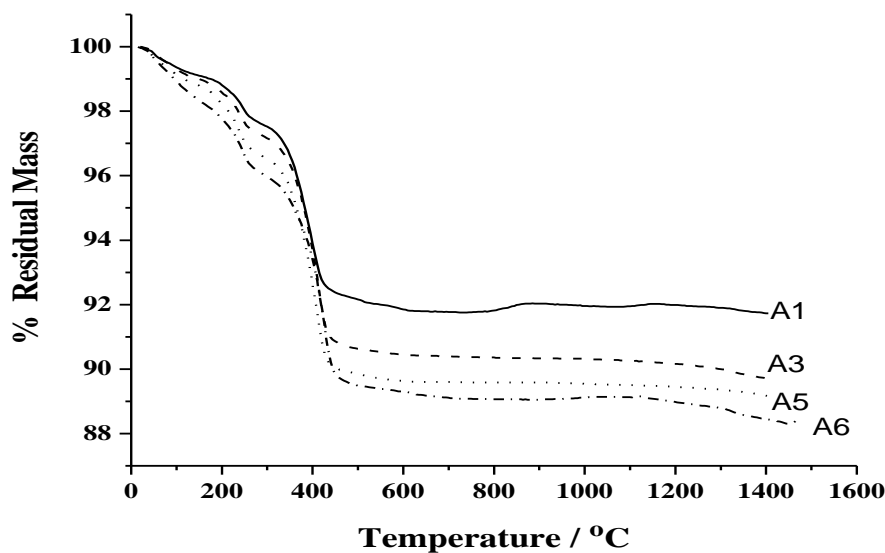


Figure 2. Non-isothermal TG curves of the cordierite mixture mechanochemically activated for different periods of time

Three mass loss steps are visible on the TG curves.

The first mass loss step occurred at temperatures up to 100°C , which indicates loss of humidity, amounting to a mass loss of $\sim 1\%$ for all samples.

The second mass loss step occurred in the temperature range from 230 °C to 300 °C. Preliminary research showed that this mass loss corresponded to the dehydration of $\text{MgCO}_3 \cdot \text{Mg}(\text{OH})_2 \cdot 3\text{H}_2\text{O}$. The mass loss was in the range from 1 % to 3 %, depending on the activation time.

The third mass loss step is very rapid and represents the greatest mass changes in the system. It occurred in the temperature range from 390 °C to 420 °C, which corresponds to the temperature range of the decomposition of magnesium hydroxyl carbonate. The mass loss in this step was 4 % for the sample activated for 5 minutes and 6 % for the sample activated for 240 minutes.

The overall mass loss of the examined samples at a temperature of 400 °C as a function of the activation time is presented in Figure 3.

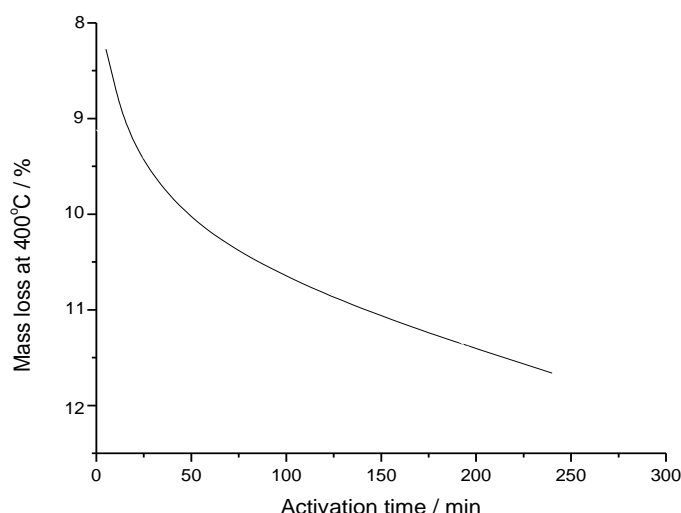


Figure 3. Total mass loss at 400 °C as a function of activation time

As seen in Figure 3, TG analyses of the cordierite mixture activated from 5 to 240 minutes exhibited a total mass loss from 8 to 12 % at 400 °C in a way that mass loss is increasing for longer activation times.

4 Conclusions

The results of an investigation of the mechanochemical activation effects on a powder mixture initially consisting of $\text{MgO} \cdot \text{Al}_2\text{O}_3 \cdot \text{SiO}_2$ in the ratio 2:2:5 have been presented. According to the obtained BET method results, with increasing duration of mechanochemical activation, the value of the specific surface area of the samples increased from 7.19 m^2/g for the sample activated 5 minutes to 8.45 m^2/g for the sample activated for 240 minutes. The mass loss, determined by TG method, after relaxation period of 24 months, occurred in three stages: at temperatures up to 100 °C, due to humidity loss; at temperatures about 240 °C, as a result of dehydration; and at temperatures around 400 °C owing to decomposition of the formed hydroxymagnesite. The total mass loss at a temperature of 400 °C increased from 8 to 12 % with increasing the activation time. Based on the obtained results, using mechanochemically activated cordierite mixture, lowering the sintering temperature of cordierite can be expected. Recommendation is to sinter the mixture as soon as possible after the activation to avoid moisture absorption by MgO .

Acknowledgments

This work was financially supported by the Ministry of Education, Science and Technological Development of the Republic of Serbia (Grant Nos. 451-03-68/2020-14/200023 and 451-03-8/2020-14/200026).

5 References

- [1] **A. I. Kingon, R. F. Davis**, "Ceramics and Sintering", Engineer Materials Handbook, vol. 2. edited by S.J. Schneider, Jr. (ASM International, Metals Park, OH, 1991).
- [2] **V.J. Powers, C.H. Drummond**, *Ceram. Eng. & Sci. Proc.* 7 (1986) 969.
- [3] **R.R. Tumlala**, *J. Amer. Ceram. Soc.* 74 (1991) 895.
- [4] **S.H. Knickerbocker, A.H. Kumar, L.W. Herron** *Amer. Ceram. Soc. Bull.* 72 (1993) 90.
- [5] **N.S. Nikolic, S.M. Radić, A.M. Maricic, M.M. Ristic**, "Cordierite Ceramics", The Fourth Yugoslav Conference "Theory and Technology of Sintering" 2001, pg.3.
- [6] **Senguttuvan TD, Kalsi HS, Sharda SK, Das BK**. Sintering behavior of alumina rich cordierite porous ceramics. *Mater Chem Phys.* 2001;67:146–50.
- [7] **Gass SE, Sandoval ML, Talou MH, Martinez AGT, Camerucci MA, Gregorová E, Pabst W**. High temperature mechanical behavior of porous cordierite-based ceramic materials evaluated using 3-point bending. *Proc Mater Sci.* 2015;9:254–61.
- [8] **Pavlović VP, Stojanović BD, Pavlović VB, Živković LM, Ristić MM**. Low temperature sintering of mechanically activated $\text{BaCO}_3\text{--TiO}_2$. *Sci Sinter.* 2002;34:73–7.
- [9] **Đorđević N, Obradović N, Kosanović D, Mitrić M, Pavlović VP**. Sintering of cordierite in the presence of MoO_3 and crystallization analysis. *Sci Sinter.* 2014;46:307–13.
- [10] **Liu C, Liu L, Tan K, Zhang L, Tang K, Shi X**. Fabrication and characterization of porous cordierite ceramics prepared from ferrochromium slag. *Ceram Int.* 2016;42:734–42.
- [11] **Filipovic S, Obradovic N, Djordjevic N, Kosanovic D, Markovic S, Mitric M, Pavlovic V**. Uticaj mehanicke aktivacije na sistem $\text{MgO--Al}_2\text{O}_3\text{--SiO}_2$ u prisustvu aditiva TeO_2 . *Tehnika–Novi materijali.* 2016;25:797–802.
- [12] **Obradović N, Đorđević N, Filipović S, Marković S, Kosanović D, Mitrić M, Pavlović V**. Reaction kinetics of mechanically activated cordierite-based ceramics studied via DTA. *J Therm Anal Calorim.* 2016;124(2):667–73.
- [13] **Kirsever D, Karakus N, Toplan N, Toplan HO**. The cordierite formation in mechanically activated talc-kaoline-alumina-basalt-quartz ceramic system. *Acta Phys Polonica A.* 2014;127:1042–4.
- [14] **Kissinger HE**. Reaction kinetics in differential thermal analysis. *Anal Chem.* 1957;29:1702.
- [15] **Kirsever D, Karakus N, Toplan N, Toplan HO**. The cordierite formation in mechanically activated talc-kaoline-alumina-basalt-quartz ceramic system. *Acta Phys Polonica A.* 2014;127:1042–4.

UTICAJ VREMENA RELAKSACIJE AKTIVIRANE SMEŠE NA SINTEZU KERAMIKE ZA NAMENU U ELEKTRONICI

IMPACT OF RELAXATION TIME OF ACTIVATED MIXTURE ON CERAMICS SYNTHESIS FOR ELECTRONICS PURPOSES

Nataša ĐORĐEVIĆ¹, Milica VLAHOVIĆ¹², Slavica MIHAJLOVIĆ¹,
Sanja MARTINOVIĆ²

¹ Institute for Technology of Nuclear and Other Mineral Raw Materials, Belgrade, Serbia

² University of Belgrade, Institute of Chemistry, Technology and Metallurgy, Belgrade, Serbia

Zahvaljujući svojim svojstvima, kordierit, $2\text{MgO} \cdot 2\text{Al}_2\text{O}_3 \cdot 5\text{SiO}_2$, danas je atraktivan keramički materijal za razne primene, ali sa vrlo visokom temperaturom sinterovanja. Mehanohemijaska aktivacija smeše početnih komponenti izvedena je da bi se snizila temperatura sinterovanja. DTA metoda je korišćena za praćenje temperaturnih promena u analiziranom trokomponentnom sistemu. Kako je ranijim istraživanjima utvrđeno da vreme relaksacije može da utiče na aktivirane komponente u smislu hemijskih promena i stepena aktiviranosti, bilo je značajno utvrditi ima li uticaj i na posmatrani aktivirani system. Uticaj vremena relaksacije na smešu aktiviranih komponentata analiziran je FT IR spektroskopijom i početnih komponenti i aktivirane smeše nakon 24h i 24 meseca perioda relaksacije.

Ključne reči: kordierit; sinterovanje; mehanohemijaska aktivacija; DTA; FT IR

Due to its properties, cordierite, $2\text{MgO} \cdot 2\text{Al}_2\text{O}_3 \cdot 5\text{SiO}_2$, is nowadays an attractive ceramic material for various applications but with very high sintering temperature. Mechanochemical activation of the initial components mixture was performed in order to decrease the sintering temperature. DTA method was used to monitor the temperature induced changes in the analyzed three-component system. Since previous research has pointed out that the relaxation time can influence the activated components in terms of chemical changes and the activation degree, it was important to determine whether it has an impact on the observed activated system. The influence of the relaxation time on the activated components mixture was analyzed by FT IR spectroscopy of both the initial components and the activated mixture after 24h and 24 months relaxation periods.

Key words: cordierite; sintering; mechanochemical activation; DTA; FT IR

1 Introduction

Cordierite, one of the most important phases of the $\text{MgO-SiO}_2\text{-Al}_2\text{O}_3$ system, has a low thermal expansion coefficient, excellent thermal shock resistance, low dielectric constant, high volume resistivity, high chemical durability, and relatively high refractoriness and mechanical strength. This ceramic material is widely used in electronics, for honeycomb-shaped catalyst carriers in automobile exhaust systems, substrate material in integrated circuit boards, and also as a refractory material, owing to its stability at high temperatures [1–3].

Cordierite ceramics can be prepared by conventional sintering methods, but it is difficult to sinter cordierite because of the narrow and sintering range (1300–1400 °C) just below its incongruent melting point [4–6]. The preparation of a homogeneous and fine cordierite powder that can be produced without sintering aids is considered to be highly desirable, due to the limiting factors of additives [7–15]. The thermodynamic principles of the kinetics of the syntheses of cordierite ceramics are given in the literature [5].

Mechanochemically activated samples have more accumulated energy compared to the inactivated initial components. Bearing this in mind, it was important to analyze the possible chemical changes of the activated system after certain periods of time (relaxation period) as they can have an

¹ Corresponding author, email: mvlahovic@tmf.bg.ac.rs

influence on the kinetics of the sintering process. The accumulated energy can induce surface and bulk chemisorption of components in the atmosphere. If no changes of an activated sample occurred during the relaxation time, then a mechanochemically activated sample can be sintered after an unlimited period of time.

The aim of this research is to decrease the sintering temperature of cordierite by mechanochemical activation of the initial mixture (caoline (Al_2O_3), quartz (SiO_2), and alkali magnesium carbonate). The free surface of the initial powders increases during the mechanochemical activation and changes in the structure of the material are induced by mechanical energy. The influence of the relaxation time of this mechanochemically activated mixture on the sintering of cordierite ceramics was investigated.

2 Experimental

In this research the next initial raw materials of technical quality were used: MgO (98.60%), Al_2O_3 (99.19%) and SiO_2 (96.10%). The mixture composed of powdered MgO , Al_2O_3 and SiO_2 in the ratio 2:2:5 was mechanochemically activated for 5, 15, 30, 60, 120 and 240 minutes (samples marked with A1-A6, respectively), in a laboratory cylindrical ceramic ball mill (VEB, model 13x10.5). Non-isothermal thermogravimetry (TG) and differential thermal analysis (DTA) were used to monitor the influence of mechanical activation on the samples. For this purpose, a METZSCH DTA instrument was employed in the temperature range 20 to 1500°C, at a heating rate of 10°C/min.

The effect of relaxation, i.e. aging, of the activated cordierite mixture on the sintering processes was monitored by analyzing the mixture activated for 120 min using FT IR spectroscopy. FFT infrared spectra of the samples were recorded on an FFT IR spectrometer BOMEM-HARTMAN & BRAUN MICHELSON MB-100, in the range of wave numbers 4000-300 cm^{-1} at a resolution of 2 cm^{-1} . Since the samples are very sensitive to the presence of moisture, the method of making a suspension with "NuJol" was used to prepare the samples. The purpose of this analysis was to identify possible chemical changes on the activated surface of the components in the mixture as well as structural changes. A non-activated sample (zero sample) was also analyzed by the same chosen methodology [8] and the obtained results were compared.

3 Results and discussion

DTA method was used to investigate the changes in the activated cordierite system during the sintering process at temperatures up to 1600 °C. The samples activated for 5, 60 and 120 minutes were chosen for this examination.

The obtained DTA curves are presented in Figure 4.

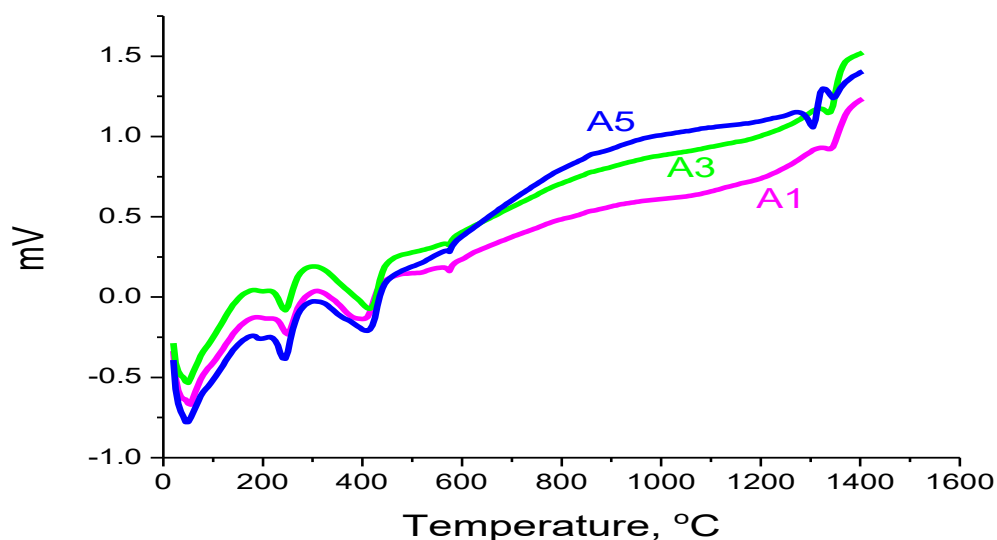


Figure 4. DTA curves of the cordierite mixture activated for 5, 60 and 120 minutes.

As seen in Figure 4, all investigated samples exhibit significant changes up to the temperature of 400 °C, while all the samples behaved quite similarly up to the temperature of 600 °C. Three characteristic peaks are visible: The first peak is up to 100 °C, resulting from loss of humidity. The second in temperature range from 230 to 300 °C which corresponds to the dehydration of $\text{MgCO}_3 \cdot \text{Mg}(\text{OH})_2 \cdot 3\text{H}_2\text{O}$, and the third peak in the range from 390 to 420 °C and it can be attributed to the decomposition of magnesium hydroxyl carbonate.

Indications of the commencement of cordierite formation were detected in the temperature range of 1200-1400 °C for the initial mixture. The corresponding endothermic and exothermic effects were shifted to lower temperatures with increasing duration of mechanical activation.

Derivative of the DTA curve of the sample activated for 5 minutes after a relaxation time of 24 months is presented in Figure 5.

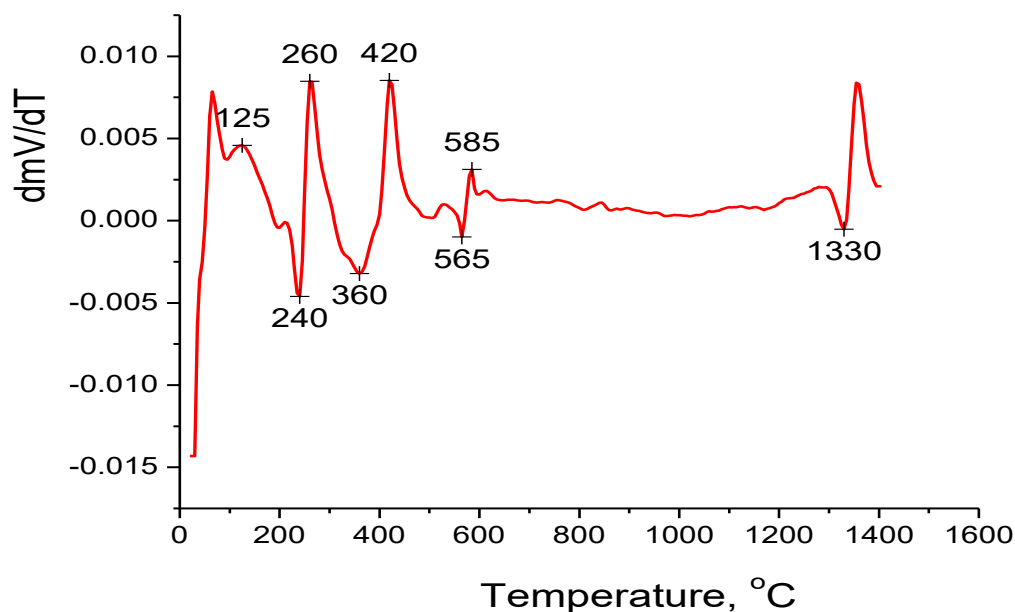


Figure 5. Derivative of the DTA curve for the sample activated for 5 minutes.

By analyzing the curve in Figure 5 it can be noticed that very rapid changes are taking place below the temperature of 600 °C. This indicates transformation reactions in the system at these temperatures. The clearly visible endothermic change at 1315 °C indicates the transformation temperature in the sintering process.

The temperature change of the endothermic effect in the cordierite sintering process from the initial cordierite mixture as a function of the mechanochemical activation duration is presented Figure 6.

As seen in Figure 6, the curve is S-shaped with two plateaus, which are separated by a region of significant changes in the system. The transformation model indicates that the temperature of cordierite sintering decreases with increasing activation time.

The first plateau lasts to 50 minutes of activation, indicating that the changes in the system in this time period were not pronounced enough to have any influence on the sintering process. From 50 to 160 minutes of activation, the changes in the reaction system cause decreasing the sintering temperature. In this range of activation times, it can be seen that the mechanochemical activation had an influence on the kinetics of cordierite sintering, i.e., the activity of the sample increased with increasing activation time. The mechanical energy was used not only for particle attrition but also for increasing the active surface of the particles. This accumulated energy has an influence on the affinity of the components to interact with each other at lower temperatures than in the non-activated systems.

After this period of change, a second plateau appeared when the reactivity of the system ceased to change. Further energy input due to mechanochemical activation results in no significant increase in the reactivity of the system and, hence, there was no further decrease in the cordierite sintering temperature. Thus, prolonging the milling would have no effect.

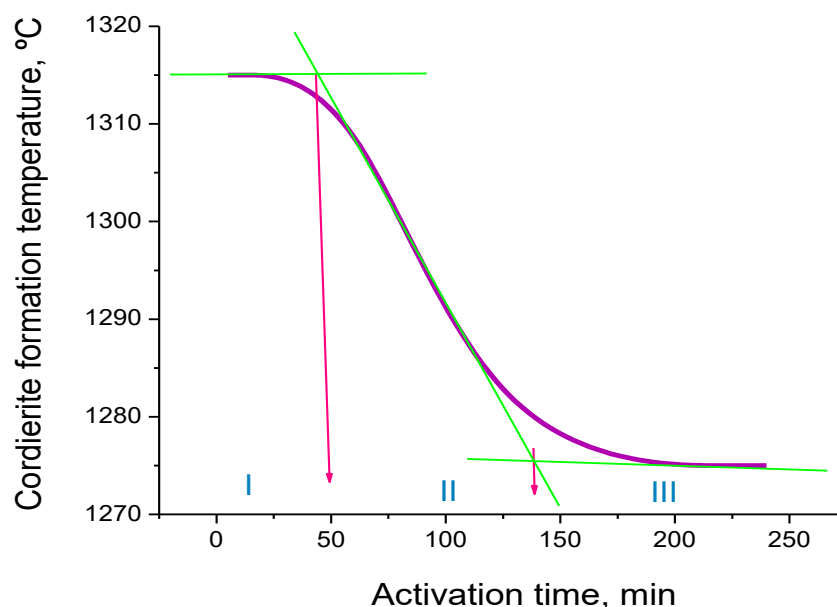


Figure 6. Temperature changes of the endothermic effect in the process of cordierite sintering as a function of the activation time

The temperature decrease of the endothermic and exothermic effects can be described by kinetic equations (Eq. 1):

$$(T_k - T_\infty) / (T_0 - T_k) = \exp(-mt) \quad (1)$$

where T_k is the characteristic endothermic or exothermic temperature effect, m is the coefficient of the process, $m = 1.5 \cdot 10^{-2} \text{s}^{-1}$. The endothermic effect favors the transformation of β -quartz to α -quartz, while the exothermic effect results from solid-state reactions between MgO and SiO₂, resulting in the formation of forsterite.

FT IR spectroscopy was used to analyze eventual chemical changes of the activated cordierite mixture during the relaxation time (ambient conditions for up to 24 months). The IR spectra of a sample activated for 120 minutes after relaxation for 24 hours and after 24 months are shown in Figure 7.

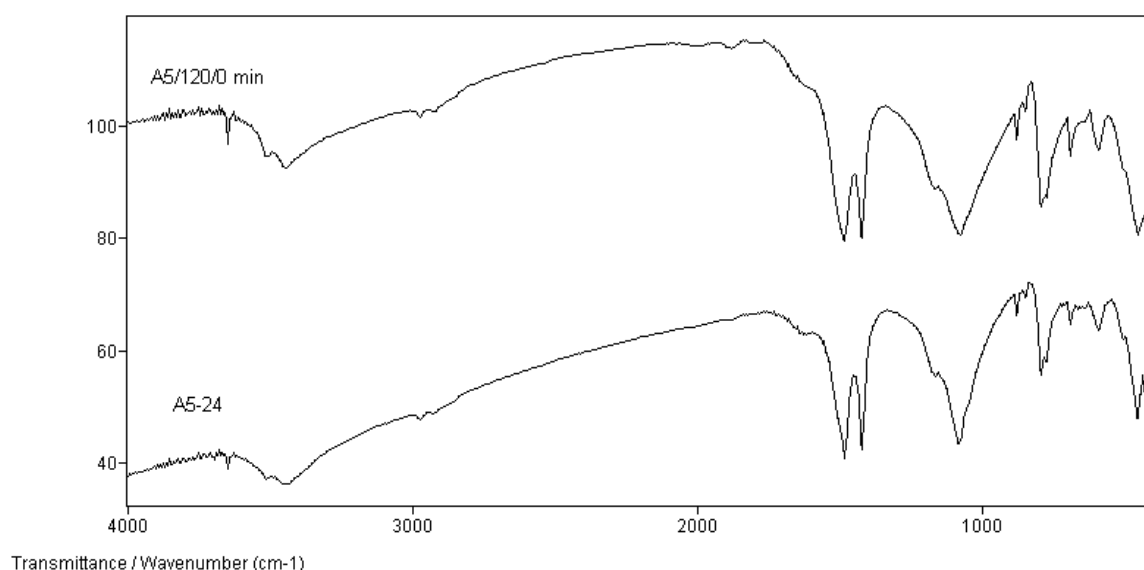


Figure 7. FT IR spectra of sample A5 after relaxation for 24 hours and 24 months.

From the spectra shown in Figure 7, it can be seen that hydroxyl- and carbonate- magnesium compounds were present as impurities in the mixture. The characteristic peaks of bound crystal water

are sharp at the wavenumbers 3445 cm^{-1} , 3512 cm^{-1} and 3649 cm^{-1} . The carbonates are visible at wavenumbers 1425 cm^{-1} and 1485 cm^{-1} , which indicates that the compounds are only impurities due to bound water and carbon dioxide, originating from the atmosphere. Since the initial components are well defined, it is supposed that this analysis proves surface adsorption of humidity and CO_2 from the atmosphere, which resulted in the formation of unstable compounds of hydromagnesite. The IR spectrum of Al_2O_3 shows the existence of $-\text{OH}$ groups at 3443 cm^{-1} , the origin of which originated is air humidity. These results are to be expected since in all experiments technical quality components were used. A relaxation period of 24 months had no influence on the sample since no noticeable changes were visible in the IR spectrum of this sample.

4 Conclusions

DTA proved that the influence of mechanochemical activation of the initial components was caused by an increase in energy of the initial cordierite mixture, which resulted in the endothermic and exothermic sintering reactions being shifted to lower temperatures. The decrease in these temperatures was about 100°C , depending on the activation time.

FT IR analyses showed that relaxation time had no influence on the activated mixtures. It can be concluded that the mechanochemically-activated samples did not change at all up to the moment of sintering, regardless of the activation time. The presented spectra explain the mass losses at the temperatures of 240 and 400°C , i.e., less-stable compounds (hydroxide and carbonate bonded to hydroxymagnesite) were generated during mechanochemical activation.

Acknowledgments

This work was financially supported by the Ministry of Education, Science and Technological Development of the Republic of Serbia (Grant Nos. 451-03-68/2020-14/200023 and 451-03-8/2020-14/200026).

5 References

- [1] **A. I. Kingon, R. F. Davis**, "Ceramics and Sintering", Engineer Materials Handbook, vol. 2. edited by S.J. Schneider, Jr. (ASM International, Metals Park, OH, 1991).
- [2] **V.J. Powers, C.H. Drummond**, *Ceram. Eng. & Sci. Proc.* 7 (1986) 969.
- [3] **R.R. Tumulala**, *J. Amer. Ceram. Soc.* 74 (1991) 895.
- [4] **S.H. Knickerbocker, A.H. Kumar, L.W. Herron** *Amer. Ceram. Soc. Bull.* 72 (1993) 90.
- [5] **N.S. Nikolic, S.M. Radić, A.M. Maricic, M.M. Ristic**, "Cordierite Ceramics", The Fourth Yugoslav Conference "Theory and Technology of Sintering" 2001, pg.3.
- [6] **Senguttuvan TD, Kalsi HS, Sharda SK, Das BK**. Sintering behavior of alumina rich cordierite porous ceramics. *Mater Chem Phys.* 2001;67:146–50.
- [7] **Gass SE, Sandoval ML, Talou MH, Martinez AGT, Camerucci MA, Gregorová E, Pabst W**. High temperature mechanical behavior of porous cordierite-based ceramic materials evaluated using 3-point bending. *Proc Mater Sci.* 2015;9:254–61.
- [8] **Pavlović VP, Stojanović BD, Pavlović VB, Živković LM, Ristić MM**. Low temperature sintering of mechanically activated $\text{BaCO}_3\text{--TiO}_2$. *Sci Sinter.* 2002;34:73–7.
- [9] **Đorđević N, Obradović N, Kosanović D, Mitrić M, Pavlović VP**. Sintering of cordierite in the presence of MoO_3 and crystallization analysis. *Sci Sinter.* 2014;46:307–13.
- [10] **Liu C, Liu L, Tan K, Zhang L, Tang K, Shi X**. Fabrication and characterization of porous cordierite ceramics prepared from ferrochromium slag. *Ceram Int.* 2016;42:734–42.
- [11] **Filipovic S, Obradovic N, Djordjevic N, Kosanovic D, Markovic S, Mitric M, Pavlovic V**. Uticaj mehanicke aktivacije na sistem $\text{MgO--Al}_2\text{O}_3\text{--SiO}_2$ u prisustvu aditiva TeO_2 . *Tehnika–Novi materijali.* 2016;25:797–802.
- [12] **Obradović N, Đorđević N, Filipović S, Marković S, Kosanović D, Mitrić M, Pavlović V**. Reaction kinetics of mechanically activated cordierite-based ceramics studied via DTA. *J Therm Anal Calorim.* 2016;124(2):667–73.

- [13] **Kirsever D, Karakus N, Toplan N, Toplan HO.** The cordierite formation in mechanically activated talc-kaoline-alumina-basalt-quartz ceramic system. *Acta Phys Polonica A*. 2014;127:1042–4.
- [14] **Kissinger HE.** Reaction kinetics in differential thermal analysis. *Anal Chem*. 1957;29:1702.
- [15] **Kirsever D, Karakus N, Toplan N, Toplan HO.** The cordierite formation in mechanically activated talc-kaoline-alumina-basalt-quartz ceramic system. *Acta Phys Polonica A*. 2014;127:1042–4.

POTENCIJAL POLJOPRIVREDNE BIOMASE U SISTEMIMA PROIZVODNJE BIOGASA U REPUBLICI SRBIJI

POTENTIAL OF AGRICULTURAL BIOMASS IN BIOGAS PRODUCTION SYSTEMS IN THE REPUBLIC OF SERBIA

**Olivera EĆIM-ĐURIĆ¹¹, Dragan KRECULJ², Danijela ŽIVOJINOVIĆ²,
Miloš VORKAPIĆ³**

¹ Univerzitet u Beogradu, Poljoprivredni fakultet, Beograd, Srbija

² Akademija tehničkih strukovnih studija, Beograd, Srbija

³ Univerzitet u Beogradu, Institut za hemiju, tehnologiju i metalurgiju, Beograd, Srbija

<https://doi.org/10.24094/mkoiee.020.8.1.63>

Biomasa predstavlja prema zvaničnim podacima najznačajniji potencijal obnovljivih izvora energije u Republici Srbiji. Ona čini oko 63% od ukupnog potencijala, ali za sada njena iskorišćenost nije na zadovoljavajućem nivou. Od ukupnih količina $14,2 \cdot 10^4$ TJ procenjuje se da je oko $9,6 \cdot 10^4$ TJ neiskorišćeno. To je i dalje evidentno veliki raspoloživi potencijal, posebno u poljoprivrednoj biomasi, izuzimajući udeo biogoriva u sektoru saobraćaja, čiji potencijal na godišnjem nivou iznosi oko $7,1 \cdot 10^4$ TJ. Glavne prepreke za intenzivniju preradu biomase i dalje predstavljaju visoki troškovi manipulacije, dispergovanost zemljišnih poseda, a naročito vremenska neusklađenost u proizvodnji, preradi i korišćenju biomase, što svakako povećava troškove skladištenja. U dosadašnjim analizama, najširu upotrebu u domaćinstvima, biomasa ima u direktnom sagorevanju i proizvodnji toplotne energije, ili u proizvodnji peleta i briketa, gde je još uvek manje zastupljena u odnosu na šumsku biomasu. Iako u poslednjih nekoliko godina trend rasta energana na biogas raste, i ukupna instalisana snaga iznosi oko 20 MW, ovaj sektor u narednim godinama ima najveći potencijal za razvoj, posebno u lokalnim zajednicama koje su primarno okrenute poljoprivrednoj proizvodnji. Rad se bavi analizom stanja proizvodnje, prerade, transporta i mogućnosti primene biomase, u cilju kogenerativne proizvodnje električne i toplotne energije. Razmatra se i uticaj korišćenja biomase na zaštitu i održivost životne sredine, kroz analizu studije slučaja na primerima teritorijalnih jedinica u Vojvodini.

Ključne reči: poljoprivredna biomasa; biogas; kogeneracija; zaštita životne sredine.

According to official data, biomass represents the most significant potential of renewable energy sources in the Republic of Serbia. It accounts for about 63% of the total potential, but for now its use is not at a satisfactory level. In total amounts of $14,2 \cdot 10^4$ TJ, it is estimated that about $9,6 \cdot 10^4$ TJ is unused. This is still evidently a large available potential, especially in agricultural biomass, with the exception of the binding share of biofuels in the transport sector, whose annual potential is around $7,1 \cdot 10^4$ TJ. The main obstacles for more intensive biomass processing continue to be the high costs of manipulation, the dispersion of land holdings and especially the time mismatch in the production, processing, and use of biomass, which certainly increases storage costs. In the former analyzes, the most widespread use in households, biomass has in direct combustion and production of thermal energy, or in the production of pellets and briquettes, where it is still less represented in relation to forest biomass. Although in the last few years the growth trend of biogas power plants is growing, and the total installed capacity is about 20 MW, this sector has the greatest potential for development in the coming years, especially in local communities, that are primarily focused on agricultural production. The paper deals with the condition analysis of the production, processing, transport, and the possibility of applying agricultural biomass, for the purpose of cogeneration electricity and heat production. The impact of the use of biomass on the protection and sustainability of the environment is also considered, through the analysis of a case study on the examples of territorial units in Vojvodina.

Key words: agricultural biomass; biogas; cogeneration; environmental protection.

¹ Corresponding author, email: nera@agrif.bg.ac.rs

1 Uvod

Primena obnovljivih izvora energije poslednjih decenija raste na globalnom nivou. Sve veće primene solarne energije, energije vetra i biomase u procesu proizvodnje električne energije, menjaju sliku svetskog tržišta energije i cene energenata [1,2]. Zakonske regulative, donete na globalnom nivou i na nivou pojedinih država, povećavaju udeo obnovljivih izvora energije u ukupnoj proizvodnji energije. Prema dopunjenoj Direktivi Evropske Unije (EU) iz 2018. godine, kao delu projekta “Čista energija za sve zemlje Evrope”, a u skladu sa zaključcima Pariskog skupa o emisiji štetnih gasova, udeo obnovljivih izvora energije do 2030. godine treba da bude najmanje 32%, tj. na svetskom nivou instalisane kapacitete treba povećati za još oko 3000 GW, čime se u pogledu zaštite životne sredine teži zadržavanju porasta temperature okoline za dva stepena na globalnom nivou [3,4]. Većina zemalja EU intenzivno radi na sve većoj primeni obnovljivih izvora energije, i postizanju planiranih ciljeva. Na žalost, zemlje Zapadnog Balkana su i dalje u velikom zaostatku za razvijenim zemljama, u široj primeni obnovljivih izvora energije, iako poseduju zavidan potencijal, tj. rezerve. Izuzimajući primenu hidro-energije, koja je tradicionalno zastupljena na području Zapadnog Balkana, ostali oblici obnovljivih izvora energije nisu još u dovoljnoj meri iskorišćeni ni u jednoj zemlji regiona. Zabrinjavajući je podatak Energetske zajednice EU iz 2019. godine da 16 termoelektrana u regionu emituje više SO₂ od 250 elektrana na području EU, što se veoma nepovoljno odražava na okolinu i ekosisteme. Poremećaji na tržištu fosilnih goriva koji se mogu javiti, u vanrednim okolnostima, u slučaju svetske pandemije, te slabije razvijene ekonomije, stavlja u nezavidan položaj pomenute zemlje pri obezbeđivanju potrebnih količina energenata.

Iako Republika Srbija raspolaže zadovoljavajućim i adekvatnim potencijalima u solarnoj energiji, energiji vetra i energiji voda, treba istaći da sektor biomase obuhvata preko 60% od ukupnih rezervi iz obnovljivih izvora energije. Veća primena biomase pre svega zavisi od stimulisanja poljoprivrednih gazdinstava za organizovanje akcije i procese prikupljanja i prerade biomase u cilju proizvodnje energije, čime bi se otvorila mogućnost stvaranja energetski nezavisnih i samoodrživih poljoprivrednih objekata. Na ovaj način, ne samo da bi se obezbedilo rasterećivanje poljoprivrede od manipulacije otpadom, koji je svakako jedan od centralnih problema, već se otvara mogućnost i za otvaranje novih radnih mesta, kao i za povećanje važne konkurentnosti poljoprivrede i razvoj lokalnih i regionalnih privrednih aktivnosti [5-7].

2 Razmatranje potencijala biomase

Ukupan potencijal biomase u Republici Srbiji u obnovljivim izvorima energije iznosi oko 63%, ili približno 12,5 miliona tona godišnje, što malo varira na godišnjem nivou. Na žalost, i dalje se veći deo ovog potencijala spaljuje na njivama, čime se ozbiljno ugrožava ekosistem, a deo se balira i koristi u kotlovima za spaljivanje biomase, čime se dobija toplotna energija dovoljna za zadovoljavanje sopstvenih energetskih potreba. Najznačajniji oblik biomase su biljni ostaci u ratarstvu, odnosno u gajenju jednogodišnjih biljaka. Prinosi i potencijal u biomasi za neke od važnijih biljnih kultura koje se gaje u Srbiji dati su u tabeli 1 [8].

Raspoređenost određene kulture teško je precizirati, ali se može zaključiti da je na području Vojvodine i centralne Srbije zastupljenija biomasa iz ratarske proizvodnje, dok u istočnoj i zapadnoj Srbiji preovlađuje šumska biomasa. Zastupljenost ratarske proizvodnje u ukupnoj poljoprivrednoj proizvodnji u Republici Srbiji prikazana je na slici 1. Iako se određen procenat (oko 30% maksimalno) ostatak mora zaorati u zemljište posle žetve, lako se može zaključiti da svake godine ostane veliki potencijal u biomasi, koja se može upotrebiti za proizvodnju energije, kroz direktno sagorevanje biomase, ili za proizvodnju biogasa. Prikaz tog potencijala za 2018. godinu dat je u tabeli 2 [8].

Ukupno posmatrano, samo u 2018. godini, raspoloživost biomase iz ratarske proizvodnje za energetske potrebe iznosila je 4748222 t ili $6,6 \cdot 10^4$ TJ. Prema nekim autorima, samo sa 1 [ha] zasada kukuruzom, može se dobiti oko 10000 [m³] biogasa, čijim sagorevanjem se dobija oko 20000 kWh električne energije, što je dovoljno za snabdevanje prosečno 5 domaćinstava na godišnjem nivou.

Tabela 1. Prinosi i potencijal u biomasi za neke od važnijih biljnih kultura

Kultura	Godina									
	2014		2015		2016		2017		2018	
	Proizv. (hilj. t)	Biomasa (hilj. t)	Proizv. (hilj. t)	Biomasa (hilj. t)	Proizv. (hilj. t)	Biomasa (hilj. t)	Proizv. (hilj. t)	Biomasa (hilj. t)	Proizv. (hilj. t)	Biomasa (hilj. t)
Pšenica	2387	2387	2428	2428	2885	2885	2276	2276	2942	2942
Raž	12	24	13	26	14	28	11	22	13	26
Kukuruz	7952	11928	5454	8181	7377	11066	4018	6027	6965	104478
Suncokret	509	1018	437	874	621	1242	541	1082	734	1468
Šećerna repa	3507	1403	2183	873	2684	1074	2513	1005	2325	930
Ukupno	14367	16760	10515	12382	13581	16295	9359	10412	12979	109844

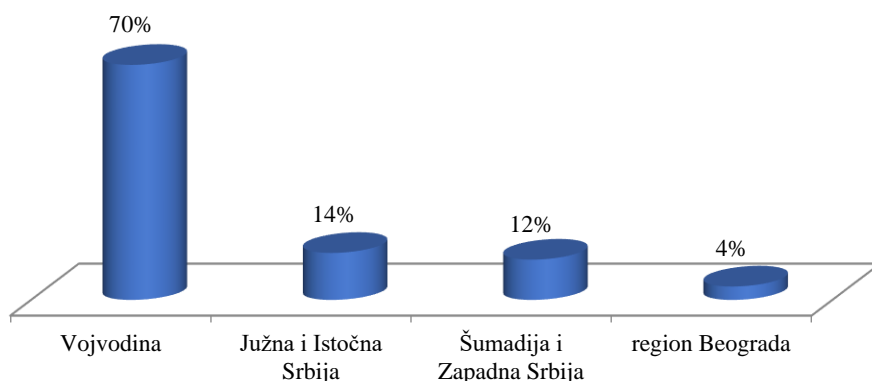
Tabela 2. Potencijal u biomasi za 2018. godinu u Republici Srbiji

Tip	Prinos		Energ. potencijal
	(t/ha)	(t)	(t)
Pšenica	4,6	2 941 601	980 534
Kukuruz	7,7	6 964 770	2 321 590
Ječam	3,9	410 138	136 713
Ovas	2,9	74 707	24 902
Raž	2,8	13 417	4 472
Šećerna repa	48,3	2 325 303	775 101
Suncokret	3,1	733 706	244 569
Soja	3,3	645 607	215 202

Stočarstvo u našoj zemlji bazirano na na uzgoju najviše svinja i živine, i u nešto manjem broju goveda, ovaca i koza. Poslednjih godina, sve više raste potražnja za organskim proizvodima, pa je i organska stočarska proizvodnja dobila na zamahu. Prema podacima iz 2018. godine, ukupna količina generisanog stajnjaka iznosila je $1,9 \cdot 10^6$ t, a na osnovu ove količine potencijalno se može dobiti $1,25 \cdot 10^4$ TJ goriva. Od raspoložive količine stajnjaka, realno se u energetske svrhe može iskoristiti oko 30%, što bi na godišnjem nivou iznosilo preko $0,37 \cdot 10^4$ TJ. Kao glavni razlog neiskorišćenosti ovih kapaciteta navodi se nedovoljan broj grla na farmama ili u domaćinstvima, kako bi proizvodnja bioagasa bila ekonomski opravdana. Godine neulaganja u stočni fond, dovele su do propadanja velikih farmi, a broj grla po domaćinstvima zaista je zanemarljiv za ozbiljna razmatranja, tj. broj grla je nazadovoljavajući za analizu i prikupljanje bi povećalo troškove proizvodnje. Odlična iskustva iz Nemačke i tzv. „energetskim selima“, gde se određen broj domaćinstava udružuje sa sirovinama, dalo bi mogućnost i našim domaćinstvima da sa više izvora obnovljive energije, proizvodnjom biogasa, obezbede svoje potrebe za električnom i toplotnom energijom, bez drastičnog povećanja troškova proizvodnje.

Dodatnu mogućnost za proizvodnju biogasa predstavlja svakako i prehrambena industrija. Potencijal u industriji prerade mleka iznosi 121 TJ, u industriji prerade mesa 487 TJ, a u industriji prerade šećera 106 TJ [9].

Raspoloživi potencijal u biomasi po regionima u Srbiji dat je na slici 1.

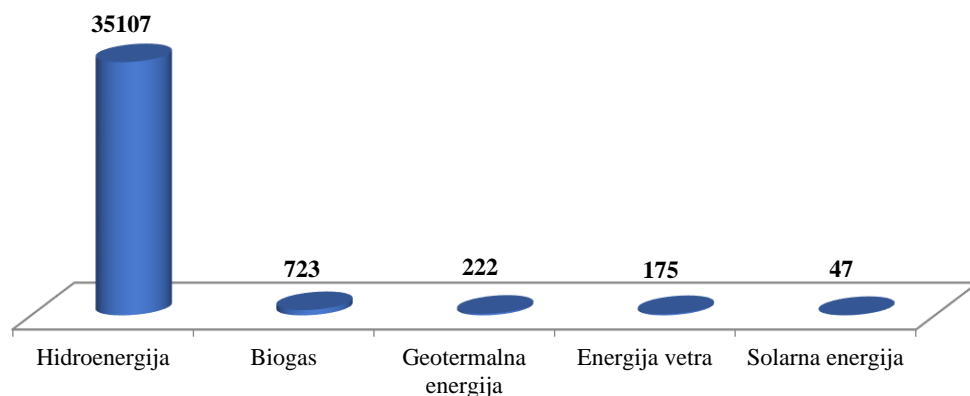


Slika 1. Raspoloživi potencijal u biomasi u Republici Srbiji

Tretman komunalnog otpada, bar njegovog biorazgradivog dela u proizvodnji biogasa, takođe ima veliki uticaj na zaštitu životne sredine. Godinama neadekvatno odlagan otpad prouzrokovao je ne samo zagađenje zemljišta, nego i vode i vazduha. Potencijal u komunalnom otpadu za proizvodnju biogasa iznosi oko 109 TJ, što je samo 20% od ukupog generisanog otpada. Glavna prepreka u korišćenju ovog energenta je unificirano razvrstavanje otpada iz domaćinstava na neorganski i organski otpad, čime se ovakav oblik energenta posebno u malim zajednicama mora odbaciti, bar za sada. Ako se uzme u obzir da se prilikom proizvodnje električne energije dobije isto toliko i toplotne energije, gotovo sve energetske potrebe pomenutih domaćinstava bile bi zadovoljene. Iako cifre pokazuju optimistične podatke, na žalost postoje brojni problemi u realizaciji, što od razuđenosti zasada, čime se povećavaju troškovi manipulacije biomase, do brojnih drugih koji ograničavaju masovniju upotrebu biomase u ove namene.

3 Analiza trenutnog stanja proizvodnje biogasa

Razvoj pojedinog sektora u proizvodnji električne energije iz obnovljivih izvora energije definisan je Zakonom o energetici Republike Srbije, Strategijom razvoja Republike Srbije do 2025. godine, a posebno podsticajnim otkupnim cenama po proizvedenom kWh iz obnovljivih izvora energije. Da bi došlo do realizacije projekta postrojenja koje koristi obnovljive izvore energije, potreban je veliki broj dozvola i licenci izdatih na lokalnom ili državnom nivou, što svakako nije jedan od razloga za masovnije ulaganje u ovaj sektor. Upravo se ovaj problem i najčešće pojavljuje u izveštajima Evropske komisije, kao jedna od bitnih prepreka bržeg popunjavanja kvota za pojedine obnovljive izvore energije. Udeo pojedinih obnovljivih izvora energije u 2017. godini u primarnoj proizvodnji energije prikazan je grafički na slici 2.



Slika 2. Primarna proizvodnja iz obnovljivih izvora energije u 2017. godini u TJ

Prema zakonskim regulativama, potencijalni proizvođači električne energije iz energana na biogas, biomasu i deponijski otpad trebali bi da računaju na podsticajne otkupne cene u vremenskom

periodu od 12 godina. Neka procena otplate investicije svodi se na period od približno 9 godina. Trenutna instalisana snaga elektrana na biogas iznosi nešto preko 20 MW, dok je slobodan kapacitet za elektrane na biogas do 2020. godine ukupno 30 MW.

Kao posebno interesantna je elektrana na biogas u okviru sistema za organsku ratarsku i stočarsku proizvodnju u Čurugu, električnog i toplotnog kapaciteta 1,27 MW (Slika 3). Poslednjih godina u ovom sektoru postoji veliko interesovanje i kvota je skoro popunjena, čime su svakako doprinele opravdane podsticajne mere u otkupnoj ceni. Pored elektrana na biogas slobodna kvota za elektrane na biomasu iznosi 100 MW, a do sada je iskorišćeno samo oko 10 MW. Za elektrane na deponijski gas kvota je 10 MW i u potpunosti je slobodna, dok je za elektrane na otpad kvota 3 MW, koja je nažalost potpuno slobodna. Za poslednje dve kategorije, kao što je ranije napomenuto, ne postoji sistematsko razdvajanje otpada, kako bi se dobila ulazna sirovina za ovu vrstu elektrana.

Prema Pravilniku iz 2018. godine podsticajne mere za elektrane na biogas, u zavisnosti od instalisane snage, kretale su se između 15 i 18 c€/kWh za 8600 sati maksimalnog efektivnog vremena rada. Za elektrane na biomasu, takođe u zavisnosti od instalisanog kapaciteta, naknada se kretala od 8 do 14 c€/kWh. Za elektrane na otpad, naknada je iznosila oko 8,5 c€/kWh. Upravo ovako povoljna naknada za otkup proizvedene električne energije iz biogasa rezultovala je većim interesovanjem za ovu oblast, što je i povećalo instalisane kapacitete. Najveći broj ovih postrojenja nalazi na području Vojvodine, shodno i većoj raspoloživosti bazne sirovine za proizvodnju [10-13].

Na žalost, početkom 2020. godine, pomenuta Uredba o merama podsticaja prestala je da važi, tako da je sada podsticajna otkupna cena za elektrane na bioagas oko 13 c€/kWh, i na nivou rentabilnosti je ovih postrojenja. Umanjene su i otkupne cene preostalih pomenutih postrojenja. Ne treba izostaviti činjenicu da ova postrojenja, za razliku od postrojenja koja koriste neke druge oblike obnovljivih izvora (na primer solarna energija i energija vetra), u mnogome utiču na životnu sredinu upravo eliminisanjem organskog otpada iz poljoprivrede, otvaraju veću mogućnost za povećanje broja radnih mesta, pa samim tim fluktuacije na tržištu energenata mogu da prouzrokuju višeznačne posledice koje se odražavaju i na druge grane privrede.



Slika 3. Elektrana na biogas kapaciteta 1,27 MW

4 Mogućnosti primene biogasa u opštinama u Vojvodini

Područje Vojvodine tradicionalno je okrenuto gajenju ratarskih kultura, pa se može zaključiti da je potencijal primene elektrana na biogas, biomasu i otpad u ovom delu Republike Srbije najveći, a to pokazuje i teritorijalna razućenost postojećih potrojenja. Neposredna blizina velikih industrijskih centara, kao i dobra pokrivenost saobraćajnicama međunarodnog karaktera, doveo je do povećanja udela industrije, preduzetništva, tako da se procenjuje da u lokalnim samoupravama koje gravitiraju bliže Beogradu, danas je udeo poljoprivredne proizvodnje oko 50%.

Na teritoriji opštine Stara Pazova ima oko 30000 [ha] obradive površine, od čega je oko 70% u privatnom vlasništvu. Dugogodišnja negativna aktivnost u tretiranju otpada iz ratarske proizvodnje, primena pesticida i mineralnih đubriva u cilju povećanja prinosa, dovela je do ozbiljne degradacije i kontaminacije zemljišta, a u zonama međunarodnih saobraćajnica došlo je do formiranja deponija i smetlišta, čime se zemljište dodatno opterećuje opasnim materijama. Netretiranje komunalnog otpada, koje ne samo da se ograničava sa izostankom selektovanja, nego i adekvatnog deponovanja,

dovelo je u pojedinim delovima ovih lokanih zajednica do ozbiljnog narušavanja održivosti ekosistema. Praveći projekcije na ostale lokalne zajednice u ovom regionu države, može se reći da lokalna zajednica Stara Pazova dobrim delom može da prezentuje ceo posmatrani region.

Odlaganje otpada udruženo sa njegovom separacijom, koje je poželjno iz više razloga, gotovo da i ne postoji. Problem uglavnom nastaje izostankom tretmana organskog otpada, pa se može zaključiti da se zagađuje ne samo zemljište, nego paralelno i vode i vazduh.

Po pitanju trošenja energetske resursa u domaćinstvima, ranije se uglavnom koristilo drvo kao energent, kojim je sama lokalna zajednica relativno siromašna. Sa povećanom gasifikacijom, potrošnja drveta se evidentno smanjila. Gotovo zanemarljiv procenat je domaćinstava koja za grejanje koriste ostatke iz primarne poljoprivredne proizvodnje, a nema podataka ni da postoji organizovano briketiranje, ili peletiranje poljoprivrednog otpada upravo za potrebe grejanja. Trenutno je u funkcionalnoj upotrebi samo jedan pogon na biogas, sa samostalnom proizvodnom jedinicom i instalisanom snagom od oko 640 kW, a koji koristi kukuruznu silažu i stajnjak kao supstrat. Razne analize koje su vršene prethodnih godina pokazale su da je oko 95% poljoprivrednih gazdinstava zainteresovano za prodaju otpada, ili za zamenu za odgovarajuća đubriva, čime bi se stvorila dobra sirovinna baza. Prilično loše interesovanje domaćinstava za prodaju poljoprivrednog otpada leži u težnjama da korisnik (elektrana) finansijski pokrije troškove baliranja, manipulacije, transporta i skladištenja.

Prikaz potencijala setvenih kultura za proizvodnju biomase predstavljen je u tabeli 3.

Tabela 3. Setvene kulture i potencijal u biomasi

	Kukuruz	Pšenica	Šećerna repa	Soja	Suncokret	Ječam
Udeo [%]	43.5	12.6	29.4	10.7	3.3	0.5
Površina [ha]	3576.4	1037.7	2420	876.7	275.7	40.8
Pr.prinos [t/ha]	6.4	4.3	52.1	4	2.8	4
Ukupan prinos t	22888.96	4462.11	126082	3506.8	771.96	163.2
Biomasa t	25177.856	4462.11	126082	7013.6	1929.9	163.2
Ukupno t	164828.7					

Od ukupne raspoložive količine biomase, 30% se može iskoristiti kao kosupstrat u proizvodnji biogasa, što na godišnjem nivou u proseku iznosi 49448,61 t raspoložive biomase. Prema dostupnim podacima, na teritoriji lokalne zajednice, sa stočarskih farmi godišnja prosečna količina stajnjaka iznosi 13574, 6 t, i uz pretpostavku da se 30% odvoji za energetske potrebe, raspoloživost iznosi 4072,4 t. U definisanju raspoloživosti izvora sirovina, treba voditi računa da ako se sirovina koristi iz sopstvenih izvora u potpunosti je besplatna, a ekonomska opravdanost transporta sirovine je prosečno oko 60 [km] ukoliko se sirovina nabavlja iz drugih izvora [14].

Od 1 m³ dobijenog biogasa moguće je proizvesti oko 2,4 kWh električne energije i oko 2,5 kWh toplotne energije, uz izvesnu količinu supstrata, koji se dobija kao ostatak iz anaerobne fermentacije. Od samo 30% raspoložive biomase na teritoriji opštine moguće je na godišnjem nivou dobiti 0,72 · 10⁶ m³ biogasa, ili 1.73 · 10⁶ kWh električne energije i 1,8 · 10⁶ kWh toplotne energije. Time bi se ne samo podmirio veći deo potreba za električnom energijom, nego bi se i ozbiljno smanjila potrošnja drugih energenata za potrebe grejanja, kao što su prirodni gas, drvo, ili električna energija. Ekološki uticaj u ovoj analizi nije zanemarljiv, a odražava se i na smanjenje emisije štetnih gasova, kao i na veliki problem rešavanja organskog otpada. Ne treba zanemariti ni dobijeni supstrat, koji se može koristiti kao đubrivo, a upravo veliki broj domaćinstava je i zainteresovan za prodaju otpada u cilju nabavke potrebnih mineralnih đubriva.

5 Zaključak

Nepopunjenost kvota za proizvodnju biogasa iz pojedinih izvora energije ukazuje da je ovaj sektor obnovljivih izvora energije još uvek neiskorišćen u svom punom kapacitetu. Kao jedna od glavnih prepreka za masovniju primenu navodi se vremenska neusklađenost proizvodnje biomase i

proizvodnje energije, stoga se biomasa mora adekvatno uskladištiti, a time se povećavaju troškovi proizvodnje. Usitnjenost i razuđenost poseda se takođe često navodi kao tehnički problem. Mnogo veći problem u masovnijoj primeni biomase je nedovoljna edukovanost stanovništva o mogućnostima tretiranja biomase i organskog otpada u energetske svrhe, i shodno tome benefitima koji proizilaze po lokalne zajednice. Ovaj problem za sobom povlači izostanak jedinstvene baze podataka proizvođača i potrošača, a svakako ne treba zaboraviti ni izuzetno komplikovanu proceduru izdavanja dozvola, koja se čak i u analizama Evropske Unije navodi kao ozbiljan problem za sve zemlje regiona. Sve ove prepreke mogu se prevazići detaljnom analizom potreba potencijalnih potrošača energije i njihove sposobnosti za proizvodnju biogasa, tj. ulaganjem u postrojenja kojima nije primarni cilj plasiranje proizvedene energije na tržište energenata, nego zadovoljavanje sopstvenih potreba primarno. Na taj način se utiče na promenu energetske slike zemlje, smanjenjem potreba za odgovarajućim fosilnim energentima.

Analiza raspoloživosti sirovine za proizvodnju biogasa pokazuje dobre rezultate za veću primenu ovakvih postrojenja upravo na lokalnom nivou. Instalisanjem samo jednog višefunkcionalnog postrojenja, rešava se niz problema, kao što je odlaganje otpada, smanjenje zagađenja obradivog zemljišta, voda i vazduha, obezbeđivanje supstrata za prehranu zemljišta. U energetsom smislu nastaje oslobađanje od zavisnosti prema fosilnim gorivima u finalnoj potrošnji toplotne i električne energije. Na žalost, trenutna situacija u praksi je drugačija, te je generalno posmatrano tretiranje biomase u energetske svrhe nedovoljno iskorišćeno. Ipak, ovaj problem bi se mogao rešiti većim animiranjem potencijalnih proizvođača biomase, njihovom boljom informisanošću o različitim mogućnostima tretiranja i benefitima, i naravno potpuno zasebnim pristupom razmatranju biomase u odnosu na ostale obnovljive izvore energije.

6 References

- [1] **Shane, S.H. Gheewala, Y. Kafwembe**, *Urban commercial biogas power plant model for Zambian towns*, Renewable Energy 103 (2017), pp. 1-14.
- [2] **Mijailovic I., Radojicic V., Ecim-Djuric O., Stefanovic G., Kulic G.**, *Energy potential of tobacco stalks in briquettes and pellets production*, Journal of Environmental Protection and Ecology 15 No 3 (2014), pp. 1034-1041.
- [3] *******, *Status Review of Renewable Support Schemes in Europe for 2016 and 2017*, Public report, Ref: C18-SD-63-03, <https://www.ceer.eu/documents/104400/-/-/80ff3127-8328-52c3-4d01-0acbdb2d3bed>, Council of European Energy Regulators, 2018.
- [4] *******, Directive (EU) 2018/2001 of the European Parliament and of the Council of 11 December <https://eur-lex.europa.eu/legal-content/EN/TXT/PDF/?uri=CELEX:32018L2001&from=EN>, 2018.
- [5] **Dodic S., Zekic V., Tica N., Dodic J., Popov S.**, *Situation and perspectives of waste biomass application as energy source in Serbia*, Renewable and Sustainable Energy Reviews Vol 14 (2010), pp. 3171–3177.
- [6] **Đurišić-Mladenović N., Kiss F., Škrbić B., Tomić M., Mičić R., Predojević Z.**, *Current state of the biodiesel production and the indigenous feedstock potential in Serbia*, Renewable and Sustainable Energy Reviews, Vol 81(1), 2018, pp. 280-291.
- [7] **Bajić, S. Dodić, D. Vučurović, J. Dodić, J. Grahovac**, *Waste-to-energy status in Serbia*, Renewable and Sustainable Energy Reviews, Vol 50 (2015), pp. 1437-1444.
- [8] *******, Republički zavod za statistiku.
- [9] **Kovačević V.**, *Dokument o stavu: Korišćenje poljoprivredne biomase za energetske potrebe u Srbiji*, <http://biomasa.undp.org.rs/wp-content/uploads/2019/01>, Srbija, 2018.
- [10] *******, *Zakon o energetici*, “Službeni glasnik RS”, br. 145/2014, Ministarstvo rudarstva i energetike, Srbija, 2014.
- [11] *******, *Nacionalni plan za korišćenje obnovljivih izvora energije (NAPOIE)*, “Službeni glasnik RS”, br. 53/2013, Ministarstvo rudarstva i energetike, Srbija, 2013.
- [12] *******, *Strategija razvoja energetike Republike Srbije do 2025. godine sa projekcijama do 2030. godine*, Službeni glasnik RS br. 101/2015, Ministarstvo rudarstva i energetike, Srbija, 2015.

- [13] ***, *Uredba o podsticajnim merama za proizvodnju električne energije iz obnovljivih izvora i iz visokoefikasne kombinovane proizvodnje električne i toplotne energije*, “Službeni glasnik RS”, br. 56/2016, Ministarstvo rudarstva i energetike, Srbija, 2016.
- [14] **Simović B., Andelković A., Kljajić M.**, *Analiza opravdanosti izgradnje postrojenja na biomasu kao baznog izvora daljinskog sistema grejanja Novog Sada*, KGH 4, pp. 357 – 365. 2018.

GASIFIKACIJA OSTATAKA BIOMASE ZA POTREBE PROIZVODNJE ELEKTRIČNE ENERGIJE

GASIFICATION OF BIOMASS WASTES AND RESIDUES FOR ELECTRICITY PRODUCTION

Marta TRNINIĆ¹,

University of Belgrade, Faculty of Mechanical Engineering, Belgrade, Serbia

Tehnologija gasifikacije predstavlja jednu od obećavajućih opcija za pretvaranje energije biomase u električnu energiju. Proces gasifikacije predstavlja process konverzije biomase (uglja itd.) u mešavinu gorivih gasova (ugljen-monoksid, vodonik, ugljen-dioksid i gasovite ugljovodonike). Proizvodni gas se može koristiti kao gorivo za motore sa unutrašnjim sagorevanjem i mikro turbine u cilju proizvodnje električne energije. Da bi se maksimalizovala efikasnost konverzije biomase, proizvedeni gas treba koristiti ne samo za proizvodnju električne energije, već i za proizvodnju toplotne energije. U ovom radu su prikazani rezultati simulacije gasifikatora povezanog sa motorom sa unutrašnjim sagorevanjem i mikro turbinom. Rezultati pokazuju odnos snage od 0,788 kWh/Nm³ za unutrašnji gasni motor i 0,553 kWh/Nm³, za mikroturbinski sistem.

Ključne reči: biomasa; električna i toplotna energija, motori sa unutrašnjim sagorevanjem, mikro – gas turbine

Gasification technology presents one of promising option for converting biomass energy into electricity. Gasification process converts carbonaceous materials into carbon monoxide, hydrogen, carbon dioxide, and gaseous hydrocarbons (producer gas). Producer gas can be supplied as fuel to internal combustion engines and micro turbines for electricity generation. In order to maximize the efficiency of biomass conversion, producer gas should be utilized not only for power generation but also for thermal production from the producer gas' sensible heat. In this paper, gasification techniques have been reviewed in depth and the main factors to be considered in the design of a gasification plant have been outlined. It is observed that there are a great number of factors involved in design and operation of a gasification plant, and many of them are critical. Additionally, modeling results for two power generation processes are analyzed. One power generation process include downdraft gasifier coupled with internal combustion engine, and other include downdraft gasifier coupled with micro gas turbine. The results show a power ratio of 0.788 kWh/Nm³ for the internal gas engine and 0.553 kWh/Nm³, for the micro turbine system.

Key words: Biomass, gasification; electricity and heat energy; internal combustion engine; micro gas turbine

1 Introduction

Ever increasing energy demand and the climate change problem caused by anthropogenic greenhouse gas emissions have resulted in the worldwide effort to find a sustainable and environmentally friendly alternative to today's fossil fuel-dominated energy supply. There is potential for biomass waste (agricultural residues, forest residues and food processing waste) to be useful in solving some of the world's energy and environmental problems, as it is widely recognized as an environmentally friendly and renewable energy source.

Agricultural waste is one of the main renewable energy resources available especially in an agricultural country such as Serbia. It is estimated that every year in Serbia, a total amount of 4.24 million tons of agricultural residues is produced, which is equivalent approximately to 1.71 million tons of oil equivalent (toe) [1].

¹ Author, email: mtrninic@mas.bg.ac.rs

Several thermochemical techniques, such as pyrolysis, gasification and combustion processes, have been proposed for biomass conversion into hydrocarbon fuels, power and thermal energy. Among the different thermochemical paths, biomass gasification is continuously receiving attention due its advantages compared to other conversion paths. A gasification process is a partial thermal oxidation, which results in mainly gaseous products (carbon dioxide, hydrogen, carbon monoxide, water vapor, methane and other gaseous hydrocarbons), and small quantities of charcoal, ash, and condensable compounds-tars [2]. The quality of produced gas from gasification, called producer gas, vary as a function of gasifying medium (air, oxygen, steam, carbon dioxide or a mixture of these) and the operating conditions. Installation of small, low-cost and efficient gasifier-engine systems can be an attractive alternative to direct combustion, considering achievable electric efficiency and costs related to storage and transport of biomass fuels [3]. The producer gas, after cleaning and conditioning, can be used as a fuel in gas engines and turbines owing to its acceptable thermochemical combustion properties (flame speed and knock tendency) [4]. Gasification is also considered as a cleaner and more efficient technology than combustion, since it enables higher electric performances at smaller scales and due to its very acceptable combustion properties coupled to a conventional Rankine cycle, giving lower NO_x and SO_x emissions, and possibilities for CO₂ capture [5].

Although gasification is widely considered as a more efficient and less polluting initial thermochemical upstream process of converting biomass to electricity than direct solid fuel combustion processes, the performance of the gasification process is highly unpredictable especially small-scale biomass gasification [6]. The major culprits are unpredictable fuel behavior[7] and unreliable operating conditions partly due to the inhomogeneous nature of biomass feedstock and the complex phenomena of a gasification process. Gasification process modeling has been suggested as a way to handle the prediction of operation behavior during normal gasification with electricity and/or heat production [7]. Furthermore, modeling can guide the preparation and optimization of experiments to be undertaken in a real system. The objective of the present article is to assess and compare the performance of electricity generation systems integrated with fixed-bed downdraft biomass gasifiers for distributed power generation. A model for estimating the electric power generation of internal combustion engines and micro gas turbines powered by syngas was developed. For model development and process simulation the Aspen Plus software was used. In this analysis, corn cob was used as a biomass feedstock (Table 1).

Table 1 Ultimate and Proximate analysis of corn cob (wt % db) [1, 7]

<i>Ultimate analysis</i>					
<i>C</i>	<i>H</i>	<i>O</i>	<i>N</i>	<i>S</i>	<i>ASH</i>
47.60	6.30	43.90	0.55	0.60	1.45
<i>Proximate analysis</i>					
<i>MC</i>	<i>VM</i>	<i>A</i>	<i>fC</i>	<i>HHV [MJ/kg]</i>	
5.18	81.08	1.45	17.47	18.63	

2 Model Formulation

2.1 Description of the system

Two different pathways for electricity generation is analyzed. The first one is the central biomass gasification and production of electricity with internal gas engine. The second one is the central gasification of biomass and production of electricity with micro turbine.

The main components of “the downdraft – internal combustion engine system” include: the gasifier, cyclone, producer gas heat exchanger, internal gas engine and heat recovery unit. The cycle involves air gasification of corn cob in a fixed bed downdraft gasifier and the producer gas obtained is then led to a cyclone in order to remove impurities such as dust and uncracked tar [1, 7]. After cleaning, the gas is fed into the heat exchanger and thereafter gas is fed into the engine to generate electricity. The exhaust gases from the internal gas engine are led to a heat recovery where drops it

temperature. Process heat or district heating or hot water heat exchange can be installed to further extract energy from the exhaust gases [7].

The main components of “*the downdraft - micro gas turbine system*” include: the gasifier, producer gas combustor/heat exchanger, indirectly fired micro-gas turbine and heat recovery unit [7]. The cycle involves air gasification of corn cob in a fixed bed downdraft gasifier and the producer gas obtained is then led to a combustor. Compressed air (to 3-5 bars) is heated up in the high temperature heat exchanger and thereafter preheated air enters the combustor where the fuel is combusted (temperature reaching 900 – 1000 °C) [8]. Hot flue gases expand through the micro turbine where mechanical work is produced. The exhaust gases from the turbine are led to a heat recovery where drops its temperature. Process heat or district heating or hot water heat exchange can be installed to further extract energy from the exhaust gases [7-9].

Plant capacity at which this technology is used ranges from 1kW_{el} – 10MW_{el} [7, 8, 10]. The efficiency is seen to be averagely 30% for 100 kW_{el} size, 35-45% for more than 1 MW_{el} [11] [12]. Also, internal combustion engines are high flexibility, long lifecycle, reliability, low cost, etc. However it should keep in mind that internal gas engines requires emission control systems because its operation produces high quality of NO_x and CO pollutants [7, 8]. In developing countries, internal combustion engine technology is used for generating electricity for small industries, residential buildings and etc. [7].

2.2 Process model simulator

Aspen Plus² is one of the sophisticated processes modeling softer package that gives a complete integrated solution to chemical processes and reactors. Aspen Plus is a steady state chemical process simulator, which uses unit operation blocks, which are the models of specific process operations (mixture, reactor, heat exchanger etc.) [7, 13]. The user places these blocks on a flow sheet, specifying material, and energy streams. An extensive built-in physical properties’ database were used for the simulation calculations [7, 13].

The simulations of two proposed CHP systems were based on the mass-energy balance and chemical equilibrium for the overall process.

2.3 Model description

Regarding to Keche A.J. et al. [13] the following assumption were considered in modeling the gasification process:

1. The whole process is in steady state and the reactions reach chemical equilibrium.
2. The heat exchange in a fixed bed is ideal and it is isothermal in the same section.
3. The heat exchange occurs instantaneously at equilibrium with volatile products including chiefly H₂, CO, CO₂, CH₄, and H₂O.
4. Tars are assumed to be negligible in the producer gas.
5. Charcoal only contains carbon and ash; ash is inert and does not participate in chemical reactions.

For the microturbine option the Capstone C200 model was chosen to be considered in calculations, while for internal gas engine Jenbacher JMS 208 GS-B.L. [7]

Figure 1 shows the modeled flowsheet for corn cobs downdraft gasification micro gas turbine system. Dry feed of corn cobs, specified as a non-conventional solid is first converted into its constituting elements (C, H, O, N, S, and ash) (block DECOMP in Figure 1) [7]. This is done by RYield model with calculations that are based on the component yield specifications. A Fortran³ statement is used to specify the yield distribution according to the ultimate and proximate analysis of corn cobs and determines the mass flow rate of each component in the blocks outlet stream [14]. The outlet stream from the block DECOMP is fed to the gasification reactor (block GASIFIER in Figure 1) where selected possible products were H₂, CO, CO₂, CH₄, and H₂O. The RGibbs was used to simulate the gasification of biomass. The RGibbs reactor calculates the producer gas composition by

² Aspen - Advanced System for Process Engineering

³ A drawback of using Aspen Plus is the lack of a library model to simulate fixed bed unit operations. However, it is possible for users to input their own models, using Fortran codes and reactions nested within the Aspen Plus input file, to simulate the operation of a fixed bed.

minimising the Gibbs free energy and assumes complete chemical equilibrium. The gasification reactor outlet enters a cyclone, which separates the ash from the produced gas. The clean product gas is cooled and combust in the Rstoic reactor (block COMB in Figure 1) with the compressed air, before the produced gas from the reaction expand through the turbine.

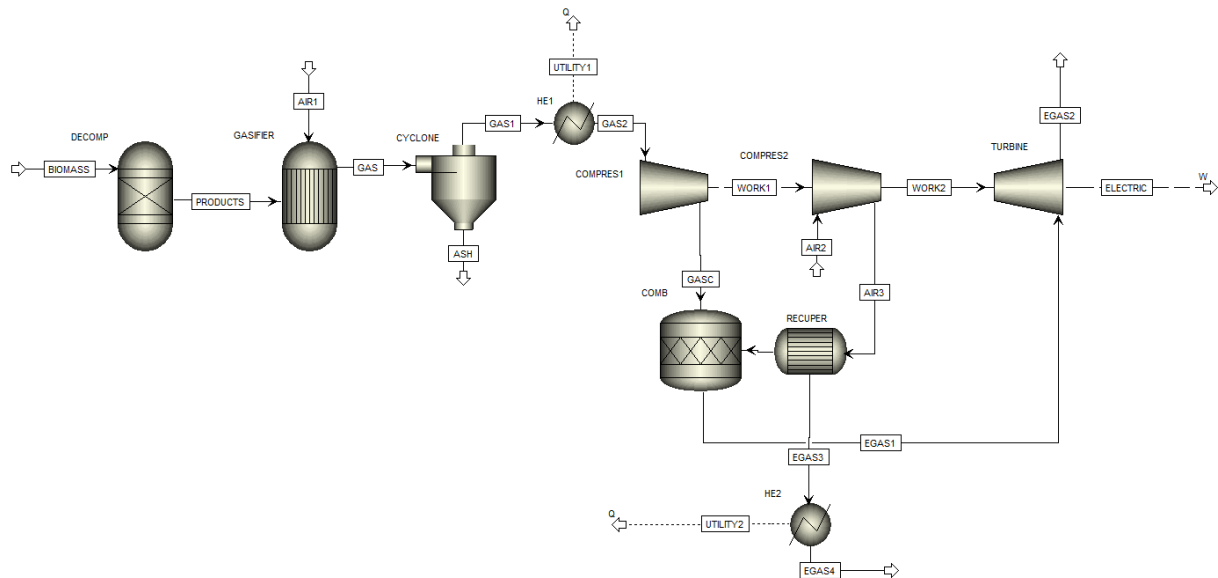


Figure 1 Corn cob downdraft gasification micro gas turbine simulation flowsheet

Figure 2 shows the modeled flowsheet for corn cobs downdraft gasification internal gas engine system. The part regarded to corn cob gasification is same as for the downdraft - micro gas turbine system, except that at the end of producer gas cooling, gas is mixed with air and compressed before entering the internal gas engine (block ENGINEIC in Figure 2) [7].

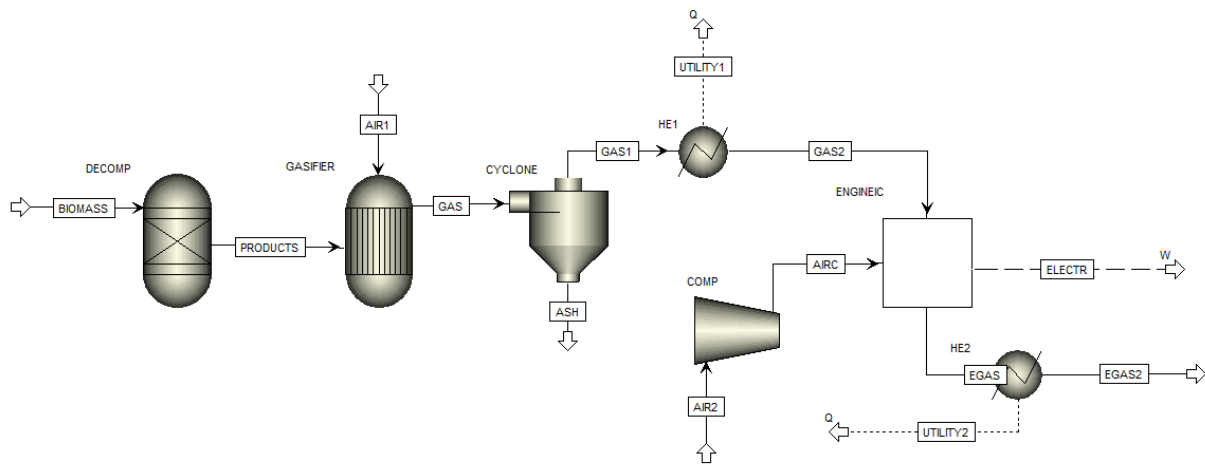


Figure 2 Corn cob downdraft gasification internal combustion engine simulation flowsheet

3 Results and Discussion

The overall process parameters are shown in Table 2.

The gasifier is fed with 100 kg/h of corn cob (HHV=18.63 MJ/kg). This yields 253.6 Nm³/h (dry basis) of producer gas with estimated low heating value of 6 MJ/Nm³ and components (by volume): H₂-16.82%, CO-21.48 %, CH₄-2.74 %, CO₂-9.63 %, N₂-40.67 and H₂O-8.66 %. Presence of water vapor and carbon dioxide molecules is due to the water-gas shift reaction during the gasification phase.

When comparing the electricity output of the two systems running, at gasification temperature of 850 °C, the power with internal combustion engine (208 kWe) is slightly higher than for the micro

gas turbine (200 kW). The electrical efficiency obtained for internal combustion engine was 37.65 % and the efficiency obtained for micro turbine was 36.20 %. Also, the systems also demonstrate higher value for thermal energy of internal gas engine (234 kW) than for micro gas turbine (135 kW). Further, the maximum attainable electricity ratio of internal gas engine (0.821 kWh/Nm³) is higher than that of micro turbine for biomass gasification (0.789 kWh/Nm³).

Simulation output result of NO_x formation in kg/kWh from all process, indicate that internal combustion engine (500 mg/Nm³) lead the chart in the production of NO_x. The micro gas turbine gave a low emission of 18 mg/Nm³ of NO_x.

Despite, higher NO_x emission compared to micro gas turbine, based on literature data, internal combustion engines are economically feasible in small scale (decentralized power investment) than that of micro gas turbine.

Table 2 Process parameters [7]

Unit	Value
<i>Gasifier</i>	
Reactor for gasification	Gibbs equilibrium reactor
Gasification media	air
Gasifier operating pressure	1 [bar]
Air entering conditions	25 [°C], 1 [bar]
Biomass LHV	17.13 [MJ/kg]
Biomass input conditions	25 [°C], 1 [bar]
Corn cob feed rate	117 [kg/h]
Thermal power input of the gasifier ($m_{\text{bio}}\text{LHV}_{\text{bio}}$)	552.5 [kW]
air/feedstock ratio	0.3 [kg/kg]
Gasification Zone	850 [°C]
Producer gas exit	253.6 [Nm ³ /h], 700 [°C]
<i>CHP with micro turbine</i>	
<i>Micro turbine</i>	
Gas inlet turbine temperature	950 [°C]
Inlet Pressure	5.5 [bar]
Turbine exhaust	1 [bar]
Nominal electricity output	200 [kW]
Electricity output	135 [kW]
Exhaust Gas Temperature	280 [°C]
Heat exchanger	1 [bar]
Pressure loss across heat exchanger	5 [%]
Efficiencies	
Electrical	33 [%]
<i>CHP with internal combustion engine</i>	
<i>Internal combustion engine</i>	
Electrical output	208 [kW]
Total recoverable thermal output	234 [kW]
Engine speed	1500 [rpm]
Exhaust gas flow	883 [Nm ³ /h]
Exhaust gas temperature	471 [°C]
Combustion air volume	742 [Nm ³ /h]
Efficiencies	
Electric efficiency	35.8 [%]

4 Conclusion

The results show that the proposed two CHP systems are feasible with self-sustaining heat generation and recovery to satisfy the process goals. The systems also demonstrate the potential of obtaining relatively high electrical efficiency. However, the maximum attainable electricity ratio of internal gas engine (0.821 kWh/Nm^3) is higher than that of micro turbine for biomass gasification (0.789 kWh/Nm^3). While on other hand, the micro gas turbine gave a low NO_x emission (18 mg/Nm^3) compared to internal combustion engine (500 mg/Nm), but are more expensive than internal combustion engines.

Unfortunately, CHP systems still characterises technical uncertainties namely operational difficulties, poor reliability and low overall efficiency that requires considerable technical advances prior to commercial viability. Therefore, there is a research need to overcome the existing technical obstacles, and to demonstrate energy-efficient biomass-fuelled CHP systems.

5 References

- [1] **Trninić, M.**, *Modeling and Optimisation of corn cob Pyrolysis*, Ph.D. thesis, Belgrade University Faculty of Mechanical Engineering, Belgrade, Serbia, 2015.
- [2] **Puig-Arnavat, M., J.C. Bruno, A. Coronas**, Modified Thermodynamic Equilibrium Model for Biomass Gasification: A Study of the Influence of Operating Conditions, *Energy & Fuels*, Volume 26 (2012), issue 2, pp. 1385-94.
- [3] **Chanphavong, L., Z.A. Zainal**, Characterization and challenge of development of producer gas fuel combustor: A review, *Journal of the Energy Institute*, Volume 92 (2019), issue 5, pp. 1577-90.
- [4] **Gautam, G.**, *Parametric Study of a Commercial-Scale Biomass Downdraft Gasifier: Experiments and Equilibrium Modeling*, MSc thesis, The Graduate Faculty of Auburn University, Auburn, Alabama – USA, 2010.
- [5] **Burgt C.H.M.**, *Gasification*, Gulf Professional Publishing, 2008.
- [6] **Musinguzi, W.B., M.A.E. Okure, A. Sebbit, T. Løvås, I. da Silva**, Thermodynamic Modeling of Allothermal Steam Gasification in a Downdraft Fixed-Bed Gasifier, *Advanced Materials Research*, Volumes 875-877 (2014), pp. 1782-93.
- [7] **Trninić, M., A. Jovović, D. Stojiljković, G. Jankes, T. Simonović, N. Tanasić, M. Stanojević**, Process Simulations of Small scale Biomass Power plant, *Proceedings V Regional Conference Industrial Energy and Environmental Protection in South Eastern Europe - IEEP 2015*, The Society of Thermal Engineers, Zlatibor, Serbia, 2015.
- [8] **Megwai, G.U.**, *Process Simulations of Small Scale Biomass Power Plant*, MSc thesis, University of Borås, Borås, Sweden, 2014.
- [9] **Lymberopoulos, N.**, *Microturbines and their Application in Bio-energy*, Centre for Renewable Energy Sources, 2004.
- [10] **Carrara, S.**, *Small-scale Biomass Power Generation*, Ph.D. thesis, University of Bergamo, Bergamo, Italy, 2010.
- [11] **Goldstein, L., B. Hedman, D. Knowles, S.I. Freedman, T. Schweizer**, *Gas-Fired Distributed Energy Resource Technology Characterizations*, National Renewable Energy Laboratory NREL, 2003.
- [12] ***Technology Data for Energy Plants, available at <https://www.energinet.dk/>. 2020.
- [13] **Keche, A., A. Gaddale, R. Tated.**, Simulation of biomass gasification in downdraft gasifier for different biomass fuels using ASPEN PLUS, *Clean Techn Environ Policy*, Volume 17 (2015), Issue 2, pp. 465-73.
- [14] **Nikoo, M.B., N. Mahinpey**, Simulation of biomass gasification in fluidized bed reactor using ASPEN PLUS, *Biomass and Bioenergy*, Volume 32 (2008), Issue 12, pp. 1245-54.
- [15] **Mavukwana, A.E., K. Jalama, K. Harding**, Simulation of South African Corncob Gasification with Aspen Plus: A Sensitivity Analysis, *Applied Mechanics and Materials*, Volume 92 (2014), pp. 386-91

POBOLJŠANJE SVOJSTAVA BETONA DODATKOM LETEĆEG PEPELA IZ TERMoeLEKTRANE ZA PRIMENU U GEOTERMALNIM SISTEMIMA

ENHANCING PROPERTIES OF CONCRETE BY ADDITION OF FLY ASH FROM A THERMAL POWER PLANT FOR APPLICATION IN GEOTHERMAL SYSTEMS

Milica VLAHOVIĆ^{1,1}, Aleksandar SAVIĆ², Sanja MARTINOVIĆ¹, Nataša ĐORĐEVIĆ³,
Zoran STEVIĆ⁴, Tatjana VOLKOV HUSOVIĆ⁵

¹ University of Belgrade, Institute of Chemistry, Technology and Metallurgy, Belgrade, Serbia

² University of Belgrade, Faculty of Civil Engineering, Belgrade, Serbia

³ Institute for Technology of Nuclear and Other Mineral Raw Materials, Belgrade, Serbia

⁴ University of Belgrade, Faculty of Electrical Engineering,
Technical Faculty Bor, CIK Belgrade, Serbia

⁵ University of Belgrade, Faculty of Technology and Metallurgy, Belgrade, Serbia

<https://doi.org/10.24094/mkoiee.020.8.1.77>

Električnu energiju u Srbiji pretežno obezbeđuju termoelektre. Svih jedanaest termoelektrana u Srbiji koriste uglj, uglavnom lignit u procesu proizvodnje električne energije, čime se godišnje generiše oko 6 miliona tona letećeg pepela. Procenjena količina letećeg pepela iz termoelektrana akumulirana na deponijama u Srbiji prelazi 200 miliona tona. S druge strane, poslednjih decenija poštovanje principa ekološki održivog razvoja nametnuto je industrijama, a jedna od njih je i građevinska. Zahvaljujući prisustvu amorfnog SiO₂ i Al₂O₃, pepeo kao pucolanski materijal pogodan je za proizvodnju betona i maltera. Zbog toga se pravilnom upotrebom letećeg pepela mogu očekivati višestruki pozitivni efekti- smanjenje deponija i poboljšanje svojstava betona. Ideja ovog istraživanja je analiziranje mogućnosti recikliranja letećeg pepela iz termoelektrane tako što će delimično zameniti uobičajeni mineralni punioci- krečnjak u proizvodnji samozbijajućeg betona (SCC). Upoređena su svojstva konvencionalnog SCC sa krečnjakom i kompozicija sa različitim sadržajem pepela. S obzirom da je u slučaju dodatka letećeg pepela potrebno da budu zadovoljeni zahtevi za SCC, kao i da svojstva betona ostanu ista ili poboljšana, ova studija je pokazala da se sve dizajnirane smeše mogu koristiti za konstrukcijske primene.

Ključne reči: samozbijajući beton (SCC); leteći pepeo; dizajn smeša; fizičko-mehanička svojstva; mikrostruktura

Electric power in Serbia is predominantly provided by thermal power plants. All of eleven existing thermal power plants in Serbia use coal, mainly lignite in the electricity production process thus generating about 6 million tons of fly ash per year. The estimated amount of fly ash from thermal power plants accumulated in Serbian landfills exceeds 200 million tons. On the other hand, during the last decades, respecting the principles of ecologically sustainable development has been imposed on industries, and one of them is the construction industry. Due to the presence of amorphous SiO₂ and Al₂O₃, fly ash as pozzolanic material is convenient for the production of concrete and mortar. Consequently, multiple positive effects can be expected by the proper consumption of fly ash- reducing landfills and improving concrete properties. The idea of this study is to analyze the possibility of recycling fly ash from a thermal power plant by replacing a part of common mineral filler- limestone in the production of self-compacting concrete (SCC). Properties of conventional SCC with limestone and compositions with different fly ash content were compared. Considering that requirements for

¹ Corresponding author, email: mvlahovic@tmf.bg.ac.rs

SCC should be satisfied and all properties remain or enhance in the case of fly ash addition, this study proved that all designed concretes can be used for structural applications.

Key words: *self-compacting concrete (SCC); fly ash; mixture design; physico-mechanical properties; microstructure*

1 Introduction

About 70 % of electric power in Serbia is generated in the existing 11 thermal power plants belonging to the Electric Power Industry of Serbia and they all use coal, mostly lignite, thus making them the largest lignite producers. In this electricity production, about 6 million tonnes of fly ash (FA) per year is obtained, which is stored in landfills covering an area around 1,800 ha. The total estimated amount of fly ash in Serbian landfills is over 200 million tonnes [1-3]. Fly ash is a fine, loose material that is being collected in the electro filters of the chimneys in thermal power plants with the particle size usually in the range of 1-150 μm .

The development of concrete additives mainly of polycarboxylate-type, led to spreading application of self-compacting concrete (SCC), considered as a revolutionary discovery in concrete technology. This concrete, owing to its own weight, fills the formwork, thus coats reinforcement bars and fulfills all available space, while achieving the highest compactness, important for hardened state properties and durability [4].

Fly ash, capable of reacting with calcium hydroxide at room temperature, due to the presence of SiO_2 and Al_2O_3 in the amorphous form, can be considered as pozzolanic material and therefore, it has been used for decades as an additive in commercial types of cement and for the production of concrete and mortar. Inhomogeneous composition is one of the disadvantages that reduce its use [5-9].

The use of fine FA particles in concrete leads to the effect of the aggregate fluidity, as well as to an increase in the solid to liquid ratio, at the same water/ cement factor; consequently, the risk of segregation and water extraction on the surface reduces.

Due to the spherical shape and glassy surface of the majority of FA particles, usually finer than the cement particles, the addition of 10 mass. % of FA in relation to the cement mass reduces the water requirement by 3-4 %.

The principles of sustainable development and ecology have been constantly and intensively promoted in all spheres. Hence, the consumption of FA will create multiple positive results, including the reduction of accumulated material at landfills and the improvement of concrete properties [5].

The idea in this study is to investigate the possibility of producing high-performance SCC using FA from Thermal Power Plant "Kolubara A", Serbia, without prior processing, for a partial replacement of mineral filler, limestone. It is presumed that small amounts of FA improve hardened SCC properties without serious deterioration of its fresh state properties. The properties of SCCs with different amounts of FA will be compared and accordingly the optimal composition will be recommended.

2 Experimental

2.1 Mixture design and samples preparation

The initial components used for SCC preparation were aggregate, cement, limestone, fly ash and superplasticizer.

Natural aggregate, from the river Danube, mostly with rounded particles, was used in three fractions: I- fine (0-4 mm), II- coarse (4-8 mm), and III- coarse (8-16 mm). The contents of coarser grains (> 4 mm) in fractions I, II, and III were 1.96 %, 5.81 %, and 0 %, respectively. The contents of fine particles in fractions II and III were 1.84 % and 0.94 %, respectively. In fraction I the contents of fine particles, < 0.063 mm and < 0.09 mm, were 0.59 % and 1.68 %, respectively.

A commercial type I Portland cement (*CEM I 42.5R, Lafarge, Serbia*) was used as a binder. Chemical composition of the cement was: 61.64 % CaO , 21.21 % SiO_2 , 2.22 % MgO , 4.81 % Al_2O_3 , 2.13 % Fe_2O_3 , 1.11 % K_2O , 0.33 % Na_2O , 0.18 % TiO_2 , and 6.37 % SO_3 .

Natural limestone (*Granit Pescar, Ljig, Serbia*), with a medium size of 250 μm was used as mineral filler. According to chemical analysis, it consists of: 54.86 % CaO, 0.21 % SiO₂, 1.10 % MgO, 0.5 % Al₂O₃, 0.09 % Fe₂O₃, 0.05 % K₂O, 0.005 % MnO, 0.5 % P₂O₅, and SO₂ in traces (LOI 43.64 %).

Fly ash, from Thermal Power Plant "Kolubara A", Serbia, was used in its original form for partial replacement of limestone. According to chemical analysis, it consists of: 58.60 % SiO₂, 21.92% Al₂O₃, 6.12 % CaO, 5.97 % Fe₂O₃, 1.77 % MgO, 1.50 % K₂O, 0.37 % Na₂O, and 0.49 % TiO₂ (LOI 3.09 %). Density of FA in the loose and compacted state was 690 kg/m³ and 910 kg/m³, respectively. The specific gravity was 2190 kg/m³.

Microstructure of FA was performed by SEM (scanning electron microscope), type JEOL JSM-5800 and the obtained microphotographs are given in Figure 1.

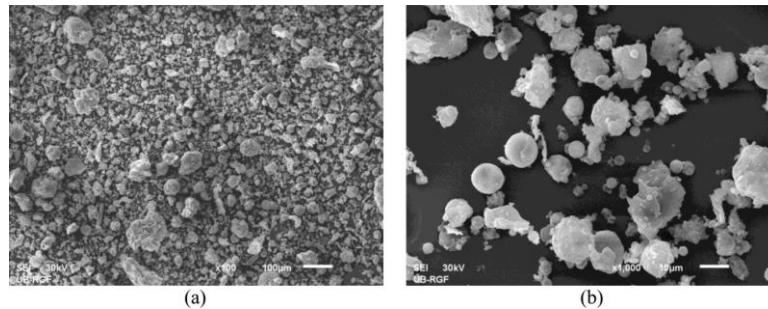


Figure 1. SEM microphotographs of fly ash taken at magnification of: a) 100 x, b) 1000 x

As seen in Figure 1, FA particles are generally spherical. Since only organic matter is lost during coal combustion, the inorganic residue remains in the ash. A large number of irregularly shaped particles is evidently present.

A polycarboxylate (Glenium Sky 690, *BASF Construction Chemicals, Italy*) additive was used as a superplasticizer that enables self-compacting capacity and improves the flowability of concrete.

The compositions of designed four SCC mixtures are shown in Table 1.

The reference SCC mixture E contains only limestone as filler. Other three SCC mixtures were made with partial replacement of FA in regard to the limestone amount: FA-10 with 10 mass. % of FA, FA-20 with 20 mass. % of FA and FA-50 with 50 mass. % of FA and with increased superplasticizer content necessary to provide workability.

Table 1. Design of SCC mixtures

	E	FA-10	FA-20	FA-50
Coarse aggregate (8-16mm) (kg/m ³)	430	430	430	430
Coarse aggregate (4-8mm) (kg/m ³)	430	430	430	430
Fine aggregate (0-4mm) (kg/m ³)	840	840	840	840
Cement C (kg/m ³)	380	380	380	380
Water W (kg/m ³)	183	183	183	183
Limestone powder LP (kg/m ³)	220	198	176	110
Fly ash FA (kg/m ³)	0	22	44	110
Superplasticizer (kg/m ³)	7.6	7.6	7.6	11.4
Water- to- cement ratio W/C	0.482	0.482	0.482	0.482

Each SCC mixture was proportioned by weight. A laboratory concrete mixer with a capacity of 60 l, fixed drum, and paddles at the vertical axel was used. The aggregate was mixed for one minute in a mixer, then the filler and cement were added and mixed for 30 s. Afterwards, water with the

superplasticizer was added and mixing continued until homogeneity (270 s). The preparation was realized at the ambient temperature (20-22 °C).

After preparation, rheological tests in fresh state of SCC were made.

Subsequently, casting was done. The specimens were removed from the molds after 24 h, and then cured in water until tests on hardened concrete were done. Each of the data obtained from testing corresponds to an average of at least three measurements.

2.2 Characterization of the SCC

The characterization of the **fresh state** of the produced SCC was performed by standard determination of density, entrained air content, flowability (Slump flow, Slump flow time (t_{500}), V-funnel time (t_v)), passing ability (L-box), and segregation resistance [10-14].

Investigations on the **hardened** SCC included: density, mechanical strength, static modulus of elasticity, water permeability, resistance against freezing in the presence of de-icing salt, and SEM analysis. Density was tested on prisms 12x12x36 cm up to the age of 180 days [15]; compressive strength on cubes at each age (3, 7, 14, 21, 28, 63, 90 and 180 days) [16]; three point bending (flexural strength) test on prisms 12x12x36 cm at the age of 28 days [17], static modulus of elasticity on cylinders with diameter of 15 cm and height of 30 cm, at the ages of 28 and 180 days [18]; water penetration at the older age of 63 days [19]; resistance against freezing in the presence of de-icing salt (3 % aqueous solution of NaCl) on special samples with the bottomless container on the top at the age of 28 days [20]. For the microstructure characterization, statistically representative samples of all mixtures were prepared and tested using the SEM (scanning electron microscope), type JEOL JSM-5800.

The SCC samples were kept in water for 180 days. They were periodically removed from water to perform measurements.

The performed qualitative analysis included comparison of the reference mixture E with the mixtures containing FA in terms of their porosity and structure.

3 Results and Discussion

3.1 Fresh SCC tests

The results of characteristic rheological tests on SCC are presented in Table 2.

According to the EFNARC, all SCC series with FA meet the requirements for the determined fresh state properties except the viscosity of FA-50. SCCs with FA exhibit lower workability than E, which is manifested in flowability and passing ability decrease as well as in segregation resistance increase. It can be concluded that the addition of FA in the higher proportion affects negatively the fluidity and workability of SCC.

Table 2. Fresh state properties of SCCs

	E	FA-10	FA-20	FA-50
Density (kg/m ³)	2397	2391	2370	2347
Entrained air content (%)	1.9	1.5	2.0	2.8
Slump flow (mm)	761.2	701.2	663.8	702.5
Slump flow time t_{500} (s)	2.62	5.71	10.91	11.32
V-funnel time t_v (s)	9.73	15.92	22.46	27.21
Passing ability L-box (H2/H1)	0.97	0.92	0.92	0.95
Segregation factor (%)	3.5	3.0	2.0	1.7

t_{500} - time required for spreading; t_v - V-funnel time; H1 and H2-heights at the beginning and at the end of the horizontal part of L-box, respectively

3.2 Hardened SCC tests

Density

Density values of tested series up to the age of 180 days are in the range of 2350-2420 kg/m³. Figure 2 shows the density change versus the logarithm of time.

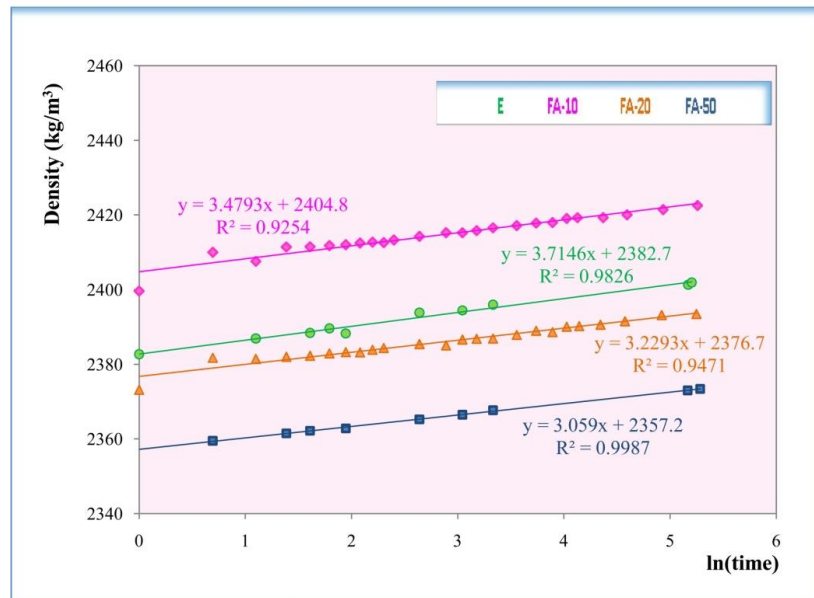


Figure 2. Density change of hardened SCCs versus time

As seen in Figure 2, at all ages, FA-50 exhibited the lowest density values, and FA-10 the highest. Unexpectedly, the density of FA-10 was higher than that of E, which is probably the result of measuring errors. Linear regression analysis gave equations with high values of correlation coefficients. Obviously, E has the greatest slope, and thus the fastest water absorption, which is in accordance with the fact that the FA addition improves the concrete structure resulting in lower water absorption [21]. Comparing only mixtures with FA, FA-10 has the greatest slope, followed by FA-20 and finally by FA-50.

Mechanical strength

The compressive strength is a basic property of hardened concrete and is often used as its quality indicator [22]. The obtained results of compressive strength are given in Figure 3.

As seen in Figure 3, the increase in FA amount leads to compressive strength decrease of SCCs at early ages and to strength increase at older ages. This is explained by the pozzolanic effect, which is more pronounced for larger FA quantities and older ages. 50 % of FA leads both to strength increase and decrease depending on age. This can be attributed to the negative effect of the mechanically weaker FA grains, especially coarser inhomogeneous, apart from the positive pozzolanic impact. However, LP-50 showed higher strength than E at all ages- from 4.3% at the age of 90 days to 16.5% at the age of 63 days. In this respect, a clear positive effect of using FA is evident. These results show that the addition of FA results in strength increase at all ages depending on its amount compared with the strength of E.

At the age of 28 days mixtures FA-10, FA-20, and FA-50 reached significantly higher strengths than E; precisely, higher for 11.3 %, 16.8 %, and 12.9 %, respectively. The 16.8 % increase for FA-20 in relation to E at 28 days of age is at the same time the largest difference among all data. This strength increment with the increasing FA content can be explained by the pozzolanic effect, which is more pronounced for larger FA quantities and at later ages.

Based on the analysis performed, a positive effect of the use of FA in SCCs is evident.

For concrete with FA, the rate of compression strength increment depends on a number of factors. Since FA, with the total content of oxides SiO₂ + Al₂O₃ + Fe₂O₃ over 80 % was used, the effect of a later increase in the concrete strength (but also a slower strength development at early ages) can be expected due to its pozzolanic reaction [23].

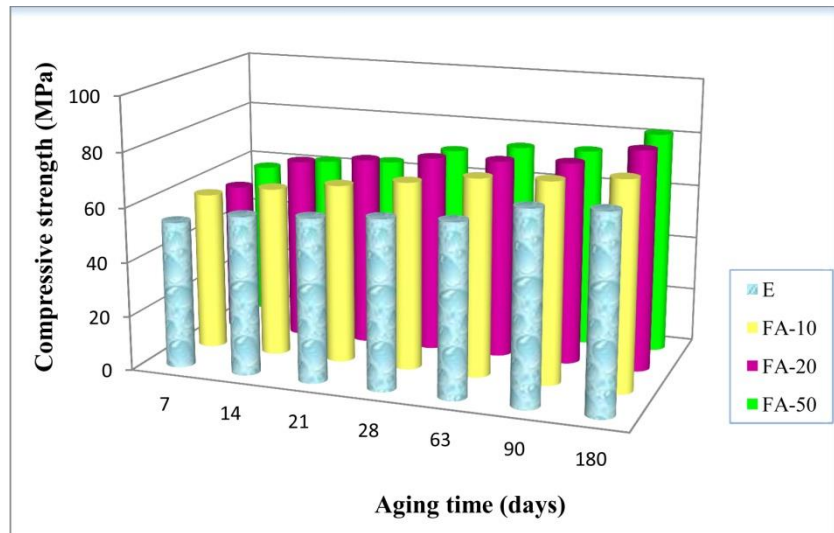


Figure 3. Compressive strength of SCC mixtures during time

Figure 4 shows the compressive strength increment of SCCs versus logarithm of time. A family of curves described by equations with high correlation coefficients was obtained by regression analysis.

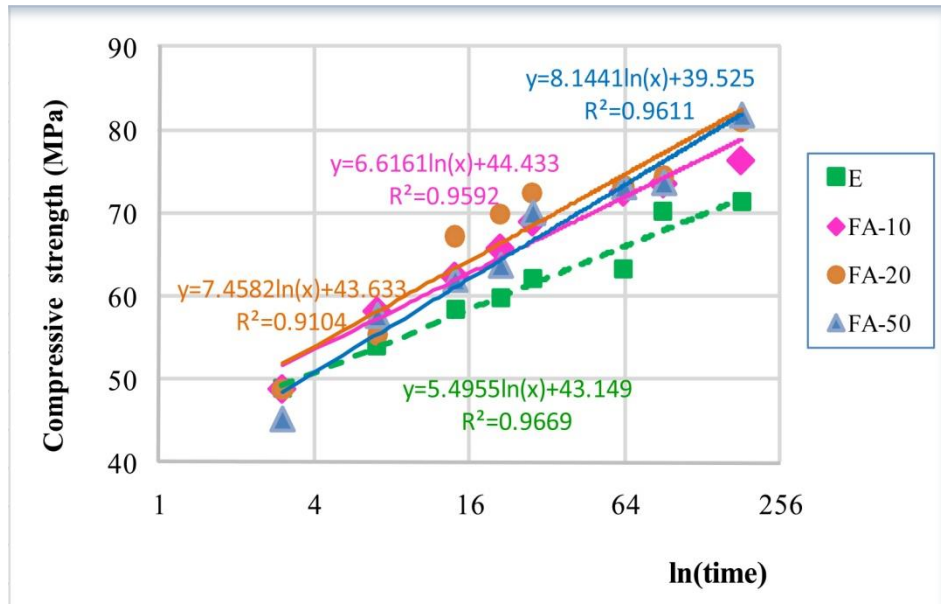


Figure 4. Compressive strength increment of SCC mixtures during the aging time

It can be observed that E represents the lower boundary of the curve family, while FA-20 the upper boundary line of the formed functional dependency family. The functional regressions derived for FA-10 and FA-50, from lower to higher, are between the two boundaries. In terms of the cement stone hardening, where the cement hydration and the pozzolanic reaction are involved, the rate of compressive strength increment, and thus the rates of the corresponding chemical reactions, can be interpreted by the slopes of the created lines. Namely, the slopes of all lines are positive- its lowest value is for E, which corresponds to the slowest rate of strength increment. A slope increment for SCCs containing FA is evident with FA content increase, which corresponds to the pozzolanic contribution to the strength enhancement. At some moment, due to the pozzolanic reaction, further significant strength increase for mixtures with FA, especially of FA-50, can be expected.

The flexural strength results for SCCs at the age of 28 days are given in Table 3.

As can be seen from Table 3, FA-10 had a 1 % lower flexural strength compared to E. FA-20 and FA-50, showed a slight flexural strength increase compared to E- 12 % and 3 %, respectively. Regarding flexural strength, the optimum FA content is 20 %.

Table 3. Flexural strength of SCC mixtures at the age of 28 days

	<i>E</i>	<i>FA-10</i>	<i>FA-20</i>	<i>FA-50</i>
Flexural strength f_{zs} [MPa]	10.3	10.2	11.5	10.6

Static elasticity modulus

The static elasticity modulus results for SCCs at the ages of 28 and 180 days are shown in Table 4.

Table 4. Static modulus of elasticity E_s [GPa] of SCCs at the ages of 28 and 180 days

Age (days)	<i>E</i>	<i>FA-10</i>	<i>FA-20</i>	<i>FA-50</i>
28	34.1	35.6	35.7	37.3
180	38.5	35.6	41.9	39.4

FA-10, FA-20 and FA-50, at 28 days of age showed higher static elasticity modulus than E- 4.4 %, 4.5 % and 9.4 %, respectively. Similarly, at 180 days of age, FA-10, FA-20 and FA-50, showed higher values than E- 8.1 %, 8.8 % and 2.3 %, respectively. Based on these results, and the evident elasticity modulus drop for FA-50 at the age of 180 days, it can be concluded that lower FA content provides better elasticity at older ages.

Water permeability

Maximal and average depths of water penetration for each specimen of each mixture, as well as the average values for each mixture are given in Table 5.

Table 5. Depths h [mm] of the water penetration

	<i>E</i>		<i>FA-10</i>		<i>FA-20</i>		<i>FA-50</i>	
Specimen	Aver.	Max	Aver.	Max	Aver.	Max	Aver.	Max
1	8	16	10	15	9	14	11	15
2	9	16	9	17	10	15	10	17
3	11	17	9	16	11	17	9	15
Average value:	9.3	16.3	9.3	16.0	10.0	15.3	10.0	15.7

It is evident that all mixtures exhibited a similarly high level of water impermeability.

Resistance against freezing in the presence of de-icing salt

Mass loss for each mixture as well as damage depth after 25 cycles of simultaneous exposure to frost and 3 % aqueous solution of NaCl is presented in Table 6.

Table 6. Mass loss and damage depth for SCC mixtures

	Mass loss (mg/mm^2)	Damage depth (mm)
E	0.12	0.6
FA-10	0.09	0.4
FA-20	0.10	0.4
FA-50	0.10	0.5

Frost resistance testing has shown some advantages concerning fly ash addition to SCC mixtures and also its contribution to improving durability in the salt environment.

The mixtures with FA after treatment underwent a certain mass loss, but lower than E. A similar effect is observed regarding the damage depth, with optimum effects for FA-10.

SEM analysis

Representative samples of all SCCs were prepared for the structure characterization by the use of SEM. Basically, the performed analysis had qualitative character.

Based on the SEM analysis, it can be observed that the homogeneity was achieved in all SCC mixtures, while the porosity was visually similar (Figure 5). Furthermore, although the contact of aggregate grains and the cement matrix is generally good, it should be noticed that this contact is better for certain grains (sandstone, limestone) than for others (quartzite), owing to the surface character and compactness of the aggregate grains themselves.

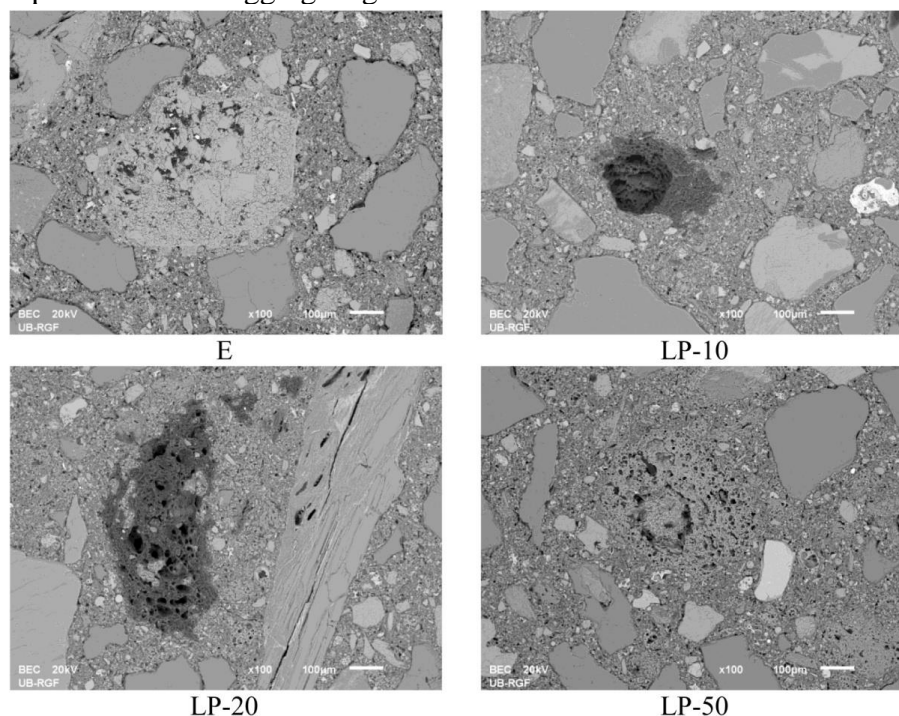


Figure 5. SEM microphotographs of SCC series

4 Conclusion

In compliance with the trends of promoting sustainable development in the field of construction, the possibility of using industrial byproduct- FA for partial substitution of the mineral filler-limestone in SCC was investigated. SCCs with the addition of FA were examined and compared with the reference mixture with limestone in order to optimize the properties and composition of these concretes.

All SCCs with FA met the standards concerning fresh state properties except the viscosity of FA-50.

Regarding hardened SCC properties, positive effect of FA is evident. Lower amounts of FA led to compressive strength increase, which was especially pronounced for FA-20 and at older ages. Flexural strength values were similar. The SCCs with FA exhibited better resistance against freezing in the presence of de-icing salt and higher values of static elasticity modulus than the reference mixture. All mixtures have similarly high impermeability and hence compactness, which was proved by SEM. Based on the SEM analysis, it can be concluded that homogeneity was achieved in all mixtures, while the porosity was visually similar. High degree of compactness of SCCs with FA is an indicator of good durability.

This study showed that it is possible to obtain a high-performance SCC using FA and that its optimal content is 20 % with respect to the total filler mass.

It is of great importance for the construction industry and should be continued towards the practical application of the designed SCC mixtures. This application may include testing of structural

elements (beams and columns) in laboratory conditions, as well as the design of construction systems in the field and their monitoring as part of full-scale feasibility studies.

Research can be widened to designing new mixtures with a higher proportion of FA as a mineral additive, which would raise the valorization of this industrial by-product in Serbia to a larger scale.

5 Acknowledgments

This work was financially supported by the Ministry of Education, Science and Technological Development of the Republic of Serbia (Grant No. 451-03-68/2020-14/200026 IHTM, 92166/3-19, 451-03-68/2020-14/20002, 451-03-68/2020-14/200135)

6 References

- [1] **Jevtić, D., Zakić, D., Savić, A., Radević, A.,** The influence of fly ash on basic properties of mortar and concrete, Proceedings Scientific conference Planning, design, construction and building renewal, Novi Sad, Serbia, 2012.
- [2] **Jevtić D., Markičević, J., Savić, A.,** Fly Ash Influence on Certain Properties of Concrete Composites, Proceedings 6th International Conference Science and Higher Education in Function of Sustainable Development, Užice, Serbia, 2013.
- [3] **Jevtić, D., Mitrović, A., Savić, A.,** Experimental investigation of fly ash content influence on cement mortars properties, Proceedings 2nd International Symposium on Environmental and Material Flow Management, Zenica, Bosnia and Hercegovina, 2012.
- [4] **Okamura, H.,** Self-compacting high-performance concrete, Concrete International 19 (1997), 7, pp. 50-54.
- [5] **Wesche, K.,** Fly Ash in Concrete: Properties and performance (Rilem Report 7), Report of Technical Committee 67-FAB Use of Fly Ash in Building, Taylor & Francis e-Library, 2005
- [6] **Jevtić, D., Savić, A., Radević, A.,** Fly ash influence on concrete composites - Contribution to sustainable construction, Proceedings 15th YuCorr, Tara, 2013.
- [7] **Jevtić, D., Zakić, D., Savić, A.,** Cementitious Composites Made With Fly Ash - A Contribution To The Sustainable Civil Engineering, Proceedings 14th International Conference Research and Development in Mechanical Industry, Topola, Serbia, 2014.
- [8] **Jevtić, D., Zakić, D., Savić, A., Radević, A.,** Properties modeling of cement composites made with the use of fly ash, Book of abstracts III International Congress Engineering, Environment and Materials in Processing Industry, Jahorina, Bosnia and Herzegovina, 2013.
- [9] **Jevtić, D., Zakić, D., Savić, A., Radević, A.,** Properties modeling of cement composites of fly ash, Materials Protection, LV, (2014), pp. 39-44.
- [10] *** SRPS EN 12350-6:2010 Testing fresh concrete - Part 6: Density.
- [11] *** SRPS EN 12350-7:2010 Testing fresh concrete - Part 7: Air content - Pressure methods.
- [12] *** SRPS EN 206-1:2011 Concrete - Part 1: Specification performance, production and conformity.
- [13] *** SRPS EN 12350-10:2012 Testing fresh concrete - Part 10: Self-compacting concrete - L box test.
- [14] *** SRPS EN 12350-11:2012; Testing fresh concrete - Part 11: Self-compacting concrete - Sieve segregation test.
- [15] *** SRPS EN 12390-7:2010 Testing hardened concrete – Part 7: Density of hardened concrete
- [16] *** SRPS EN 12390-3:2010 Testing hardened concrete - Part 3: Compressive strength of test specimens.
- [17] *** SRPS ISO 4013:2000 Concrete - Determination of flexural strength of test specimens
- [18] *** ASTM C469/ C469M 10: Standard Test Method for Static Modulus of Elasticity and Poisson's Ratio of Concrete in Compression, (2005).
- [19] *** SRPS U.M1.015:1998 Concrete - Hardened concrete - Determination of the depth of penetration of water under pressure.
- [20] *** SRPS U.M1.055:1984 Concrete - Method of test for resistance of concrete against freezing

- [21] **Assie, S., Escadeillas, G., Marchese, G., Waller, V.**, 2006. Durability properties of low-resistance self compacting concrete, Magazine of Concrete Research 58 (2006), 1, pp. 1-7.
- [22] **Muravljov, M.**, Osnovi teorije i tehnologije betona, Građevinska knjiga, Beograd, 2011.
- [23] ASTM C 618: Standard specification for coal fly ash and raw or calcined natural pozzolan for use in concrete, (2003).

PRIMENA OBNOVLJIVIH IZVORA ENERGIJE U ZGRADARSTVU

APPLICATION OF RENEWABLE ENERGY RESOURCES IN BUILDINGS

Njegoš DRAGOVIĆ^{1,1}, Milovan VUKOVIĆ¹, Igor UROŠEVIĆ²,

¹ Univerzitet u Beogradu, Tehnički fakultet u Boru, Bor, Srbija

² Univerzitet u Beogradu, Arhitektonski fakultet, Beograd, Srbija

<https://doi.org/10.24094/mkoiee.020.8.1.87>

Struktura objekata koji se grade moraju biti projektovani tako da budu energetske efikasne. Doprinos svakog objekta za stanovanje ili za poslovne, proizvodne i skladišne potrebe mora biti posmatran u kontekstu ušteda energije i transformacije kroz centralizovan sistem. Značajan doprinos energetske efikasnosti u zgradarstvu daju obnovljivi izvori energije, koji mogu da se međusobno kombinuju i kroz transformacije termalne u električnu energiju, ostvare ogromne uštede. Pored ušteda i efikasnosti, OIE utiču i na izgradnju objekata koji se uklapaju u životni prostor i kompenzuju modalitete grejanja-hlađenja-transformacije-čuvanja-prodaje viška energije.

U radu se analizira trenutno stanje izdavanja dozvola, projektovanje i izgradnja objekata, kao i davanje upotrebnih dozvola uz osvrt na ugradnju „zelenih“ materijala i stvaranja odgovarajuće atmosfere koja podržava obnovljive izvore energije i energetske efikasnosti.

Ključne reči: Obnovljivi izvori energije; energetska efikasnost; zgrade; „zeleni materijali“; arhitektura

The structure of the facilities under construction must be designed to be energy efficient. The contribution of each residential or business, production and storage facility must be viewed in the context of energy savings and transformation through a centralized system. Renewable energy sources (RES) make a significant contribution to energy efficiency in buildings, which can be combined with each other and through huge transformations from thermal to electricity, achieve huge savings. In addition to savings and efficiency, RES also affect the construction of facilities that fit into the living space and compensate for the modalities of heating-cooling-transformation-storage-sale of excess energy.

The paper analyzes the current state of licensing, design and construction of facilities, as well as the issuance of use permits with reference to the installation of "green" materials and the creation of an appropriate atmosphere that supports renewable energy sources and energy efficiency.

Key words: Renewable energy sources; energetic efficiency; buildings; "Green materials"; architecture

1 Renewable energy sources

Energy resources were previously considered limited and unavailable for widespread use. However, with the development of technology of transfer, reception, processing and supply, its appearance and use form is viewed in a different way.

Dependence on traditional energy is increasing due to technological development and real needs for sustainable energy. Unlike these sources, renewable energy sources have consistency and are environmentally friendly. Their renewability does not depend on the consumption of resources but on a continuous inflow through the development of technological capacities, such as turbines, photovoltaic cells, thermal sensors and rods, mechanical pendulums and propellers. As a renewable energy source (RES) we know biomass (wood and waste) and biofuels (biogas), wind energy, solar energy, hydropower (watercourses, small hydropower plants, sea currents, tides), wave energy, geothermal

¹ Corresponding author, email: njegdr@gmail.com

energy and the Earth's internal heat, geothermal water), as well as combined forms of renewable energy sources (water, air, light, waves). The use of RES has become an important part of the design and development of green building (Hashim H, HoWS, 2011).

The main difference between energy used in the world and in our country is that the developed world cares about reducing environmental pollution, consumption of traditional energy sources and trying to increase the energy efficiency of individual households, either through incentives and regulations or through greater availability of renewable materials and technologies centralized supply system. Figure 1 shows the connection of different forms of renewable energy that a building can use to meet the thermal needs for heating water and premises, as well as the production of electricity from its own sources.

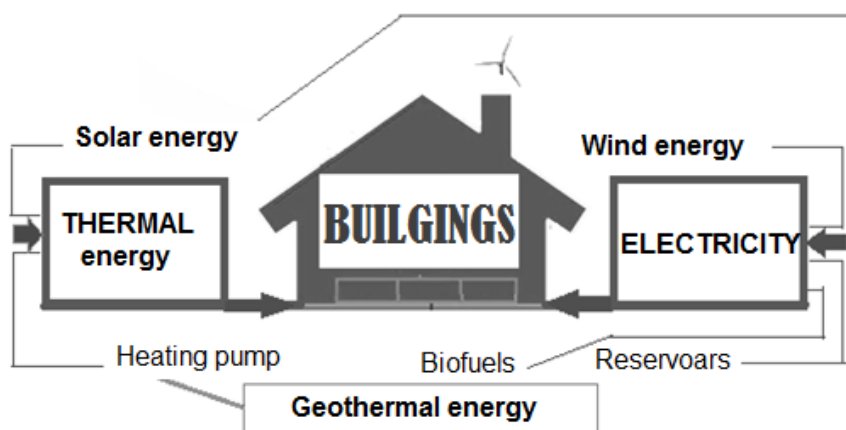


Figure 1. Integration of different forms of RES in buildings

1.1 Solar energy in buildings

Solar radiation is a completely pure form of energy that has no harmful consequences, because it is far enough away from the source and has a protective coating that is damaged by the use of fossil fuels in some layers. The application of solar energy is under great care because it is free of harmful gases; it is used in photovoltaic systems, for solar water heating and a hybrid photovoltaic solar system (Golić, Kosorić and Furundžić, 2011).

Most often, the sun's energy is used directly by means of solar panels, creating thermal energy for heating water or an object. Since solar energy is an inexhaustible source of supply, its renewability is unquestionable, but the problem occurs with day-night phases or seasonal oscillations of weather conditions. The possibility of using nanomaterials in the production of solar panels and solar cells due to toxic semiconductors that emit harmful gases is increasingly being investigated.

So much solar energy is transferred on Earth during two hours that it is enough for the year-round energy needs of all humanity. Hot water heaters can save 10-15% of energy consumption and a solar heating system can create 45% energy savings in buildings (China wind power and solar photovoltaic industry association).

Passive solar energy technology is applied in houses and for ventilation. A passive solar house requires the rationality of the interior and exterior so that the position of the building is chosen, materials that will enable the collection of heat rays in cold periods or in the mountains. These passive houses are usually built, cheap, adaptable to life but with larger temperature changes. Solar ventilation technology uses hot air pressure to increase the effect of solar radiation so that internal ventilation grows and refreshes, cools and removes gases (Shule Wei, 2018).

Solar water heating technology is an energy saving system by converting solar rays through a collector, storage device and pipe, whose air collector is placed on the roof.

1.2 Biomass in buildings

Although biomass is a renewable energy source, it can produce a lot of energy, heat but also produce harmful gases in the environment. By building high chimneys, it is possible to reduce suspended particles, but the central heating systems must be technologically improved by installing

filters and purifiers. In addition to the environment in which trees are planted, it can create a comfortable space near buildings, protecting them from the heat during the summer months. The installation of natural materials in buildings is a trend that the architectural profession returns and integrates into the space, by introducing partition walls in the rooms for easier fluctuation of air and heat, and it can also have a pleasant sound effect.

1.3 Wind energy and buildings

Primitive forms of wind use existed in China or Japan, so that windmills began to work in Europe only in the 12th century. Wind energy is quite expensive for individual needs, and the biggest drawback is insufficient efficiency and installation.

The use of wind energy is possible with the systematic monitoring of the atlas with the characteristics, wind speed, height at which it has a satisfactory strength, wind intensity and pressure. It is desirable that wind farms be located where the average wind speed is higher than 4.5 m / s. Wind power changes over time, and forecasting is acceptable in a longer time interval where there is a balance of electricity produced and consumed. The most common problem is that the regulations for planning and construction on facilities are not sufficiently developed, so independent installation of wind turbines is not recommended due to low power, only in combination with other sources, and in a windy place.

1.4 Hydropower and buildings

Large hydroelectric power plants are buildings that change the natural features, animal habitats, populated areas and reduce the navigability of rivers due to dams. Particularly interesting types of hydroelectric screens are small HPPs, which can destroy mountain rivers and fish stocks, tourist sites and the agrarian existence of households. In the case of buildings, hydropower can be interesting at the time of the influx of torrential rivers, floods in order to use mechanical energy to pump out excess water, generate electricity or reheat or dry buildings through heat pumps.

1.5 Geothermal energy in buildings

In the interior of the Earth, there is heat that is concentrated in the core, and which is heated by constant movement and cracking of the rocks. The energy generated through the various spheres of decomposition, transmission and transmission in the depths of our planet represents geothermal energy.

Hot water can be used directly to heat houses and greenhouses, and the island is a good example of that. Indirectly, geothermal water and steam can drive a generator motor to produce electricity, but the temperature must be above 100 degrees Celsius. Hydrogeothermal resources can currently be used up to a depth of 3 km, and in households they can be installed through heat pumps arranged horizontally and vertically. Horizontally immersed rods have a variable ratio to the outside temperature, while vertical ones are characteristic of narrower areas with a constant temperature due to the depth. For housing needs in individual and collective residential buildings, geothermal energy requires large initial costs of investment in installations with which comes a fixed cost in the form of a heat pump that heats the buildings with electricity (Dragović, 2015).

Surface water in the form of rivers, lakes and rainwater near buildings can drain into the depths and be a source of supply for heat pumps. This exchanges surface water temperatures with groundwater in the rocks, so the system is not expensive, but you should take care of problems with corrosion and freezing during the winter. Groundwater heat pumps have a direct and indirect system, and are characterized by significant savings.

1.6 Biofuels in facilities

Biofuels are in a fluid state and the most well-known form is bio-oil, ie biodiesel and pure vegetable oil, while there is also bioalcohol as ethanol fuel. Biodiesel fuel can be used with minor processing in diesel engines that are primarily designed to run on vegetable oil. Natural plant material, such as corn stalk or sugar beet, is specially grown to produce ethanol to supply internal combustion engines and all of this can be applied in rural areas where there are crops.

Biogas occurs by the decomposition of organic waste generated in a landfill or in a wastewater treatment plant. The entire production of this fuel is accumulated from residues after the production of sugar (cane, colaseed), paper and cardboard, animal residues (dung) and fecal waste.

In order for biofuels to be used in buildings as a heat source for heating water and rooms, filtration devices must be installed, and it is important not to install them in the basement of buildings because there is high humidity and accelerated corrosion of equipment, which means that biofuels are not an adequate choice for buildings in urban areas, and is ideal for RES for rural facilities.

2 Building - comparative analysis in the world and Serbia

Building could be defined as a space intended for a shorter or longer stay, where non-industrial services, cultural and sports events, education, etc. are performed. As an energy sector, it is composed of a large number of small consumers, who use about 40% of primary energy worldwide. Energy consumption in buildings in Serbia (public and private sector) in final energy consumption is 36%, which is more than industry and transport alone. Electricity consumption in buildings is about 60%

With the adoption of the National Strategy for Sustainable Development of the Republic of Serbia in 2008, with the Action Plan for Implementation, energy efficiency was identified as a priority measure to adopt the First National Plan for Energy Efficiency in 2010 and since then Serbia has been working intensively on implementing energy efficiency. 2010/31/ EU of the European Parliament and of the Council of 19 May 2010 on the energy performance of buildings (Manual for the energy certification of buildings, 2017).

According to the consumption sectors, most final energy was consumed in the household sector - 36%, followed by industry - 29%, then in the transport sector - 23%, while other sectors participated with 12%. Of the energy sources, final energy consumption is dominated by oil with 30% and electricity with 28%, followed by coal with 8%, natural gas with 12%, thermal energy with 9%, while renewable energy sources (firewood) participate with 13% (Ministry of Mining and Energy, 2015).

The greatest potential for energy savings is related to the improvement of thermal protection of buildings, in order to reduce heat losses. In the housing sector, most of the construction stock was built more than 30 years ago. The average consumption of thermal energy, which is around 170 kWh / m², compared to 70-130 kWh / m² in Western European countries (Šumarac et al., 2010).

At the EU level, about 2/3 of consumption in buildings is realized in residential buildings (Institute for European Environment Policy, 2015). In Serbia, about 45% of total energy consumption is realized in households and in the public and commercial sector (based on the Energy Balance of the Republic of Serbia, 2016).

There are over 2.2 million housing units in Serbia, with a total floor area of 290 million m². It is estimated that they consume 65 million MWh of heating energy annually, while the average consumption of heating energy is 224 kWh / m² per year, which is far higher than the EU average. The average consumption in residential buildings in the European Union is 138 kWh / m², Denmark 96 kWh / m², Poland 90-120 kWh / m². Average old houses consume 200 -300 kWh / m² of heating energy per year, standard insulated houses under 100, modern low-energy houses about 40, and passive 15 kWh / m² and less (Manual for energy certification of buildings, 2017).

The ways of heating buildings in Serbia are as follows: 26% of the total area is heated from district heating systems and local boiler rooms with central heating (14% from district systems and 12% from local boiler rooms), 14% from the electricity system, 10% from the natural gas system and 50% of the total area uses solid fuels in local furnaces (coal, firewood, agricultural biomass, waste, etc.).

3 Construction and adaptation of buildings

The construction and adaptation of residential buildings has the greatest potential for development, primarily when the recommendations of construction experts and the scientific preferences they bring through energy strategies are taken into account. Energy savings have been identified as the most important area because over two-thirds of the energy invested is lost through outdated installations, lack of insulation and energy inefficiency.

There are many plans for energy savings, which focus on thermal amenities in buildings, such as walls, floors, doors or windows (Marszal, Heiselberg, Bourrelle, Musall, Voss, Sartori, & Napolitano, 2011). Passive and active energy saving strategies achieved in heating, cooling and lighting come into consideration (Sadineni, Madala, & Boehm, 2011). One of the important decisions in building is the orientation of the building in relation to energy consumption, due to thermal amenities, ventilation and lighting. In the room simulation, the energy consumption of the north-south facades is close to the east-west by close to 10%, with a reduced annual consumption of 13% (Ashmawy&Azmy, 2018).

Sustainable green buildings have several advantages such as 26% lower energy consumption, 13% lower cumulative maintenance costs, 27% higher customer satisfaction and as much as 33% lower CO2 emissions (GSA Public Buildings Service, 2008).

A proposal for an architectural system and optimization algorithm called Green Charge can efficiently manage renewable energy and storage to reduce electricity bills (Sawant&Patil, 2017). This system supports a smart server that monitors electricity prices over the Internet, household consumption, the inclusion of renewable sources and the sensor status of battery charging. Special mention should be made of auxiliary software for modeling energy efficient buildings such as Design Builder, insight 360, TRNSYS, Skellion.

Serbia has adopted regulations, typology of residential buildings and trained experts to introduce the Central Register of Energy Passports (CREP), which is available online with data on energy certification of buildings, location and licensed contractors. All new facilities, which are currently being reconstructed or energy rehabilitated, must have an energy passport according to the law on construction, and energy efficiency has been introduced as a public interest where municipalities will be able to allocate funds for which housing communities will apply.

Most residential buildings in Serbia have inadequate thermal insulation (windows, doors) and excessive heating installations (boilers, heating stations). The recommendation for building owners is to put a good thermal insulation layer on the facade, to insulate the roof (with mineral stone wool), to replace damaged windows and put insulating strips on doors and windows, to remove double panes or to install thicker or triple glazing. The benefits of investing in energy efficiency are that electricity expenditures will be reduced, internal temperatures will rise and the value of the facility will increase.

3.1 Integration of renewable energy sources in buildings

The buildings are used for residential, service, production needs and combined purposes, so it is recommended that the construction of new facilities be in accordance with regulations, using technological solutions in construction, the use of materials that contribute to energy savings, moderate heating and easy maintenance. The essence is to find materials at the construction site that will not disturb the ambience, and which will contribute to light being available during the day in work spaces, not rooms, and for geothermal energy to be conducted to the place where it is necessary during cold periods.

It is very difficult to integrate all renewable energy sources in the same facility, and apart from the lack of funding for such a project, the problem may be the lack of wind, light, water, biomass, biofuels, while geothermal energy is not in question. A complete system would include quality installation in an individual power supply system (solar cells, wind generators, mini-hydropower plants) and a thermal profile (solar panels, biofuels and geothermal heat pumps).

Figure 2 shows a model that enables a combined supply of thermal and electricity from renewable sources for homes, businesses and public institutions (schools, health facilities, buildings of local and state authorities).

Most often, integration is carried out in business buildings, in facilities for health care and education, as an example that should be followed by others, but without the help of the state or local communities, that investment is impossible. Increasingly, this concept is said to integrate renewable energy and the IT sector into smart homes or facilities, making it the term smart cities, which are managed remotely over the Internet.

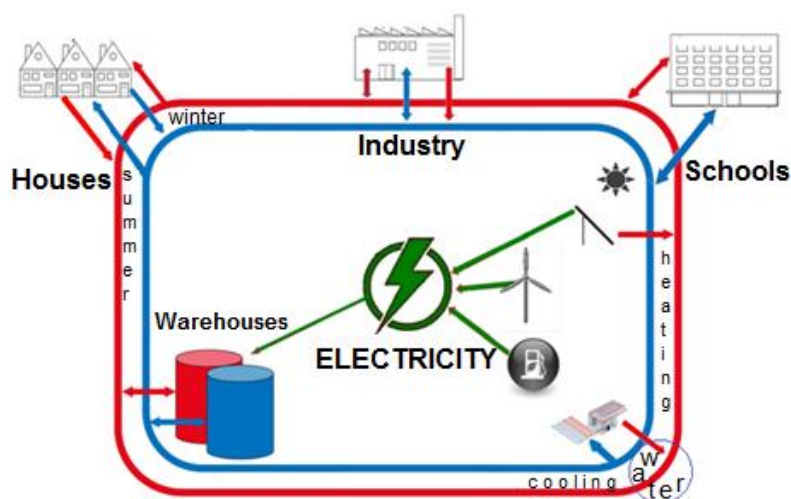


Figure 2. Combined model of thermal and electric power supply

4 Green construction and energy efficiency of buildings

Green construction supports the use of materials from the environment (stone, wood) with integration with the space so that it rests on rocks or land, which fits into the proctor.

Directive 2002/91 / EC of the European Parliament and of the Council on the energy performance of buildings, which aims to promote improvements in the energy performance of buildings within the community, lays down a set of requirements for the energy performance of buildings, including energy certification of buildings.

Table1. Energy efficiency classes of buildings (http://ec.europa.eu/environment/index_en.htm)

Classes	Heating Indicator [kWh/m ² year]	Energy efficiency level
A	0-30	BEST ENERGY EFFICIENCY
B	31-50	HIGH ENERGY EFFICIENCY
C	51-70	ENERGY EFFICIENT BUILDING
D	71-120	AVERAGE ENERGY EFFICIENT BUILDING
E	121-160	UNSATISFACTORY ENERGY EFFICIENCY
F	161-200	VERY ENERGY EFFICIENT BUILDING
G	201+	COMPLETELY ENERGY EFFICIENT BUILDING

Energy efficiency of buildings can be implemented in several ways individually or in combination, starting from the most available:

- Replacement of light bulbs in households, industry, public institutions,
- Switching from heating to electricity,
- Improving building insulation
- Window and door replacement,
- Electronic energy management,
- Application of construction standards,
- Change of heating consumption calculation (from lump sum to consumption).

Introduction of energy efficiency certification of the building (a prerequisite for a building permit, and old ones for a better price).

5 RES application model in buildings

The building must have several levels of savings and sustainability, such as:

- Sustainability of building materials (construction, interior, roof),
- Sustainable construction environment (adapted to the site, without landslides),
- Good ventilation and ventilation (windows, solar lighting and fan),
- Efficient heating and cooling (panels, cells, heat pumps, water),
- Savings (insulation, facade, solar roof-no tile).

The materials from which the building is built or renovated must meet quality standards, crack resistance and serve as noise insulation, retain heat and be waterproof. It is important to make a quality selection of insulation materials and install double insulation on the corners of the building, while the floor and ceiling insulation with mineral and stone wool is necessary. The airiness of the building is important because of the daylight in the rooms, but also because of the evening needs for light that is accepted from the solar panels that can be fixed on the roof. Windows and doors are sealed, which contributes to reducing heat loss, while increasing daylight and indirectly heating the space. Heating of the building is possible with solar collectors that heat water for hygiene, as well as through heat pumps that heat the building. Ventilation is done to let in fresh air, and warm air can circulate and heat up.

The model of integration of some of the RES in buildings can be called hybrid energy of buildings: solar-wind-electricity system; solar-wind-battery, solar-wind-biogas-hydrogenerator; solar-wind generator-rain and groundwater. In order for the process of integration of RES and the building to be successful, there must be an architectural design of the building, energy design, structural design, IT design and evaluation of the introduction of innovations.

Architectural scheme involves site selection and fitting design. When choosing a position, it is important to match the appearance of the building with the space that will be next to the energy source, dimensions and spatial features with software simulations when choosing solar collectors, wind turbines on the location or size of rooms and windows, tree positions and daylight, nesting or close to water tank. The fitting design requires integration with the building material, entrance or functionality of the building, such as the roof, wall or balcony, roof integration is a choice in which solar panels are placed aesthetically above the tile, as a mobile or fixed part, or instead of the tile itself, where good roof ventilation is important, integration with the wall is a large space in which there is the possibility of painting in a darker color for indirect heating or placing panels on the wall, integration with elements such as balcony, window is important if greenery is added or reflective glass is installed.

Energy design is an important part of new buildings and includes software, equipment selection, consumption determination, space estimation, heat source selection based on input data. Construction design is based on materials, size and needs to meet space and cost goals in order to integrate hallways, staircases or balconies with RES. Information design is a structure that includes the installation of programs for the operation of machines, RES that starts working at a given moment, saving energy and electricity. Assessing the introduction of innovations in a building is a process that includes repaying investments, saving on RES, reducing pollution, and assessing working and maintenance conditions.

6 Conclusions

The building sector is large, and the savings that can be achieved by using renewable energy sources are multiple, because they are free energy sources, economical and environmentally friendly. Energy efficiency enables individuals who have realized the benefits of responsible use of energy in the form of renewable sources (biomass, solar energy, wind energy, geothermal energy, etc.) to see savings in payment and rationally control costs because they decided to solve the long-term energy stability of their construction object.

Buildings that consume less energy have a sustainable pleasant temperature, programmed lighting and the ability to easily switch from one renewable energy source to another and all with the

concept of a smart building. If an efficiently insulated building consumes less energy in winter for heating and in summer for cooling, the stay is of better quality, and the long-term use value is higher.

7 Literatures

- [1] **Ashmawy R. E., Neveen Y. A.**, Buildings Orientation and its impact on the Energy Consumption, *The Academic Research Community Publication*,
- [2] *** DOI:10.21625/archive.v2i3.344, (2018), pp.35-49
- [3] **Dragović Nj.**, Opravanost upotrebe geotermalnih resursa u proizvodnim procesima i za zagrevanje objekata, 46. *Međunarodni kongres i izložba o KGH*, 2015, 263-269
- [4] **Golić K., V. Kosorić, AK. Furundžić**, General model of solar water heating system integration in residential building refurbishment—potential energy savings and environmental impact. *Renewable and Sustainable Energy Reviews*, 15 (2011), 3, pp. 1533–1544.
- [5] **Hashim H**, HoWS, Renewable energy policies and initiatives for a sustainable energy future in Malaysia. *Renewable and Sustainable Energy Reviews*, 15(2011), 9, pp.4780–4787.
- [6] **Marszal, A. J., Heiselberg, P., Bourrelle, J. S., Musall, E., Voss, K., Sartori, i., & Napolitano, A.** Zero Energy Building—A review of definitions and calculation methodologies. *Energy and buildings*, 43 (2011) 4, pp.971-979
- [7] **Sadineni, S. B., Madala, S., & Boehm, R. F.** Passive building energy savings: A review of building envelope components. *Renewable and Sustainable Energy Reviews*, 15 (2011) 8, pp.3617-3631.
- [8] **Sawant Ajinkya, S. B .Patil**, GreenCharge: Managing Renewable Energy in Smart Buildings, *international Journal of Engineering Research & Technology (iJERT)*, Vol. 6 issue 05, May – 2017, pp.152-160
- [9] **Shule Wei**, Renewable Energy Technologies Applied in Architecture and its innovative Research, *iOP Conf. Series: Earth and Environmental Science* (2018) 012007.
- [10] **Šumarac D., Todorović M., Đurović-Petrović M., Trišović N.** Energy Efficiency of Residential Buildings in Serbia, *Thermal Science*, Vol. 14, (2010). pp. S97-S113.
- [11] ***, GSA Public Buildings Service, *Assessing building performance: A post occupancy evaluation of 12 GSA buildings research*, 2008
- [12] ***, Ministarstvo rudarstva i energetike, M. Banjac, B. Ramić, D. Lilić, A. Pantić: *Energija u Srbiji*, Kosmosd.o.o. Beograd, 2015.
- [13] ***, Priručnik za energetska sertifikaciju zgrada – Vodič za investitore, izvođače I projektante, Maja Todorović, Aleksandar Rajčić, 2017
- [14] ***, *Plate solar water heater leading carbon revolution*, China wind power and solar photovoltaic industry association, <http://www.cwpva.org/html/taiyangnenjishu/2010/0416/147.html>.
- [15] ***, Institute for European Environment Policy, 2015
- [16] ***, <https://www.grenef.com/energetska-efikasnost-u-zgradama/>
- [17] ***, http://ec.europa.eu/environment/index_en.htm

EFIKASNA SINHRONIZACIJA DIZEL GENERATORA U USLOVIMA PROMENLJIVE FREKVENCije

IMPROVED SYNCHRONIZATION OF DIESEL GENERATORS IN VARIABLE FREQUENCY CONDITIONS USING PREDICTIVE METHOD

Zoran NIKOLIĆ^{1,1}, Dušan NIKOLIĆ²

¹ Institute of the technical sciences of the SASA, Beograd, Srbija

² Enernet Global, Australia

<https://doi.org/10.24094/mkoiee.020.8.1.95>

U radu je razmatrana sinhronizacija dizel generatora ostrvskog napajanja nominalne snage 2MW koji se često uključuju na mrežu. Efikasno korišćenje vetrogeneratora sa promenljivim generisanjem energije podrazumeva brzo i efikasno uključivanje i sinhronizaciju dizel agregata kako potrošači ne bi ostali bez napajanja. Razmatrana metoda prediktivne sinhronizacije ima znatnih prednosti nad konvencionalnih metoda sinhronizacije jer omogućuje sinhronizaciju generatora za najkraće vreme. Primena adaptivnih neuro-fuzi sistema je metoda koja daje najbolje rezultate.

Ključne reči: ostrvsko napajanje; sinhronizacija dizel generatora; prediktivna sinhronizacija; neuro-fuzi logika

The synchronization of diesel generators of island power supply with a nominal power of 2MW, which are often connected to the network is discusses in this paper. Fast and efficient switching on and synchronization of diesel generators so that consumers do not run out of power implies efficient use of wind turbines with variable energy generation. The considered method of predictive synchronization has significant advantages over conventional synchronization methods because it enables generator synchronization in the shortest time. The application of adaptive neuro-fusion systems is the method that gives the best results.

Key words: Island power supply; synchronization of diesel generators, predictive synchronization, neuro-fusion logic

1 Introduction

The main sources of electricity in isolated power systems (IPS) are traditionally diesel generators. Diesel generators are a proven technology. With IPS, the maintenance of these systems has higher costs, so they must be robust enough to reduce maintenance costs. Some IPSs introduce wind turbines to reduce the cost of electricity generation and greenhouse gas (GHG) emissions. The large share of wind turbines is caused by large variations in the frequency of the system, which results in a long-term synchronization process, especially when diesel generators are synchronized. Long synchronization can compromise network stability, especially with small IPSs.

Unlike conventional networks, IPSs not only deliver less power (usually MW, not GW), but are also much smaller in space. Consequently, consumption is less predictable. Being smaller on the surface means that the supply from the RE source is more variable - such as a higher percentage of RE generators that are likely to be affected by the same weather events (e.g. wind calm or cloud formation).

In smaller IPS, the problem of variation is much smaller because mainly rechargeable batteries are used to stabilize the frequency [01] and satisfactory results are obtained.

¹ Corresponding author, email: zoran.nikolic@itn.sanu.ac.rs

2 Standard generator synchronization

An example of a load curve for IPS with wind turbines is shown in Figure 1. The high variability of the load makes the operation of the diesel engine heavier and less efficient and requires more generator start-up during the day. As a result, the synchronization equipment installed for diesel generators works more often and in more difficult operating conditions.

The synchronization process enables the connection of the generator to the power system, so that the generator is set to correspond to the frequency and phase of the power network. When these two signals are close enough to each other, it is allowed to close the generator switch and after that the generator is electrically connected to the power supply system.

Classic analog synchronizers use signals for system voltage and generator phases. Based on the generator status signal and the power supply phase phase system, standard synchronization generator This signal is processed using an internal PI synchronizer (proportional-integral) controller. After processing, the signal is sent to the diesel engine controller. Diesel engines have a delay in responding to changes in steering, which is usually around 250 ms. When the generator starts to respond to the speed correction signal, it slowly changes to a new value [02]. When the synchronizer sees that the diesel generator and mains frequencies and phases are within the allowable limits, it commands the switch (CB) to react. The automatic synchronizer provides automatic connection of the unit to the network at the time of equalization of voltage, frequency and phase voltage of the generator and the network, ie reducing their difference to defined limits, where there are no excessive electromechanical stresses that could lead to damage or disconnection.

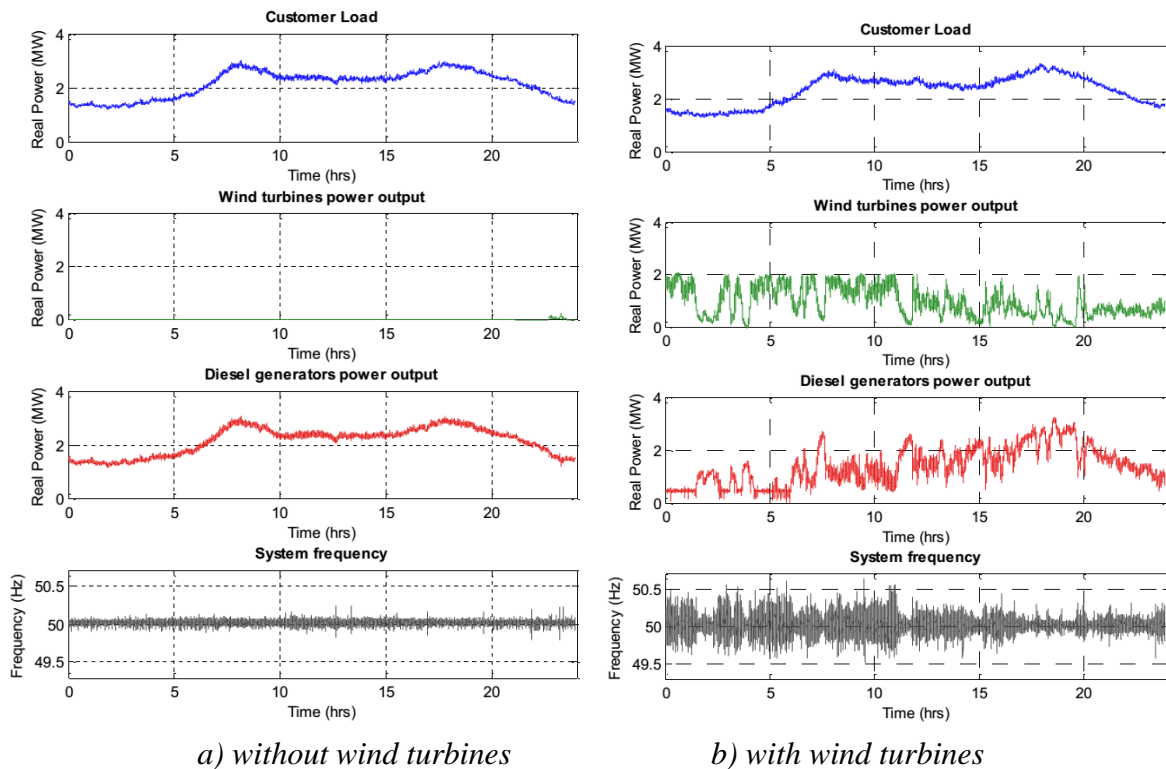


Figure 1. Network frequency in IPS, as a consequence of load during the day and generation of electricity from wind turbines and diesel generators

Classic synchronizers use PID control loops and differ only in the way the state is calculated. [03]. A normal synchronization process takes less than 8 seconds, and extended synchronization can take more than 30 seconds.

3 Predictive synchronization method

Although a large share of wind has clear advantages because it uses cost reduction and emissions on the one hand, and on the other hand prolongs the process of synchronization of diesel

generators and endangers the energy stability of the system. To maintain high wind usage while avoiding generator synchronization problems, a predictive synchronizer model has been developed to reduce synchronization time [04].

The basic idea of this predictive synchronizer is to predict the frequency and phase of the system two seconds into the future and then set the generator to meet that prediction. If the prediction is accurate accurate (e.g. $\pm 10^\circ$ phase), hunting between the synchronizing diesel and the system will be avoided.

The predictive synchronizer, whose functional diagram is shown in Figure 2, differs from the classic synchronizers in two ways:

a) It compares predicted, instead of current, frequency and phase signals to the power system frequency and phase. This is presented in Figure 3 as an additional functionality of the signal conditioning module.

b) It does not use a PID loop, but sends a step change into the governor speed reference signal. This is presented in the Figure 3 as a Step Command Module. Engine time delay is the same as diesel engine delay presented in figure 3. Operation of the predictive synchronizer can be described as a five-step process (Figure 3):

1. At the start of the synchronization process, the system frequency (f_{SYS}), the synchronizing generator frequency (f_{GEN}) and their phases (ϕ_{SYS} and ϕ_{GEN} , respectively) are measured from voltage signals V_{SYS} and V_{GEN} at a specific time interval and recorded. (Figure 3(a) shows this for system frequency only.) The differences between the system and generator frequencies ($\Delta f = f_{SYS} - f_{GEN}$) and the system and generator phases ($\Delta \phi = \phi_{SYS} - \phi_{GEN}$) are calculated.
2. Based on the recorded time-series of the system frequency, $f_{SYS}(t-n), \dots, f_{SYS}(t-2), f_{SYS}(t-1), f_{SYS}(t)$ and the system phase, $\phi_{SYS}(t-n), \dots, \phi_{SYS}(t-2), \phi_{SYS}(t-1), \phi_{SYS}(t)$, a predictive module calculates the (very near) future values for the system frequency, $f_{SYS}(t+n)$ and its phase $\phi_{SYS}(t+n)$, as presented in Figure 3(b). This figure practically shows system frequency brought a few seconds ahead in time based on the prediction.
3. Using frequency and phase difference ($\Delta f, \Delta \phi$) plus the predicted values for system frequency and phase ($f_{SYS}(t+n)$, and $\phi_{SYS}(t+n)$), the speed reference signals for the synchronizing generator governor are calculated based on the equal area criterion [05] and issued to the governor. Because both frequency and phase need to be within allowed limits, the synchronizer will issue two speed step commands to the synchronizing generator governor. The first step shifts the generator phase to the desired value, while the second step puts the generator in the predicted position for synchronization. The two steps are communicated as a step-up signal issued at t , and a stepdown signal at t , (Figure 3(c)).
4. After a short delay (engine delay), the generator responds to given speed correction commands from the synchronizer (Figure 3(d)).
5. If the frequency and phase predictions are within allowable limits, this adjustment of the speed will result in matching generator frequency and phase to the system. Synchronization has been achieved, so the Check Synch module issues CB close signal at (Figure 3(e)) to bring the generator online.

Correct prediction of the system frequency and phase on a very short-term time scale is a vital part of the proposed approach to synchronization in IPSs. In this chapter, very short-term prediction is defined as look-ahead period of 2 seconds. However, there is no reliable system for very short-term time-series prediction.

Both the frequency and phase represent a time series which can be defined as a set of observations of a parameter, or set of parameters, taken at a number of time intervals. These intervals are usually (although not always) of a regular length. Real-world time series are diverse. Some time series data changes slowly and relatively smoothly, for example monthly electricity demand. Other time series can exhibit chaotic behaviour, making their prediction very challenging. A frequency time series of an IPS with high wind penetration, such as in Figure 3, possesses these characteristics.

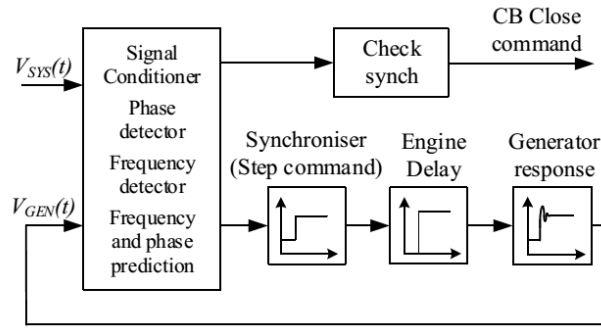


Figure 2. Functional diagram of the predictive synchronizer control loop.

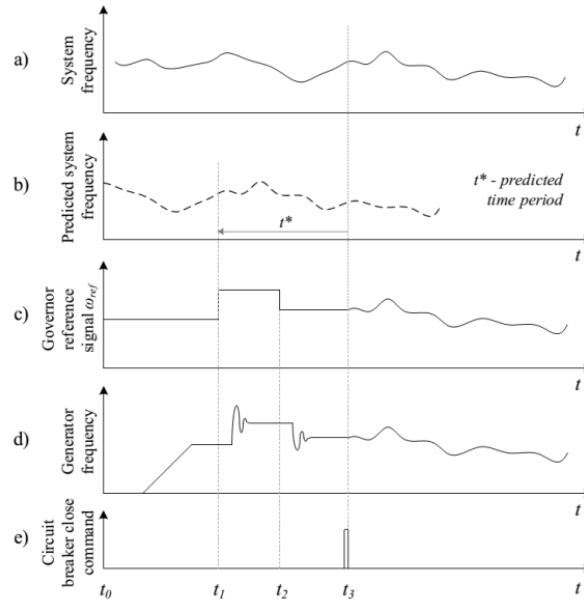


Figure 3. Operation of the predictive synchronizer.

The time scale is important when trying to create a prediction system. Two main classes of techniques have been used for very short-term predictions. These are statistical methods and methods based upon artificial neural networks (ANN). The statistical methods are autoregressive. This means they use the difference between the predicted and actual values in the immediate past to tune the model parameters. The neural networks use past data taken over a longer time-frame to learn the relationship between the input data and output wind speeds. The accuracy of these methods degrades rapidly with increasing prediction lead time.

Prediction research is a growth area and increasingly often this research involves the use of artificial intelligence. In next text, a hybrid approach was investigated – a combination of an ANN and fuzzy logic for very short-term system frequency and phase prediction.

4 Application of neuro-fusion logic

The application of fuzzy (i.e. fuzzy logic based) and adaptive neuro-fuzzy (i.e. neural networks incorporating fuzzy logic) interference system (ANFIS) techniques for application in power systems with wind turbines and diesel generators has been proposed by several authors [06-08].

Two ANFIS systems have been developed for system frequency and phase prediction, one for frequency prediction and the other for phase prediction. ANFIS model proposed by Roger Young [09] is a modern neural network. ANFIS uses a hybrid algorithm that combines least squares estimation and gradient drop methods. First, the initial activation functions are assigned to each membership neuron. The functional centers of the neurons connected to the input are set so that the domain is divided equally, and the widths and slopes are set to allow sufficient overlap of the corresponding functions. In the ANFIS training algorithm, each training epoch is composed of back and forth passes.

In the anterior transition, a set of input pattern training (input vector) is presented to ANFIS, the neuron outputs are calculated at The layer-by-layer and parameters that follow from the rules are identified. A detailed description of ANFIS is given in [10].

It should be mentioned that the regulator helps maintain the stability of the power system during faults and transient processes. This is achieved by using subfrequency load rejection (UFLS), where some loads are switched off, so that most of the system loads are saved. Because dynamic processes occur very quickly during faults (within a few seconds), the diesel generator synchronization process cannot be used.

5 Results of application of the predictive synchronization method

Finally, a synchronizer using ANFIS as a prediction technique is simulated. The result shows an average time of 18 s, which is an improvement over both the conventional synchronizer and the simulated synchronizer with the basic prediction technique.

It is important to note that the simulation results show that the predictive synchronizer has achieved statistically better performance compared to the classical synchronizer. However, the presented result does not mean that the predictive synchronizer will work better in every possible scenario.

It is also interesting to compare the accuracy of the prediction between the moving average and the ANFIS prediction technique. error prediction frequency than ANFIS.

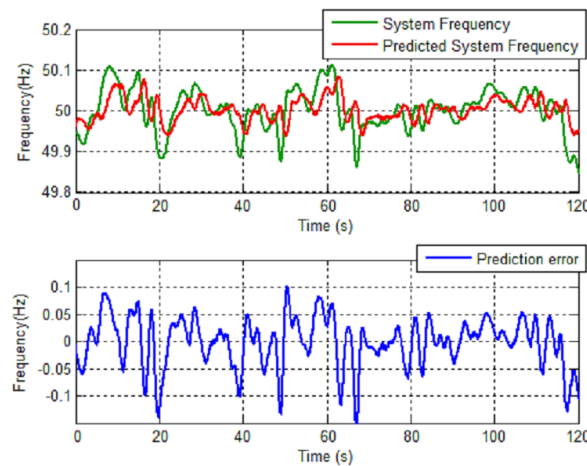


Figure 4. Moving average prediction results. Mean frequency prediction error was $\sim 0.043\text{Hz}$.

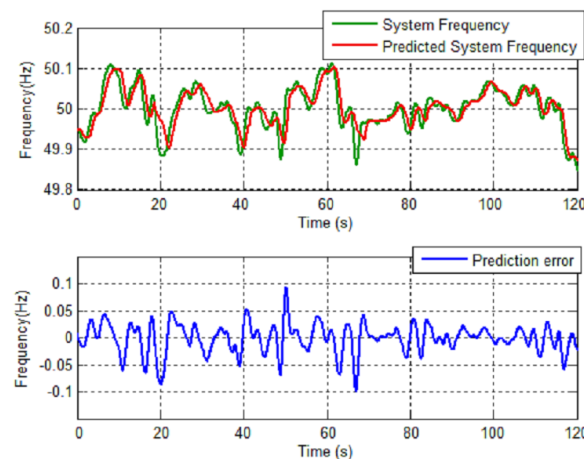


Figure 5 ANFIS prediction results and prediction error example.
Mean frequency prediction error was $\sim 0.019\text{Hz}$

Although only examples of frequency prediction are shown in Figure 4 and Figure 5, phase prediction shows similar results.

6 Conclusion

This chapter identifies some synchronization challenges in IPSs with strong wind penetrations. As a solution to the problem of extended synchronization, the concept of the proposed synchronization of diesel generators in these IPSs in future synchronizers for diesel generators operating in IPSs with high RE penetration is proposed. The model of the predictive synchronizer was developed and tested on the recorded data of the actual wind power supply system.

Two main conclusions can be drawn from Figure 4 and Figure 5:

a) ANFIS prediction technique is more suitable for use in predictive synchronization of processes due to higher prediction accuracy.

b) ANFIS technique is accurate enough to be used in the IPS diesel generator synchronization process, because it reduces the synchronization time and thus increases the stability of the system

Finally, further ANFIS neural network adjustments, better processing power, and future prediction techniques could predict even better results in the next prediction of synchronization devices.

The simulation results showed that the predictive synchronizer provides statistically better performance results compared to the classical synchronizer. This results in a significantly reduced synchronization time (on average) of diesel engines during periods of strong wind penetration.

7 References

- [1] **Nikolić Z., Shiljkut V. M., Nikolić D.**, Diesel-solar electricity supply for remote monasteries, *J. Renewable Sustainable Energy* 5, 041815 (2013); <http://dx.doi.org/10.1063/1.4813068>
- [2] **Woodward.** (2012). SPM synchronisers product. Available: www.woodward.com/synchronizers.aspx
- [3] **ABB.** (2012). Synchrotact Synchroniser product. Available: <http://www.abb.com>
- [4] **Nikolic D.**, Enabling Technologies for Increasing Renewable Energy Penetration in Isolated Power Systems, Phd theses, University of Tasmania, Hobart, Australia, 2019.
- [5] **Best R. J., Morrow D. J., Mc Gowan D. J., and P. A. Crossley**, "Synchronous Islanded Operation of a Diesel Generator," *Power Systems, IEEE Transactions on*, vol. 22, pp. 2170-2176, 2007.
- [6] **Chedid R., Karaki S., Chemali C.**, "Adaptive fuzzy control for wind-diesel weak power systems," in *Power Engineering Society Winter Meeting, 2000. IEEE, 2000*, p. 1426 vol.2.
- [7] **Bevrani H., Daneshmand P. R.**, "Fuzzy Logic-Based Load-Frequency Control Concerning High Penetration of Wind Turbines," *Systems Journal, IEEE*, vol. 6, pp. 173-180, 2012.
- [8] **Marzband M., Sumper A., Gomis-Bellmunt O., Pezzini P., Chindris M.**, "Frequency control of isolated wind and diesel hybrid MicroGrid power system by using fuzzy logic controllers and PID controllers," in *Electrical Power Quality and Utilisation (EPQU), 2011 11th International Conference on*, 2011, pp. 1-6.
- [9] **Jang S. R.**, "ANFIS: adaptive-network-based fuzzy inference system," *IEEE Transactions on Systems, Man, and Cybernetics*, vol. 23, pp. 665-685, 1993.
- [10] **Negnevitsky M.**, *Artificial Intelligence: A Guide to Intelligent Systems*. Harlow, England: Addison Wesley, 2011.

KORIŠĆENJE OBNOVLJIVIH IZVORA – PRETVARANJE GEOTERMALNE ENERGIJE U ELEKTRIČNU

UTILIZING RENEWABLE RESOURCES – CONVERTING GEOTHERMAL ENERGY TO ELECTRICITY

Miljan VLAHOVIĆ¹, Milica VLAHOVIĆ^{1,2}, Zoran STEVIĆ³,

¹ Public Company Nuclear Facilities of Serbia, Belgrade, Serbia

² University of Belgrade, Institute of Chemistry, Technology and Metallurgy, Belgrade, Serbia,

³ University of Belgrade, Faculty of Electrical Engineering, Technical Faculty Bor,
CIK Belgrade, Serbia

<https://doi.org/10.24094/mkoiee.020.8.1.101>

Prema zvaničnoj definiciji, koju je odobrilo Evropski savet za geotermalnu energiju (European Geothermal Energy Council- EGEC), geotermalna energija je energija akumulirana kao toplota ispod površine čvrstog tla. Geotermalna energija je toplotna energija koja se generiše i skladišti u Zemlji. Generalno se definiše kao deo geotermalne toplote koji se može direktno koristiti kao toplota ili pretvoriti u druge oblike energije. Geotermalni resursi se razlikuju u zavisnosti od lokacije i dubine u odnosu na jezgro Zemlje. Njihova primena moguća je za različite svrhe u zavisnosti od njihove temperature. Ovaj rad prikazuje upotrebu geotermalnih resursa za proizvodnju električne energije. Postoje tri osnovna principa rada geotermalnih elektrana: suva para (dry steam), separisanje pare (flash steam) i binarni (binary cycle). Postrojenja na suhu paru izbacuju vruću paru iz unutrašnjosti Zemlje u turbine, a ona napaja generator koji daje električnu energiju. Postrojenja sa separisanjem pare pumpaju toplu vodu iz unutrašnjosti Zemlje u hladniji rezervoar. Nastala para pokreće generator električne energije. Postrojenja sa binarnim ciklusom pumpaju toplu vodu iz unutrašnjosti Zemlje kroz izmjenjivač toplote čime se greje drugi fluid i pretvara u paru koja pokreće generator. U svim pomenutim sistemima korišćeni fluidi se recikliraju. Može se zaključiti da geotermalne elektrane rade slično kao i druge elektrane, ali paru za pokretanje turbine obezbeđuju iz unutrašnjosti Zemlje. Činjenica da se korišćeni fluidi vraćaju u zemlju čini geotermalne izvore energije obnovljivim.

Ključne reči: geotermalna energija; električna energija; geotermalna elektrana; obnovljivi izvori

Abstract. According to the official definition, approved by the European Geothermal Energy Council (EGEC), geothermal energy is energy accumulated as heat below the surface of solid soil. Geothermal energy is thermal energy generated and stored in the Earth. It is generally defined as the part of geothermal heat that can be directly utilized as heat or converted into other types of energy. Geothermal resources vary by location and depth towards the Earth's core. Their use is possible for different purposes depending on their temperature. This paper presents the harnessing geothermal resources for electricity generation. There are three main types of geothermal power plants: dry steam plants, flash steam plants, and binary cycle plants. Dry steam plants pipe hot steam from underground into turbines, which powers the generator to provide electricity. Flash steam plants pump hot water from underground into a cooler flash tank. The formed steam powers the electricity generator. Binary cycle plants pump hot water from underground through a heat exchanger that heats a second liquid to transform it into steam, which powers the generator. In all mentioned systems the used fluids are recycled. It can be concluded that geothermal power plants work similarly to other power plants, but providing the steam for starting the turbine from the earth's interior. The fact that used fluids return to the ground makes geothermal energy resources renewable.

Key words: geothermal energy; electricity; geothermal power plant; renewable resources

¹ Corresponding author, email: mvlahovic@tmf.bg.ac.rs

1 What is geothermal energy

Geothermal energy is the natural heat of the Earth, accumulated in fluids and rock mass, which is estimated to be 5500 °C or even up to 7000 °C in the core. This heat is derived from the original formation of the planet (by exothermic chemical reactions in the Earth's crust such as oxidation of sulfides, by crystallization and hardening of molten rocks, as well as by friction during the movement of tectonic masses) and from the decay of the radioactive elements in the Earth's crust. It is transferred to the subsurface by conduction and convection. The rate of temperature increases with depth, which is called geothermal gradient [1].

In nature, geothermal energy most often appears in the form of geysers, volcanoes and hot springs.

People learnt to use different temperatures and apply them for various purposes. For centuries, geothermal springs have been used for bathing, heating and cooking.

Since ancient times geothermal resources have played a significant role in human societies. Probably the most ancient one is the use of the geothermal hot springs. Nothing can compare to thermal bathing and geothermal waters have been long known for their healing properties. The use of thermal waters dates straight back to 3000 BC when the Indus Valley civilizations used natural hot and mineral springs.

Geothermal waters are highly beneficial, especially for improving health and well-being, treat arthritis, skin diseases, and high blood pressure. Thermal waters contain a lot of minerals. Nowadays, a lot of wellness centers offer a variety of geothermal by-products such as soaps, shampoos, bath powders and facial cremes with thermal water.

In the early 20th century people started to consider the heat from inside the Earth as a practical source of energy with huge potential. Geothermal energy is now used to produce electricity, to heat and cool buildings as well as for other industrial purposes like grain and lumber drying, pulp and paper processing, fruit and vegetable cultivation, soil warming and many others.

Geothermal energy history is presented in Figure 1.

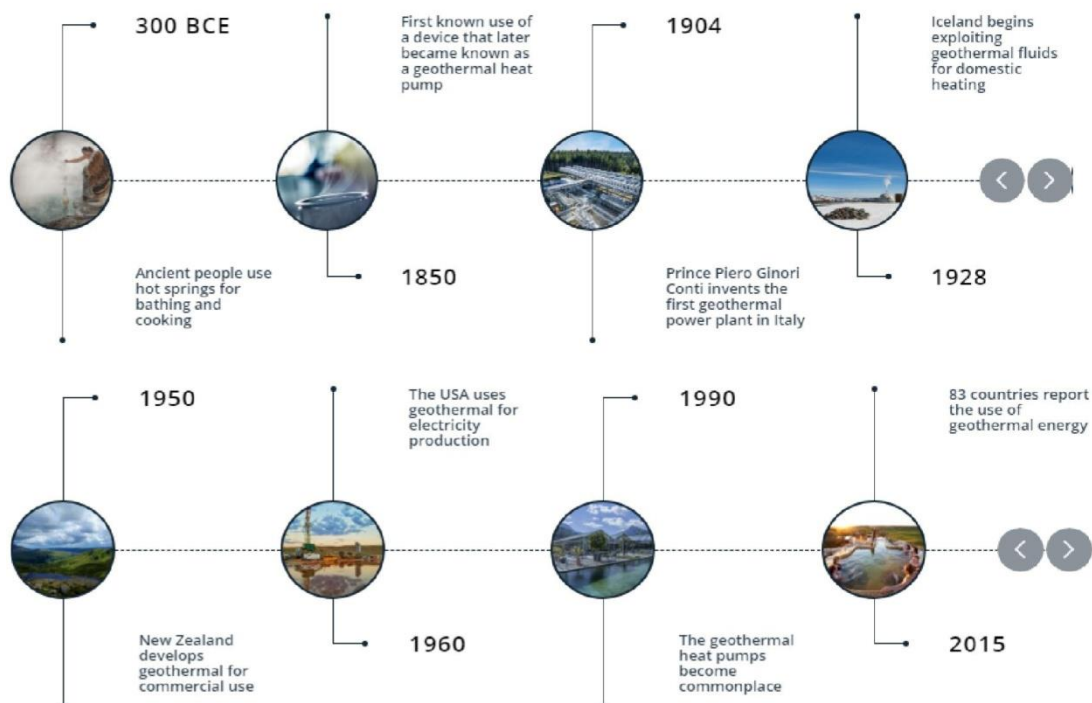


Figure 1. Geothermal energy history [2].

Geothermal energy has become established as a reliable and environmentally friendly source of power. High availability and load factors with no dependence on outer sources make geothermal energy one of the key resources in a sustainable energy future. Only a small fraction of the world's

geothermal potential has been developed so far, which leaves possibility for growth and development in both electricity and direct use sectors [1].

2 How much geothermal energy is available

Only several kilometres under the Earth's surface temperatures can exceed 250 °C and it increases by 1 °C for every 30-50 metres of depth, pointing to the conclusion that the Earth's geothermal potentials are immense. The estimated stored thermal energy down to 3 km within the continental crust is roughly 43×10^6 EJ, and that's why geothermal energy is treated as a renewable energy source, and is as such suitable for use in various sectors in an environmentally-friendly manner (World Energy Council, 2016). The main advantage of geothermal energy is its easy use with relatively simple and low-cost technology. However, when it comes to geothermal rock energy, today's technology is limited to a drilling depth of up to 10 km, and therefore exploitation to these depths is possible. Modern technological solutions enable simple and cost-effective use of low-temperature energy sources and, in that context, the European Union redefined the term of geothermal energy as "energy stored in the form of heat beneath the surface of solid earth" under the Directive on renewable energy sources [3].

Hydrogeothermal resources are technically much more usable and cost-effective, although there are fewer of them. If the possibility of using this energy to a depth of 3 km is considered, its global reserves are 2,000 times larger than coal reserves.

In order to assess whether a certain area meets the conditions for the exploitation of geothermal energy, it is necessary to determine the proximity and temperature of the hot mass in relation to the earth's surface. Hot water and steam can be delivered to the surface and used regardless of whether their reservoirs are located in shallow surface layers or at a depth of several kilometers, and the choice of exploitation technology as well as application of the obtained energy primarily depends on the deposit temperature. However, it is most practical to use this energy in areas where the hot mass is close to the earth's surface [4].

Geothermal potential is the amount of energy that can be utilized from a geothermal energy. The potential of geothermal energy in the world is huge, 50000 times greater than the energy that can be obtained from oil and gas.

The geothermal energy of the Earth can be estimated at 12.6×10^{24} MJ, and of the crust at 5.4×10^{21} MJ, which is almost 35 billion times more than today's energy needs, but only a small part of this potential can be used efficiently (only to a depth of 5000 m) [5].

2.1 Geothermal potential of Serbia

Geothermal resources in the Republic of Serbia are divided as follows:

- Classification of geothermal energy according to location in the Earth's crust where it is accumulated and exploited:
 - Hydro-geothermal energy (accumulated in water),
 - Petro-geothermal energy (accumulated in solid rock mass),
 - Aero-geothermal energy (accumulated in gases), and
 - Magma-geothermal energy (accumulated in magma).
- Classification of hydro-geothermal resources according to fluid temperature:
 - Low enthalpy resources – fluid temperature < 100 °C,
 - Medium enthalpy resources – fluid temperature 100-200 °C, and
 - High enthalpy resources – fluid temperature > 200 °C.

All geothermal phenomena identified in Serbia so far are low enthalpy geothermal resources, with fluid temperature below 100 °C.

Geothermal resources of the Republic of Serbia are quantified according to the following sub-groups:

- Subgeothermal resources of temperature of up to 30°C (sub-hydro-geothermal and sub-petro-geothermal resources),
- Geothermal resources in the strict sense, of temperature between 30°C and 100°C,
- Geothermal resources of temperature over 100°C (hydro-geothermal resources and hot dry rock energy - HDR) [6].

According to available data, Serbia has 360 springs of thermal and thermo-mineral waters with a temperature of 14 to 98 °C. With the amount of geothermal heat- heat that erupts on the Earth's surface, calculated per m² per second, which averages 100 MW/m², Serbia exerts with significant hydrogeological and geothermal resources compared to the average values in Europe of 60 MW/m². However, although experts state that the total amount of heat of geothermal resources in Serbia is about twice greater than the heat that would be generated from domestic coal reserves, this potential has not been exploited at all. Water from geothermal springs or wells is mainly used for therapeutic purposes in numerous thermal spas and sports and recreation centers, although in an irrational and inefficient way. On the contrary, in Iceland and El Salvador, more than 25 % of total electricity is produced in geothermal plants, and many other countries are increasingly taking advantage of this energy source (USA, Italy, Germany, France, New Zealand, Mexico, Nicaragua, Costa Rica, Russia, Philippines, Indonesia, China, Japan) [7].

Figure 2 presents hot water flowing artesian well in Jošanička Banja spa.



Figure 2. Hot water flowing artesian well in Jošanička Banja spa of temperature of 78 °C [6].

3 Utilizing geothermal resources

There is a natural source of power found below the surface of the earth that has been around for centuries. Underground, far below, there are pools of water, geothermal reservoirs, heated by magma (or molten rocks). Water or steam can escape from cracks in the earth in the form of geysers or (or sometimes as magma from a volcano). Harnessing the power of the earth's temperatures to power, heat or cool homes and businesses is the essence of geothermal power.

Geothermal power does not require the burning of any fossil fuels. The hot water or steam used is returned to the ground after it is used where it can be used again, which makes it a renewable energy source as well [8].

The use of geothermal resources is possible for various purposes.

Modern conversion technologies enable the use of geothermal resources in electricity generation, district heating in cities, at industrial plants, for the heating of buildings, sports and recreation facilities and spa resorts, in family homes and in agriculture.

High-temperature geothermal sources (>150 °C) are suitable for electricity generation. Medium and low temperatures of resources (<150 °C) are suitable for various applications (in balneotherapy, agriculture, industry, tourism etc), while resources with temperatures below 20 °C are used with heat pumps (Figure 3) [6].

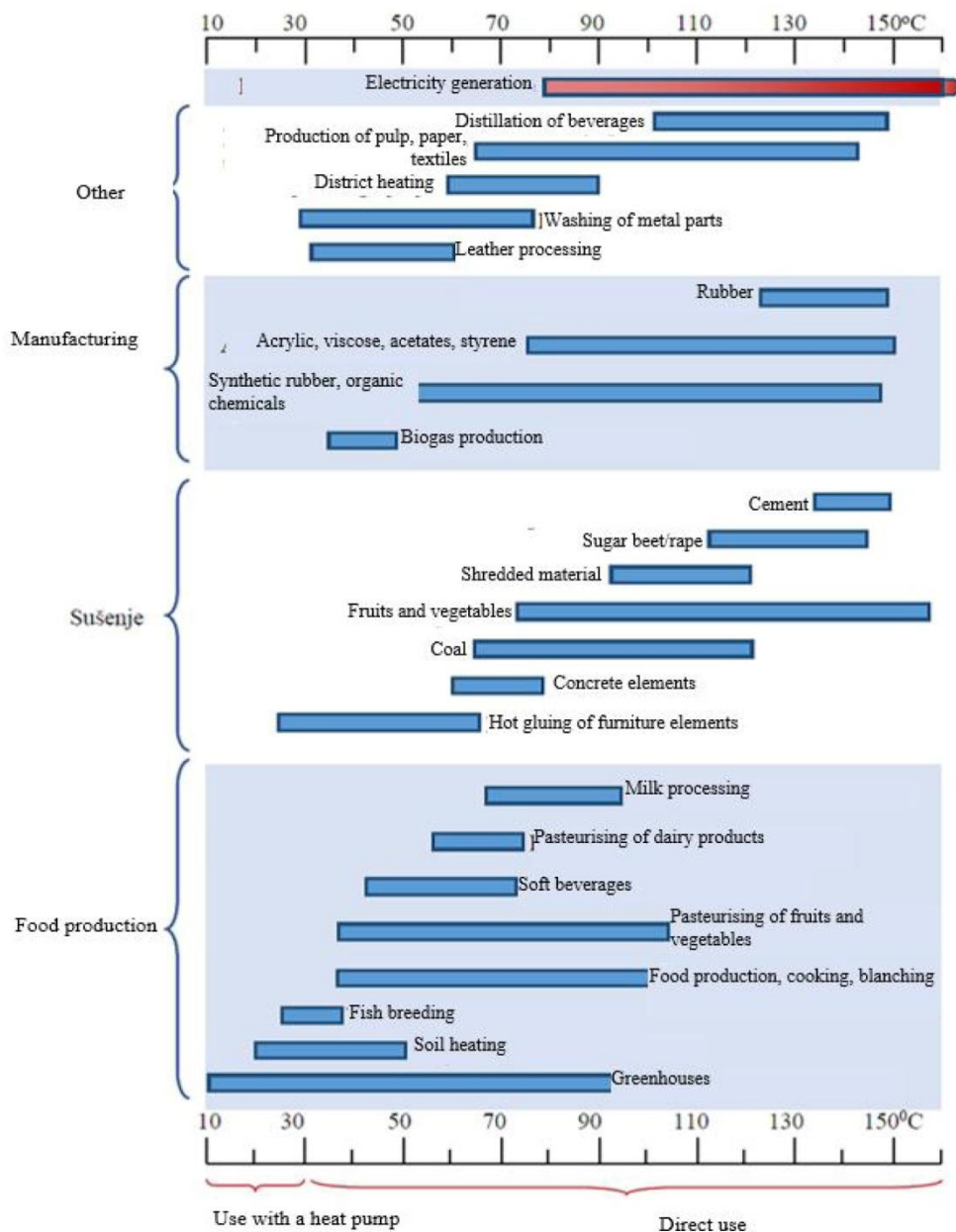


Figure 3. Use of geothermal resources [6].

There are also numerous classifications of these resources in relation to usability. One of the basic classifications divides geothermal resources according to the possibility of utilization depending on the temperature into two groups [9]:

- Geothermal resources for electricity generation;
- Geothermal resources for thermal energy production.

The most important way of using geothermal energy is the production of electricity whereby hot water and steam from the Earth are used to power the generator, which means that there is no burning of fossil fuels and subsequently no emission of harmful gases into the atmosphere, only water vapor is released. Also, an advantage is that such power plants can be implemented in a variety of natural environments.

4 Geothermal resources for electricity generation- geothermal power plants

By the end of the 19th Century, Prince Piero Conti conceived an idea to harness the natural steam of the Larderello geothermal field in Italy to produce electric energy; he started technical experiments in 1903, and a year later, the first geothermal-electric energy that lighted five 5-watts-lamps was produced.

In 1913, Conti put in commercial operation a power plant of 250 kW fed by pure steam, and in 1916 two power units of 3.5 MW each. This is how geothermal power production was born [2].

There are currently geothermal plants in over 80 countries according to the Geothermal Energy Association and although the United States is currently the global leader of geothermal power, other countries like Indonesia, Turkey and Kenya are all in the process of expanding their power capacities as well. The first geothermal plant in the United States was built in 1960 at an area called The Geysers, in the Mayacamas Mountains north of San Francisco. Today, California is the world's largest geothermal field with 22 geothermal power plants, known as The Geysers Complex.

Geothermal power plants function in a similar way as any other power plant, with the difference that the steam needed to start the steam turbine is obtained from the earth's interior. Existing power plant technologies enable generation of electricity either directly from high temperature steam, from steam-water mixtures, or from geothermal water with intermediate temperature. After passing through the turbines, the steam goes to the condenser, turns into a liquid state, and returns to the underground or is further cascaded.

There are different ways to get electricity from geothermal resources. The method that will be chosen in the construction of the geothermal power plant in the certain region depends on the characteristics of the geothermal energy source- temperature, depth and quality of water and steam. In all cases, the condensed steam is returned to the well, which increases the abundance of the geothermal source.

Three main types of geothermal energy plants that generate power in slightly different ways are as follows:

- Geothermal power plants with dry steam,
- Geothermal power plants with flash steam, and
- Geothermal power plants with binary cycle.

Geothermal power plants with dry steam

This is the simplest and oldest system, and at the same time the cheapest, applied for the first time in Lardarello, Italy. Fluids above 220 °C are used. Dry steam geothermal power plants are the most common types of geothermal power plants, accounting for about half of the installed geothermal plants. This direct method works by piping hot steam from underground reservoirs into turbines from geothermal reservoirs, which powers the generators to provide electricity. After powering the turbines, the steam condenses into water and is piped back into the earth via the injection well.

Schematic presentation of a dry steam geothermal power plant is given in Figure 4 and photograph of one of 22 dry steam geothermal power plants in the Geysers (Northern California) is shown in Figure 5.

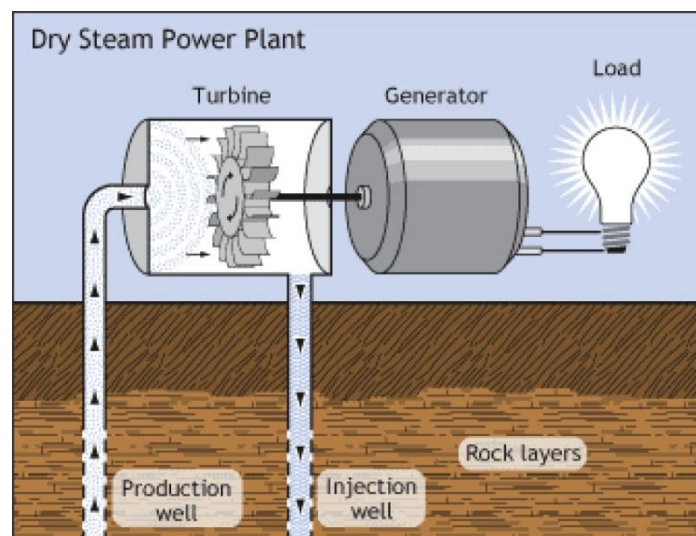


Figure 4. Dry steam geothermal power plant [10].



Figure 5. Dry steam geothermal power plant, The Geysers, California, USA [11]

Geothermal power plants with flash steam

This indirect method is characterized by the double use of water and steam. Fluids above 180 °C are used. Flash steam geothermal power plants differ from dry steam because they pump hot water, rather than steam, directly to the surface. These flash steam plants pump hot water at a high pressure from below the earth into a "flash tank" on the surface. The flash tank is at a much lower temperature, causing the fluid to quickly "flash" into steam. The steam produced powers the turbines. The steam is cooled and condenses into water, where it is pumped back into the ground through the injection well. Most modern geothermal power plants work on this principle.

Schematic presentation of a flash steam geothermal power plant is given in Figure 6 and photograph of one flash steam geothermal power plant in Iceland is shown in Figure 7.

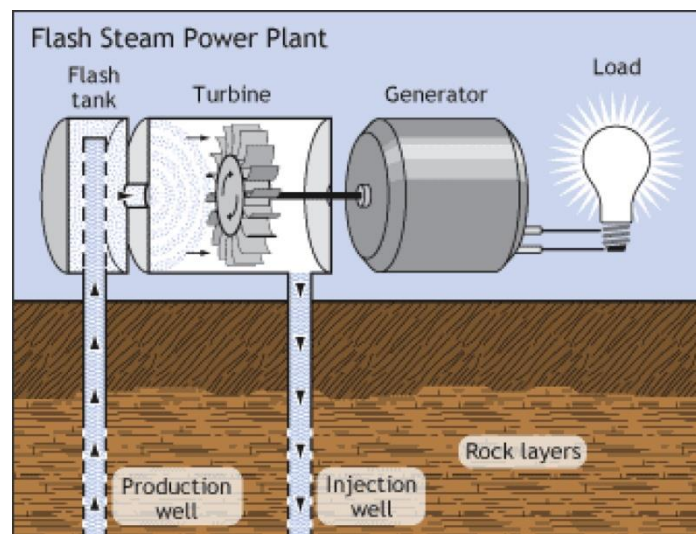


Figure 6. Flash steam geothermal power plant [10].

Fluid temperatures for such mixed method range from 100 °C and above. In these binary cycle geothermal power plants, the main difference is that the water or steam from below the earth never comes in direct contact with the turbines. Instead, water from geothermal reservoirs is pumped through a heat exchanger where it heats a second liquid- like isobutene, freon, ammonia, alcohols (with a lower boiling point than water). This second liquid is heated into steam, which powers the turbines that drives a generator. The hot water from the earth is recycled into the earth through the injection well, and the second liquid is recycled through the turbine and back into the heat exchanger where it can be used again. The advantage of this principle is higher efficiency and greater availability of the required geothermal reservoirs. Also, an advantage is the complete closure of the system since the used water is returned back to the reservoir, so heat loss is reduced, and there is almost no water loss. Most of the planned new geothermal power plants will use this principle.



Figure 7. Flash steam geothermal power plant in Iceland [11].

Geothermal power plants with binary cycle (ORC Rankin cycle)

Schematic presentation of a binary cycle geothermal power plant is given in Figure 8 and photograph of one binary cycle geothermal power plant in Nevada, USA is shown in Figure 9.

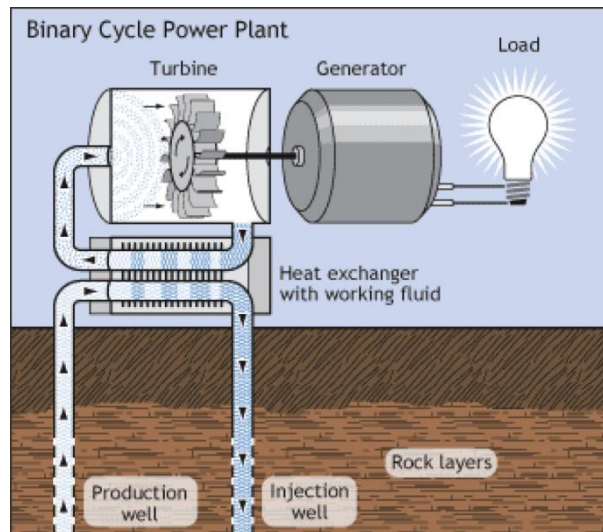


Figure 8. Binary cycle geothermal power plant [10].



Figure 9. Binary cycle geothermal power plant in Nevada, USA [11]

In addition, there are combined or hybrid plants that comprise two or more of the above basic plant types to improve versatility, increase overall thermal efficiency, and improve load-following capability. Cogeneration plants, or Combined Heat and Power plants (CHP), produce both electricity

and hot water for district heating at significantly higher efficiency than can be achieved by just generating electricity or supplying heat [1].

5 Advantages and disadvantages of geothermal power plants

Advantages are as follows:

- **Renewable, sustainable and permanent source**

Geothermal energy is end-less, it will always exist and geothermal power will work. It can provide a constant supply of energy unlike other renewable energy sources.

- **Ecologically clean**

Geothermal power plants use a renewable heat source with a constant supply unlike coal-fired power plants and emit only 5% of greenhouse in the contrary with coal-fired power plants.

- **Low operating costs, more electricity with stable prices**

Geothermal power stations require minimal maintenance compared to conventional power plants, thus being reliable and cheap in operation. They have the great capacity that can meet the growing energy demand and offer stable electricity price because it does not depend on varying fuel costs.

- **Small area**

They occupy less space than their fossil fuels equivalents.

- **Low noise work**

Geothermal energy is produced with a little noise; the main is by the fans in the cooling systems which can easily be reduced.

- **Energy security**

Using local geothermal resources, supplying from other countries reduces, thus lowering dependence on external influences and helping in increasing energy security.

Disadvantages are as follows:

- **Geographical limits and seismic instability**

Geothermal activity is the highest along the tectonic fault lines in the earth's crust where the geothermal energy has the greatest potential. Therefore, only few countries can use geothermal resources: the USA, Iceland, Kenya, Indonesia, the Philippines, Mexico. Geothermal structures can cause seismic activity which is usually insignificant.

- **Expensive construction**

Although they have low operating costs, the construction costs of geothermal power plants are high. Much expenses concerns the exploration and drilling of geothermal energy resources as well as special heating and cooling systems and other equipment resistant to high temperatures.

- **Ecological problem**

High consumption of fresh water can be a loss for the environment, which can lead to its deficit. Liquids extracted from the earth during drilling contain toxic chemicals (including arsenic and mercury), as well as greenhouse gases (such as hydrogen sulfide, carbon dioxide, methane, ammonia and radon) that have to be properly treated.

- **Possible exhaustion**

Without careful management, geothermal sources can be exhausted thus making the geothermal power plant unnecessary until the tank restoration. The only inexhaustible option is to get geothermal energy directly from the magma, but this is still in the developing stage [11].

6 Conclusion

Geothermal energy has a rather serious potential and will play an important role in the future. In Europe, geothermal heat is used for different needs, but most of all for electricity generation, heating, and cooling of buildings.

With the estimated total amount of geothermal energy that could be used significantly higher than the total amount of energy sources based on oil, coal, and natural gas, more importance should certainly be given to geothermal energy, especially having in mind that it is cheap, a renewable energy

source and also environmentally friendly. Since geothermal energy is not easily available everywhere, accessible places, such as edges of tectonic plates, should definitively be used and thus the pressure on fossil fuels would be at least slightly reduced, which would help the Earth to recover from harmful gases.

Serbia's current energy strategy does not treat geothermal energy as a significant resource several times larger than the total coal reserves in Serbia, which is present in every place at all times.

The whole of Europe is striving to reduce energy dependence and is trying to increase its energy production; the only possibility for that is to significantly increase the share of renewable energy sources in the overall energy balance. Serbia is in a similar energy dependence on imports and that is why it is very important to urgently start increasing the use of geothermal energy.

7 Acknowledgments

This work was financially supported by the Ministry of Education, Science and Technological Development of the Republic of Serbia (Grant Nos. 451-03-68/2020-14/200026)

8 References

- [1] *** Geothermal Quick guide, International Geothermal Association Inc., 2018.
- [2] *** <https://www.geothermal-energy.org/explore/what-is-geothermal/>
- [3] *** Directive 2009/28/EC of the European Parliament and of the Council of 23 April 2009 on the promotion of the use of energy from renewable sources and amending and subsequently repealing Directives 2001/77/EC and 2003/30/EC (European Council. 5 June 2009. Retrieved 19 September 2016).
- [4] *** <https://www.energetskiportal.rs/obnovljivi-izvori-energije/geotermalna-energija/>
- [5] *** <https://www.gradjevinarstvo.rs/tekstovi/1828/820/geotermalna-energija-osnovni-pojmovi>
- [6] *** <http://zelenaenergija.pks.rs/ZelenaEnergija.aspx?id=140&p=4&>
- [7] *** Energy Sector Development Strategy of the Republic of Serbia for the Period by 2025 with Projections by 2030 (Official Gazette of RS No. 101/15)
- [8] *** <https://www.saveonenergy.com/how-geothermal-energy-works/>
- [9] **Milenić, D., Vranješ, A.**, Istraživanje i valorizacija subgeotermalnih energetske resursa, University of Belgrade, Faculty of Mining and Geology, Belgrade, Serbia, 2015.
- [10] **Mohr, M.**, Geothermal power in the Long Valley Caldera and Beyond, Student research, Indiana University Geological Sciences G188, Collings Living-Learning Center L130, 2014.
- [11] *** <https://avenston.com/en/articles/geothermal-pp-pros-cons/>

OBNOVLJIVI IZVORI ENERGIJE, POTENCIJALI I PRIMENA U SVETSKIM OKVIRIMA I U SRBIJI

RENEWABLE ENERGY SOURCES, POTENTIALS AND APPLICATIONS WORLDWIDE AND IN SERBIA

Miomir MIKIĆ¹, Sanja PETROVIC, Zorica SOVRLIĆ, Daniela UROŠEVIĆ
MMI Bor, Serbia

Oko 80% globalne potrošnje energije (struje i toplote) proizvode se sagorevanjem fosilnih goriva. Ovakav vid goriva je ograničen u svojoj količini, a nakon obavljenih alarmantnih podaka o posledicama emisije gasova sa efektom staklene bašte, koji nastaju upravo sagorevanjem fosilnih goriva, sve više država se opredeljuje za obnovljive izvore energije. Obnovljivi izvori energije se nalaze u prirodi i obnavljaju u celini ili delimično. Upotreba obnovljivih izvora energije se nameće kao vrlo prihvatljiva mogućnost u osiguranju energije za budućnost i za zaustavljanje dalje degradacije životne sredine.

Ključne reči: obnovljivi izvori energije; energija; životna sredina.

Approximately 80% of global energy use (electricity and heat) is produced by burning fossil fuels. The need for the use of renewable energy sources has surfaced over the past several decades since alarming data has been released on the effects of greenhouse gases emitted by combustion of fossil fuels, which are limited in nature. Renewable energy sources are in nature and are renewed in whole or in part. The use of renewable energy sources is imposed as a very acceptable option in providing energy for the future and for stopping further environmental degradation.

Key words: renewable energy sources; energy; environmental.

1 Introduction

The most acute problem in terms of energy resources is the pace and how they are exploited and used. It is estimated by experts that the maintenance of current trends will lead to an increase by 2050 in terms of resource extraction up to five times higher than at present [1].

Based on the concept of sustainable development of human society, the current consumptions must be analyzed and predictions must be made on the trends in use of traditional energetic resources [1].

In addition to finite deposits of fossil and mineral fuels such as oil, gas, coal and uranium, the earth also offers various natural, auto-regenerative - or renewable - sources of energy that derive from sun insolation, geothermal activity and gravitational forces.

Theoretically, the global supply of energy from such renewable sources by far exceeds the earth's present total energy demand. The supply of energy is subject in part to pronounced technical and economic utility limitations, e.g., the disparity between the temporal/spatial demand for energy and the actually available supply of renewable energies, and the latter's modest power density compared to conventional energy vehicles.

The main renewable energy (RE) sources are:

1. Insolation, i.e., the direct radiant energy of the sun (made useful by collectors, solar cells, etc.)
2. Energy obtained from biomass; biochemical energy of photosynthetic products; made useful by:
 - burning (of wood, straw, etc.)
 - gasification (of wood, etc.)
 - anaerobic digestion (= biogas)

¹ Corresponding author, email: miomir.mikic@itmbor.co.rs

- alcoholic fermentation
- 3. The kinetic energy of wind
- 4. The kinetic energy of moving water:
 - low-pressure systems
 - high-pressure systems
 - micro-hydropower plants
 - tides, waves, ocean currents
- 5. Miscellaneous
 - geothermal energy
 - thermal energy deriving from differences in seawater temperature
 - osmotic energy deriving from concentration gradients between saltwater and freshwater.

Energy is closely linked to economic development and the quality of the environment. It is central to the world economy, providing the strength needed for industrial production, transportation and (increasingly) agriculture. Energy makes a major contribution to health, well-being and productivity, enabling the existence of services that include heating, lighting and cooling. The energy chain that provides these services begins by collecting or extracting a primary energy source - for example, coal - that can be transformed into another form of energy, such as electricity, transported or transferred to the point of use and eventually used to power some equipment as which is a heater, lamp or motor. Figure 1 shows an energy chain, which uses coal, as an energy source, as an example.

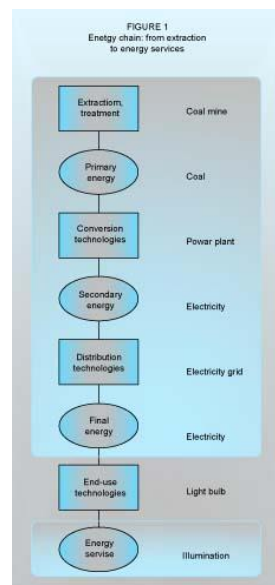


Figure 1. Energy chain: from exploitation to energy services

2 Energy production and distribution in world frames

Primary energy sources include fossil fuels (coal, oil, natural gas) and renewable sources such as biomass (wood, other plant sources, fertilizer), hydropower, solar energy, wind energy, tidal energy and geothermal energy. A small but significant part of the world's electricity is also provided by nuclear energy. The ways in which these primary sources are extracted, transformed, delivered and used have a huge impact on the environment locally and globally. They also have both positive and negative effects on human health. Figure 2 shows global primary energy sources and totals. Between 1973 and 1997, the total amount of primary energy used in energy production increased by almost 60%. Nuclear power plants, which were almost non-existent in 1973, provided more than 6% of the world's energy by 1997. Much of the primary energy is used to produce electricity, especially in the developed world.

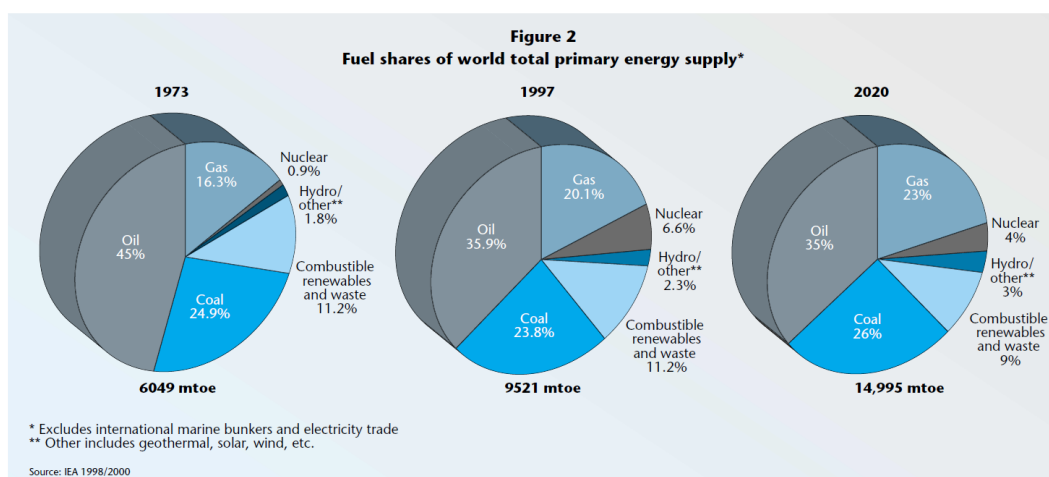


Figure 2. Share of fuel in total world primary energy consumption (source: IEA 1998/2000)

* Other energy sources are: geothermal, solar, wind, etc.

The share of fossil fuels, renewables and nuclear energy in electricity generation is shown in Table 1. Estimates of future energy use are based on “as usual” scenarios, in which current trends continue [2]. There are huge differences in the primary energy resources of different countries and regions (Figure 3), as well as the way these resources are used (Figure 4) - for example, whether they are converted into secondary energy or consumed directly in the household [3]. Although less primary energy is used as a whole for transport than for energy production, transport is the most important oil-consuming sector [4].

Tabela 1. World electricity generation (source: IEA 1998/2000)

					Share of total, %*	
	1971	1995	2010	2020	1995	2020
Electricity generation (TWh)	5248	13204	20852	27326		
Solid fuels	2131	5077	7690	10490	38	38
Oil	1100	1315	1663	1941	10	7
Gas	691	1932	5063	8243	14	30
Nuclear	111	2332	2568	2317	18	8
Hydroenergy	1209	2498	3445	4096	19	15
Other renewables	5	49	154	239	0,4	0,9

In Africa traditional biomass energy sources provide roughly 37% of total energy used, with commercial sources providing the remainder [5]. However, there are huge variations among the different parts of Africa: biomass sources account for some 84% of all energy use in East Africa and the islands of the Indian Ocean, but only about 3% of that in North Africa [5].

In Europe and Central Asia there has been a transformation of the energy industries since the 1960s, when coal was the primary source of energy for electricity generation, industry and domestic heating in most parts of these regions [5]. In Western Europe oil, natural gas and nuclear power are now the primary sources for energy production, while Central and Eastern Europe and Central Asian countries have reduced their coal use and moved increasingly towards oil, natural gas, and hydro and nuclear power for electricity generation [5].

Two of Asia’s giant economies, China and India, rely heavily on coal and will continue to do so in the next few decades due to its abundance and easy availability [5]. West Asia (Iran, Iraq, Syria and the Arabian Peninsula) relies on its abundant oil and gas reserves for virtually all of its energy needs [5].

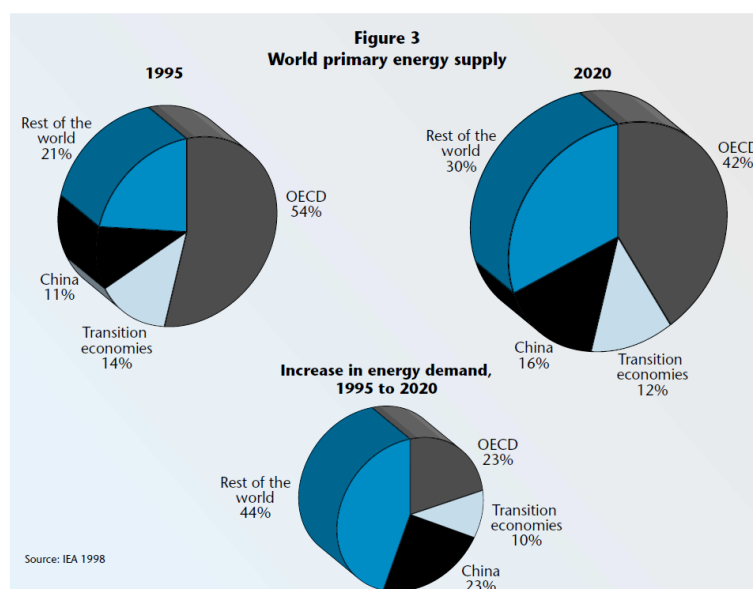


Figure 3. World primary energy supply

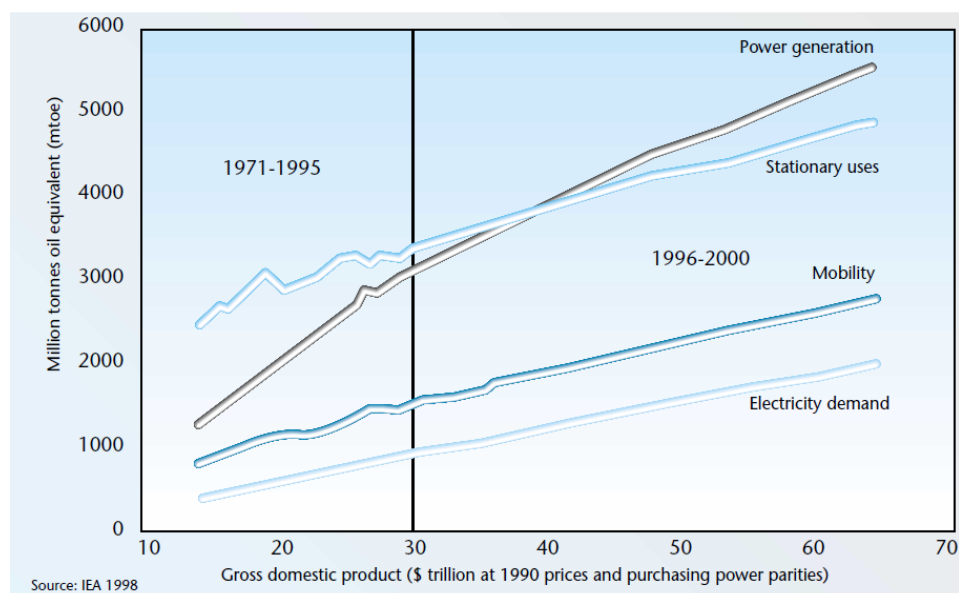


Figure 4. World energy-related services, 1971-2020.

Primary energy sources in Latin America and the Caribbean countries vary widely. Mexico and Venezuela, which have important oil and gas resources, use them for much of their energy; in Central America over 50% and, in Brazil, some 70% of electricity is generated by hydro power [5]. Drought in recent years has made hydro power supplies uncertain in some areas. And there is a trend in Argentina, Brazil and Colombia, for example, to move from renewable energy to fossil fuels in both the electric power and transportation sectors following deregulation of the energy sector [5].

North America has enormous coal, oil, natural gas and hydro resources. Coal is used to produce some 40% of its electricity. It's well developed transportation sector, and the high rate of vehicle ownership, make North America a major oil consumer as well. The United States is the world's largest oil importer, but also the second largest oil producer after Saudi Arabia [5].

3 Renewable energy sources in Serbia and its potentials

Serbia is a middle-income country with a great potential for fast economic development, as the country is endowed with natural and mineral resources and fertile and arable agricultural land. Serbia's GDP fell dramatically in the 1990s. However, since 2000 the GDP has increased steadily and in 2006 it was nearly 30% higher than in 2000. Strong economic progress has been achieved since 2001, particularly in expanding private sector participation in the economy. Macroeconomic stability,

achieved swiftly in the first years of transition, has been broadly maintained although economy is currently hit by global downturn. Serbia has a total dependence of 40%, and compared to the energy dependence of other EU27+ countries [6] the country's energy dependence is considered average.

Serbia has extensive unused potential for greater energy efficiency and RES production. Serbia's renewable energy potential can cover almost half of its primary energy needs. Moreover, projections suggest that with minor adjustments in the regulatory system, RES could easily rise to one-third of Serbia's overall primary energy consumption, which now relies on fossil fuels for 93% of its supply [7].

The wind energy potential is about 1,9 Mtoe a year (2,3 TW h/year). This potential is based on the long-term data of the existent hydro-meteorological stations that carry out measuring on 10 m altitude and on the new data where measuring was carried out on 100 m altitude [8,9].

According to the available data, use of photovoltaic solar energy is currently almost negligible. Solar energy is used for water and space heating in the domestic and tourist sectors, but there are no figures on the extent of this use. The country's solar energy exploitation potential is approximately 0.64 Mtoe a year. In Serbia the solar energy potential is vast, as the number of solar irradiation hours is much higher than in some other European countries reaching approximately 2000 h/year [10].

The unused hydropower potential (0.9 Mtoe) in Serbia is situated mainly in the catchments of Drina and Morava rivers and it can be utilized for large as well as for small HPPs. According to the electricity utility company Elektroprivreda Srbije, this potential may be used in 52 large HPPs that would have average capacity of around 25 MW [11]. Around 0,4 Mtoe a year are found in small streams, where the smaller hydro-electric power stations could be built. This estimation is based on the land register of small hydro-electric power stations where there are 856 locations suitable for building small power stations of 90 kW to 8,5 MW, of the total power of 450 MW and 1590 GW by which around 90% of locations have the technical potential under 1 MW [12].

Table 2. Total technically available potential of renewable energy sources

<i>RES</i>	<i>Available technical potential used (Mtoe/year)</i>	<i>Unused available technical potential (Mtoe/year)</i>	<i>Total available technical potential (Mtoe/year)</i>
BIOMASS	1,054	2,394	3,448
Agriculture biomass	0,033	1,637	1,67
Agriculture remains	0,033	0,99	1,023
Residues in fruit growing, viticulture and pre-fruit production		0,605	0,605
Liquid manure		0,042	0,042
Wood (forest) biomass	1,021	0,509	1,53
Energy crops			NA
Biodegradable waste	0	0,248	0,248
Biodegradable municipal waste	0	0,205	0,205
Biodegradable waste (except municipal)	0	0,043	0,043
HYDROENERGY	0,909	0,77	1,679
For installed capacities up to 10 MW	0,004	0,151	0,155
For installed capacities up to 10 MW up to 30 MW	0,02	0,102	0,122
For installed capacities over 30 MW	0,885	0,517	1,402
WIND ENERGY	≈0	0,103	0,103
SOLAR ENERGY	≈0	0,24	0,24
For the production of electricity	≈0	0,046	0,046
For the production of thermal energy	≈0	0,194	0,194
GEOTHERMAL ENERGY	≈0	0,1	0,18
For the production of electricity	≈0	≈0	≈0
For the production of thermal energy	0,005	0,175	0,18
TOTAL OF ALL RES	1,968	3,682	5,65

With 55% of its territory being arable land, and 25% under forests, Serbia has high biomass potential. This potential lays around 2,7 Mtoe annually, (63% share in the total RES potential), where

1.1 Mtoe represents the wood biomass potential (woodcutting and wood mass refuse produced in its primary and/ or industrial processing) and more than 1,6 Mtoe constitute agricultural biomass (agricultural and farming cultivation residues, including also liquid manure) [10]. Production of pellets is also considered as very promising, having a potential of 250–350 kt/year from sawmill waste [11].

The total technically available potential of renewable energy sources in the Republic of Serbia is estimated at 5,65 million tons per year. Of this potential, 1,054 million tons of biomass (mostly as firewood) and 909 thousand tons of hydropower are already used [13].

3.1 Share of renewable energy sources in Serbia

In Serbia, most of the energy comes from coal, which is used the most in addition to oil and natural gas. Coal is the dominant raw material in electricity generation. In Serbia, only hydro potential and biomass have been used to a greater extent from renewable sources. In the production and consumption of energy from renewable sources, large hydropower plants are also calculated according to EU regulations, but those in the field of environmental protection are not considered ecological plants due to the harmful effects of dam construction on the environment. In this context, without large hydropower plants, the share of electricity from renewable sources is very small.

Regarding the current situation in Serbia, it must be emphasized the lack of quantitative indicators in the planned areas of application of renewable energy sources, as well as the need for much more pronounced efforts to promote their use [14]. The share of energy from renewable sources in Serbia is about 6% (including large hydropower plants) and is projected to remain stable in the coming period. The Energy Development Strategy until 2015 envisages that the share of new renewable sources (excluding large hydropower plants) in total primary energy consumption should increase from 1.07 to 1.21% in 2015, (Table 3) [15].

Table 3. Share of energy from renewable sources in total primary energy consumption, according to the Energy Development Strategy, scenario of dynamic economic development. [15].

	2006	2009	2012	2015
Total primary consumption energy	615	647	715	753
Share of energy from renewal. Sources (without large hydropower plants)	0,8	1,1	1,05	1,1

The share of energy obtained in Serbia from renewable sources is small. Currently in Serbia, only about 1% of energy is obtained from alternative sources, which is negligibly small, if we take into account the natural potentials and requirements of the Kyoto Protocol.

4 Conclusion

Serbia has significant energy potential in renewable energy sources, but it has not been sufficiently used. The use of energy from renewable sources is still in its infancy in the world, except in some developed countries, and the biggest challenge is the transition to cleaner technologies while achieving economic profitability.

In addition to environmental, the use of renewable energy sources has economic significance - it can contribute to reducing the import of fossil fuels, the development of local industry and job creation, but also enable savings for households.

Thank-you note

To the Ministry of Education, Science and Technological Development of the Republic of Serbia and call for a contract: Agreement on the implementation and financing of scientific research work of NIO in 2020, Record number: 451-03-68 / 2020-14 / 200052.

5 References

- [1] **Florin Faur, Maria Lazăr, Dunca Emilia, Daniela Ionela Ciolea**, Critical analysis of the trends in use of classical energetic resources, 15th International Multidisciplinary Scientific

GeoConference SGEM 2015, www.sgem.org, SGEM2015 Conference Proceedings, ISBN 978-619-7105-33-9 / ISSN 1314-2704, Volume: 3, At: Albena, Bulgaria, 2015.

- [2] *** International Energy Agency (IEA) (1998), World Energy Outlook, pp. 63-4.
- [3] *** UNEP (1999) Global Environmental Outlook 2000 (GEO-2000); IEA 1998.
- [4] *** US Department of Energy (US DOE) (2000), International Energy Outlook 2000, p. 1.
- [5] *** Industry and environment, ISSN 0378-9993 Industry and Environment Volume 23 No.3, July – September 2000, A publication of the United Nations Environment Program Division of Technology, Industry and Economics
- [6] *** Eurostat, Energy dependence, % of net imports in gross inland consumption, 2009, <http://epp.eurostat.ec.europa.eu/tgm/table.do?tab=table&init=1&language=en&pcode=tgigs360&plugin=1S>.
- [7] *** Jefferson Institute, Serbia's capacity for Renewables and Energy Efficiency, Project Promoting European Energy Security, ISBN978-86-86975-05-8, Jefferson Institute, Policy Association For an Open Society (PASOS), Serbia, 2009.
- [8] *** Statistical Office of the Republic of Serbia, Economic Trends in the Republic of Serbia, 2010, Number 364, Statistical Office of the Republic of Serbia, Belgrade, 2010.
- [9] **Golusin M, Tesic Z, Ostojic A.** The analysis of the renewable energy production sector in Serbia. Renewable of Sustainable Energy Reviews 2010;14: 1477–83.
- [10] **Michaleva E, Angeon V.** Local challenges in the promotion of renewable energy sources: the case of Crete. Energy Policy, 2009; 37: 2018–26.
- [11] *** Larive Serbia, Croatia, Serbia and Bosnia –Herzegovina – Renewable energy. Dutch Ministry of Economic Affairs, EVD – The Agency of International Business and Cooperation
- [12] **Zenic Zeljkovic J,** Serbian experience in regulating the infrastructure services, UNCTAD—United Nations Conference on Trade and Development, Geneva, 2010.
- [13] *** Kjoto Protokol uz Okvirnu konvenciju Ujedinjenih nacija o promeni klime (1997)
- [14] **Kolaković S.,** „Hidro-energetski potencijal hidrosistema Dunav-Tisa-Dunav“, Fakultet tehničkih nauka, Trg Dositeja Obradovića 6, Novi Sad, Srbija
- [15] *** Ministarstvo rudarstva i energetike Republike Srbije (2015), Strategija razvoja energetike Republike Srbije do 2025.godine sa projekcijama do 2030.godine.

OCENA ŽIVOTNOG CIKLUSA BIOENERGETSKIH SISTEMA

LIFE CYCLE ASSESSMENT OF BIOENERGY SYSTEMS

Slobodan CVETKOVIĆ^{*1}, Mirjana KIJEVČANIN²

¹ Ministarstvo zaštite životne sredine Republike Srbije, Beograd, Srbija

² Univerzitet u Beogradu, Tehnološko-Metalurški fakultet, Beograd, Srbija

Svi energetske sistemi utiču na životnu sredinu. Bioenergetski sistemi se smatraju ključnim rešenjem u povećanju budućih potreba za energijom i ublažavanju emisija gasova sa efektom staklene bašte. Jedna od metoda za procenu uticaja bioenergetskih sistema na životnu sredinu je analiza životnog ciklusa (LCA). Cilj ovog istraživanja je da predstavi sveobuhvatne informacije o LCA za bioenergetske sisteme. Ova studija može da pruži bolje razumevanje globalnih žarišta u specifičnim istraživanjima vezanim za LCA za bioenergiju, ali takođe može da pruži korisne informacije za širenje istraživačkog područja bioenergije u Republici Srbiji.

Ključne reči: Bioenergetski sistemi, energija, LCA analiza

All energy systems have an impact to the environment. Bioenergy systems are considered as a crucial solution in the increasing future energy demand and mitigation of greenhouse gas emissions. One of method to assess influence of bioenergy systems to the environment is the life cycle analysis (LCA). The objective of this reseach is to present the comprehensive informations about LCA for bioenergy systems. This study can provide a better understanding of global hotspots in the specific research related to the LCA for bioenergy, but may also provide useful information to broaden research area of bioenergy in the Republic of Serbia..

Key words: Bioenergy system, energy, LCA analysis

1 Uvod

Da bi se izvršila kompletna analiza uticaja proizvodnih procesa i sistema na životnu sredinu, oni se moraju posmatrati u svom celokupnom životnom ciklusu (od projektovanja do finalne upotrebe ili prestanka korišćenja). Imajući ovo u vidu, uveden je koncept analize životnog ciklusa (eng. Life cycle assesment-LCA) proizvodnih procesa ili proizvoda u posmatranju njihovih uticaja na prirodno okruženje [1]. Ovaj koncept razmatra uticaje na životnu sredinu od ekstrakcije sirovina za proizvodni proces ili proizvod pa do finalne upotrebe proizvoda, odlaganja proizvoda na deponiju ili ponovne upotrebe proizvoda. Ekstrakcija prirodnih resursa i njihovo korišćenje se određuje i uključuje u razmatranje uticaja ovih procesa na ključne ekološke resurse kao što su vazduh, voda i zemljište.

Analiza obuhvata: snabdevanje resursima, proces proizvodnje, transport, distribuciju, ponovnu upotrebu, reciklažu i odlaganje proizvoda ili kraj proizvodnog procesa. Svi tokovi materijala i energije su obuhvaćeni LCA analizom.

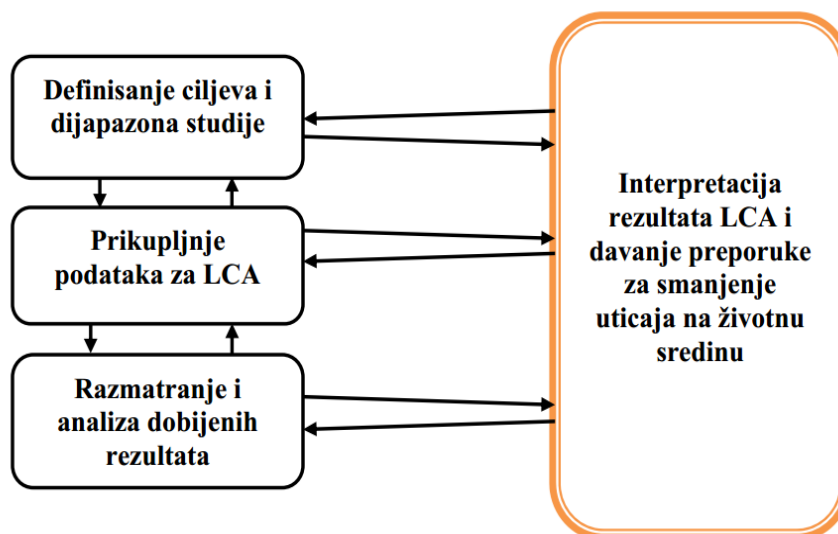
Prve LCA studije pojavile su se sredinom šezdesetih godina 20. veka. Osnivanje organizacije SETAC (Society for Environmental Toxicology and Chemistry), doprinelo je da LCA analiza postane jasnija i standardizovanija [2]. Standardizacija ove metodologije je uspostavljena 1993. godine, kada su objavljeni prvi ISO standardi za razvoj međunarodne norme i pravila za LCA metodologiju. Ova standardizacija je postavila osnovu za sve buduće LCA studije. U 2006. godini izvršeno je revidiranje ovih standarda, kada su uspostavljena dva nova standarda serije ISO 14040: 2006 [3,4]. Faze LCA anlize prikazane su na Slici 1.

Ove faze obuhvataju:

- definisanje ciljeva i opsega studije sa definisanjem granica sistema za analizu,
- prikupljanje podataka, pri čemu se sakupljaju svi ulazi unutar granice sistema za analizu i u kome se izlazi određuju i prezentuju,

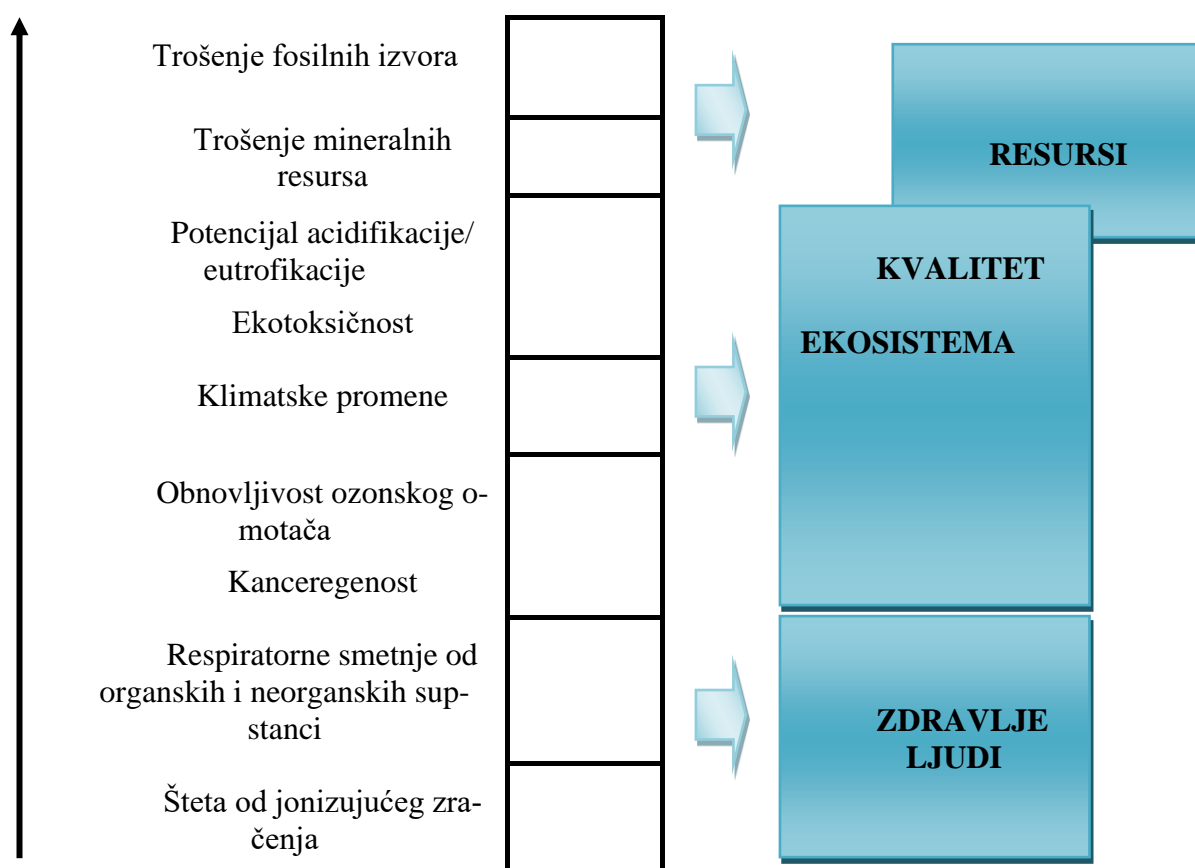
^{*} Corresponding author, email: ing.slobodancvetkovic@yahoo.com

- procena uticaja životnog ciklusa na životnu sredinu, pri čemu su uticaji određeni i kvantifikovani,
- analiza rezultata zasnovanih na prethodnim fazama gde su opisani uticaji na životnu sredinu i date preporuke za smanjenje uticaja na životnu sredinu procesa ili proizvoda.



Slika 1. Faze LCA analize [2,3]

Kao što se može videti sa Slike 2., LCA analiza razmatra uticaj procesa ili proizvoda na nivo korišćenja fosilnih i mineralnih resursa, na kvalitet ekosistema kao i uticaj na zdravlje ljudi. Tokom LCA analize moguće je razmatrati sve ove navedene uticaje ili samo neke pojedinačno, u zavisnosti od granice sistema za analizu i vrste procesa.



Slika 2. Šematski prikaz mogućih uticaja procesa i proizvoda na životnu sredinu koji se razmatraju kroz LCA analizu [5]

2 LCA analiza bioenergetskih sistema

Pod bioenergetskim sistemima podrazumevamo proizvodne sisteme koji za proizvodnju energije koriste biomasu ili energente nastale iz biomase. Studije životnog ciklusa bioenergetskih sistema mogu se svrstati u tri grupe [6,7]:

- analiza tokova energije u životnom ciklusu (LCEA), koja je fokusirana na razmatranje trošenja fosilnih resursa, energetske efikasnost ili karakterizaciju biogoriva sa aspekta obnovljivosti,
- procena emisije GHG gasova tokom životnog ciklusa,
- procena životnog ciklusa, u kojoj se razmatra uticaj različitih kategorija koje su prikazane na Slici 2. i njihov uticaj na životnu sredinu.

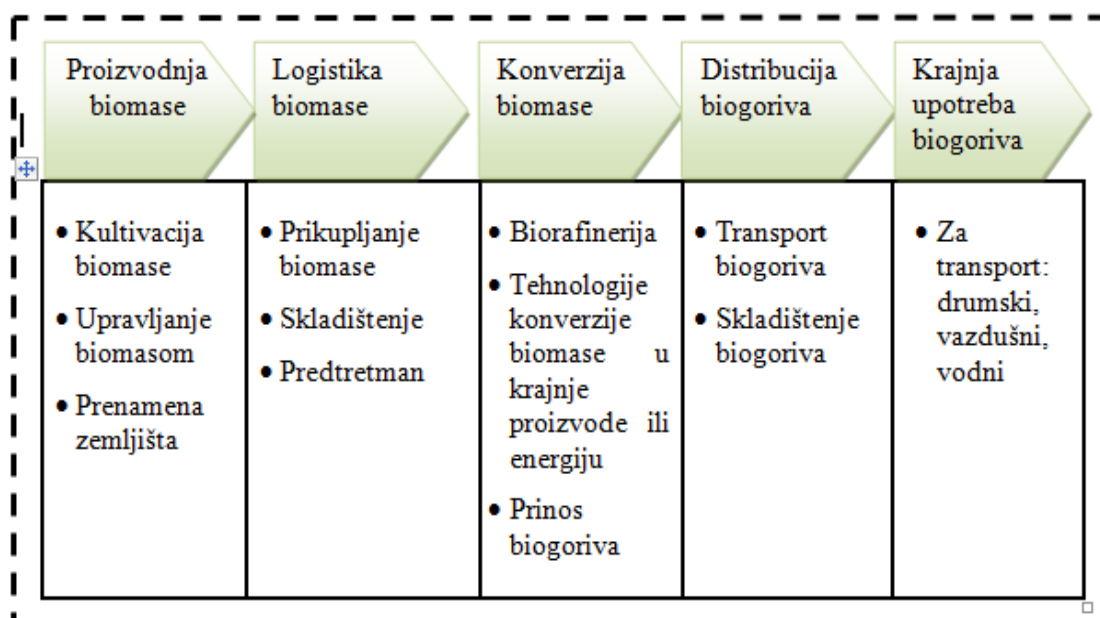
Osim toga, LCA studije bioenergetskih sistema se mogu podeliti [8] na:

- komparativne studije LCA, u kojima se bioenergetski sistemi upoređuju sa energetske sistemima koji koriste fosilne resurse (ove analize se koriste u cilju kreiranja energetske politike kada treba izvršiti supstituciju nekog fosilnog izvora),
- LCA studije bioenergetskih sistema koje se koriste za dobijanje uvida u najveće uticaje na životnu sredinu u lancu proizvodnje energije iz određenog izvora biomase, i
- LCA studije bioenergetskih sistema koje se koriste da identifikuju glavne faze u životnom ciklusu proizvodnje energije iz biomase, sa ciljem da kompanije koje proizvode energiju iz biomase poboljšaju efikasnost u tim fazama.

Važni metodološki izazovi u oblasti LCA bioenergetskih sistema odnose se na izbor jedinične veličine na osnovu koje se porede ulazne i izlazne vrednosti za posmatranu granicu sistema. Najčešće se ova jedinična veličina iskazuju [9]:

- u pređenom 1 km u određenom vozilu koje koristi biogorivo koje je predmet analize;
- po 1 MJ proizvedenog biogoriva;
- po 1 kg proizvedenog biogoriva;
- po 1 litar proizvedenog biogoriva; i
- po 1 ha zemljišta za proizvodnju biomase iz koje je proizvedeno biogorivo koje je predmet analize.

Na slici 3. prikazan je bioenergetski sistem sa fazama životnog ciklusa.



Slika 3. Prikaz bioenergetskog sistema sa fazama životnog ciklusa [10]

Bilans energije i razmatranje uštede gasova sa efektom staklene bašte, zahtevaju uspostavljanje odgovarajuće referentne osnove. Najčešće se kao referentne osnove koriste fosilna goriva (benzin ili dizel). Izbor granice sistema za koji se vrši LCA analiza je od ključne važnosti za krajnje rezultate i njihovu interpretaciju. Granica sistema može obuhvatiti sve ili pojedinačne faze životnog ciklusa procesa ili proizvoda sa svim materijalnim i energetske tokovima.

3 Zaključak

Ocena životnog ciklusa nekog procesa uspostavlja maseni i eneregtski bilans u ispitivanom bioenergetskom sistemu analizom svih ulaza i izlaza procesa tokom čitavog njegovog životnog ciklusa ili tokom nekih faza životnog ciklusa. LCA obezbeđuje sistematski i multidisciplinarni pristup u kvantifikaciji opterećenja u životnoj sredini i njihovim potencijalnim uticajima tokom čitavog životnog ciklusa proizvodnje energije u bioenergetskom sistemu. Uključivanje faktora životne sredine zasnovanih na konceptu životnog ciklusa u procese donošenja odluka o većoj primeni obnovljive energije od velikog je značaja za vladine institucije, kompanije i industrijske organizacije. LCA metodologija se još uvek razvija šireći svoje granice ka sveobuhvatnoj proceni održivosti tehnoloških procesa.

4 Literatura

- [1] **Ahmadi, L., Kannangara, M., Farid Benseba, F.**, Cost-effectiveness of small scale biomass supply chain and bioenergy production systems in carbon credit markets: A life cycle perspective, *Sustainable Energy Technologies and Assessments*, 37, 2020, 100627
- [2] **Sonnemann, G., Castells, F., Schumacher, M.**, 2003. *Integrated Life-Cycle and Risk Assessment for Industrial Processes*. 1 ed. Lewis Publishers, London
- [3] *** ISO 14044, *Environmental management - Life cycle assessment - Requirements and guidelines*. International Organization for Standardization, 2006
- [4] *** ISO 14040, *Environmental management - Life cycle assessment - Principles and framework*, International Organization for Standardization, 2006
- [5] *** Tutorial, 2006. SimaPro 7. Tutorial.
- [6] **Liska, A.J., Cassman, K.G.**, Towards Standardization of Life-Cycle Metrics for Biofuels: Greenhouse Gas Emissions Mitigation and Net Energy Yield. *J. Biobased Mater. Bioenergy* 2, 2008, 187–203
- [7] **Cherubini, F., Strømman, A.H.**, Life cycle assessment of bioenergy systems: state of the art and future challenges. *Bioresour. Technol.* 102 (2), 2011, 437-51
- [8] **van der Voet, E., Lifset, R.J., Luo, L.**, Life-cycle assessment of biofuels, convergence and divergence. *Biofuels*, (3), 2010, 435-449
- [9] **Malça, J., Freire, F.**, Life-cycle studies of biodiesel in Europe: A review addressing the variability of results and modeling issues. *Renew. Sustain. Energy Rev.* 15 (1), 2011, 338-351
- [10] **Zhang, F., Johnson, D.M., Wang, J.**, Life-Cycle Energy and GHG Emissions of Forest Biomass Harvest and Transport for Biofuel Production in Michigan. *Energies*, 2015, 8, 32

VETROTURBINE SNAGE PREKO 20 MW – TEHNOLOŠKA PERSPEKTIVA

WIND TURBINE BEYOND 20 MW – TECHNOLOGY PERSPECTIVE

Aleksandar SIMONOVIC*, Aleksandar KOVAČEVIĆ¹, Toni IVANOV¹,
Miloš VORKAPIĆ²

¹ University of Belgrade, Faculty of Mechanical Engineering, Belgrade, Serbia

² University of Belgrade, ICTM - CMT, Belgrade, Serbia

<https://doi.org/10.24094/mkoiee.020.8.1.123>

Trend razvoja vetroturbina ima poseban značaj u eksploataciji obnovljivih izvora energije. Vetroturbine velikog prečnika rotora i visokih tornjeva sve se više razmatraju u istraživačkim i razvojnim centrima širom sveta. Upotrebom vetroturbina na većim visinama gde je brzina vetra znatno veća ostvaruje se mogućnost boljeg iskorišćenja ovog obnovljivog izvora energije. Razvoj novih tehnologija otvara mogućnost za novu generaciju vetroturbina snage preko 20 MW. U poslednjih nekoliko godina razne studije izvodljivosti su pokazale da koncept vetroturbine velikog prečnika rotora koji se nalazi na visokim tornju daje pozitivne rezultate sa aspekta analize strukturalnih i aerodinamičkih parametara. Posebna pažnja posvećena je smanjenju ukupne mase i prigušenju vibracija korišćenjem novih materijala. U ovom radu prezentovan je razvoj vetroturbina velike snage, dat je pregled tehnoloških mogućnosti u proizvodnji osnovnih komponenti kao i perspektiva za realizaciju vetroturbina snage preko 20 MW.

Ključne reči: *vetroturbine; elementi vetroturbine; nove tehnologije; materijali; perspektiva*

The trend of wind turbine development has a special significance in the exploitation of renewable energy sources. At higher altitudes, we have better wind energy utilization higher speed and their conversion are achieved in the best possible use of wind turbines. The development of new technologies opens space for a new generation of wind turbines with a 20MW rated power. In recent years, various feasibility studies have shown that wind turbines with large rotor diameter and high towers give positive shifts in the analysis of structural and aerodynamic parameters, with a focus on reducing overall mass and damping vibrations due to the use of new materials. In this paper, the evolution of high power wind turbines and an overview of the technological development of the basic components of the turbine will be presented. Perspectives in the further development of wind turbines with rated power above 20MW will be also considered.

Key words: *wind turbine, turbine elements, new technologies, materials, perspective;*

1 Introduction

There are many different ways in which devices can convert the energy of wind into mechanical work. Today there are a lot of divisions of wind turbines (WT). According to the location WT can be onshore, offshore and airborne. According to Jacobson et al. [1], onshore WT in 139 countries cover the area of 1105000 km², while offshore WT occupy 653200 km² of global water area. The realization of wind turbines from idea to final product implies a multidisciplinary approach. The development of a WT follows the increase in dimensions and weight. Therefore, designers tend to use different tools and techniques, to project, optimize, realize the construction, and extend the exploitation life of WT. The policies of an increasing number of countries are to produce the most percent of electrical energy from wind power. Improvements in the production of wind generators involve a larger and heavier construction to get lower energy costs from renewable energy sources. It's where big problems arise.

* Corresponding author, email: asimonovic@mas.bg.ac.rs

Global annual and cumulative installed wind capacity from 2001 to 2017 is shown in Figure 1 following Global Wind Report - Annual market update [2].

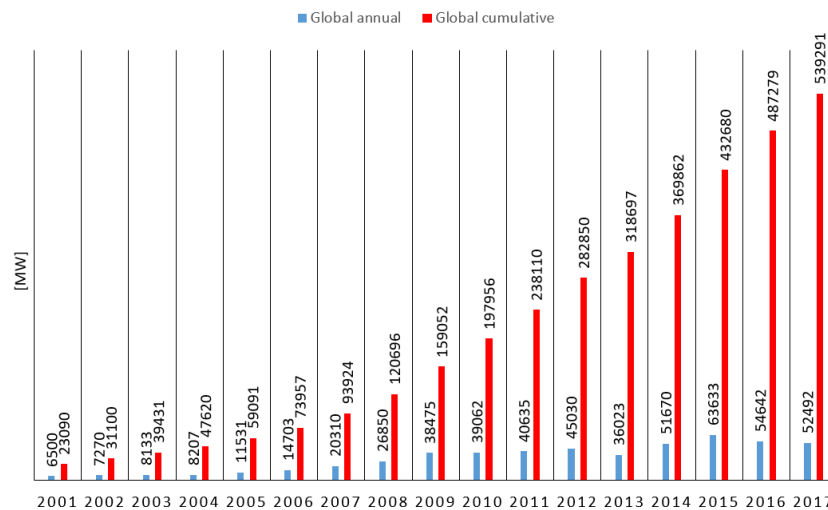


Figure 1 - Global annual and cumulative installed wind capacity

According to [2], overview of total installed WT power for 2017 in developed and developing countries is shown in Table 1.

Table 1 - Global installed wind power capacity

Regional distribution	Country	Total installed capacity to 2017 [MW]	Wind power capacity added in 2017 [MW]	Number of turbines	Share of wind generated in electricity consumption
Asia	PR China	188392	19666	104934	4.8
	India	28700	4184	32136	4.35
North America	USA	89077	7017	54430	6.3
Europe	Germany	56132	6581	150000	16.1
	France	13759	1964	6000	4.8
Latin America	Brasil	12763	2022	6491	7.44
Mid. East and Africa	South Africa	1467	618	961	2.15

PR China planned to produce 30 GW of electric energy by WT to 2020. Although, because of huge technological progress, this plan is achieved in [3]. According to that plan, China took over the leadership from the USA in the field of producing electric energy by WT. British petroleum gives a comparison between using oil and all other energy sources. In 2017 consumption of energy produced by all other sources increased 2.2% relative to oil energy consumption. The development and supply chain of electricity from renewable sources of energy is projected for the period 2015-2050. Forecast of increasing is given respectively: 2015 (5.6 %), 2020 (20%), 2025 (56%), 2030 (80%), 2040 (95%), 2050 (100%) [1]. Today, the realization of wind turbines with large powers exceeding 20MW has become imperative. In general, there is little data on the research of these WT. Starting from the structure, the realization of the tower and rotor wind generators becomes more and more complex. A multidisciplinary approach is increasingly used in optimizing the design of WT. This involves obtaining a new aero-elastic tower and rotor design including problems that can occur through: removal

of ice from the leading edge of the blade, load distribution, modal frequency appearance, velocity at the tip of the blade, and the appearance of fatigue damage [4].

Table 2 - A chronological overview of companies who developing WT [12, 47]

Company	Name	Country	Year	Power [MW]	Diameter [m]	Hub height [m]
Poul La Cour	-	Denmark	1891	0.035	20	-
FL Smidth	-	Denmark	1941	0.05	17	24
Smith Company	Smith Puntam	USA	1941	1.25	53	36
Tvind	Tvindkraft	Denmark	1978	2	54	53
Aeolus	WTS-75	Sweden	1983	2	75	77
NASA	MOD 5B	Hawaii, USA	1987	3.2	97.5	61
Adwen	Adwen AD 5-135	Germany	2004	5	135	95
Ming Yang	Ming Yang SCD 6.0	China	2014	6	140	100
Siemens	Siemens Gamesa Sg 8.0-167	Unitet Kingdom	2017	8	167	155
Vestas	MHI Vestas V164 - 9.5	Unitet Kingdom	2018	9.5	164	140

The starting point of this paper is to investigate the feasibility of WT outputs larger than 20 MW and to provide an appropriate model for reducing energy costs. In the period from 1999 to 2012, the use of wind energy to a total of 283 GW increased sharply, while for 2020 it is expected that this number will reach 760 GW [5]. Table 2 shows the trend of increasing of hub height, the diameter of the rotor, and the power of WT from 1941 to 2018. Chronologically, the major steps were made in 2005 with the implementation of a 5 MW wind generator [6]. Then there were transient solutions for expansion of power from 7-8 MW, so in 2012 there was a wind turbine power of 8 MW with a rotor diameter of 164 m. A step further, Bak et al. [7] presented the WT power of 10 MW. It is a rotor with three blades for a speed range from 5 m/s to 25 m/s. As for research for this WT, CFD analysis was performed to obtain detailed aerodynamic characteristics of the rotor [8].

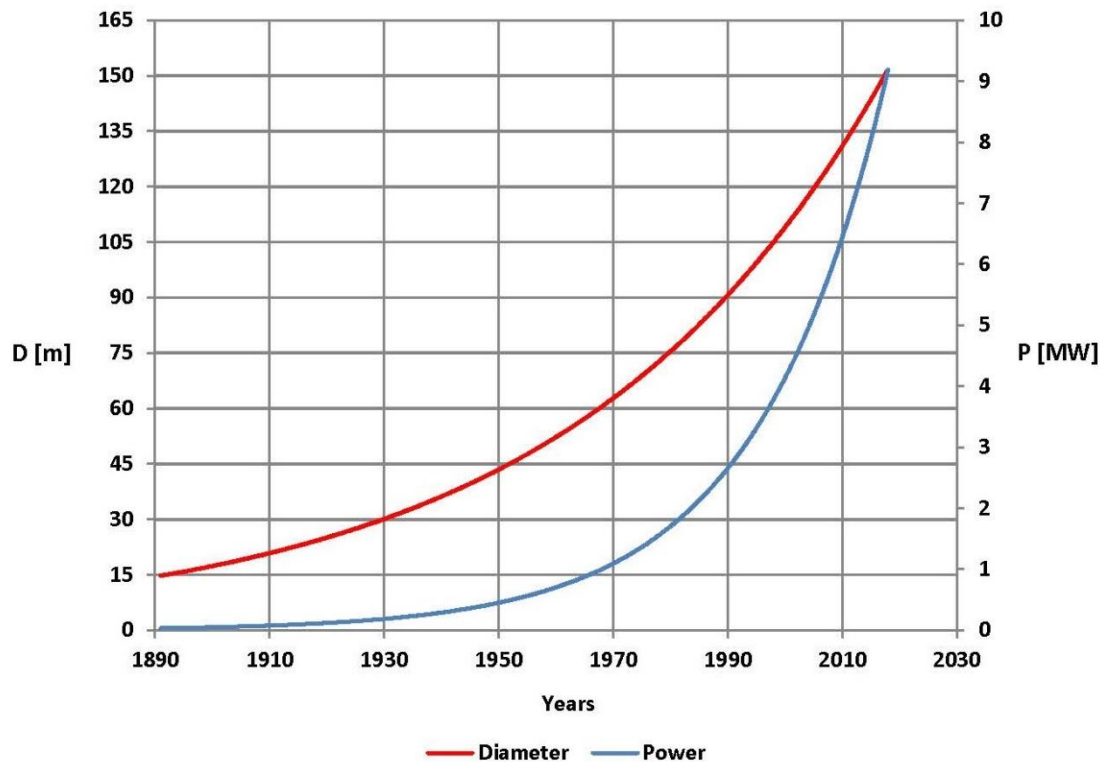


Figure 2 - The trend of increasing rotor diameter and power of WT

Peeringa et al. [9] presented the preliminary WT design of 20 MW and controller design. In this context, the WT of 5 MW is being upgraded as a starting point for the analysis of the reference WT of 20 MW. The concept of wind turbines with multiple rotors on one tower is being considered [10]. The conclusion is that the price of a 20 MW multirotor type wind turbine is less 80% compared to four 5 MW single-rotor type WT. These researches depend on many assumptions, but they indicate that the concept of multirotor deserves more intense research. In this paper, we will talk about WT with a horizontal axis of rotation (HAWT). HAWT has much higher efficiency for the same wind conditions relative to the vertical axis wind turbine (VAWT). Also, their blades are connected to the hub [11]. The biggest disadvantages are reflected in the noise production, large space they occupy, and price. Generator and gearbox are on the tower, which is also a problem in case of failure.

2 Rotor

The WT blade is one of the most important components of WT. In this sense, the manufacturing of a WT blade requires innovative design approaches, material selection, and manufacturing processes. The current and future development blades are related to the construction, selection, development of materials, and production. The design of the blade must fulfill two basic conditions: an analysis of structural requirements and achieving aerodynamic efficiency. For large diameter rotors, the airfoil selection is important. The aerodynamic efficiency of the blade increases with the choice of the thinner airfoil. In the blade construction, the four objectives are set: optimization of aerodynamic design, blade length, blade design and, production requirements, and reliability of blades testing. The multidisciplinary optimization is becoming more and more common for the complex calculation of WT components [13]. Composite materials are increasingly used today for the production of WT blades. Blades that are made of these materials are light in weight but at the same time have good structural characteristics as strength, stiffness, and fatigue resistance [14]. Very easy shaping is one of the most important characteristics of composite materials. This characteristic is very important in the case of complex body geometry. Also, new materials contribute to reducing the costs of producing blades [15]. On the other hand, WT manufacturers are not able to provide proper quality control related to the elimination of defects in manufacturing such as waves and wrinkles [16] and porosity [17]. The development of the rotor and usage of new materials, the weight of the blades increases

nonlinearly with their length [18]. The comparison rotor diameter of WT with a wingspan of big planes is presented by the Figure 3. Here appear large structural loads due to blades suppleness. Therefore, these loads and the phenomenon of natural bladder frequency must be reduced.

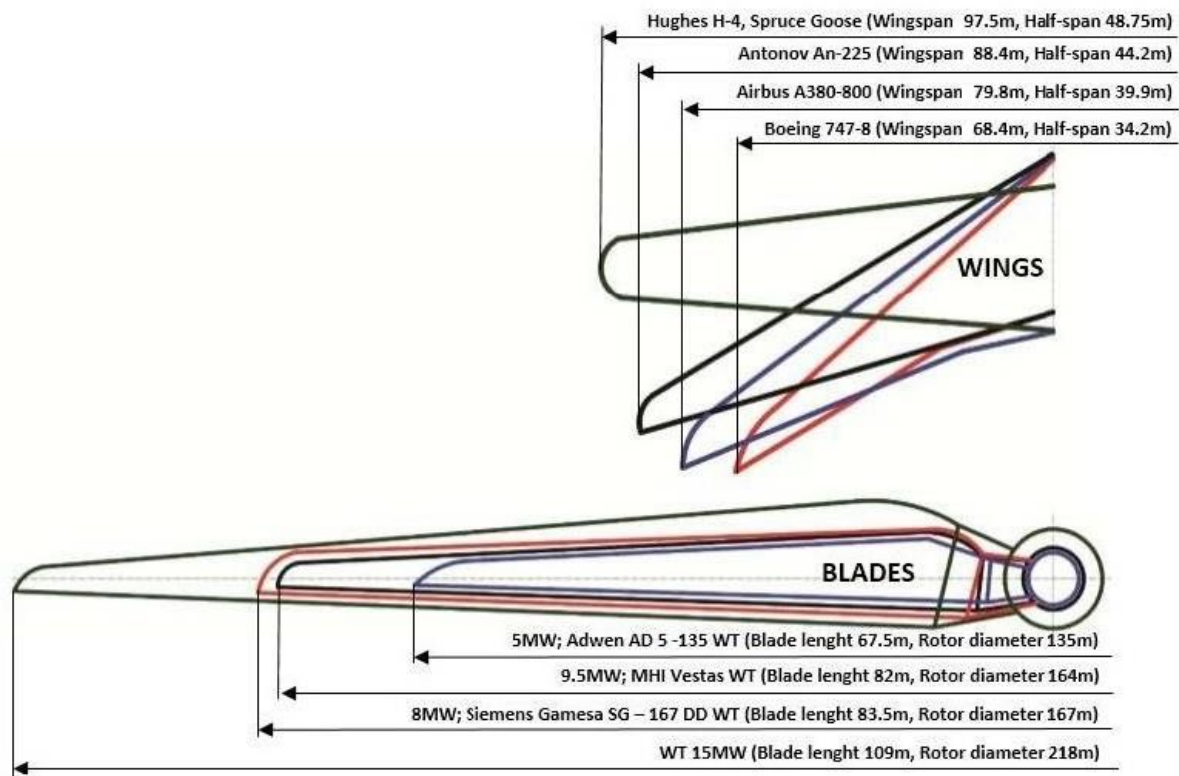


Figure 3 - Comparison rotor diameter of WT with wingspan of big planes

The future research and directions of the rotor development are: increasing the diameter of the wind turbine rotor whose goal is to exploit wind energy at higher altitudes, efficient optimization of all data, considering the potential costs of innovative materials, and improving quality control to reduce defects in rotor production.

3 Transmission

One of the classifications of WT is the concept of transmission. In accordance with this classification, WT can be geared type and gearless type [19]. Both type have their own advantages and disadvantages which will be more explained in further text.

3.1 Wind turbines with gearbox

The WT gearbox has the function of increasing the shaft angular speed that is connected with a generator of electrical energy. Block scheme [20] of the conversion of mechanical energy to electrical energy in wind turbines is given in Figure 4. Most commonly used is a three-stage WT gearbox [21]. The first stage is a planetary gear train, which has three planet gears, one sun gear, and one ring gear. The second and the third stages are parallel gear trains that each have a pair of gears. This gearbox uses eight pairs of helical gears, nine in total, to perform its operation. The dimensions of drive gears are much larger than the driven gear [22,23]. The speed of the input shaft is around 25 rpm while the output shaft speed is about 1500 rpm [24]. Parallel gears transmission with parallel axis units is used for speeds with medium and higher transmission ratio, while gearboxes with planetary transmission are used for speeds with a lower transmission ratio.

Gearboxes for high-power WT (MW type) are usually used with three-speed transmission [25]. All vibrations from the rotor and the wind are transmitted to the gearbox. There are various failures: from damage and breakage of all gears to damage to the input shaft, due to poor lubrication and

damage to the housing [26]. Because of all mentioned, the gearbox is the source of the failure of many wind turbines, which prevents them from reaching a projected lifetime [27].

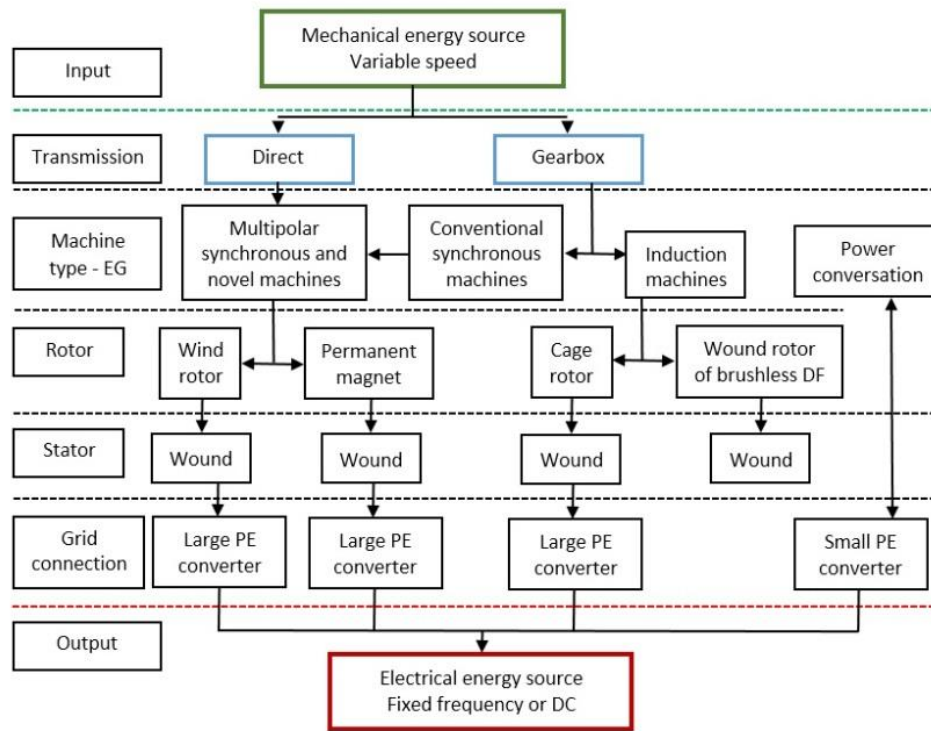


Figure 4 - Block diagram of conversion mechanical energy to electrical energy using wind turbine

3.2 Gearless wind turbines

The idea of a direct connection of the rotor with the electric generator is now more and more in use. This solution is slowly applied to avoid the use of the gearbox to reduce the weight of the WT. The advantages and disadvantages of geared and gearless WT are presented in Table 3.

Table 3 - Advantages and disadvantages of geared and gearless WT

Type of wind turbine	Advantages	Disadvantages
Gearless wind turbines	<ul style="list-style-type: none"> - Simplified drive train - Increased energy yield - Higher reliability - Reducing total weight 	<ul style="list-style-type: none"> - Heavy electric generator - Large rotor shaft diameter - Large torque
Magnetic	<ul style="list-style-type: none"> - Cheaper - Low weight of electric generator - Low torque on high speed shaft 	<ul style="list-style-type: none"> - Failure fatigue - Problems with maintenance - A lot of parts

4 Electric generator

In order to maximize and use gained power and reduce costs, WT with different engineering solutions have been developing simultaneously. The classification of electro generators is being done by power level and the working principle. Synchronous generators featuring new engineering solutions are the most common generators existing in market. They can also be classified as inductive generators [28]. More and more WT are being included in electrical network. Frequency is still being controlled by conventional thermal power stations. The question is how to maintain frequency in a predefined domain. Nowadays, conventional generators are equipped with primary and secondary control. More and more WT are being included in the electrical network. Frequency is still being

controlled by conventional thermal power stations. The question is how to maintain frequency in a predefined domain. Nowadays, conventional generators are equipped with primary and secondary control. The direct wind energy method is part of primary frequency control [29]. In normal conditions, WT are not supplying available energy to the electrical network, so the limits stay defined by power control. A considerable amount of kinetic energy is accumulated in the rotating mass of blades of wind generators. This energy is contributing to network inertia in case of constant speed WT, but in case of varying speed, rotation is isolated from network frequency by the electric power converter. Considering this, additional control by means of "hidden inertia" can be acquired by inertia imitating and limited time primary frequency control [28]. As important representatives in the realization of electro generators in this paper, the most common technologies will be presented: generator with planetary magnets and HTS (High Temperature Superconductor) technology. The principal of superconductor generator technology is shown in Figure 5.

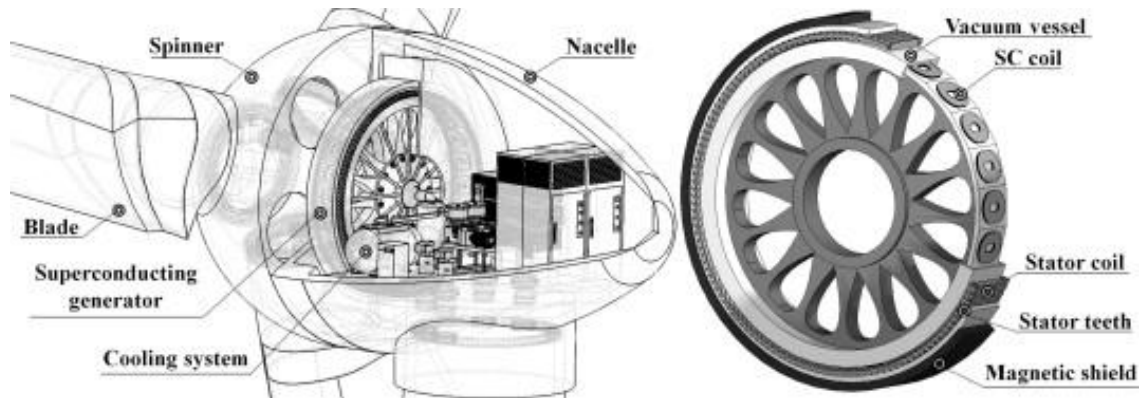


Figure 5 - Basic elements of superconductor generator technology [19]

The generator with permanent magnets is connected to the main rotor assembly through the main rotor bearing clutch and separated generator bearings [30]. In general, switching generators with permanent magnets has three concepts: PM radial flux (RFPM machines), PM with the axial flow (AFPM machines), and PM transverse flow (TFPM machines) [31]. RFPM machines produce magnetic flux in a radial direction with radial orientated PM [32]. These machines are a better economical solution for big WT with direct drive. AFPM machines produce magnetic flux in an axial direction with PM. These toroidal-stator machines have some advantages: compact design, reduced length in an axial direction, appropriate connection with motor [33]. They are designed for small power machines [31]. TFPM machines point that the direction of magnetic flux is perpendicular to the direction of motor rotation. These machines provide more space for coil, but at the same time reduce available space for main flux [34]. They also feature big specific torque and a large number of parts, which represents discussing a matter of maintenance and elements optimization [35]. High temperature superconductor (HTS) technology is present nowadays which allows generators to operate with a third of mass and half of the loss compared to conventional machines [36-38]. HTS coil operates at extremely high and low temperatures [32]. Size and weight reduction of 10MW wind generators are accomplished by this technology, with a consequence regarding reducing pure energy costs compared to copper generators and permanent magnet generators. Also, this technology is practical and allows an economical approach to maintenance. HTS technology eliminates separated gearbox generator assembly, i.e. flexible structure is mounted in that part. Integrated multipolar permanent magnet generators enable the creation of a technically simple and at the same time innovative design of WT with high efficiency. This type of generator achieves a nominal power even at an angular speed of 12 rpm. In addition to reducing the weight of the WT, this concept also ensures low noise during its operation.

5 Tower

The WT tower transmits the load of the gondola and the WT rotor to the ground. The most common are made from steel, concrete, or composite materials. Also, there are hybrid solutions that

represent a combination of concrete and steel. Depending on the height, different solutions to the construction of the columns are applied. According to the de la Fuente [39], an overview of the realization of the rotor with its basic characteristics is given in Table 4.

Table 4 - Wind turbine towers: Applications, strengths and weaknesses

Type of tower	Height [m]	Diameter of base [m]	Weight/Height [t/m]	Strengths	Weaknesses
Steel (Tubular)	60-120	3-4.5	2-5	Less material and optimal transport for $h < 80$ m	High transport and assembly costs for $h > 80$ m
Concrete (On-site)	60-115	3-8.5	8-19	Monolithic, durability and stiffness	Weather conditions vulnerability
Steel + Concrete	60-146	3-5	3-15	Expected to solve weaknesses of previous alternatives	In experimental stage
Active Composite	80-146	3-5	-	Possibility of damping wind vibration	The inability to dampen the vibrations

5.1 Steel tower

The steel tower consists of steel profiles interconnected by wire links or welded together at the position of the WT. Such constructions allow for realization at altitudes from 60m to 160m. For height greater than 80m, conical cast iron poles are most often used, with the main advantage of the transport and material optimization [40]. The main goal is how to achieve a small mass of the tower for different conditions as well as obtaining a lower load [41]. Enercon has developed a new method for assembling sections of tubular steel towers using a grout joint [42]. The new Enercon design is based on the separation of the tower pillars into the longitudinal sections. These sections are much easier to transport from place to place.

5.2 Concrete tower

Towers of WT are generally made of ferroconcrete. Following Grünberg and Göhlmann [43] company Enercon made a WT E126/6 MW with characteristics (hub height 135 m and rotor diameter 126 m). WT tower is divided in both horizontal and vertical direction, and design improvement of the ferroconcrete tower is made. On the other side, minimal costs of manufacturing ferroconcrete towers are provided by Ma and Meng [44]. High quality of tower construction is obtained by using FEM analysis, and they made optimization to obtain the minimum concrete cost. Lofty [45] designed a new kind of tower in which the cross section is a triangle shape. The ferroconcrete towers are cheaper in comparison with steel towers.

5.3 Hybrid tower

Dutch company Mecal has set up a hybrid tower for WT of 2.3 MW for a hub height of 133m. The concrete tower has five rings, and each ring is divided into four quarter-circle and four flat elements for easy transportation. One of the advantages of a hybrid tower is the possibility of replacing the steel part after 20 years because the lifetime of the concrete is 40 years. However, for the latest generation of hybrid towers, the data is not available and is still in the development phase.

5.4 Composite tower

The construction of a WT tower of materials such as steel profiles or sheet metal is heavy, expensive to manufacturing, and require special conditions for transporting materials. Besides this lacks of steel, concrete, and hybrid constructions, the main disadvantage is the inability to dampen the vibrations. In this respect, composite materials have a significant advantage in comparison with other designs due to the possibility of damping wind vibration, which reduces vibration loads, which is very important for high construction. Another significant advantage is that tower production can be done on-site. This way of production allows reducing the cost of production facilities, where the mold manufacturing equipment fits into the existing standards [46].

6 Conclusion

Wind energy has been gaining more and more important as the element of renewable energy resources. Hence, the chronological development of wind turbines points to a rapid increase in active power. The analysis of achieved technical solutions has been done throughout the basic elements of the wind turbine in this paper. Using composite materials in designing rotor blades, reducing the size of the gearbox, new technological achievements in improvements of generator performances, and acquiring more usable power are all the factors that will be researched in future development. Knowing this, aerodynamic characteristics and structural components must be designed in terms of mass reduction and maximizing wind potential at nominal and extreme work conditions. New technologies and materials are in expansion. It means a multidisciplinary approach in designing and manufacturing wind turbines. The usage of new materials gives many advantages and limitations at the same time. At high altitudes, the speed of the wind is greater and that provides more wind exploitation.

Knowing this, aerodynamic characteristics and structural components must be designed in terms of mass reduction and maximizing wind potential at nominal and extreme work conditions. WT with power beyond 20 MW have a significant role in increasing tower height, rotor diameter, and dimensions of other elements. All of this increases the total mass of the WT possibility of damping wind vibration. The tendency is to reduce the total mass of the WT as well as the simplification of the structure with the usage of new composite materials and technical solutions. Using composite materials in designing rotor blades, reducing the size of a gearbox, new technological achievements in improvements of generator performances, and acquiring more usable power are all the factors that will be researched in future development.

7 Acknowledgement

This paper is the part of TR-35035 project of the Ministry of Education, Science and Technological Development of the Republic of Serbia.

8 References

- [1] **Jacobson, M. Z., M. A. Delucchi, Z. A. Bauer, S. C. Goodman, W. E. Chapman, M. A. Cameron, J. R. Erwin**, 100% clean and renewable wind, water, and sunlight all-sector energy roadmaps for 139 countries of the world, *Joule*, 1(2017), 1, pp. 108-121.
- [2] Web page: Global Wind Energy Council, Source: <http://files.gwec.net/files/GWR2017.pdf>
- [3] (Accessed 09.06.2020).
- [4] **Wang, Q**, Effective policies for renewable energy - the example of China's wind power-lessons for China's photovoltaic power, *Renewable and Sustainable Energy Reviews*, 14(2010), 2, pp. 702-712.
- [5] **Ashuri, T., J. R. Martins, M. B. Zaaier, G. A. van Kuik, G. J. van Bussel**, Aeroservoelastic design definition of a 20 MW common research wind turbine model, *Wind Energy*, 19(2016), 11, pp. 2071-2087.
- [6] **Blaabjerg, F., K. Ma**, Future on power electronics for wind turbine systems, *IEEE Journal of emerging and selected topics in power electronics*, 1(2013), 3, pp. 139-152.

- [7] **Jonkman, J., S. Butterfield, W. Musial, G. Scott**, Definition of a 5-MW reference wind turbine for offshore system development (No. NREL/TP-500-38060), National Renewable Energy Lab., Golden, CO (United States), 2009.
- [8] **Bak, C., R. Bitsche, A. Yde, T. Kim, M. H. Hansen, F. Zahle, J.J. Wedel Heinen, T. Behrens**, Light Rotor: The 10-MW reference wind turbine, *Proceedings of the European Wind Energy Association (EWEA) Annual Event*, EWEA, Copenhagen, Denmark, 2012.
- [9] **Zahle, F., C. Bak, N. N. Sørensen, S. Guntur, N. Troldborg**, Comprehensive aerodynamic analysis of a 10 MW wind turbine rotor using 3D CFD, *In 32nd ASME Wind Energy Symposium*, ASME, National Harbor, Maryland (USA), 2014.
- [10] **Peeringa, J., R. Brood, O. Ceyhan, W. Engels, G. De Winkel**, Upwind 20MW Wind Turbine Pre-Design (Paper No. ECN-E-11-017), *ECN*, Netherland, 2011.
- [11] **Jamieson, P., M. Branney**, Multi-rotors; a solution to 20 MW and beyond?, *Energy Procedia (Selected papers from Deep Sea Offshore Wind R&D Conference)*, EERA, Trondheim, Norway, 2012.
- [12] **Sieros, G., P. Chaviaropoulos, J. D. Sørensen, B. H. Bulder, P. Jamieson**, Upscaling wind turbines: theoretical and practical aspects and their impact on the cost of energy, *Wind energy*, 15(2012), 1, pp. 3-17.
- [13] **Hau, E., H. von Renouard**, Wind turbines: fundamentals, technologies, application, economics, *Springer Science & Business Media*, 2003, pp. 669-675.
- [14] **Lambe, A. B., J. R. Martins**, Extensions to the design structure matrix for the description of multidisciplinary design, analysis, and optimization processes, *Structural and Multidisciplinary Optimization*, 46(2012), 2, pp.273-284.
- [15] **Mishnaevsky Jr, L., P. Brøndsted, R. Nijssen, D. J. Lekou, T. P. Philippidis**, Materials of large wind turbine blades: recent results in testing and modeling. *Wind Energy*, 15(2012), 1, pp. 83-97.
- [16] **Lantz, E.**, Clean Energy Manufacturing: US Competitiveness and State Policy Strategies (Presentation) (No. NREL/PR-6A20-61265), National Renewable Energy Lab., Golden, CO (United States), 2014.
- [17] **Riddle, T., D. Cairns, J. Nelson**, Characterization of manufacturing defects common to composite wind turbine blades: Flaw characterization. In *52nd AIAA/ASME/ASCE/AHS/ASC Structures, Structural Dynamics and Materials Conference 19th AIAA/ASME/AHS Adaptive Structures Conference 13t*, ASME, Denver, CO (United States), 2011.
- [18] **Lambert, J., A. R. Chambers, I. Sinclair, S. M. Spearing**, 3D damage characterisation and the role of voids in the fatigue of wind turbine blade materials, *Composites Science and Technology*, 72(2012), 2, pp. 337-343.
- [19] **Fingersh, L., M. Hand, A. Laxson**, Wind turbine design cost and scaling model (No. NREL/TP-500-40566), National Renewable Energy Lab., Golden, CO (United States), 2006.
- [20] **Sung, H. J., G. H. Kim, K. Kim, M. Park, I. K. Yu, J. Y. Kim**, Design and comparative analysis of 10 MW class superconducting wind power generators according to different types of superconducting wires, *Physica C: Superconductivity*, 494(2013), pp. 255-261.
- [21] **Hansen, L. H., P. H. Madsen, F. Blaabjerg, H. C. Christensen, U. Lindhard, K. Eskildsen**, Generators and power electronics technology for wind turbines, *In Industrial Electronics Society (The 27th Annual Conference of the IEEE)*, IEEE, Denver, CO (United States), 2001.
- [22] **Zhao, M., J. Ji**, Dynamic analysis of wind turbine gearbox components. *Energies*, 9(2016), 2, pp.110.
- [23] **Ding, F., Z. Tian, F. Zhao, H. Xu**, An integrated approach for wind turbine gearbox fatigue life prediction considering instantaneously varying load conditions, *Renewable Energy*, 129(2018), pp. 260-270.
- [24] **Nejadkhaki, H. K., S. Chaudhari, J. F. Hall**, A design methodology for selecting ratios for a variable ratio gearbox used in a wind turbine with active blades, *Renewable Energy*, 118(2018), pp. 1041-1051.

- [25] **Shanbr, S., F. Elasha, M. Elforjani, J. Teixeira**, Detection of natural crack in wind turbine gearbox, *Renewable Energy*, 118(2018), pp. 172-179.
- [26] **Xu, X., P. Dong, Y. Liu, H. Zhang**, Progress in Automotive Transmission Technology, *Automotive Innovation*, 1(2018), 3, pp. 187-210.
- [27] **Salameh, J. P., S. Cauet, E. Etien, A. Sakout, L. Rambault**, Gearbox condition monitoring in wind turbines: A review. *Mechanical Systems and Signal Processing*, 111(2018), pp. 251-264.
- [28] **Herbert, G. J., S. Iniyan, E. Sreevalsan, S. Rajapandian**, A review of wind energy technologies, *Renewable and sustainable energy Reviews*, 11(2007), 6, pp. 1117-1145.
- [29] **Piwko, R., N. Miller, J. Sanchez-Gasca, X. Yuan, R. Dai, J. Lyons**, Integrating large wind farms into weak power grids with long transmission lines, *In Power Electronics and Motion Control Conference*, IEEE, Portoroz, Slovenia, 2006.
- [30] **Sørensen, P., A. D. Hansen, F. Iov, F. Blaabjerg, M. H. Donovan**, Wind farm models and control strategies, Risø National Laboratory (DK-4000 Roskilde), Denmark, Risø, 2005
- [31] **Bang, D., H. Polinder, G. Shrestha, J. A. Ferreira**, Review of generator systems for direct-drive wind turbines, *In European Wind Energy Conference & Exhibition*, EWEA, Brussels, Belgium, 2008.
- [32] **Badrzadeh B**, Qualitative performance assessment of semiconductor switching device, converter and generator candidates for 10 MW offshore wind turbine generators, *Wind Energy*, 14(2011), 3, pp. 425 - 448.
- [33] **Slemon, G. R., X. Liu**, Modeling and design optimization of permanent magnet motors, *Electric Machines & Power Systems*, 20(1992), 2, pp. 71-92.
- [34] **Wu, W., E. Spooner, B. J. Chalmers**, Design of slotless TORUS generators with reduced voltage regulation, *IEE Proceedings-Electric Power Applications*, 142(1995), 5, pp. 337-343.
- [35] **Chang, J., D. Kang, J. Lee, J. Hong**, Development of transverse flux linear motor with permanent-magnet excitation for direct drive applications, *IEEE Transactions on Magnetics*, 41(2005), 5, pp. 1936-1939.
- [36] **Harris, M. R., G. H. Pajooman, S. A. Sharkh**, Performance and design optimisation of electric motors with heteropolar surface magnets and homopolar windings, *IEE Proceedings-Electric Power Applications*, 143(1996), 6, pp. 429-436.
- [37] **Schiferl R.**, High-temperature superconducting synchronous motors: economic issues for industrial applications, *IEEE Trans IndAppl*, 44(2008), 5, pp. 1376–1384.
- [38] **Snitchler, G., B. Gamble, C. King, P. Winn**, 10 MW class superconductor wind turbine generators, *IEEE Transactions on Applied Superconductivity*, 21(2010), 3, pp. 1089-1092.
- [39] **Badrzadeh B.**, Qualitative performance assessment of semiconductor switching device, converter and generator candidates for 10 MW offshore wind turbine generators, *Wind Energy*, 14(2011), 3, pp. 425 - 448.
- [40] **de la Fuente, A.,**. New system of precast concrete towers for wind farms, *Academic Project*, Technical University of Catalonia (UPC), Barcelona, Spain, 2007.
- [41] **Agbayani, N. A., R. E. Vega**, The rapid evolution of wind turbine tower structural systems: a historical and technical overview, *In Structures Congress 2012*, ASCE, Chicago, IL (United States), 2012.
- [42] **Yoshida, S.**, Wind turbine tower optimization method using a genetic algorithm, *Wind Engineering*, 30(2006), 6, pp. 453 - 469.
- [43] Web page: *Enercon*, Source:
- [44] https://www.enercon.de/fileadmin/Redakteur/MedienPortal/wind-blatt/pdf/WB_032016_GB.pdf (Accessed 16.06.2020).
- [45] **Grünberg, J., J. Göhlmann**, *Concrete structures for wind turbines*, Erns & Sohn, Berlin, Germany, 2013.
- [46] **Ma, H., R. Meng**, Optimization design of prestressed concrete wind-turbine tower, *Science China Technological Sciences*, 57(2014), 2, pp. 414-422.

- [47] **Lofty, A.**, Prestressed concrete wind turbine supporting system, MSc. Thesis, University of Nebraska, Lincoln, NE (United States), 2012.
- [48] **Zheng, D., L. D. Willey, W. W. Lin**, *U.S. Patent No. 7,927,445*, U.S. Patent and Trademark Office, 2011.
- [49] **Ackermann, T.**, *Wind power in power systems*, John Wiley & Sons, Chichester, England, 2005.

NUMERIČKA PROCENA AERODINAMIČKIH PERFORMANSI ROTORA VETROTURBINE SA VERTIKALNOM OSOM OBRTANJA I KONCENTRATOROM

NUMERICAL EVALUATION OF AERODYNAMIC PERFORMANCES OF VERTICAL-AXIS WIND TURBINE ROTOR WITH FLOW CONCENTRATOR

Jelena SVORCAN^{*1}, Ognjen PEKOVIĆ¹, TONI IVANOV¹, Miloš VORKAPIĆ²,

¹ University of Belgrade, Faculty of Mechanical Engineering, Belgrade, Serbia

² ICTM – CMT, University of Belgrade Serbia

<https://doi.org/10.24094/mkoiee.020.8.1.135>

Usled stalnog porasta iskorišćenja energije vetra, interesovanje za male vetroturbine za urbane sredine se takođe širi. Kako ovakve mašine često funkcionišu u nepovoljnim radnim uslovima (Zemljinom graničnom sloju, vrtložnom tragu okolnih objekata, pri maloj i promenljivoj brzini vetra), moguće je instalirati dodatne elemente čija uloga je da lokalno povećaju brzinu kroz rotor i olakšaju pokretanje vetroturbine. Ovaj rad istražuje prednosti dodavanja optimizovanog koncentratora struje vazduha rotoru vetroturbine sa vertikalnom osom obrtanja. Prostorne, nestacionarne simulacije turbulentnog, nestišljivog opstrujavanja izolovanog rotora koji sadrži tri prave lopatice kao i rotora sa koncentratorom izvedene su u softverskom paketu ANSYS FLUENT metodom konačnih zapremina za nekoliko različitih radnih režima. Ova vrsta proračuna je izazovna jer su napadni uglovi visoki, javljaju se brojni strujni fenomeni i nestabilnosti dok interakcija između lopatica i odvojenih vrtloga može biti značajna. Obrtno kretanje lopatica rešeno je pristupom klizajućih mreža. Strujno polje modelovano je nestacionarnim Navije-Stoksovim jednačinama osrednjenim Reynoldsovom statistikom (URANS) koje su zatvorene k- ω SST turbulentnim modelom. Prikazane su i kvantitativne i kvalitativne analize dobijenih numeričkih rezultata. Naročito je izvršeno poređenje dve krive koeficijenta snage i naglašene su prednosti instaliranja koncentratora struje vazduha.

Ključne reči: vetroturбина; koncentrator; proračunska aerodinamika; koeficijent snage

With wind energy extraction constantly increasing, the interest in small-scale urban wind turbines is also expanding. Given that these machines often work in adverse operating conditions (Earth's boundary layer, vortex trails of surrounding objects, small and changeable wind speeds), additional elements that locally augment wind velocity and facilitate turbine start may be installed. This paper investigates possible benefits of adding an optimized flow concentrator to a vertical-axis wind turbine (VAWT) rotor. Three-dimensional, unsteady, turbulent, incompressible flow simulations of both isolated rotor consisting of three straight blades and a rotor with flow concentrator have been performed in ANSYS FLUENT by finite volume method for several different operational regimes. This type of flow simulations is challenging since flow angles are high, numerous flow phenomena and instabilities are present and the interaction between the blades and detached vortices can be significant. The rotational motion of the blades is solved by the unsteady Sliding Mesh (SM) approach. Flow field is modeled by Unsteady Reynolds Averaged Navier-Stokes (URANS) equations with k- ω SST turbulence model used for closure. Both quantitative and qualitative examinations of the obtained numerical results are presented. In particular, the two computed power coefficient curves are compared and the advantages of installing a flow concentrator are accentuated.

Key words: VAWT; flow concentrator; CFD; power coefficient

^{*} Corresponding author, email: jsvorcan@mas.bg.ac.rs

1 Introduction

The growing and widespread consciousness of the fossil fuels finality in the past few decades has also led to an accelerated development of the techniques for the energy extraction from renewable resources. Apart from solar, wind energy offers the greatest possibilities for technological advancement and economic exploitation [1]. Wind farms have become a common sight all over the world, Serbia included. Although the first thing that comes to mind when talking about wind farms are large-scale structures with horizontal axis of rotation, there is another option. It is also possible to install small-scale vertical-axis wind turbines (VAWTs) in densely populated areas and urban surroundings where winds are weaker and highly changeable in both space and time [2-3].

Main advantages of VAWTs are their low production and maintenance costs, omnidirectional operability in "dirty", slower winds and decreased noise. On the other hand, their efficiency is low compared to horizontal-axis wind turbines (HAWTs), but can be significantly improved by adequate design, installation and control or by addition of outer elements whose purpose is to direct the flow and locally augment the wind speed, and consequently generated power. This paper investigates the possible benefits of the flow concentrator to the aerodynamic performances of a small-scale VAWT.

Here, the two halves of the flow concentrator are shaped like half-ellipsoids whose semi-major a and semi-minor b axes were optimized in one of the previously performed studies with respect to the oncoming undisturbed velocity profile (defined in accordance with the Earth's boundary layer).

In order to accurately estimate aerodynamic performances of VAWTs many computational models have been tried [4-5], ranging from the simplest momentum models to the full Navier-Stokes equations. However, due to the complex, unsteady aerodynamics and numerous flow phenomena that might appear, contemporary approach to resolving the flow around VAWTs usually assumes performing detailed, spatial and transient CFD simulations [6-10]. The performed numerical study is therefore quite challenging due to the non-uniform wind speed, high values of instantaneous angles-of-attack α and significant interaction between the blades and detached wakes.

2 Numerical simulation

Aerodynamic performances of both an isolated and shrouded (by flow concentrator) wind turbine rotor were estimated by finite volume method in the commercial engineering software package ANSYS FLUENT [11]. The following subsections provide details of the adopted computational approach and made assumptions as well as computational choices/compromises.

2.1 Geometric model

The characteristics of the small-scale straight-bladed VAWT rotor used in this computational study and illustrated in Figure 1 are as follows: rotor radius is $R = 0.75$ m, blade length is $L = 1.5$ m, number of blades is $N_b = 3$, blade chord is $c = 0.10$ m resulting in rotor solidity $\sigma = (N_b c)/(2R) = 0.2$. This lower solidity value generally provides greater values of maximal power coefficient. In order to decrease the rotor production costs, blades are straight and untwisted with the cross-section shaped like a NACA 0018 airfoil.

Flow concentrator comprises two parts, lower and upper half-ellipsoids defined by the values of its semi-major and semi-minor axis. Geometric parameters of the lower part are $a_2 = 2.2$ m and $b_2 = 0.97$ m, and of the upper part are $a_1 = 1.92$ m and $b_1 = 1.0$ m. These values were obtained after an optimization study that was performed for a power-law velocity profile assumed along the inlet boundary:

$$V(h) = V_o \left(\frac{h}{h_o} \right)^\alpha. \quad (1)$$

For the sake of comparison and validation of the performed shape optimization study, an arbitrary flow concentrator geometry was also numerically investigated. This was done in order to observe the differences between the flow fields that appear around an optimized and ordinary concentrator geometry.

The rotational zone of the computational domain is shaped like a hollow cylinder encircling the three blades. Its inner and outer diameters are $d = 1.25$ m and $D = 1.75$ m, respectively. It is also depicted in Figure 1. In order to make the grid generation possible, its height is slightly bigger than the length of the blades.

The extents of the outer stationary sub-domain are: $-5a$ fore and $12a$ aft the central wind turbine shaft along the longitudinal x -axis, $\pm 5a$ along the lateral y -axis and $5L$ along the vertical z -axis starting from the ground where $z = 0$ m.

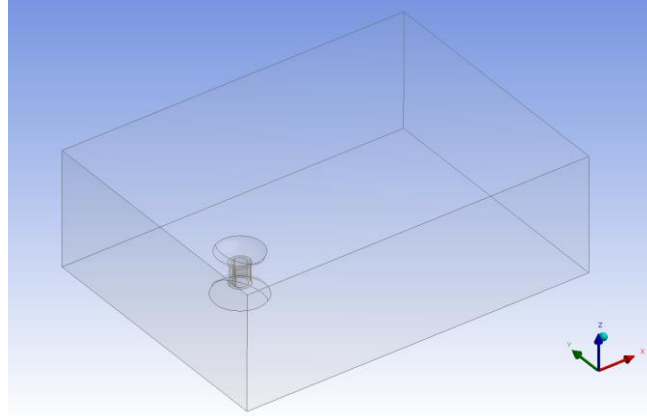


Figure 1. Computational domain with boundaries and separate zones, VAWT rotor and flow concentrator

2.2 Computational grid

Hybrid unstructured computational meshes containing approximately 3-3.2 million cells were used in computations. These medium fine grids were adopted as a compromise between the significant computational complexity on one hand, and limited computational recourses on the other.

Global size functions are applied across the computational domain. They are used to refine the interface surfaces (face sizing 2.5 cm) and ensure that small edges and surfaces are represented correctly (proximity & curvature option). Size functions are also defined along the blade edges, in the chord- and span-wise directions (number of elements is 50 and 60, respectively, while the ratio of the biggest-to-smallest edge size is 5), enabling the creation of the structured mesh along the blade upper and lower surfaces. Cells grow larger in the radial direction from the central shaft towards the outer boundaries.

For modeling the flow adjacent to blade walls as the most critical (in the rotational part of the computational domain), $N = 25$ layers of prismatic cells with a growth rate $q = 1.2$ and the first layer thickness $y_1 = 0.07$ mm resulting in dimensionless distance from the wall $y^+ < 5$ were created. Boundary layers were somewhat relaxed around the flow concentrator ($N = 20$, $q = 1.2$, $y_1 = 0.5$ mm) and ground ($N = 30$, $q = 1.2$, $y_1 = 1.0$ mm) surfaces in order to reduce the total number of elements. Figure 2 provides a detail of one of the used computational meshes.

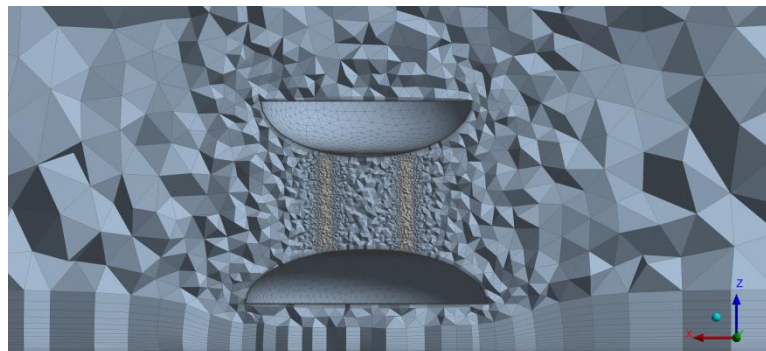


Figure 2. Detail of the used computational grid

2.3 Zonal and boundary conditions

Fluid flow around the wind turbine rotor with and without the flow concentrator is modeled as unsteady and viscous (turbulent). Due to the small velocities, fluid, air, was considered as incompressible gas of constant dynamic viscosity.

The following boundary conditions are defined. At the "velocity inlet" the height-varying magnitude and direction of the undisturbed wind speed V_o together with turbulent quantities – intensity $t = 5\%$ and relative turbulent viscosity $\nu_t/\nu = 10$ are assumed. At the "pressure outlet" the constant value of gauge pressure is set $\Delta p = 0$ Pa. Blades are considered as no-slip rotational walls, while the concentrator walls are stationary.

In order to accomplish different values of tip-speed ratio $\lambda = R\Omega/V_o$ at constant undisturbed wind speed, the rotational motion of the inner zone with angular velocity Ω varied is modeled by the "sliding mesh" approach where the nodes and cells of the rotor mesh zone perform a rigid body rotational motion relative to the outer stationary zone [11]. The interpolation of flow quantities is performed along a non-conformal interface surface separating the two sub-domains.

2.4 Numerical set-up and schemes

Unsteady Reynolds-averaged Navier-Stokes equations are closed by a two-equation $k-\omega$ SST turbulence model, based on Boussinesq hypothesis, that presents a combination of standard $k-\omega$ model near the walls and $k-\varepsilon$ in the outer layer. Its features (modifications) make it more accurate and reliable for flows including airfoils, adverse pressure gradient flows, etc. [12].

Since the flow is considered as incompressible, pressure-based solver is employed, with SIMPLEC pressure-velocity coupling scheme. All spatial derivatives are approximated by 2nd order schemes, while the temporal discretization is of the 1st order.

Time step, $dt = T/180$, corresponds to $\Delta\theta = 2^\circ$ angular increment. Ten iterations per time-step were performed. Simulations for each working regime lasted 3-5 revolutions until reaching quasi-convergence of aerodynamic moment coefficients.

3 Results and discussion

3.1 Quantitative analysis

During each simulation, the values of instantaneous torque Q around the rotation axis are registered. Figure 3 illustrates the computed fluctuations of the torque throughout a single rotation at tip-speed ratio $\lambda = 3.5$ for all three investigated geometries. The highest values obtained with the optimal flow concentrator are marked by a solid black line.

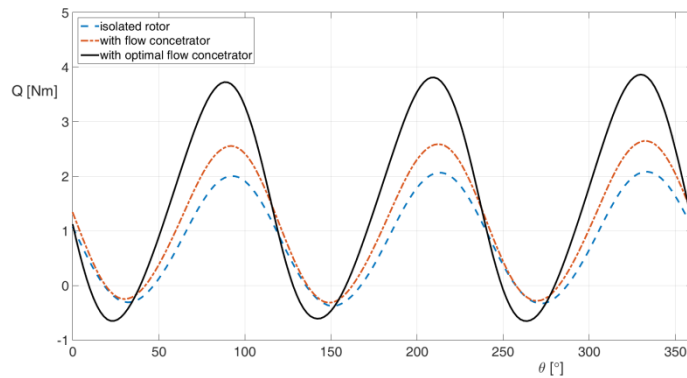


Figure 3. Torque curves during rotor rotation at $\lambda = 3.5$

Mean rotor power P can then be computed as the product of total shaft torque averaged per rotation Q_{mean} and its angular velocity Ω . Power coefficient presents the portion of attainable wind energy. It is estimated as:

$$C_P = \frac{P}{0.5\rho V_o^3 A}. \quad (2)$$

Computed power coefficient curves $C_P(\lambda)$ of all three considered geometries are presented in Figure 4.

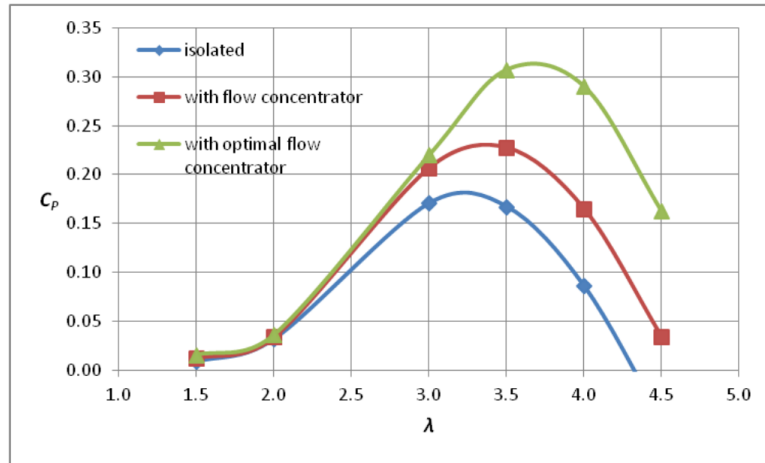


Figure 4. Computed power coefficient curves $C_P(\lambda)$

Figure 4 demonstrates several important facts: wind turbine rotor can be started at low wind speeds, $\lambda_{\min} \approx 1.0$, both without and with the flow concentrator, i.e. the addition of flow concentrator to the rotor does not reduce the starting qualities of small-scale VAWTs, and the maximal expected power coefficient of an isolated rotor of $C_{P,\max} \approx 0.17$ achieved at optimal working regime $\lambda_{\text{opt}} \approx 3.1$ can be increased to $C_{P,\max} \approx 0.31$, i.e. more than 80%, achieved at $\lambda_{\text{opt}} \approx 3.5$ with the optimized geometry of the flow concentrator. This significant increase of both the power coefficient C_P and extracted power P is primarily due to two circumstances: *i*) the accelerated flow field through the flow concentrator, i.e. the increase in available wind power, but also *ii*) more efficient deceleration through the rotor shrouded by the flow concentrator which is precisely what a wind turbine rotor should do – slow down the oncoming air flow and turn the extracted kinetic energy of translational motion to rotational. The changes of velocity profiles across the isolated rotor and the rotor shrouded by the optimal flow concentrator are depicted in Figure 5. The presented values of x -coordinate are measured with respect to the rotational axis where $x = 0$ m, while $x = -0.75$ m and $x = 0.75$ m lie fore and aft of the axis.

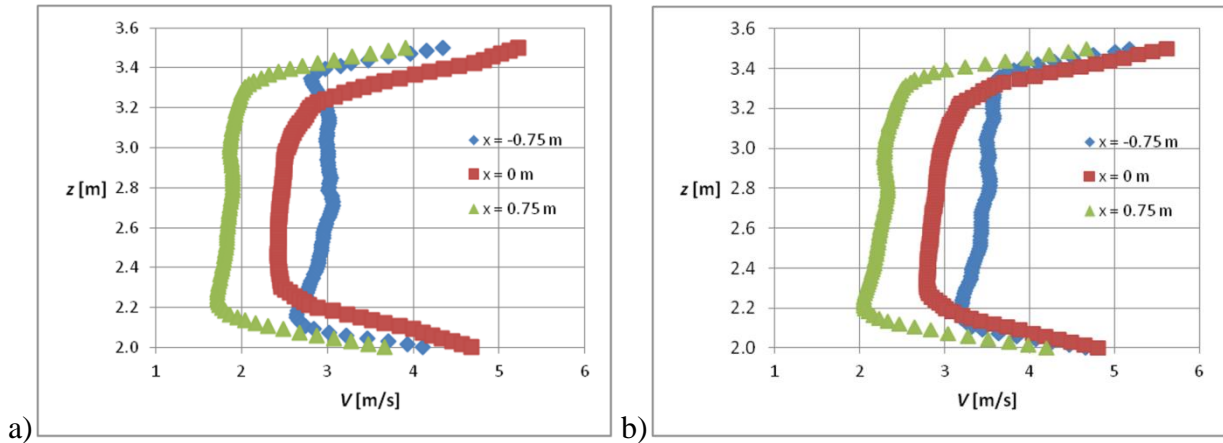


Figure 5. Computed velocity profiles for: a) the isolated rotor and b) the rotor with the optimal flow concentrator

3.2 Qualitative analysis

Finally, instantaneous flow visualizations in the shape of velocity contours and streamlines, respectively, are depicted in Figures 6-7 for $\lambda = 3.5$ and the two rotors, without and with optimal flow concentrator. The effects of both the rotor and flow concentrator on the oncoming air stream are apparent through decelerated zones marked in the dark shades of blue.

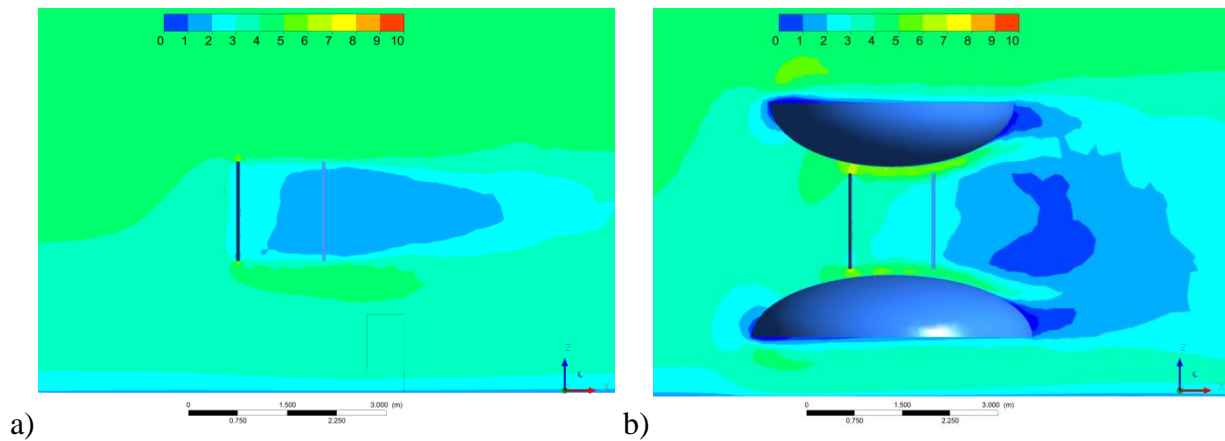


Figure 6. Computed velocity contours around: a) an isolated rotor and b) a rotor with optimal flow concentrator

Apart from locally augmenting the wind speed by making the streamlines through the rotor more compact, the flow concentrator enables the increased deceleration of wind speed by greater expansion of the streamlines downstream of the rotor, i.e. increased energy extraction resulting in higher values of power coefficient. Its benefits are numerous and can be further optimized for a particular location by a proper definition of its geometric parameters.

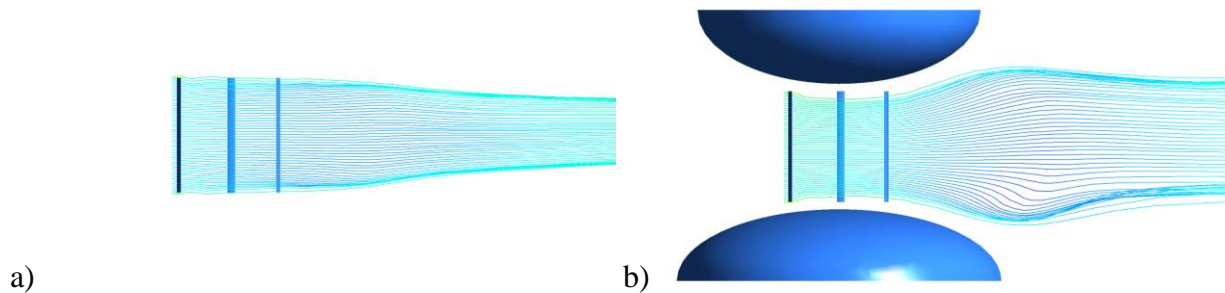


Figure 7. Computed streamlines around: a) an isolated rotor and b) a rotor with optimal flow concentrator

4 Conclusions

The most important conclusions from the performed study can be summed up as follows.

The paper provides a detailed description of all the necessary steps for performing numerical simulation of the 3D, unsteady fluid flow around a vertical-axis wind turbine rotor.

It also investigates the means to improve VAWT efficiency in urban environments by adding additional elements.

By installing a flow concentrator of optimal geometry for a particular location and wind speed profile, the estimated efficiency improvement amounts to more than 80% at tip-speed ratios close to optimal.

Future work will include a more detailed study of the flow concentrator on high-solidity VAWT rotors where the interference between the blades and the shed wakes is more significant.

5 Acknowledgement

This research work was supported by the Ministry of Education, Science, and Technological Development of Republic of Serbia through contracts no. 451-03-68/2020-14/200105 and 451-03-68/2020-14/200026.

6 References

- [1] ***, **IRENA**, Renewable capacity statistics 2019, International Renewable Energy Agency (IRENA), Abu Dhabi, UAE, 2019.

- [2] Bhutta, M. M. A., N. Hayat, A. U. Farooq, Z. Ali, Sh. R., Jamil, Z. Hussain, Vertical axis wind turbine – A review of various configurations and design techniques, *Renewable and Sustainable Energy Reviews*, 16(2012), 4, pp. 1926–1939.
- [3] Stathopoulos, T., H. Alrawashdeh, A. Al-Quraan, B. Blocken, A. Dilimulati, M. Paraschivoiu, P. Pilay, Urban wind energy: Some views on potential and challenges, *Journal of Wind Engineering and Industrial Aerodynamics*, 179(2018), pp. 146–157.
- [4] Islam, M., D. S. -K. Ting, A. Fartaj, Aerodynamic models for Darrieus-type straight-bladed vertical axis wind turbines, *Renewable and Sustainable Energy Reviews*, 12(2008), 4, pp. 1087–1109.
- [5] Manwell, J. F., J. G. McGowan, A. L. Rogers, *Wind energy explained, Theory, Design and Application*, 2nd edn, John Wiley & Sons Ltd., Chichester, UK, 2009.
- [6] Howell, R., N. Qin, J. Edwards, N. Durrani, Wind tunnel and numerical study of a small vertical axis wind turbine, *Renewable Energy*, 35(2010), pp. 412–422.
- [7] Nini, M., V. Motta, G. Bindolino, A. Guardone, Three-dimensional simulation of a complete Vertical Axis Wind Turbine using overlapping grids, *Journal of Computational and Applied Mathematics*, 270(2014), pp. 78–87.
- [8] Balduzzi, F., J. Drofelnik, A. Bianchini, G. Ferrara, L. Ferrari, M. S. Campobasso, Darrieus wind turbine blade unsteady aerodynamics: a three-dimensional Navier-Stokes CFD assessment, *Energy*, 128(2017), pp. 550–563.
- [9] Franchina, N., G. Persico, M. Savini, 2D-3D Computations of a Vertical Axis Wind Turbine Flow Field: Modeling Issues and Physical Interpretations, *Renewable Energy*, 136(2019), pp. 1170–1189.
- [10] Guillaud, N., G. Balarac, E. Goncalves, J. Zanette, Large Eddy Simulations on Vertical Axis Hydrokinetic Turbines – Power coefficient analysis for various solidities, *Renewable Energy*, 147(2020), pp. 473–486.
- [11] ***, ANSYS Fluent Theory Guide, Release 16.0, ANSYS, Inc., Canonsburg, USA, 2015.
- [12] Menter, F. R., M. Kuntz, R. Langtry, Ten Years of Industrial Experience with the SST Turbulence Model, In: *Proceedings of the 4th International Symposium on Turbulence, Heat and Mass Transfer*, pp. 625–632, Begell House Inc., West Redding, USA, 2003.

UPRAVLJANJE PRETVARAČIMA U VETROTURBINAMA

CONTROL OF CONVERTERS IN WIND TURBINES

Stevan JOKIĆ*, Zoran STEVIĆ*

School of Electrical Engineering, University of Belgrade, Belgrade, Serbia

U ovom radu predstavljen je algoritam upravljanja pretvaračem koji se koristi u vetroturbinama. Zbog stohastičkog karaktera brzine i smera vetra potrebno je izvršiti konstantnu kontrolu kako bi se obezbedio maksimalni koeficijent iskorišćenja vetroturbine, a samim tim i maksimalna snaga koja se prenosi konvertorom. Mašina koja se koristi za ovu svrhu je asinhroni generator. On je povezan preko ispravljača na DC link koji je dalje preko invertora i izlaznog filtra povezan na mrežu. Ova simulacija je odrađena za proizvoljni profil brzine vetra i to u Simulink simulacionom paketu.

Ključne reči: vetar, turbine, pretvarači, kontrola, ispravljač, inverter, DC link

In this paper, the control algorithm of converters used in wind turbines is presented. It is necessary to perform a constant control of the stochastic character of the wind speed and direction in order to ensure the maximum efficiency of wind turbines, and thus the maximum power transmitted by the converter. The machine used for this type of turbine is an induction generator. It is connected via a rectifier to a DC link which is connected to the grid via an inverter and an output filter. This simulation is done for a random profile of wind speed in the Simulink simulation package.

Key words: wind, turbines, converters, control, rectifier, inverter, DC link

1 Introduction

With the increased fear of climate change, there is an increased use and application of energy sources that have reduced emissions of carbon dioxide and other greenhouse gases into the atmosphere during their use. First of all, there is an expansion of the use of machines that convert wind energy into electricity. The process itself must be carefully designed because wind is a rather unpredictable source of energy. Namely, the wind speed and its direction are constantly changing. When connecting such sources to the grid, several parameters must be observed. Namely, parameters such as frequency, power and torque must be fully adjusted in order to successfully connect to the network. Also, the network itself is characterized by three important parameters: the frequency of the grid voltage, the electrical angle of the grid and its amplitude value. Therefore, before the advancement in power electronics, connecting such sources to the grid was practically impossible. Today, power converters are so advanced that they perform all the necessary functions with minimal response time and energy consumption. The converter itself consists of several parts. On the machine-turbine side, we use a rectifier based on IGBT transistors, which we control using pulse-width modulation. The machine we use in this simulation is an induction generator, primarily because it is often used in the real case because as it is easiest to place in a wind turbine. It is connected to the wind turbine via a gearbox. Further, the converter contains a single capacitor (DC link) which has the role of maintaining the power supply in the event of sudden voltage drops. Finally, we use an inverter based on IGBT transistors, which we also control by pulse-width modulation. The layout of the entire simulation is given in Figure 1. Figure 2 shows the subsystem of the wind turbine itself.

2 Wind model

For winds of arbitrary density and speed, the effective wind speed can be calculated, which gives the same wind power but respects its standard density of $1,225 \text{ kg/m}^3$. The model for calculating the effective wind speed is given in Figure 3. The inputs to the model are wind speed and density, while the output is the effective wind speed.

* Authors', emails: jokicstevan@gmail.com; zstevic@live.com

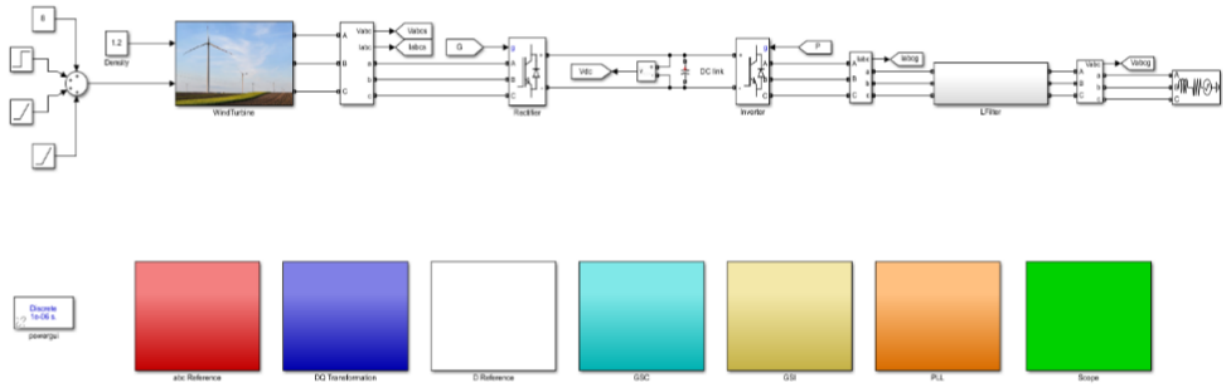


Figure 1 Simulation layout

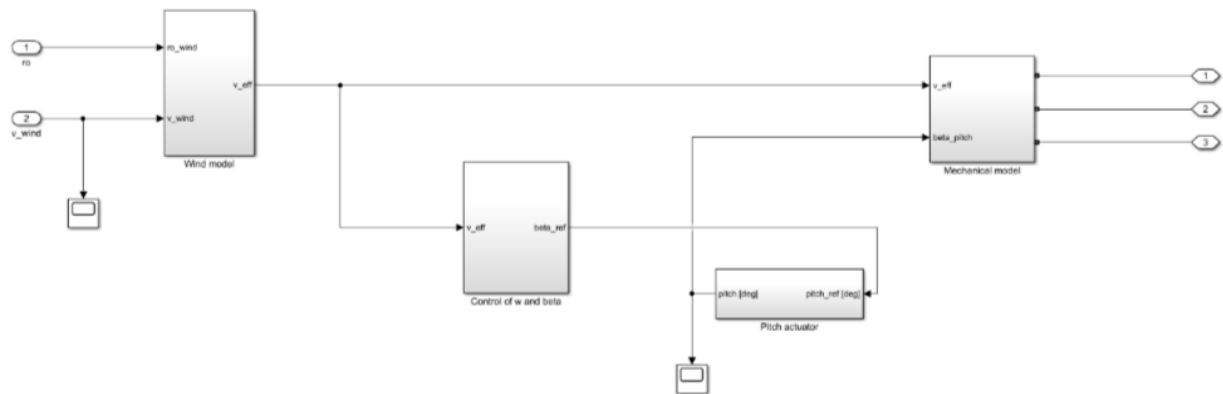


Figure 2 Windturbine subsystem

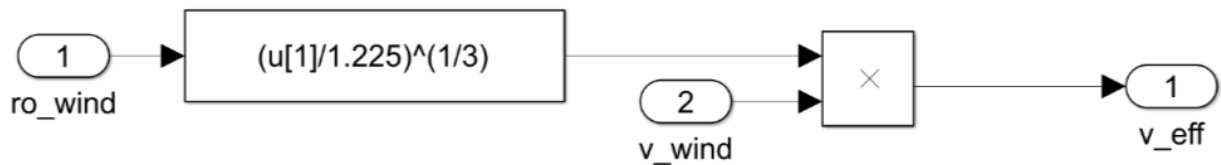


Figure 3 Wind speed model

Figure 4 shows the algorithm for calculating the turbine output power.

The mechanical power extracted from the wind can be expressed as follows [5]:

$$Pm = 0.5 * Cp(\lambda, \beta) * \rho * A * v^3$$

where Pm is the mechanical power output of the wind turbine, $Cp(\lambda, \beta)$ is the power coefficient, λ is the tip-speed ratio (TSR) of the turbine blade, while β is the pitch angle of the blade. The constant ρ represents the density of air, A is the area covered by the wind turbine blades, and v is the wind speed. The gearbox transfers power from the rotating part of the wind turbine shaft to the rotating shaft of the generator. The angular velocity of the generator ω_m is related to the angular velocity of the wind generator ω_t through the following equation:

$$\omega_m = G * \omega_t$$

where G is the gearbox ratio. The ratio of the line speed of the blade tip is related to the angular speed of the wind generator ω_t and the angular speed of the generator ω_m through the following equation:

$$\lambda = \frac{R * \omega_t}{v}$$

where R is the radius of the turbine blades. The power coefficient C_p is a nonlinear function of λ ; several nonlinear C_p models can be found in the literature. In this paper, the power coefficient model is adopted [5]:

$$C_p(\lambda, \beta) = a_1 * \left(\frac{a_2}{\lambda} - a_3 * \beta - a_4 \right) * e^{\frac{(-a_5)}{\lambda}} + a_6 * \lambda$$

with $a_1 = 0,5109$, $a_2 = 116$, $a_3 = 0,4$, $a_4 = 5$, $a_5 = 21$, $a_6 = 0,0068$, $a_7 = 0,08$ and $a_8 = 0,035$.

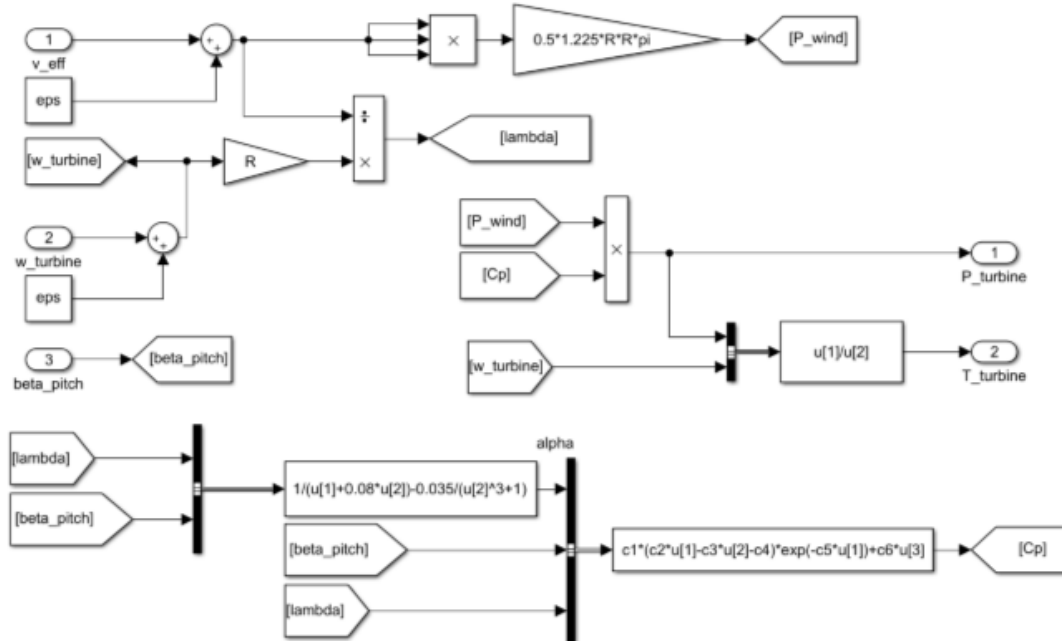


Figure 4 Calculating turbine power

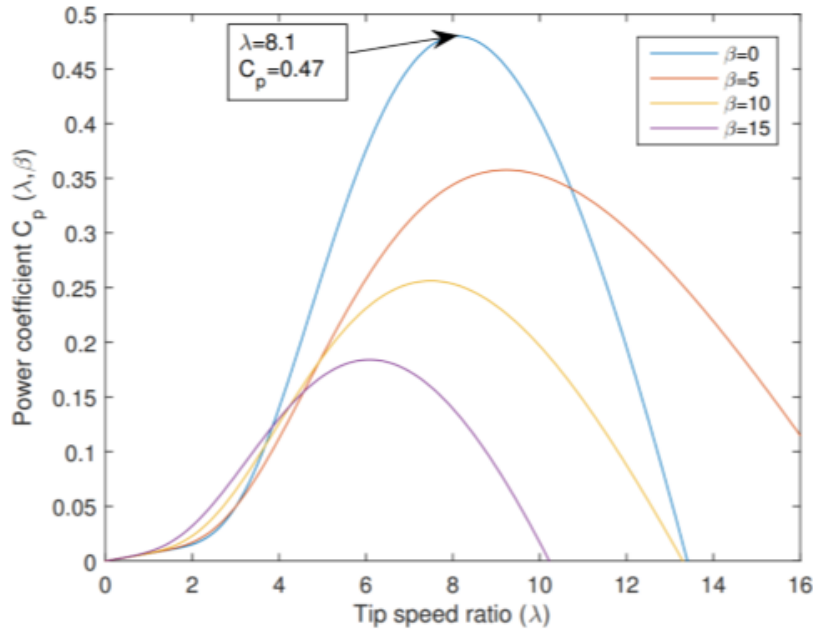


Figure 5 Power coefficient as a function of a tip speed ratio

From Figure 5, which shows the dependence of the power factor on the TSR, can be seen that the maximum value of the power factor C_p is $C_{pmax} = 0.47$. This value is obtained when the angle of inclination β is equal to zero degrees and the corresponding optimal peak velocity ratio is $\lambda_{opt} = 8.1$. In Figure 6 we see the dependence of mechanical power on rotor speed for different wind speeds.

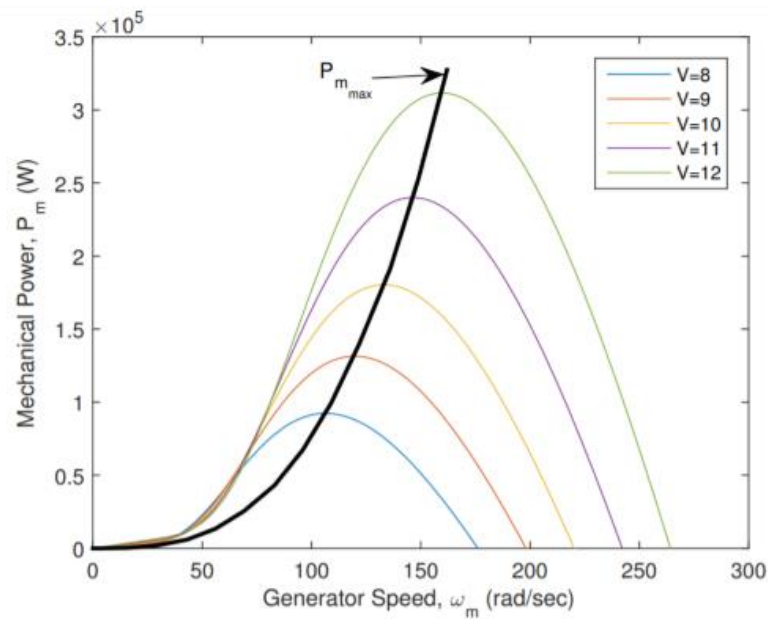


Figure 6 Mechanical power extracted as a function of generator speed

3 Mechanical model of turbine

Figure 7 shows the mechanical part of the turbine, with the following inputs: effective speed, blade angle while the output is the rotor speed. The picture shows that there is a conversion of torque and speed (due to the existence of a reducer).

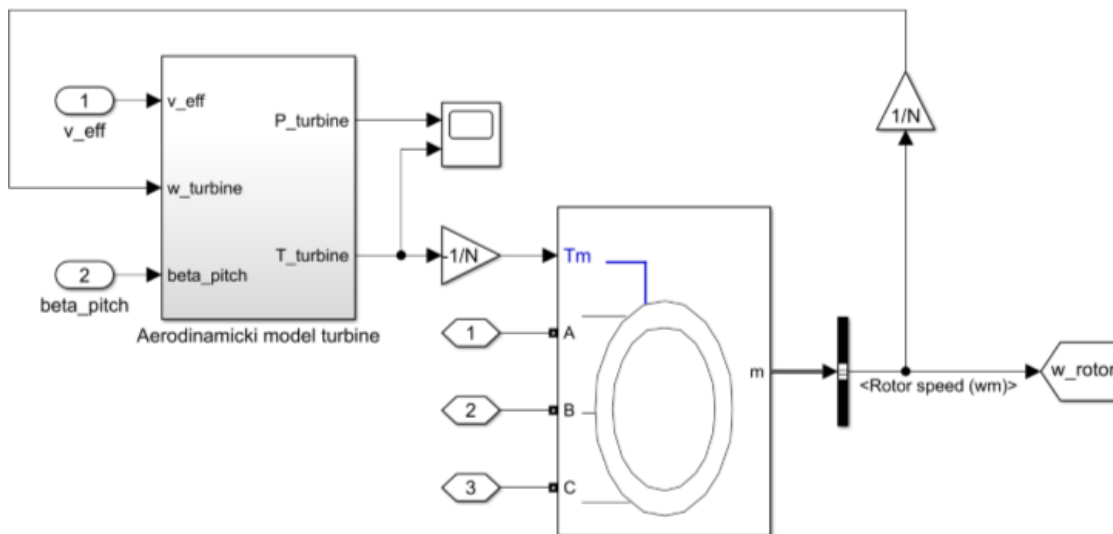


Figure 7 Mechanical part of turbine

Control of induction generator

One of the biggest challenges in designing such converters is to control an induction generator. In this simulation, the method of indirect vector control was used.

The very concept of indirect vector control appeared in the late 1960s, when K. Hasse in his doctoral dissertation explained the method of uncoupled flux and torque control of an induction motor, thus practically reducing asynchronous motor control to DC motor control. The essence of this approach is based on a complex mathematical model of an asynchronous machine and the existence of an energy converter with which we can achieve the necessary phase voltages on it. The mathematical model of a real three-phase asynchronous machine would be very complex and impractical for application, therefore by successive application of Clarke's, three-phase-two-phase, and Park, rotational, transformations from real three-phase machine we make a mathematically equivalent,

imaginary, two-phase machine whose windings rotate synchronously (the so-called Blondel transformation).

By setting the reference dq system so that the entire flux of the rotor is in the axis d ([Equation]), we achieve the set goal, i.e. unbundled control of the flux and torque of the induction machine.

Thus, by setting the value of the stator current in the d axis, we control the flux in the machine, and by using the value of the stator current in the q axis, we control the torque of the machine. The realization of the set values of the stator currents is achieved by means of 2 PI current regulators. If we want the generator to work in speed control mode, we need to add another PI controller which will be superior to the current regulator in the q axis. In order to achieve the regulation described in this way, it is necessary to measure the stator currents as well as the rotor speed. It is necessary to mention that the regulation performed in this way requires double application of Blondel's transformation, in which the frequency of rotor currents is performed by estimation based on reference values of stator currents in the d and q axes, which follows from the equations mentioned above. In Figure 8 we can see the implementation of determining the rotor reference speed at which there is a maximum turbine efficiency.

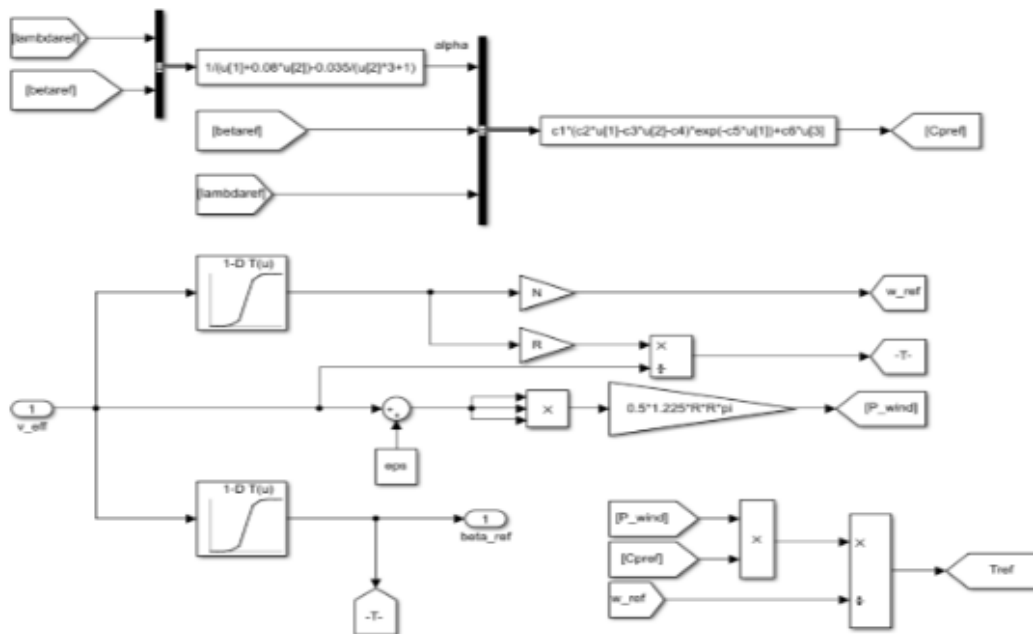


Figure 8 Calculating reference speed of rotor

Figure 9 shows how to control the pitch of the blade (pitch angle).

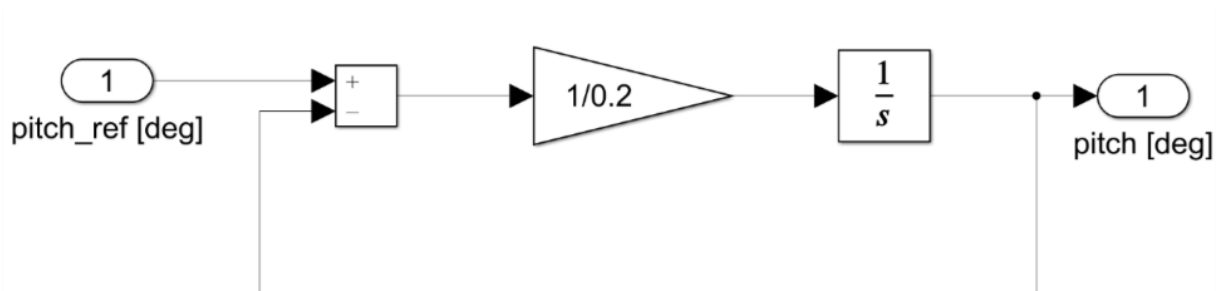


Figure 9 Pitch angle control

Figure 10 shows the control of the converter connected to the generator.

4 Calculating of PI parameters in d and q axis

The parameters of the current regulators in the d and q axes are determined by the principle of optimization of the amplitude characteristic, using the modular optimum, where the parameters of both regulators are the same. We represent a three-phase inverter bridge through its gain and delay,

which is determined on the basis of the carrier frequency, by means of which the pulse width is modulated. The connection between the voltage and the stator current is described via gain and delay, which are obtained from the RL circuit of an equivalent replacement circuit of an induction motor that is in short circuit (ignoring the rotor resistance). The current regulation loop is given in Figure 11 [4].

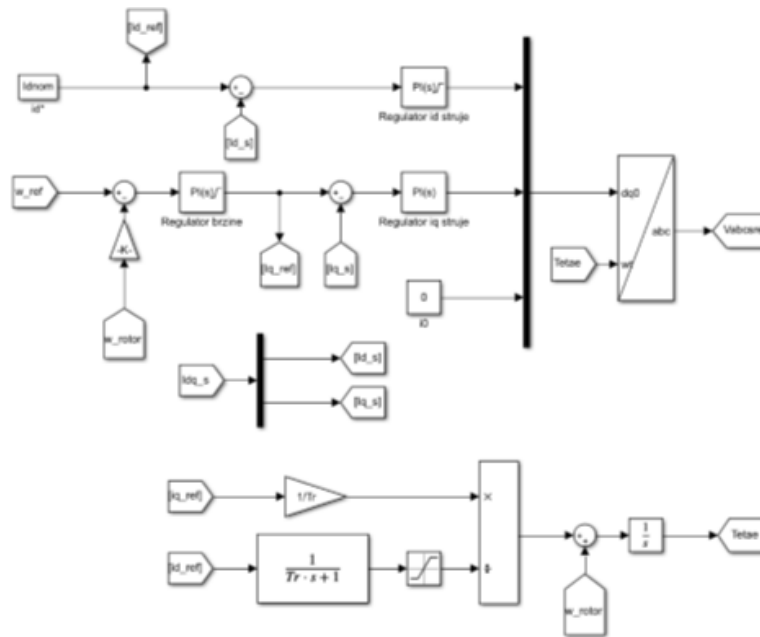


Figure 10 Control of GSC

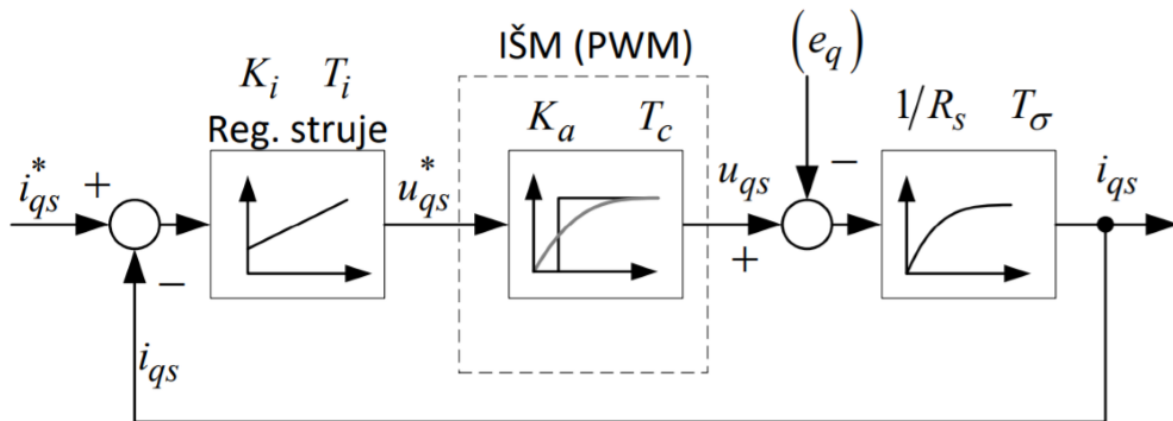


Figure 11 q axis current control

5 Calculating of PI parameters of speed

The parameters of the speed regulator are determined according to the principle of optimization of the amplitude characteristic, applying a symmetrical optimum. The previously solved current loop is equivalent using one transfer function. In the speed feedback, there is a filter whose role is to suppress the noise in the measured speed signal, which has a dominant component at a frequency of 30 Hz at 10% of its value. The gain in the filter branch is determined by the type of speed sensor used. The speed control loop is given in Figure 12 [4].

6 Control of inverter

To convert DC voltage to mains voltage we need an inverter. It consists of 3 branches with 2 switches each. In this analysis, the voltage of the capacitor (DC link) was considered to be constant and can be equivalent to a battery. Each branch is controlled independently.

Inverter control (GSC block) is performed by pulse-width modulation. It was performed in a dq synchronously rotating system because of the reasons presented in the previous part of the paper. Within this control, voltage control with a DC link has been implemented, in order to ensure the transmission of complete active power.

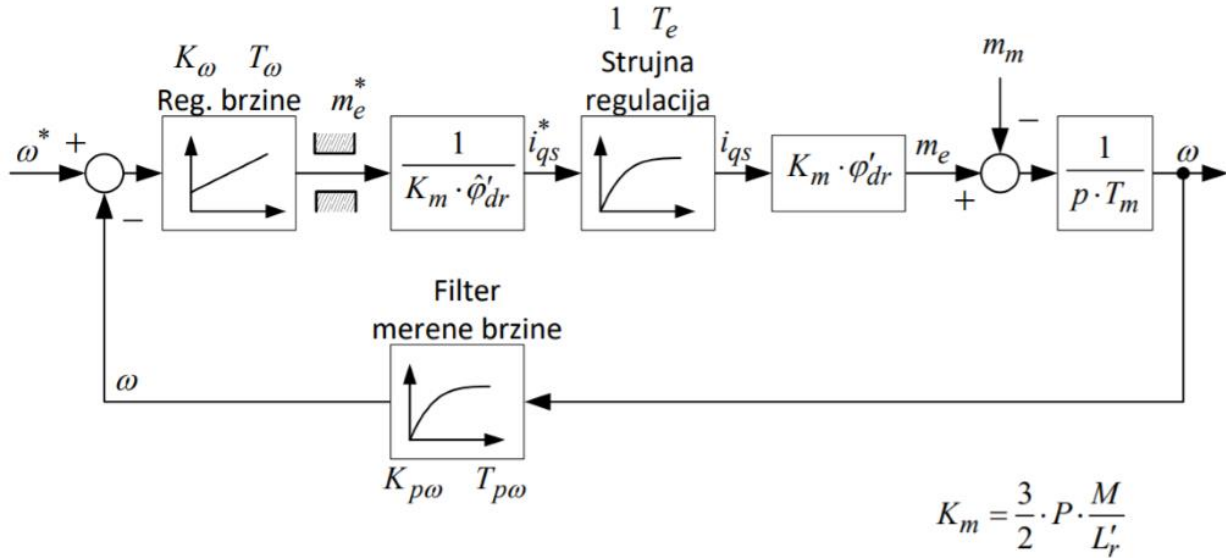


Figure 12 Control of rotor speed

0 The corresponding active and reactive power in a synchronously rotating system are:

$$P = 1.5 * (vd * id + vq * iq)$$

$$Q = 1.5 * (vq * id - vd * iq)$$

By setting the voltage along the q axis to zero, we obtain a completely uncoupled control. Due to the nature of the output provided by the inverter (the current has a saw shape), it is necessary to install an additional filter, which will reduce these ripples. That is why it is necessary to calculate the voltage drops on it in order to perform synchronization (for a given reference of active and reactive power). The equations that apply in this case can be expressed by the following connections:

$$\begin{pmatrix} \frac{dia}{dt} \\ \frac{dib}{dt} \\ \frac{dic}{dt} \end{pmatrix} = \begin{pmatrix} \frac{-R}{L} & 0 & 0 \\ 0 & \frac{-R}{L} & 0 \\ 0 & 0 & \frac{-R}{L} \end{pmatrix} \begin{pmatrix} ia \\ ib \\ ic \end{pmatrix} + \frac{1}{L} * \begin{pmatrix} ua - va \\ ub - vb \\ uc - vc \end{pmatrix}$$

$$\begin{pmatrix} \frac{did}{dt} \\ \frac{diq}{dt} \end{pmatrix} = \begin{pmatrix} -R & \omega L \\ -\omega L & -R \end{pmatrix} \begin{pmatrix} id \\ iq \end{pmatrix} - \frac{1}{L} * \begin{pmatrix} vd \\ vq \end{pmatrix} + \frac{1}{L} * \begin{pmatrix} ud \\ uq \end{pmatrix}$$

$$ud = \left(Kp + \frac{Ki}{s} \right) * (id^* - id) - \omega * L * iq + vd$$

$$uq = \left(Kp + \frac{Ki}{s} \right) * (iq^* - iq) + \omega * L * id + vq$$

The layout of the corresponding block diagram is given in the figure below. The input is represented by the current values of the currents in the d and q axes as well as the voltage value on the capacitor. They are controlled by appropriate PI controllers. This control is shown in Figure 13.

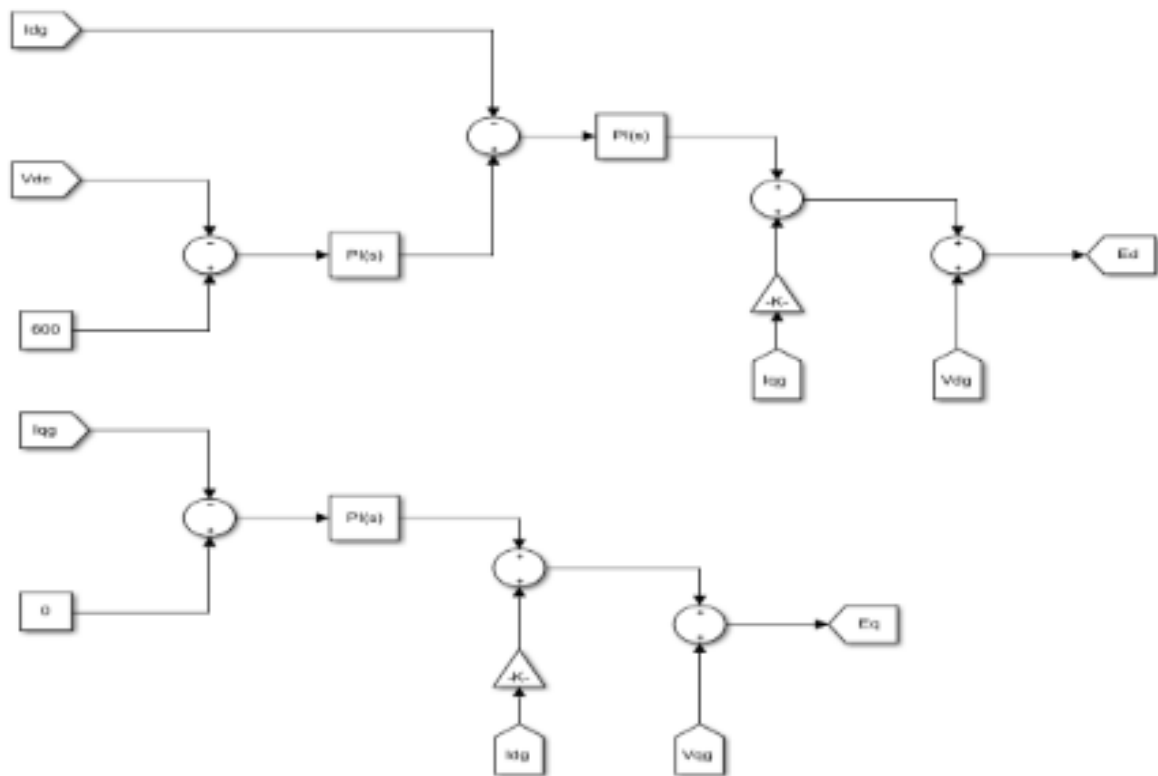


Figure 13 Control of inverter

PLL

In order to perform proper synchronization, it is necessary to determine the electrical angle of the network at the time of sampling. The diagram in the figure below (PLL) is used for this purpose. The input to this loop is the q voltage component that is compared to 0 to determine the difference between the required and current frequency.

In the end, the current frequency is obtained, the integration of which gives the grid angle. This loop is shown in Figure 14.

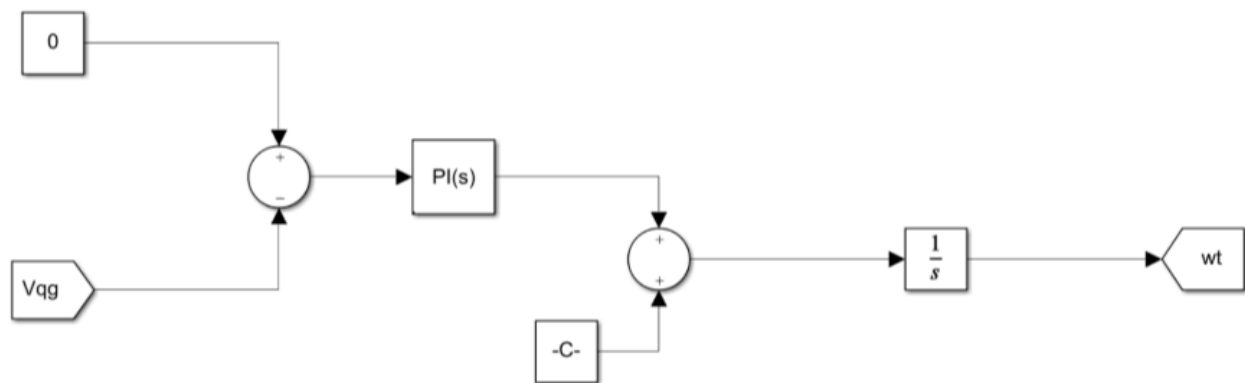


Figure 14 PLL

7 Simulation results

The figures below show the parameters and results of the simulation (lasts about 15s). It is clear from the pictures that the control is designed correctly because the responses are almost instantaneous. The simulation parameters are shown in Figure 15.

```

Editor - C:\Users\Stevan Jokić\Downloads\Konferencija.m
Konferencija.m
1 %Parametri
2 fc=10000;
3 Rs=0.6;
4 Rr=0.23;
5 Landa_s=0.00522;
6 Landa_r=0.00522;
7 M=0.171867;
8 Ls=M*Landa_s;
9 Lr=M*Landa_r;
10 Ts=(Ls*Lr-M^2)/(Lr*Rs);
11 Sn=29266.77/3;
12 Un=380;
13 Ugrid=220;
14 sn=-0.016;
15 nn=1500*(1-sn);
16 idn=3.706*sqrt(2);
17 Fir_n=idn*M;
18 ign=14.351*sqrt(2);
19 igmax=1.5*ign;
20 Mmax=1.5*2*M*igmax*Fir_n/Lr;
21 Mn=1.5*2*M*ign*Fir_n/Lr;
22 J=0.5;
23 p=1;
24 Tr=Lr/Rr;
25 Vdc=1000;
26 Ka=380*sqrt(2)/sqrt(3);
27 Ta=1/fc;
28 Tm=J;
29 Tp=((1/0.2)^2-1)/(2*3.14159*400);
30
31 %Parametri filtra
32 Kpw=1/15;
33 Tpw=sqrt((1/0.1)^2-1)/(2*3.14159*30);
34 Te=Ta;
35
36 %Parametri regulatora
37 Ti=Ts;
38 Ki=Ti*Rs/(2*Ka*Ta);
39 Tw=4*(2*Te+Tp);
40 Kw=2*Tm/(Tw*Kpw*1.5*p*M*Fir_n/Lr);
41

```

Figure 15 Simulation parameters

In Figure 16 we see the appearance of wind speed. This input parameter can be selected arbitrarily.

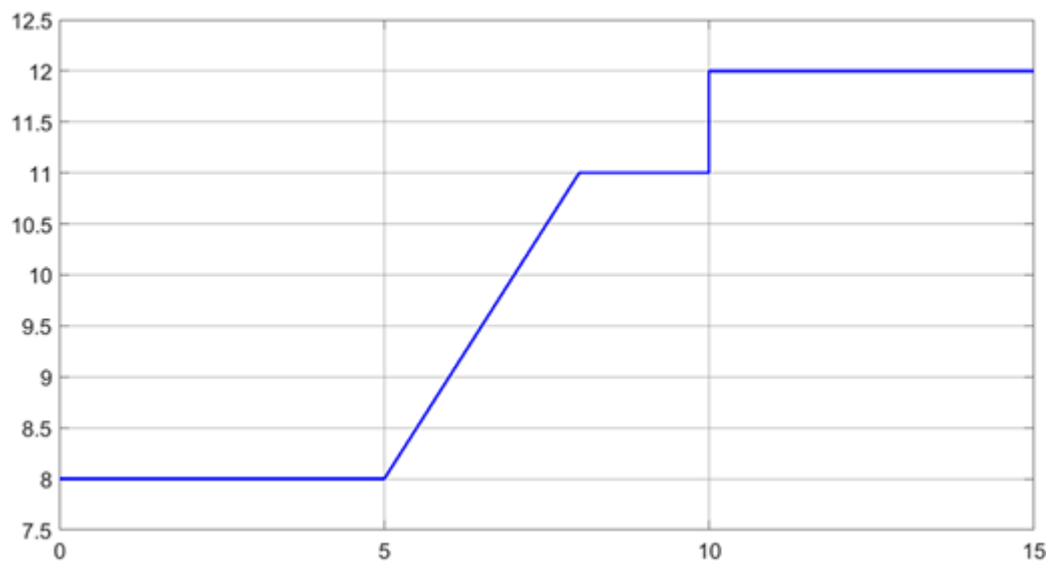


Figure 16 Wind speed

The figures below (17-21) show the simulation results.

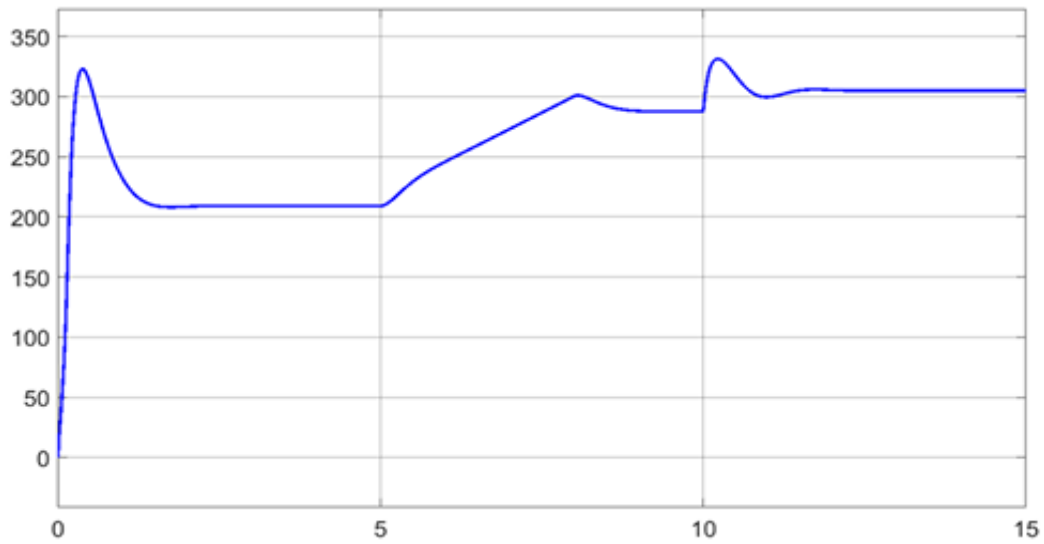


Figure 17 Rotor speed

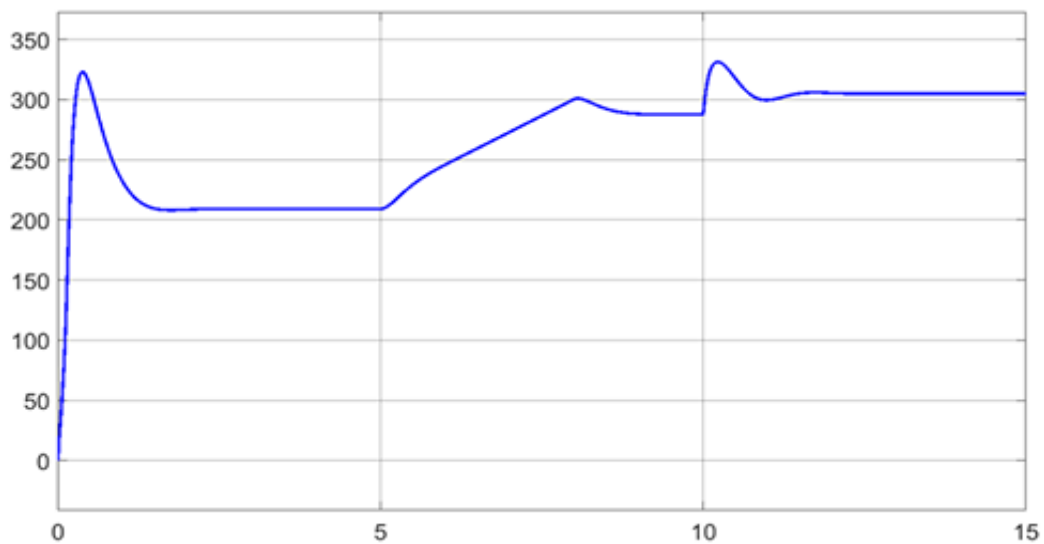


Figure 18 Grid current

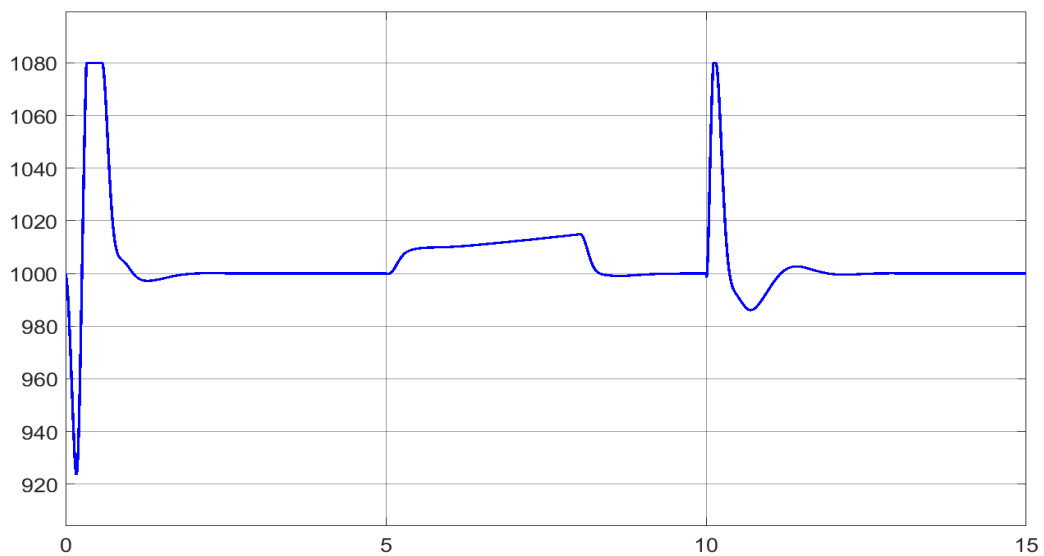


Figure 19 DC link voltage

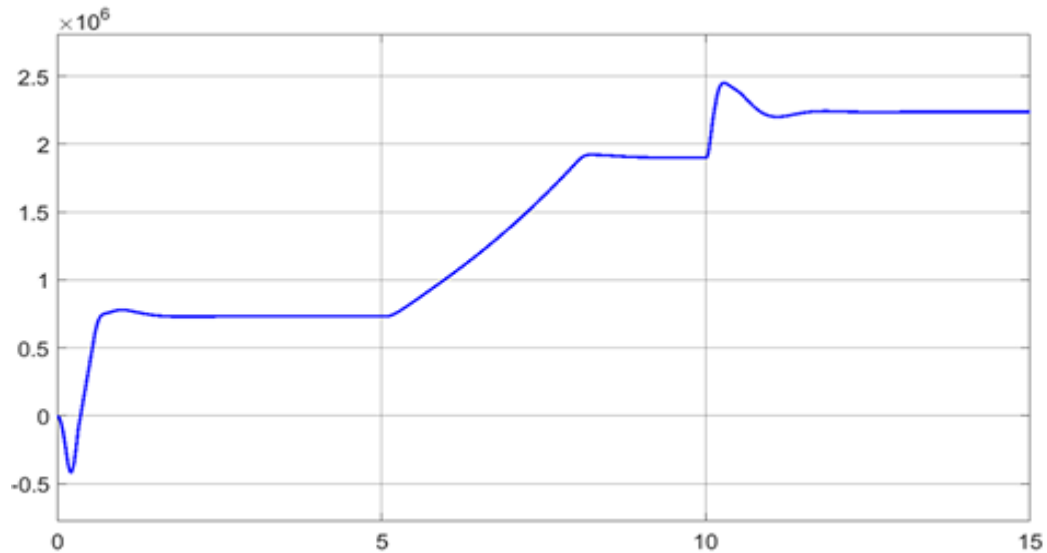


Figure 20 Active Power transmitted to the grid

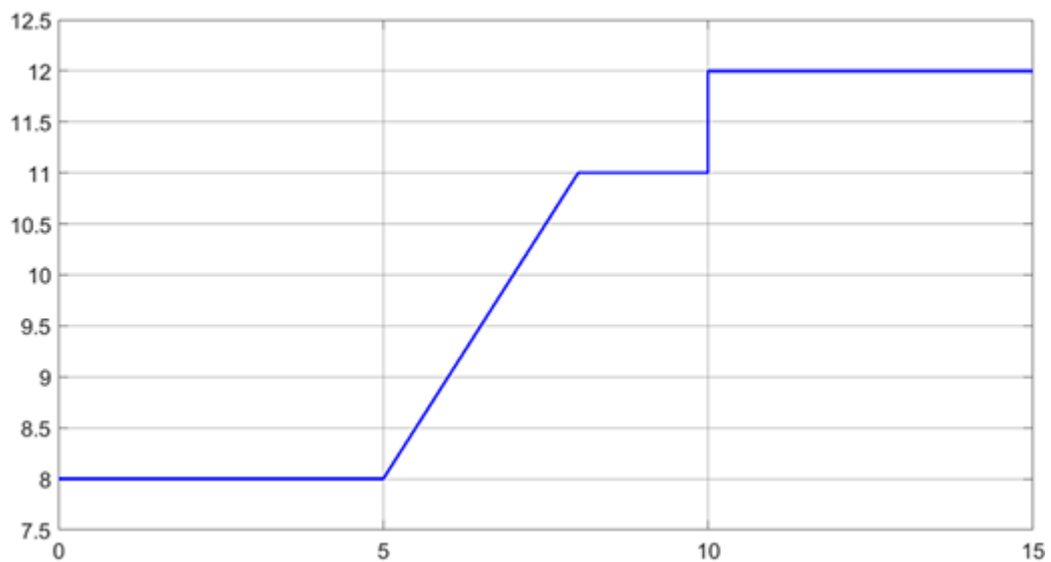


Figure 21 Reactive Power transmitted to the grid

8 Literature

- [1] **Vladan Vučković**, “ Električni Pogoni“, Akademska misao, Belgrade 2002,
- [2] **Slobodan Vukosavić**, “ Električne Mašine“, Akademska misao, Belgrade 2010,
- [3] *** Materials from website www.pogoni.etf.bg.ac.rs,
- [4] *** Materials from website <http://ees.etf.bg.ac.rs/>,
- [5] *** Sliding Mode Control of a Variable- Speed Wind Energy Conversion System Using a Squirrel Cage Induction Generator, *Mohamed Zribi, Muthana Alrifai * and Mohamed Rayan*

NAPREDNI SOFTVERSKI SISTEM ZA MONITORING SOLARNOG NAPAJANJA

ADVANCED SOFTWARE SYSTEM FOR MONITORING OF SOLAR PANELS

Vuk JOVANOVIĆ^{*1}, Ilija RADOVANOVIĆ², Zoran STEVIĆ³

¹ School of Electrical Engineering - University of Belgrade, Computing center
School of Electrical Engineering in Belgrade, Serbia

² School of Electrical Engineering - University of Belgrade, Innovation center of
School of Electrical Engineering in Belgrade, Serbia

³ School of Electrical Engineering - University of Belgrade, Technical Faculty Bor,
University of Belgrade, CIK, Belgrade, Serbia

<https://doi.org/10.24094/mkoiee.020.8.1.155>

Predstavljen napredni solarni sistem za proizvodnju električne energije sa akcentom na softversko unapredjenje monitoringa, prikaz i analizu podataka od značaja u cilju povećanja energetske efikasnosti. Računarski monitoring sistema prikazan je na bazi LabView softverskog alata sa proširenjima i unapredjenjima korišćenjem drugih specifičnih tehnologija i tehnika za obradu podataka. Sistem je testiran, a zatim i pusten u rad u laboratoriji za energetske pretvarače na Elektrotehničkom fakultetu u Beogradu.

Ključne reči: solarni sistemi; obnovljivi izvori energije; monitoring; LabVIEW, Java

In this paper an advanced solar system for power supply is presented, with special attention on software improvement of system monitoring, data display and analytics in order to achieve better energy efficiency. Computer monitoring is displayed using LabView software tool with extensions and improvements using other specific techniques and technologies for data analysis. System was tested, then commissioned in laboratory for power converters, School of Electrical engineering in Belgrade.

Key words: PV system, renewable energy, monitoring, LabVIEW, Java

1 Introduction

Nowadays, the important part of the energy production from renewable energy sources is to cut the costs and to create the more efficient systems. The monitoring of such a system, environment and the conditions in which the energy production is happening is crucial [1]. For PV systems the monitoring of the environmental conditions, as well as its operation is high priority task, following the exposure to different sources of performance degradation and faults especially in urban areas. Different application services are needed in order to convert raw data from sensors to useful information. Since the obtained information is time dependent and corresponds to the measured physical property in the exact time instance, the data volume that would be transferred between end devices and data base should be significantly decreased, so that real-time operations would not be effected [1-3].

Modern era advancement in technology brought the need for fast data exchange, acquisition and processing in almost any field of work. Software solutions are present in every aspect of everyday life and its job is to help us get results, statistics and representation of figures easier, faster and with less trouble than before. Nowadays it is important to have different kinds of reports about the acquired data, with ways to get valuable information from them that can help make future adjustments, decisions and right steps in order to upgrade the system as a whole. PV systems are widely spread and used, with different software solutions used for data acquisition, monitoring and exchange. This paper

^{*} Corresponding author, email: vuk.jovanovic@etf.bg.ac.rs

presents an open source monitoring solution, developed for the PV system at hand. Its purpose is to acquire and parse the data that is generated by the LabView software tool using File I/O protocol [4]. Process and store the data to the relational database and make it available to the end user at real time.

Monitoring software solution developed for the PV system in this paper integrate four very important aspects of Big Data, Volume, Velocity, Variety and Veracity. LabVIEW software tool is used for reading the data from the PV system once every second, and storing it to an output file, at first glance the volume of this data is small, but as this is a continuous reading, the data is linearly growing high velocity data acquiring. Variety of data at the moment is low, but with future addition of different types of sensors and the upgrade of the PV system, the potential of variety in data collected is very high. Using File I/O protocol, as well as scheduling and polling system, the software at hand utilizes periodical file check. It accesses the file location, reads the contents of the file and checks if the file has grown since the last file check operation and by how much. Then it reads and parses the differential between already stored and processed data and the new one in the file. This is the new data acquired by the LabVIEW application from the PV system since the last data check. Once the data is processed and stored to the relational database, it is displayed to the end user in different data-table and chart views which allows different sets of actions and manipulation.

2 Implementation

Modern monitoring systems in various branches of engineering often use one or more different software tools in their line of work. Though not directly associated with IT technologies PV systems have a wide range of possible applications and coexistence with informational technologies. This paper shows only a fragment of possibilities how different technologies can work and cooperate with diverse applications and software tools. As shown, this newly developed software system communicates with existing LabVIEW software tool via File I/O protocol, thereby enabling the cooperation of these two, from the implementational point of view, completely different software packages. It enables the cross-origin communication between two unrelated programs using a simple file I/O protocol, this way enabling data encapsulation, manipulation and processing in real time.

Above described monitoring software is a secure web application developed using a three-layer architecture stack additionally adapted for PV system functionalities. First (bottom) layer used for data storage is implemented using open source RDBMS PostgreSQL, a popular solution known by its performance and stability. Second (middle) layer is used for two purposes. Firstly, for Big data manipulation, reading and processing data retrieved from the PV system, and the process of storing it using Hibernate ORM and JPA included in Spring Data package. Second usage is for delivering data upon client request via secure RESTful web services. This layer is implemented using JAVA based technologies, Spring framework, Spring REST[5], Spring data, OAuth 2.0, JAVA IO etc. Third (front) layer is a javascript (typescript) web client, a frontend application implemented in Angular v.10[6], one of the most advanced open source frameworks, with various extension packages such as PrimeNG, Bootstrap, ngx-charts and others. These three layers communicate securely and share data in order to get the wanted result and present it to the end user via web browser over intranet or internet.

The figure 1. shows the software architecture stack of the system developed and used with the PV system described in this paper as well as the directional flow of data between certain parts of the application.

On the hardware side, the signals from PV panels and the LM35 temperature sensor were led to the input channels (from AI CH0 to AICH7) of the analog-to-digital converter (ADC USB 6009) [7]. The obtained digital signals through the USB port are connected to the computer (PC) in order to be processed by the software.

The application for primary measuring, displaying and storing the data was implemented in the software package LabVIEW [8,9]. Analog signals from the sensors are measured by DAQ Assistant, standard module of the LabVIEW package for the data acquisition.

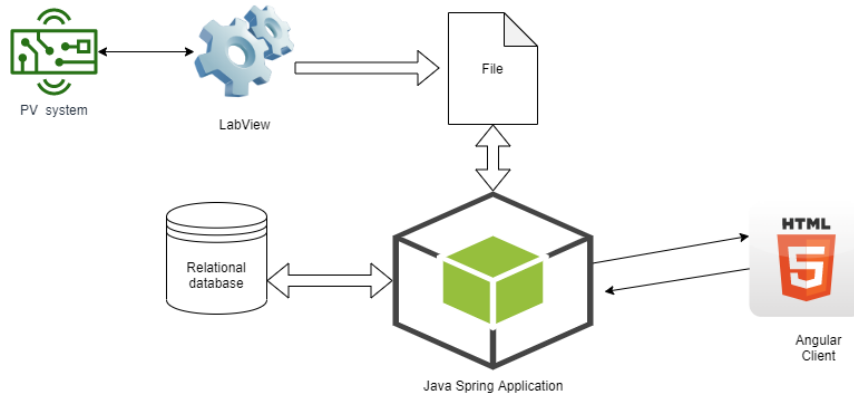


Figure 1. Software technology stack diagram

3 Results

Over a period of 5 days in August data was collected and monitored using the software system described in this paper. The data was continuously read from the PV system and stored to the files via Labview. The files were read accordingly, and parsed values were stored in the database.

The Figure 2. shows data-table data representation, the columns hold values averaged over one minute of time. The functionalities allow the end user to search the table over a period, at exact moments etc. and the search results as well as the initial set of data, can be sorted in ascending or descending order, thereby allowing the user to recognize the points of interest in the data pool presented.

SPR software

Table data representation

Data retrieved from solar panel every 1 second, stored in database, averaged over one minute period, then represented in database

Hour	Minute	Time	V1	V2	Temperature	Power1	Power2	Date
16	46	16:46	17.860V	17.740V	34.117C	6.110W	6.423W	16/08/2020
16	47	16:47	17.790V	17.660V	34.546C	6.436W	6.379W	16/08/2020
16	48	16:48	17.710V	17.580V	33.980C	6.451W	6.320W	16/08/2020
16	49	16:49	17.640V	17.510V	33.813C	6.100W	6.271W	16/08/2020
16	50	16:50	17.560V	17.430V	33.813C	6.322W	6.220W	16/08/2020
16	51	16:51	17.580V	17.450V	33.889C	6.286W	6.160W	16/08/2020
16	52	16:52	17.500V	17.370V	33.887C	6.488W	6.408W	16/08/2020
16	53	16:53	16.980V	17.390V	33.883C	6.456W	6.376W	16/08/2020
16	54	16:54	16.280V	16.750V	33.883C	6.826W	6.736W	16/08/2020
16	55	16:55	16.410V	16.260V	33.883C	6.917W	6.827W	16/08/2020
16	56	16:56	16.310V	16.390V	33.881C	6.982W	6.902W	16/08/2020
16	57	16:57	16.340V	16.430V	33.883C	7.213W	6.937W	16/08/2020
16	58	16:58	16.130V	16.420V	33.883C	7.007W	6.924W	16/08/2020
16	59	16:59	16.480V	16.370V	33.881C	6.977W	6.887W	16/08/2020
17	0	17:00	16.420V	16.320V	33.883C	6.826W	6.886W	16/08/2020
17	1	17:01	16.280V	16.180V	33.883C	6.826W	6.736W	16/08/2020
17	2	17:02	16.100V	16.080V	33.883C	6.886W	6.812W	16/08/2020
17	3	17:03	17.080V	17.210V	33.883C	6.138W	6.477W	16/08/2020
17	4	17:04	17.730V	17.890V	33.786C	6.476W	6.386W	16/08/2020
17	5	17:05	17.330V	17.450V	33.786C	6.271W	6.214W	16/08/2020

No. of records : 8271

Figure 2. Data-table representation of derived data stored in the database

Second part of the application is a graphic representation of data over time. Averaged values over one minute of time are shown in Figure 3. as a multi-valued, multi-axis chart with additional functionalities such as period selection, data series inclusion and exclusion, data point focusing with value comparison etc. For further analysis it is possible to zoom each interval needed, as shown for one-day interval in Figure 4.

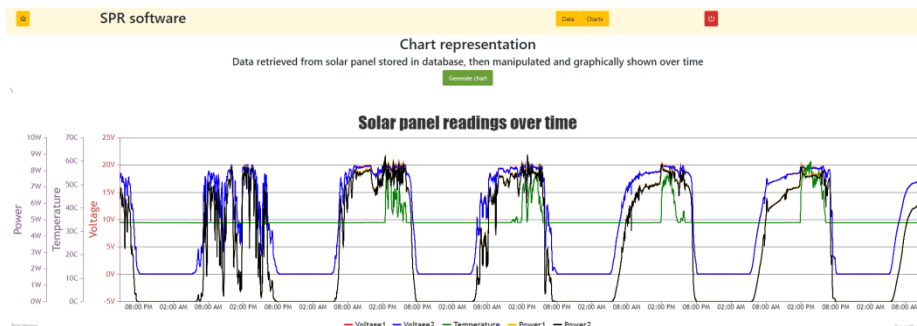


Figure 3. Multi-chart representation of derived data over a 5 day period

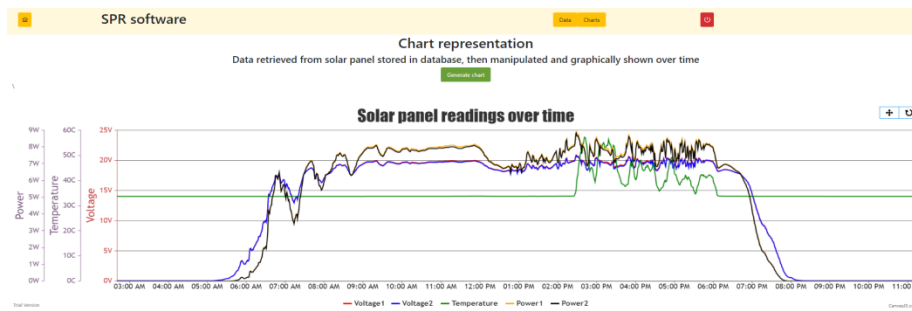


Figure 4. One-day multi-chart representation of derived data

4 Conclusion

Benefits of monitoring PV systems are highly diverse. From better insight to power management to identifying flaws and making decisions for future improvement. The system at hand is a scalable web application that can be easily upgraded to collect additional data and at a higher volume than now. Though developed locally and for the purpose of improvement of the scientific PV system at hand, the plan is to make this application available for educational purposes at all times, so the data is accessible via personalized user accounts. Another upgrade that is planned is a feature that will allow the software not only to monitor, but also to send certain command to the LabView application. Aside from mentioned functionalities there are little limits to improvements that can be made for the software to be more complete and have more use-cases available to the end user.

5 Acknowledgement

The authors gratefully acknowledge financial support from the Ministry of Education and Science, Government of the Republic of Serbia.

6 References

- [1] **I. Radovanović**, Multi channel sensor Measurements in fog computing architecture for renewable energy sources systems monitoring, V MKOIEEE Conference, Beograd, October 2017.
- [2] *** OpenFog Reference Architecture for Fog Computing, OpenFog Consortium, 02/2017.
- [3] **M. Abdelshkour**, "Iot, from cloud to fog computing," March 2015. [Online]. Available: <https://goo.gl/7zNxEd>.
- [4] *** File I/O protocol integration documentation - <https://www.enterpriseintegrationpatterns.com/patterns/messaging/Chapter1.html>
- [5] *** Spring REST protocol implementation documentation - <https://docs.spring.io/spring-restdocs/docs/2.0.4.RELEASE/reference/html5/>
- [6] *** Angular v10 framework official documentation - <https://angular.io/docs>
- [7] *** NI USB-6008/6009. National Instruments, USA, 2015, <http://www.ni.com/pdf/manuals/371303n.pdf>.
- [8] *** National Instruments. LabVIEW Basic I Course Manual. September 2006. Part Number 320628G-01.
- [9] *** National Instruments. User Manual, 2010 Edition. Part Number 320999C-01.

ANALIZA I POREĐENJE RAZLIČITIH METODA MPPT KOD PV SISTEMA NAPAJANJA

ANALYSIS AND COMPARISON OF DIFFERENT MPPT METHODS IN PV POWER SYSTEMS

Zoran STEVIĆ^{*1}, Miša STEVIĆ², Ilija RADOVANOVIĆ³

¹ School of Electrical Engineering - University of Belgrade, Technical Faculty Bor,
University of Belgrade, CIK, Belgrade, Serbia

² Mikroelektronika, Belgrade

³ School of Electrical Engineering - University of Belgrade, Innovation center of School of
Electrical Engineering in Belgrade, Serbia

U radu su dati pregled stanja i uporedna analiza različitih metoda praćenja tačke maksimalne snage (MPPT – Maximum Power Point Tracking) PV sistema napajanja. Za date konfiguracije i uslove predložene su optimalni algoritmi.

Ključne reči: MPPT; PV sistemi; uslovi delimičnog zasenčenja; procena efikasnosti

The paper presents an overview of the state and comparative analysis of different methods of the maximum power point tracking (MPPT - Maximum Power Point Tracking) of the PV power system. Optimal algorithms have been proposed for the given configurations and conditions.

Key words: MPPT; PV systems; partial shading conditions; performance evaluation

1 Introduction

The voltage and current of the solar panel, ie its power, depend on several factors, the most important of which are the intensity of solar radiation and ambient temperature. Typical curves of current and power of the solar panel on its voltage are given in Fig. 1.

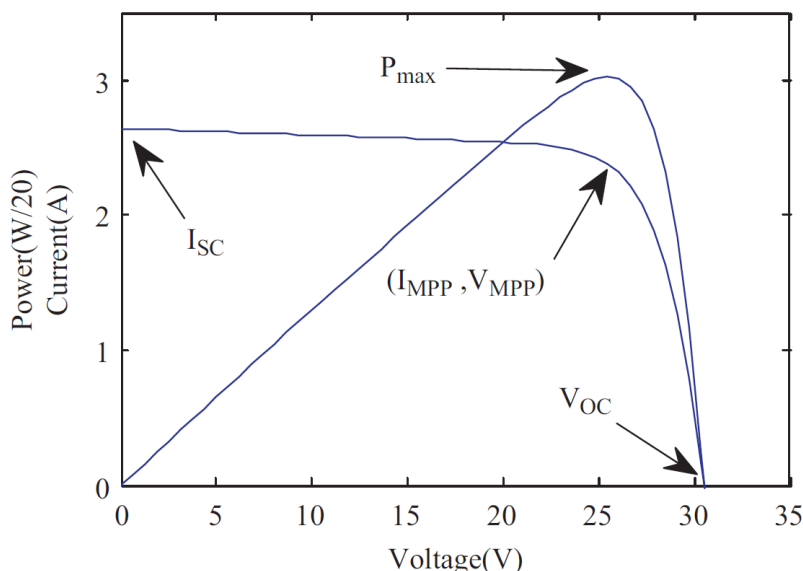


Figure 1. I-V and P-V characteristics of solar cell [1]

In the given operating conditions, there is still only one point at which the power of the solar panel is maximum. Considering the low degree of efficiency of solar panels and the existence of only one point of their maximum power under certain operating conditions, it is very important to obtain and monitor the maximum power from solar panels. In order to obtain the maximum power from

^{*} Corresponding author, email: zstevic@tfbor.bg.ac.rs

them, the load must be constantly adjusted to their operating point, ie the load line of the load must intersect the point of maximum power of the solar panels. Therefore, it is necessary to insert a converter (DC / DC or DC / AC) between the solar panel and the load, which have the function of finding and monitoring the maximum power point of the solar panel, or adjusting the load to the operating conditions of the solar panel. The process of tracking the maximum power point of solar panels is called the MPPT (Maximum Power Point Tracking) procedure. MPPT algorithms also determine the operating point of the inverter.

Several different MPPT algorithms have been developed, such as: P&O (perturbation and observation), incremental conductance method, no-load voltage methods, solar panel short-circuit current methods, phase-logic method, neural network-based methods, etc. [1] .

The solar power system generally consists of three basic parts: a solar panel, a converter and a load. The MPPT procedure is impossible to perform without the existence of a converter between the solar panel and the load. There are many different topologies for both DC and AC solar power systems. In recent times, a voltage buck-boost converter is most commonly used. Depending on the value of the duty cycle of the control pulses, this inverter can either a lower or raise the voltage [2].

2 MPPT methods

MPPT algorithms can be evaluated by various criteria, such as complexity, number of required sensors, convergence rate (reaching the point of maximum power of the solar panel), adaptability to rapid changes in atmospheric conditions, price, efficiency, application in certain applications, implementation hardware, etc. .

2.1 Perturbation and observation algorithm (P&O)

The perturbation and observation algorithm is based on the perturbation of the DC-DC converter duty cycle and the perturbation of the DC line operating voltage between the photovoltaic module and the converter. The change in voltage is caused by the perturbation of the converter duty cycle. If there is an increase in power, the perturbation is maintained in the same direction, and if the power decreases, the direction of the next perturbation changes [3].

2.2 Incremental conductance algorithm

The incremental conductance algorithm modifies the voltage relative to the voltage corresponding to the point of maximum power. It is based on the incremental and instantaneous conductivity of the photovoltaic module. Figure 2 illustrates the principle of operation of this algorithm [3].

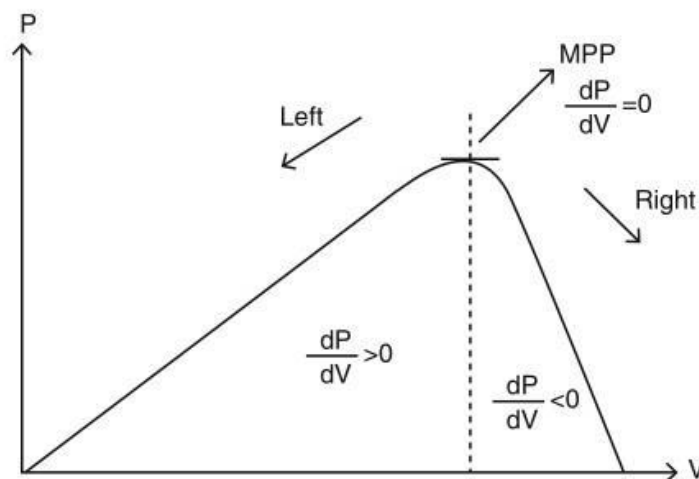


Figure 2. Illustration of the principle of operation of the incremental conductance algorithm [3]

At the point of maximum power, the slope of the voltage and power curve is equal to zero. To the left of the point of maximum power is positive, and to the right of it is negative. The speed of

reaching the maximum power depends on the size of the increment, but this speed is higher in relation to the perturbation and observation algorithm [4]. Negative features of this method are the possibility of faulty monitoring the conditions of rapid changes in atmospheric parameters and setpoints oscillations around the point of maximum power.

2.3 Idle fractional voltage algorithm

The no-load fractional voltage algorithm is based on an almost linear relationship between the no-load voltage and the voltage at the point of maximum power of the photovoltaic module, through variable values of temperature and radiation [5]:

$$V_{MPP} \approx k_1 V_{OC}$$

The coefficient of proportionality depends on the type of photovoltaic module and needs to be determined. Most often, its value ranges from 0.71 to 0.78 [3]. This method works by periodically measuring the no-load voltage, which requires a short-term shutdown of the converter. To avoid this, an unloaded pilot cell is installed, from which the no-load voltage is determined. After that, the closed voltage on the converter asymptotically reaches the appropriate voltage. The pilot cell should represent the characteristics of the photovoltaic module. Linearity is an approximation, so that in reality work is never achieved at the point of maximum power, but for certain applications and situations the accuracy is satisfactory. The good side of this method is the cheap implementation. However, in cases of partial illumination of the module, several local maximums of the voltage-power curve appear, so that the coefficient is not valid in this case, so this method cannot be applied. The problem also arises if the atmospheric conditions on the implemented pilot cell are different from the conditions on the photovoltaic module [3-5].

2.4 Fractional short circuit current

Just like in the fractional open circuit voltage method, there is a relationship, under varying atmospheric conditions, between the short circuit current I_{SC} and the MPP current, I_{MPP} , as is shown by:

$$I_{MPP} \approx k_2 I_{SC}$$

The coefficient of proportionality k_2 has to be determined according to each PV array, as in the previous method happened with k_1 . The constant k_2 is between 0.78 and 0.92.

2.5 Extremum Seeking Control method (ESC)

ESC is a robust and adaptive control techniques for non linear dynamic uncertain systems. It is based on theories namely averaging theory, adaptive control and singular perturbation techniques. The objective of ESC is to rapidly reach the MPP despite uncertainties and disturbances on the PV panel and the load. The reference current is perturbed by a sinusoidal modulation. The power got at the output of the PV system is high pass filtered, to get only effect of the perturbation.

2.6 Artificial neural network (ANN)

ANN is a representation of interconnected artificial neurons (nodes), similar to the structure of the biological brain. In general ANN consists of three layers: input, hidden and output. A simple configuration of ANN to identify MPP in PV is illustrated in Fig. 3. The irradiance, temperature, V_{oc} , and I_{sc} are normally used as input layer, while the output may be in the form of voltage, duty cycle or current depending. In each layer the numbers of nodes are defined by the user and varied based on the requirement [2].

2.7 Comparison of MPPT methods

Each of these methods has its advantages and disadvantages. That is why we are constantly working on modifying the standard methods and setting up new ones, and often resort to hybrid methods. Table 1 shows the basic characteristics for the most commonly used methods, so that the optimal method can be chosen according to the circumstances.

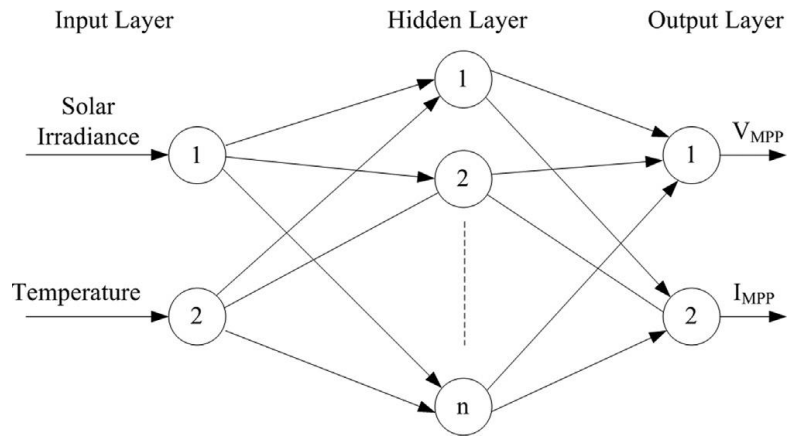


Figure 3. A typical ANN structure for MPPT [2]

Table 1. Comparison of MPPT methods

MPPT method	Complexity	Convergence speed	Sensed parameters	Efficiency
Open circuit voltage	Low	Medium	Voltage	Low (86%)
Short circuit current	Medium	Medium	current	Low (89%)
Artificial neural networks	High	Fast	Depends	High (98%)
Fuzzy logic	High	Fast	Depends	High
P&O (fixed perturbation size)	Low	Low	Voltage and current	Low
P&O (variable perturbation size)	Medium	Fast	Voltage and current	High (96%)
ESC	Medium	Fast	Voltage and current	High (97%)
IncCond	Medium	Depends	Voltage and current	High

3 Conclusion

The advantages and disadvantages of the most commonly used MPPT methods are discussed, including ease of implementation, costs as well as all hardware requirements. The requirements are often conflicting, so it is always necessary to find the optimal solution. In addition to the developed optimization methods, the experience and creativity of the designer are also required. In further research, special attention will be paid to the integration of microprocessor control MPPT and related electronics, the application of embedded systems and IoT.

4 Acknowledgement

The authors gratefully acknowledge financial support from the Ministry of Education and Science, Government of the Republic of Serbia.

5 Literature

- [1] **Ali Reza Reisi, Mohammad Hassan Moradi, Shahriar Jamasb**, Classification and comparison of maximum power point tracking techniques for photovoltaic system: A review Renewable and Sustainable Energy Reviews 19 (2013) 433–443
- [2] **Jubaer Ahmed, Zainal Salam**, A critical evaluation on maximum power point tracking methods for partial shading in PV systems, Renewable and Sustainable Energy Reviews 47 (2015) 933–953
- [3] **L. Ashok Kumar, P. Surekha, S. Sumathi**, Solar PV and Wind Energy Conversion Systems, Springer, 2015
- [4] **F. H. Math Bollen**, Integration of distributed generation in the power system, 2011
- [5] **M. I. Ioan Viorel Banu**, "Modeling of Maximum Power Point Tracking Algorithm for Photovoltaic Systems," 2012.

SOLARNA ENERGIJA U SRBIJI

SOLAR ENERGY IN SERBIA

Sanja PETROVIĆ*, Miomir MIKIĆ, Daniela UROŠEVIĆ

Mining and Metallurgy Institute Bor

Razvoj obnovljivih izvora energije je od izuzetnog značaja za svaku zemlju. Srbija ima znatno veći broj časova Sunčevog zračenja nego većina evropskih zemalja, a najbolji uslovi su u jugoistočnom delu naše zemlje. Najveći deo tehnologija obnovljivih izvora energije se direktno ili indirektno napaja iz Sunca. Direktno korišćenje energije Sunca podrazumeva korišćenje solarnih panela ili kolektora pri čemu se solarna energija pretvara u toplotnu energiju i kao takva se uglavnom koristi za zagrevanje vode. Drugi vid direktnog korišćenja solarne energije jeste koncentrisanje solarne energije u jednu tačku u kojoj se tečnost zagreva i kao takva se koristi za proizvodnju električne energije. Korišćenje energije Sunca ostvaruje se i primenom solarnih ćelija, odnosno pretvaranjem solarne energije direktno u električnu energiju.

Ključne reči: obnovljivi izvori energije; solarne ćelije

The development of renewable energy sources is extremely important for every country. Serbia has a significantly higher number of hours of solar radiation than most European countries, and the best conditions are in the southeastern part of our country. Most renewable energy technologies are directly or indirectly powered by the sun. Direct use of solar energy implies the use of solar panels or collectors where solar energy is converted into thermal energy and as such is mainly used to heat water. Another type of direct use of solar energy is the concentration of solar energy in one point where the liquid is heated and as such is used to produce electricity. The use of solar energy is also achieved by using solar cells, ie by converting solar energy directly into electricity.

Key words: renewable energy sources; solar cells

1 Introduction

Solar energy is a renewable and unlimited source of energy. Therefore, the development of solar technology is extremely important. Using this type of energy can ensure the production of hot water and electricity from renewable energy sources without the emission of harmful gases into the atmosphere. There are two types of solar systems that are used for the production of electricity:

- Photovoltaic modules that convert solar energy into electricity (the atoms emit electrons at the absorption of luminous energy and thus creating photoelectric effect) and
- Solar energy is focused on mirrors and concentrators at the point of maximum production of heat energy from which electricity is produced by using conventional methods (steam turbine or otherwise).

Photovoltaic cells or PV cells can be producer in many different ways as well as from a many different materials. The most common material for solar panel construction is silicon which exhibit semiconducting properties [1]. Several of these solar cells are required to construct a solar panel and many panels make up a photovoltaic array.

In effect, there are three main types of PV cell technologies which are the most common in the world market: monocrystalline silicon, polycrystalline silicon and thin film. Due to high cost, high-efficiency PV technologies, including gallium arsenide and multi-junction cells, are rarer, but on the other hand, they are ideal for use space applications as well as in the in concentrated photovoltaic systems The actual PV cell technologies include Perovskite cells, dye-sensitized solar cells and quantum dots as well as organic solar cells [2].

Concerning PV module production in 2019, China (main land) holds the lead with a share of 66%, followed by Rest of Asia-Pacific & Central Asia (ROAP/CA) with 18%. Europe contributed

* Corresponding author, email: sanja.bugarinovic@irmbor.co.rs

with a share of 3%; USA/CAN contributed 4%. In 2019, Europe's contribution to the total cumulative PV installations amounted to 24% (compared to 25% in 2018). In contrast, installations in China accounted for 36% (same value as the year before) [3]. PV Module Production by Region - Global Annual Production is presented in Figure 1.

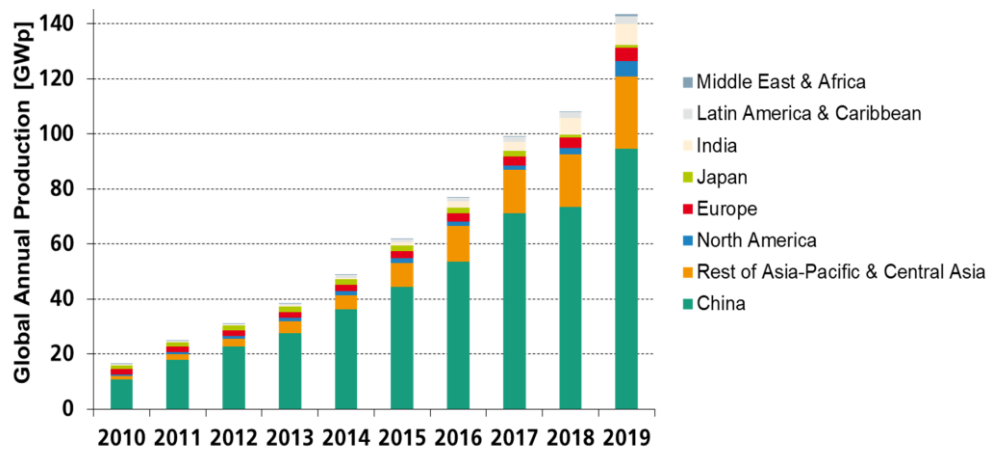


Figure 1. PV Module Production by Region - Global Annual Production [3]

2 Solar energy in Serbia

The number of hours of solar radiation is significantly higher in Serbia than in many European countries (between 1500 and 2200 hours per year) [4]. The assessment of the solar energy share in the total RES potential is 0.64 millions toe annually (16.7%) in Serbia. The most favorable conditions are in the southeastern part of the country. At the annual level, the average value of global radiation energy for the territory of the Republic of Serbia is 1200 kWh/m²/year. In north western Serbia, the average value of global radiation energy is up to 1550 kWh/m²/year. In the central part of Serbia, this value is about 1400 kWh/m²/year. The degree of radiation utilization depends on the characteristics of the built-in heat receiver, so that the average value of available useful energy in the Republic of Serbia is about 700 kWh/m² per year [5]. The average daily energies of global radiation on the horizontal surface in Serbia are presented in Figure 2 [6, 7, 8].

For the first time, the Government of the Republic of Serbia provided the opportunity for the construction of solar power plants in Serbia through subsidies with the by introducing the By-law on Feed-in tariffs for the production of energy from renewable energy sources and combined heat and power generation from 2009. Also, the government further increased the capacity and reduced the subsidized price through two new Regulations from 2013 and 2016 [9].

The currently prescribed quotas of the Government of the Republic of Serbia for solar are 10 MW, and it is divided as follows:

- 4 MW for solar power plants on facilities, with half of this power provided for small solar power plants up to 30kW, and the other half for solar power plants from 30 to 500 kW;
- 6 MW is prescribed for solar power plants on the ground.

3 Solar plant

Investment in larger solar power plants can lead to profit. On the other hand, for construction of such plant, it is necessary to meet technical, administrative and financial conditions and obtain a series of permits and approvals issued by competent state authorities. According to unofficial data, about 15 000 m² of solar collectors are installed annually in Serbia. In Kikinda, the first phase of the solar power plant was built in October 2015. Regarding all renewable sources it can be said that solar parks are the most active in Serbia from all renewable sources and 8.5 MW of these investments have been implemented since the planned 10 MW [8]. This one plant in the Kikinda is one of the largest and the second largest in Vojvodina and the fourth in Serbia. The incentive purchase price of electricity from solar energy is on average 20 eurocent·kWh⁻¹ [10].

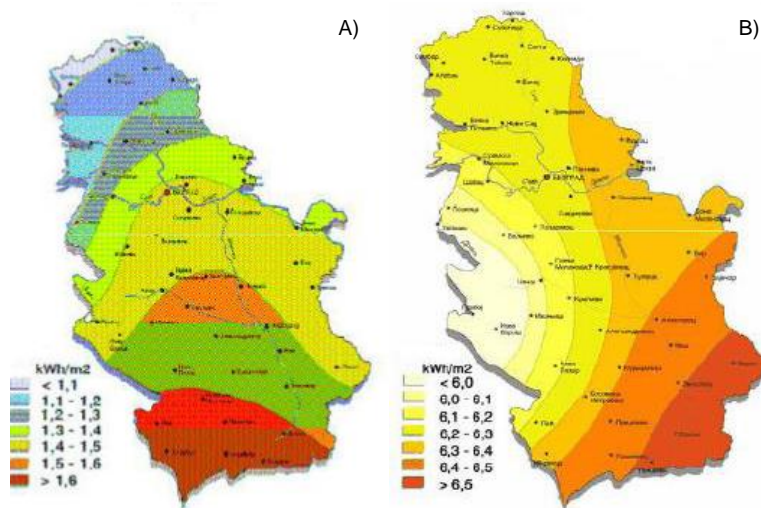


Figure 2. Average daily energy of global radiation on the horizontal surface in Serbia A) January, B) July [6,7]

Average purchase prices of electricity produced from renewable energy sources is presented in Table 1.

Table 1. Average purchase prices of electricity produced from renewable energy sources [10]

Type of power plant	The price of the installed power (Euro·kW ⁻¹)	Average purchase price (eurocent·kWh ⁻¹)
Small hydroelectric power plants	2000	9
Wind power plant	1000	9.5
Solar power plant	2000	20

4 Conclusion

Solar energy represents the energy potential of the Republic of Serbia, which can be used for the production of heat or electricity. The Republic of Serbia has favorable climate conditions for use of solar energy. Developments in the world in the field of electricity production have dictated that many plants used solar energy in the next years. Serbia's energy resources in renewable sources are a potential that needs to be used, both for the development of the local economy and society, and for energy efficiency in the country.

5 Acknowledgement

The research presented in this paper was done with the financial support of the Ministry of Education, Science and Technological Development of the Republic of Serbia, within the funding of the scientific research work of Scientific Research Organization in 2020 according to the contract with registration number 451-03-68 / 2020-14 /200052.

6 References

- [1] *** <http://www.altenergy.org/renewables/solar/common-types-of-solar-cells.html>
- [2] *** https://energyeducation.ca/encyclopedia/Types_of_photovoltaic_cells.
- [3] *** <https://www.ise.fraunhofer.de/content/dam/ise/de/documents/publications/studies/Photo-voltaics-Report.pdf>
- [4] *** Ministarstvo rudarstva i energetike Republike Srbije (2015), Strategija razvoja energetike Republike Srbije do 2025. godine sa projekcijama do 2030.godine.
- [5] <http://www.solarisenergy.co.rs/solarna-energija-u-srbiji>.
- [6] **Lambić, M.** *Solar Technique, Solar Energy Society*. Serbia Solar, Zrenjanin, Serbia, 2004.

- [7] **Lambić, M., D. Tolmač**, *Energetic efficiency – management, rational consumption, efficiency*. Serbia Solar, Zrenjanin, Serbia, 2004.
- [8] **Tolmač J., S. Prvulović, M. Nedić, D. Tolmač**, Analysis of the development opportunities of solar systems in Serbia, *Agricultural Engineering*, 23 (2019), 2, pp. 85-92.
- [9] *** <https://www.energetskiportal.rs/obnovljivi-izvori-energije/energija-sunca>
- [10] **Prvulović S., D. Tolmač, M. Matic, Lj. Radovanović, M. Lambić**, Some aspects of the use of solar energy in Serbia, *Energy Sources Part B-Economics Planning and Policy*, 13 (2018), 4, pp. 237-245.

MOGUĆNOSTI IMPLEMENTACIJE FOTONAPOSNKIH SOLARNIH PANELA U PODRUČJIMA NAMENJENIM VIŠEPORODIČNOM STANOVANJU

THE POSSIBILITIES FOR IMPLEMENTATION OF PHOTOVOLTAIC SOLAR PANELS IN MULTI-FAMILY HOUSING AREAS

**Borjan BRANKOV^{*1}, Ana STANOJEVIĆ², Mila PUCAR¹,
Marina NENKOVIĆ-RIZNIC¹**

¹ Institute of Architecture and Urban&Spatial Planning of Serbia, Belgrade, Serbia

² Faculty of Civil Engineering and Architecture, University of Niš, Serbia

<https://doi.org/10.24094/mkoiee.020.8.1.167>

Usled dinamičnije promene klime i porasta broja ljudi u gradovima obnovljivi izvori energije (OIE) sve više doprinose racionalnijem korišćenju energije. Imajući u vidu značaj koji upotreba OIE u stanovanju donosi u pogledu finansijske uštede i smanjenja emisije CO₂, rad ispituje mogućnost upotrebe OIE u područjima višeporodičnog stanovanja sa aspekta sakupljanja i konverzije solarne energije odnosno implementacije fotovoltaičnih panela i generisanja električne energije. Kod višeporodičnog stanovanja, problem održivosti i primene OIE je složen zadatak, prvenstveno zbog postojećih načina korišćenja prostora i vlasništva koje je višeslojno, ali i postojanja potrebe za aktivnim uključenjem cele stambene zajednice u procesu donošenja odluka i pokretanja inicijativa. Istraživanje analizira prednosti i mane za postavljanje solarnih panela i to na krovovima i fasadama objekata, i u okviru zajedničkih otvorenih prostora u bloku, postavljanjem solarnih svetiljki, solarnog napajanja za električna vozila, solarnih punjača itd. Ispitivanje mogućnosti za korišćenje solarne energije sprovedeno je na primeru stambenog Bloka 29 na Novom Beogradu, urbanističkom analizom uz podršku odgovarajućih podataka o solarnoj radijaciji za analizirano područje i softvera Skelion i PVGIS-a za numeričku i grafičku ilustraciju količina energije koje je moguće dobiti postavljanjem fotonaponskih solarnih panela. Rad sagledava dva različita scenarija: kada se paneli instaliraju na krovovima stambenih objekata i kada se oni postavljaju na otvorenim prostorima, istovremeno analizirajući potencijale svakog od njih i preduslove za njihovu realizaciju u praksi. Dobijeni rezultati imaju za cilj da uporede kolicine električne energije dobijene proračunom za dva različita scenarija.

Ključne reči: solarna energija, fotovoltaični solarni paneli, električna energija, višeporodično stanovanje, stambeni blok, Novi Beograd

Due to the increasingly dynamic climate change and the increase in the number of people in cities, renewable energy sources (RES) are contributing to a more rational use of energy. Given the importance that the use of RES in housing directly brings in terms of financial savings and reduction of CO₂ emissions, the paper examines the possibility of using RES in multi-family housing from the aspect of solar energy collection and conversion respectively implementation of photovoltaic panels and electricity generation. In multi-family housing, the problem of sustainability and implementation of RES is a complex task, primarily due to the existing ways of using space and ownership, which is multi-layered, but also the need for the active involvement of the entire housing community in decision-making and initiatives. The research analyzes the advantages and disadvantages of installing solar panels on the rooftops and facades of buildings, and within the common open spaces in the block, by installing solar lamps, solar power for electric vehicles, solar chargers, etc. The examination of the possibilities for using solar energy was conducted on the example of the residential Block 29 in New Belgrade, using urban analysis supported by appropriate data on solar radiation for the analyzed area and Skelion software for a numerical and graphical illustration of the amount of energy that can be obtained by installing photovoltaic solar panels. The paper considers two different

^{*} Corresponding author, email: sanja.borjan@iaus.ac.rs

scenarios: when panels are installed on the roofs of buildings and when they are installed in open spaces, analyzing the potential of each and the prerequisites for their implementation in practice. The results aim to compare the quantities of electricity obtained by calculation for two different scenarios.

Key words: solar energy, photovoltaic solar panels, electrical energy, multifamily housing, housing block, New Belgrade

1 Introduction

Renewable energy sources (RES) are an indispensable part of sustainable postulates of urban development and modern life, which, in addition to a high standard, also require the protection of the environment and the active struggle of humanity against climate changes. Globally, many cities are leaders in the use of new RES within the dense urban matrix. Solar technology based on the use of ecologically clean solar energy in the form of light and heat, which is used by conversion to obtain heat or electricity, is the most common form of using RES. Namely, solar radiation is available all over the planet, while nowadays technological progress enables simple and financially cost-effective energy independence of users from connections to the electricity distribution network and the provision of hot water from an energy source that does not emit harmful gases. Sustainable solutions that rely on solar design are increasingly present in single-family housing, applying passive principles of energy transmission and accumulation, as well as installing solar panels on the rooftops of buildings. Given that passive solar systems require adequate considerations in the earliest stages of urban planning and design, implementing bioclimatic principles [1], improving the energy performances of already built facilities, and reducing energy consumption in residential and working spaces is often achieved using active solar systems [2].

Active solar systems mean the use of solar thermal or photovoltaic receivers for the conversion of solar energy into heat or electricity [3]. Solar collectors and panels are most often installed on the rooftops of buildings, on their facades, or the ground. Drawing energy from the Sun to heat water and air, through different types of collectors, is one of the oldest forms of using solar energy. Nowadays, solar water heating systems are used in single-family housing, educational institutions, restaurants, hospitals, agricultural buildings and for the needs of various technological processes in industrial production where large amounts of hot water are used [4]. The absorbed solar energy is successfully transformed into energy that heats the air inside the building, using advanced SolarWall technologies [5]. Nevertheless, the researches show that photovoltaic power is the strongest growth of all RES technologies, with recent annual growth rates of around 40% [6]. In Europe, the average amount of electricity generated per year from solar radiation on one square meter of horizontal ground surface is 1.000kWh [7]. Photovoltaic (PV) solar panels composed of photovoltaic cells in which there is a difference in the electric potential after the sun shines on their surface, and direct conversion into electricity, are most often placed on the rooftops. Merging the cells in several rows leads to the desired energy characteristics of solar panels, which also depend on the type of photovoltaic cell or its chemical composition [8]. For buildings that are located away from the distribution network, it is possible to form a self-contained, independent photovoltaic system (for example single-family buildings). Photovoltaic systems connected to the distribution network, i.e. solar power plants, are used in buildings with a larger roof area or are built as independent plants.

The number of hours of solar radiation on the territory of Serbia is between 1500 and 2200 hours per year, with an average intensity of solar radiation from 1.1 kWh /m²/day in the north to 1.7 kWh/m²/day in the south - during January, and from 5.9 to 6.6 kWh/m²/day - during the month of July [9,10]. Based on the currently available electricity capacities in Serbia, for the provision of tertiary reserves, the maximum usable capacity of solar power plants is 450 MW i.e. their technically usable potential is 540 GWh/per year (0.046 million toe/per year) [10,11]. By Decrees on incentive measures for the production of electricity from renewable sources from 2009, 2013, and 2016, the RS Government provided the opportunity to build solar power plants on the territory of the country using subsidies, whereby such plants become economically viable with a return on an investment after a period of six years. From 2009, when the National Action Plan for the Utilization of Renewable

Energy of RS was adopted in the legislative sense, which encourages investment in renewable energy sources, until October 2016, 104 solar power plants with a capacity of 8.8 MW were built [12].

Given the fact that practice shows that solar panels are most often used in single-family housing, as well as in larger public and industrial buildings, the paper explores the possibilities of using solar energy in the field of multi-family housing. Searching for realistic options for the implementation of photovoltaic panels in housing blocks, the paper aims to test the capacity of contemporary multi-family housing in Serbia and their associated open spaces for the use of solar power energy based on PV systems. Testing the possibility of generating electricity using a renewable source of solar radiation was conducted on the example of Block 29 in New Belgrade with the support of PVGIS and Skelion software [13]. The research compares two possible scenarios:

- Scenario 1: installation of PV panels on the rooftops of the buildings;
- Scenario 2: installation of PV panels within common open spaces.

The paper takes into account various parameters on which the final energy characteristics of solar power plants significantly depend: quality and length of solar radiation exposure in a given area, depending on the season and meteorological conditions, availability of solar panels on the national market, type of photovoltaic solar panel - in terms the type of solar cell being used.

2 Multi-family housing and RES in Serbia - the case study of Block 29 in New Belgrade

Housing has always been a dynamic space, while various intensified changes in cities, society, and family structure lead to more condensed housing in cities and changes in user patterns. In that sense, housing is often an ideal polygon for possible "upgrading" of how space is designed and used. Multi-family housing has always followed residents' needs and overall shifts in global changes and demands in the residential sphere. In the contemporary context, the change in the use of multi-family housing is mutually conditioned by social and other changes both in Europe and later at the global level. Possibilities and progress of the architectural design of multi-family assemblies are related to the current needs of solving social and spatial problems, both in different periods of the 20th century and today. Multi-family housing in the second half of the 20th century in former Yugoslavia is a good example of experimenting with new and improved functions and spatial dispositions as it was also focused a lot on the well-being of residents through different dwelling and common areas design [14,15].

The improvement of energy resources and the possibility of introducing PV panels as a common good of all tenants is one of the possible new common benefits. On the one hand, common functions generally tend to improve the comfort and possibilities of a multi-family housing complex by offering additional collective facilities to users and raising the quality of living space [16]. Emphasizing the better use of the building is an important aspect of multifamily housing, with residents expanding their sphere of privacy outside the dwelling [17]. The use of common energy resources of the building for tenants can mean a better understanding of the potentials of the building (spatial and energy potential). Therefore renewable energy sources in housing can show the importance and value of common space and the significance of the community to an individual resident. This paper also examines the possibility of how a residential complex can be upgraded in terms of energy efficiency during its lifetime and how much the collective sphere of space in multi-family housing can be an advantage over individual housing.

The focus of this paper analysis is the residential complex Block 29, which is located in the northwestern part of the central zone of New Belgrade (Fig. 1). The block is divided into two parts: the residential part of the block and the part for the regional center (which was never built and its place occupied a newer residential complex after the 2000s). The focus of the analysis in the paper will be only the original residential part of Block 29. DOCOMOMO Serbia has included this Block in its Atlas of housing as modern heritage in Serbia and emphasized its significance [18].

The competition for the design of Block 29 was announced in 1967, and the construction of Block took place in the period from 1969 to 1974. The designer of the urban solution of the Block is Milutin Glavički, while the authors of the building designs are the architects Dr. Mihailo Čanak and

Milosav Mitić. The contractor for Block 29 was the construction company "Rad" from Belgrade. The structure of the residential part of the block consists of 7 residential buildings, each with 7 above-ground floors, built in the IMS system, with a total of 1129 apartments and a projected population of 4358. Within the block, there is a local community building (today it is also a commercial space) and kindergarten, while the planned primary school was never built [15,19]. The residential buildings in the block are in the form of a two-lane road (Fig. 1,2). Open spaces include the central zone of the park, the zones around residential buildings, and along the perimeter of the block, as well as the basketball court. Road traffic is solved along the perimeter of the block, while the central part of the block is mostly reserved only for pedestrians.



Figure 1: View of the Block 29 residential complex

Source: <https://mapio.net/pic/p-15908646> (left) <https://www.designed.rs> (right)

Within residential buildings, the architects used the parallel two-track so that in the communication zone (staircase and elevator) the space next to the apartments would not be a corridor but a common space for apartment owners (four apartments on the floor - common areas for two neighboring apartments) [15]. All residential buildings have the same number of floors and a sufficient distance between them, which why they are suitable for installing photovoltaic panels on their roofs (Fig. 2). The double tract in this case also corresponds to the fact that, in relation to the residential towers, it has more roof area, with a larger flat surface for the panels. However, on the other hand, the buildings are compact enough in the sense that the number of the residents and organization of one building for these types of energy improvements is feasible and the panels can be partially done from building to building. Compared to, for example, Blocks 21 and 28, buildings are mostly towers or long lamellas and it significantly increases the organization, and agreement between residents can be more complicated. This type of intervention overall enables better participation of users in the use of common space/resources and direct benefits within the living space, and the paper proposal includes two levels of common spaces (roofs and open spaces) [20].

3 Research Metodology

The methodology framework for this study was formulated in four main stages: (1) analyzing the solar radiation and urban morphology of the study area; (2) defining possible scenarios for implementing PV panels; (3) choosing the market available type of solar panels to be installed; (4) modeling solar gains using PVGIS and Skelion software.

3.1 Analyzing the solar radiation and urban morphology of Blok 29

The older multi-family housing part in Block 29 is situated in the zone of New Belgrade at N 44°49' latitude and E 24°25' longitude. Regarding solar energy potential, as the main precondition for the construction of solar power plants, the territory of New Belgrade is suitable for the use of active solar systems in the form of PV panels. Namely, in Belgrade, the annual average daily solar radiation received on a surface ranges between 3,76kWh/m² and 3,86kWh/m² [21]. The highest amount of solar energy is available in the period between April and September. The mean solar power per unit area per year (global solar radiation on a horizontal surface) is approx. 1.300 to 1.400kWh/m² per year, while average daily solar radiation received on a horizontal surface ranges from 3,4 to 4,0kWh/m². There are 2019 sunny hours per year, with an average cloud coverage of 5-6%. Previous data indicate the convenience of using solar energy in the study area. The optimum angle for installing the PV

panels in the area of New Belgrade is 44° . To maximize the electricity production, it is necessary to install PV panels at an angle of 35° , thus adapting the angle to the summer period and using this period of higher radiation to the maximum extent [21]. During the construction, solar panels should also be oriented towards the south.

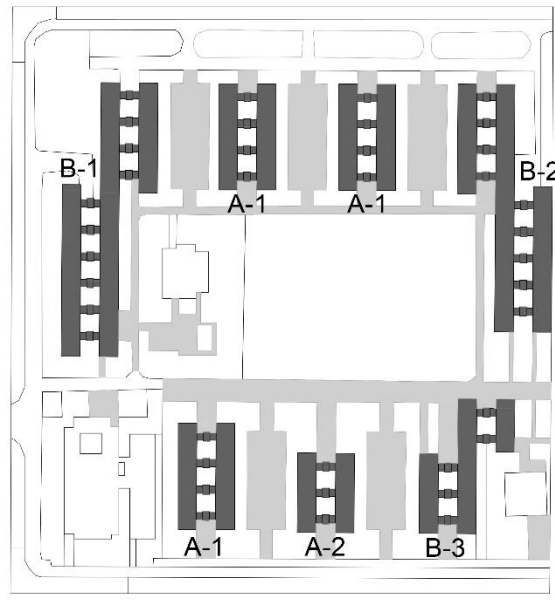


Figure 2: Urbanistic map with disposition of multi-family housing divided by type into A (compact) and B (longer and more complex) and its subtypes Source: Authors

Residential buildings organized in the form of parallel two-trackt, extend on their longer side in the direction northeast-southwest, with a deviation of 33° to the north, providing good insolation within the block and housing units. The distance between the residential buildings is optimally 33m, so there is no danger of creating a shadow between them, which would cover their roofs. The total area of the part of the Block that is the subject of analysis in the paper is 89.178m^2 , where the area of the block under the buildings is 15.347m^2 while the open common areas occupy an area of 73.830m^2 .

3.2 Defining possible scenarios for implementing PV panels

The urban analysis of the area of Block 29, which included the analysis of the orientation of the buildings, their position on the plot, distances and character of non-residential facilities and open common areas, has defined two possible scenarios for the implementation of solar power plant (PV panel installation). *Scenario 1* involves the installation of PV panels on all rooftops of multi-family housing buildings in the block, assuming that the generated electricity delivered to the distribution network is deducted from the electricity consumed in the housing units in the buildings, reducing the financial costs of users (Fig. 3). *Scenario 2* concerns the installation of solar panels on public areas, where we recognized the possibility of integrating panels within pedestrian paths and their installation in the part of the area intended for parking, assuming that parking zones will be covered with canopies (Fig. 3). The obtained electricity would either be deducted from the costs of electricity in housing units, or would be used in part or in full to illuminate the area. The conducted research did not consider the possibility of installing panels on public buildings in the complex (kindergarten, business-commercial building), nor the possibility of creating solar trees, and similar solar design solutions within the outdoor urban space for recreation.

3.3 Choosing the market available type of solar panels

For the paper purposes, the use of stationary PV panels is adopted. Due to the fact that the surfaces of all roofs of residential buildings are flat, Scenario 1 requires the use of free-standing PV panels, while the panels will be integrated into the path surfaces in Scenario 2. It is assumed that the parking lot will be covered with a construction that will have a flat roof, suitable for free-standing PV panels. The availability of solar panels on the national market is an indispensable factor in the process

of creating a solar power plant project. The Serbian market offers a large number of PV panels that serve the smaller needs of users (for example weekend houses), but also offer the construction of power plants that can seriously contribute to energy independence. Individual PV panels are sold in different dimensions: 35x48.5cm; 67x46,5cm; 67x84,5cm; 67x148cm; 99x165cm etc., while based on their technology, they can be made of mono or poly-crystal structure, or rarely as thin-film panels. Their price depends on their dimensions and power, and it goes from 3.500 to 32.000 dinars. Some of the panels that are usually used in Serbia are: MONO 310W EXE (mono-crystal, 1658x990mm, 310Wp, 18.35% efficiency), EXE Solar EXP285 (poly-crystal, 1650x991, 285Wp, 17,50% eff.), LX270P Luxor (poly-crystal, 1640x992, 270Wp, 16,63% eff.), etc. For the simulation research purposes we chose the solar panels Sanyo Electric HIP-270NJE1 (mono-crystal, 270Wp, 16,2% eff.) to be installed on the rooftops of the multi-family buildings and on the canopy of the parking space, with the dimension of single one 1600x100mm. For the pedestrian paths we have used Solar Roadways panels (270Wp) which is not available on our market yet, but are the most effective type of the panels that can be walked or even driven upon.

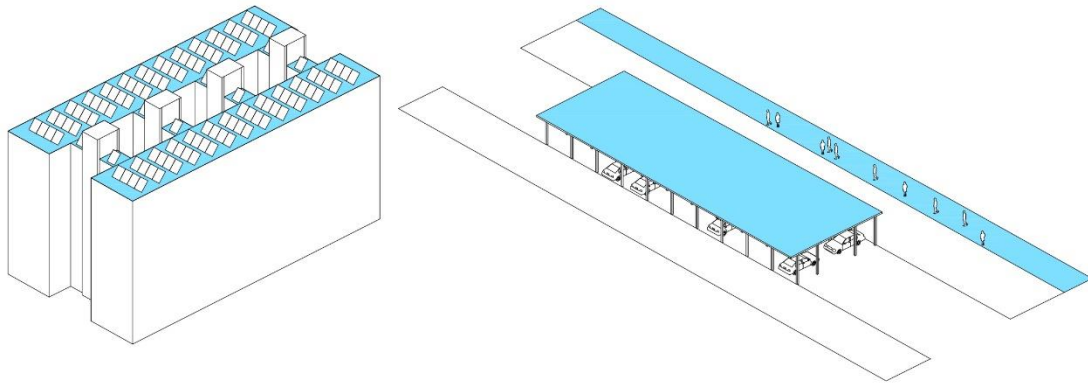


Figure 3: Scenario 1(left) - installation of PV panels on all rooftops of multi-family housing buildings in the block, Scenario 2(right) - installation of solar panels on public areas in the complex – parking canopies and pedestrian pathways Source: Authors

4 Results - Modelling energy gains provided by solar panels

The amount of electricity generated using the solar panels for set scenarios is calculated using the PVGIS (Photovoltaic Geographical Information System) and Skelion software, which is used as a plug-in for the Sketch up program. The calculation is conducted for the shadows at winter solstice noon 21.12.2020. (Fig. 4). In Tables 1, the analytic data gain from Skelion simulation for Scenario 1 are given, representing number of installed panels and they total power, and price per different types of buildings in block and in total. Table 2 represents the analytic data gain from PVGIS for Scenario 1 with average monthly electricity production (E_m) and average monthly sum of global irradiation per square meter received by the modules of the given system (H_m), per months. In Tables 3 and 4 the same type of analytic data using Skelion and PVGIS are presented for Scenario 2.



Figure 4: Modelling of PV panels on all rooftops of multi-family housing buildings and on public areas in the complex – parking canopies and pedestrian pathways Source: Authors

Table 1: The analytical data gain from Skelion simulation of creating solar power plant on the rooftops of the buildings (PV panel: Sanyo Electric HIP-270NJE1, nominal power 270W)

Scenario 1	Roof area [m²]	No.	No. of panels	Total power [kW]	Energy [kWh]	Yield [kWh/kWp]
Rooftop A-1	1.240	3	356	96,12	113.159	1177,27
Rooftop A-2	930	1	264	71,28	83.887	1176,88
Rooftop B-1	3.085	1	865	233,55	276.606	1184,35
Rooftop B-2	2.780	1	799	215,73	253.916	1177,01
Rooftop B-3	1.500	1	442	119,34	140.424	1176,68
In total*	12.015m²		3438	928,26	1.094,31	8.246,73
*the total values consider all buildings in area including three buildings type A-1						

Table 2: The analytical data gain from PVGIS for Scenario 1 (Em- kWh/month; Hm- kWh/m²/month)

Scen. 1	A-1		A-2		B-1		B-2		B-3		In total*
	Em	Hm	Em	Hm	Em	Hm	Em	Hm	Em	Hm	Em
January	3952	54.59	2928	54.58	9825	54.59	8866	54.59	4901	54.58	38.376
February	5251	72.40	3892	72.39	13057	72.40	11781	72.40	6514	72.38	50.997
March	9375	128.8	6949	128.7	23143	128.8	21036	128.8	11632	128.7	90.885
April	11756	161.5	8715	161.5	28768	161.5	26380	161.5	14589	161.5	113.720
May	12874	177.2	9545	177.1	31360	177.2	28891	177.2	15980	177.1	124.398
June	13350	183.9	9899	183.9	32419	183.9	29962	183.9	16573	183.9	128.903
July	14960	205.8	11093	205.7	36223	205.8	33574	205.8	18572	205.7	144.342
August	14385	197.4	10665	197.4	34860	197.4	32282	197.4	17855	197.4	138.817
Septem.	10486	143.9	7772	143.9	25564	143.9	23528	143.9	13010	143.9	101.332
October	8037	110.3	5956	110.3	19755	110.3	18031	110.3	9969	110.3	77.822
Novem.	5391	74.21	3995	74.20	13345	74.21	12093	74.21	6686	74.19	52.292
Decem.	3337	46.15	2472	46.14	8282	46.15	7485	46.15	4138	46.14	32.388
*the total values consider all buildings in area including three buildings type A-1											

Table 3: The analytical data gain from Skelion simulation of creating solar power plant on the canopy of parking lots and at the pedestrian paths

Scenario 2	Area [m ²]	No. of panels	Total power [kW]	Energy [kWh]	Yield [kWh/kWp]
Parking lot	9224	3165	704,16	829.357	1177.80
Paths	6413	2304	622,08	657.632	1055.32
In total	15.637	5469	1.326,24	1.486,989	2.233,12

Table 4: The analytical data gain from PVGIS for Scenario 1 (Em- kWh/month; Hm- kWh/m²/month)

Scen. 2	parking		paths		In total		parking		paths		In total
	Em	Hm	Em	Hm	Em		Em	Hm	Em	Hm	Em
January	28983	54.62	17265	39.32	46.248	July	109609	205.8	99820	211.2	209.429
Febr.	38504	72.44	25361	56.39	63.865	Augst	105417	197.4	87491	186.6	192.908
March	68726	128.8	49779	108.3	118.505	Septe.	76867	144.0	57403	124.3	134.270
April	86163	161.6	70249	150.3	156.412	Oktob.	58930	110.4	37990	84.28	96.920
May	94333	177.2	84182	178.6	178.515	Nove.	39532	74.26	22539	51.47	62.071
June	97814	183.9	91197	192.8	189.011	Decem.	24473	46.18	14349	32.90	38.822

5 Conclusion

Multi-family housing is a polygon not only for creating new solutions for the organization of dwelling plans due to changes in family structure and living conditions, but is an excellent indicator of how much and in what way the common sphere of housing can contribute to an individual user in the complex. This type of housing differs from individual housing, and if common spaces and common interest are not used and stimulated, the value and the whole point of this type of housing is questioned. Thus, the paper emphasizes one aspect of the improvement of multi-family housing, which can contribute not only to the financial savings of residents, but also to achieving greater comfort and sustainability. These aspects are especially important in dense urban areas, which are increasingly attacked by enormous new construction, reduced greenery and lack of resources of all kinds, especially space. The potential of unused spaces of buildings (as roofs) that can be turned into an energy generator for the neighborhood is something refreshing and necessary.

Paper analysis has shown that in the case of Block 29 photovoltaic panels on the roofs of buildings generates less energy than parking lots and pedestrian paths in this Block. Bearing in mind that not all footpaths were used for this type of panel covering and also that spaces of non built types of spaces have not been taken into account, this area and consequently the energy gains can be higher. On the other hand, the capacity of electricity generated on the roofs of buildings is significant, which brings the autonomy of buildings in relation to the entire complex and can be managed independently of other buildings, while placing panels on public areas requires the involvement of the entire community of about 5,000 people. Another advantage of roofs is that it is the easiest space to place the PV panels compared to a parking lot that requires canopy, while paths are much more financially demanding.

Interesting aspect of making these kind of interventions in Serbia is that this is still a pilot solution, comparing to other countries. This can be also a type of “advertisement” of RES use in residential complexes and can drive more communities into this process.

There are some important aspects of such interventions which are beyond technical design. One is the problem of placing canopies above parking as an institutional and legislative problem, due to that design must fallow the legislative, also the question is who will have the jurisdiction, considering that parking spots are usually on public (city) owned land. The other possible problem is the issue of user participation in the endeavor. Organization of the community in these interventions is of high importance. This paper did not address this, but in further research it is necessary to look not only at the technical characteristics and benefits of RES systems in housing but also at potential problems that are not directly related to space or technology itself. Observing the condition of multi-family housing areas, non-maintenance, and even illegal construction within housing complexes, it is possible to expect that the aspect of user participation and initiative in this regard can prove to be one of the most difficult steps besides the financial aspect for this type of intervention.

6 References

- [1] **Pucar, M., M. Pajević, M. Jovanović-Popović**, *Bioklimatsko planiranje i projektovanje - urbanistički parametri*, IP Zavet, Beograd, Srbija, 1994.
- [2] **Milošević, M., D. Milošević, D. Stević, V. Dimić, A. Stanojević**, The analysis of energy efficiency indicators and renewable energy sources for existing buildings, *Proceedings of 5th International Conference on Renewable Electrical Sources, SMEITS, Belgrade, Serbia, 2017*, pp. 205-212.
- [3] **Kosorić, V.**, *EKOloška kuća, Građevinska knjiga*, Beograd, Srbija, 2012.
- [4] **Ogueke, N.V., E.E. Anyanwu, O.V.Ekechukwu**, A review of solar water heating systems, *Journal of renewable and sustainable energy*, 1 (2009), pp. 043109.
- [5] **Saadatian, O., C.H. Lim, K. Sopian, E. Salleh**, A state of the art review of solar walls: Concepts and applications, *Journal of Building Physics*, 30 (2013), issue 1, pp. 55-79.
- [6] **Pavlović, T., D. Milosavljević, I. Radonjić, L. Pantić, A. Radivojević, M. Pavlović**, Possibility of electricity generation using PV solar plants in Serbia, *Renewable and Sustainable Energy Reviews*, 20 (2013), pp. 201-218.
- [7] **Radovanović, M., S. Popov, S. Dodić**, *Sustainable Energy Management*, Elsevier, Oxford, UK, 2013.
- [8] **Rabaia, M.K.H., M.A.Abdelhareem, E.T. Sayed, K.J. Chae, T. Wilberforce, A.G. Olabi**, Environmental impacts of solar energy systems: A review, *Science of The Total Environment*, Available online 29 August 2020, 141989, In press
- [9] **Pucar, M., M. Nenковиć-Riznić**, Application of renewable sources of electrical energy from the aspect of economical, ecological and social sustainability, *Proceedings of the 4th International Conference on Renewable Electrical Sources, SMEITS, Belgrade, Serbia, 2016*.
- [10] **Energy Sector Development Strategy of the Republic of Serbia for the period by 2015 with projections by 2030**, The Republic of Serbia, Ministry of Mining and Energy, Belgrade, 2016.
- [11] **Dimić, V., M. Milošević, D. Milošević, D. Stević**, Adjustable Model of Renewable Energy Projects for Sustainable Development: A Case Study of the Nišava District in Serbia, *Sustainability* (2018), issue 10, pp. 775.
- [12] **Progress Report on the Implementation of the National Renewable Energy Action Plan of the Republic of Serbia**, The Republic of Serbia, Ministry of Mining and Energy, Belgrade, 2016.
- [13] <http://www.pvresources.com/en/software/software.php> (5.9.2020)
- [14] **Brankov, B.**, Zajednički prostori u razvoju višeporodičnog stambenog sklopa, *Arhitektura i urbanizam*, 49 (2019), pp. 32-39.
- [15] **Marušić, D.** Prikaz konkursnih projekata 1965 – 1975, *Arhitektura i urbanizam*, 1975, str. 74-77.
- [16] **Brankov, B.**, Common areas in multi-family housing in Serbia: case study of Cerak Vinogradi, *Proceedings of the 3rd International doctoral-postdoctoral conference FACING POST-SOCIALIST URBAN HERITAGE*, Faculty of Architecture, Budapest University of Technology and Economics, Budapest, Hungary, pp. 42-45.
- [17] **Ilić, D.** Višespratne stambene zgrade – kolektivno porodično stanovanje u novim uslovima. U Stanovanje u višeporodičnim spratnim zgradama u novim tržišnim uslovima - Stanovanje 1. 1996, Prosveta, Niš, Srbija, 1996
- [18] **Docomomo Serbia**, Atlas stanovanja: Blok 29 centralne zone Novog Beograda., [online]) Available at: <http://www.docomomo-serbia.org/atlas/blok-29-centralne-zone-novog-beograda/>, Available online 30 August 2020.
- [19] **Bodlović, V.** Stambeni blok 29 u Novom Beogradu. *Izgradnja*. 1973. br. 12, str. 53- 58.
- [20] **Brankov, B., A. Stanojević**, Diferenciranje upotrebljivosti otvorenih zajedničkih prostora u višeporodičnom stanovanju, *Zbornik radova Međunarodnog naučno-stručnog skupa 16. Letnje škole urbanizma*, Udruženje urbanista Srbije, Prolom Banja, Srbija, 2020., pp. 143-152.
- [21] **Pucar, M., B. Brankov**, Possibility of using the solar energy by installing the PV panels on flat roofs of public buildings. Case Study: Market in Block 44 in New Belgrade-model-based approach, *Proceedings of 5th International Conference on Renewable Electrical Sources, SMEITS, Belgrade, Serbia, 2017*, pp. 163-168.

ПРИМЕНА СОЛАРНЕ ЕНЕРГИЈЕ У ФУНКЦИЈИ ОДРЖИВОГ РАЗВОЈА У ЈП ЕПС, ОГРНАК РБ "КОЛУБАРА"- ОРГ. ЦЕЛ. ПРЕРАДА

APPLICATION OF SOLAR ENERGY IN THE FUNCTION OF SUSTAINABLE DEVELOPMENT IN PC EPS, BRANCH OF RB "KOLUBARA" - ORG. CEL. PROCESSING

Момчило МОМЧИЛОВИЋ*, Милисав ТОМИЋ
ЕПС ПДРБ "Колубара"-Лазаревац

Енергетска климатска политика Европе дефинише амбициозне циљеве за стварање одрживог, безбедног и конкурентног енергетског система. Употреба соларне енергије само је једна од области употребе обновљивих извора енергије. Европска унија има стратегију да у будућности све више промовише употребу обновљивих извора енергије, са низом мера којима би се подстакле инвестиције у објекте са применом обновљивих извора енергије. Потребно је повећати производњу из обновљивих извора енергије а постепено смањивати традиционалну производњу која је уједно и највећи загађивач животне и радне средине или модернизовати системе, чиме би се испоштовале дозвољене норме загађујућих материја које се емитују у животну и радну средину. У раду је представљен пример примене соларних панела на објектима "РБ Колубара, оц-Прерада", где је приказана количина произведене ел. енергије, количина смањења емисије CO₂, новчана добит и уштеда, као и друге погодности које се остварују применом соларних панела за производњу електричне енергије. За потребе рада разматрани су објекти са најбољим карактеристикама (оријентација, нагиб крова, конструкција, површина), такође и потрошња ел.ен. у самим објектима.

Кључне речи: соларна енергија; обновљиви извори енергије; соларни панели; CO₂.

Europe's energy and climate policy defines ambitious goals for creating a sustainable, secure and competitive energy system. The use of solar energy is only one of the areas of use of renewable energy sources. The European Union has a strategy to increasingly promote the use of renewable energy sources in the future, with a series of measures to encourage investment in renewable energy facilities. It is necessary to increase the production from renewable energy sources and gradually reduce the traditional production which is also the biggest polluter of the living and working environment or to modernize the systems, which would respect the allowed norms of pollutants emitted into the living and working environment. solar panels on the facilities "RB Kolubara, oc-Prerada", where the amount of produced electricity, the amount of reduction of CO₂ emissions, monetary gain and savings, as well as other benefits that are realized by using solar panels for electricity production are shown. For the needs of the work, the facilities with the best characteristics (orientation, roof slope, design, surface) were considered, as well as the consumption of electricity in the facilities themselves.

Key words: solar energy, renewable energy sources, solar panels, CO₂.

1 Увод

Велики потенцијал лежи у соларним електранама. Према процени „Међународне агенције за енергетику“ (ИЕА), у периоду од 2005 до 2025. године се очекује увећање потрошње примарне енергије за 40%. То говори о неопходности да се развој енергетике стратешки планира и детаљно анализира са свих аспеката. Србија се налази међу 20 најинтензивнијих земаља по емисији угљеника.

Заменом постојећих капацитета новим капацитетима значајно би се повећала ефикасност. Овим међутим неће бити довољно да се оствари систем производње енергије са ниским

* Corresponding author, email: momcilo.momcilovic@rbkolubara.rs

нивоом емисије угљеника тј. смањење емисије гасова са ефектом стаклене баште за 80% до 2050. године. Потребно је повећати производњу из обновљивих извора енергије а постепено смањивати традиционалну производњу која је уједно и највећи загађивач животне и радне средине или модернизовати системе, чиме би се испоштовале дозвољене норме загађујућих материја које се емитују у животну и радну средину. Производња електричне енергије из фотонапонских ћелија (ПВ) има стопу раста 50-60 % на годишњем нивоу. Гледајући прогнозу „S&P Global Platts Analytics“, просечне цене на четири највећа тржишта у Европи за 2019 год., биле су 58 €/MWh у односу на 54 € колико је била у 2018. и 37 €/ MWh у 2016. Поскупљење је тако од 2016. до 2020. достигло око 56%, а као главни разлог наводи се раст цена CO₂ са 8 на 24 € по тони. Одбор директора Европске инвестиционе банке (ЕИБ) одобрио је нову политику кредитирања енергетског сектора, која предвиђа и престанак финансирања пројеката повезаних са фосилним горивима, од краја 2021. године. "ЕИБ" (Европска инвестициона банка) је издала саопштење да неће више разматрати нова финансирања за пројекте који се односе на фосилна горива, укључујући и природни гас, од краја 2021. године. Осим тога, банка је поставила нови стандард о емисијама (Emissions Performance Standard) од 250 грама CO₂ по киловату-сату (кWh), који ће заменити важећи стандард од 550g CO₂/кWh. Претходна ревизија политике кредитирања енергетике, обављена 2013 год., већ је омогућила, да "ЕИБ" буде прва међународна финансијска институција, која је ефикасно окончала финансирање производње електричне енергије из угља применом строгог стандарда за емисије (<https://balkangreenenergynews.com>). У електроенергетском сектору "EBRD" (Европска банка за обнову и развој), све више се ради на подршци "ОИЕ" (Обновљиви извори енергије), и енергетској ефикасности, али између 2014. и 2017. и даље је велики проценат одобрених кредита у сектору енергетике (41%), био намењен за фосилна горива. Нова политика кредитирања у енергетици "EBRD"-а, усвојена 2018, скоро да уопште није била усклађена са "Париским" споразумом, али банка сада има шансу да то надокнади приликом усвајања Стратегије за усклађивање са овим споразумом (Pirra Gallop, 2019).

Европски Парламент континуирано подржава ове циљеве. Европско Веће је такође презентовало своје дугорочно опредељење за декарбонизацијом енергетског сектора са циљем да ЕУ и друге индустријске земље сниже своје емисије за 80÷95% до 2050. године. Када је у питању политика ОИЕ у свету она може постати најјефтинија технологија у наредним годинама.

2 Анализа потенцијала сунчевог зрачења на Колубарском подручју

Србија има знатно већи број сати сунчевог зрачења од већине европских земаља (између 1500 и 2200 сати годишње зависно од локације). Најбољи услови су у југоисточном и централном делу наше земље где је просечна годишња вредност енергије зрачења до 1550 kWh/m². Енергија зрачења у централном делу износи око 1400 kWh/m². Идеални природни услови за изградњу соларне електране се могу наћи на југу Србије на територији Ниша, Враћа, Пирота, као и у централном делу око Крагујевца и Краљева као и у западној Србији.

Просечан интензитет сунчевог зрачења на територији Републике Србије се креће од 1,1 KWh/m²/дан на северу до 1,7 KWh/m²/дан на југу током јануара, а од 5,9 до 6,6 KWh/m²/дан, током јула. Србија има просечно више сунчаних дана од већег дела Европе где се увелико примењују соларни системи као што су Немачка, Аустрија, Швајцарска... Југ и централни део Србије имају више сунчаних дана од Војводине и источне Србије.

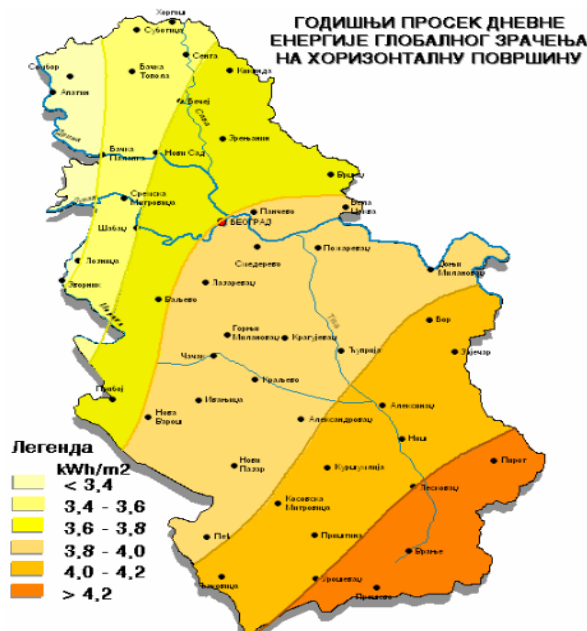
На слици бр.3., је приказан дијаграм са месечним вредностима сунчаних, делимично облачних, облачних и кишних дана. Дани са облачношћу мањом од 20% се сматрају сунчаним, од 20-80% као делимично облачни, а са облачношћу већом од 80% као облачни дани. Слика бр.4., приказује карту са проценом соларног фотонапонског потенцијала за производњу енергије представља укупне просечне дневне / годишње количине електричне енергије из 1kW вршне снаге соларне електране, израчунату за период од 25 последњих година. Прорачун соларне електричне енергије заснован је на подацима о соларним ресурсима високе резолуције и софтверу за ПВ моделирање - "SOLARGIS". Прорачун узима у обзир соларно зрачење,

температуру ваздуха и терен, да симулира претварање и губитке енергије у соларним модулима и осталим компонентама соларне електране. У симулацији су процењени губици услед прљавштине и прашине од 3,5%. Кумулативни ефекат осталих губитака претварања се рачуна да је 7,5% (засенчење, неусклађеност, претварачи, каблови, трансформатори, итд.) Сматра се да је расположивост соларних електрана 100%. Енергија сунца се израчунава из атмосферских и сателитских података, временског периода од 15 и 30 минута, и просторне резолуције од 1000m. Ову карту је "SOLARGIS" припремио према уговору са Светском банком (The World Bank) на основу базе података о соларним ресурсима коју "SOLARGIS" поседује и одржава.



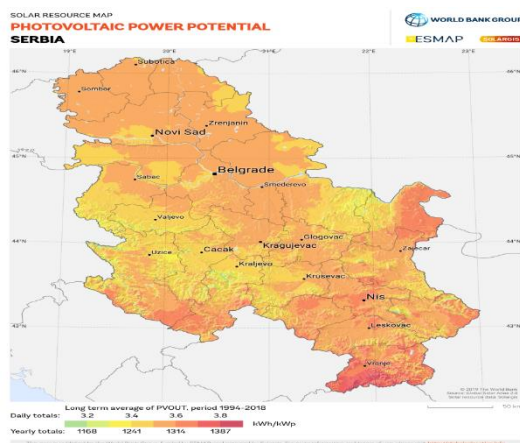
Слика бр.1: Мапа сунчевог зрачења у Србији на нагнуту површину од 30°

*Преузето из "Студије енергетског потенцијала Србије за коришћење сунчевог зрачења и енергије ветра", Институт за мултидисциплинарна истраживања



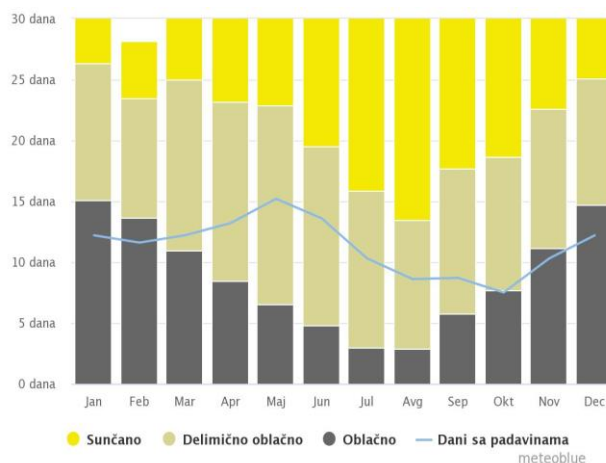
Слика бр.2: Мапа сунчевог зрачења у Србији на хоризонталну површину

*Преузето из "Студије енергетског потенцијала Србије за коришћење сунчевог зрачења и енергије ветра", Институт за мултидисциплинарна истраживања



Слика бр.3: Дијаграм месечних вредности сунчаних, делимично облачних, облачних и кишних дана за територију општине Лазаревац

*Преузето са сајма: www.meteoblue.com



Слика бр.4: Соларни потенцијал панела kWh/kWp

*Преузето са сајма: <https://globalsolaratlas.info/map>

3 Могућност изградње соларних система („on-greed“) на објектима "РБ Колубара - орг. целине „Прерада", Вреоци

3.1 Концепт пројекта

Предложени пројекат укључује развој фотонапонских електрана у ПДРБ "Колубара". Фотонапонске електране ће бити изграђене на крововима објеката организационе целине Прерада, који су најпогоднији за постављање панела. Укупна номинална електрична снага свих инсталираних соларних електрана тј., панела ће бити 1870 KWp. Произведена електрична енергија ће покрити очекивану годишњу потрошњу за објекте на којима се предвиђа постављање панела, али ће бити и вишка произведене енергије. Предвиђени соларни системи неће имати батерију за уштеду електричне енергије, већ ће вишак произведене електричне енергије продати на тржишту или преусмерити на друге потрошаче. Снабдевање електричном енергијом вршиће се из електричне мреже када је то потребно. Ово ће значајно смањити почетна улагања а самим тим и обезбедити објектима тј., корисницима соларне енергије континуитет у снабдевању ел. енергијом. У разматрање је узето 28 објекта на локацији поменуте организационе целине који су својом конструкцијом, површином и географским положајем најповољнији за постављање соларних панела.

Орјентација кровних површина је у правцу Југ, Југозапад, Запад и Исток. Тачније 11 кровних површина је орјентисано у правцу Југ- Југозапад, док је 17 кровних површина орјентисано у правцима Исток и Запад. Укупна кровна површина разматраних објеката износи око 14740 m². Површина која одговара за постављање соларних панела износи око 12130 m². Кровне површине орјентисане ка Југу и Југозападу износе око 2430 m², док је кровна површина орјентисана у правцу Исток - Запад око 9700 m².



Слика бр.5: Орг.цел."Прерада",погон
Оплемењивање



Слика бр.6: Орг.цел."Прерада",погон
Жел.транспорт

Укупан број разматраних објеката, расположива кровна површина за постављање панела и потрошња електричне енергије објеката, приказани су у следећој табели.

Табела бр.1.: Број објеката, површина крова и потрошња ел. ен.

Орјентација кровних површина објеката	Југ-Југозапад	Исток-Запад	Укупно
Број објеката	11	17	28
Одговарајуће кровне површине за постављање панела (m ²)	2430	9700	12130
Потрошња ел.ен. разматраних објеката (кWh/год)	1 614 346,00		
Потрошња ел.ен. разматраних објеката (кWh/год) од 07-15h	1 012 752,00		

Кровне површине на којима је могуће постављање панела су добијене множењем стварне површине основе објеката са коефицијентом за одговарајући нагиб крова за исте објекте. У обзир су узете кровне површине орјентисане ка Југу, Југозападу, Истоку и Западу.

Очекивана количина произведене ел. енергије представљена је у Табели бр.2.

Табела бр.2.: Инсталисана снага и количина произведене ел.ен. соларних панела

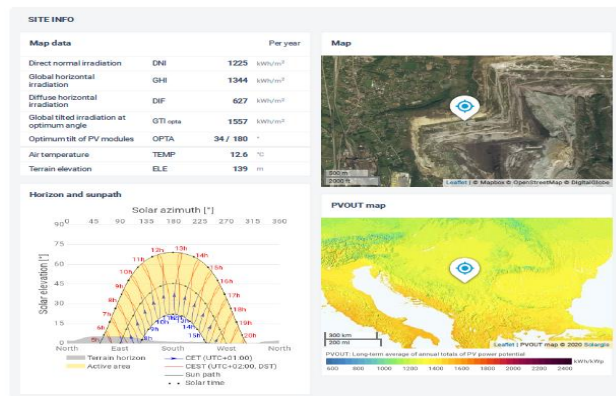
Орјентација објекта	Југ-Југозапад	Исток	Запад	Укупно
Инсталисана снага соларних панела у kWp	370	750	750	1870
Очекивана количина произведене ел. ен. на годишњем нивоу у kW/h	452 105,00	764 120,00	755 379,00	1 971 604,00

3.2 Соларни прорачун произведене електричне енергије

Очекивана количина произведене ел.енергије добијена је на основу соларног прорачуна у софтверу "SOLARGIS". Рађени су прорачуни за површине орјентисане ка Југу и за кровне површине орјентисане ка Истоку и Западу.

GLOBAL SOLAR ATLAS
BY WORLD BANK GROUP

Lazarevac
44°26'23", 20°17'50"
Lazarevac, Novi Grad, Serbia
Time zone: UTC+01, Europe/Belgrade (CET), Daylight saving time not considered
Report generated: 28 Jul 2020



WORLD BANK GROUP ESMAP SOLARGIS © 2020 The World Bank Group

Lazarevac 1 / 4

Слика бр.7: Соларне Карактеристике терена

GLOBAL SOLAR ATLAS
BY WORLD BANK GROUP

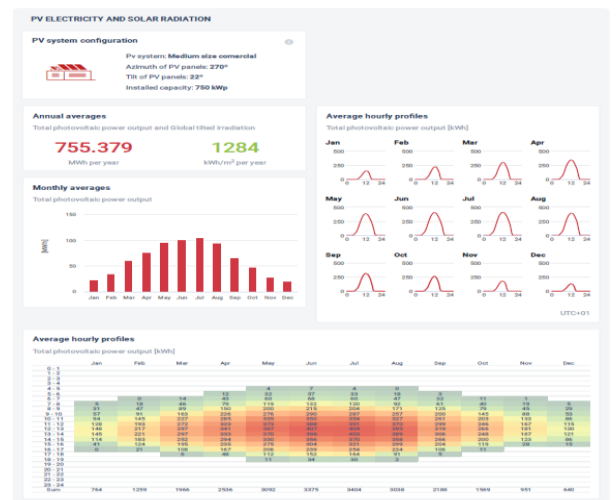


WORLD BANK GROUP ESMAP SOLARGIS © 2020 The World Bank Group

Lazarevac 2 / 4

Слика бр.8 : Соларни прорачун за кровне површине орјентисане ка Југу

GLOBAL SOLAR ATLAS
BY WORLD BANK GROUP



WORLD BANK GROUP ESMAP SOLARGIS © 2020 The World Bank Group

Lazarevac 2 / 4

Слика бр.9: Соларни прорачун за кровне површине орјентисане ка Западу

GLOBAL SOLAR ATLAS
BY WORLD BANK GROUP



WORLD BANK GROUP ESMAP SOLARGIS © 2020 The World Bank Group

Lazarevac 2 / 4

Слика бр.10: Соларни прорачун за кровне површине орјентисане ка Истоку

4 Могућност изградње соларних паркинга на локацији "РБ Колубара - орг. целина „Прерада“, Вреоци

Паркинг простори су изгубљено земљиште и захтевају веома мало пажње, па су самим тим идеални за израду соларних паркинга у виду соларних надстрешница. На тај начин би паркинг простор поред своје првобитне намене производио ел.енергију преко соларних панела и самим тим допринео заштити животне средине кроз смањење емисије CO₂ и повећању удела ОИЕ (обновљиви извори енергије). Велика предност соларних паркинга је та што им није потребно додатно земљиште као што је то случај са соларним електранама на земљи. Као резултат тога, носачи соларних панела нуде ефикаснију употребу простора у односу на соларне системе монтиране на земљи. Носачи соларних панела имају мање ограничења у односу на соларну електрану на земљи, па се могу сматрати пожељнијим у многим околностима. Неки од примера соларних паркинга могу се видети на следећим сликама.

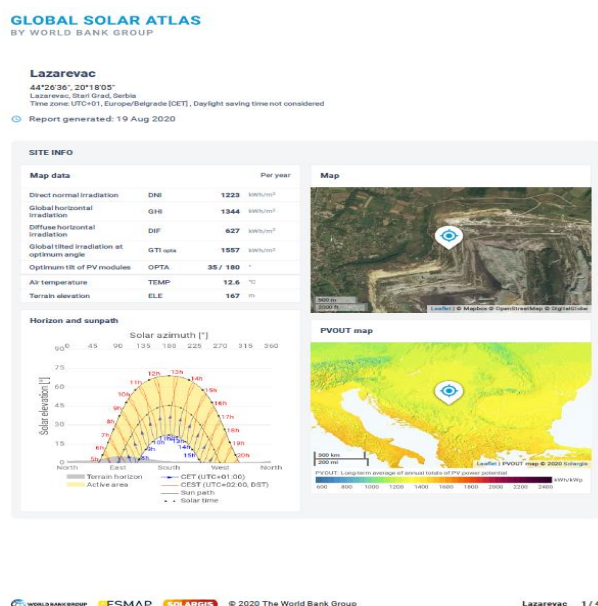
На основу расположиве површине постојећих паркиралишта на локацији орг.јед."Прерада", може се одредити јачина соларних електрана које би се поставиле на металне конструкције. Прорачун произведене ел.ен., укупна снага соларних панела као и површина паркинга дата је у табели бр.3.

Табела бр.3.: Прорачун Соларних паркинга

Локација сол.паркинга	Расположива Површина паркинга (m ²)	Снага сол. панела (kWp)	Очекивана количина произведене ел.ен. (kWh)
Стара Управа	2866	472	577 373,00
Топлана	2464	405	495 415,00
Дирекција Прераде	500	82	100 306,00
Сува Сепарација	550	90	110 092,00
Нови Водовод	440	72	88 074,00
УКУПНО	6820	1121	1 371 000,00

4.1 Соларни прорачун за предвиђене паркинг површине

Прорачун је рађен уз помоћ софтвера „SOLARGIS“ збирно за све паркинг површине.



Слика бр.11: Соларне карактеристике терена



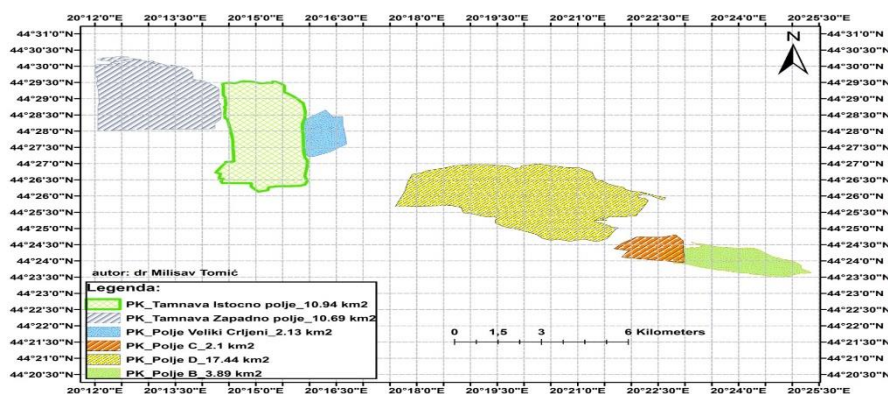
Слика бр.12: Соларни прорачун за паркинг површине

Соларни паркинзи су замишљени тако да се изнад паркинг простора подигне носећа конструкција на коју би се поставили соларни панели. Тако изграђен соларни паркинг има

вишеструку намену од производње електричне енергије до заштите аутомобила од сунца. Предност у односу на соларне електране на земљи је та што се ради адаптација постојећег паркинга у виду металне конструкције на коју се стављају соларни панели уместо уобичајних наткривних материјала, док за соларне електране на земљи мора да се ради читав низ послова, од препарцелације ако је потребна, пренамене земљишта до припреме терена и остало. Соларни паркинзи имају могућност да сву произведену енергију шаљу у дистрибутивни систем за интерну потрошњу. Тиме се остварује највећа финансијска добит с обзиром да је према „Одлуци о интерним ценама ел.енергије за 2020 годину“, формирана цена ел.енергије произведене из соларних електрана које нису стекле статус повлашћених произвођача у износу од 10,519 дин/ kWh. Постоји могућност да се један мали део електричне енергије складишти у батеријама и да се користи ноћу за осветљење самог паркинг простора. Такође постоји могућност и да се део или сва количина генерисане ел.ен.испоручује оближњим потрошачима чиме би се смањио укупни рачун за утрошену струју и такође остварила значајна финансијска уштеда. С обзиром на све већу потребу за обновљивим изворима енергије, потребно је и обезбедити нове површине за соларне електране. Најповољније су површине које нису више употребљиве за првобитну намену или постојеће површине где се неће угрозити њихова првобитна намена. Такво решење нуде соларни паркинзи.

5 Могућност изградње соларне електране на земљи

У Републици Србији постоји доста простора, где не постоји пољопривредна производња тј., није могућа, као што су јаловишта и неплодна земљишта. Такви простори могу бити искоришћени за соларне електране. Рударски басен Колубара је идалан по том питању јер има велике површине земље где је завршена експлоатација угља. Такво земљиште је деградирано и да би се довело у стање погодано за пољопривредну производњу потребно је инвестирати у послове рекултивације земљишта и све пропратне радове. С'тога се може рећи да би изградња соларне електране на земљи била оправдана са стране искоришћења земљишта. У Србији је подстицајна ("feed inn") откупна цена за соларну енергију драстично опала у односу на 2010. годину. За само четири године висина подстицајна откупна цена је са 23 с€/кWh пала на вредност од 20,66 до 16,25 с€/кWh и зависно од инсталисане снаге и начина инсталације (на објекту или земљи). Нова подстицајна регулатива из 2016. године још више је оборила цене, нарочито за соларне електране на земљи, која сада износи 9 с€/кWh. Систем би био исплатив у случају да се сва или већина произведене ел.ен., користи за сопствену потрошњу из разлога тенденције поскупљења ел.ен., или да се сва ел.ен. наплаћује по интерној цени ЕПС-а од 10,519 дин/кWh или у случају да се оствари ткзв. "feed inn" тарифа од државе, која се издаје на период од 12 година чиме би се гарантовала једна цена за тај период у току ког би се и систем отплатио.



Слика бр.13: Површински копови у РБ "Колубара"

Са ове слике се може видети да РБ Колубара има огроман потенцијал кад су у питању соларне електране на земљи с'обзиром да располаже великом површином земљишта на којима се врши експлоатација угља а такође и површином где је завршена експлоатација, с'тим да се

константно повећава површина на којој је експлоатација завршена и самим тим добијају нове површине које су погодне за изградњу соларних електрана. Примарна намена соларне електране је производња ел.енергије, али би поред тога служила и у едукативне сврхе а свакако би била и туристичка атракција.

6 Заштита животне средине кроз смањење емисије CO₂

Замена електричне енергије произведене из обновљивих извора, тачније из соларних система у односу на тренутну праксу из фосилних горива ће резултирати значајним смањењем емисије CO₂. Средња вредност специфичне емисије CO₂ из термоенергетских блокова ТЕНТ-а износи 1,132 kg CO₂/kWh_{el.en.}, или 1,132 t CO₂/MWh_{el.en.} [6]. На основу тога се може израчунати уштеда у смањењу емисије CO₂.

6.1 Смањење емисије CO₂ применом соларних електрана на објектима орг.јед. "Прерада"

Просечна годишња производња електричне енергије из соларних фотонапонских електрана на објектима ће смањити емисију CO₂ како је приказано у наставку:

$$\text{Смањење Емисије CO}_2 = 1971,6 \frac{\text{MWh}}{\text{год}} \times 1,132 \frac{\text{t CO}_2}{\text{MWh}} = 2231 \frac{\text{t CO}_2}{\text{год}}$$

У овом случају инсталирањем соларних електрана на разматраним објектима би се остварило смањење емисије CO₂ штетних гасова у количини од $2231 \frac{\text{t CO}_2}{\text{год}}$.

6.2 Смањење емисије CO₂ применом соларних паркинга

Просечна годишња производња електричне енергије соларних паркинга ће смањити емисију CO₂ како је приказано у наставку:

$$\text{Смањење Емисије CO}_2 = 1371 \frac{\text{MWh}}{\text{год}} \times 1,132 \frac{\text{t CO}_2}{\text{MWh}} = 1552 \frac{\text{t CO}_2}{\text{год}}$$

У овом случају инсталирањем соларних електрана на разматраним објектима би се остварило смањење емисије CO₂ штетних гасова у количини од $1552 \frac{\text{t CO}_2}{\text{год}}$.

6.3 Смањење емисије CO₂ реализацијом оба објекта

У случају реализације оба пројекта годишње би се смањила емисија CO₂ за 3753 тоне, чиме би се у знатној мери допринело очувању животне и радне средине.

$$\text{Смањење Емисије CO}_2 = 2231 \frac{\text{t CO}_2}{\text{год}} + 1552 \frac{\text{t CO}_2}{\text{год}} = 3783 \frac{\text{t CO}_2}{\text{год}}$$

Овиме би се такође смањило емитовање загађујућих материја које утичу на загађење животне средине и глобално загревање.

Ту се поред угљен диоксида (CO₂), мисли и на смањење емисије:

- азотних оксида (NO_x/NO₂),
- сумпорних оксида (SO_x/SO₂),
- чврстих прашкастих честица (PM).

Поменути загађења настају у термоелектрани као последица сагоревања угља за производњу топлотне и електричне енергије, приликом чега долази до емитовања загађујућих материја у атмосферу.

Смањењем емисије CO₂ и осталих загађујућих материја се поштују директиве ЕУ из области заштите животне средине као и принципи међународних конвенција на које се Република Србија обавезала да ће их спроводити.

7 Финансијска добит

Систем соларних електрана остварује новчану добит на више начина који су представљени у даљем раду.

7.1 Финансијска добит и исплативост соларних система на објектима у орг. цел. "Прерада"

7.1.1 Прва варијанта

1. Део произведене електричне енергије се директно користи за сопствену потрошњу у објектима на којима су инсталирани соларни панели. На тај начин се директно утиче на смањење рачуна за утрошену струју чиме се остварује финансијска уштеда.

2. Вишак произведене електричне енергије се шаље директно у мрежу, односно дистрибутивни систем. Предата количина електричне енергије се наплаћује по тренутно важећој цени чиме се такође остварује директна финансијска добит.

У овом случају би се за сваку годину рачунала садашња цена (7,7 дин/ kWh) по којој РБ Колубара Прерада плаћа утрошену ел.енергију. Цена по којој би се наплаћивао вишак ел.енергије тренутно износи 10,519дин/kWh(интерна цена у ЕПС-у за произведену ел.ен.из соларних електрана).

За објекте на којима је предвиђена инсталација соларних панела утврђено је да на годишњем нивоу троше око 2 218 994,00 kWh ел. ен. од чега се у првој смени (07h - 15h) потроши око 1 012 752,00 kWh .

Уштеда услед умањења рачуна за утрошену ел.ен., износи:

$$\text{Добит}(1) = 1\,012\,752,00 \text{ kWh/год} * 7,7 \text{ дин/ kWh} = 7\,798\,190,00 \text{ дин/год.}$$

Резултат је добијен множењем количине утрошене ел.ен., из соларних панела, са ценом по којој би се плаћала та иста ел.ен. (тренутно 7,7 дин). Укупан вишак струје који се произведе се предаје дистрибутивном систему по интерној цени која тренутно износи 10,519 дин/ kWh.

*Добит (2) од продаје вишка ел.ен.,износи: 958 852,00 kWh. * 10,519 дин/ kWh.= 10 086 164,00 дин/год*

Очекивана годишња добит: Добит(1)+Добит(2) = 17 884 354,00 дин/год.

7.1.2 Друга варијанта

Ако би се вишак произведене електричне енергије преусмерио на друге потрошаче у орг.јед.,„Прерада" уместо у мрежу, тада би се практично сва произведена ел. енергија користила за сопствену потрошњу на нивоу орг. јед. „Прерада". У овом случају је рачуната садашња цена (7,7 дин/ kWh).

*Очекивана годишња добит : 1 971 604,00 kWh * 7,7 дин/ kWh*=15 181 350,00дин*

Ово је најнеисплативији сценарио који уједно и није реалан с обзиром на тенденцију раста цене ел.енергије.

7.1.3 Трећа варијанта

У овом случају би се сва произведена ел.енергија из соларних електрана користила за потрошњу унутар ЕПС-овог система, тј. за потребе РБ Колубара, по тренутно важећој интерној цени у оквиру ЕПС-а од 10,519 дин/ kWh, с обзиром да је потрошња много већа од произведене количине ел.енергије из соларних система,

*Очекивана годишња добит : 1 971 604,00 kWh * 10,519 дин/ kWh = 20 739 302,00 дин.*

Ово је најисплативији сценарио, с'тим да постоји тенденција раста интерне цене ел.ен. из соларних електрана које нису стекле статус повлашћеног произвођача.

7.2 Финансијска добит и исплативост соларних паркинга у орг. цел. "Прерада"

Соларни паркинзи су замишљени тако да се на постојећим паркинзима изгради конструкција налик надстрешници на коју би се поставили соларни панели. Сваки соларни паркинг представља засебну соларну електрану са свим својим елементима.

7.2.1 Прва варијанта

Произведена електрична енергија се може предавати директно у мрежу, тј., у дистрибутивни систем и на тај начин остварити финансијска добит. Интерна цена произведене ел.ен. за соларне електране које нису у систему повлашћених произвођача износи 10,519 дин/ kWh.

Очекивана годишња добит : $1\,371\,000,00\text{ kWh} * 10,519\text{ дин/ kWh} = 14\,395\,500,00\text{ дин}$

7.2.2 Друга варијанта

Подразумева могућност да се сва електрична енергија шаље потрошачима који се налазе у погону тј., организационој целини "Прерада". Орг.цел "Прерада" на годишњем нивоу троши око 65 GWh/god. ел.енергије, где су највећи потрошачи енергије погон "Оплеменењавање" са потрошњом од око 26 GWh/god и PJ Топлана са потрошњом од око 14 GWh/god. С обзиром да се у непосредној близини налази највећа површина предвиђених соларних паркинга, може се рачунати да ће сва произведена ел.ен. бити употребљена за сопствену потрошњу чиме се остварије уштеда кроз смањење рачуна за утрошену ел.ен.

Очекивана годишња добит = $1\,371\,000,00\text{ kWh/god} \times 7,7\text{ дин} = 10\,556\,700,00\text{ дин}$

За случај да се цена електричне енергије додатно повећа што је реално с обзиром на тренд повећања и ситуације на берзи као и садашњу цену електричне енергије, тада би годишња добит била већа а то би знатно утицало на период исплативости инвестиције

7.3 Финансијска добит на основу произведене ел.ен. из соларних система

Производњом електричне енергије из соларних система растеређује се енергетски систем за произведену количину ел.ен., а то се односи и на РБ "Колубара". Да би се иста та количина електричне енергије из соларних система произвела у термоенергетским постројењима, потребан је читав низ послова и радова. То са собом повлачи трошкове целокупног поступка производње електричне енергије, од планирања, експлоатације, прераде, транспорта до сагоревања угља у термоблоковима уз све пропратне радове, ангажман људства и механизације, потрошње енергената као и трошкове експропријације.

На слици испод дат је прорачун коштања производње електричне енергије.

Contracting Party	Plant type (fuel)	Operating expenses	Return on equity	Direct coal subsidies	Assumed carbon costs	Estimated full costs of production per plant type	Average full costs of production of electricity
		EUR/MWh	EUR/MWh	EUR/MWh	EUR/MWh	EUR/MWh	EUR/MWh
Bosnia and Herzegovina	coal	44,17	6,09	3,64	20	73,89	61,81
	hydro	27,20	11,55			38,76	
Kosovo*	coal	26,81	2,31	2,93	20	52,05	51,50
	hydro	30,82				30,82	
Montenegro	coal	61,99	5,11	1,23	20	88,33	63,78
	hydro	29,71				41,26	
North Macedonia	coal	60,57	5,31	0,70	20	86,59	54,32
	hydro	32,32				32,32	
Serbia	coal	38,58	5,07	3,87	20	67,51	54,36
	hydro	23,38				23,38	
Ukraine	coal	47,3	5,00	5,69	20	77,99	53,85
	other	43,22				43,22	

Слика бр.14.: Прорачун коштања производње електричне енергије.

* Analysis of Direct and Selected Hidden Subsidies to Coal Electricity Production in the Energy Community Contracting Parties

Ако се узме у обзир разлика у цени произведене количине ел.ен. из разматраних соларних система и цени коштања производње исте количине ел.ен., из термоелктрана, остварује се годишња уштеда од око 223.836,00 €.

Кад се на то додају и претходно разматране добити од соларних система на објектима (сва три случаја) и соларних паркинга онда се остварије укупна годишња добит од 441 955,00 € до 521 588,00 € , зависно од разматране опције.

8 Користи од примене соларних панела у ЈП "ЕПС"- Огранак "РБ Колубара"

Главне користи за ЈП ЕПС, огранак РБ "Колубара" су следеће:

- Уштеда у смањеним рачунима за утрошену електричну енергију.
- Могућност остваривања прихода од продаје ел. енергије.
- Допринос борби против климатских промена и већем коришћењу ОИЕ.
- Растеређење система кроз смањење експлоатације примарног енергента за производњу ел.ен., за количину произведене ел.ен. из соларних система.
- Нова радна места за потребе соларних система.
- Боље повољности код ЕУ фондова и Европских банака.

– Маркетинг фирме.

Коришћењем произведене електричне енергије за сопствену потрошњу би се смањио укупни годишњи рачун за утрошену електричну енергију. Вишак произведене ел.ен., или сва количина би се могла продавати држави или на слободном тржишту. Производњом електричне енергије из соларних панела би се произвело око **3 342 604 kWh**. Самим тим би се смањила потреба за експлоатациом угља ради производње исте количине ел.ен., и растеретио рударски систем у одређеној мери.

Додатне уштеде које се могу остварити су:

– Смањени ангажман људских ресурса, конкретно радне снаге за послове експлоатације угља ради производње ел.ен.

– Смањена потрошња струје потребне за експлоатацију оне колчине угља која је потребна за производњу 3,342 GWh, ел.ен., у термоелектранама.

– Смањење потрошње горива за рад машина за потребе експлоатације угља.

– Амортизација и одржавање механизације потребне за послове експлоатације угља потребног за производњу 3,342 GWh.

– Рационалнија експлоатација угља као необновљивог извора енергије што значи и дужи век трајања самог рударског басена.

Држава добија:

– Повећано коришћење ОИЕ.

– Унапређење стања и система заштите животне средине кроз смањење емисије гасова са ефектом стаклене баште, пре свега CO₂, као и прашкастих материја.

– Смањене потребе за инвестиције у велике електране.

– Повећана сигурност снабдевања кроз дистрибуирану производњу.

– Смањене потребе увоза електричне енергије а самим тим и додатна новчана уштеда са могућношћу продаје вишка ел.ен.

Електродистрибутивне компаније себи обезбеђују:

– Позитиван утицај на смањење губитака у електродистрибутивној мрежи

– Децентрализација система.

– Отварање нових пословних могућности.

– Повећану сигурност снабдевања.

9 Закључак

Повећање енергетске ефикасности треба посматрати и у контексту сигурности снабдевања енергијом, као и очувања енергената за будуће генерације, односно у функцији одрживог развоја. ЕУ потенцира енергетску ефикасност као економски најефективнији начин да се смање емисије гасова, унапреди енергетска стабилност и конкурентност, доступност енергије за потрошаче, као и да се повећа запосленост односно отворе нова радна места. Енергија сунца је најперспективнији облик енергије у еколошком смислу. У визији Европске Уније (ЕУ) за фотонапонске системе одређено је да ће се до 2030.године у ЕУ инсталирати соларне електране чија ће снага достићи 200 GW, што је 4% укупне светске производње електричне енергије. До 2050. године сва произведена електрична енергија из соларних система требало би да достигне преко 25% од укупне електричне енергије, произведена на класичан начин, у целом свету. Ако би се соларни системи применили на свим одговарајућим објектима и паркинг просторима на нивоу целе фирме односно целог предузећа, онда би сви позитивни ефекти били значајно израженији и приметнији. С'обзиром да је РБ Колубара корисник средстава "Европске банке за обнову и развој" ("EBRD" банака) остварили би се доста повољнији услови и добила већа средства приликом аплицирања за исте. Једна од главних ставки које "EBRD" банка и друге сличне организације гледају приликом додељивања средстава јесте смањење емисије CO₂. Поготово ако би се изградила соларна електрана на земљи за сопствену потрошњу ел.ен., (по интерним ценама ЕПС-а) или продају по "feed in" тарифи, тада би се сви позитивни резултати додатно повећали. Соларни системи ће бити све исплативији и све више фондова ће одобравати и подржавати пројекат. Ако се узму у обзир све претходно наведене чињенице и погодности које се остварују овим системима као и то да већина компанија које се баве изградњом сол.електрана има праксу смањења цене услуге уградње ако се ради већа

површина (као у случају овог пројекта), онда се долази до закључка да се соларни системи отплаћују у кратком року и да су вишестуко корисни и исплативи.

10 Литература

- [1] *** *Analysis of direct and selected hidden subsidies to coal electricity production in the energy community contracting parties*, Секретаријат енергетске заједнице, Септембар 2019
- [2] *** Водич за инвеститоре 2016 - Изградња постројења и производња електричне енергије у фотосоларним електранама у Републици Србији
- [3] *** *Energy 2020 – A strategy for competitive, sustainable and secure energy*. European commission, 2010
- [4] *** Енергетски биланс Републике Србије за 2019 ("Службени гласник РС", број 105-18)
- [5] *** Енергија у Србији, Министарство рударства и енергетике, 2010.
- [6] **З. Марковић и др.**, Прорачун специфичне емисије угљен диоксида из термоелектрана Никола Тесла А и В:, Термотехника, 2016, 25-36.
- [7] *** Закон о енергетици ("Сл. гласник РС", бр. 145/2014 И 95/2018).
- [8] *** Закон о планирању и изградњи („Службени гласник РС”, бр. 72/09, 81/09 – исправка, 64/10 – УС, 24/11, 121/12, 42/13 – УС, 50/13 – УС, 98/13 – УС, 132/14 И 145/14).
- [9] *** Закон о просторном плану републике србије (Сл. гласник РС, бр.88/10).
- [10] *** Закон о заштити животне средине, (Сл.гласник РС, бр.135/04,36/09 И 14/16).
- [11] *** Извештај о спровођењу националног акционог плана за обновљиве изворе енергије 2018. Министарство рударства и енергетике
- [12] **Katalin Bódis, Ioannis Kougias, Nigel Taylor and Arnulf Jäger-Waldau**, Solar photovoltaic electricity generation: a lifeline for the european coal regions in transition.
- [13] **K. Vickery, R.J. Baron**, Solar photovoltaic energy production comparison of east, west, south-facing and tracked arrays.
- [14] *** Национални акциони план за коришћење обновљивих извора енергије (напоие) („Службени гласник РС“, број 53/2013).
- [15] *** Стратегија развоја енергетике Републике Србије до 2025. године са пројекцијама до 2030. године, („Службени гласник РС“, број 101/2015).
- [16] *** **Студија енергетског потенцијала србије за коришћење сунчевог зрачења и енергије ветра**, Институт за мултидисциплинарна истраживања, Београд 2004 год.
- [17] *** Уредба о подстицајним мерама за производњу електричне енергије из обновљивих извора и из високоефикасне комбиноване производње електричне и топлотне енергије, („Службени гласник РС“, БРОЈ 56/2016).
- [18] *** <https://balkangreenenergynews.com/rs>.
- [19] *** <https://ec.europa.eu/>.
- [20] *** <https://energize.rs/en/contact/>
- [21] *** <https://www.esolarfirst.com>
- [22] *** <https://www.klima101.rs/pariski-sporazum/>
- [23] *** [https://www.noleko.rs /contact/](https://www.noleko.rs/contact/)
- [24] *** <http://www.plan-net.si/index.php/contact/>
- [25] *** [http://www.telefon-inzenjering.co.rs/ contact/](http://www.telefon-inzenjering.co.rs/contact/)

ENERGETSKA EFIKASNOST U SEKTORU JAVNIH ZGRADA NA TERITORIJI GRADA KRAGUJEVCA – STUDIJA SLUČAJA OŠ „MILUTIN I DRAGINJA TODOROVIĆ“

ENERGY EFFICIENCY IN THE PUBLIC BUILDINGS SECTOR IN THE TERRITORY OF THE CITY OF KRAGUJEVAC – CASE STUDY OF "MILUTIN AND DRAGINJA TODOROVIĆ" ELEMENTARY SCHOOL

Ana RADOJEVIĆ*, Aleksandar NEŠOVIĆ, Jasmina SKERLIĆ,
Dušan GORDIĆ, Danijela NIKOLIĆ
Fakultet tehnički nauka, Kragujevac, Srbija

Obrazovne ustanove (OU), sa udelom od oko 38%, predstavljaju najveću kategoriju objekata u sektoru javnih zgrada (SJZ) na teritoriji grada Kragujevca po pitanju potrošnje električne energije, koja na godišnjem nivou iznosi preko 10 GWh. Sprovedenjem odgovarajućih mera koje podrazumevaju obaveznu upotrebu obnovljivih izvora energije (OIE) u kombinaciji sa vođenjem odgovorne energetske politike na gradskom nivou, potrošnja električne energije u navedenom sektoru može biti značajno redukovana, uz niz pozitivnih efekata, od energetske i ekonomskih, do ekoloških. U ovom radu korišćeni su softverski paketi EnergyPlus i Google SketchUp kako bi se ispitala mogućnost postavljanja fotonaponskih (FN) panela na krov zgrade OŠ „Milutin i Draginja Todorović“, sa osnovnim ciljem da se u bližoj budućnosti ovaj model implementira i na ostale javne zgrade čime bi se obezbedila veća energetska nezavisnost i stabilnost čitavog sektora.

Ključne reči: sektor javnih zgrada (SJZ); obrazovne ustanove (OU); osnovne škole (OŠ); fotonaponski (FN) paneli; EnergyPlus.

Educational institutions (EI), with a share of approximately 38%, represent the largest category of facilities in the public buildings sector (PBS) in the City of Kragujevac when it comes to electric power consumption, which annually amounts to over 10 GWh. By implementing appropriate measures, including the mandatory use of renewable energy sources (RES) in combination with a responsible energy policy at the city level, electricity consumption in this sector can be significantly reduced, with a number of positive effects – from energy and economic to environmental ones. In this paper, the software packages EnergyPlus and Google SketchUp were used to examine the possibility of installing photovoltaic (PV) panels on the roof of "Milutin and Draginja Todorović" Elementary School (ES) building, with the main goal to implement this model in other public buildings in the near future, thus providing greater energy independence and stability of the whole sector.

Key words: public buildings sector (PBS); educational institutions (EI); elementary schools (ES); photovoltaic (PV) panels; EnergyPlus.

1 Introduction

According to the data available in the Energy Efficiency Program of the City of Kragujevac [1], the electric power consumption in PBS is 10089395.48 kWh/a (Fig. 1). EI contribute the most to this consumption with approximately 3857881.2 kWh (38%), followed by HI (1624609.61 kWh/a) and SO (1299957.83 kWh/a). Among EI in the city of Kragujevac, the ES are the most numerous (69 of them), which is why they have the highest consumption of electric power (1909274.03 kWh/a), while the second highest are HS with the consumption share of 12% (1223935.83 kWh/a).

In order to reduce the consumption of electricity in EI, and even in the entire PBS, the use of PV panels can play a key role, which has been tested and shown in a large number of papers around the world [2-7].

* Corresponding author, email: aradojevic@kg.org.rs

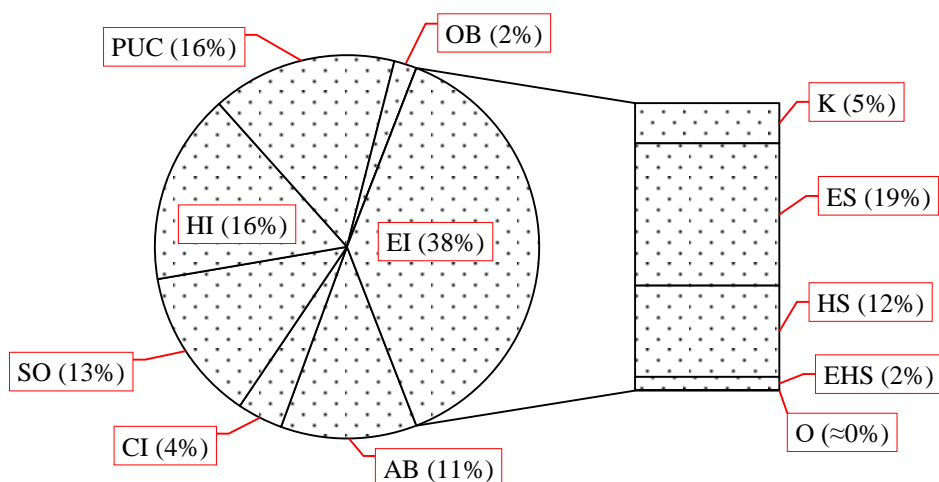


Fig. 1. The electric power consumption in PBS in the City of Kragujevac according to the facility structure [1]

EI – Educational Institutions; AB – Administrative Buildings; CI – Cultural Institutions; SF – Sports Objects; HI – Health Institutions; PUC – Public Utility Companies; OB – Other Buildings; K – Kindergarten; ES – Elementary School; HS – High School; EHS – Elementary and High School; O – Other

The study conducted in Portugal [8] dealt with the implementation of PV panels on the roofs of school buildings, taking into account the following: the potential of use of the roofs of school buildings, investment costs, return of investment period, reduction of greenhouse gases. *Shaari and Bowman* simulated the operation of BIPV applications on a standard school building in Malaysia, showing that the potential for using PV technologies is much higher [9]. A study conducted on a school building in Turkey [10] showed that the use of PV panels can cover 28-80% of electricity needs, depending on the month of the year. In [11] 265 PV panels were used on the roof of the school in Izmir to meet 65% of its own electricity needs. In one school building in the United Arab Emirates [12], 62 PV panels (total installation power of 7936 W) were used in conjunction with 62 batteries (each 12 V), which proved that the produced electricity can be used for an in-school water treatment plant and night decorative lighting. *Leena Cholakal* took a specific example of a school building in Blacksburg (Virginia) and used multiple linear regression in order to develop a model that would be used to assess the cost-effectiveness of a structurally integrated PV roof system connected to a electric power grid [13]. In [14] eQUEST software package was used to (among other things) examine the production of electricity from the PV system in a school building located in a humid climate, in Hong Kong. By using BIPV for facades, 97.5% of electricity needs can be met, and by installing PV panels on the roof, complete energy independence of the building can be ensured.

In Serbia, the use of PV panels is still very low, although the potential for using solar energy is higher than the European average. One of the main reasons is that there are no legal regulations for the return of "surplus" electricity produced into the power grid, free of charge, which is why solar systems are sized according to the needs of the users in the building (regardless of its purpose).

In this research, the roof of the "Milutin and Draginja Todorović" Elementary School building is used for the installation of PV panels in order to reduce the consumption of electricity in it. The goal is to accelerate the use of solar energy through greater implementation of PV systems in PBS, which would ensure energy and environmental stability of the City of Kragujevac.

2 Materials and methods

The subject of the research is the "Milutin and Draginja Todorović" Elementary School building (Fig. 2). The building has four floors with a total area of 4424.74 m², as follows: basement (683.3 m²), ground floor (1986.94 m²), first floor (823.55 m²) and second floor (930.95 m²). The main entrance is oriented to the southwest (SW).

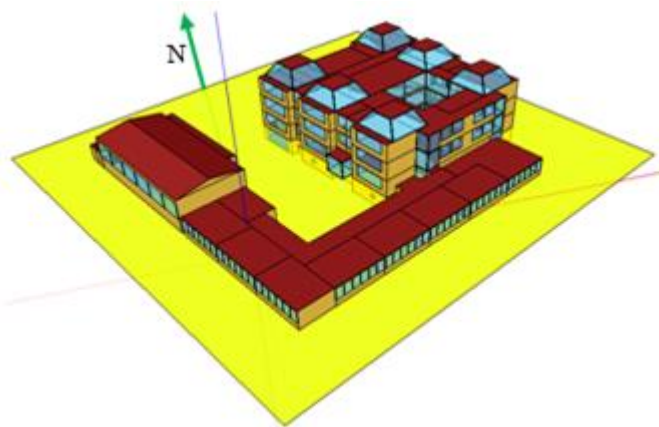


Fig. 2. Isometric view of the ES "Milutin and Draginja Todorović"

Kragujevac (located in GMT+1 h time zone) is characterized by a moderate continental climate with distinct seasons. Summers are hot and humid, with temperatures reaching +37°C. On the other hand, winters are cold (temperatures drop to -12°C) with snow. The city is located at 44°02' N and 20°92' E, at the altitude of 209 m [15]. Meteorological data for the city of Kragujevac are given in Tab. 1.

Tab. 1. Meteorological data for the city of Kragujevac [15]

Month	t_D [°C]	t_W [°C]	I_{DIFF} [W/m ²]	I_{DIR} [W/m ²]	ϕ [%]	a [deg]	c [m/s]
January	-0.24	-1.44	33.30	63.63	79.92	213.17	2.01
February	0.88	-0.46	49.39	86.66	79.82	210.60	2.02
March	5.57	3.29	77.08	106.12	72.06	207.98	2.35
April	10.87	7.74	92.65	149.02	67.92	209.06	2.27
May	16.06	12.18	113.30	176.45	66.57	210.08	1.77
June	18.85	14.99	109.50	208.94	69.42	209.51	1.69
July	20.78	16.04	110.60	228.12	64.49	198.04	1.62
August	20.38	15.69	96.25	215.40	64.05	211.45	1.51
September	16.68	13.30	75.54	166.92	71.21	203.79	1.68
October	11.18	8.83	57.34	119.43	76.40	222.28	1.69
November	6.08	4.45	39.83	64.51	79.80	210.38	2.06
December	1.13	0.09	28.66	58.86	83.51	208.33	1.87

t_D – Dry bulb temperature; t_W – Wet bulb temperature; I_{DIFF} – Diffuse solar radiation;
 I_{DIR} – Direct solar radiation; ϕ – Relative humidity; a – Wind Direction; c – Wind speed

Taking into account the specific factor of the building shape and orientation, the Fig. 3. shows potential roof surfaces for the installation of PV panels. The characteristics of the listed roof surfaces are given in Tab. 2.

It is possible to install 72 monocrystalline PV panels, measuring 1940×990×40 mm in size, with the total installed (maximum) power of 24480 W [16] on the Roof 1. Taking into account the optimal angle of inclination of the PV panels, which is 37.5° for the city of Kragujevac [17], the recommendations from [18] related to the method of assembly and installation of PV panels, the impact of shadow due to the factor of orientation and shape of the building (Fig. 4), as well as the formula (Eq.1 [19]) for determining the optimal distance between the rows of PV panels (Fig. 5), it is possible to place a total of 88 monocrystalline PV panels (of same dimensions) with the total installed (maximum) power of 29920 W on the Roof 3.

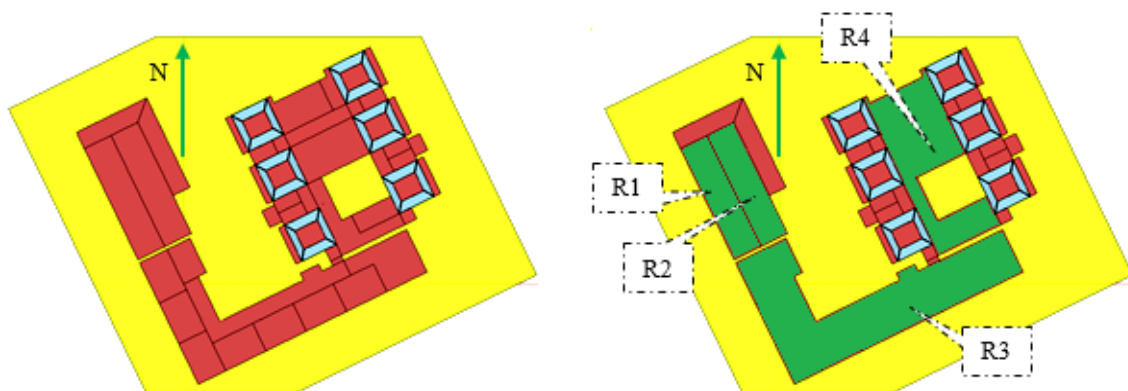


Fig. 3. View of the roof flats of the ES "Milutin and Draginja Todorović"

Tab. 2. Characteristics of potential roof surfaces for installing PV panels

Name	Designation	P [m ²]	Characteristic	I _{TOT} [kWh/m ² /a]	Conclusion
Roof 1	R1	145.24	Hip roof (≈9.6° to SW)	1367.52	Suitable for installing PV panels
Roof 2	R2	145.24	Hip roof (≈9.6° to NE)	1247.63	Not suitable for installing PV panels
Roof 3	R3	647.95	Flat roof	1278.14	Suitable for installing PV panels
Roof 4	R4	366.35	Flat roof	1242.86	Not suitable for installing PV panels

P – Roof area; I_{TOT} – Total solar radiation incident on roof area

$$Z = H \cdot \frac{\sin(180^\circ - (\alpha + \beta))}{\sin \beta} = 1.94m \cdot \frac{\sin(180^\circ - (37.5^\circ + 22.5^\circ))}{\sin 22.5^\circ} = 2.24m \quad (\text{Eq. 1})$$

The impact of the shadow (the so-called shadow line) is determined for the spring (March 21) and autumn (September 23) equinox, when the length of the day and night is 12 hours each.

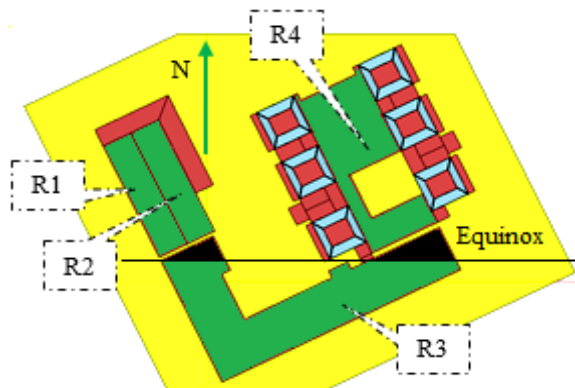


Fig. 4. Net roof surface for PV panel installation on the Roof 3

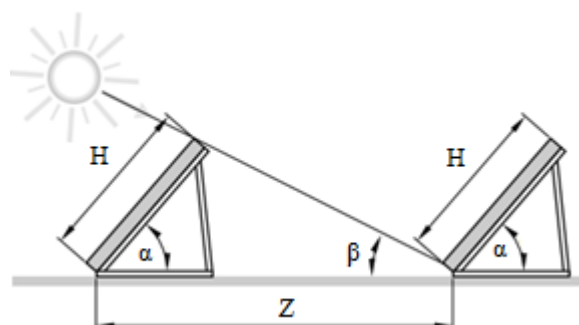


Fig. 5. Optimal distance between the rows of PV panels

Isometric view of the conceptual design of the solar power plant on the roof of the "Milutin and Draginja Todorović" Elementary School building with a total installed (maximum) power of 54400 W is shown in Fig. 6.

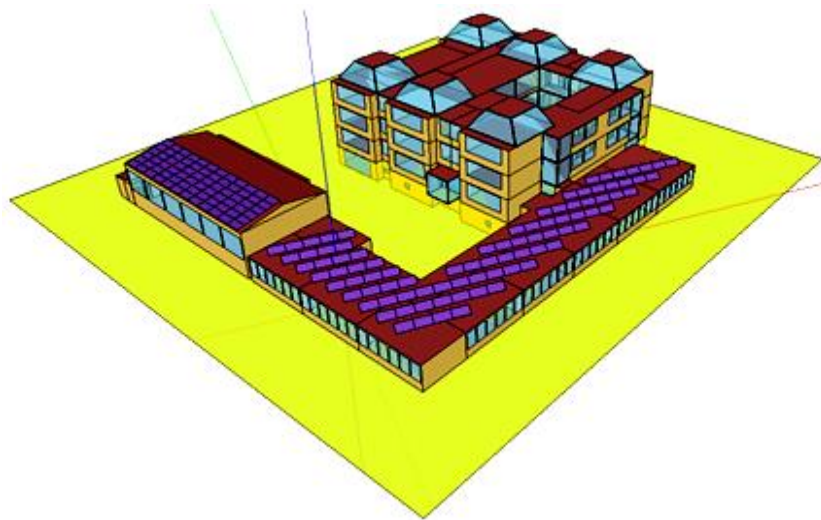


Fig. 6. Isometric view of the conceptual design of the solar power plant on the roof of the "Milutin and Draginja Todorović" ES building

3 Research results

Electric power consumption in the "Milutin and Draginja Todorović" Elementary School building, by months, for the period 2015-2019, is shown in Fig. 7.

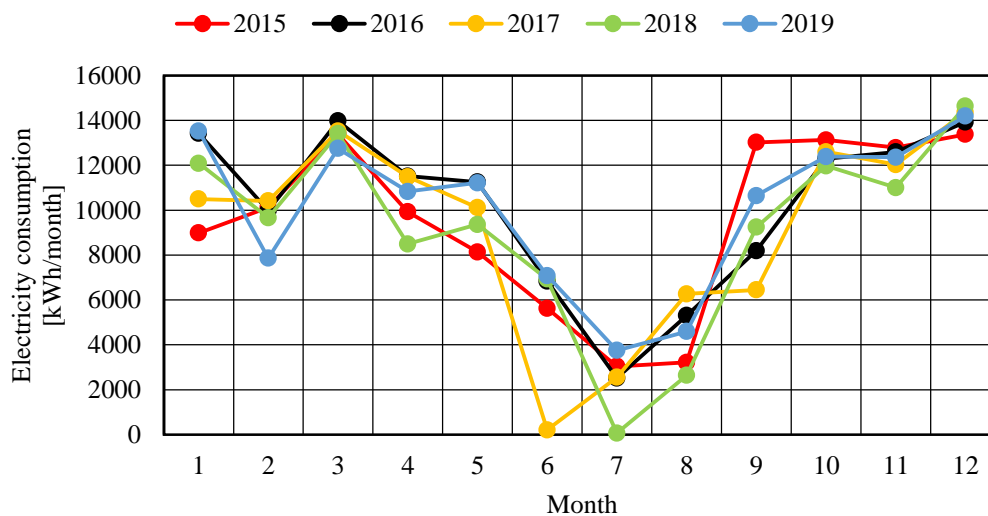


Fig. 7. Monthly consumption of electricity in "Milutin and Draginja Todorović" ES building (2015-2019)

Fig. 7. shows that consumption of electric power is very uneven if the same months are observed during the analyzed period. It can also be noticed that electricity consumption during the summer season is much lower (from March to October) compared to electricity consumption during the heating season. The reason lies in the school calendar that includes summer vacation, but also in low-usage of air-conditioning split systems that are utilized as a supplementary heating source during the winter season.

Fig. 8. shows the relationship between the monthly production of electricity from the solar power plant and its average consumption in the period from 2015 to 2019 in the analyzed building.

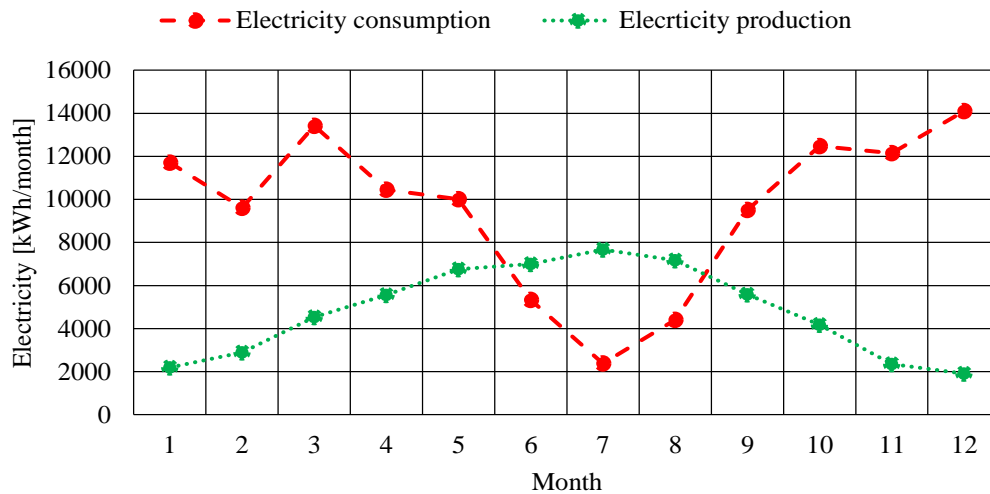


Fig. 8. Relationship between the monthly production of electricity and its average consumption in "Milutin and Draginja Todorović" ES building

The first thing to be noticed is that the solar power plant is not able to fully compensate for the school's needs for electric power from September to May, that is, school's electricity needs are much higher than the solar power plant potentials. It can also be noticed that the production of electricity is the highest in June, July and August, when the needs are the least (the production of electricity exceeds the needs of the building). As the legislation in Serbia is still not on the side of the privileged producers of electricity, the surplus electricity can be stored and then used depending on the needs of the building. This would give much more even production and consumption curves (Fig. 9).

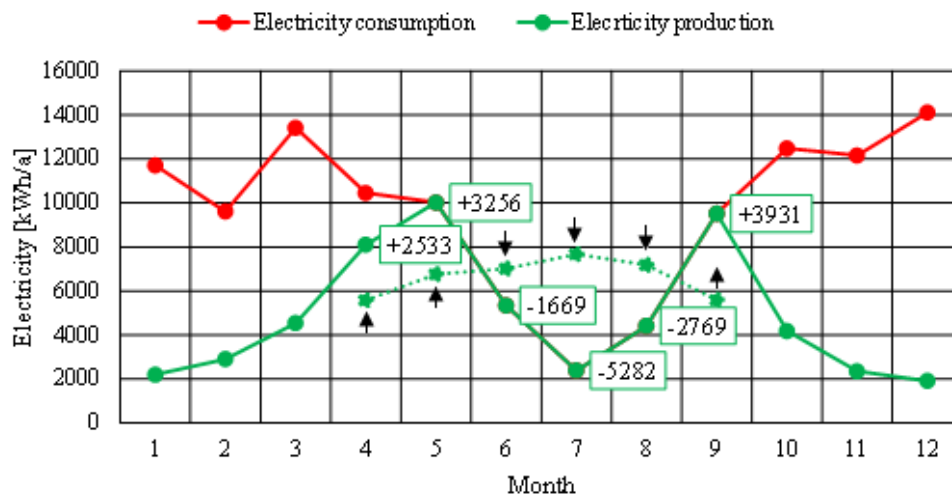


Fig. 9. Balancing of electricity consumption in "Milutin and Draginja Todorović" ES building

As the average annual electricity consumption in the analyzed period is around 115558 kWh/a, and the average electricity production is 57795 kWh/a (with a system efficiency of 90% during the first 15 years), it can easily be concluded that, by installing a solar power plant on the roof of the "Milutin and Draginja Todorović" Elementary School building, savings in consumption of about 50% can be achieved, which means that a significant reduction in CO₂ emissions and primary energy consumption can be achieved as well (Fig. 10, Fig. 11).

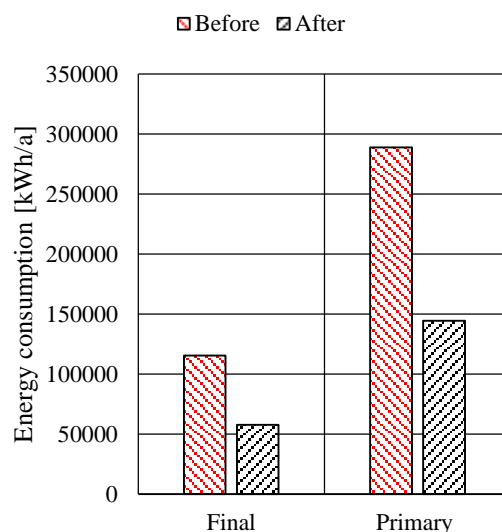


Fig. 10. Final and primary energy consumption in "Milutin and Draginja Todorović" ES building before and after energy efficiency measures [20]

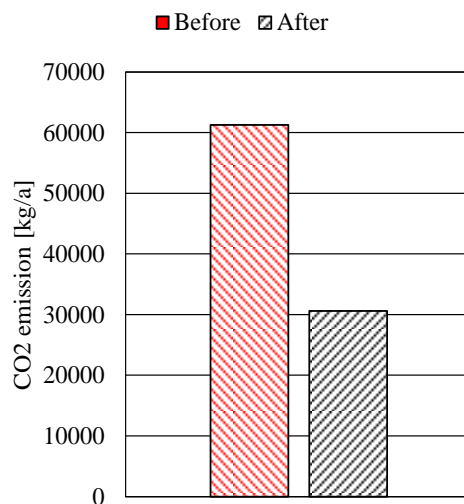


Fig. 11. CO₂ emissions in "Milutin and Draginja Todorović" ES building before and after energy efficiency measures [20]

4 Conclusion

Educational institutions (EI), with a share of approximately 38%, represent the largest category of facilities in the public buildings sector (PBS) in the City of Kragujevac when it comes to electric power consumption, which annually amounts to over 10 GWh. By implementing appropriate measures, including the mandatory use of renewable energy sources (RES) in combination with a responsible energy policy at the city level, electricity consumption in this sector can be significantly reduced, with a number of positive effects – from energy and economic to environmental ones.

In order to reduce electricity consumption in EI, and even in the entire PBS, the use of PV panels can play a key role, which has been tested and shown in a number of papers around the world. It is possible to install a solar power plant with a total installed (maximum) power of 54400 W on the roof of the "Milutin and Draginja Todorović" Elementary School building in Kragujevac.

The solar power plant is not able to fully compensate for the school's needs for electric power from September to May, that is, school's electricity needs are much higher than the solar power plant potentials. The production of electricity is the highest in June, July and August, when the needs are the least (the production of electricity exceeds the needs of the building).

By installing a solar power plant on the roof of the "Milutin and Draginja Todorović" Elementary School building, savings in consumption of about 50% can be achieved, which means that a

significant reduction in CO₂ emissions and primary energy consumption can be achieved as well. As the legislation in Serbia is still not on the side of the privileged producers of electricity, the surplus electricity can be stored and then used depending on the needs of the building.

5 Acknowledgments

This paper is a result of two investigations: (1) project TR33015 of Technological Development of Republic of Serbia, and (2) project III 42006 of Integral and Interdisciplinary investigations of Republic of Serbia. The first project is titled “Investigation and development of Serbian zero-net energy house”, and the second project is titled “Investigation and development of energy and ecological highly effective systems of poly-generation based on renewable energy sources”. We would like to thank the Ministry of Education and Science of Republic of Serbia for their financial support to these investigations.

6 References

- [1] Energy efficiency program of the city of Kragujevac for the period 2018-2020, http://www.aarhus.org.rs/wp-content/uploads/2018/11/Program_energetske_efikasnosti_grada_Kragujevca.pdf (accessed on June 2020).
- [2] **Al-Otaibi, A., Al-Qattan, A., Fairouz, F., Al-Mulla, A.**, Performance evaluation of photovoltaic systems on Kuwaiti schools’ rooftop, *Energy Conversion and Management*, Vol. 95 (2015), Issue 1, pp. 110-119.
- [3] **Bilir, L., Yildirim, N.**, Photovoltaic system assessment for a school building, *International Journal of Hydrogen Energy*, Vol. 42 (2017), Issue 28, pp. 17856-17868.
- [4] **Economou, A.**, Photovoltaic systems in school units of Greece and their consequences, *Renewable and Sustainable Energy Reviews*, Vol. 15 (2011), Issue 1, pp. 881-885.
- [5] **Ubertini, S., Desideri, U.**, Performance estimation and experimental measurements of a photovoltaic roof, *Renewable Energy*, Vol. 28 (2003), Issue 12, pp. 1833-1850.
- [6] **Alihodzic, R., Murgul, V., Vatin, N., Aronova, E., Nikolić, V., Tanić, M., Stanković, D.**, Renewable Energy Sources Used to Supply Pre-School Facilities with Energy in Different Weather Conditions, *Applied Mechanics and Materials*, Vol. 624 (2014), Issue 1, pp. 604-612.
- [7] **Ibrik, I., Hashaika, F.**, Techno-Economic Impact of Grid-Connected Rooftop Solar Photovoltaic System for Schools in Palestine: A Case Study of Three Schools, *International Journal of Energy Economics and Policy*, Vol. 9 (2019), Issue 3, pp. 291-300.
- [8] **Kadyan, H., Berwal, Dr. A. K.**, Design of A 12 kWp Grid Connected roof top Solar Photovoltaic Power Plant on school building in the Rohtak District of Haryana, *International Journal of Applied Engineering Research*, Vol. 13 (2018), Issue 1, pp. 11354-11361.
- [9] **Shaari, S., Bowman, N.**, Photovoltaics in buildings: A case study for rural England and Malaysia, *Renewable Energy*, Vol. 15 (1998), Issues 1-4, pp. 558-561.
- [10] **Yilmaz, S., Binici, H., Ozcalik, R. H.**, Energy supply in a green school via a photovoltaic-thermal power system, *Renewable and Sustainable Energy Reviews*, Vol. 57 (2016), Issue 1, pp. 713-720.
- [11] **Bilir, L., Yildirim, N.**, Photovoltaic system assessment for a school building, *International Journal of Hydrogen Energy*, Volume 42 (2017), Issue 28, pp. 17856-17868.
- [12] **Elmasry, S. K., Haggag, M. A.**, Whole building design for a green school building in Al-Ain, United Arab Emirates, *WIT Transactions on Ecology and the Environment*, Vol. 150 (2011), Issue 1, pp. 165-176.
- [13] **Cholakkal, L.**, *Cost-benefit analysis of a Building Integrated Photovoltaic Roofing system for a school located in Blacksburg, Virginia*, M. Sc. thesis, Faculty of the Virginia Polytechnic Institute and State University, Blacksburg, USA (Virginia), USA, 2006.
- [14] **Lou, S., Tsang, E. K. W., Li, D. H. W., Lee, E. W. M., Lam, J. C.**, Towards Zero Energy School Building Designs in Hong Kong, *Energy Procedia*, Vol. 105 (2017), Issue 1, pp. 182-187.
- [15] EnergyPlus: Energy Simulation Software (Weather File).

- [16] Prostar 72 solar cells monocrystalline 340 W,
<https://www.prostarsolar.net/product-details/prostar-72-solar-cells-monocrystalline-340w-solar-panel-cost> (accessed on June 2020).
- [17] **Skerlić, J., Bojić, M.**, *Optimization of solar collector performance by using EnergyPlus and Hooke-Jeeves algorithm*, Proceedings of the 41st International congress on heating, refrigerating and air – conditioning, Association of Mechanical and Electrical Engineers and Technicians of Serbia SMEITS, Belgrade, Serbia, 2010.
- [18] BOSH, installation and maintenance manual,
<http://bosch-rs.boschtt-documents.com/download/pdf/file/6720808645.pdf> (accessed on June 2020).
- [19] Viessmann, design instructions,
https://webapps.viessmann.com/vibooks/api-internal/file/resources/technical_documents/RS/sr/VPA/5815440VPA00014_1.PDF?#pagemode=bookmarks&zoom=page-fit&view=Fit (accessed on June 2020).
- [20] Rulebook on energy efficiency of buildings, Law on Planning and Construction of the Republic of Serbia 2011,
<https://www.mgsi.gov.rs/sites/default/files/PRAVILNIK%20O%20ENERGETSKOJ%20EFIKASNOSTI%20ZGRADA.pdf> (accessed on June 2020).

SIMULACIJA INVERTORA ZA INDUKCIONO GREJANJE

SIMULATION OF INVERTER FOR INDUCTION HEATING

Biljana BAKOVIĆ^{*1}, Zoran STEVIC²,

¹ School of Electrical Engineering - University of Belgrade, Serbia

² School of Electrical Engineering - University of Belgrade, Technical Faculty Bor,
University of Belgrade, CIK, Belgrade, Serbia

Sistemi za indukciono grejanje koriste se u elektrotermiji za zagrevanje predmeta obrade (šarže) u cilju dobijanja željenog oblika i hemijskih i mehaničkih osobina. Indukciono zagrevanje zasniva se na pojavi elektromagnetne indukcije, odnosno indukovanju vrtložnih struja u zagrevanom predmetu kada se on nalazi u promenljivom magnetskom polju induktora. Zbog toga je indukciono zagrevanje ograničeno na obradu metala. Proticanje indukovanih struja kroz šaržu dovodi do generisanja toplotne energije zbog Džulovih gubitaka. Veoma važnu ulogu igra i površinski efekat, odnosno pojava neravnomerne raspodele struja po poprečnom preseku šarže. Usled površinskog efekta, gustina indukovane struje najveća je na površini i opada ka njenoj unutrašnjosti. Brzina opadanja struje zavisi od električnih i magnetnih osobina materijala i od učestanosti magnetnog polja, pri čemu je veća na većim učestanostima. Posledica toga je da se toplotna energija generiše u sloju određene debljine na površini šarže, pri čemu je debljina određena osobinama materijala i učestanošću magnetskog polja. Za napajanje indukcionog grejanja većih i velikih snaga mogu se koristiti polumosni i mosni invertori, kao i paralelna veza više invertora. U ovom radu prikazana je simulacija jednog polumosnog invertora koji napaja indukcionu peć.

Ključnereči: Indukciono grejanje; Energetska efikasnost; Polumosni inverter; Simulacija

Induction heating systems are used in electrothermy to heat the object to obtain the desired shape and chemical and mechanical properties. Induction heating is based on the occurrence of electromagnetic induction, ie induction of eddy currents in the heated object when it is in a changing magnetic field of the inductor. Therefore, induction heating is limited to metal processing. The flow of induced currents through the object leads to the generation of thermal energy due to Joule losses. The surface effect also plays a very important role, ie the appearance of uneven current distribution across the batch cross-section. Due to the surface effect, the density of the induced current is highest on the surface and decreases towards its interior. The rate of a current drop depends on the electrical and magnetic properties of the material and the frequency of the magnetic field, being higher at higher frequencies. The consequence is that thermal energy is generated in a layer of a certain thickness on the surface of the batch, where the thickness is determined by the properties of the material and the frequency of the magnetic field. Semi-bridge and bridge inverters, as well as a parallel connection of several inverters, can be used to supply induction heating of higher power. In this paper, a simulation of a half-bridge inverter supplying an induction furnace is presented.

Key words: Induction heating; Energy efficiency; Half-bridge inverter; Simulation

1 Introduction

1.1 Power inverters

Inverters are switching regulators [1] used to supply consumers with an alternating voltage of variable RMS value and/or variable frequency. Depending on the power supply method, they can be a voltage (voltage source inverters - VSI) or current (current source inverters - CSI). In this project, a voltage half-bridge inverter will be analyzed.

The voltage-powered single-phase inverter should generate an alternating voltage of the given amplitude, waveform, and frequency at the output, taking energy from the DC voltage source at the

^{*} Corresponding author, email: bljn.bakovic@gmail.com

input. This voltage consists of a procession of voltage pulses that are formed by the process of modulating the pulse duration. Using a simple periodic modulating signal, the inverter output voltage spectrum will consist of a fundamental harmonic, which is the desired load voltage, and a series of higher harmonics that are removed by a low-pass bandpass filter. The field of application of inverters is very wide and they are most often used for regulation of electric motor drives, in uninterruptible power supply systems, for power supply of consumers from renewable energy sources, for energy transfer from renewable energy sources to the distribution network, and so on. This paper will discuss the application of inverters in induction heating.

1.2 Induction heating

Induction heating systems are used in electrothermy to heat the object to obtain the desired shape and chemical and mechanical properties. Induction heating is based on the occurrence of electromagnetic induction, ie induction of eddy currents in the heated object when it is in a changing magnetic field of the inductor. Therefore, induction heating is limited to metal processing. The flow of induced currents through the object leads to the generation of thermal energy due to Joule losses. The surface effect also plays a very important role, ie the appearance of uneven current distribution across the batch cross-section. Due to the surface effect, the density of the induced current is highest on the surface and decreases towards its interior. The rate of a current drop depends on the electrical and magnetic properties of the material and the frequency of the magnetic field, being higher at higher frequencies. The consequence is that thermal energy is generated in a layer of a certain thickness on the surface of the batch, where the thickness is determined by the properties of the material and the frequency of the magnetic field.

The variable frequency magnetic field is obtained by the flow of current through the inductor winding inside when the batch is placed (Figure 1). The frequencies with which induction heating is performed depending on the desired depth of penetration of induced currents in the batch, which is dictated by the technological process, dimensions, and material of the batch and range from the network frequency (50 Hz) to several hundred kilohertz. For frequencies other than the network frequency, the inductor is powered from an inverter with an adaptive resonant circuit. Inverters enable the supply of inductors with a current in the desired frequency range, with the possibility of regulating the heating power [2].

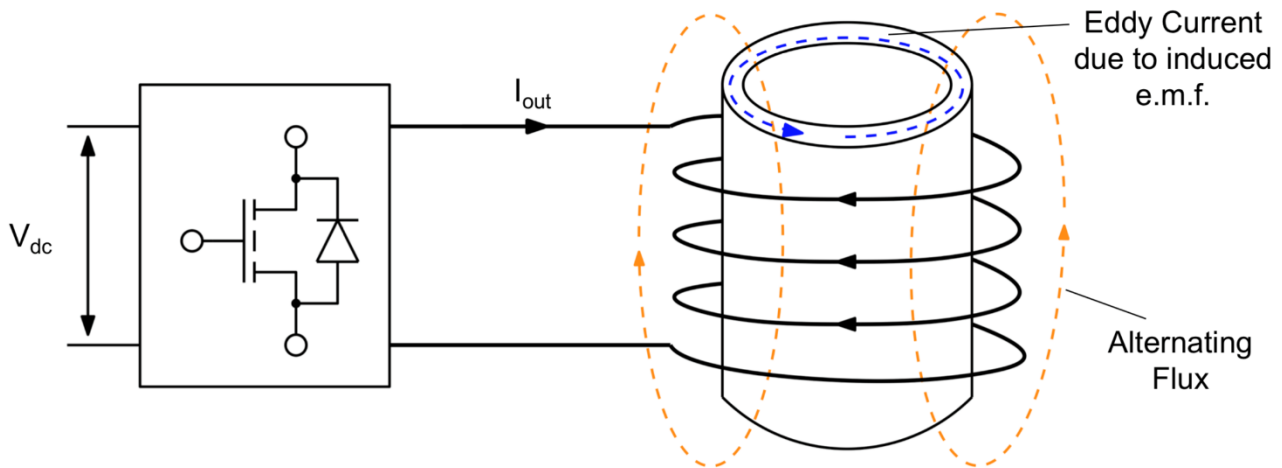


Figure 1. Induction Heater for Melting Aluminum [3]

2 The simulation

The parameters used in the simulation can be seen in the figure (Figure 2.1). The inverter is supplied with a DC voltage of 560V, the frequency in the control circuit ranges from $f_{sw}=10\text{kHz}$ to 100kHz with a step of 10kHz. The inductance L (pure inductive load) is adjusted manually. Values are given in the range of 100uH to 800uH in steps of 100uH.

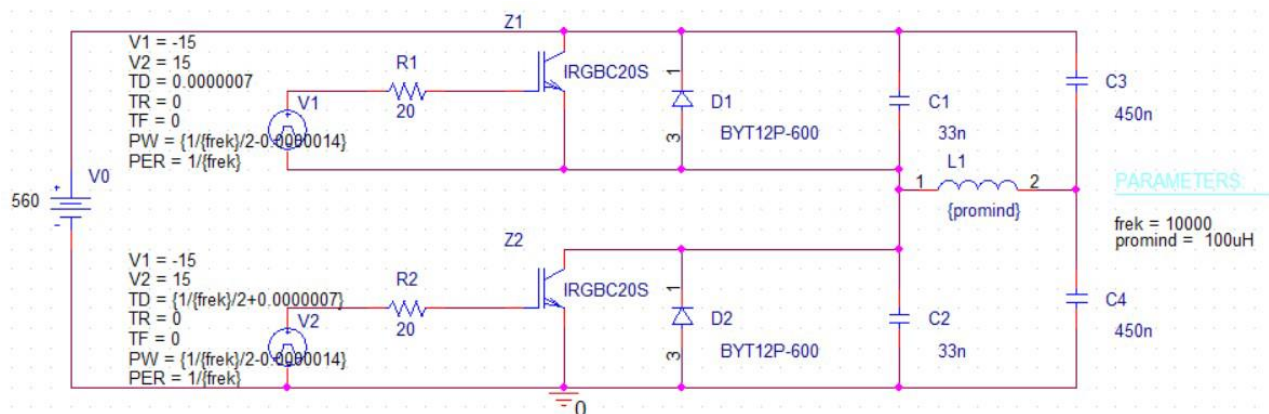


Figure 2.1. Inverter scheme

A model with real components was used. How the time and frequency of the simulation are set (Figure 2.2), and the frequency, period, and time of delay of the rectangular voltage of the switching circuit of the transistor (Figure 2.3), can be seen in the figures below.

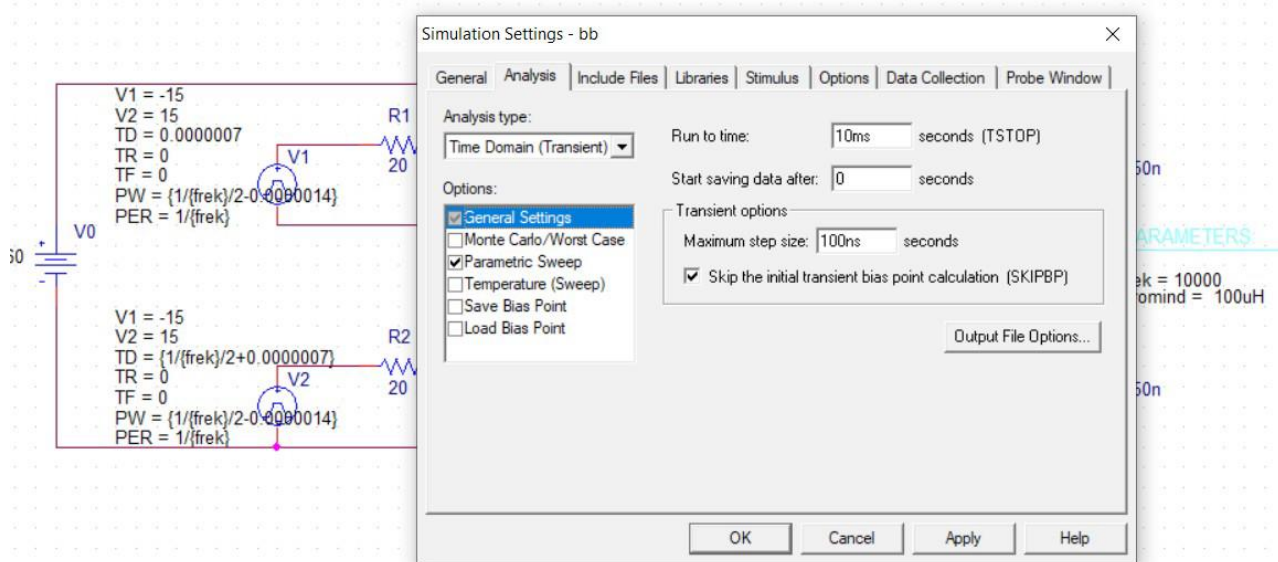


Figure 2.2. The simulation time setting

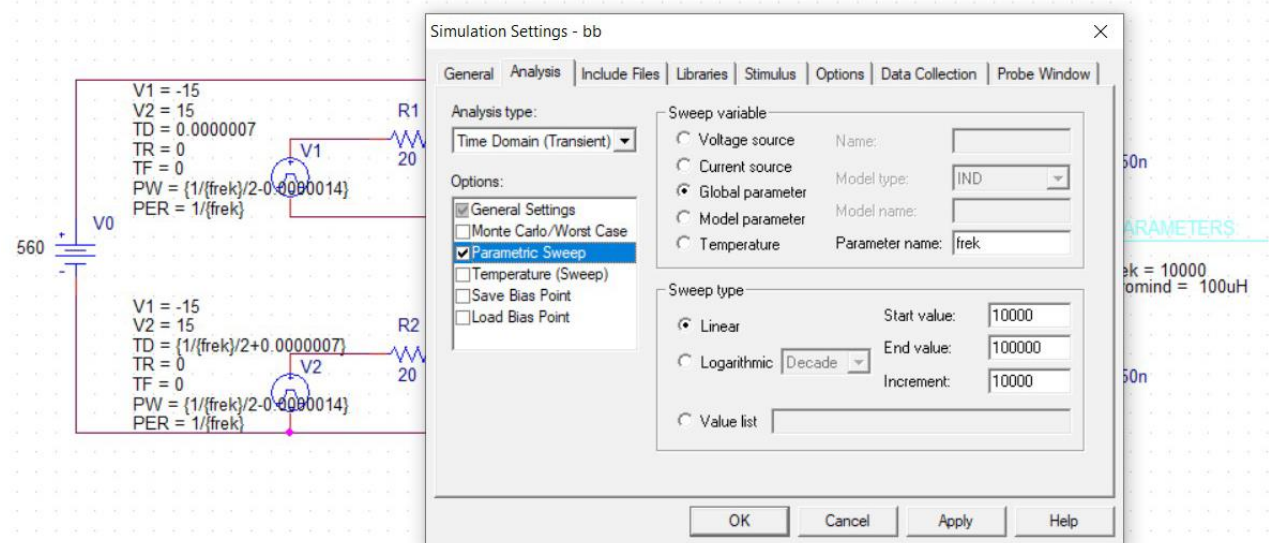


Figure 2.3. Setting f_{sw}

3 The results of the simulation

The graphs obtained as a result of the simulation show the currents and voltages for each frequency from the range $f_{sw}=10\text{kHz}$ to 100kHz with a step of 10kHz . This means that each graph shows 10 currents/voltages and they are marked with different symbols (circle, square, triangle, inverted triangle, and so on). The following figures (Figure 3.1, Figure 3.2, Figure 3.2, Figure 3.3) show graphs of currents and voltages in the frequency domain for induction values $L=100\mu\text{H}$ and $L=800\mu\text{H}$:

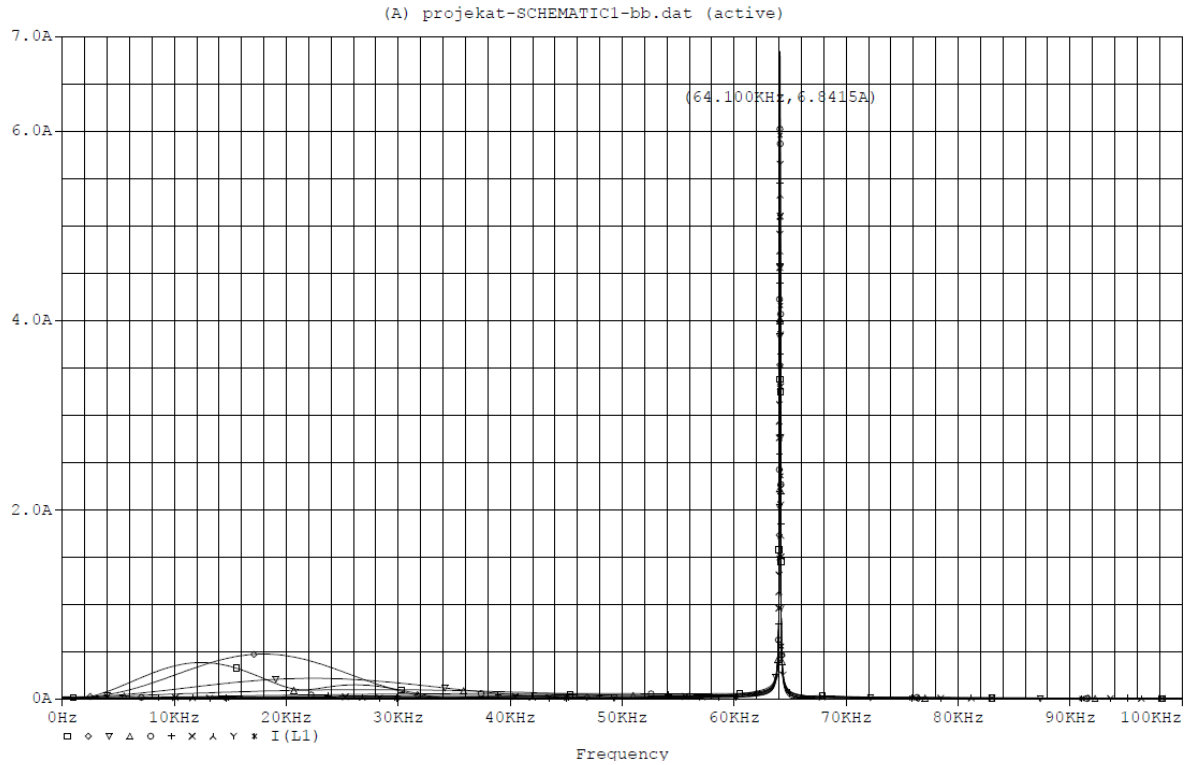


Figure 3.1. A plot of currents for $f_{sw}=10\text{kHz}$ to 100kHz and $L=100\mu\text{H}$

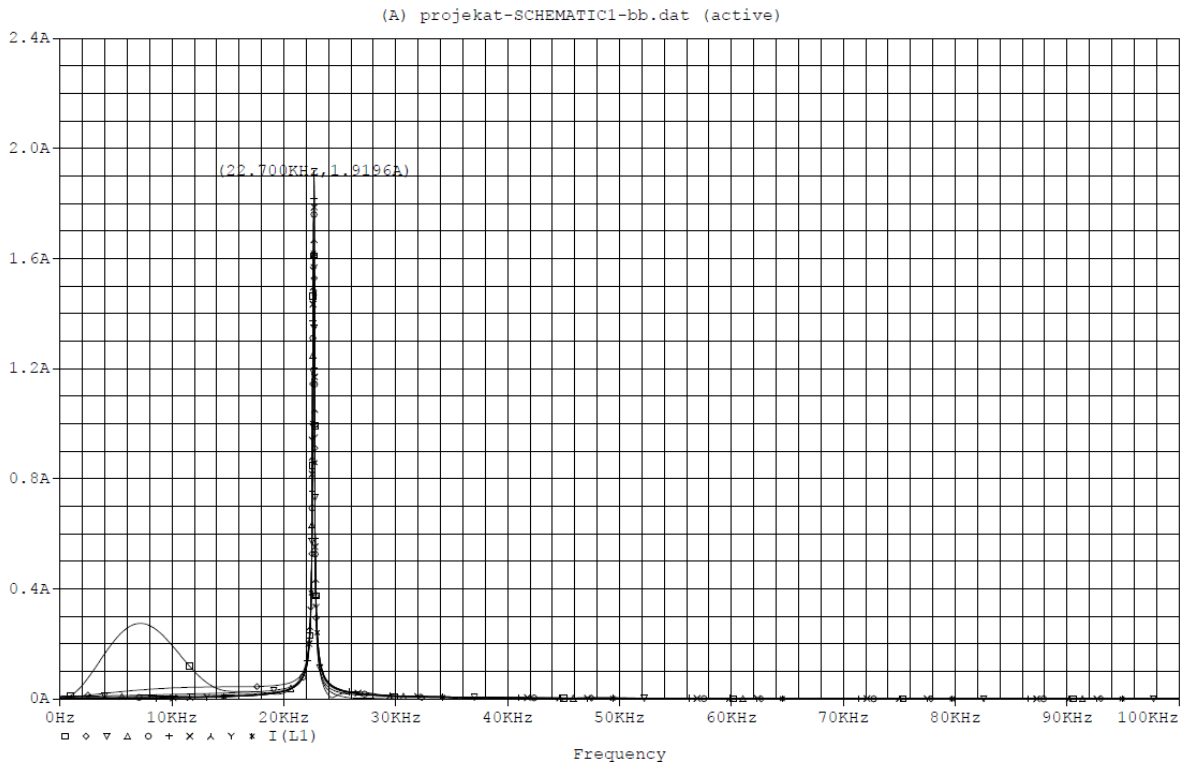


Figure 3.2. A plot of currents for $f_{sw}=10\text{kHz}$ to 100kHz and $L=800\mu\text{H}$

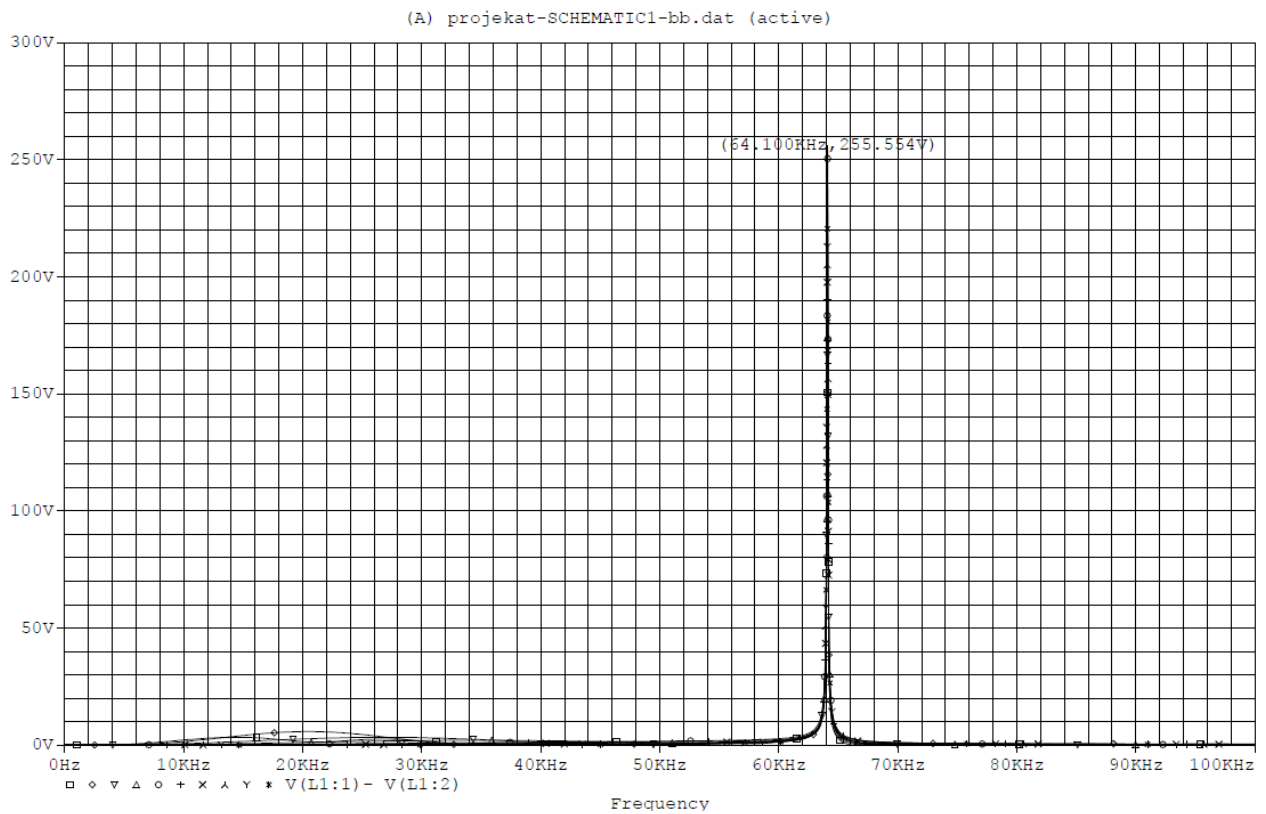


Figure 3.3. A plot of voltages for $f_{sw}=10\text{kHz}$ to 100kHz and $L=100\mu\text{H}$

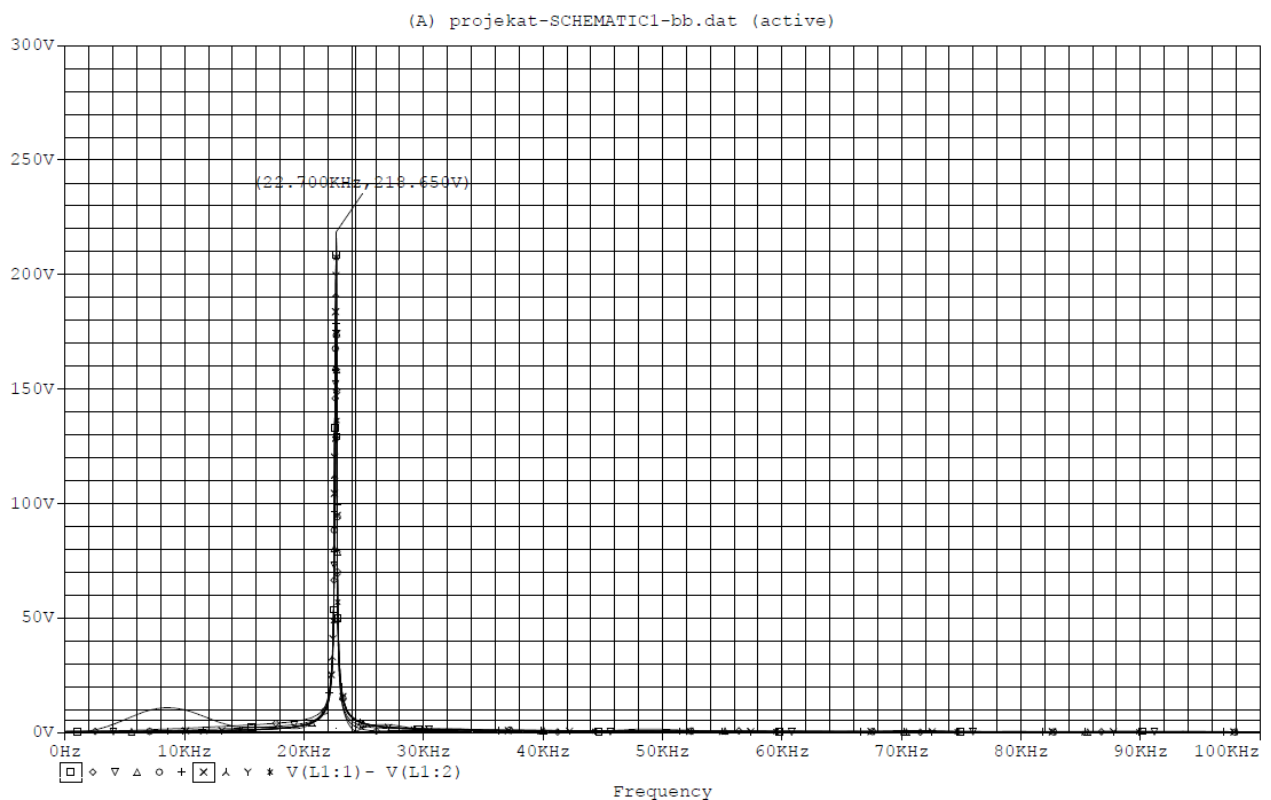


Figure 3.4. A plot of voltages for $f=10\text{kHz}$ to 100kHz and $L=800\mu\text{H}$

When it comes to the time domain, currents and voltages for inductance $L=100\mu\text{H}$ are observed, because it is in the interest only to see whether the correct sinusoids are obtained at the output of the inverter, ie at the load. This can be seen in the pictures (Figure 3.5 and Figure 3.6):

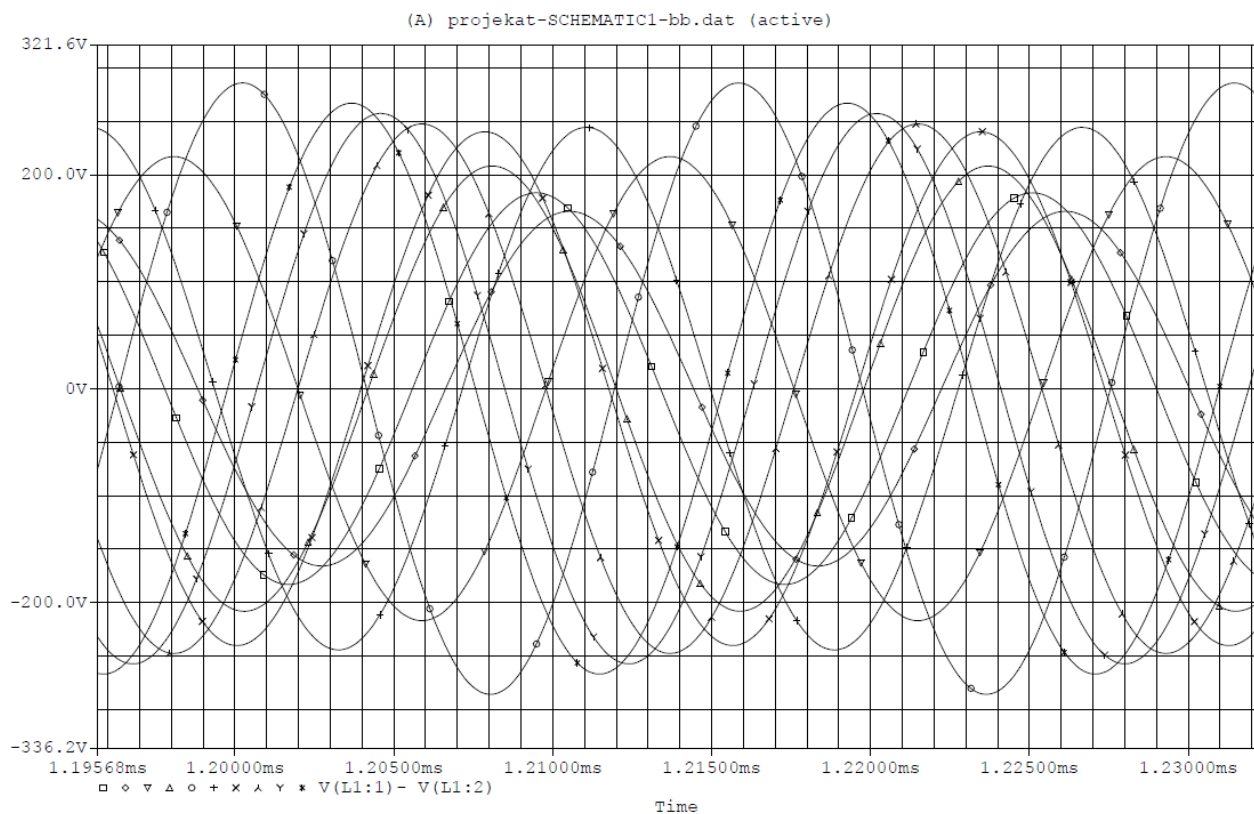


Figure 3.5. Inverter output voltages plot for $f=10\text{kHz}$ to 100kHz and $L=100\mu\text{H}$

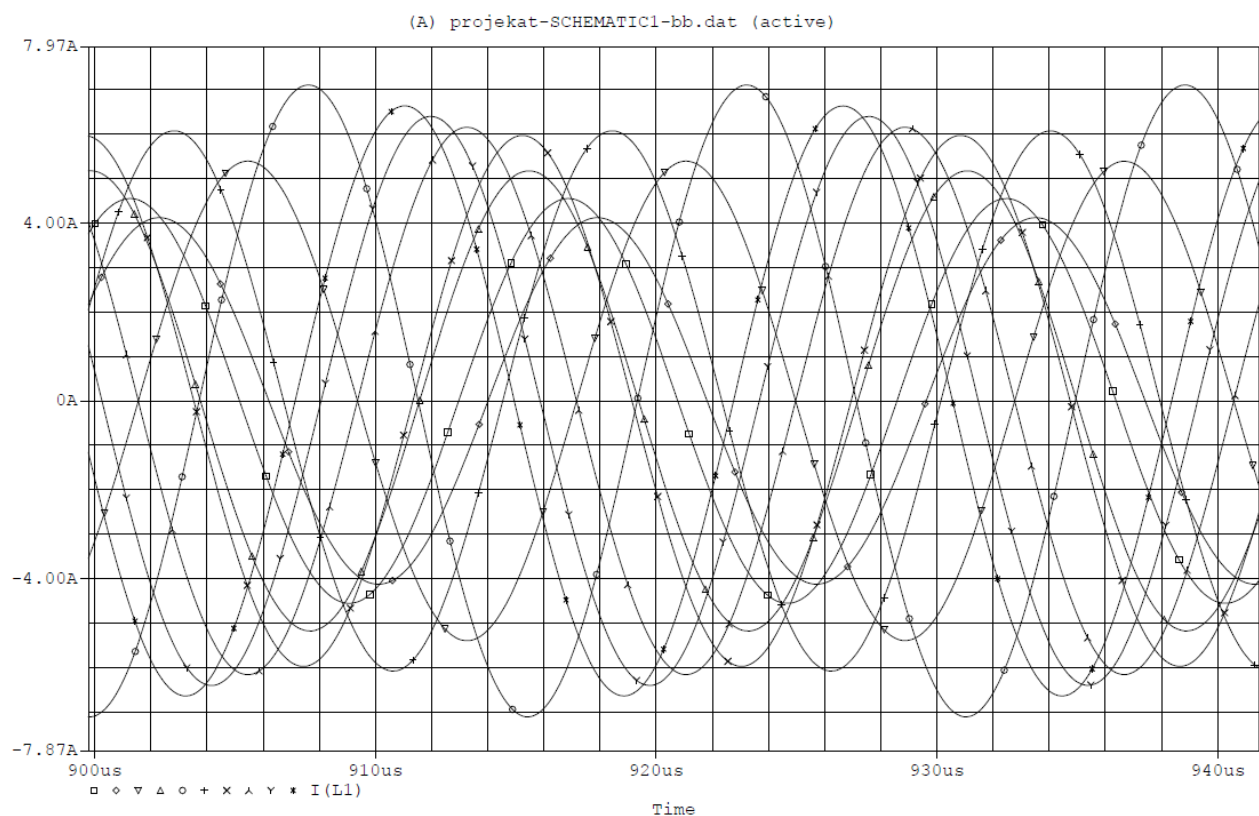


Figure 3.6. Inverter output currents plot for $f=10\text{kHz}$ to 100kHz and $L=100\mu\text{H}$

4 Conclusion

On the graphs of currents and voltages in the time domain, it can be noticed that the sinusoidal alternating voltages are correct, so the choice of components of this inverter is good.

The resonant frequency is shown on graphs with a frequency horizontal axis. This is the frequency for which the currents/voltages from the entire switching frequency range (10kHz-100kHz) have the maximum value.

On the graphs in the frequency domain, it can be seen that with increasing inductance, the current decreases as well as the resonant frequency. Such a result was also expected considering that it can be concluded from the formula for the natural frequency that with increasing inductance the natural frequency decreases. In contrast to the frequency, small deviations for some inductance values were seen in the current.

Finally, since the simulation works with variable parameters all the time, it is expected that the output voltage will change. Inverters are usually designed to give a certain value of the voltage at the output depending on the load and this could be adjusted by introducing certain changes in the control circuit.

5 Acknowledgement

The authors gratefully acknowledges financial support from the Ministry of Education and Science, Government of the Republic of Serbia.

6 References

- [1] **Miloš R. Nedeljković, Srđan L. Srdić**, Power converters 1 - Basic topologies of power converters(2016), University of Belgrade School of Electrical Engineering, Akademska misao, Belgrade, 114-117
- [2] **Miloš R. Nedeljković**, Power converters 2 – The topologies of power converters(2016), University of Belgrade School of Electrical Engineering , Akademska misao, Belgrade, 85-91
- [3] **Yuvn Kokuhennadige, Md Masum Billah, Joni-Markus Hietanen, Jaakko Lind**, Induction Heater for Melting Aluminum, Aalto University, School of Electrical Engineering, Automation and Electrical Engineering (AEE) Master's Programme, Project, Helsinki, Finland, 2019

PRIMENA SUPERKONDENZATORA U ELEKTRIČNIM VOZILIMA

APPLICATION OF SUPERCAPACITORS IN ELECTRIC VEHICLES

Zoran STEVIĆ^{*1}, Ilija RADOVANOVIĆ², Miša STEVIĆ³,

¹ School of Electrical Engineering - University of Belgrade, Technical Faculty Bor,
University of Belgrade, CIK, Belgrade, Serbia

² School of Electrical Engineering - University of Belgrade, Innovation center of
School of Electrical Engineering in Belgrade, Serbia

³ Mikroelektronika, Belgrade, Serbia

U radu su dati pregled stanja i pravci daljeg razvoja sistema za skladištenje električne energije na bazi superkondenzatora. Kritičnu komponentu svakog hibridnog ili čisto električnog vozila predstavlja skladište električne energije. Superkondenzatori su danas jedina dostupna tehnologija koja može obezbediti veliku specifičnu snagu i veliki broj ciklusa po povoljnoj ceni. Superkondenzatori imaju i druge karakteristike koje ih čine atraktivnim u električnim vozilima, kao što su mogućnost potpune upotrebe energije (tzv. regenerativno kočenje) za povećanje energetske efikasnosti, bez dodatnog održavanja, malo toksičnosti i lako odlaganje nakon upotrebe.

Ključnereči: Superkondenzatori, EV, Skladištenje energije

The paper gives an overview of the state and directions of further development of the Electricity Storage Systems based on supercapacitors. Critical component at each hybrid or pure electrical vehicle presents electrical storage. Supercapacitors are nowadays the only available technology, which can provide great specific power and great number of cycles at reasonable price and save and reliable work. Supercapacitors have other characteristics that make them attractive in hybrid vehicles such as possibility of complete energy using (so called regenerative braking) for increasing energy efficiency, with no additional maintenance, great recovery of electrical energy, little toxicity and easy disposal after usage.

Key words: Supercapacitors, EV, Energy storage

1 Introduction

Electric drive vehicles present one of the most important technological advances having in mind spread of this kind of nature pollution. Lately there is increased world interest for so called hybrid vehicles that have reduced fuel consumption and much less pollutants emission than regular vehicles. Hybrid vehicles can in broadest sense be described as vehicles utilizing combination of production and storage of energy. Good properties of conventional vehicles are combined (long range and acceleration, very good supply network) and electrical vehicles (zero emission, quiet operation, regenerative use of braking energy) [1,2].

Two kinds of these vehicles are in consideration - so called parallel and series hybrids. In parallel hybrids there is a connection between power generator and driving wheels, while in series that relation is not present. Series hybrids have substantial advantages compared to parallels due to their mechanical simplicity, flexibility in terms of design and ability of simple new technologies incorporation [2,3]. Supercapacitors are increasingly used in the power supply of electric motor drives, as well as electronic circuits in EVs.

2 Supercapacitors vs. accumulator batteries and fuel cells

Supercapacitors are relatively new type of capacitors distinguished by phenomenon of electrochemical double-layer, diffusion and large effective area, which leads to extremely large capacitance per unit of geometrical area (in order of multiple times compared to conventional capacitors). They

^{*} Corresponding author, email: zstevic@tfbor.bg.ac.rs

are taking place in the area in-between lead batteries and conventional capacitors. In terms of specific energy (accumulated energy per mass unity or volume) and in terms of specific power (power per mass unity or volume) they take place in the area that covers the order of several magnitudes. Supercapacitors fulfill a very wide area between accumulator batteries and conventional capacitors taking into account specific energy and specific power [1,2]. Batteries and fuel cells are typical devices of small specific power, while conventional capacitors can have high specific power, but at a very low specific energy. Electrochemical capacitors improve batteries characteristics considering specific power or improve capacitors characteristics considering specific energy in combination with them. In relation to other capacitor types, supercapacitors offer much higher capacitance and specific energies, as illustrated in Figure 1 [2].

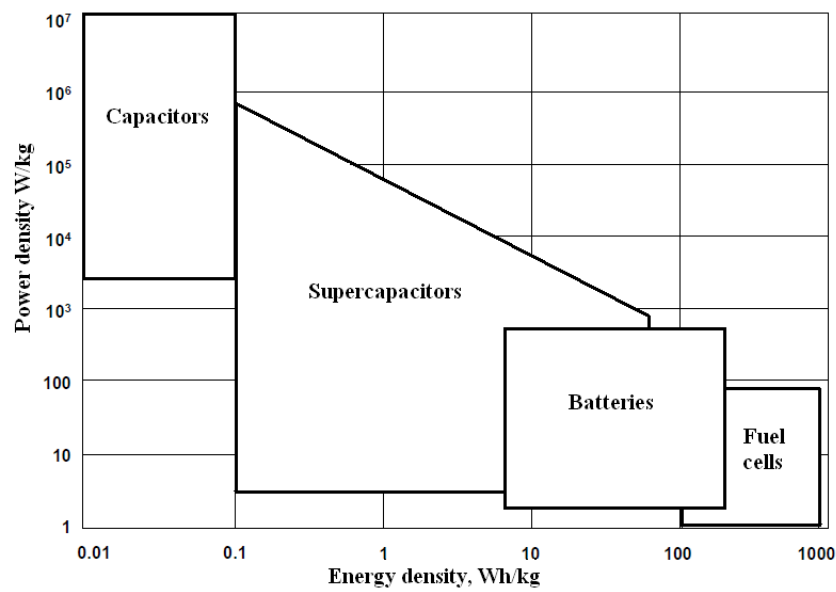


Fig. 1 Area diagram for various energy storage systems [2]

Accumulator batteries and low temperature fuel cells are typical devices with low specific power, where conventional capacitors may have specific power over 1 MW/dm^3 , but at very low specific energy. Electrochemical capacitor can improve characteristics of batteries in terms of specific power and improve properties of capacitors in terms of specific energy when they are combined with them [4].

Supercapacitors store charge in a similar way to conventional capacitors, but the charge does not accumulate in two conductors, but in the interface between the surface of a conductor and an electrolytic solution. Devices consist of two electrodes which allow a potential to be applied across the cell, therefore they present two double-layers, one at each electrode/electrolyte interface [5]. An ion-permeable separator is placed between the electrodes in order to prevent electrical contact, but still allows ions from the electrolyte to pass through. The electrodes are made with high effective surface materials, such as porous carbon or carbon aerogel [6]. Two principal technologies are used [7]: aqueous (maximum voltage of 1.2 V and work voltage of 0.9 V) and organic (voltage near 3 V but with a much higher series resistance).

The principal supercapacitor characteristic that makes it suitable for using in energy storage systems (ESS), is the possibility of fast charge and discharge without loss of efficiency, for thousands of cycles. This is because they store electrical energy directly. Supercapacitors can recharge in a very short time having a great facility to supply high and frequent power demand peaks [8].

Data given in Table 1 clearly show supercapacitor characteristics that make those devices adequate for purposes requiring great specific energy and great specific power combination or long life-time denoted by charging and discharging number of cycles. In other words, capacitors have retained classical capacitors positive property to achieve almost unlimited charging and discharging number of cycles [2].

Table 1 Capacitor, supercapacitor and accumulator basic characteristics

Characteristic	Classical capacitor	Supercapacitor	Accumulator
Discharging time	$\mu\text{s} - \text{ms}$	$\text{ms} - \text{weeks}$	min - months
Charging time	$\mu\text{s} - \text{ms}$	$\text{ms} - \text{minutes}$	hours
Specific energy	$< 0,01 \text{ Wh/dm}^3$	$0,5 - 5 \text{ Wh/dm}^3$	$< 500 \text{ Wh/dm}^3$
Specific power	$> 10^4 \text{ W/dm}^3$	$(1-3) 10^3 \text{ W/dm}^3$	$< 500 \text{ W/dm}^3$
Cycles number	$10^6 - 10^8$ (unlimited)	$10^6 - 10^8$	200 - 1000

3 Supercapacitor applications in EV

Considering applying, there are four groups of supercapacitors. Depending on applying place, different characteristics of supercapacitors can be more or less taken into account. Some of them are of crucial importance for capacitor choice, and some of them can be of no importance at all [2].

Most strict requirements are related to capacitors of fourth group applying in electric haulage, i.e. for vehicles of the future. Nowadays, batteries of several hundreds farad capacitance are with working voltage of several hundred volts have been produced. Beside great capacitance and relatively high working voltage, these capacitors must have great specific energy and power (because of limited space in vehicle). Considering their specific power, they have great advantage in relation to accumulator batteries, but, on the other side, they are incomparably weaker considering specific energy. Hence, ideal combination is parallel connection of accumulator and condenser batteries. In an established regime (normal drawing) vehicle engine is supplied from accu-battery, and in the case of rapidly speeding, from supercapacitor. Very important is the fact that in the case of abrupt breaking, complete mechanical energy could be taken back to system by converting into electrical energy only in presence of supercapacitor with great specific power. Because of mentioned reasons, inner resistance of these supercapacitors has to be extremely small. Leakage current is not of essential importance. Vehicles with such drive are not still in wide use, and the reasons for that are for sure economic [2].

In Figure 2 the scheme of an electrical drive vehicle in which supercapacitor is used for energy storage and so-called regenerative breaking is presented.

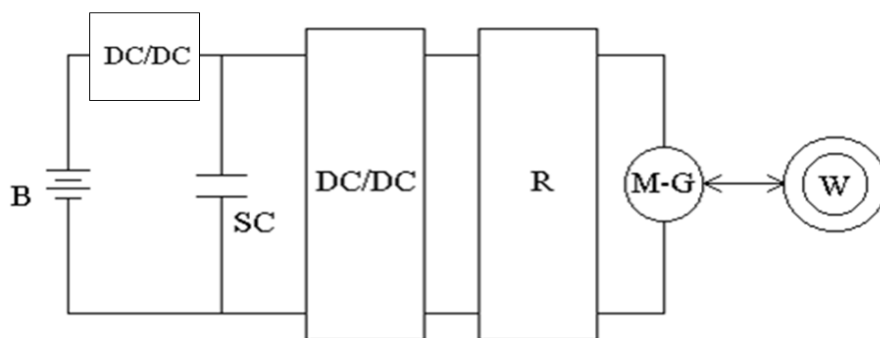


Fig. 2 Scheme of electrical drive vehicle with supercapacitor with possibility for using breaking energy; B – one-way voltage source, SC – supercapacitor; DC/DC – direct voltage converter; R – regulator; M-G – engine – generator (depending on working regime; W – drive wheels [2]

4 Conclusion

Critical component in every hybrid or purely electrical vehicle is energy storing. Possible solutions are accumulators, supercapacitors, flying wheels, hydraulic devices and new special materials for hydrogen storing. Supercapacitors are only available technology today that can provide high power and great cycle numbers at acceptable price. Supercapacitors have other properties that makes them interesting in hybrid vehicles, and it's ability of complete regeneration of energy of braking (so

called regenerative braking), which increases energy efficiency, no special maintenance needed, great utilization of electric energy, small toxicity and easy storage after use.

Batteries with large capacitance of several hundred Farads and few hundred volts of working voltages are already produced. Apart from large capacitance and relatively high working voltage those capacitors also must have high specific energy and power (for reason of limited vehicle space). They have huge advantage in terms of specific power compared to accumulator batteries, but they are incomparably worse in terms of specific energy. That's why the ideal combination becomes parallel connection of accumulator and capacitor batteries. In steady state (normal drive) vehicle motor is supplied from accu-battery and at sudden accelerating it is fed from supercapacitor. Very important fact is that at sudden breaking all mechanical energy can be returned to a system by transforming to electric energy only with presence of supercapacitors with high specific power.

5 Acknowledgement

The authors gratefully acknowledge financial support from the Ministry of Education and Science, Government of the Republic of Serbia.

6 Literature

- [1] **Van Voorden, A.M.; Ramirez Elizondo, L.M.; Paap, G.C.; Verboomen, J. & Van der Sluis, L.**, The Application of Super Capacitors to relieve Battery-storage systems in Autonomous Renewable Energy Systems. *Power Tech*, (2007). pp. 290-295.
- [2] **Zoran Stević, Mirjana Rajčić-Vujasinović, Supercapacitors as a Power Source in Electrical Vehicles**, Book title: *Electric Vehicles – The Benefits and Barriers / Book 1*, Edited by: Seref Soyulu, Intech, Rijeka (2011)
- [3] **Stević, Z.; Rajčić-Vujasinović, M. & Stanković, Z.**, Galvanostatic investigations of copper sulfides as a potential electrode material for supercapacitors, PO 320, *Book of Abstracts 3rd International Conference of the Chemical Societies of the South-Eastern European Countries on Chemistry in the New Millennium – an Endless Frontier*, Vol.II, pp. 97, Bucharest, Romania, September 22-25, 2002.
- [4] **Stević, Z.** Supercapacitors based on copper sulfides, Ph.D. Thesis, University of Belgrade, 2001F. H. Math Bollen, Integration of distributed generation in the power system, 2011
- [5] **Bugarinović, S.; Rajčić-Vujasinović, M. & Stević, Z.** Construction of double layer capacitors, *Proceedings of 39th International October Conference on Mining and Metallurgy*, pp. 470-476, ISBN 987-86-80987-52-1, Sokobanja, Serbia, October 7-10, 2007
- [6] **(Bugarinović, S.; Rajčić Vujasinović, M. & Stević, Z.**, Supercapacitors based on activated carbon, *Proceedings on 40th International October Conference on Mining and Metallurgy*, pp. 417-422, ISBN 978-86-80978-60-6, Sokobanja, Serbia, October 5-8, 2008.
- [7] **Stević, Z.; Rajčić-Vujasinović, M.; Nikolovski, D. & Antić, D.**, Hardware and software of a system for electrochemical and bioelectrochemical investigations, *Book of abstracts on CD ISIRR 2010, 11th International Symposium on Interdisciplinary Regional Research*, pp. 139, Szeged, Hungary, October 13-15, 2010.
- [8] **Kotz, R. & Carlen, M.**, Principles and applications of electrochemical capacitors. *Electrochimica Acta*, Vol.45, No15-16, (May 2000), pp. 2483-2498

ENERGETSKI EFIKASAN SISTEM ZA STERILIZACIJU DRVETA

ENERGY EFFICIENT SISTEM FOR WOOD STERILIZATION

Miloš MARJANOVIĆ^{*1}, Miša STEVIĆ², Miloš MILEŠEVIĆ³, Žarko ŠEVALJEVIĆ³,
Sanja PETRONIĆ⁴, Marta TRNINIĆ⁵, Zoran STEVIĆ⁶

¹ VISER, Belgrade, Serbia

² Mikroelektronika, Belgrade, Serbia

³ University of Belgrade, School of electrical engineering, Belgrade, Serbia

⁴ Innovation center of Mechanical faculty, Belgrade, Serbia

⁵ University of Belgrade, Mechanical faculty, Belgrade, Serbia

⁶ University of Belgrade, School of electrical engineering, TF Bor, CIK Belgrade, Serbia

U radu je opisan dizajn energetske efikasnog sistema za sterilizaciju drveta. U zatvorenom sistemu automatskog upravljanja temperaturom primenjen je kontinualni PID regulator sa trofaznim tiristorskim faznim regulatorom na izlazu. Merenje temperatura u 5 zona komore sa drvetom izvedeno je Pt1000 sondama i one su po određenom algoritmu iskorišćene za definisanje referentne temperature PID regulatora koji upravlja snagom grejača generatora vodene pare.

Ključne reči: energetska efikasnost, sterilizacija drveta, PID regulator, tiristorski fazni regulator, regulacija temperature

The paper describes the design of an energy efficient wood sterilization system. In a closed automatic temperature control system, a continuous PID controller with a three-phase thyristor phase controller at the output was applied. Temperature measurement in 5 zones of the chamber with wood was performed with Pt1000 probes and they were used according to a certain algorithm to define the reference temperature of the PID controller that controls the power of the steam generator heater.

Key words: energy efficiency, sterilization of wood, PID regulator, thyristor phase regulator, temperature control

1 Specific requirements for heat treatment (HT) treatment

Specific requirements for wood heat treatment processes, which are the subject of this paper, are given in Annex 1, IPSM standard 15.

The guidelines given in this appendix apply to the thermal treatment of wood in conventional heat chambers (dry kilns) commonly used for drying wood. Newer treatments involving dielectric heating (eg radio frequency, microwave ovens), hot water baths, etc. are not considered. Although, as mentioned earlier, these treatments can be equally effective in combining temperature and time to destroy pests [1].

Research has confirmed that heating a tree, including its core, to a minimum temperature of 56 ° C for a period of 30 minutes is effective in destroying pests. Recent results have shown that this method of heat treatment also kills many fungal organisms that can be found in wood .

Heat treatment is achieved by regulating the temperature inside the heat chamber. The chamber temperatures required for effective treatment depend on:

- types and conditions of the treatment chamber;
- volume and direction of air flow through beams / piles of trees;
- moisture content in the surrounding air surrounding the trees during treatment;
- initial wood temperatures;
- moisture content in the wood;
- wood density;
- dimensions of the tree;

^{*} Corresponding author, email: milosmarjanovich@gmail.com

- the species of wood to be treated, and
- the amount of heat applied in the chamber, which is determined by the heating system.

The air flow inside the closed chamber depends on:

- capacity of the equipment in the air movement chamber;
- dimensions of the wood being treated;
- size of airspace, and
- the degree of separation between the pieces of wood within the pile .

Given the influence of the above factors, heat treatment is based on the development of a treatment procedure and the definition of procedures that minimize variations in these components during and between treatments.

The NPPO should establish specific heat treatment parameters, including processes to measure treatment efficacy and audit by authorized manufacturers. The guidelines given in this Annex 1 require verification that the treated wood is subjected to sufficient heating as prescribed in ISPM 15. It is not stated to what extent the NPPO may prescribe individual requirements for individual producers or parameters necessary to effectively verify those requirements. This should be determined in relation to the type of facility in which heat treatment is performed and in relation to the degree of specificity of the approach to heat treatment [1].

1.1 Technical elements of thermal treatment

The standard lists some technical elements that should be taken into account in thermal treatment.

Technical requirements relate to:

1. Heat chamber;
2. Filling the heat chamber;
3. Air circulation;
4. Venting;
5. Humidification.

1.1.1 Heat chamber

The heat chamber can be made of different materials. The materials used in the construction should not affect the functioning of the chamber. It can be used through heat sources, including natural gas, oil, electricity, solar energy and biofuels.

Chamber construction can affect the effectiveness of treatment. Some criteria that should be met are:

- the door of the heat chamber must not be damaged and should be sealed in order to prevent heat loss from the chamber;
- the chamber itself should be built in a way that reduces heat loss;
- the air flow must be uninterrupted through a bundle of wood and equipment must be used to direct the air flow, such as baffles;
- fans should be used for air circulation in the chamber;
- fans should meet the requirements of the chamber and work in accordance with the manufacturer's specification. If more than one fan is used, they must all work in such a way as to maximize the air flow in the same direction and direction;
- venting used in the chamber should ensure even temperature distribution;
- temperature sensors, including cables, must be in good condition;
- valves and motors used to reverse or change the air flow should work properly;
- the appearance of moisture on the floors can be an indicator that the measurement of moisture in the building is inadequate, that there is not enough air circulation or other causes that require resolution.

1.1.2 Charging the heat chamber

The way in which the heat chamber is filled affects the flow of air through the wood beam, and therefore care should be taken about the location of "cold spots " (places where the set temperature

is reached most slowly) in the chamber and the position of the wood in these positions. To ensure proper airflow through the wood beam, the following should be considered:

- The wooden beam should be lifted off the ground to allow efficient air flow under the tree and to avoid the effects of cooling from the ground.

- The beam must not be overloaded so as to prevent the flow of air over the top of the beam.

- The space should contain enough free space to allow sufficient, uniform air flow through the wood beam.

- The material to be treated should be the same (eg pallets only or slabs only) to ensure a homogeneous heat distribution. Mixing materials such as pallets and boxes can make it difficult to reach the recommended temperature and more temperature sensors may be needed to confirm that the appropriate mode has been achieved.

- Sheaves of sawn wood should be stored with spacers or stickers between the boards. The spacers must be placed parallel to the direction of air flow. Some heat chambers may require the use of special perforated stickers to allow the required airflow.

- In cases when the chamber is not filled along the entire cross-section, it is necessary to install partitions to direct the flow of air through the wood beam. Where bulkheads are not used, air will move through the lowest air resistance (Figure 1, right) [1].

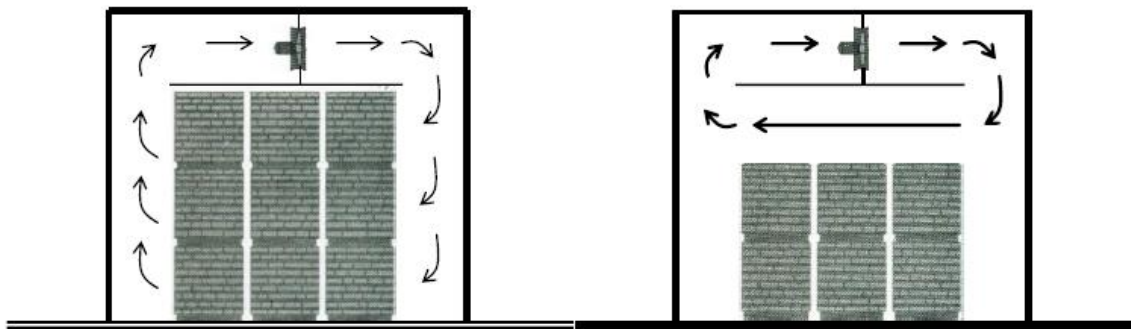


*Figure 1. Schematic cross-section of the chamber, **Left** : Filled chamber; the air circulates through the entire beam, and the heating is more uniform. **Right** : Insufficiently filled chamber , air circulates over the beam of wood, due to which the free space heats up faster than the beam*

1.1.3 Air circulation

Air circulation fans help to ensure the controlled movement of heated air in the chamber. Air flow can be measured using an anemometer. These can be fixed units that perform constant automatic measurements or manual units that periodically record the air flow to determine if the fans are operating within the desired parameters. A minimum air flow of 0.5m / s (100ft / min) is recognized as necessary for normal operation in the chamber [1].

The installation of the fan ensures the movement of air in the desired direction. Directing the flow of air during the treatment helps to ensure even heating on all sides of the wood. Changing the air flow ensures that the wood in the chamber is heated to the maximum temperature. As the air moves through the wood beam, it cools due to the evaporation of water from the wood. By directing the air with the fans, the processing time is reduced, reducing the influence of this cooling effect by the constant circulation of warm air. Depending on the position of the air directing fan, the position of the "cold spots " (places where the wood heats up the slowest) is estimated , and temperature sensors should be installed in these places to ensure that the required temperature is reached at all critical points. However, in chambers where fans are not used to direct the air flow, the wood is effectively treated by achieving a higher ambient temperature or compensated by a much longer heating duration [1]..

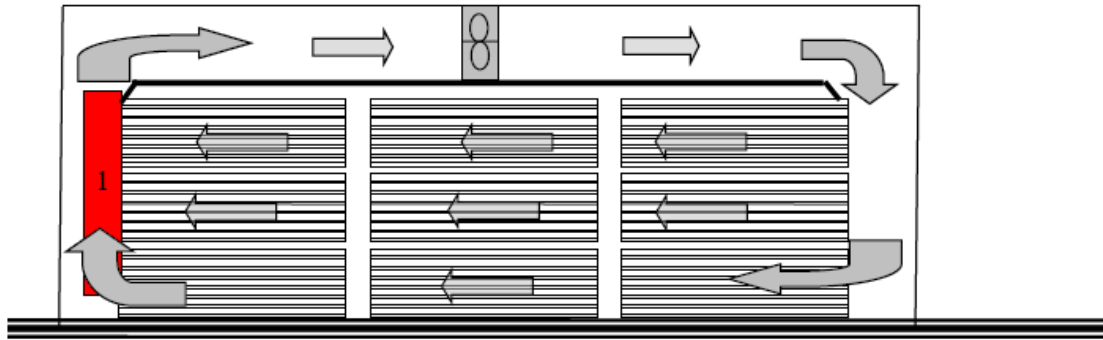


Figure 2. Heating chamber in which the heating pipes are placed with a fan above the wood bundle . The "cold spot " is probably located on the outlet side of the beam, so the temperature sensor should be placed where the air exits the wood beam (marked "1").

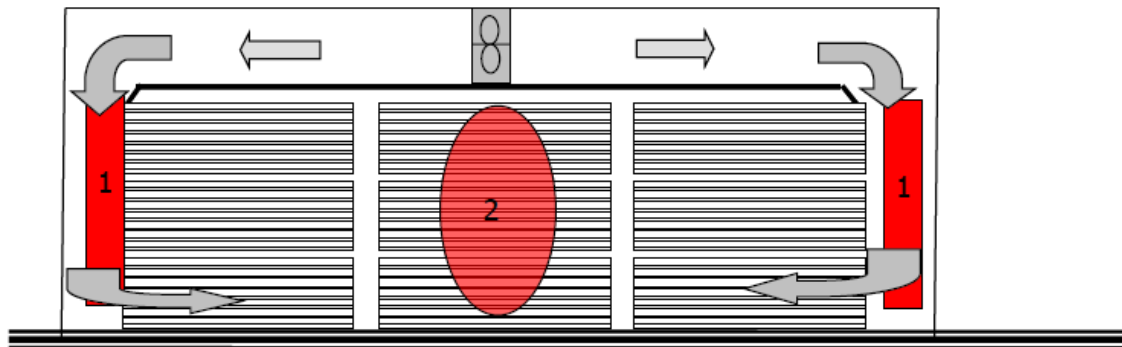


Figure 3. Heating chamber in which the heating is two-way. If the intended treatment is long, the "cold spot " may be on the side outlets of the beam (marked 1). Temperature sensors should be placed along the walls of the chamber. If the intended treatment is shorter, the "cold spots " are probably in the center of the beam (marked "2") and the sensors should be placed there.

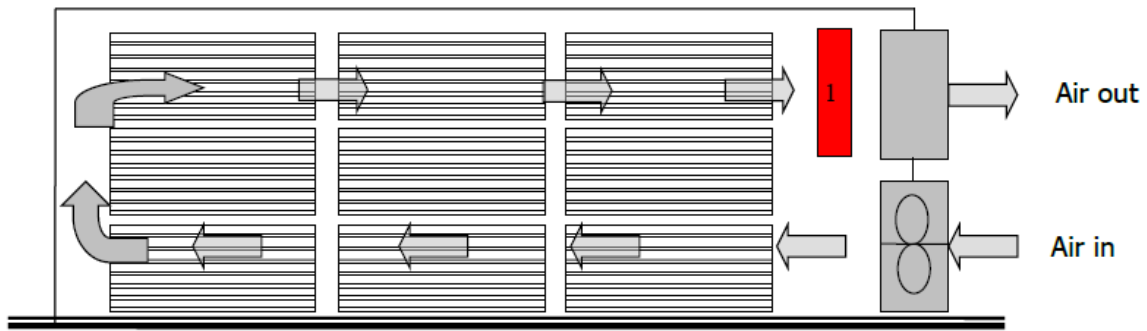


Figure 4. Heating chamber in which heating occurs on one side of the floor. The temperature sensor is placed at the air outlets from the wood beam (marked with "1").

2 . System construction

A modern process control system has been upgraded to the existing wood sterilization system in order to increase energy efficiency, reliability, product quality and user comfort. The existing ON / OFF temperature controller has been replaced by a continuous PID controller with a three-phase thyristor phase controller at the output. The existing temperature measurement in the zones of the chamber with wood was retained, but the same signals were introduced in the new system, where they were used according to a certain algorithm to define the reference temperature of the PID controller [2,3].

2.1 Three-phase phase controller SCR -380 D 100 P

SCR -380 D 100 P, from LeiChuang TEC, is an integrated module for phase voltage regulation. It consists of three anti-parallel connections of two thyristors and one chip that serves to generate the ignition signal. It has good output voltage symmetry, precise control and high operating stability. This module has the following parameters:

- Rated voltage (U_n) : 400 V AC ;
- Rated frequency: 50Hz / 60Hz;
- Rated current: 100A,
- Output voltage asymmetry: $\leq 5\%$;

There is a built-in power supply for the steering wheel that is powered by 230V AC. In Figure 5 is a schematic of internal connections, and in Figure 6 the wiring diagram of this module is given.

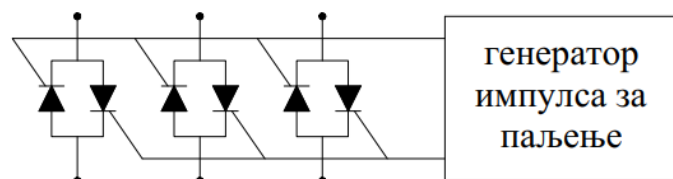


Figure 5. Scheme of internal connections of the module

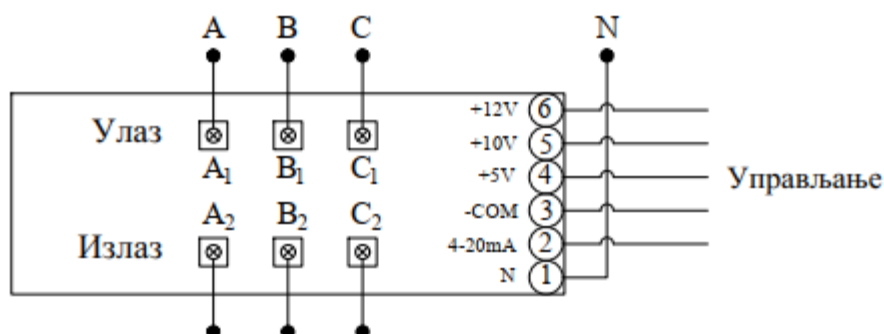


Figure 6. Module connection diagram

This inverter can be operated in five different ways (Figure 7). Control methods 1, 2, 3 and 4 use an internal power source, and method 5 an external one. Method 4 involves manual control, via a potentiometer [4].

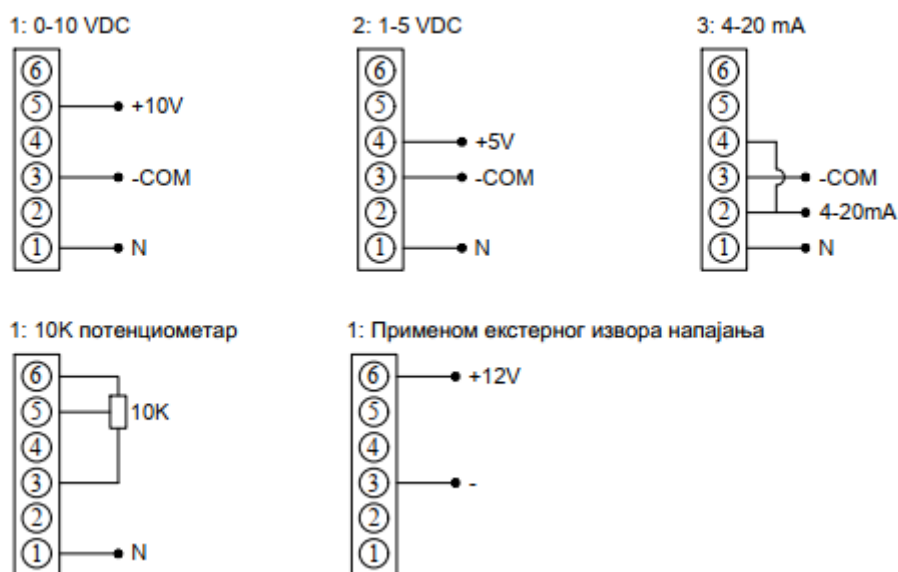


Figure 7. Module management methods

Given the output voltage range of the NI USB -6001 card [5], the module will be controlled by a voltage signal in the range of 0 to 10 V and the control inputs will be connected as in Figure 7 for the specified range.

In Figure 8 the scheme of the control - energy part of the system with the phase regulation of the power of the steam generator heater is shown .

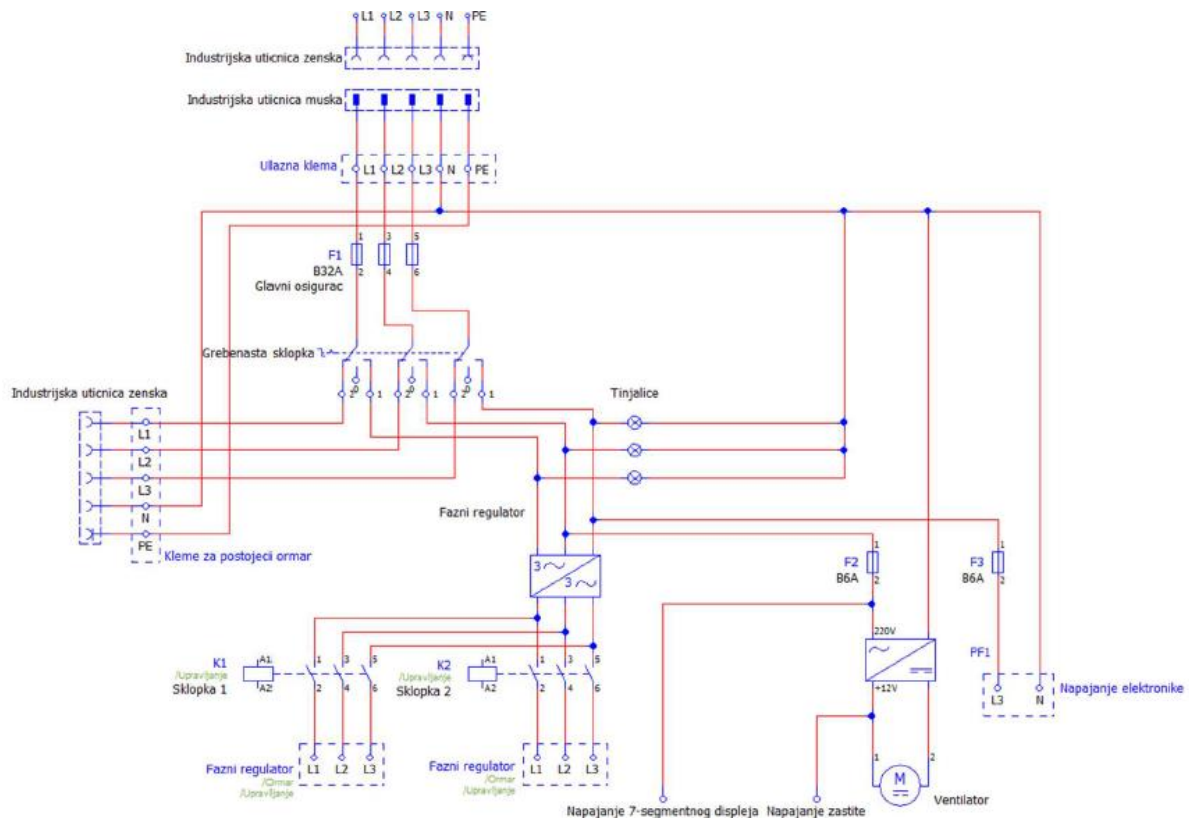


Figure 8. Scheme of control cabinet

3 Acknowledgement

The authors gratefully acknowledge financial support from the Ministry of Education and Science, Government of the Republic of Serbia.

4 References

- [1] **Sela, S., et al.** Explanatory document for ISPM 15 (Regulation of wood packaging material in international trade). [ed.] IPPC Secretariat. s.l. : FAO, Approved in 2014, published in 2017..
- [2] **Marjanović M.**, Optimization of electrical installations in the technological process of wood thermal treatment in small dryers, Master Thesis, School of Electrical and Computer Engineering of Applied Studies, Belgrade, 2020
- [3] **Радовановић, И., Стевић, З.** Завршни извештај пројекта унапређења процеса термотретирања дрвета са становишта поузданости и енергетске ефикасности. Београд : Иновациони центар електротехничког факултета, 2019.***, Standard title, Publisher, year
- [4] ***, SCR-380D100P thyristor power controller product manual. <https://chinese.alibaba.com/product-detail/100A-SCR-power-controller-three-phase-62248833692.html>. [Online]
- [5] USER GUIDE: N1 USB-6001/6002/6003 Low-Cost DAQ USB device. <http://www.ni.com/pdf/manuals/374259a.pdf>. [Online]

KOJE VEŠTINE SU POTREBNE U PROIZVODNJI LITIJUM-JONSKIH BATERIJA ZA ELEKTRIČNA VOZILA

WHAT SKILLS ARE NEEDED IN PRODUCTION OF LITHIUM-ION BATTERIES FOR ELECTRICAL VEHICLES

Zoran KARASTOJKOVIĆ*

Institut za hemijske izvore struje, Technoexperts, Beograd, Srbija

Baterije kao deo obnovljivih izvora energije uglavnom se koriste u električnim i hibridnim vozilima, dok su vetrogeneratori pogodniji za korišćenje u ruralnim sredinama. U međuvremenu, od 1990-tih, ovakve baterije su u velikom broju počele da se koriste u laptopovima, mobilnim telefonima i dr. U ovim baterijama, litijum-jon baterije su privukle veliku pažnju, kako u proizvodnji tako i korišćenju, kao punjive dnevno ili u bilo kojem nivou napunjenosti, nasuprot olovnim ili nikl-kadmijum baterijama.

U arhitekturi ovih baterija, mnogi anodni i katodni materijali su uključeni i primenjeni, uglavnom od oksida (kao što su: LiCoO_2 , LiMn_2O , $\text{Li}(\text{Ni}_x\text{Mn}_y\text{Co}_z)\text{O}_2$, zatim vanadium fosfati, čak i grafit ili još neki alkalni metali, idr.), što znači da je elektrohemija široko uključena u njihovu proizvodnju i primenu. Sa te tačke gledišta se javlja pitanje: šta je cilj u ogromnom broju studenata ekonomije, prava i/ili menadžmenta nad brojem studenata tehničkih nauka?

Ključne reči: Punjive baterije, elektrohemija, broj studenata

Batteries as a part of renewable sources of energy are preferably for using into electric and hybrid cars, while wind generators are particularly suitable for rural areas. In the mean time, from 1990, these batteries in a large scale came in use in laptop computers, mobile phones, etc. At those batteries, the lithium-ion batteries have attracted a great attention, both in producing and using, as rechargeable daily or at any state of using or charge level, in contrary to lead-acid or nickel-cadmium batteries.

In the architecture of these batteries, many anodic/cathodic materials are included and applied, almost from oxides (as like: LiCoO_2 , LiMn_2O , $\text{Li}(\text{Ni}_x\text{Mn}_y\text{Co}_z)\text{O}_2$, further from vanadium fosfates, even from carbon or some alkali metals, etc.), it means that the (electro)chemistry is widely incorporated in their production. From that point arises the question: what is our goal with a huge number of students on economy, law and/or management over the number of students on technical sciences?

Key words: Rechargeable batteries, electrochemistry, number of students.

1 . Introduction

No doubt that the energy is one of the crucial factors for human life, and therefore is a subject of further researching and development. Renewable energy sources are dedicated for production of energy which is collected from renewable sources as like sunlight, wind and geothermal heat, or other less important. Those energy sources serve almost for electricity generation and/or for water heating-up. Some types of electrical sources, as like wind generators, are particularly suitable for rural areas in developing countries, while batteries are preferably for electric cars.

Hybrid vehicles became popular, because they achieve lower emissions than conventional combustion engines. But, it should be noticed that the internal combustion engine is better for maintaining high speed than electric motor.

Batteries in electrical cars are in using to power the electric motor or to power the hybrid electric vehicle, since the late of 1990s, when also came in use in laptop computers, mobile phones, etc. From that time to now, we have an opportunity to react as a state, first of all on the kind of profiles which

* Author's email: zoran.karastojkovic@gmail.com

will be educated, firstly for the production schedules of energy sources. Our answer, as a developing country, was resulted in dominance by number of students at economy, law and management over the number of natural or technical sciences. But, does this represents an usefull choice? Here will be given an effort in analysing the skills which are needed in production of renewable sources for electric cars.

2 . Short view on batteries for electric vehicles

In modern electric vehicles, the most common battery types are lithium-ion and lithium polymer, which posses high ampere-hour capacity and according that they show high energy density compared to their weight. Lithium-ion batteries usually are rechargeable, daily or at any state of using or charge level, in contrary to lead-acid or nickel-cadmium batteries. It should be noticed that motors on liquid fuels still have a greater *specific energy* (power to weight ratio) in comparison to batteries. Another task for such batteries is small weight, reducing the weight of the vehicle. So, are the economists, lawyers or managers able to improve the performances of those batteries? They are able only to see that there are some batteries.., as could be seen from Fig. 1.

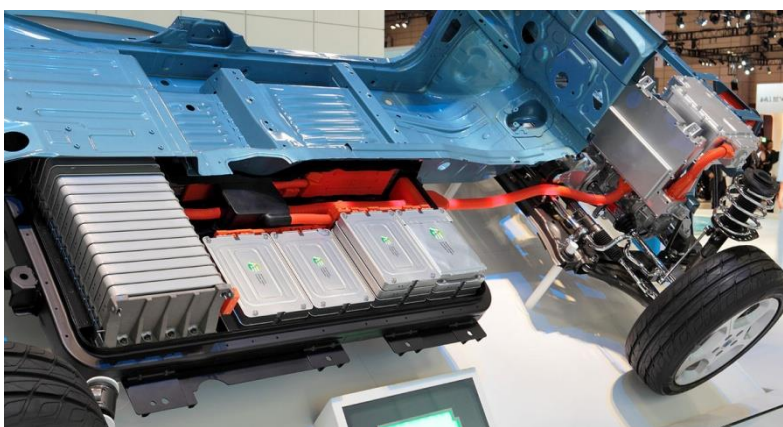


Fig. 1. One view on batteries in an electrical car

On that way they are only a *good buyer* and nothing more. But, the real question becomes: is the right choice only in importing and buying all kinds of goods? For trade, it is however quite enough. What about the employing of young people? Are they only the consumers of imported goods? Why we, as a state, continuously educated in great scale proffesions which are unable to produce many of needed goods?

3 . Configuration and materials in lithium-ion batteries for electric vehicles

Common lead-acid batterries, nickel-cadmium, nickel–metal hydride, and less commonly were overgrowned on behalf of huge efforts/developments only by technicians but not from econimists, lawyers or managers. The most known batteries now are based on lithium. Lithium-ion batteries in the first generation were designed on spinel structure and further on a layer structure.

Another criteria for assessing of battery capacity is the cruising distance, according to the amount of electricity stored in batteries is measured and expresed on a simple manner - in kilowat-hours, in Table 1. are shown results according to Nissan classification.

At almost cars still is the problem in starting during cold periodes, it means in winter. At freez-ing temperatures, the batteries lose their capacity, even a lithium-ion batteries. In these researches are included many of electrochemists, for discovering which materials are the most desired either as anode or cathode material. The electrochemical reactions are of the crucial role in all of those batter-ies.

Table 1. Cruising distance for various batteries (Nissan motor corporation)

Battery	Cruising distance (WLTC/JC08 mode)	
24kWh	2010	(200km@JC08)
	2012	(228km@JC08)
30kWh	2015	(280km@JC08)
40kWh	2017	322km@WLTC Mode (400km@JC08 Mode)
62kWh	2019	458km@WLTC Mode (570km@JC08 Mode)

In simplified form, the scetch of Li/ion battery is shown in Fig. 2a) and its form in reality in Fig. 2b).

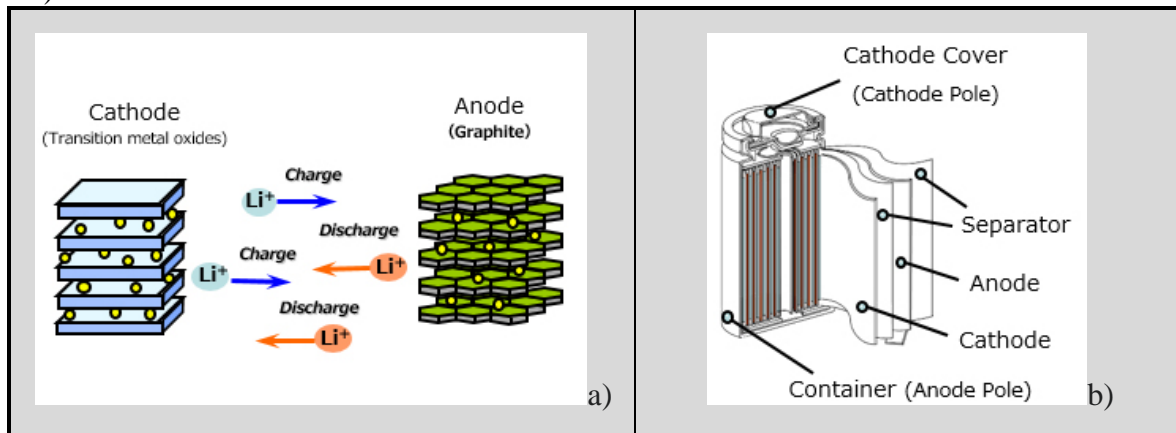


Fig. 2. Configuration of Li-ion battery with graphite anode a) and in 3D form b)

Short review of some other configurations and materials in lithium-ion batteries for electric vehicles are shown in figs. 3.

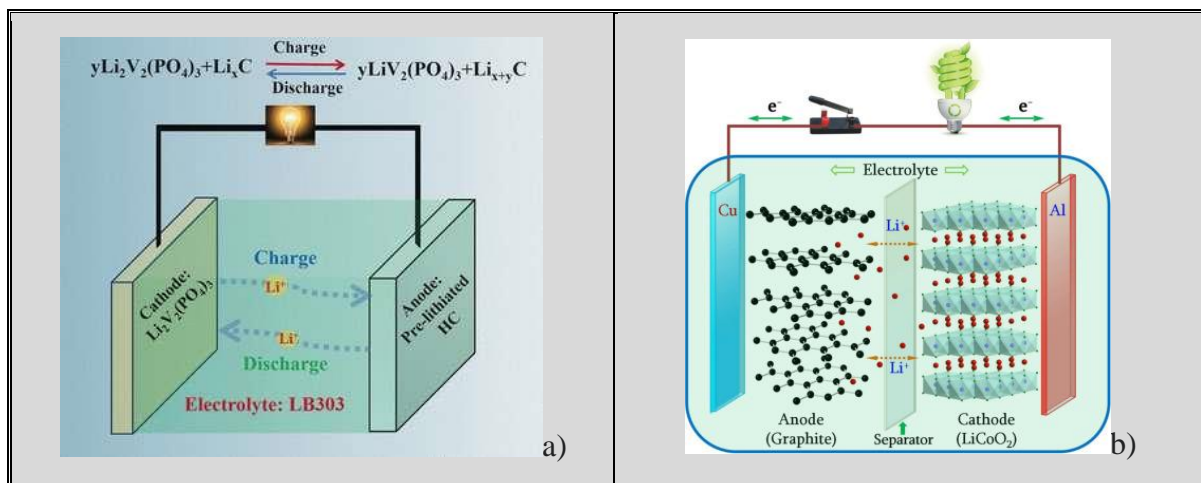


Fig. 3. Schematic diagrams of bateries with different materials for anode&cathode

However, one of the serious problems with lithium-air cells reported to date is that a solid reaction product (Li_2O or Li_2O_2), which is not soluble in organic electrolyte, clogs the air electrode (cathode) in the discharge process. If the air electrode is fully clogged, O_2 from atmosphere cannot be reduced any more.

Another improvement is made by using the air instead of oxygen, Fig. 4.

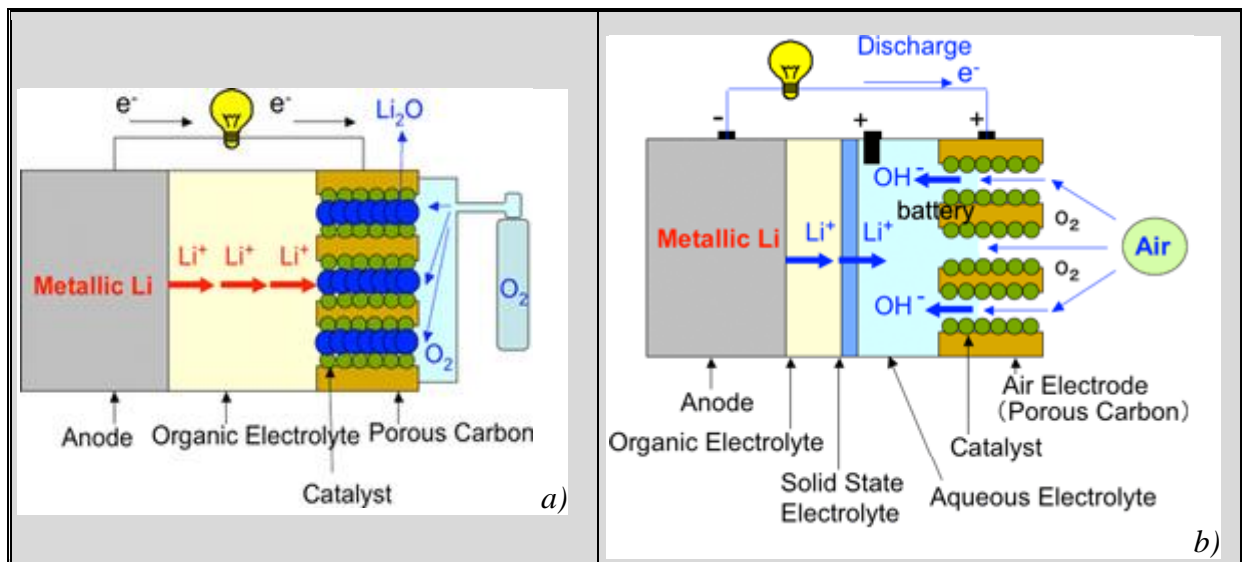


Fig. 4. Configuration of: a) conventional lithium-oxygen battery and b) new lithium-air cell b)
Source: Japan's AIST (National Institute of Advanced Industrial Science and Technology)

Some of the main cathodic materials in lithium batteries are on the oxide basis, as: LiCoO_2 , LiMn_2O_4 , or $\text{Li}(\text{Ni}_x\text{Mn}_y\text{Co}_z)\text{O}_2$, Fig. 5, or further vanadium oxides, etc. Carbon may be included in both electrodes, Fig. 5b).

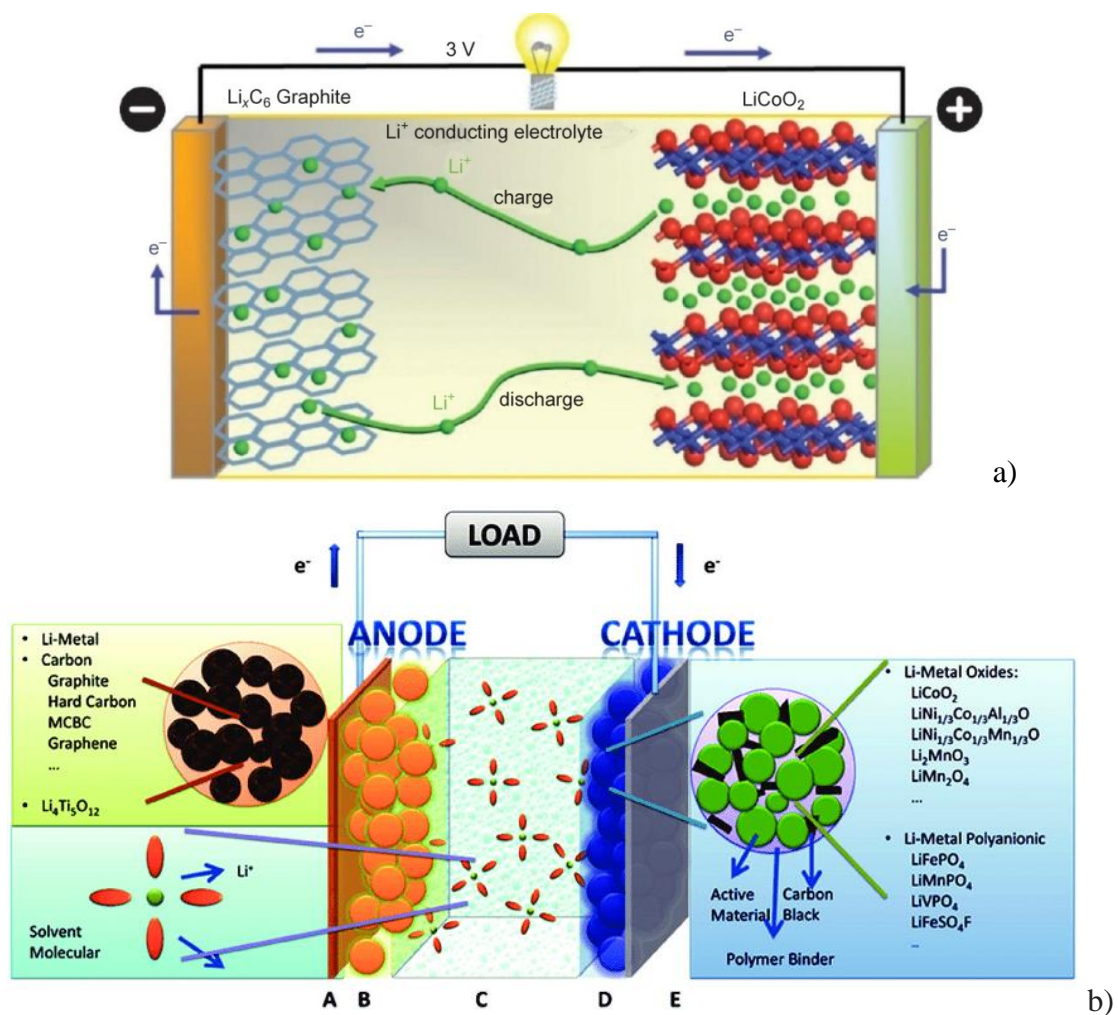


Fig. 5. More complex materials used for anode and cathode

4 Sodium-ion batteries are potential power technology of future

Batteries are constantly developing, one of the potential useful design, with promising application in the future, is shown in Fig. 6.

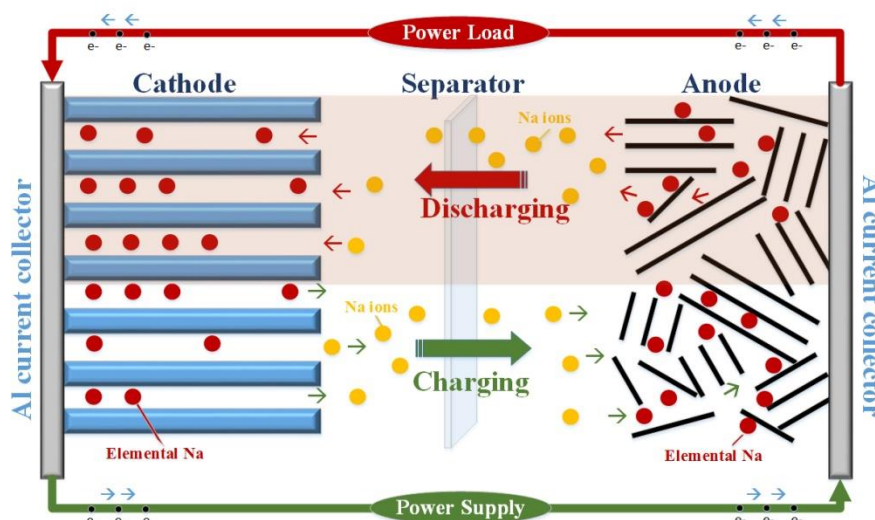


Fig. 6. One concept of battery based on sodium

Except of here presented, there are present a versatility in kinds of used materials, both for anode or cathode.

5 Discussion

Lithium air battery is one of the most promising power technologies in the future because it has theoretical specific energies 100 times that of the state of the art Li-ion battery. One of the main obstacles in the development of Li-air battery technology is the stability of electrolyte. Here arises the question: is the stability of electrolyte the product of electrochemists or economists, lawyers and managers? For every step is needed many experiments in laboratories, about fast-charging, high volumetric capacity, etc. This is a real challenge for a society.

Most people even today know and use the lead-acid battery (accumulator), but from that time many improvements have happened. It is evident that any clever solution, from whatever discipline in human life, will not “fall from the sky”, just contrary - many efforts should be provided.

Some of the used materials might be harmful for environment and/or people. Batteries for electric vehicles should be characterized by their relatively high power-to-weight ratio. Also, they have to be small, for reducing the weight of the vehicle and therefore improve its performance. Compared to fossil fuels, most current battery technologies still have much lower specific energy, and a lot of work must be done.

6 Conclusion

The architecture of any kind of contemporary battery is not simple, just contrary. Many efforts must be involved in designing of every detail from battery, it means anode, cathode and electrolyte chemistry. Without an adequate knowledge/skills from (electro)chemistry it is impossible to make any step in designing&production of batteries for electrovehicles, laptops, and similar equipment from our every day needs. Who will be at first identify and farther produce the radically different methods or approaches for electrical energy storage? (Non)toxicity of used materials also must be the subject of any solution, it means after batteries will be spent.

In the mean time we will be convicted on economists, lawyers, managers... in importing and buying the such goods. So, what is the target in the progress of society/state?

6. References

- [1] **Y. Miao, P. Hynan 2, A. von Jouanne, A. Yokochi:** Current Li-Ion Battery Technologies in Electric Vehicles and Opportunities for Advancements, *Energies*, 2019, 12, 1074;
- [2] **D. Deng:** Li-ion batteries: basics, progress, and challenges, *Energy Science and Engineering*, 2015, str. 385-415.
- [3] **N-y. Kim, G. Lee, J- Choi:** Fast-Charging and High Volumetric Capacity Anode Based on $\text{Co}_3\text{O}_4/\text{Cu}@\text{TiO}_2$ Composites for Lithium-Ion Batteries, *Chemistry Europe*, 2018.
- [4] **N. Nitta, F. Wu, J.T. Lee, G. Yushin:** Li-ion battery materials: present and future, *Materials today*, 18/2015/, str. 252.264.
- [5] **F. Wu, J. Maier, Y. Yu:** Guidelines and trends for next-generation rechargeable lithium and lithium-ion batteries, *Chemical Society Reviews*, 2020.
- [6] **B. Yang, S. Liu, H. Song, J. Zhou:** Carbon nanonio-assembled microspheres for excelent gravimetric and volumetric Ni-Ion storage, *Science Direct*, 153/2019/, str. 298-307.
- [7] *** Wikipedia: Electric vehicle battery, (accessed on 22.6.2020.)
- [8] **J.R. Dahn, J.A. Seel:** Energy and Capacity Projections for Practical Dual Graphite Cells, *J. of The Electrochemical Society*, 3/147.
- [9] **C. P. Grey:** New Materials For and Challenges in Lithium Ion Battery Research, *Stony Brook State University of New York*, str. 1-66.
- [10] **Z. Karastojković, M. Srećković, N. Bajić, Z. Janjušević:** Energy consumption and education of personal needs, VII Int. Conf, of Renewable Electric Energies, Belgrade 2019.

PRIMENA LASERA U AUTOMOBILSKOJ INDUSTRIJI

APPLICATION OF LASERS IN AUTOMOTIVE INDUSTRY

Milesa SREČKOVIĆ^{*1}, Nenad IVANOVIĆ², Stanko OSTOJIĆ³, Aleksander KOVAČEVIĆ⁴,
Nada RATKOVIĆ KOVAČEVIĆ⁵, Zoran KARASTOJKOVIĆ⁶, Sanja JEVTIĆ⁷

¹ Faculty of Electrical Engineering, University of Belgrade, Belgrade, Serbia

² Institute of Nuclear Sciences, University of Belgrade, Belgrade, Serbia

³ The Academy of Applied Technical Studies Belgrade, Department of
Tehnikum Taurunum, Belgrade, Serbia

⁴ Institute of Physics, University of Belgrade, Belgrade, Serbia

⁵ The Academy of Applied Technical Studies Belgrade,
Department of Computer-mechanical Engineering, Belgrade, Serbia

⁶ IHIS Techno Experts, Belgrade, Serbia

⁷ Academy of Technical and Art Applied Studies, Department of Railway Studies, Belgrade, Serbia

<https://doi.org/10.24094/mkoiee.020.8.1.223>

Uloga lasera i sprežanja sa solarnom energijom i problemima „tematike“ vozila je vrlo široka. U ovom radu su analizirani principi, savremeni razvoj specifičnih disciplina i posmatranja sa tehničko/ naučno/ inženjersko/ metroloških tačaka gledišta. Ova oblast je u širem smislu vezana za „istoriju“ naše planete ili, u užem, sredinu prošlog veka i zlatno doba kvantne elektronike. Neki od generalnih problema su rešavani sporo, ali sa druge strane, posmatranjem sadašnjeg stanja nekonvencionalnih napajanja vozila/ automobila i realizovanih komponenti, neke karakteristike su menjale konvencionalne pristupe realizovanju i kapacitansama u sistemima napajanja. Glavni cilj je da se analiziraju problemi koji bi rešavanjem povećali gradijente budućeg razvoja solarne energije i njene primene u automobilskoj industriji, putem multidisciplinarnih pristupa. Uz podsećanja na potrebe, razmotrena su sprežanja kroz teoretsko inženjerske pristupe u polju tehnologije, metrologije i generisanja snage/ energije, i transformacije u području razvoja, primene i rada lasera, automobila i solarne energije.

Ključne reči: laser; Sunce; obnovljivi izvori energije; vozilo; tehnologija; metrologija; solarno pumpanje lasera; holografija; plazma

Laser role and couplings with vehicles and solar power are numerous and in this paper we analyzed the principles, contemporary development of special areas and observation from the scientific/ engineering, or from the metrological point of view. This area is, in broader sense, connected to history of our planet, or since the midst of the previous century and golden age of quantum electronics. Some of the general problems have rather slow dynamics of solving, but on the other hand, considering contemporary state-of-the-art of unconventionally powered vehicles and realized components, some characteristics change conservative opinions on the realizable capacities. The main goal of this consideration is to point to the unity of problems, which might speed up the gradients of the developments in solar technology of automotive technology, by multi-disciplinary approach. Overall, we have considered both theoretical approaches and currently developed systems in the fields of technology, metrology and power production and transformation.

Key words: laser; Sun; renewable energy sources; vehicle; technology; metrology; solar laser pumping; holography; plasma

1 Introduction

Main parts of electrical power system bring to mind the importance of electrical power, production, distribution, consumption and production capacities of Serbia and neighboring countries

^{*}Corresponding author, email: esreckov@etf.rs

(BiH - Republic of Srpska, Montenegro, Romania), as well as Europe and other continents. There are issues of small/ large hydro-, thermo-, wind and geothermal power plants and systems (and others) concerning planned and realized capacities. Wind energy transformation, properties of energy, transmission/ distribution/ development of networks, distribution facilities, photographs, questions of consumers and areas, generation of local area diagrams and averaging of capacities are still contemporary topics. The question and the stance of education of necessary theoretical and practical knowledge, as well as the skills for education systems are of special importance. Detailed data regarding climate and weather, like wind charts, etc. should be constantly recorded, due to (debatable) changes of climate.

1.1 Sun and wind

Almost entire renewable energy and also fossil fuel energy originate from the Sun's energy. Sun as a star rotates with the speed of 30 km/s around its axis with period of 27 days at Sun's equator and of around 31 day at Sun's poles. In the core, temperatures are estimated at 10^7 K, pressure 10^{14} Pa and density 10^5 kg/cm³. Here the thermonuclear fusion of hydrogen to helium takes place, generating vast quantity of energy which is transferred to the surface and from there transmitted into Space in the form of electromagnetic radiation.

Photosphere, chromosphere, corona (seen during eclipse) and heliosphere (reaching out towards Space) are areas which parameters are expressed with temperature - T , pressure - p , radiation/ solar constants, state of ionized particles and gases. The temperature at the photosphere is $T = 5769$ K and radiating power 64MW/m. Sun attributes, like the change of irradiation power with the distance from the Sun to the Earth is decreasing and solar constant drops to ≈ 2353 W/m. The causes of wind formation could be found. One parallel is that laser motor was known although it did not work on laser with solar drive. Other parallels are lasers pumped by solar power.

For a long time, Germany was leading in wind power production capacity. In 2008 Germany had dropped to the second place and in 2010 to third, with the China taking the precedence. The development of wind energy in the first two decades of the 21st century and the factsheet on the wind power in Germany from various references are shown, Figs. 1-3. Consumption management in the smart power grids with variable production puts on line issues: electrical power, distributed sources, smart network, response, consumption, load, prognosis, management, peak power, variable production. Nowadays, economic and ecologic interests are often opposed and are the topics of everyday consideration and debate [1-22].

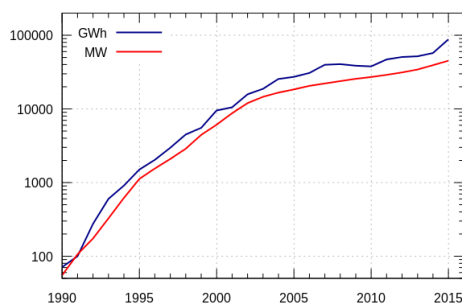


Figure 1. Wind power in Germany from 1990 to 2015 [2]

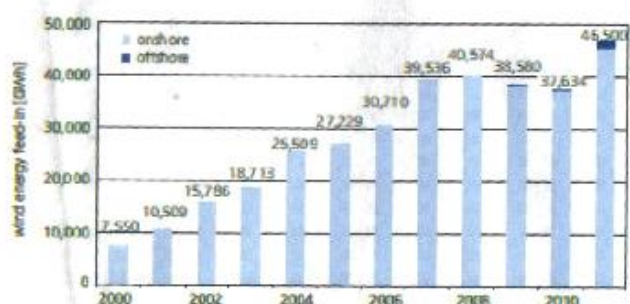


Figure 2. Development of wind energy supply in Germany

2 Technological and metrological application

The use of lasers in automotive/ vehicle industry, aircrafts and shipbuilding - maritime industry [23-27], for civil and military purposes is increasing. Historically, a series of references describing application of lasers in certain area of everyday life contain it as a topic. As devices, lasers were developed in scientific disciplines worldwide and used in advances to Space, medicine, in art and heritology as well [23-27]. Here, several examples are presented existing in generally all categories

covering material processing [27-34], a role in vehicle sensors, state of tires and similar, concluding with laser motors (engines) and laser rocket engines (motors) [35-54].

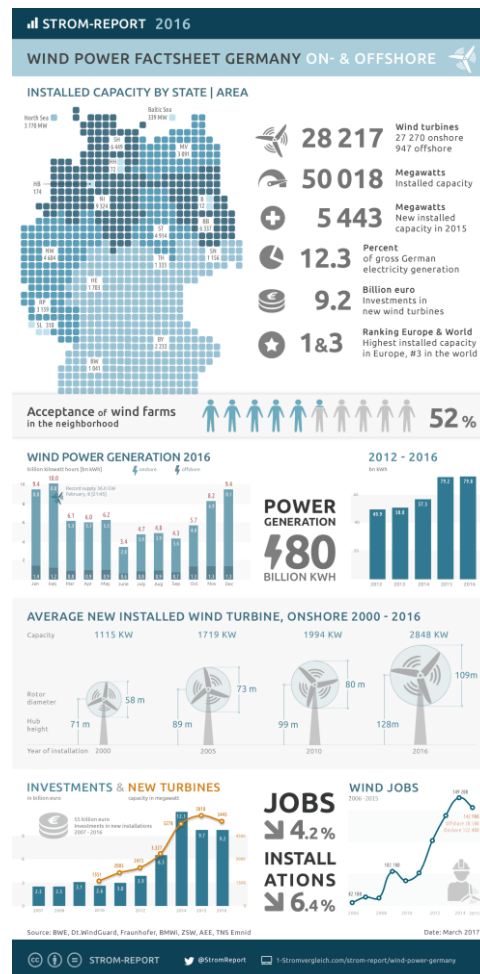


Figure 3. The factsheet on wind power in Germany in 2016 [1]

The application of lasers in automated visual inspection systems, quality management and in the measurement technique of vehicle production and control are among the measurements developed on the basis of coherent sources for non-destructive testing (NDT) of: fatigue, vibration, deformation, flow and combustion processes. The attributes are: simplicity, easy handling, ergonomic design of the car interior, methods of geometric and physical optics, profiles and surface positions, detection of defects and optical vibration measurement and monitoring.

To control oil purity and combustion processes, a number of spectroscopic methods are used. For other features linked to automotive industry and vehicle operating, laser based methods of frequent use are anemometric methods, interferometry, holography, tomography, however speckle based methods are also implemented. In many methods, quantum generators are widely used as sources. In the field of precision mechanics and analogous problems, Moiré methods were known as more classic. Some developments that are linked to all the methods mentioned above are: CCD batteries and the development of small computers including more *conservative classical methods*.

In *pure* processing of materials in automotive industry, laser role is included through the tasks of engraving, printing on metal parts, drilling, cutting, welding (machining/ processing of objects of various geometries), printing through glass or layers of other material, after the system has been assembled. Printing techniques are known in the methods of masks (in photolithography) and matrix or scaffolding in 3D printing and are connected to branching procedures and artificial intelligence. Monitoring by camera is also performed in the vehicle industry, especially in the automotive industry. The trend in general is to replace the human work with robotic or digitalized solutions. Once upon a time, acquiring an image of a work piece in good illumination was sufficient for further analysis, which excluded the necessity to observe or to have access to the work piece. Pro-

cessing speeds and solutions depend on the complexity of the part to be produced and the current technology. In perspective, the quality of acquired images improves with illumination by coherent sources. As an example, lasers were included in bar code technology much later after it was introduced. Much of the theoretical work has been invested and many technological operations were developed until laser centering of automotive parts became common in many car repair centers in *almost every town*. A large number of possible, potential or current laser applications are sketched in Fig. 4.

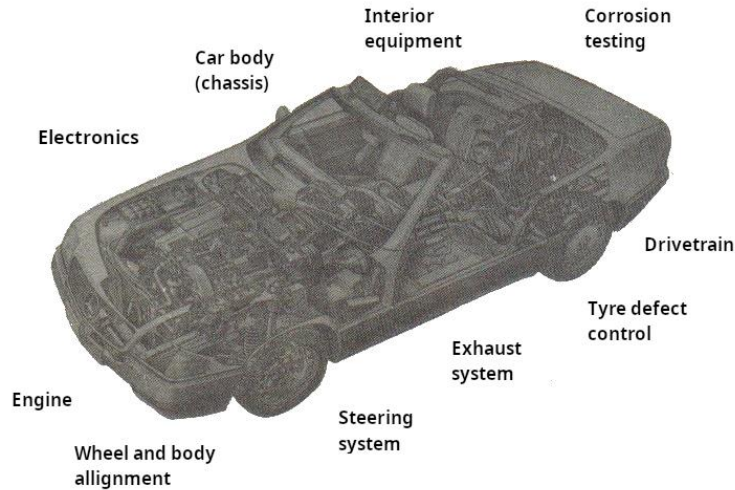


Figure 4. Typical points of inspection and quality control in vehicles. Emphasis is on the measuring role of the quantum generator, but it was not taken into account that the laser methods also participated in the construction of a particular component or assembly

Characteristic places of inspection and quality control in vehicles are steering wheel and measuring elements, engine, drive unit, electronics, exhaust gases, interior equipment, car body, centering of gears and wheels, control of tires, corrosion testing, measuring of vehicle speed and wheel rotation speed, topographic types of control, performed at normal speed of movement. For instance, poorly centered pneumatics cause vehicle vibrations and have serious impact on the car suspension and support system. The implementation of such systems, Figs. 4-8, has been developed by car and tires manufacturers, Michelin among the others.

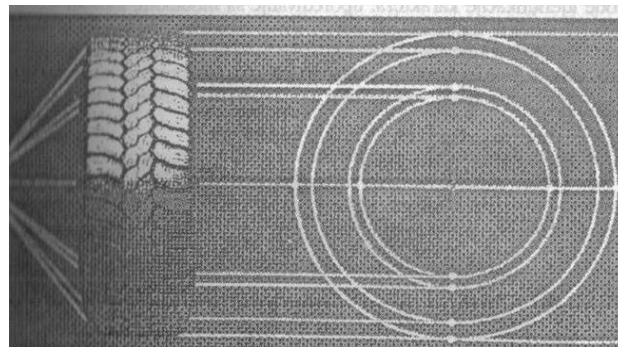


Figure 5. Control (monitoring) of tires with a laser beam

Profile and surface quality examination, and the surface position measurement are also performed by laser. In contour measurements, a sharpened probe is used maintaining the mechanical contact with the surface of interest. Changing the position causes the probe to move, which further evaluates the contours of the surface profile. Mechanical devices in various areas verify the thickness of details and determine the surface parameters in the process of automatic control by using the servo systems and feedback by adequate comparison. For the exact reproduction of the 3D representation, the method of profilometry of the template is used.

Optical solutions in profilometry have the following advantages: no damage to the work surface, no wear of instruments, measurements can be performed with templates made of various mate-

rials. Developed models range from polished materials of various degrees of metal surface quality to plastic and matt surfaces. Accessories with wedge-shaped components and topography recording are increasing in numbers. Measurements provide a profile, horizontal map, object thickness, as in Fig. 9a.

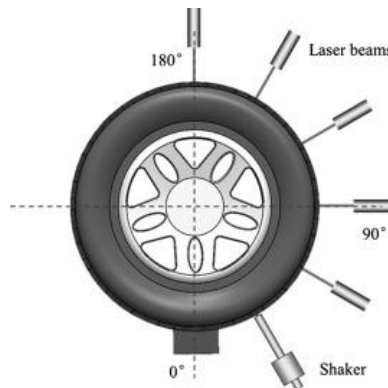


Figure 6. Control of a tyre with a laser beam [24]

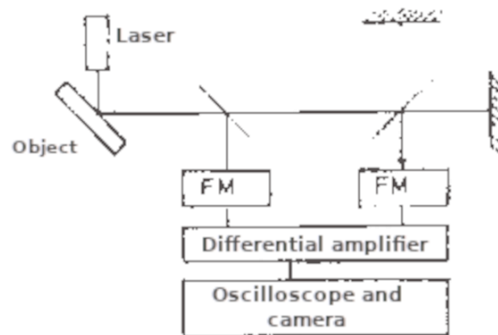


Figure 7. Displacement measurement scheme

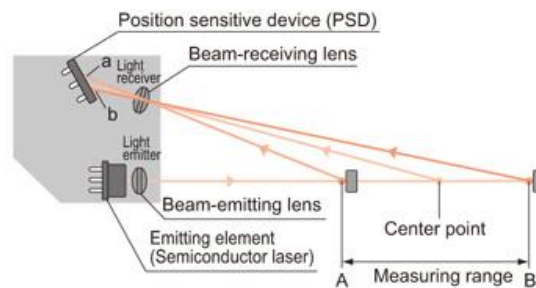


Figure 8. Laser displacement measurement [25]

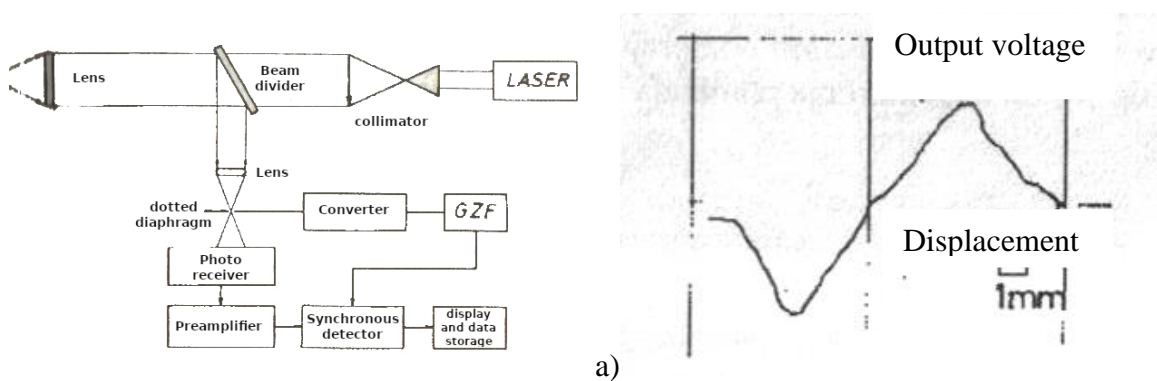


Figure 9. a) Block diagram for measuring the surface profile; b) synchronous detector output

In the surface profile measurement system, Fig. 9, the laser beam is focused at a small spot on the surface of the examined object. Scattered radiation is collected by lenses and focused through

the diaphragm vibrating at sound frequencies onto the photodetector. The variable component is amplified and detected by synchronous detection in relation to the frequencies of the generator. Diaphragm dimension is 250 μm , and vibration frequency is 525 Hz. The sign of the output signal depends on the direction of movement in relation to the focus. This is how maps are recorded (2D analysis).

2.1 Systems for defect search and diagnostics

The advantages of laser quality inspection and control methods come to the fore when it is difficult to provide automatic control. There are various cases: surface quality, mass production, rapid control of multilayer materials, small details in the automotive industry. The system works on the principle of light scattering (laser beam). For cylindrical geometry, the He Ne laser beam is transformed into a line, which follows the workpiece with a mechanical manipulator of the auto-revolver type. Various optical signals are collected from the surface of the working part, transmitted through a system of fibers and other optical elements, and detected by a photomultiplier. The frequency spectrum of the obtained signals is compared with/ to the spectra obtained from the surfaces without defects.

2.2 Optical vibration measurements

The character of vibrations of one structural part during harmonic excitation is measured. Complex processes in engines, brakes, body parts and testing areas at several points can be analyzed. For instance, Volkswagen used the contactless methods for obtaining the data for analysis, holographic and laser Doppler measurement techniques. Among them, there are two-pulse holography, LDA measurements of vibrations in small volume (SOVAS technique); Tabs.1 and 2 give characteristics of laser methods during time.

Table 1. General methods of vibration measurement

	Real time holography	Pulse holography	SOVAS
Object	Single construction elements	Construction blocks, aggregates, chassis	Construction blocks, aggregates, movable parts of chassis
Measuring quantity	Amplitude	Analysis regarding laser pulse	Speed
Measuring interval	0.2 μm - 0.5 μm	0.2 μm - 200 μm (extrapolated)	0.001 m/s - 1 m/s
Excitation	Harmonic	Harmonic or auto-excitation	Harmonic or auto-excitation and excitation of noises
	Frequency variation	Dominant frequency time filtering	Spectral analysis
State of vibrations	Forced	Transitional regime	Stationary regime
Mode of operation	Surface	Surface	30 dots \times 30 dots
Duration of measurement	Several seconds	Instantly	10 s - 300 s

Table 2. Methods of holographic interferometry

	Real time holography	Pulse holography	Holographic interferometry with averaging in time
Operations	Hologram exposure, loading the object	Hologram exposure, loading the object, secondary exposition	Hologram exposure during object moving and development
Advantages	Total information on object changes	Easy realization, one-for-all single setup, constant emulsion	Easy realization and easy interpretation of results
Drawbacks	Difficulties in interpretation, necessity of repeating the setup, emulsion, distortions	Pure information, difficulties in interpretation	Not suitable on immobile surfaces

Applications	Analysis of mechanical stresses, defects	Analysis of mechanical stresses, defects, Analysis of transitional processes	Analysis of vibrations
--------------	--	--	------------------------

2.3 Active holography - real-time holography

With the help of a real-time holography, the vibrations caused by the construction elements are visualized. The vibration distributions are observed on a monitor with a video camera. Resonances are established by varying the excitation frequency. The measuring area relates to the area of the interference fringes $0.1 \mu\text{m} - 5 \mu\text{m}$. The interferometer must be on a special stand with insulation from vibrations of a mechanical nature. There is also the holographic working camera, the control of the illumination of the object, excitation and the stroboscopic device. For structural vibrations of the engine block, the range above 1 kHz is reached.

Another application with laser technique is related to the technique of optimization of brakes from the stress-strain point of view, Fig. 10. The problems of real-time holography are related to: a) placing the hologram in the exposure position, b) distorting the photoemulsions and c) detailed interpretation of the interference image in relation to the theory of local zones.

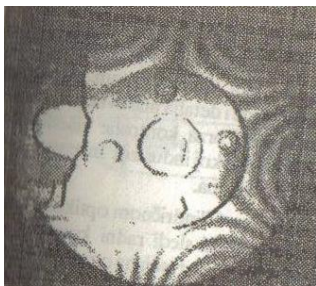


Figure 10. Vibration: technical optimization by holographic interferometry

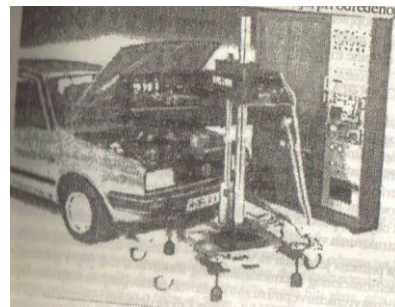


Figure 11. Holocamera

2.4 Two-pulse holography

Pulse holography has long been used outside of optical laboratories. Illumination with two pulses is used for the analysis of transient modes with a holocamera and adequate electronics, Figs. 7, 10, 11, which evaluate the vibrations (displacement/ dynamic) of the car body and the sub-systems. Free and forced vibrations are monitored. The resulting interference distribution showed the exact position and time (moment) of the vibration at a certain frequency. In addition, structural material weaknesses, noise sources and material strength are also examined. One of the first applications of holography in general, including this method, is based on the examination of pneumatics and defects in production and exploitation, Figs. 12, 13. Compared to the methods of real-time HRV holography, the method is less flexible and cannot monitor continuous deformation. The problems are in the interpretation, localization of zones, etc., Figs. 13, 14. The existence of both defects and places of different loads causes the occurrence of thickening and deformation.

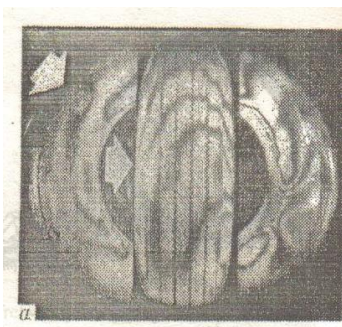


Figure 12. Holographic tests of tires; interference fringes



Figure 13. Detail of hologram for defect analysis

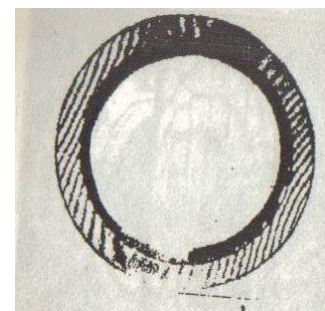


Figure 14. Changes on disk couplings examined by holographic techniques (mechanical and thermal stresses)

2.5 Laser Doppler methods: LDA and LDV

Holographic interferometry, HI, with time averaging does not demand that the detail, the construction ensemble and the scene are without vibrations of the environment (“without moving”), and that mechanical displacements are less than $\lambda/4$, where λ is the wavelength of the applied quantum generator. The characteristic of the beam intensity dependence on x , taken by one of the holographic schemes, is connected to $D(x)$ – surface displacement from the equilibrium state (or undeformed state) – and to λ . The surface analysis and estimation of its dynamics is possible if the condition $4\pi D/\lambda \gg 1$ is fulfilled.

In general, if the Doppler effect is present, the methods inherit its name. It is often used with the systems that follow both the development of techniques/ technology and the widening of our experience from acoustics to area where relativistic effects had to be taken into account for the case of EM radiation. HI methods are based on the optical path manipulation and on obtained visualization of hologram. The image is closely connected to vibrations, resonant frequencies, provoked deformations, and stresses of the objects or system. The vibrometer uses the direct and referent beams. Laser beam reflected from the object is recorded in the measuring system. The laser beam operates with defined number of measuring. In the case of vibrations, vibration processes are imprinted in signals. The obtained spectrum is the principal task for analysis and from the depth of modulation characteristic (resonant) frequencies and the local distribution of the vibrations can be obtained, Figs.15. Besides the first known application in violin resonator (or other musical instruments), and in turbine blades, HI methods with time averaging are applied in automotive, aircraft and other vehicle industries.

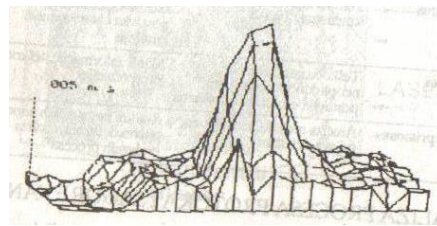


Figure 15a. SOVAS techniques define resonance frequencies of component, part of the system or in general recorded area (valve dynamics)

The analyses of the combustion processes have been performed by the methods of laser beam scattering and have been used for monitoring of engine operation, and for monitoring of turbulent processes. The Schlieren method is commonly used in this case, Fig. 15b.

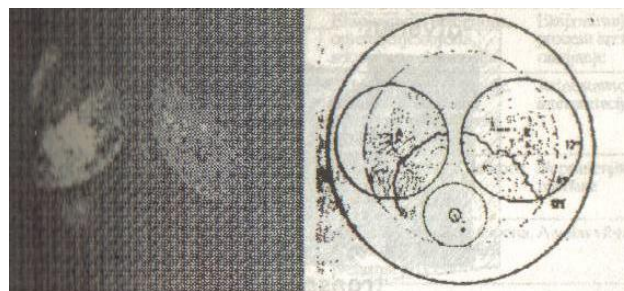


Figure 15b. Schlieren method applied in motor dynamic control/ monitoring

2.6 Laser Rocket Motors

New trends in the development of rocket techniques have opened new possibilities for lasers to be implemented and for solving problems related to classical motors used in interplanetary flights. In this paper, some aspects of the design and construction of laser rocket motors as well as the implementation of exchange of laser power are presented. A lot of debate concerning the types of optimal design of the systems of energy transformation in cosmic investigation still exists, and new technologies in recent years have opened up many new possibilities.

Laser rocket motors run on various energy types: electrical (electrostatic, electromagnetic and electrothermal), nuclear, solar, magneto-hydrodynamic and numerous types of chemical fuel, and

more. They all have many advantages and disadvantages, with different degrees of efficiency. Solar-powered laser motors also exist. Both solar into thermal energy transformation and motors (ionic or plasma) are considered for the cosmic travel. However, it seems that the ideas concerning classical – thermal – motors are still dominant in the field of contemporary solutions in the Earth's atmosphere. The link between reactive motors and laser as a power source is still a topic of discussion as also is the grouping of laser power transmission into several groups based on the principle of operation, thermal, electric and hybrid.

One possible solution of laser implementation is where a directed, focused laser beam is absorbed in some solid, liquid or gas fuel, or for laser-ignited combustion, Fig. 16. The basic mechanisms of absorption in heat exchange devices are: Bremsstrahlung radiation, CW absorption, molecular absorption and particle-level absorption.

The implementation of pulsed, periodical laser beams, or CW laser beams depends on the combustion material type. The essential part of the design is linked to the current generator in the motor nozzle. In our terminology, the motor nozzle means establishing plasma in the working material, and combustion is the main process in sustaining the plasma.

The aerodynamic windows are especially important when working with high-power lasers. There exist non-linear optic solutions in surmounting window-related problems; these solutions are based on multi-layered materials and inverse-population processes. Optoelectronic systems are used for energy transport from Earth to orbital stations; the purpose of these systems is the transmission of CO₂ and free electron laser beams, Fig. 17.

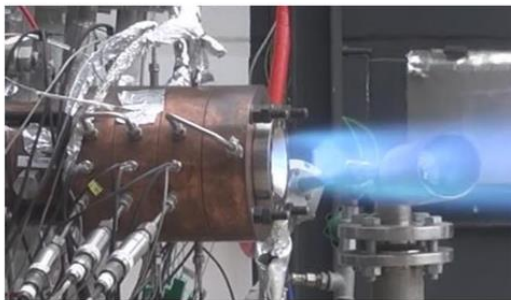


Figure 16. Laser-ignited combustion [50]

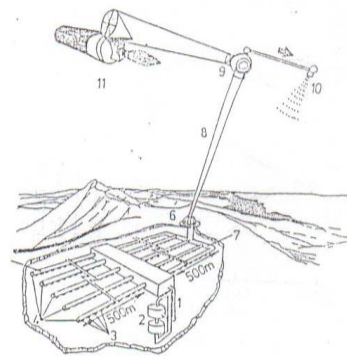
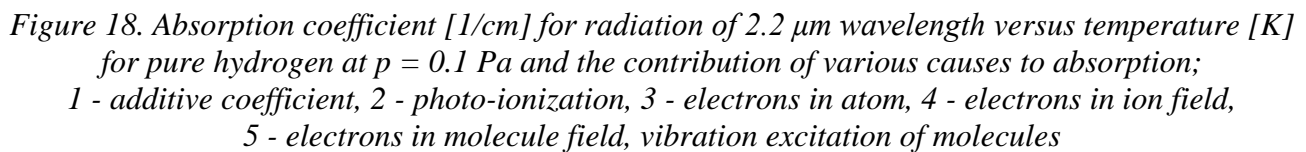


Figure 17. One of the first schemes of transmission of energy from free electron lasers on Earth to cosmic satellites. This scheme relies on the application of reflection and refraction processes

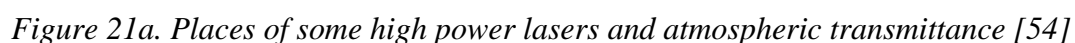
The station is built on high altitudes to minimize loss of power/ energy in the atmosphere. The principal parts of the system are: the free electron accelerator, powering sources, vacuum pumps, the transmitting mirror, the optical resonator, the collector/ concentrator of radiation; beam trajectory, geostationary orbital retranslator, etc. The feedback with the power station and the interorbital rocket with laser motor are also important aspects of the complex.

Laser rocket motors produce pressure based on the transformation of the beam energy into kinetic energy of fuel molecules via heating and expansion processes in the nozzle. The gases involved are of low molecular mass, and are therefore heated to very high temperatures. The principal tasks for the practical realization of motors of this type are: fulfilling the conditions for optimal absorption mechanisms of the laser beam, selection of the wavelength, the minimization of energy losses in all phases of motor's functioning, the design of the motor, and even the choice of materials or fuel, Figs. 18, 19.

Characteristic values are linked to simple approach to 1D modeling of flow, cylindrical geometry of the nozzle of constant cross section. These are the first approximations related to the real absorption of the laser beam, when effects of detonation, laser plasma wave transmission, supersonic processes and deflagration are possible. For CO₂ laser beam wavelength and hydrogen, at 0.1 MPa, power threshold is 10^{10} W/cm².



In Figs. 21-22, some characteristic results and facts from literature are presented.



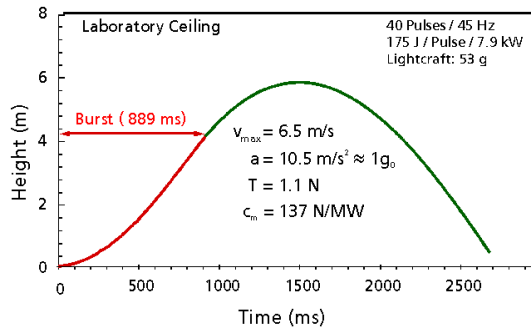


Figure 21b.



Figure 22. Gabarites in contemporary systems.

3 Laser Cladding on Exhaust Motor Valves

3.1 Plasma and Laser Cladding on Stainless Steel for Exhaust Motor Valves

The exhaust motor valves are exposed to high temperature of hot combustion gasses, followed by the pressure at the contact surface with the valve seat. The valves for fossil fuel motors are manufactured from stainless steel materials, but many of which do not have satisfactory wear properties at high temperatures. The thermal stability can be improved by cladding. For that purposes, hard and corrosion resistant material should be used, such as Co- or Ni-based materials. Due to high boiling and melting points, the plasma spraying and laser cladding must be used for fast melting. Laser cladding is distinguished from plasma cladding in a smaller fusion area at the parent metal and in producing a well metallurgical bond of the hardfaced material. Furthermore, the combustion of vaporized liquid fuel produces specific kind of high-temperature corrosion. Many attempts have been done in choosing the material with adequate properties. The Ni alloys for motor engine valves must contain strengthening elements, commonly Co, Al, and Ti. Due to lower price, the Co coating alloys are superior to stainless steel as a surface material. The industrial acceptance of laser cladding is still slow.

Powders. Typical stainless steel for exhaust motor valve has contributions of five elements (percent): C (0.50), Cr (21.0), Mn (9.0), Ni (4) and N (0.4). After quenching from 1140 °C- 1180 °C in aqua, steel retains the austenitic structure; it means that hardness values are not increased. As corrosion resistant and hardfaced materials for exhaust motor valves, available are Ni-Cr-B-Si and Co-Cr-W alloys (Stellite 6 or similar) in powder form [27]. For melting of those alloys, the high energy welding methods should be used.

Characteristics of cladding methods for engine valves. The contact surface between the engine valve and its seat, assigned by an arrow in Fig. 23a, subjected to the pressure in the atmosphere of combustion gases, achieves a remarkable wear. In order to decrease the wear, surfaces should be cladded/ hardfaced, Fig. 23b. This surface is rough, Fig. 23c, and has to be grinded.

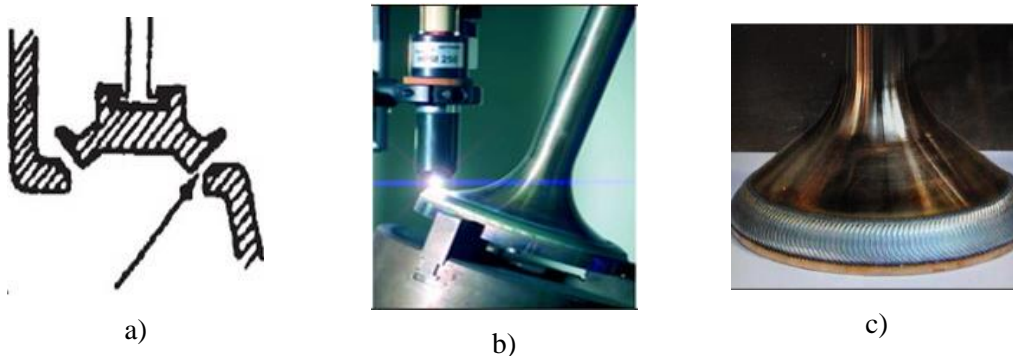


Figure 23. a) Contact surfaces between valve and seat, b) Surface during cladding, c) Cladded surface at the edge of motor engine valve

It is possible to achieve high energy torch in the plasma gun (*plasmatron*), Fig. 24a, where the stream of high velocity gases does not carry the molten particles. The plasma gun enables achieving high temperatures ($> 4000\text{ K}$), fast and strong stream of formed plasma gas, so that different powders could be melted at the valve edge.

The laser beam produces high temperatures in interaction, even more than plasma torch. Powder for laser cladding could be fed from one or both sides, Fig. 24b. It is possible to produce a thinner layer by laser beam than by plasma torch. One of the main advantages of laser beam is in lower dissipation of an expensive powder material to be melted and cladded. Depending on used powders, the hardness values of cladded material range from $\approx 390\text{ HV}$ to $\approx 550\text{ HV}$. It is reasonable to consider hardfacing. In plasma or laser cladding, different technological parameters are applicable in a wide range: speed of beam travel, powder mass flow rate, used plasma or shielded gas, pulse frequency, energy of beam, etc.

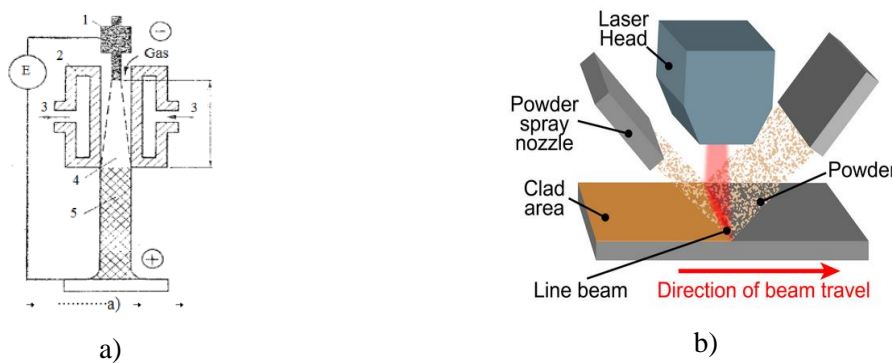


Figure 24. Cross section through: a) plasma gun and b) laser head, for cladding;
1-W electrode, 2-Cu nozzle, 3-cooling water, 4- created plasma, 5-plasma stream, E-current source

For laser cladding of Co alloys, when sufficient energy of the beam reaches levels of $> 18\text{ J/pulse}$, CO_2 or pulsed $\text{Nd}^{3+}:\text{YAG}$ lasers are used [27]. Heat affected zone, HAZ, and especially interface layers are very small after laser cladding, Fig. 25. The pores occurring in microstructure after laser cladding are rare and small, Fig. 25a.



Figure 25. Microstructures of cladded layers: a) stellite-6 layer and small interface on the parent metal; b) parent metal (left), HAZ and Ni-Cr-C-S alloy (right), magnification $300\times$ [27]

The dilution of cladded layer with parent material is higher with plasma method than with laser cladding method. Surface roughness, R_a , after grinding of cladded layer on motor engine valves [27] has to be on level $< 1.8\text{ }\mu\text{m}$.

Following statements are for further analysis. Plasma and laser claddings are cost effective methods for improving the wear- and corrosion- resistance characteristics of motor engine valves. Therefore, for surfaces, a material with better properties than the parent metal must be used. After cladding, the surface is rough. Industrial lasers are controllable power sources, meaning that the control of the heat input into the workpiece is better with the laser cladding than with the plasma gun cladding. The plasma cladding gives significantly higher power input into the workpiece, which is usually disadvantage in the sense of higher distortion of treated machine component. Lower distortion means smaller grinding thickness, which is of importance for manufacturing schedule. In both processes, it is possible to employ high-hardness alloys, even mixtures containing WC, SiC or similar intermetallic compounds, for a variety of applications [27].

4 Conclusion

Characteristics of plasma and laser cladding methods could be emphasized as: plasma and laser methods for cladding of motor engine valves dominate in automotive industry. In laser cladding the higher power density is achieved at the small target area than in plasma method. Hard and corrosion resistant materials may be easily melted by both methods. Obtained hardness values are in closer relation to chosen chemical composition of clad material rather than the used method for deposition of a layer. The negative role of strong plasma stream is the blowing of powder material to be clad. The smaller dissipation of powder material is achieved by using laser beam instead of plasma torch. The dilution of melted layer is lower in laser than plasma cladding. Both methods are available for producing new parts, as well as in additive manufacturing and for rebuilding of partially worn surface(s).

The main branches of the field of laser processing are: the study of technical characteristics of laser systems and laser types, as well as the study of other optical components, mechanical systems and the specificity of the designed devices. Since the era of MILK and the first PhD theses in former Yugoslavia about the industrial applications of lasers, there have been numerous other studies about basic functioning and practical applications: namely, about laser pumping, beam shaping, transportation, reflection and refraction processes. There have also been studies about systems based on fluid mechanics, system cooling, thermostating for increasing laser stability. It is important not to forget about the social and health aspects of research, i.e. the education in the application of the developed systems and demand to provide the necessary protective measures. Note that some of the old terminology for the deviation of the actual results from the nominated/projected/fabricated results (for example, drilling diameter, surface roughness, precise contour cutting) needs to be updated – for example, the term “error” should be replaced by “uncertainty”; this not just a matter of terminology. Considering the variable nature of energy transformation, a multidisciplinary approach is inevitable.

From the economic perspective, there is no doubt about the fact that quality is the best investment, and this is true for the vehicle industry as well. In order to establish a system of quality in the automotive industry, one must have: technical documentation depending on the type of the vehicle, production equipment, personnel, realization monitoring, environmental conditions and ecological trends.

Several highly trained people are required to study on large and complex array of machines. One engineer today with a laptop can do more sophisticated studies of much larger systems. Steady-state flows are simulated as the positive sequence equivalent, presented by several π sections connected in series. Each of them represents a length of line as shunt capacitors and series reactive elements. The system was replaced on a large panel, the face of which was a maze of physical connection links. Unbalanced faults required an interconnection of three networks, each one for positive, negative and zero sequence. Dynamics were simulated by a step-by-step process with some representation.

Lasers are used in various ways for technical verification purposes. New measuring methods for displacement and sizes are constantly being developed, but they are all based on geometrical and physical optics, diffraction, interference, holography, holographic interferometry, etc. Methods for the measuring of vibrations in general as well as stresses and stress distribution are also based on the aforementioned physical disciplines and processes. Many of these methods are in essence classical, where the laser is only a substitute for a natural source of energy; however, many others can only be realized with the use of lasers/coherent beams. The term “coherent” should be used both in the spatial and temporal sense, but in practice, it usually refers to only one of these two. Because of the development of lasers with very short pulse (ns-ps-fs), certain measurements, which could previously only be done in a laboratory, can now be performed in the field.

Laser measuring methods are often cheaper, simpler and faster than their more classical counterparts. Lasers are also used in systems which measure displacements caused by static and dynamical loadings, which are a very important aspect of monitoring in the automotive industry. One such example is the tuning and positioning of car suspension. Also, corrosion is nowadays monitored by

small portative devices. All of these processes are carried out from a distance, without interrupting the production processes. Laser-based microanalysis of materials (like LIBS, ...) has numerous advantages over other microanalysis methods (chemical, ion and electron beams, SEM and TEM, ...). Many practical applications rely on laser plasma. Laser-based microanalysis methods are very precise even for very small samples ($< 1\mu\text{g}$). There are numerous illustrations for the state of *know-how technology* and potential laser implementations.

Although they have their own histories, the topics of laser propulsion and rocket motors have connected several contemporary disciplines in recent years, initiating much theoretical research, as well as large international projects on the applied side of the areas.

A detailed examination of the comparison and current state of contemporary laser motors, which would consider both the theoretical and practical point of view, would necessarily be a very long/demanding project. Therefore, in this paper, only rough sketches of the subject matter have been given. From an educational point of view, one should neither dismiss the historical dynamics of the development of laser motors, nor the current state of today's most promising designs. The lasers have been given a special place in this paper, because many commercial and non-commercial quantum generators exist (laser transitions). One of the most important areas of research concerning lasers is the transfer of mechanical magnitudes by optical systems: buoyancy force or the transformation of electromagnetic energy to other ranges. In order to improve the functioning of laser motors, the most important aspect is increasing the efficiency of absorption (multi-layer material, coating, concentrator, etc.).

The theoretical foundations have existed for almost 30 years. The realization depends on both the needs and currently available technology. When minimizing losses in the application of lasers in motors, one must pay special attention to the processes in: plasma, transmission of energy to the working fluid, flow regulation, the mixing of hot and cold materials, the transfer of heat into the motor walls by convection and radiation, and in the protection of walls. Other important points of view include the gasdynamics of the flow through the plasma and the nozzle design. It is important to select the optimal laser wavelength for laser motors (engines), due to very large number of quantum generators. In particular, aerodynamical windows require many new solutions on their own. To reach the goals, the activities of today implement more and more, but efficient models, and also increase the level of approximation of the thermodynamic and other real processes. This can be achieved by developing better numerical models and more mathematical complex representation or mathematical symbolism/ formalism. The technical side consists of decreasing the project costs, increasing reliability, safety, "user-friendliness", simplification of design and ease of maintenance. The contemporary development of laser techniques is moving towards amelioration of laser beam characteristics and performance, stability (of frequency, polarization and mechanical one), increasing the range of applications and the choice of wavelength in the total range of the EM spectra and power (ranging from kW to MW). The emission and absorption processes in the atmosphere should be constantly studied and evaluated. That influences both the quality and the power magnitude of the laser beams entering the rocket engine from the station, located on the surface of the Earth. The contemporary development of material technology will lead to many new discoveries in the construction of new adequate materials with high hardness to temperature and pressure.

Acknowledgements

The authors are grateful for the help in preparing this manuscript to MSc Zivojin Petrovic and MSc Matija Sreckovic for professional discussion.

5 References

- [1] *** *Infographic "Germany: Wind Power Factsheet 2016,"* from Stromvergleich.de (<https://1-stromvergleich.com/wind-power-germanygermany-wind-power-2016>), accessed September 4th, 2020.
- [2] *** *Annual Wind Power in Germany 1990-2015,* from Wikipedia: Wind Power in Germany (https://en.wikipedia.org/wiki/Wind_power_in_Germany), accessed September 4th, 2020.

- [3] **Mitrašević, Lj.**, *Eolske elektrane. Perspektive razvoja i eksploatacije*, B.Sc. Thesis, Faculty of Electrical Engineering, University of Belgrade, Belgrade, Serbia, 2001.
- [4] **Adetifa, B. O., A. K. Aremu**, Influence of a Base Reflector on the Performance of Double Exposure Box Type Solar Cooker with and without Heat Storage Materials, *FME Trans.*, 46 (2018), issue, pp. 567–574.
- [5] **Satputte, J. B., J. A. Rahan**, *FME Trans.*, 46 (2018), issue, pp. 575–584.
- [6] **Vanucchi de Camargo, F., C. Gragassa, et al.**, *Analysis of the Suspension Design Evolution in Solar Cars*, from ResearchGate (https://www.researchgate.net/publication/315797146_Analysis_of_the_Suspension_Design_Evolution_in_Solar_Cars), accessed September 4th, 2020.
- [7] **Belić, I.**, *Modern industrial complex MILK for metal processing*, Ph. D. Thesis, Faculty of Mechanical Engineering, University of Belgrade, Belgrade, Serbia, 1990.
- [8] **Šiljkut, V.**, *Demand side management in smart power grids with variable generation*, Ph. D. Thesis, Faculty of Electrical Engineering, University of Belgrade, Belgrade, Serbia, 2015.
- [9] **Milovanović, Z. N., Knežević, D., Milašinović, A., et al.**, Analysis of solutions for electrical energy storage inside the policy for development of improved technologies based on renewable energy sources, *Energija ekonomija ekologija*, pp. 127–140 (www.savezenergeticara.org.rs).
- [10] **Babić, M., A. Babić**, Proposal a new concept for development and exploitation of electric cars, *Energija ekonomija ekologija*, pp. 102–107 (www.savezenergeticara.org.rs).
- [11] **Lazić, B.**, *Solar PV cells*, B. Sc. Thesis, University of Belgrade, Beograd, Srbija, 2003 (in Serbian).
- [12] **Despotović, Ž., M. Jovanović, I. Stevanović, M. Majstorović**, Pressure control in mobile off-grid solar system for irrigation of crops, *Proceedings 6. Sajam Obnovljivi izvori energije*, SDIT, Požarevac, Serbia, 2018, pp. 35–44.
- [13] **Pavlović, T.**, *The Sun and Photovoltaic Technologies* (eBook), ISBN 978-3-030 -22403-.
- [14] **Obradović, D., Obradović, D.**, The effect of energy efficiency on ecological and economic parameters, *Proceedings 6. Sajam Obnovljivi izvori energije*, SDIT, Požarevac, Serbia, 2018, pp. 60–69.
- [15] **Trifunović, M.R., Stanković, M. E. , Grujić, N. R.**, Doprinos SITJ Požarevca u promociji mogućnosti korišćenja obnovljivih izvora energije, *Proceedings 6. Sajam Obnovljivi izvori energije*, SDIT, Požarevac, Srbija, 2018, pp. 70–78.
- [16] A) **Obradović, D.**, Ugalj i dalje glavni energent, *Tehnika*, 57 (2020), 57, pp. 52–61. B) **Crnčević, M., Vukašinović, V., Nikolić, M.**, Prezentacija projektnih rešenja i gradnje solarnih kolek tora u domu učenika poljoprivredne škole „Sonja Marinković”, *Proceedings 6. Sajam Obnovljivi izvori energije*, SDIT, Požarevac, Srbija, 2018, pp. 79–88.
- [17] A) **Bindra, A.**, Electric Vehicles Batteries Eye Solid State Technology, *Power Electronics*, 7 (2020) 1, pp.16-19. B) **Milošević, S.**, 25s/11, Dnevnik praktične nastave Ikarbus, Škola Politehnika, Beograd, Srbija, p. 41. C) **Bindra, A.**, Electric Vehicles Enter a New Era, *Power Electronics*, 7(2020) 1, pp.14-17.
- [18] **Nikolić, Z. D.**, The Results of the PV Supply testing in Belgrade and one method of ecological power supply of the republic of serbia electric energy, *Proceedings 6. Sajam Obnovljivi izvori energije*, SDIT, Požarevac, Serbia, 2018, pp. 1-7.
- [19] **Stanojević, M., Z. Stević, D. Todorović**, Energy balance of the digester waste processing and biogas production, *Proceedings 6. Sajam Obnovljivi izvori energije*, SDIT, Požarevac, Serbia, 2018, pp. 11-17.
- [20] **Grujić, N.R., M. Trifunović**, Use of renewable energy sources in agriculture, *Proceedings 6. Sajam Obnovljivi izvori energije*, SDIT, Požarevac, Serbia, 2018, pp. 18-27.
- [21] **Bahaghigal, M., S. A. Motamedi**, Vision Inspection and monitoring of wind turbine farms in emerging smart grids, *Facta Universitatis*, 31 (2018) 2, pp.267-301.

- [22] **Srećković, M., M. Kutin, M. Hribšek, et al.**, *Primena elionskih tehnika i drugih tehnika u merenju, kontroli i obradi materijala i procesa*, Institut Goša - Društvo za tehničku dijagnostiku Srbije - Katalog univerzitetskih izdanja, Beograd, Srbija, 2009.
- [23] **Liu, X., Q. Feng**, Structure-borne vibrations of tire, *Automotive Tire Noise and Vibrations – Analysis, Measurement and Simulations*, (2020), issue, pp. 149–183.
- [24] *** *Laser Displacement Sensor*, from Panasonic (https://www3.panasonic.biz/ac/ae/service/tech_support/fasys/tech_guide/measurement/laser/index.jsp), accessed September 4th, 2020.
- [25] **Srećković, M., Petrović, Ž., Pavićević, M.**, Lasers in automotive industry, *Zastava* 7(1989), 2, pp. 23-35.
- [26] **Srećković, M. (Ed.)**, *Lasers and application; metrology and material processing*, SITJ, Beograd, Srbija, 1990 (in Serbian).
- [27] **Janjušević, Z., Karastojković, Z., Bajić, Z. et al.**, “Characteristics of plasma and laser cladding of stainless steel for exhaust motor valves,” *Proceedings 48th Int. October Conf. on Mining and Metallurgy*, Bor, Serbia, 2016, pp. 309-312.
- [28] A) **Jendrzewski, R., Conde, A., De Damborenea, J. G., Sliwincki, G.**, Characterization of the laser-clad stellite layers for protective coatings, *Materials&Design*, 23(2002), pp. 83-88.
B) **Davies, A.C.**, *The science and practice of welding, Vol. 2: The practice of welding*, Cambridge University press, Cambridge, 1994, pp. 189-195.
- [29] **Rykalin, N., Uglov, A., Zuev, I., Kokora, A.**, *Laser and electron beam material processing (Handbook)*, Mir Publishers, Moscow, USSR, 1988, pp. 314-324.
- [30] **Sun, S., Durandet, Y., Brandt, M.**, Parametric investigation of pulsed Nd:YAG laser cladding of stellite 6 on stainless steel, *Surface and Coat. Technol.* 194 (2005) 2-3, pp. 225-231.
- [31] **Zhu, Y.-Z., Z.-M. Yin, H. Teng**, Plasma cladding of Stellite 6 powder on Ni76Cr19AlTi exhausting valve, *Trans.Nonferrous Met. Soc. China*, 17(2007), , pp. 35-40.
- [32] **Aihua, W., Zengui, T., Beidi, Z.**, Laser Beam Cladding of Seating Surfaces on Exhaust Valves, *Welding Research Supplement*, (1991), April, pp. 106-109.
- [33] **Walsh, R. A.**, *Machining and Metalworking Handbook*, McGraw-Hill Handbook, New York, USA, 1993, pp. 571-757.
- [34] **Cavenz, I. H. (Ed.)**, *Space: state and perspective*, Mir, Moskva, SSSR, 1988 (in Russian).
- [35] **Atanackov, B. E., Bregalin, A. F., Tišin, A. P.**, *Theory of rocket motors* (3rded.), Mašinostroenie, Moskva, SSSR, 1980 (in Russian).
- [36] **Sutton, P.**, *Rocket Propulsion Elements*, J. Wiley&Sons, New York, USA, 1986.
- [37] **Kantrowitz, A.**, Propulsion to Orbit by Ground Based Lasers, *Astronautics&Aeronautics*, 10 (1972), , pp.74-76.
- [38] **Pirri, A.N., Monsler, M. J., Nebolsine, P. E.**, Propulsion by Absorption of Laser Radiation, *AIAA J*, 12 , 9, pp.1254-1261.
- [39] **Piks, P. K., Pirri, A. N.**, Stability of Laser heated flows, *AIAA J*, 14 (1976), pp.390-392.
- [40] **Gudzenko, I.I.**, *Plasma Lasers*, Atomizdat, Moskva, SSSR, 1987 (in Russian).
- [41] **Gerrx, E., J.D. G.**, The Laser Future, *Astronautics &Aeronautics*, (1979), pp.66-67.
- [42] **Thygaryak, K., A. K. Gathal**, *Lasers, Theory and Applications*, PlPr, New York, USA, , March, pp.66-67.
- [43] **Henderson, W.D.**, Space based Lasers, Ultimate ABM System, *Astronautics & Aeronautics*, 20 (1982), May, pp. 44-53.
- [44] **Bunkin, F.V.**, Applications of lasers sources of power for design of reactive tjagi, *UFN*, 119 (1983), pp. 425-428 (in Russian).
- [45] **Voronkov, G.T.**, *Optical Technology in Space*, Mašinostrenie, Leningrad, USSR, 1984.
- [46] **Glemb, R., H. Krier**, Principl and state of laser motors design, *Aerokosmiceskaya tehnika*, (1985) 1, pp.119-132(in Russian).
- [47] **Gudzenko, I.I.**, *Plasma Lasers*, Atomizdat, Moskva, SSSR, 1987 (in Russian).
- [48] **Marshall, T.C.**, *Free electron Lasers*, Nauka, Moscow, USSR, 1987.
- [49] **Sutton, P.**, *Rocket Propulsion Elements*, J. Wiley&Sons, New York, USA, 1986.

- [50] **Meek J.M., Craggs, I. D.**, (Eds.), *Electrical Breakdown in Gases*, J. Wiley & Sons, New York, USA, 1989.
- [51] **Kroupa, G., Boerner, M.**, Miniaturized high-energy laser for rocket engines, Proc. *SPIE*, SPIE, , USA, 2019, 11180, p. 11805I, doi: 10.1117/12.2536117.
- [52] **Ristić, S., Srećković, M., Anastasijević, Z., Čitaković, S.**, Raketni motori na laserski pogon, *NTP*, 44 (1994), 10, pp.24-32.
- [53] **Komurasaki, K., Wang, B.**, *Laser propulsion*, 2010, <https://doi.org/10.1002/97804780470686652.eae123>.
- [54] **Eckel, H.A.**, *Laser Propulsion - An Innovative Launcher Technology*, 207, April, <https://www.researchgate.net/publication/224986072/>.

RASTVARANJE KATODNOG MATERIJALA IZ LIB U SUMPORNOJ KISELINI U PRISUSTVU AZOTA

DISSOLUTION OF LIBs CATHODE MATERIAL IN SULFURIC ACID IN THE PRESENCE OF NITROGEN

**Dragana V. MEDIĆ*, Snežana M. MILIĆ, Slađana Č. ALAGIĆ, Zoran M. STEVIĆ,
Boban R. SPALOVIĆ, Maja M. NUJKIĆ, Ivan N. ĐORĐEVIĆ**

University of Belgrade, Technical faculty Bor, Vojske Jugoslavije 12, 19210 Bor, Serbia

Dobro je poznato da litijum-jonske baterije (LIB), sa kratkim životnim vekom (od 1 do 3 godine), čine veliki udeo u elektronskom otpadu. Pored opasnih materija (uglavnom soli litijuma rastvorene u organskim rastvaračima), LIB sadrže i značajnu količinu vrednih metala (pre svega Co i Li), čija valorizacija u velikoj meri doprinosi konceptu održivog razvoja. Postupci reciklaže LIB odnose se na fizičke, hemijske i biološke procese i mogu se generalno podeliti na: hidrometalurške, pirometalurške i biološke procese. U cilju smanjenja emisije štetnih gasova i optimizacije procesa, u novijim istraživanjima prednost se daje hidrometalurškom pristupu. U ovom radu ispitana je mogućnost izluženja kobalta iz katodnog materijala istrošenih LIB u sumpornoj kiselini u prisustvu azota. Postupku luženja prethodio je specifičan višefazni tretman pripreme pojedinačnih ćelija. Kako bi se odredili optimalni uslova luženja, ispitan je uticaj različitih procesnih parametara, i to: koncentracija kiseline, odnos čvrsto/tečno, temperatura i vreme trajanja procesa. Pri optimalnim uslovima luženja (2M H₂SO₄, 33 g/L, 85°C i 100 min) postignuta je efikasnost izluženja Co od oko 40%. Niska efikasnost izluženja Co može se objasniti jakom hemijskom vezom između Co i O₂, te se može zaključiti da je za potpuno rastvaranje LiCoO₂ u H₂SO₄ potrebno prisustvo redukujućeg sredstva.

Ključne reči: kiselinsko luženje; kobalt; LIB; reciklaža; azot

It is well known that the short-lasting (1-3 years) lithium-ion batteries (LIBs) represent a large part of electronic waste. Except hazardous materials (mainly Li-salts in organic solvents), LIBs contain a significant quantity of valuable metals such as Li and cobalt (Co); namely, their valorization contributes to the concept of sustainable development. Recycling LIBs procedures refer to physical, chemical and biological processes, so that, they can be divided into the hydrometallurgical, pyrometallurgical, and biological processes. In order to reduce waste gases emissions and to enhance the optimization of the process, the novel researches force the hydrometallurgical approach. In this work, the possibilities for Co leaching from the cathode material of spent LIBs were investigated using sulfuric acid in nitrogen presence. Before the leaching, a specific multi-stage preparation treatment was applied to each cell. In order to determine the optimum leaching conditions, different influential parameters were investigated such as: acid concentration, solid to liquid (S/L) ratio, temperature, and the process duration. Under the optimal leaching conditions (2M H₂SO₄, 33 g/L, 85°C and 100 min), the leaching efficiency of Co was about 40%. Low leaching efficiency of Co can be explained by the strong chemical bond between Co and O₂, which leads to a conclusion that the total dissolving of LiCoO₂ in H₂SO₄ requires the presence of a reducing agent.

Key words: acid leaching; cobalt; LIBs; recycling; nitrogen

1 Introduction

Lithium-ion batteries (LIBs) have a key role in the further development of electric vehicles, energy storage and the renewable sources of energy. It is considered that LIBs are going to contribute to the reduction of global carbon-dioxide emission. Higher demand for this specific type of batteries in the fields of portable electronics and transportation has sparked the interest for the recycling process of LIBs [1].

* Corresponding author, email: dmedic@tfbor.bg.ac.rs

LIBs are composed of battery cylindrical case, anode, cathode and separator. Main components of anode are the graphite and binder, while the cathode is composed of carbon and lithium-transition metal oxides, such as: LiCoO_2 , LiNiO_2 , LiMn_2O_4 , and $\text{LiCo}_x\text{Mn}_y\text{Ni}_z\text{O}_2$. Content of Co, Ni and Li in cathode material varies and reaches from 5% up to 15% for Co, 2-7% for Ni, and 0.5-2% for Li; with other elements (Au, Al, Fe, etc.) that are present in lower concentrations [2].

Most commonly used cathode material is LiCoO_2 . The content of Li and Co in spent LIBs remains around 10-20 wt.%, which in some cases exceeds the content of said elements in the ores found in nature [3].

According to the European Union, certain components of LIBs, such as Co, P and graphite are classified as „Critical Raw Materials“, because of their economic significance and high supply risk [1].

Generally, for the valorization procedure of valuable metals from expired LIBs, it is necessary to include and comprehend two main processes: Separation of active cathode material from the current collector, and the extraction of precious metals [4].

Taking into consideration the structural composition of cathode material, separation of aluminum foil from the active cathode material represents the decisive step in the recycling process [5].

Three methods are used for the separation of aluminum foil from the active cathode material: mechanical separation, dissolution of current collector and the removal of the binder [4].

In the extraction process of valuable metals, they are firstly dissolved via leaching process; then the separation, purification and the preparation of the final product follows. Among all of these steps, the leaching process is the most accountable one [4].

A common leaching processes used in this case are: leaching via inorganic and organic acids, alkaline leaching and bioleaching. Some experiments have confirmed that the use of inorganic acids provides better results in the term of leaching efficiency, unlike the use of organic acids. Inorganic acids can also effectively dissolve all the metals present in the cathode material, however, the organic acids dissolve metals selectively, and the leaching efficiency of Co extraction is relatively low [6,7].

In this paper, optimal conditions for the extraction process of Co from the cathode material via leaching process are discussed. Experiments were conducted in sulfuric acid in the presence of nitrogen. Raw material for the leaching process is obtained after multiphase treatment of individual cells.

2 Experimental

2.1 Materials and methods

Cathode material collected from 40 LIBs, was treated thermally, via procedure explained in previous work/paper of Medić et al. (2020) [8]. Chemical composition of examined material was determined using inductively coupled plasma optical emission spectrometry (ICP-OES). For the dissolution of cathode material, 65% HNO_3 and 36% HCl (Merck, Darmstadt, Germany) in ratio 1:3, were used. All reagents were of analytical purity and the solutions were prepared by deionized water. For the continuous assessment of Co concentration, UV-VIS spectrophotometry was used (Beckman DU-65).

2.2 Leaching tests

Leaching experiments were carried out in a reactor with measuring tube (diameter of 1 cm), which was used to determine absorbance. The apparatus was placed inside the spectrometer. Spectrometer working conditions, gas flow and temperature were controlled via device based on the microcontroller STM32F103. The obtained data was processed and given in a form of Python scripts.

Before the leaching process, mass of the material was determined and precisely measured. In the reactor was added 60 ml H_2SO_4 of known concentration and thermostated until desired temperature was reached, with constant gas flow rate of 2 L/min. Upon reaching this temperature, predetermined amount of cathode material was added. Spectra were recorded every 3 minutes, with 10 s pause of mechanical mixing before every reading/recording. Cobalt concentration was determined by calibration curve method, previously obtained by reading standard of known concentration CoSO_4 in

H₂SO₄. Because of light dissipation on the material used in leaching, slight corrections were conducted.

Leaching efficiencies were calculated using eq 1 [9]:

$$\text{Leaching efficiency} = \frac{\text{Metal content in leachate}}{\text{Total amount of metal in cathodic materials}} \times 100\% \quad (1)$$

3 Results and discussion

3.1 Chemical Composition of the Cathode Active Material before leaching

Chemical analysis results of examined cathode material are shown in Table 1. According to the obtained results, it can be concluded that the cathode material is composed mainly of LiCoO₂, while the presence of Al can be explained via pretreatment of the batteries. In the analyzed sample, it has been determined high content of Li and Co, which has led to the consideration of these batteries as an important source of said metals.

Table 1 Metal contents found in the obtained cathode active material

Metal element	Li	Co	Al
Content [wt. %]	5.98	49.81	0.01

3.2 Leaching of waste cathode material

3.2.1 Effect of acid concentration on leaching

The effect of the initial concentration of sulfuric acid (0.5–3M) on leaching efficiency of cobalt from cathode material was investigated at constant conditions: temperature 35°C, solid-liquid ratio 33 g/L, nitrogen flow rate 2 L/min, total time of the experiment 100 min. From the obtained results and according to the Fig. 1, it can be concluded that the leaching efficiency of Co was increasing with the increase of H₂SO₄ concentration until 2M. At this specific concentration, leaching efficiency of cobalt was around 35%.

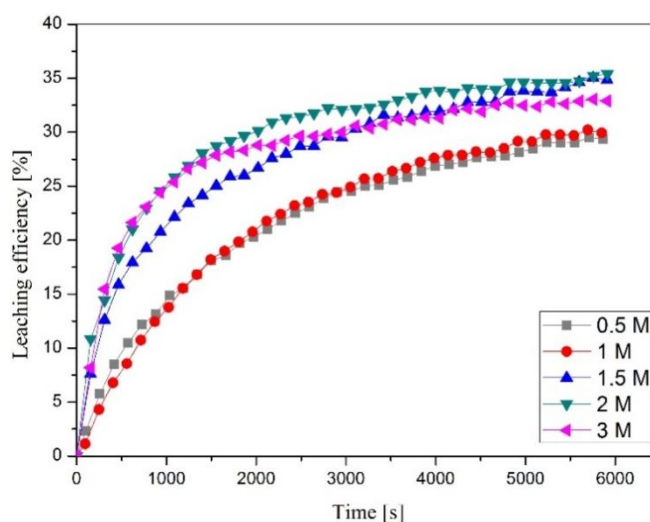


Fig.1 Effect of H₂SO₄ concentration on the leaching of waste LiCoO₂

However, a continued increase in concentration resulted in the decrease of leaching efficiency (from 35% to 33 %). As described by Swain et al. (2007) [10], the lower concentration of H₂SO₄ results in the better leaching efficiency of LiCoO₂ as Co(II), while the strong acid solution causes the lower leaching efficiency of cobalt - Co(III) is more unstable than Co(II). Taking into account the obtained results, 2M sulfuric acid solution was selected as the optimum concentration for the leaching of Co.

3.2.2 Effect of the solid-to-liquid ratio on leaching

In terms of investigating the effect of solid-liquid ratio on leaching efficiency of cobalt, an experiment has been performed at: solid-liquid ratio 10-67 g/L, acid concentration of 2 M, temperature 35°C, nitrogen gas flow 2 L/min and total time of the experiment of 100 min. Obtained results are shown in Fig. 2, where it can be seen that curves representing leaching efficiency of cobalt during a given time period indicate that the leaching efficiency of cobalt declines with the increase of solid-liquid ratio. With the increase of solid-liquid ratio of 10-67 g/L, leaching efficiency is lowered from 36% to 32%.

The lower leaching efficiency at higher solid/liquid ratio was due to the higher viscosity of the mixture, the higher resistance of diffusion mass transfer, and acid deficiency [11].

However, a large solid-liquid ratio is usually required to facilitate proper operational efficiency in practical applications and therefore solid-liquid ratio was chosen to be 33 g/L in accordance to Fig. 2 [12].

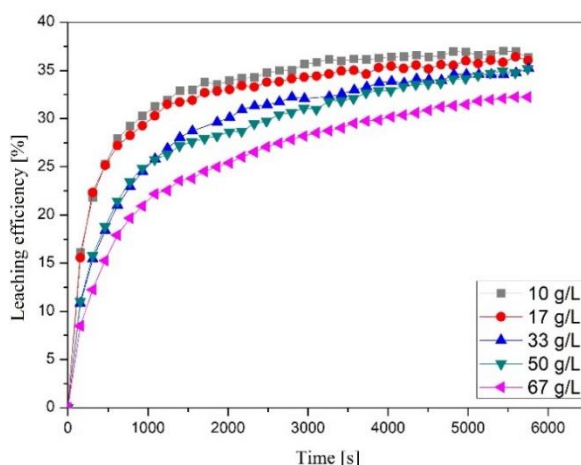


Fig. 2 Effect pulp density on the leaching of waste LiCoO_2

3.2.3. Effect of temperature on leaching

The effect of temperature on leaching efficiency, was investigated in the temperature range from standard room temperature up to 85°C in 2M sulfuric acid, at 33 g/L solid-liquid ratio, nitrogen flow rate 2 L/min and total time period of 100 min. The results of this experiment are shown on Fig. 3, where it can be seen that leaching efficiency increases from 29% to 40% with the increase of temperature from 35 to 85°C. Similar results were reported by He et al. (2017) [13].

It can also be noted that by the shape of the dissolution curves, temperature in the initial stadium of the process has a significant impact on the rate of dissolving the cathode material obtained from the expired LIBs.

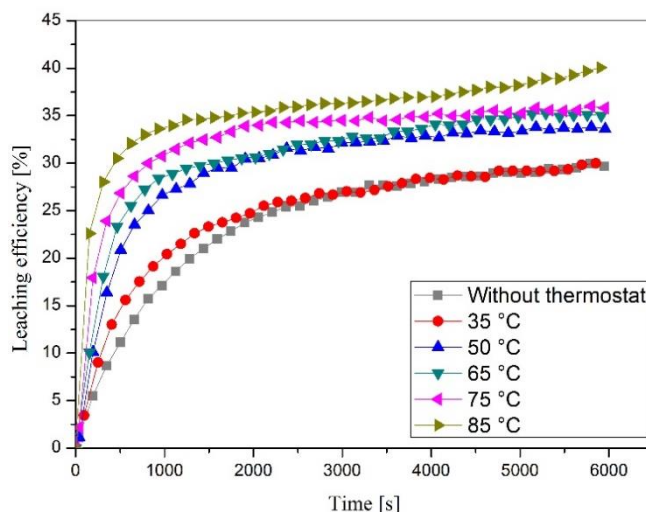


Fig. 3 Effect of leaching temperature on the leaching of waste LiCoO_2

Conclusion

Taking into consideration all of the results obtained from the conducted experiments, it can be concluded that the LIBs are deemed to be a significant source of Co. Using the H_2SO_4 in the leaching process of the cathode material obtained from the spent LIBs, low leaching efficiency of Co is achieved (around 40%). In view of the fact that a strong chemical bond between Co and O_2 in the LiCoO_2 is/can be formed, for a high leaching efficiency usage of an adequate reducing agent is necessary. Maximum cobalt leaching efficiency is achieved at the concentration of leachate being 2 M, solid-liquid ratio being 33 g/L, nitrogen flow rate being 2 L/min and at the temperature of 85°C . Obtained results have shown that with the increase of both - temperature and the solid-liquid ratio, leaching efficiency of cobalt increases. Also, based on the shape of LiCoO_2 dissolution curves, it can be noted that the leaching efficiency increases with the increase of the sulfuric acid concentration, until 2 M concentration of H_2SO_4 is reached, when the further increase of concentration leads to reduction in leaching efficiency.

Acknowledgments

The research presented in this paper was done with the financial support of the Ministry of Education, Science and Technological Development of the Republic of Serbia, within the funding of the scientific research work at the University of Belgrade, Technical Faculty in Bor, according to the contract with registration number 451-03-68/2020-14/ 200131.

4 References

- [1] **Cerrillo-Gonzalez M.M., M. Villen-Guzman, C. Vereda-Alonso, C. Gomez-Lahoz, J.M. Rodri-guez-Maroto, J.M. Paz-Garcia**, Recovery of Li and Co from LiCoO_2 via Hydrometal-lurgical–Electrodialytic Treatment, *Applied Sciences*, 10 (2020), 7, pp. 2367.
- [2] **Chen D., S. Rao, D. Wang, H. Cao, W. Xie, Z. Liu**, Synergistic leaching of valuable metals from spent Li-ion batteries using sulfuric acid- L-ascorbic acid system, *Chemical Engineering Journal*, 388 (2020), pp. 124321.
- [3] **Verma A., G. H. Johnson, D. R. Corbin, M. B. Shiflett**, Separation of Lithium and Cobalt from LiCoO_2 : A Unique Critical Metals Recovery Process Utilizing Oxalate Chemistry, *ACS Sustainable Chem. Eng.*, 8 (2020), pp. 6100–6108.
- [4] **Wang W., Y. Zhang, L. Zhang, S. Xu**, Cleaner recycling of cathode material by in-situ ther-mite reduction, *Journal of Cleaner Production*, 249 (2019), pp. 119340.
- [5] **Zhao S., W. Zhang, G. Li, H. Zhu, J. Huang, W. He**, Ultrasonic renovating and coating mod-ify-ing spent lithium cobalt oxide from the cathode for the recovery and sustainable utilization of lithium-ion battery, *Journal of Cleaner Production*, 257 (2020), pp. 120510.
- [6] **Yang Y., S. Lei, S. Song, W. Sun, L. Wang**, Stepwise recycling of valuable metals from Ni-rich cathode material of spent lithium-ion batteries, *Waste Management*, 102 (2020), pp. 131–138.
- [7] **Chu W., Y. Zhang, X. Chen, Y.G. Huang, H.Y. Cui, M. Wang, J. Wang**, Synthesis of $\text{LiNi}_{0.6}\text{Co}_{0.2}\text{Mn}_{0.2}\text{O}_2$ from mixed cathode materials of spent lithium-ion batteries, *Journal of Power Sources*, 449 (2020) pp. 227567.
- [8] **Medić D., S. Milić, S. Alagić, I. Đorđević, S. Dimitrijević**, Classification of spent Li-ion bat-teries based on ICP-OES/X-ray characterization of the cathode materials, *Hemijska Industrija – Article in press*, 74 (2020).
- [9] **He L-P., S. Sun, Y-Y. Mu, X. Song, J. Yu**, Recovery of lithium, nickel, cobalt, and manganese from spent lithium-ion batteries using L-tartaric acid as a leachant, *ACS Sustainable Chemistry & Engineering*, 5 (2017) pp. 714–721.
- [10] **Swain B., J. Jeong, J-C. Lee, G-H. Lee, J-S. Sohn**, Hydrometallurgical process for recovery of cobalt from waste cathodic active material generated during manufacturing of lithium ion batteries, *Journal of Power Sources*, 167 (2007), pp. 536–544.

- [11] **Jiang F., Y. Chen, S. Ju, Q. Zhu, L. Zhang, J. Peng, X Wang, J.D. Miller**, Ultrasound-assisted leaching of cobalt and lithium from spent lithium-ion batteries, *Ultrasonics-Sonochemistry*, 48 (2018), pp. 88–95.
- [12] **Gao W., X. Zhang, X. Zheng, X. Lin, H. Cao, Yi Zhang, Z.H.I. Sun**, Lithium Carbonate Recovery from Cathode Scrap of Spent Lithium-ion Battery – a Closed-loop Process, *Environmental Science & Technology*, 51 (2017), pp. 1662–1669.
- [13] **He L-P., S-Y. Sun, X-F. Song, J-G. Yu**, Leaching process for recovering valuable metals from the $\text{LiNi}_{1/3}\text{Co}_{1/3}\text{Mn}_{1/3}\text{O}_2$ cathode of lithium-ion batteries, *Waste Management*, 64 (2017), pp. 171–181.

INTEGRACIJA DISTRIBUIRANIH PV SISTEMA U PAMETNIM SREDINAMA KORISTECI FOG COMPUTING ARHITEKTURU

INTEGRATION OF DISTRIBUTED PHOTOVOLTAIC SYSTEMS IN THE SMART ENVIRONMENT THROUGH FOG COMPUTING ARCHITECTURE

Ilija RADOVANOVIC*, Ivan POPOVIC²

¹ School of Electrical Engineering - University of Belgrade, Innovation center of School of Electrical Engineering in Belgrade, Serbia

² School of Electrical Engineering - University of Belgrade, Belgrade, Serbia

<https://doi.org/10.24094/mkoiee.020.8.1.247>

U ovom radu je predstavljen koncept integracije distribuiranih PV sistema u pametnim sredinama. Prikazani su detalji integracije, greske pri funkcionisanju PV sistema povezane sa smanjenom izlaznom snagom istih, kao i implementacija mikroservisa i specifičnosti korišćene FOG arhitekture.

Ključne reči: PV sistemi; pametna sredina; otkrivanje grešaka rada sistema; Fog Computing arhitektura

This paper presents the concept of the integration of distributed photovoltaic systems in the smart environment. The details of the proposed integration and its operation faults related to the reduced power output of the photovoltaic system, design and implementation of services as well as architecture-related details are presented.

Key words: Photovoltaic systems; smart environment; fault detection; Fog computing architecture

1 Introduction

Due to the world, development where the living spaces requirements increases, the challenges and opportunities are to create such environment founded on a foresight understanding and pragmatism. Enormous and complex congregations of people in urban areas inevitably tend to become disordered places. Making an environment smart is emerging as a strategy to mitigate the problems generated by the urban population growth and rapid urbanization [1].

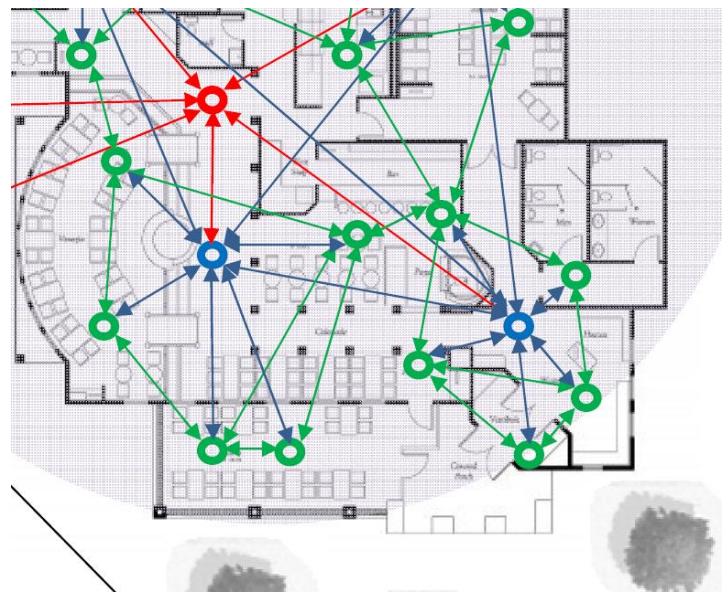
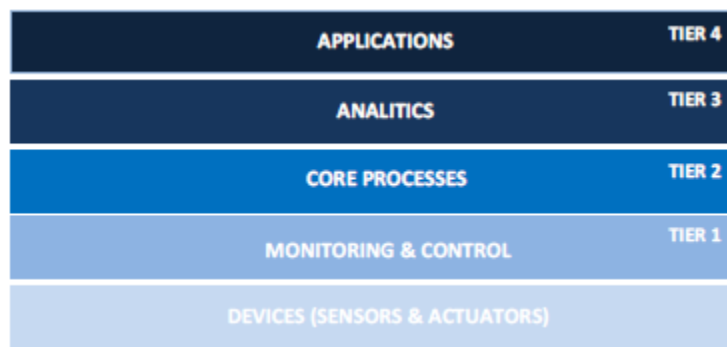
The concept is essentially aiming to develop a system for following up the activities electronically in the smart environment. The advantage of adopting such systems is the high level of integration and systems interoperability, which expanding the view of daily controlling. The goal is to provide the initial necessary guidelines to improve operations and maintenance, reduce the cost of operation, provide enhanced energy management capabilities and provide scalability and freedom for future. A smart city relies, among others, on a collection of smart computing technologies applied to critical infrastructure components and services [2]. Distributed generation of clean and cost effective energy can provide an adequate tool to deal with energy reliability and to successfully implement the principals of the renewable energy [3].

2 System architecture

The distributed PV systems with its sensors of interest represent single sensor node. This concept of sensor nodes along with its services is usefully implemented in fog computing architecture providing increased performance, energy efficiency, reduced latency, quicker response time, scalability, and better localized accuracy for different applications in energy network [4]. The solution enables efficient way of real-time monitoring and provides crucial information for further integration in smart environments.

* Corresponding author, email: ilija.radovanovic@ic.etf.rs

On the other hand, the fog computing architecture concept is based on the tiered architecture [5]. It enables the modularity and efficient upgrade of the implemented overall systems. The particular node functionalities vary based on its role and position in N-tiered fog architecture. The nodes at the edge of the network infrastructure located at Tier 1, collect or provide the data for/from connected end devices at tier 0. Following the complexities of the network itself, the nodes at the higher tier (Tier 2) are focused on data filtering, edge analytics, and support for time-critical processing/services. The nodes closer to the network core are capable for extensive processing and communication, supporting higher-level analytics [4-6]. The layer scheme of the system based on Fog computing architecture is presented in figure 1. The deployment view of particular indoor sensor node system based on the fog computing architecture concept is shown in figure 2.



3 Implementation and results

The bottom level of the fog node application service layer is reserved for the fog connector service (FCS). The FCS is used as an interface to different front-end devices. On the device side, the local service management layer (LSM) is providing the interface to the corresponding fog node. Device-to-node pathways are given as a collection of end-to-end data communications. The individual communication context is managed through the service agent as a dedicated system level component

[5]. The service agent operation is positioned at the top of the data link layer supporting legacy point-to-point communication technologies. From the application point of view, service agents are given in the form of configurable micro services as a part of fog connector operation. The operation of service agent might be either time-triggered or event-based, supporting the request-response and publish-subscribe message exchange pattern with end-device [5].

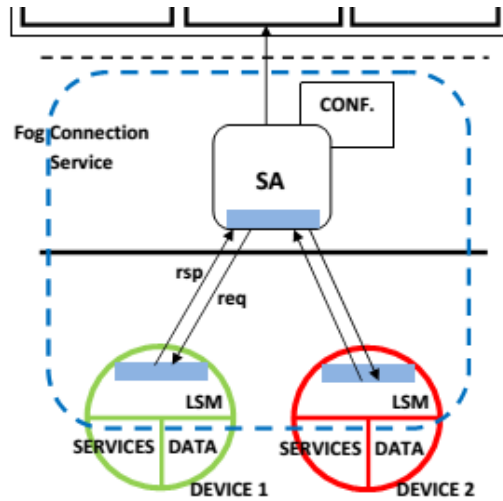


Fig. 3. Fog node architecture for multi channel sensing applications

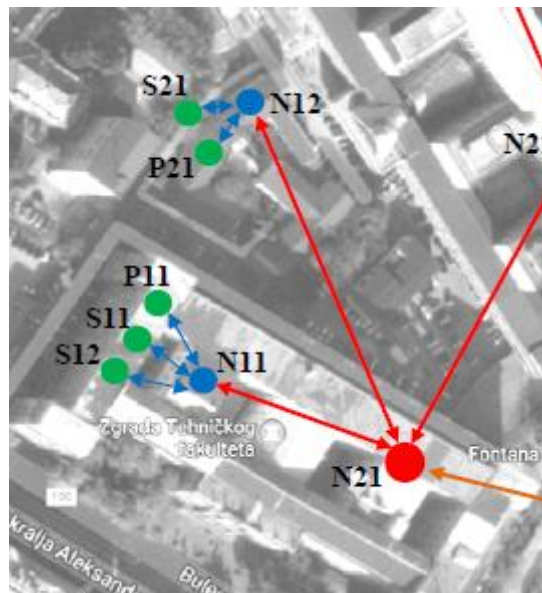


Figure 4. Deployment view of the integrated sensor nodes

The deployment scenario presenting the tiered fog architecture in the local area is given on the Figure 4. The area includes several University buildings and research facilities located in separate buildings. PV panel 1 together with other end devices (set of sensors S1), are connected to the fog node N11 located at the RES lab at the Technical Faculty building. They are integrated into the fog architecture through building area node N11 residing at tier 1. Similarly, the PV panel 2 and environmental sensors are located at the ICEF research lab and they are connected to the building area node N12. Higher-level services are supported through the technical faculty infrastructure node N21. Further integration toward core services is supported through local area nodes N3X. The set of sensors S1 is used for temperature, humidity, PM and other environmental and air quality measurements.

4 Conclusion

The presented solution enables efficient way of integrating distributed PV systems in smart environments. Depending of its use, the integration might vary in complexity and systems interoperability. The utilized fog computing infrastructure enables the further integration of locally generated

information and knowledge, and provides basis for further system upgrades. The onsite results have shown that the presented approach is adequate for real-time or near real-time constrained application. The further system integration would consist of the detailed smart environment map with different groups of sensors.

5 Acknowledgement

The authors gratefully acknowledge financial support from the Ministry of Education and Science, Government of the Republic of Serbia.

6 References

- [1] **M. Al-Hader; A. Rodzi; A. R. Sharif; N. Ahmad**, Smart City Components Architecture, International Conference on Computational Intelligence, Modelling and Simulation, IEEE Computer Society, 2009.
- [2] **Ishida T., Isbister K. (Eds.)**, Digital Cities: Technologies, Experiences, and Future Perspectives, Springer-Verlag, 2000.
- [3] **Popovic and I Radovanovic**, Methodology for detection of photovoltaic systems underperformance operation based on the correlation of irradiance estimates of neighboring systems, Journal of Renewable and Sustainable Energy, 10 (2018).
- [4] **I. Radovanović, DJ. Klisić, I Popović**, Multi channel sensor Measurements in fog computing architecture for renewable energy sources systems monitoring, V MKOIEE Conference, Beograd, October 2017.
- [5] **I. Radovanovic, I. Popovic and D. Drajić**, Multi channel sensor measurements in fog computing architecture, 2017 Zooming Innovation in Consumer Electronics International Conference (ZINC), Novi Sad, 2017, pp. 9-12.
- [6] OpenFog Reference Architecture for Fog Computing, OpenFog Consortium, 02/2017
- [7] **I. Radovanović, I Popović**, Analysis of the pv system operation using the system efficiency factor - η_{SF} , VI MKOIEE Conference, Beograd, October 2018.
- [8] **A. Khanna**, An architectural design for cloud of things, Facta universitatis-series: Electronics and Energetics 29 (3), 2016, pp. 357-365.

PRIMENA METODOLOGIJE PAMETNIH MREŽA U DISTRIBUCIJI ELEKTRIČNE ENERGIJE

SMART GRID TECHNOLOGY IN POWER DISTRIBUTION SYSTEMS

Ivan POPOVIĆ*

Innovation center of School of Electrical Engineering in Belgrade, Belgrade
School of Electrical Engineering, University of Niš, Niš

Ovaj rad opisuje primenu pametnih mreža u sistemima za distribuciju električne energije. Izloženi su sistemi za automatizaciju trafostanica koji omogućavaju nadzor, merenja i kontrolu u realnom vremenu

Ključne reči: pametne mreže; distribucija električne energije; automatizacija trafostanica

This paper discusses implementation of smart grid technology in power distribution systems. Substation automation that will handle real time monitoring, metering and control is proposed.

Key words: smart grid; power distribution; substation automation

1 Introduction

Smart technologies are changing the way we live and work today. Smart devices connected to the Internet or private network provide us with a large amount of information. Implementing such a smart technology in a power network makes it more efficient and reliable. Most outages in the low voltage network are caused by faults on the medium voltage side. Automated substations can reduce outage duration through fault location and remote control of switching equipment. Automated remotely controlled switchgear will help to isolate faulty areas from the rest of the network.

2 Smart grid in power distribution network

Smart grid consists of control center, automated substations and pole mounted switchgears and radio system for remote monitoring and control. Control center is equipped with SCADA (supervisory control and data acquisition) system for presenting the data and controls to their human operators. Automated substation is equipped with smart device that combines secure communication and protocol converter with telemetry.



Figure 1- SCADA system in control center. It represents different analog and digital parameters collected from automated substations. It also enables human operator to remotely control substations.

* Corresponding author, email: ivan.popovic@netico-group.com



Figure 2 - Smart device in substation. It both talks to intelligent unit and control center over radio network. Intelligent unit measures current, voltage, power and other important parameter and sends them to smart device. It also detects faults on guidelines and use protection function to protect substation. All information from smart device are sent to control center.

3 EDB medium voltage automation

In order to modernize existing distribution system and make it less sensitive to power supply interruptions EDB upgraded their medium voltage network with a smart grid. The implemented system is used to remotely monitor and control equipment across a large geographic area within the city of Belgrade and rural communities. The whole system is controlled from a single control center.

Telecommunication network is divided in 5 remote sub-systems. There are two independent master radio systems in control center for communication between 5 data concentrators in remote sub-systems and SCADA system in control center through DNP3 protocol. Five remote slave radio sub-systems communicate with NetMan equipment in each sub-system.

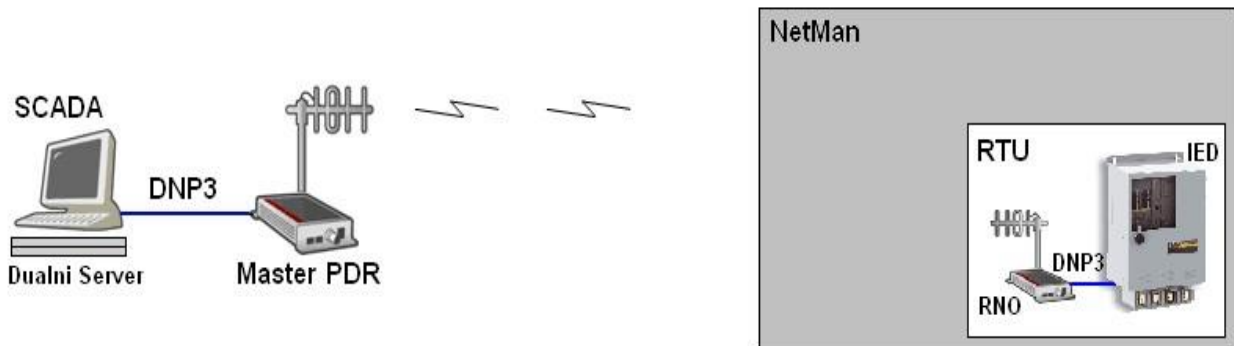


Figure 3 - Communication between SCADA system and NetMan equipment in one sub-system.

In each sub-system, NetMan equipment consists of data concentrator and automated substations or pole mounted switchgears. Data concentrator is the heart of NetMan equipment and it controls all automated stations in that sub-system. Communications between data concentrator and remote stations is accomplished over UHF radio network. Measurements data from each remote station consists of 48 digital statuses and 8 analog measurements.

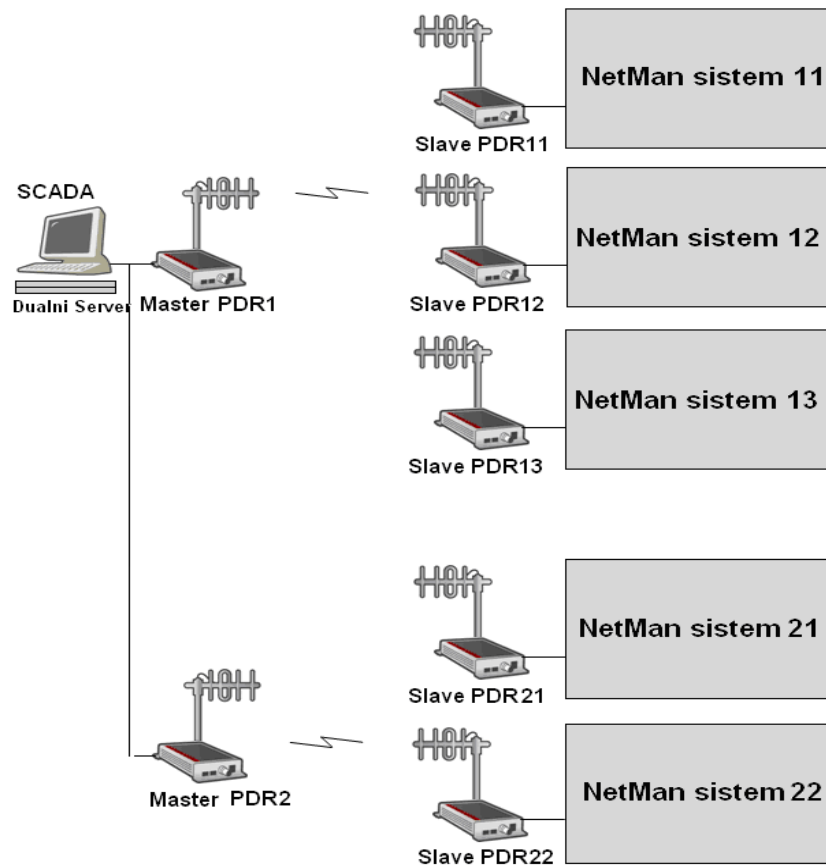


Figure 4 - Communication in the whole system.

4 Conclusion

By modernizing Belgrade power network with smart grid technology, a lot of benefits are achieved:

- Fast and reliable fault localization and isolation
- Reduced outage time
- Fast energy supply restoration
- Increased overall system reliability
- High degree of future expansion possibilities

In the future, this system could be expanded up to 500 automated substations and switchgears. DNP3 protocol could be implemented in communication between data concentrators and remote locations. It will enable new parameters, such as time stamping, to be transmitted.

5 Acknowledgement

The authors gratefully acknowledge financial support from the Ministry of Education and Science, Government of the Republic of Serbia.

6 References

- [1] **Harry R. Anderson**, *Fixed Broadband Wireless system design*, John Wiley & Sons Ltd, 2003.
- [2] **Roger L. Freeman**, *Radio System Design for Telecommunications*, John Wiley & Sons Ltd, 2007.
- [3] **Andreas F. Molisch**, *Wireless communications*, John Wiley & Sons Ltd, 2011.
- [4] **K.Hak-Man, L.Jong -Joo, K. Dong-Joo**, "A Platform for smart substation", in *Future Generation Communication and Networking*, 2007.
- [5] **Electric Utility of Belgrade**, "Medium Voltage Automation", 2014.

MOGUĆNOSTI PRIMENE IIOT PLATFORME U ELEKTROENERGETSKIM SISTEMIMA

POSSIBILITIES OF IIOT APPLICATION PLATFORMS IN THE ELECTRICAL POWER SYSTEMS

Vojkan NIKOLIĆ^{*1}, Zoran STEVIĆ², Stefana JANIĆIJEVIĆ³, Dragan KRECULJ⁴

¹ University of Criminal Investigation and Police Studies, Belgrade

² Technical Faculty Bor and School of Electrical Engineering Belgrade,
University of Belgrade, CIK Belgrade

³ Comtrade SI, Belgrade

⁴ Technical College of Vocational Studies Belgrade

<https://doi.org/10.24094/mkoiee.020.8.1.255>

Na tržištu postoje različiti internet inteligentni uređaji (IoT) koji se primenjuju u elektroenergetskim sistemima. IoT uređaji mogu biti fizički ili virtuelni, umreženi interoperabilnim komunikacionim protokolima i inteligentnim interfejsima. IoT tehnologije obezbeđuju njihovo povezivanje na internet, kao i povezivanje sa servisima i aplikacijama. Elektroenergetski sistemi imaju tradicionalno Sisteme za upravljanje resursima preduzeća (ERP), Sisteme za nadzor, praćenje, arhiviranje i kontrolu industrijskih sistema (SCADA), Distribuirane kontrolne sisteme (DCSs), kao i tradicionalnu industrijsku automatizaciju za postizanje integracije između nivoa upravljanja kompanijom i nivoa proizvodnje. Industrijske IoT (IIoT) platforme treba da prevaziđu jaz između okruženja Informacionih tehnologija (IT) i Operativnih tehnologija (OT). Ove platforme pružaju pogodniju arhitekturu podataka za savremenu industrijsku automatiku. U radu je dat pregled savremenih rešenja.

Ključne reči: IIoT platforma, informacione tehnologije, operativna tehnologija, poslovna inteligencija

Nowadays in the market there are different Internet of Things (IoT) devices, that are used in electrical power systems. Such IoT devices can be physically, or virtually networked, with interoperable communication protocols and intelligent interfaces. IoT technologies provide their connection to the internet, as well as connection to special services and applications. Electrical power systems have traditional Enterprise resource planning (ERP), Supervisory control and data acquisition (SCADA), Distributed control systems (DCSs), as well as traditional industrial automation stack to achieve functional integration between the company management level and the production level. Industrial IoT (IIoT) platforms should overcome the gap between Information technology (IT) and Operational technology (OT) environments. These platforms providing a more suitable data architecture for the modern industrial automation stack. The paper presents the overview of one modern solution with the Claroty IIoT platform. Claroty delivers comprehensive and reduces the complexity of OT security.

Key words: *IIoT platform, information technology, operational technology, business intelligence, claroty*

1 Introduction

Traditional IT are separate from OT. IT and OT have evolved independently for a long time. IT refers to the application of network, storage, and compute resources towards the generation, management, storage, and delivery of data throughout and between organizations, while OT refers to technology that monitors and controls specific devices and processes within industrial workflows. [1]

^{*} Corresponding author, email: vojkan.nikolic@kpu.edu.rs

Recently, there has been an increasing convergence and integration of these two technologies. The convergence of IT and OT in IoT has been going on for a while and there isn't a strict division between them in the real world. With IT and OT converging, the scope of CIO authority may cater to the needs of planning and coordinating a new generation of operational technologies alongside existing information- and administration-focused IT systems. [2]

In addition to the fact that IT and OT are increasingly converging with each other, they are also increasingly connecting to the internet. This integration provides IoT in such a way as to achieve a greater degree of integration, functionality and flexibility, as well as central management in accordance with the decisions that arise as a result of the complex algorithms of the Big Data concept. IoT is a global network infrastructure that provides connectivity of "smart" devices with interoperable communication protocols and intelligent interfaces.

IIOT represents the application of IoT in the industrial environment in order to increase industrial efficiency, productivity, safety and transparency. "...the industrial internet is an internet of things, machines, computers and people enabling intelligent industrial operations using advanced data analytics for transformational business outcomes, and it is redefining the landscape for business and individuals alike". [3]

IoT platforms are a software and hardware platform for efficient development of IoT systems. With the number of connected IoT devices in a manufacturing facility, cyber security has become important to industrial companies and workers safety and productivity.

IIoT platforms are specialized IoT platforms for industrial environments. The development and implementation of the IIoT platform is a very dynamic area of the software and hardware environment. For the development of IIoT platforms used in electrical power systems, as well as for the development of any IoT platforms, it is necessary to consider the IoT devices to be used, communication components that will provide connectivity within the platform, services to perform, ways to manage platform functionality, security aspects of platforms and application components that allow end users to monitor, use functionality, and manage platforms.

With the development of mobile business technologies, the Internet of intelligent devices and social media, the amount of data stored in the company's information systems is increasing. [4]

Companies acquire a large amount of data every day that they cannot use by using traditional databases. Therefore, new approaches for storage, rapid retrieval and analysis of large amounts of data in real time, based on Big Data (BD) technology are being developed. [5]

In order for IIoT platforms to get their full functionality, it is necessary to apply BD analytics (BDA). Some studies showed that the adoption of BDA increase companies output and productivity; while IoT enables companies to have more information and control in physical resources, processes and environments. BDA is expected to provide operational and customer level intelligence in IIoT systems. Although many studies on IIoT and BDA exist, only a few of them have explored the convergence of these two paradigms. [6]

The paper presents the Claroty IIoT platform that provides deep integration between IT and OT, as well as BDA, and its implementation in electrical power systems significantly contributes to the quality of management and efficiency.

2 Information technology (IT) and Operational technology (OT) convergence

IT/OT convergence is the integration of information technology (IT) systems used for data-centric computing with operational technology (OT) systems used to monitor events, processes and devices and make adjustments in enterprise and industrial operations. A comparative analysis of these two technologies is presented in Table 1. [7]

IT/OT convergence improves automation and efficiency, provides interoperability conditions and accelerates innovation. In terms of business benefits, they are reflected in the reduction of risks due to the use of proven technologies and protocols, the reduction of costs due to the connection of distributed entities and the reduction of implementation time due to reduced complexity by introducing IoT technology.

Table 1. A comparative analysis between IT and OT [7]

	Information Technologies (IT)	Operational Technologies (OT)
Function	It refers to telecommunications equipment. Information Technology focuses on the storage, recovery, transmission, manipulation and protection of data	OT is more oriented to the control of processes or their change through the monitoring and control of devices
Use, area	Business-oriented	Industrial-oriented
Access	Connected with the outside world	Very restricted access. Limited to people with certain privileges
Assets Vs workers	The number of assets is usually equal (or close) to the number of professionals	More autonomous More devices than professionals
Frequency change	Constantly changing: new employees joining the company (=new devices connected) and former employees leaving the company (=devices that are disconnected)	Less changing environment (there may be no changes for months to years)
Environment	Controlled, stable and constant	OTs endure adverse weather conditions (extreme temperatures or humidity levels, among others)
Interface and Network	Web browser, keyboard, device	Sensors, coded or touch screens
Main priority	Data security (usually confidential data)	Uptime, the availability and integrity of the legacy and no longer system devices is essential
Updates	Constant due to software updates Service interruptions are tolerable and, in some cases, programmable outside of working hours	Updates must be tested carefully in advance and, usually involve restarting or stopping the machines Consequently legacy systems are very frequent
Life cycle	Shorter life cycles (3-5 years)	OT systems have longer life cycles (15-20 years) As a result, legacy systems and no longer supported ones are frequent
Processing requirements	Minutes-days	Milliseconds-Seconds
Objective	Logical security (no lives at risk) The objective is to protect confidential information from any potential risk (human error, natural disasters, cyberattacks, etc.)	The objective is to protect the environment, people and infrastructures
Operating System	Standard operating systems	Specific purpose equipment with proprietary Operating Systems (Custom-developed software)

Ready-made solutions can be used to implement IIoT platforms, or own platforms can be developed. IIoT platforms as ready-made solutions are commercial, ie. proprietary platforms and they represent complete and closed solutions that, immediately after purchase and installation, connect to IoT hardware and configure. After that, they are ready for the use. These platforms usually have APIs for connecting to other software solutions. Their main advantage is fast implementation and low price. On the other hand, like most proprietary software solutions, these platforms are closed to third-party devices and software components. Developing personal IIoT platform requires a significantly higher level of technical knowledge and a longer implementation time. The main advantages of one's own development are flexibility and openness.

The quality of the IIoT platform also depends on the ability to provide the required flow of information in real time. In order to ensure that, the application of the Big Data concept is needed. BD has the ability to collect and store large amounts of data generated by IoT devices, as well as their processing.

3 Claroty IIoT platform

The Claroty platform bridges the gap and provides integration between information technology and operational technology environments. Claroty's converged IT/OT solutions, ensures the integration of an organizations IT solutions with OT critical infrastructure, where existing IT infrastructure and existing OT infrastructure can be used to a large extent. This platform provides the use of existing IT processes and security technology to improve the availability, safety, and reliability of their OT assets and networks seamlessly and without requiring downtime. The result is more uptime and greater efficiency across business and production operations. With Claroty product enterprises increase the utilization of IoT devices to drive digital transformation and increase the operation efficiency.

The Claroty Platform comprises Claroty's Continuous Threat Detection (CTD), Enterprise Management Console (EMC) and Secure Remote Access (SRA) systems. This single, agentless solution seamlessly integrates with existing IT security infrastructure. Also platform provides for the industry broadest range of OT security controls across four essential areas: visibility, threat detection, vulnerability management, and triage & mitigation. [8]

Claroty OT Security Solution is visible in the Figure 1.

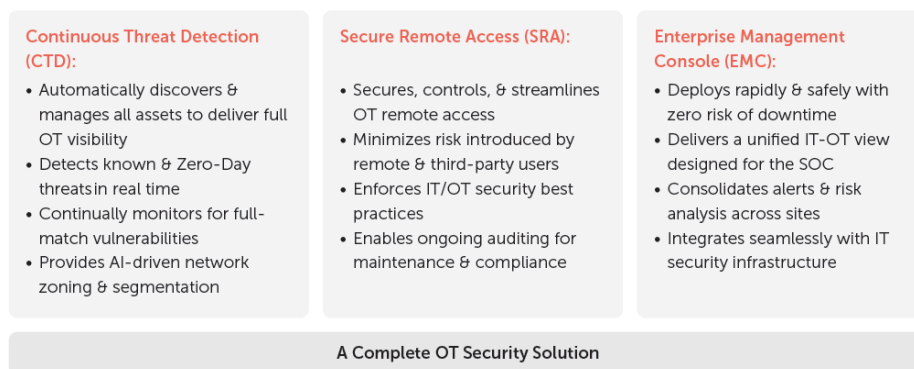


Figure 1. Claroty OT Security Solution [8]

Claroty CTD minimizes the considerable risks inherent to IT-OT convergence by extending fundamental security controls to OT environments. These controls can be implemented rapidly and safely, do not require downtime, or OT expertise, and span four key areas:

1. Asset Identification & Management;
2. Network Segmentation & Micro-segmentation;
3. Security Monitoring & Threat Detection;
4. Risk & Vulnerability Management. [9]

CTD provides complete OT visibility and asset management controls using OT protocols and passive, active, and AppDB scanning capabilities. One of the main advantages of the Claroty platform

is that it provides visibility into all three variables of risk in OT environments: asset visibility, network visibility, and process visibility. CTDs intuitive interface offers a single-pane view into all assets, processes, sessions, and related risks & vulnerabilities in your OT environment (Figure 2).

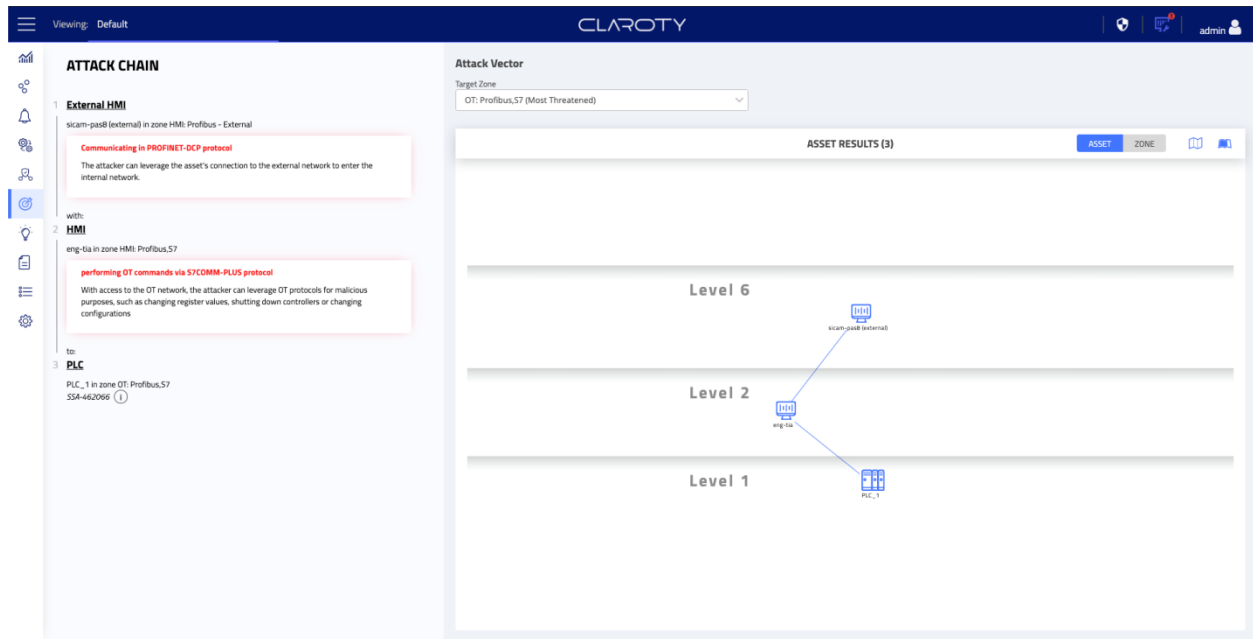


Figure 2. Claroty Threat Detection [8]

Claroty SRA provides simple, secure, highly controlled remote access to OT environments for both internal and third-party users. Key features and capabilities include:

- Automatic enforcement of granular role- and policy-based administrative controls in accordance with Least Privilege and Zero Trust principles;
- Over-the-shoulder monitoring and full recording of all remote sessions for live supervision and troubleshooting, painless audits, and streamlined investigations;
- A secure and clientless interface through which all remote users connect prior to performing software upgrades, periodic maintenance, and other support or auditing activities in OT environments.

[9]

The unique Claroty platforms with the components are presented in Figure 3.

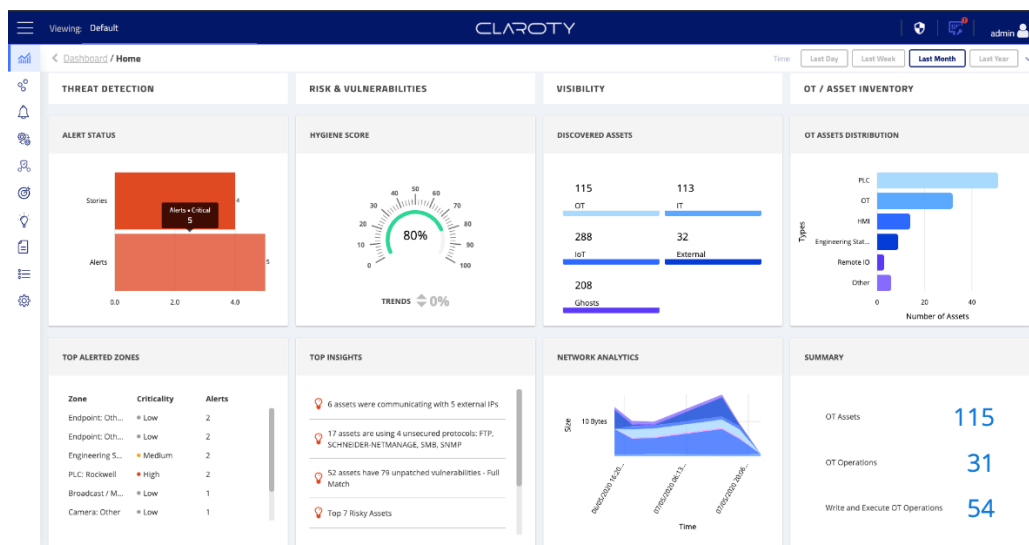


Figure 3. Claroty platform [9]

Then Claroty EMC is a centralized management interface that aggregates data from Claroty products deployed across multiple sites. It displays a unified view of all assets, activities, alerts, and

access controls spanning the entirety of each customers OT environment. The key features include the following:

- Pre-built reports, customizable analytics dashboards, and contextualized risk scoring;
- Seamless integration with SIEM, SOAR, firewall, NAC, and other existing security infrastructure components;
- Single-pane-of-glass visibility and governance structure ideal for security operations center (SOC) deployments. [9]

4 Conclusion

The disagreement that exists between internet technologies and operating technologies is successfully bridging through the IoT. The IoT devices are increasingly appearing in electrical power systems, which on the one hand, need to be integrated into certain system; and on the other hand, to ensure the connection of this system with traditional IT solutions already owned by companies. This task is achieved by using IIoT platforms that can be proprietary solutions, or can be developed independently. With adequate platforms, after purchase and installation, they are connected to IoT hardware and configurations, so they can be completely used. The main advantages of these platforms are low prices and fast implementation. The independent development of the IIoT platform is reflected in the fact that a higher degree of technical knowledge and a longer implementation time are required, while the advantages of this approach are flexibility and openness.

With the advanced and cutting-edge technologies, the electric power industry has more options to control, monitor, analyze and utilize the collected data, in order to create intelligent decisions automatic. Through intelligence concept the IIoT allows this industry to evolve and to make its functions more efficient.

Claroty is supposed as high-quality commercial IIoT platform. It enhanced continuous threat detection and secure remote access. This platform is successfully applied in various electrical power systems. One of the main advantages of the Claroty platform is that it provides visibility into all three risk variables in OT environments: asset visibility, network visibility and process visibility. In addition, it ensures a high protection degree at all critical points of the complete system, as well as the necessary analytics for the data that collects and stores from IoT devices, and the processing of those data in real time.

Many energy companies in the electric industries rely on Claroty platform in order to enhance OT availability, integrity and safety. The Claroty platform comprehensive protects electric control systems and continuously monitors industrial networks to prevent dangerous cyber threats.

5 References

- [1] *** <https://www.coolfiresolutions.com/blog/difference-between-it-ot/> (Retrieved june 2020.).
- [2] *** <https://www.gartner.com> (Retrieved june 2020.).
- [3] **H. Boyes, B. Hallaq, J. Cunningham, T. Watson**, The industrial internet of things (IIoT): An analysis framework, *Computers in Industry* 101 1–12, 2018.
- [4] **B. Radenković, M. Despotović-Zrakić, Z. Bogdanović, D. Barać, A. Labus**, *Electronic Business*, Faculty of Organizational Sciences Belgrade, 2015.
- [5] **B. Radenković, M. Despotović-Zrakić, Z. Bogdanović, D. Barać, A. Labus, Ž. Bojović**, *Internet of intelligent devices*, Faculty of Organizational Sciences Belgrade, 2017.
- [6] **M.H. Rehman, I.Yaqoob, K. Salah, M. Imran, P. P. Jayaraman, C. Perera**: The role of big data analytics in industrial Internet of Things, *Future Generation Computer Systems*, Volume 99, Pages 247-259, 2019.
- [7] *** <https://randed.com/information-technologies-it-vs-operational-technologies-ot/?lang=en> (Retrieved june 2020.).
- [8] *** [claroty_platform_overview_april2020](#) (Retrieved june 2020.).
- [9] *** <https://claroty.com> (Retrieved june 2020).

ISTRAŽIVANJE UTICAJA RELATIVNE VLAŽNOSTI I TEMPERATURE NA IOT REŠENJE ZASNOVANO NA JEFTINIM SENZORIMA ZA PRAĆENJE KVALITETA VAZDUHA

INVESTIGATION OF THE INFLUENCE OF RELATIVE HUMIDITY AND TEMPERATURE ON THE IOT SOLUTION WITH LOW COST AIR QUALITY MONITORING SENSORS

Ivan VAJS*, Dejan DRAJIĆ, Ilija RADOVANOVIĆ

School of Electrical Engineering - University of Belgrade,
Innovation center of School of Electrical Engineering in Belgrade, Serbia

<https://doi.org/10.24094/mkoiee.020.8.1.261>

Usled porasta zagađenosti vazduha u gusto naseljenim oblastima, potreba za pouzdanim i pristupačnim sistema za praćenje kvaliteta vazduha je u porastu. Jeftini komercijalni senzori predstavljaju dobru početnu tačku sa praćenje kvaliteta vazduha s obzirom na njihovu dostupnost na tržištu i nisku cenu ali zaostaju u smislu tačnosti i pouzdanosti izmerenih podataka u odnosu na javne merne stanice. U ovom radu, ispitan je uticaj relativne vlažnosti i temperature vazduha na tačnost merenja ovih senzora. Različiti tipovi statističkih modela su korišćeni kako bi modelovali grešku merenja senzora prouzrokovanu relativnom vlažnošću i temperaturom vazduha. Dobijeni rezultati pokazuju da se tačnost senzora može poboljšati adekvatnom kompenzacijom greške merenja i time povećati preciznost i pouzdanost ovakvog sistema za praćenje kvaliteta vazduha.

Ključne reči: IoT; senzori; kvalitet vazduha; monitoring; neuralne mreže

Due to the rising air pollution in densely populated areas, the need for reliable and cost-effective air monitoring systems is on the rise. Low-cost off-the-shelf air quality sensors available on the market provide a good starting point as they are readily available and inexpensive but fall short when it comes to accuracy and reliability. In this paper, the influence of relative humidity and temperature on the accuracy of these sensors is analyzed. Different types of statistical models are used in order to model the measuring error of the sensors caused by relative humidity and temperature. Obtained results show that the accuracy of the off-the-shelf system can be improved by adequate compensation and a more reliable, yet inexpensive air monitoring systems could be implemented.

Key words: IoT; sensors; air quality; monitoring; neural networks

1 Introduction

The estimation of the World Health Organization (WHO) is that by the year 2050, 70% of people in the world will live in cities [1]. This trend is unavoidable but overpopulation in urban areas can significantly affect the quality of life of the citizens. Their health can be put at great risk due to the rising air pollution trends [2]. Air quality guidelines were issued by the WHO with a goal to direct activities in polluted areas [3]. In order to recognize what actions should be taken, there is a need for air monitoring IoT systems that can track the air pollution in urban areas. The number of air monitoring stations, however, is low due to the high cost per station as well as the annual calibration cost. The potential solution to this problem is using low-cost off-the-shelf sensors to monitor the air quality. These sensors unfortunately tend to have low accuracy and calibration issues. The reason for this is that the accuracy of the measurements is highly influenced by temperature and relative humidity. In this paper, two methods for calibrating off-the-shelf air quality sensors are proposed. One uses the Least Squares Method to fit the data and the other uses a neural network which further improves the calibration by using the relative humidity and temperature data [4,5]. Both methods were

* Corresponding author, email: ivan.vajs@ic.etf.bg.ac.rs

implemented so that they can be used in real-time and provide a basis for a low-cost air monitoring IOT solution. In section 2. system architecture is presented and calibration methods are explained. Section 3. provides results and discussion, while Section 4. concludes the paper and gives directions for future work.

2 System architecture and calibration methods

Device with a Plantower PMS 7003 PM low cost sensor [6] is collocated with the public monitoring station, whose measurements are used as reference measurements for the calibration. Measurements from the PM sensor are collected every minute and sent to the cloud where raw data is stored and available for further processing. Data available from public monitoring station is averaged hourly values.

Two calibration methods were implemented in this paper. The first consisted of linear calibration and the second included a simple neural network (Figure 1).

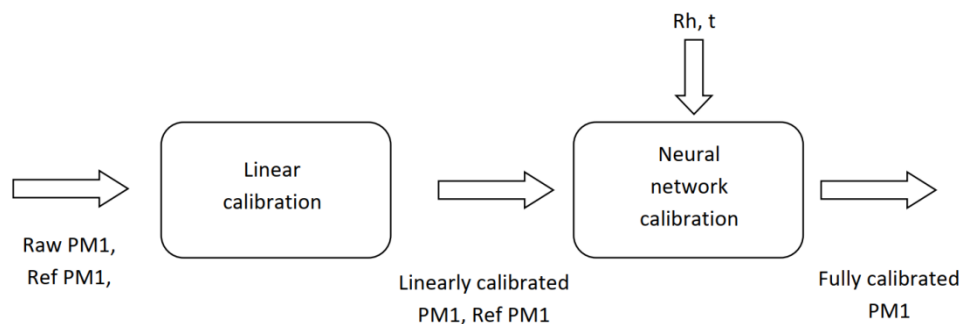


Figure 1. Calibration algorithm.

Linear calibration was performed using the Least Squares Method [7] curve fitting. Under the assumption that the data is linearly dependent, the least Squares Method can be applied to fit the raw data to the reference data.

After linear calibration a neural network model was trained in order to further improve the accuracy of the measurements. The model consisted of two hidden layers containing 1000 and 200 neurons, respectively. The Relu activation functions were used in the neural network, the inputs to the network were relative humidity, temperature and linearly calibrated data and the desired output was the reference data. The model was trained with a 9:1 split of the training data into training and validation sets.

3 Results and performance evaluation

The data used in this paper was acquired during the months of June and July of 2020. The reference system made hourly measurements while the low-cost sensors made measurements every minute. In order to compare the values from these two systems, the measurements from the low-cost sensors were averaged for each hour and furthermore synchronized with reference system measurements. The input data for the calibration process consists of PM1 measurements from the low-cost sensors and the relative humidity and temperature from the reference sensors. The parameters for the calibration process were fit based on the first group of data and tested on the second group. The input parameters for the calibration process of the test data are shown in Figure 2.

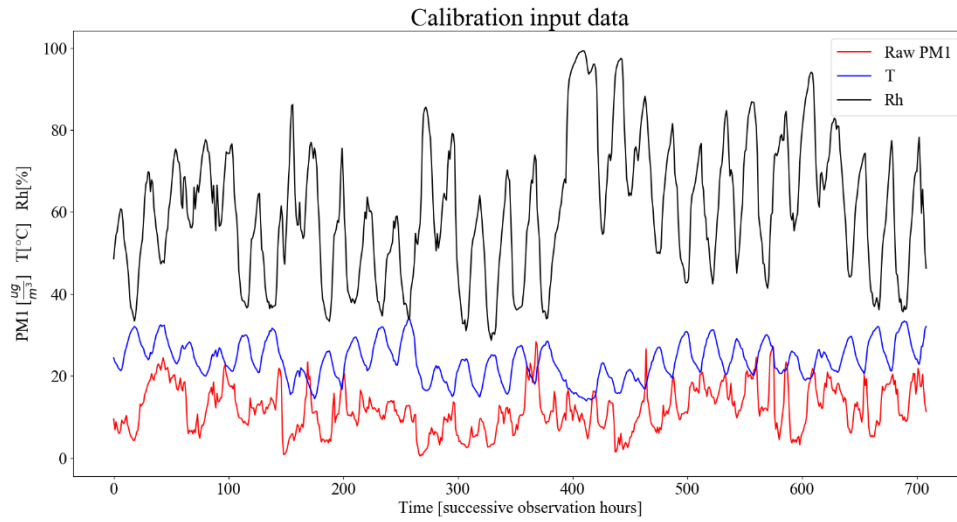


Figure 2. Calibration input data, Raw PM1 measurements (red), temperature (black) and relative humidity (blue).

After applying the linear calibration to the test data, a RMSE of $1.15 \frac{ug}{m^3}$ was obtained. The reference data and the linearly calibrated data are shown in Figure 3.

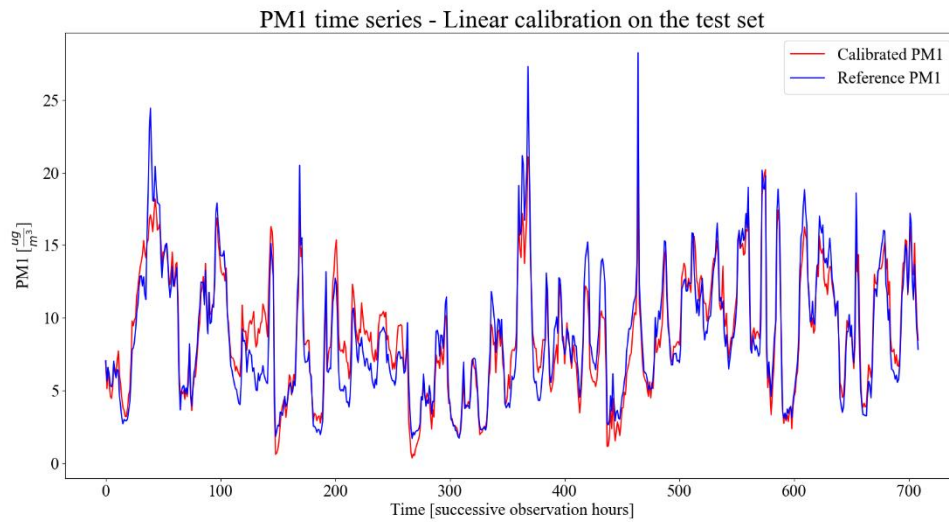


Figure 3. PM1 time series. PM1 concentration after linear calibration (red) and reference PM1 concentration (blue).

After the linear calibration, neural network calibration was performed. The RMSE of $0.87 \frac{ug}{m^3}$ was achieved using the neural network which shows an improvement from the RMSE parameter calculated after using only the linear calibration. The time series for the reference data and for the data after the neural network calibration is shown in Figure 4.

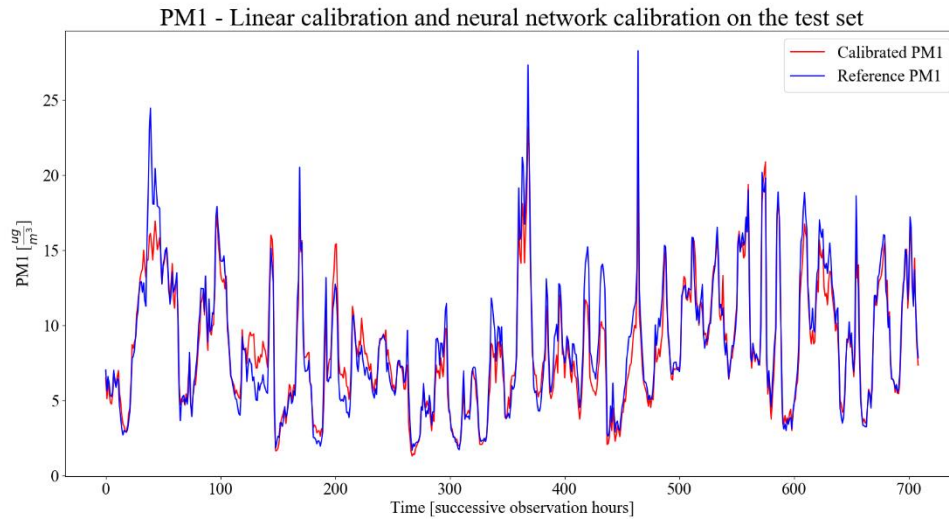


Figure 4. PM1 time series. PM1 concentration after linear and neural network calibration (red) and reference PM1 concentration (blue).

Regarding the R2 measure, a value of 0.88 was obtained using only linear calibration and a value of 0.92 was obtained after using the neural network. The calibration plot for both methods is shown in Figure 5.

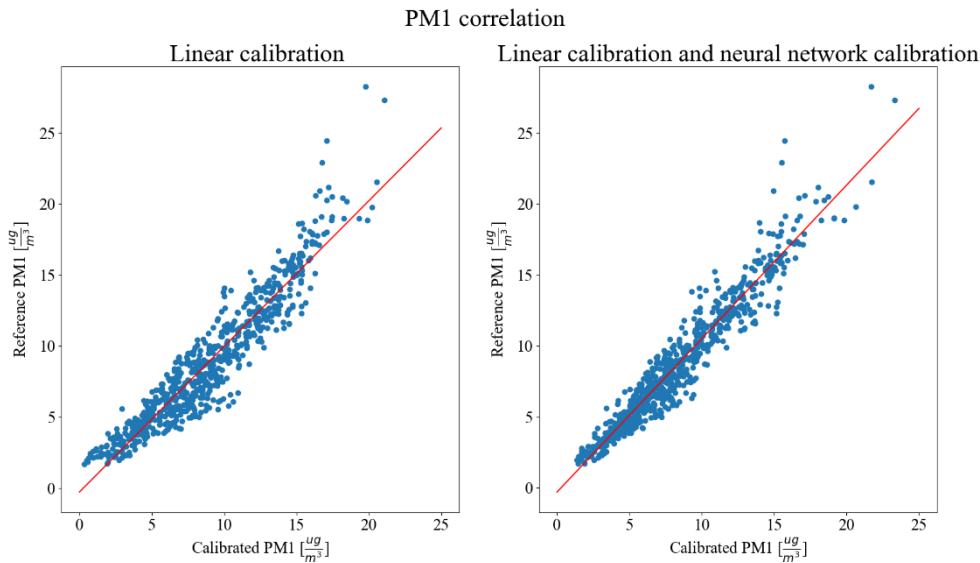


Figure 5. PM1 correlation scatter plot. Only linear calibration (left) and linear calibration with neural network calibration (right).

From the figures shown, it can be deduced that the use of a low-cost PM sensor shows quite a good correlation with the measurements of the public monitoring station, and that the usage of neural networks could further improve the correlation and increase the R2 value.

4 Conclusion

In this paper, we have presented a novel method for increasing the accuracy of a calibration by using a combination of a linear calibration with a neural network. It is shown that the used PM sensor has quite a good correlation with the reference measurements and the correlation coefficient is further improved by using a neural network. It is obvious that the temperature and relative humidity have an influence on the measurements and that they should be taken into account in order to increase the accuracy of the measurements. The measurements were conducted during June and July. The temperature was high and relative humidity was low during this period, and in future work we will

implement the calibration during autumn and winter in order to see the influence of these parameters during that part of the year. Furthermore, we will do a calibration of PM2.5, PM10 and other low-cost gas sensors, like CO and NO₂.

5 Acknowledgment

The authors gratefully acknowledge financial support from the Ministry of Education and Science, Government of the Republic of Serbia.

6 References

- [1] *** World Health Organization (WHO), Global Health Observatory (GHO) data. [Online]. Available: https://www.who.int/gho/urban_health/situation_trends/urban_population_growth_text/en/
- [2] **P. Kumar et al.**, “The rise of low-cost sensing for managing air pollution in cities”, *Environment International*, vol. 75, pp. 199–205, 2015. DOI: 10.1016/j.envint.2014.11.019.
- [3] *** Air quality guidelines for Europe, 2nd ed., WHO regional publications, European series, no. 91, 2000. [Online]. Available: www.euro.who.int/document/e71922.pdf
- [4] **Drajić D. et al.**, “Reliable Low-Cost Air Quality Monitoring Using Off-The-Shelf Sensors and Statistical Calibration”, *Elektronika ir Elektrotehnika*. 2020 Apr 25;26(2):32-41.
- [5] **Specht D.**, “A general regression neural network”, *IEEE transactions on neural networks*, 1991 Nov 1;2(6):568-76.
- [6] *** <https://www.espruino.com/PMS7003>
- [7] **M. Engelhardt and L. J. Bain**, *Introduction to Probability and Mathematical Statistics*. Brooks/Cole, 2000.

RAČUNARSKO UPRAVLJANJE ENERGETSKI EFIKASNIM SISTEMOM ZA STERILIZACIJU DRVETA

COMPUTER CONTROL OF ENERGY EFFICIENT WOOD STERILIZATION SYSTEM

Miša STEVIĆ^{*1}, Miloš MARJANOVIĆ², Ilija RADOVANOVIĆ³, Zoran STEVIĆ⁴

¹ Mikroelektronika, d.o.o., Belgrade, Serbia

² MS Kablovi, d.o.o., Paraćin, Serbia

³ Innovation center of School of Electrical Engineering in Belgrade, Serbia

⁴ University of Belgrade, Technical faculty Bor, School of Electrical engineering,
CIK, Belgrade, Serbia

Na postojeći sistem za sterilizaciju drveta nadograđen je savremeni sistem za regulaciju procesa u cilju povećanja energetske efikasnosti, pouzdanosti, kvaliteta proizvoda i komfora korisnika. Postojeći ON/OFF regulator temperature zamenjen je kontinualnim PID regulatorom sa trofaznim tiristorskim faznim regulatorom na izlazu. Zadržano je postojeće merenje temperature u zonama komore sa drvetom ali su isti signali uvedeni i u novi sistem, gde su po određenom algoritmu iskorišćeni za definisanje referentne temperature PID regulatora.

Ključnereči: PID regulator; sterilizacija drveta; energetska efikasnost; merenje; temperatura

This paper describes the design of hardware and software for computer control of energy efficient wood sterilization system. The existing ON / OFF temperature controller has been replaced by a continuous PID controller with a three-phase thyristor phase controller at the output. Temperature measurements in 5 zones of the chamber with wood was performed with Pt1000 probes and they were used according to a certain algorithm to define the reference temperature of the PID controller that controls the power of the steam generator heater

Key words: PID regulator; sterilization of wood; energy efficiency; measurement; temperature

1 Introduction

A modern process control system has been upgraded over the existing wood sterilization system in order to increase energy efficiency, reliability, product quality and user comfort. The existing ON / OFF temperature controller has been replaced by a continuous PID controller with a three-phase thyristor phase controller at the output [1-4]. The existing temperature measurement in the zones of the chamber with wood was retained, but the same signals were brought to the new system, where they were used according to a certain algorithm to define the reference temperature of the PID controller [5,6].

2 Implementation

2.1 Hardware

Temperatures in the five zones of the chamber with wood are measured by PTC sensors Pt1000 which, combined with 10kΩ resistors, form voltage dividers connected to the multiplexer 4051 from which negative pulses are obtained as a "call" of an individual sensor. The sensors were immersed in hot water whose temperature was changed in the range from 50 °C to 80 °C and the signal level at the distributor output was measured, which determined the temperature of the output signal in a given temperature range:

$$T = -1666,7 U - 320$$

^{*} Corresponding author, email: misa.stevic@live.com

where T is the temperature of the observed zone in $^{\circ}\text{C}$, and U is the output voltage of the distributor [1].

Figure 1 shows the shape of the output signals for the temperature $T = 70^{\circ}\text{C}$, while on the Figure 2 signal amplification and conditioning from the Pt1000 sensors and input to the 5 analog inputs of the AD / DA converter NI 6001 USB are shown [7,8].

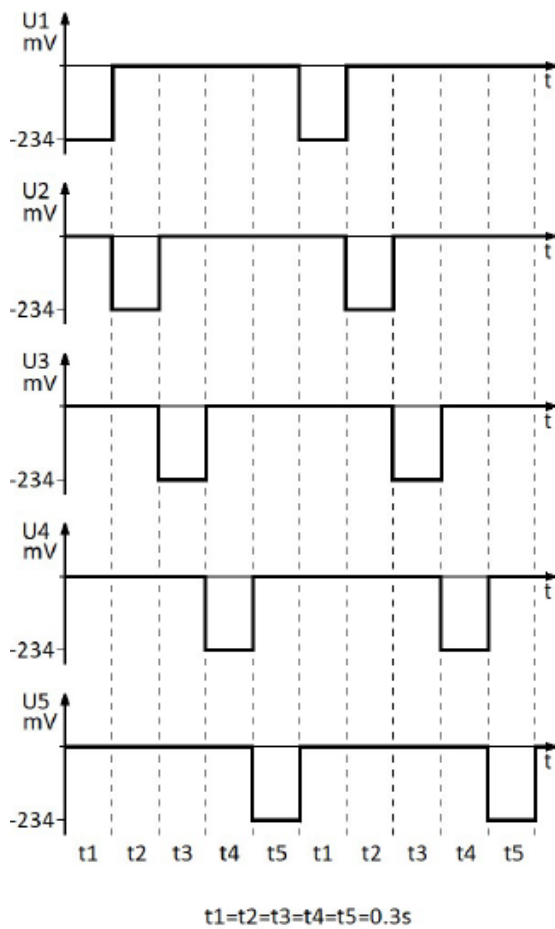


Figure 1. Signal shape from the temperature sensors

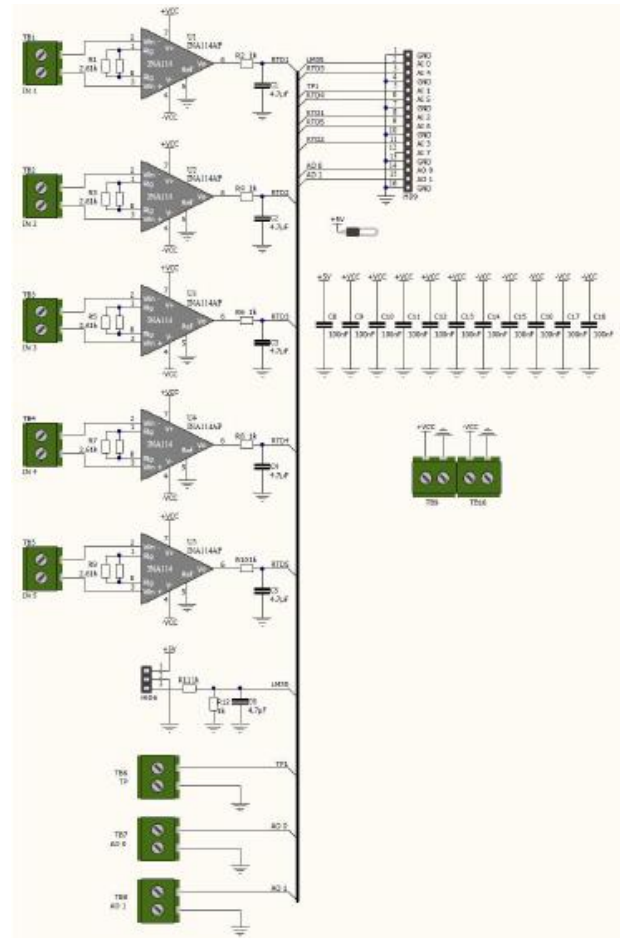


Figure 2. Signal amplification and conditioning

2.2 Software

The signal processing and process control are performed within the LabVIEW environment. Signals from the analog inputs of the DAQ card are imported into this environment via the DAQ Assist block (Figure 3). The output of this block is a dynamic structure consisting of six signals. A signal corresponding to the output of the protection module appears at the first output of the DAQ Assist block, which is averaged, multiplied by the appropriate constant and finally displayed on the Temperature indicator in the steam generator [1]. At the next five outputs, signals corresponding to the voltages of the Pt1000 sensor appear. These signals are averaged, their offset is adjusted as well, and converted to temperature using the calculation block (Formula Node), according to equation, and displayed on the diagram (XY Graph). The chamber zone temperature data define the setpoint for the PID steam generator temperature controller (PID) according to the algorithm in Figure 4. At the output of the PID block, a Control signal is obtained, which is displayed on the indicator and on the time diagram.

Other elements of the program block diagram are numerical constants, numerical indicators and graphical indicators, as well as control blocks for setting the gain of the controller, reference temperature and channel selection frequency [1].

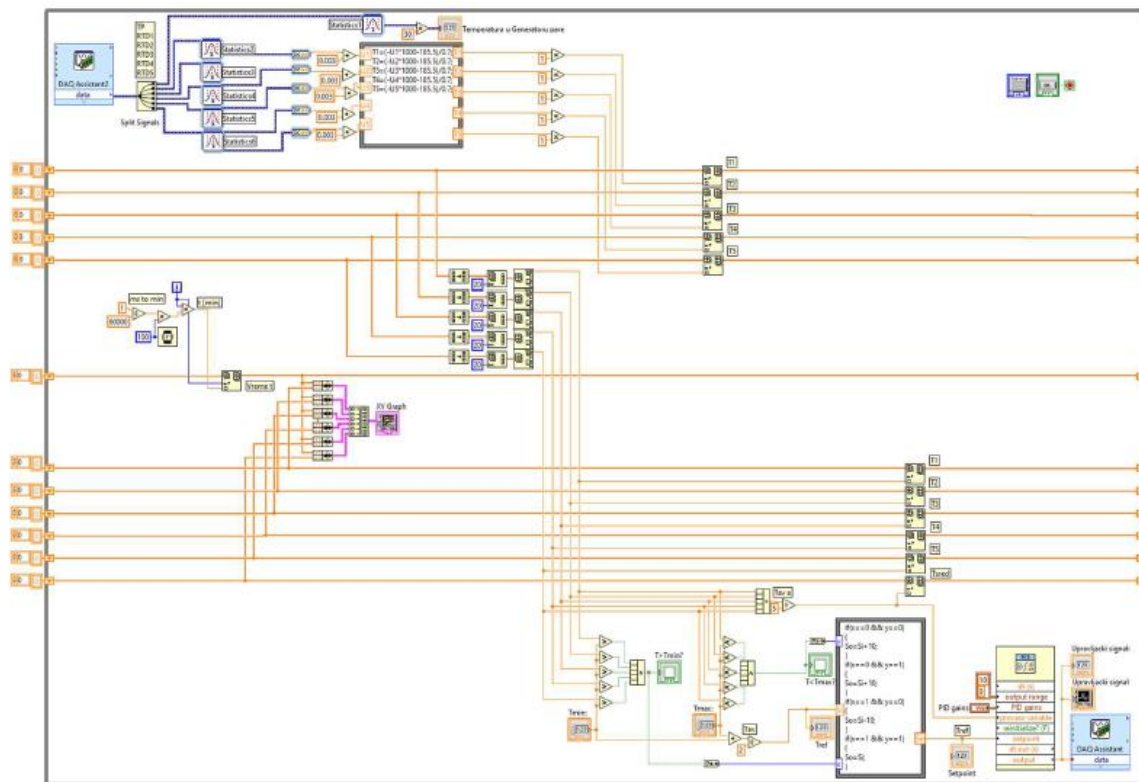


Figure 3. Block diagram in LabVIEW

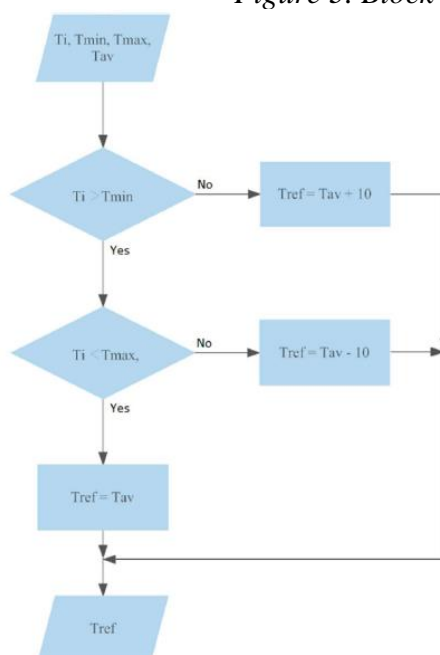


Figure 4. Algorithm for determining the setpoint temperature of the steam generator

In Figures 5 and 6 parts of the Front Panel are shown, within which the temperature and output signal are monitored, as well as the setting of the selection frequency, reference temperature and gain of the PID controller.

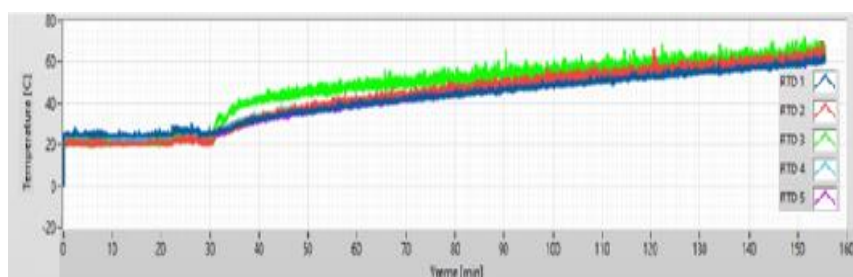


Figure 5. Front panel (monitoring the temperature signal)

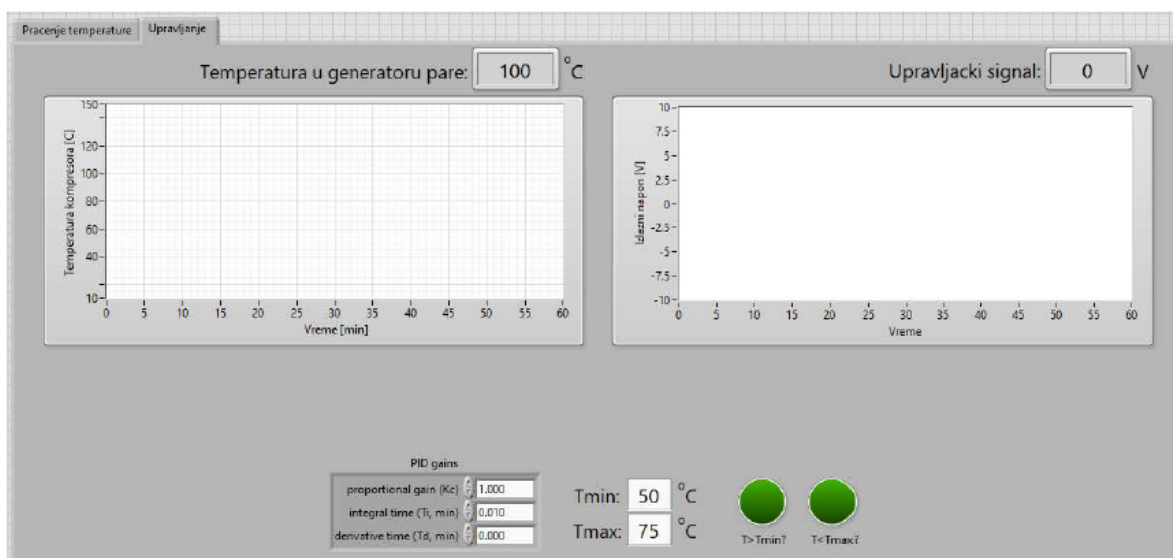


Figure 6. Front panel (setting controller parameters and monitoring output voltage)

3 Results

Based on the presented construction documentation, a system for wood sterilization was realized in DOO MS Kablovi in Paraćin. The system is based on an existing plant where the ON / OFF controller has been replaced by a PID controller. The new solution also brings a higher degree of protection against accidents. Significant energy savings are also achieved by the optimization algorithm for defining the set temperature of the steam generator based on the temperatures of the zones in the chamber. Computer measurement and control was performed in a LabVIEW environment, with its own application software solution (1).

4 Acknowledgement

The authors gratefully acknowledge financial support from the Ministry of Education and Science, Government of the Republic of Serbia.

5 References

- [1] **Marjanović M.**, Optimization of electrical installations in the technological process of wood thermal treatment in small dryers, Master Thesis, School of Electrical and Computer Engineering of Applied Studies, Belgrade, 2020
- [2] **Naleg, T., Kosik, S. and Fuhlborn, D.** What you need to know about SCR power controllers - Functions, features and efficiencies. <https://www.advancedenergy.com/globalassets/resources-root/white-papers/what-you-need-to-know-about-scr-power-controllers.pdf>.
- [3] *** The many benefits of SCR power control. IEEE Globaspec Media Solutions, Advanced Energy Industries, Inc., Septembar 2017.
- [4] **Isailović, M.** Temperature control using a three-phase thyristor phase controller, Thesis. Belgrade: School of Electrical Engineering, 2019.
- [5] **Hurem, Nedim**, Drying and thermal wood processing from the phytosanitary requirements aspect. Visoko, Bosnia and Herzegovina : s.n., 2019.
- [6] **Park, R., M., et al.**, Manual on the use of thermocouples in temperature measurement, 4th edition., s.l. : ASTM Committe E20 on temperature measurement, 1993.
- [7] *** USER GUIDE: N1 USB-6001/6002/6003 Low-Cost DAQ USB device. <http://www.ni.com/pdf/manuals/374259a.pdf>. [Online]
- [8] *** Accurate calculation of PT100/PT1000 temperature from resistance.
- [9] *** <https://techoverflow.net/2016/01/02/accurate-calculation-of-pt100pt1000-temperature-from-resistance/>. [Online]

VAŽNOST PRIMENE ANALIZE RIZIKA KOD OPREME POD PRITISKOM KOJA SE ISPITUJE PO POSEBNOM PROGRAMU

IMPORTANCE OF APPLYING RISK ANALYSIS TO PRESSURE EQUIPMENT TESTED BY A SPECIAL PROGRAM

**Sanja PETRONIĆ^{*1}, Marko JARIĆ¹, Katarina ČOLIĆ¹,
Suzana POLIĆ², Dimitrije MALJEVIĆ³**

¹ Innovation Centre of the Faculty of Mechanical Engineering in Belgrade, Belgrade, Serbia

² Central Institute for Conservation, Belgrade, Serbia

³ Faculty of Mechanical Engineering in Belgrade, University of Belgrade, Belgrade, Serbia

Oprema pod pritiskom se prema PED 2014/68 i Pravilniku o tehničkim zahtevima za projektovanje, izradu i ocenjivanje usaglašenosti opreme pod pritiskom deli na opremu visokog i niskog nivoa opasnost, u zavisnosti od vrste opreme, stanja i grupe fluida i proizvoda zapremine i pritiska, odnosno akumulirane energije. Ova oprema se ispituje prema Pravilniku o pregledu opreme pod pritiskom tokom veka upotrebe. Međutim, postoji određeni broj opreme pod pritiskom koji ne može da se ispituje po redovnom programu, najčešće zbog svoje konstrukcije, ili radnog fluida. Ova oprema se ispituje po posebnom programu koji se pravi za svaku opremu posebno. U sklopu ovog programa potrebno je uraditi i analizu rizika. U ovom radu će biti pojašnjena važnost primene analize rizika i biće prikazana njena primena na određene sklopove opreme.

Ključne reči: oprema pod pritiskom, PED, analiza rizika

According to PED 2014/68 and the Regulation on technical requirements for design, manufacture and conformity assessment of pressure equipment, pressure equipment is divided into high- and low-level risk level equipment, depending on the type of equipment, condition and group of fluids and products of volume and pressure, i.e. accumulated energy. This equipment is tested according to the Regulation on the inspection of pressure equipment during its service life. However, there are a number of pressure equipment that cannot be tested according to a regular program, most often due to their construction, or working fluid. This equipment is tested according to a special program that is made for each equipment particular. As part of this program, it is necessary to do a risk analysis. This paper will explain the importance of applying risk analysis and will show its application to certain sets of equipment.

Key words: pressure equipment, PED, risk analysis

1 Introduction

The Ordinance on technical requirements for the design, manufacture and conformity assessment of pressure equipment (1) and PED 2014/68 (2) define the conditions and obligations under which the pressure equipment is designed, manufactured and assessed, while the Ordinance on inspections of pressure equipment during life time (3) defines requirements for the safety of pressure equipment during the service life, regular and extraordinary inspections at the place of use, procedures and deadlines for inspection and testing of pressure equipment in use and the requirements to be met by the inspection bodies in order to be designated for the classification of pressure equipment and/or inspections and tests of pressure equipment, then the obligations of the user and the inspection body on inspections of pressure equipment in operation. Ordinance (3) provides for a pre-commissioning inspection, a first inspection, a regular periodic inspection and an extraordinary inspection. There are three types of regular periodic inspection: external, internal and pressure testing. In special cases, the internal examination may be replaced by an equivalent method, as well as a pressure test. However,

^{*} Corresponding author, email: sanjapetronic@yahoo.com

depending on the technical construction and / or operating conditions, there are exceptions in which the equipment needs to be tested according to a special program.

Croatian Ordinance (4) contains an appendix which lists the pressure equipment that requires treatment according to a special program. Our Ordinance (3) maintained that the Special Periodic Inspection Program is defined in the technical documentation of the pressure equipment manufacturer. This documentation contains the scope and deadlines of the examination. However, there are exceptions when the manufacturer does not provide a special program, and the equipment is subject to a special inspection program because due to the specific working conditions and technical complexity cannot be inspected according to the regular program of periodic inspections. The practice solves these problems, with the approval of Ministry of mining and energy Republic of Serbia, in a way that the user makes a special program, and the body for inspection and testing of pressure equipment approves and certifies it.

The ordinance does not define in detail what a special program for periodic inspection of pressure equipment should contain. This paper will present the role of risk analysis in compiling a special program of periodic inspections of pressure equipment, will provide an overview of standards related to risk analysis, discussed examples of pressure equipment that can not be tested by regular periodic program and analyzed and discussed example of membrane battery for which a special program was made.

2 Risk analysis and pressure equipment tested according to a special program

Risk analysis is the process of assessing the probability that negative events will occur within a system, and in our case a pressure vessel. The purpose of risk analysis and assessment is to make and implement measures and decisions in order to treat certain risks and eliminate them, based on the information and evidence obtained.

Risk-based inspection (RBI) is a methodology and procedure of analysis which, unlike condition-based inspection, requires a qualitative or quantitative assessment of the probability of failure (PoF) and the consequences of failure (CoF) associated with each item of equipment, assemblies or pipelines included in a particular process unit. Properly implemented RBI program allocates individual pieces of equipment according to their risks and gives priority to inspection based on this categorization.

The ISO 31000 (Risk management - Guidelines) standard (5) defines risk management and its assessment methodology. This standard has performed a number of applied risk-based concepts, such as Quantitative Risk Assessment (QRA), Risk-Based Control (RBI), Risk-Based Control and Maintenance (RBMI), Reliability-Based Maintenance (RCM), Risk-based age management (RBLM), or simply, Risk-based management (RBM).

Standard ISO 31010 Risk management - Risk assessment techniques defines risk management, and one of the important phases is risk analysis. Cause analysis identifies risks and causes, as well as their relationship, i.e. the impact of causes on risk, assesses the probability and consequences of risk realization, proposes measures for their elimination, defines parameters for monitoring and more. The ISO 31010 standard (6) is an auxiliary standard for ISO 31000 and provides guidance on the selection and application of systematic risk assessment techniques. A risk assessment conducted in accordance with this standard contributes to other risk management activities.

Other international engineering standards dealing with this issue are: API 571: Damage Mechanisms Affecting Fixed Equipment in the Refining Industry (7), API 580: Risk-Based Inspection - Recommended Practice (8), API 581: Risk Based Inspection Methodology - Recommended Practice (9) and ASME PCC-3: Inspection Planning Using Risk-Based Methods (10).

Risk-based inspection (RBI) is a method in which assets are identified for inspection based on their associated risks, as opposed to a predetermined time interval. In other words, it is a planning and prioritization tool, predominantly used in the oil and gas industry, that helps identify high-priority items (i.e., high-risk ones) relative to low-priority items (i.e., low-risk items). Those with low risk). This approach allows users / property owners to increase the efficiency of their inspection

resources by concentrating them on those assets that pose the greatest risk and do not spend resources on assets that have essentially no impact.

In a risk-based inspection, the risk is calculated as a result of the probability of failure and the consequences associated with the failure.

$$\text{Risk} = \text{probability of failure} \times \text{consequences of failure}$$

Risk is usually considered a better measure of priority than the probability of failure or the consequences of failure individually, because it describes the actual damage or loss more. For example, if you have to determine the advantage of two assets where one asset has a high probability of failure but a low consequence of failure and the other asset has a low probability of failure but a high consequence of failure, the analysis will give completely opposite results if you consider only one or the other factor. The use of risk eliminates this ambiguity. The probability of failure (POF) is determined using the applicable damage factors (mechanisms), the frequency of generic failures and management system factors (10):

$$\text{POF}(t) = 1 - e^{-\text{gff} \times \text{FMS} \times \text{Df}(t)}$$

where: gff is the generic failure frequency, FMS is the control system factor and Df (t) is the overall failure factor.

The frequency of generic failures is based on industry averages of equipment failures. The management system factor is a measure of how well the plant's management and workforce are trained to handle the plant's day-to-day activities and any emergencies that may arise due to an accident. Total damage factor is a combination of different damage factors that are applicable to a particular piece of equipment being analyzed. The consequence of a failure is calculated as a combined value of the consequences of damage to damaged equipment, damage to surrounding equipment, loss of production, costs due to injury per person and damage to the environment. The consequence of a failure may include both a financial consequence (FC) and an area safety (CA) consequence (10).

Some of the pressure equipment that requires a special program of periodic inspection due to the specifics of construction or operating conditions are: pressure equipment in electrical switches and switchgear, fire protection devices, pressure equipment operating in a closed circuit, silencers, equipment under pressure intended for fire extinguishing, pressure equipment with outer shell or wall, pressure equipment for gases and gas mixtures operating at temperatures below -10°C and others.

3 Special program for periodic inspections of the oil / nitrogen membrane pressure accumulator

3.1 Technical characteristics of the membrane pressure accumulator

Figure 1 shows a membrane oil / nitrogen pressure accumulator, manufactured by HYDAC Technology GmbH, D-66280 Sulzbach / Saar, Germany. The technical characteristics of this vessel are listed in Table 1.

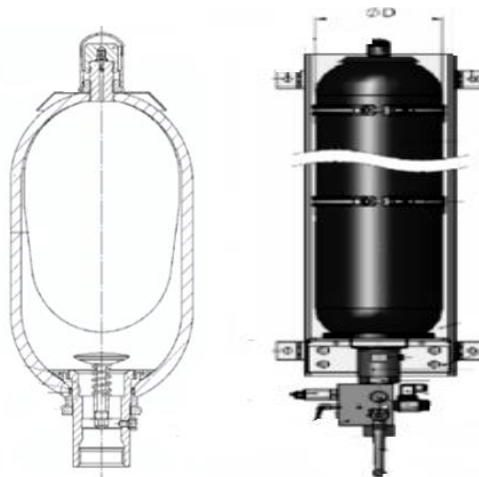


Figure 1. Membrane pressure accumulator

Table 1. Operating characteristics of a membrane pressure accumulator

Operating parameters		Unit	Value
Max allowed working pressure	PS	[bar]	330
Test pressure	PT	[bar]	472
Volume	V	[l]	10
Max allowed working temperature	TS	[°C]	100
Working fluid		-	Oil/nitrogen
Category of the pressure vessel			IV

The category of a membrane pressure accumulator is determined according to diagram 2 in (3) and belongs to the equipment of high level of danger: IV category. According to Annex III - Deadlines for regular periodic inspections, Ordinance on inspection of pressure equipment during the service life (3), the membrane accumulator should be tested according to the following dynamics: for 2 years external inspection, for 5 years internal inspection and for 10 years pressure test.

The problem that arises is the complexity of the construction in which there are no conditions to do an internal inspection or pressure test. Internal inspection can be replaced by ultrasonic measurement of wall thickness, while pressure testing by an equivalent non-destructive testing method. Considering that the accumulator is made of a seamless pipe and that there are no welded joints, it is reduced that the pressure test should be replaced by ultrasonic measurement of the wall thickness, ie two tests should be replaced by the same method. For these reasons, a special testing program is needed to conduct a risk analysis.

3.2 Risk analysis of the membrane pressure accumulator

Risk assessment can be quantitative, which requires a complicated procedure based on a large number of input data, or qualitative, which is reduced to assessing the degree of risk of individual components and their positioning in the risk matrix. Although the results are not as accurate as in the quantitative analysis, this approach is fully justified for pressure equipment where the operating conditions are such that there is virtually no risk of corrosion (stored medium is nitrogen / oil) and brittle fracture (negligible risk of pressure overload). In addition, in the case of the analyzed equipment under pressure for regulating the turbine plant, there are no mechanisms to reduce the wall thickness, especially if we keep in mind that the equipment is seamless, i.e. there are no welded joints, so the probability of failure is practically zero which is confirmed by history of such plants. Accordingly, the position in the risk matrix depends only on the estimated consequence, which in the worst case would be field B1, Table 2, i.e. (very) low risk.

Table 2 shows Numerical Values Associated with POF and Area-Based COF Categories taken from API 581 (9). Consequence area for this accumulator is 25m² and damage factor is 1. Based on these data and according to Table 2 the membrane pressure accumulator belongs to B1 category, i.e. low risk.

Table 2. Numerical Values Associated with POF and Area-Based COF Categories (9)

Category	Probability Category		Consequence Category	
	Probability Range	Damage Factor	Range Category	Range (m2)
1	$P_f(t) \leq 3.06E-5$	$D_f \leq 1$	A	$CA \leq 9.29$
2	$3.06E-5 < P_f(t) \leq 3.06E-4$	$1 < D_f \leq 10$	B	$9.29 < CA \leq 92.9$
3	$3.06E-4 < P_f(t) \leq 3.06E-3$	$10 < D_f \leq 100$	C	$92.9 < CA \leq 929$
4	$3.06E-3 < P_f(t) \leq 3.06E-2$	$100 < D_f \leq 1000$	D	$929 < CA \leq 9290$
5	$P_f(t) > 3.06E-2$	$D_f > 1000$	E	$CA > 9290$

Figure 2 presents Iso-Risk Plot for Consequence Area taken from API 581 (9). The values in this iso-risk plot are given in ft² and CA for this case is 269 ft², damage factor is 1, and the accumulator is in field B1, marked with the “X”.

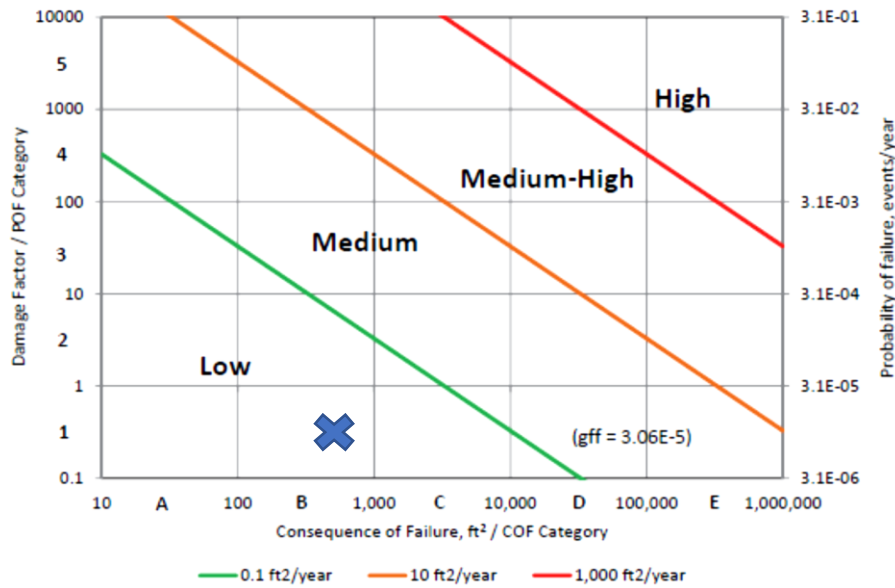


Figure 2. Iso-Risk Plot for Consequence Area (9)

Table 3 shows Numerical Values Associated with POF and Financial-Based COF Categories taken from API 581 (9). Financial risk for this accumulator is below 10000\$ and damage factor is 1. Based on these data and according to Table 3 the membrane pressure accumulator belongs to A1 category, i.e. very low risk.

Table 3. Numerical Values Associated with POF and Financial-Based COF Categories (9)

Category	Probability Category		Consequence Category	
	Probability Range	Damage Factor	Range Category	Range ()
1	$P_f(t) \leq 3.06E-5$	$D_f \leq 1$	A	$FC \leq 10000$
2	$3.06E-5 < P_f(t) \leq 3.06E-4$	$1 < D_f \leq 10$	B	$10000 < FC \leq 100000$
3	$3.06E-4 < P_f(t) \leq 3.06E-3$	$10 < D_f \leq 100$	C	$100000 < FC \leq 1000000$
4	$3.06E-3 < P_f(t) \leq 3.06E-2$	$100 < D_f \leq 1000$	D	$1000000 < FC \leq 10000000$
5	$P_f(t) > 3.06E-2$	$D_f > 1000$	E	$FC > 10000000$

Figure 3 presents Iso-Risk Plot for Financial Consequence taken from API 581 (9). The values in this iso-risk plot are given in \$ and FC for this case is 1000\$ and damage factor is 1, and the accumulator is in field A1, marked with the “X”.

The risk matrix is presented in Figure 4, and fields related to the membrane pressure accumulator are marked with “X”.

This assessment is also influenced by the fact that the risk of accident is lower than the risk of testing, i.e. discharge of this type of pressure equipment, even when controlled, could cause severe consequences.

For this level of risk, the prescribed program for measuring wall thickness every 5 years is conservative because it prevents all possible adverse events and ensures safe operation of the plant.

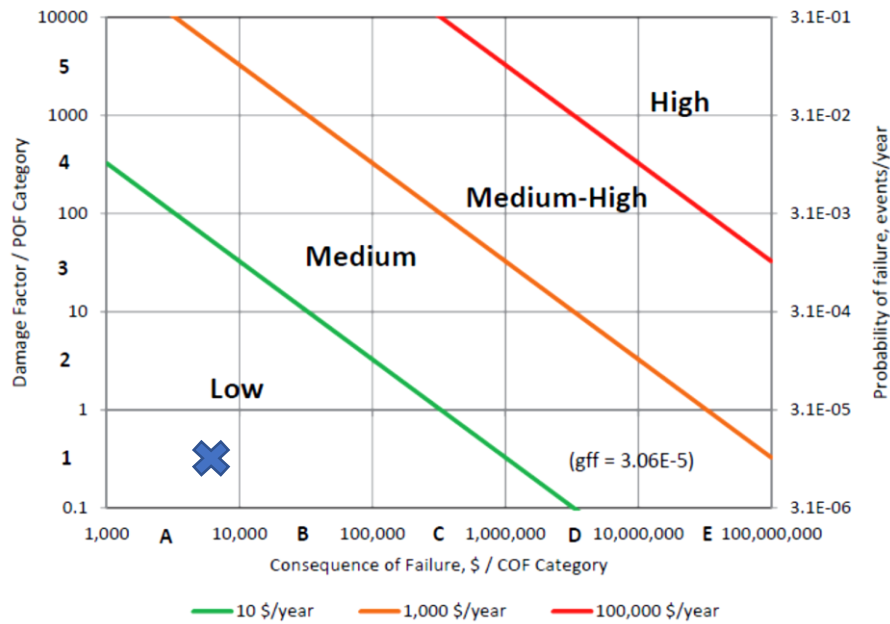


Figure 3. Iso-Risk Plot for Financial Consequence (9)

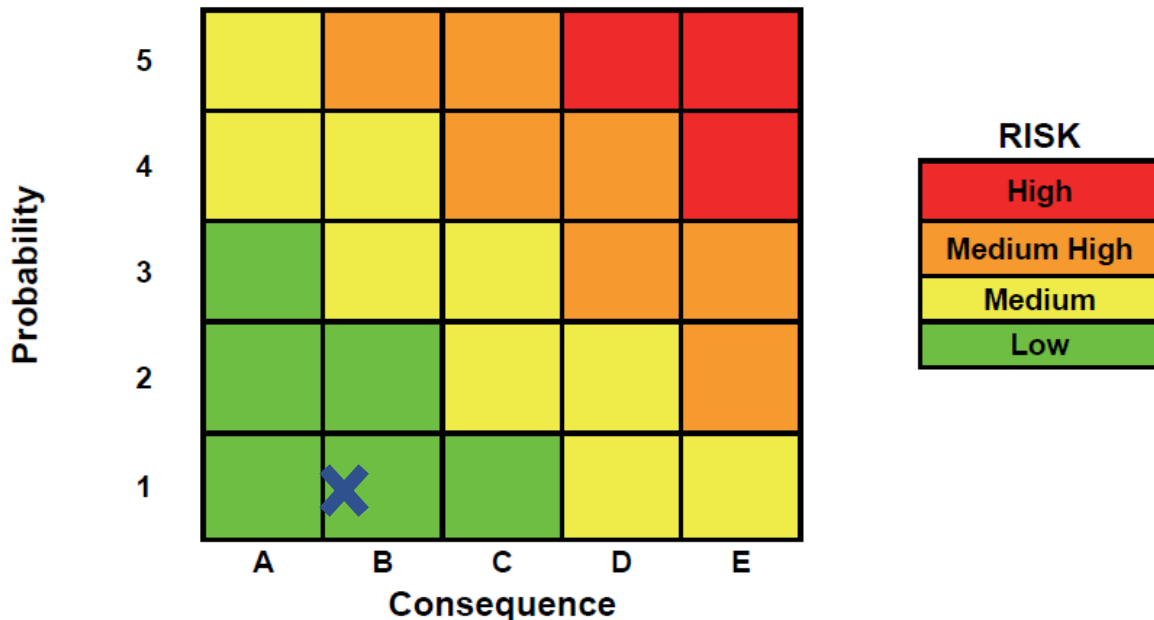


Figure 4. Risk matrix

3.3 Determining the periodicity of subsequent inspections according to the Special Program

External inspection (every 2 years) according to the inspection period assigned in the Ordinance on inspection of pressure equipment during the service life (3).

Visually inspect every two years to check:

- whether there are irregularities and deviations in relation to the technical documentation,
- general condition of membrane accumulator, condition of the supporting structure, connections, accompanying pipelines and safety devices,
- condition of the working environment and plant in which the equipment is located,
- anti-corrosion protection of external surfaces of equipment,
- whether the equipment is used in accordance with the purpose.

Ultrasound wall thickness measurement (every 5th year)

Measurement of wall thickness by ultrasound of cylindrical shells of membrane pressure accumulator should be performed every five years according to the schema given in Figure 5.

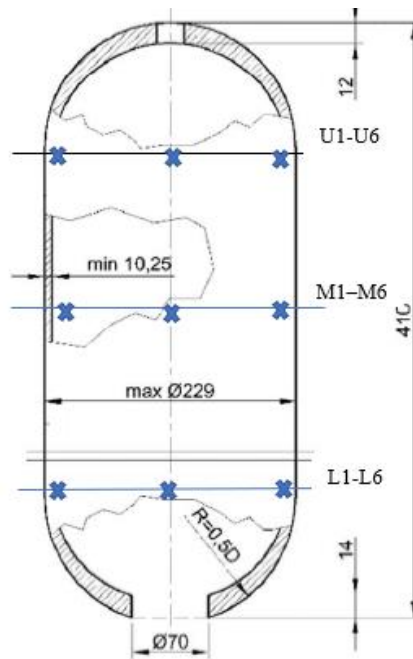


Figure 5. Measuring points U1-U6, M1-M6 and L1-L6 on the membrane accumulator

The minimum wall thickness of the seamless cylindrical shells of membrane pressure accumulators according to the strength calculation is 10.25 mm.

Table 3 gives the results of ultrasound measuring the wall thickness at the measuring points shown in Figure 5.

Table 3. Results of ultrasound measurement of the wall thickness

Point of measurement Line of measurement	1	2	3	4	5	6
U	11, 3	11, 2	11, 3	11, 3	11, 1	11, 1
M	11, 1	11, 4	11, 2	11, 1	11, 1	11, 4
L	11, 3	11, 3	11, 1	11, 2	11, 2	11, 2

The minimum measured wall thickness of seamless cylindrical shells of membrane pressure accumulators must not be less than the minimum wall thickness as required by the manufacturer and the required wall thickness given in the strength calculation. The derived wall thickness of the lower and upper hemispherical bottom is from 10.25 to 14 mm. The membrane pressure accumulator has no welded joints. Due to the operating conditions, the working medium and the large difference between the required and derived wall thickness, it is not necessary to measure the wall thickness of the lower and upper hemispherical bottoms of membrane accumulators.

4 Conclusion

This paper presents and explains the importance of risk analysis in the preparation of inspections and tests of pressure equipment according to a special program.

The paper presents an example of risk analysis and test periodicity for membrane pressure accumulators.

It has been shown that the risk of accidents is very small and that tests can be performed for 5 years, which would save money.

The risk analysis showed that no critical high risk positions were observed, and that none of the elements of membrane accumulator tends to move to the category of higher risk in the case when the review and testing program is realized in the next review and testing dates given in this program.

5 Reference

- [1] *** Rulebook on technical requirements for design, manufacture and conformity assessment of pressure equipment, Official Gazette RS, 87/2011, 2011
- [2] *** DIRECTIVE 2014/68/EU OF THE EUROPEAN PARLIAMENT AND OF THE COUNCIL of 15 May 2014 on the harmonisation of the laws of the Member States relating to the making available on the market of pressure equipment, Official Journal of the European Union, 2014
- [3] *** Rulebook on inspections of pressure equipment during the service life, Official Gazette of RS, 87/2011 i 75/2013
- [4] *** Ordinance on the inspection and testing of pressure equipment, Official Gazette of Croatia, 80/2013 i 14/2014
- [5] *** ISO 31000: 2018 Risk management – Guidelines, International Organization for Standardization, 2018.
- [6] *** IEC 31010: 2019, Risk management – Risk assessment techniques, International Organization for Standardization, 2019.
- [7] *** API 571: Damage Mechanisms Affecting Fixed Equipment in the Refining Industry, American Petroleum Institute, 2020.
- [8] *** API 580: Risk-Based Inspection - Recommended Practice, American Petroleum Institute, 2016.
- [9] *** API 581: Risk Based Inspection Methodology - Recommended Practice, American Petroleum Institute, 2016.
- [10] *** ASME PCC-3: Inspection Planning Using Risk-Based Methods, The American Society of Mechanical Engineering, 2017.

AUTOMATIZACIJA PROCESA PROIZVODNJE BAKARNE ŽICE METODOM LIVENJA U VIS – PODSISTEM ZA INDUKCIONO ZAGREVANJE

AUTOMATION OF A COPPER WIRE MANUFACTURING PROCESS USING UP-CASTING METHOD – SUBSYSTEM FOR INDUCTION HEATING

Nada RATKOVIĆ KOVAČEVIĆ^{*1}, Misa STEVIĆ², Milos MILEŠEVIĆ³,
Srđan MAKSIMOVIĆ⁴, Đorđe DIHOVIČNI⁵, Zoran STEVIĆ⁶

¹ The Academy of Applied Technical Studies Belgrade, Belgrade, Serbia

² Mikroelektronika, Belgrade, Serbia

³ School of Electrical Engineering, University of Belgrade, Belgrade, Serbia

⁴ The Academy of Applied Technical Studies Belgrade, Belgrade; Trizma, Belgrade, Serbia

⁵ The Academy of Applied Technical Studies Belgrade, Serbia

⁶ School of Electrical Engineering, University of Belgrade, Technical faculty in Bor,
University of Belgrade; Central Institute of Conservation, Belgrade, Serbia

<https://doi.org/10.24094/mkoiee.020.8.1.279>

Cilj ovde predstavljenog istraživanja je da se projektuje i implementira sistem za automatsku proizvodnju bakarne žice, metodom livenja u vis (eng. up-casting). Podsystem indukcionog zagrevanja obuhvata automatsku kontrolu temperature bakra, topljenog kao i žarenog, automatsko regulisanje snage indukcionog zagrevanja, kako bi se omogućilo pravilno grejanje bakarne žice, tako da se može dostići potrebna temperatura, i postiglo žarenje ili topljenje. Zavojnica je izrađena od bakarne cevi i njena temperatura se reguliše pomoću prisilnog proticanja ulja kroz cev. Sistem se može lako prilagoditi za automatsko žarenje čelične žice ili žice od železa, imajući u vidu električna i magnetska svojstva železa i čelika. Sistem je proizveden, testiran i stavljen u funkciju.

Ključne reči: automatizacija; indukciono zagrevanje; mehatronika; žarenje

The aim of the research presented here is to design and implement a system for automatic production of copper wire, by the method of up-casting. The subsystem for induction heating includes automatic control of the temperature of the melted as well as annealed copper, automatic regulation of the induction heating power. The induction coil was designed and made to provide proper heating of the copper wire that is produced, so that the necessary temperature can be reached and its annealing or melting obtained. The coil is made of copper tube and its temperature is regulated using forced oil flow through the tube. The system can be easily adapted to be used in automation of the process of steel wire or iron wire annealing, having in mind the electrical and magnetic properties of the steel and iron. The system was produced, tested and put to work.

Key words: annealing; automation; induction heating; mechatronics

1 Introduction

Induction heating is the process of heating an electrically conducting object (usually a metal) by electromagnetic induction, through heat generated in the object by eddy currents [1]. Induction heating is based on conversion of electro-magnetic field energy into heat [2]. This conversion is obtained through electromagnetic induction which is performed in systems for induction heating. The systems for induction heating can be with or without magnetic core [2].

An induction heater consists of an electromagnet and an electronic oscillator that passes a high-frequency alternating current (AC) through the electromagnet [1]. The rapidly alternating magnetic field penetrates the object, generating electric currents inside the conductor, called eddy currents. These currents flowing through the material cause the metal to be heated by Joule heating, because

^{*} Corresponding author, email: nratkovicmf@gmail.com

of materials electric resistance [1]. Joule heating is exploited here for melting copper to produce copper wire, and is applied afterwards on the copper wire produced to obtain its annealing.

In ferromagnetic (and ferrimagnetic) materials such as iron, heat may also be generated by magnetic hysteresis losses. Since the generated alternating magnetic field is of high frequency, eddy currents are also having high frequency, which causes another effect to take place – the skin effect. The frequency of current used depends on the object size, material type, coupling (between the work coil and the object to be heated) and the penetration depth [1] - [4].

Both heating causes, eddy currents and hysteresis, occur in electric machines, however these are there referred to as energy losses, i. e. the losses in copper and losses in iron, whereas losses in iron could be due to hysteresis and eddy currents [5] - [7]. In contrast to that, both are intentionally induced heating effects in systems for induction heating.

In case of steel, its properties could be with or without significant ferromagnetic characteristics, depending of its composition and intended application.

Induction heating of copper is done with induction coil made out of copper as well. Since the frequency of the AC supply used in the copper coil is very high, skin effect occurs in the coil. This allowed that the coil is made out of helicoidally twisted copper tube rather than a copper rod or wire. Since the material of the inductive coil is hollow, the flow of oil through the copper tube is used to provide regulation of the coils temperature.

Skin effect is the tendency of an alternating electric current (AC) to become distributed within a conductor in such a way that the current density is largest near the surface of the conductor and decreases exponentially with increase in depths in the conductor [3], [4]. The electric current flows mainly at the "skin" of the conductor, between the outer surface and a level called the skin depth. Skin depth depends on the frequency of the alternating current; as frequency increases, current flow moves to the surface, resulting in thinner skin depth. Skin effect reduces the effective cross-section of the conductor and thus increases its effective resistance. Skin effect can be caused by opposing eddy currents induced by the changing magnetic field resulting from the alternating current. At 60 Hz in copper, the skin depth is about 8.5 mm [4]. At high frequencies the skin depth becomes much smaller [3], [4].

The upward continuous casting method, better known as the UPCAST® system, was originally developed within the Finnish Outokumpu Group in the late '60s [8]. According to [8], the outcome resulted from a synthesis of innovative thinking and long production experience. The first UPCAST® production line was installed in 1971 at the facilities owned by the Group, located in Pori, Finland, and is still in operation and up to date, thanks to a number of modernizations. This first production line has been followed by a continuous string of others delivered worldwide, establishing UPCAST® as the undisputed market leader in its field [8].

As a result of Outokumpu Group's decision to divest its copper business, a new, independent company UPCAST OY was established in 2006 to carry the UPCAST® legacy into the future. UPCAST OY is the exclusive supplier of the original UPCAST® process, as stated in [8].

2 Half Bridge with IGBT and Low Pass Filtering

The Insulated Gate Bipolar Transistor, (IGBT) is semiconductor switching device that has the output characteristics of a bipolar junction transistor, (BJT), but is controlled like a metal oxide field effect transistor, (MOSFET) [9]. IGBT combines the insulated gate (hence the first part of its name) technology of the MOSFET with the output performance characteristics of a conventional bipolar transistor, (hence the second part of its name). The result of this hybrid combination is that the "IGBT Transistor" has the output switching and conduction characteristics of a bipolar transistor but is voltage-controlled like a MOSFET [9].

IGBTs are mainly used in power electronics applications [9], such as: inverters, converters and power supplies, where the demands of the solid state switching device are not fully met by power BJTs and power MOSFETs. High-current and high-voltage BJTs are available, but their switching speeds are slow, while power MOSFETs may have higher switching speeds, but high-voltage and high-current devices are expensive and hard to achieve, as stated in [9].

Because the IGBT is a voltage-controlled device, it only requires a small voltage on the Gate to maintain conduction through the device, unlike BJT's which require that the Base current is continuously supplied in a sufficient enough quantity to maintain saturation [9]. One of the main advantages of the IGBT transistor is the simplicity by which it can be driven "ON" by applying a positive gate voltage, or switched "OFF" by making the gate signal zero or slightly negative allowing it to be used in a variety of switching applications. It can also be driven in its linear active region for use in power amplifiers. Also the IGBT is a unidirectional device, meaning it can only switch current in the "forward direction", that is from Collector to Emitter, unlike MOSFET is which have bi-directional current switching capabilities (controlled in the forward direction and uncontrolled in the reverse direction) [9].

In figure 1 is given simplified equivalent circuit of a IGBT (on the left), and IGBT symbol (on the right), taken from [9].

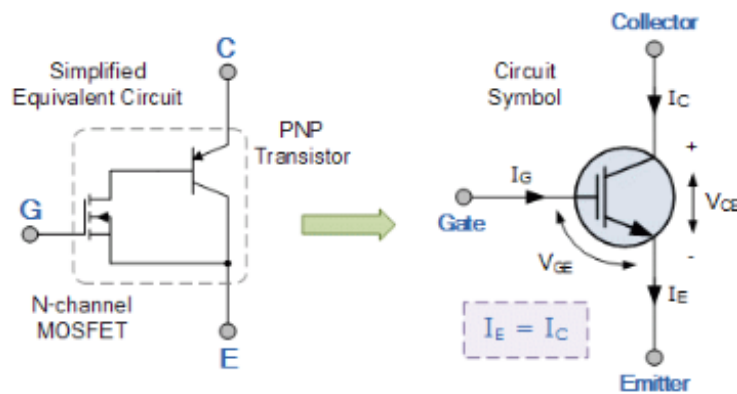


Figure 1 IGBT: simplified equivalent circuit (on the left), and IGBT symbol (on the right) [9]

A general comparison between BJT's, MOSFET's and IGBT's is given in the table 1, as taken from [9].

Table 1 Comparison between BJTs, MOSFETs and IGBTs [9]

Device Characteristic	Power BJT	Power MOSFET	IGBT
Voltage Rating	High <1kV	High <1kV	Very High >1kV
Current Rating	High <500A	Low <200A	High >500A
Input Drive	Current, $h_{FE} = 20 - 200$	Voltage, $V_{GS} = 3 - 10V$	Voltage, $V_{GE} = 4 - 8V$
Input Impedance	Low	High	High
Output Impedance	Low	Medium	Low
Switching Speed	Slow (μs)	Fast (ns)	Medium
Cost	Low	Medium	High

The principal of operation and Gate drive circuits for the IGBT are very similar to that of the N-channel power MOSFET. The basic difference is that the resistance offered by the main conducting channel when current flows through the device in its "ON" state is very much smaller in the IGBT. Because of this, the current ratings are much higher when compared with an equivalent power MOSFET, as described in [9].

The main advantages of using the **IGBT** over other types of transistor devices are its high voltage capability, low ON-resistance, ease of drive, relatively fast switching speeds and, combined with zero gate drive current, these make it a good choice for moderate speed, high voltage applications such as in pulse-width modulated (PWM), variable speed control, switch-mode power supplies or solar powered DC-AC inverter and frequency converter applications operating in the hundreds of

kilohertz range. With its lower on-state resistance and conduction losses as well as its ability to switch high voltages at high frequencies without damage, makes the **IGBT** ideal for driving inductive loads such as coil windings, electromagnets and DC motors [9].

Here a half-bridge with a pair of IGBTs is used to supply inductive load, used for inductive heating of a wire. The half-bridge, depicted in schematics in figure 2, is implemented to provide current to supply to an induction coil – an output load (not in figure 2). The current waveform is sinusoidal approximate. A coil is to be connected as output inductive load of the half-bridge in figure 2. When the coil is connected, it forms an oscillatory circuit with conducting capacitors - during one half period with C_4 , or during other half period with C_5 . C_2 and C_3 also contribute to this behavior. According to [10], both IGBTs and diodes have capacitances that have to be taken into account.

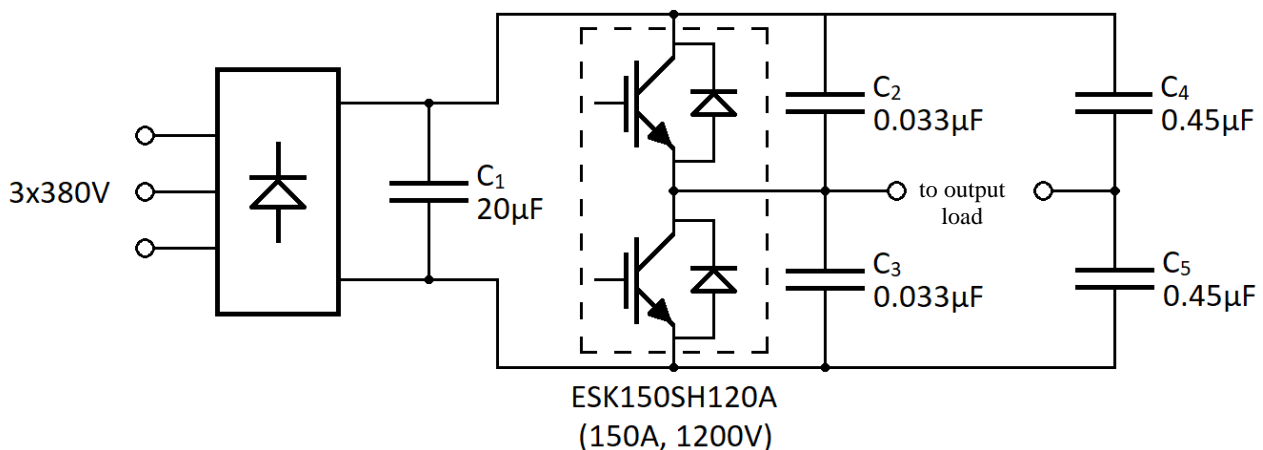


Figure 2 Half Bridge with IGBT Transistors and Low Pass Filtering

Diodes in figure 2 between Emitter and Collector of either IGBTs are freewheeling diodes or fly-back diodes [11]. These diodes are used to protect switches from arcs or sparks of current when inductive load is powered, during IGBT transition from its forward state to its blocking state, while another IGBT is at the same time to be in transition from its blocking state to forward state. When the current of inductive load is switched off, a transient response occurs, preventing the immediate drop to zero of the inductance current. This transient current could damage IGBT that is in its blocking state, if there would not be the diode between IGBTs Emitter and Collector that will turn on when is in its forward state and protect the IGBT. It is of utmost importance to prevent that both IGBTs are in their forward state at the same time, since it would make the shortcut of the power supply unit and almost certainly cause its failure. According to [10] capacitive effects of diodes during reverse recovery process should be modeled as well. In [10] extensive research work is derived and presented, analysis is performed and calculation of power switching losses in IGBTs of a half-bridge two level converter is performed.

3 Automated System for a copper wire manufacturing process using up-casting method

In building systems such as this one, where expert knowledge in several areas is required, it is wise to implement mechatronic approach to design. Concise description of the mechatronics is given in [12] whereas in [11] it is presented in more detail. Mechatronic approach to design has several stages, and is often referred to as the V-Model or V scheme [13], [14].

The V-Modell is a guideline for the planning and execution of development projects, which takes into account the whole life cycle of the system. In this process the V-Modell defines the results that have to be prepared in a project and describes the concrete approaches that are used to achieve these results. It also defines the responsibilities of the individual participants in the project, as stated in [15]. In the V-Model every stage in the designing and planning process has its counterpart in the timeline of testing and verification (and this outline even resembles the form of letter V, so it is named after this letter).

Suggestions on how to increase reliability in mechatronics systems are given in [16].

Some good advices and best practice recommendations for the implementation of mechatronics systems and computer-controlled systems can be found in [11] and [17].

The system designed and described here has electronics and electrical subsystem, mechanical subsystem, and it is used in a metallurgy process for heat treating (sometimes referred to as thermal treatments) [18], [19]. Mechanical part is twofold: hydraulic is one and moving and storing the wire is another. Hydraulic part has to provide oil circulation through the inductive coil, in order to obtain the temperature regulation. Drive of the wire is implemented using step motor, for a step-by-step moving of the processed wire and storing is done in wrapped turns of the annealed wire.

The inductive coil is part of the electrical subsystem as well as part of the hydraulic system, for cooling of the coil with the flow of oil through its interior. Along the axis of inductive coil a wire is drawn that is heated using inductive heating, until it is being annealed. Knowledge in signals and systems and automatic control is necessary to design and produce automated regulation of several variables: frequency of the input converter, temperature of the core wire, temperature of the induction coil (or the flow of the oil, which is cooling it), speed of the pulling of the wire, etc.

Furthermore, the plants specialized and used for this kind of manufacturing and processing usually are huge factories with lots of machinery and spacious halls (as can be seen in a video in [8]), while this system is of size small enough to be placed on the desktop (figures 3 and 4).



*Figure 3 a) On the left, the finished device, with control unit having half bridge with IGBT transistors visible in the upper left corner and induction coil in front of the cabinet.
b) On the right, the Control unit enclosed in casing, with visible connectors.*

Figure 3 a) and b) are the photos of the finished device. Photo on the left, figure 3.a) is the interior of the electrical cabinet, with control unit visible in the upper left corner, two fans on the upper right side, and induction coil in front of the cabinet. The control unit has half-bridge with two IGBT transistors. Photo on the right, figure 3.b) depicts the control unit enclosed in casing, with connectors visible on its right side.

The whole device for automated annealing completed is shown in the figure 4. The inductive coil in the figure 4 is being connected both to its electrical wiring as well as to the hydraulic installation providing oil flow for the regulation of the coils temperature.

The system was successfully put in operation on 22. 07. 2020. which can be seen in figure 4.



Figure 4 Finished system for induction heating: the electrical cabinet is situated on the left, and induction coil is placed on the wooden holder (on the right) while being connected to both electrical and hydraulic installation.

4 Conclusion

The aim of the research presented here was also the object of a project mentioned in Acknowledgements - it is to design and implement a system for automatic production of copper wire, by the method of up-casting. The goal of the project was completely fulfilled. The system was produced and tested and put to work. The system can be easily adapted to be used in automation of the process of steel wire or iron wire annealing, having in mind the electrical and magnetic properties of the steel and iron.

5 Acknowledgments

This investigation was funded by the Ministry of Education, Science and Technological Development of Republic of Serbia under the projects OI 172060 for the period 2011-2020.

6 Nomenclature

AC/DC - Alternating Current/ Direct Current,
BJT - Bipolar Junction Transistor,
DC - Direct Current,
IGBT - the **Insulated Gate Bipolar Transistor**,
MOSFET - Metal oxide semiconductor Field Effect Transistor,
NDT - Nondestructive testing,

PWM - pulse-width modulation (noun), pulse-width modulated (adverb),
UCT Company - Up Cast Technologies Company.

7 References

- [1] *** Wikipedia article on Induction heating, (accessed on 24. 07. 2020.)
https://en.wikipedia.org/wiki/Induction_heating
- [2] **Kostić, M. M.**, Teorija i proračun elektromagnetnih sistema za indukciono grejanje, (in Serbian), Elektrotehnički Institut Nikola Tesla, University of Belgrade, Beograd, Serbia, 2013.
- [3] *** Wikipedia article on Skin effect, (accessed on 24. 07. 2020.)
https://en.wikipedia.org/wiki/Skin_effect
- [4] **Bajić, D.**, Električna i elektronska kola, uređaji i merni instrumenti I, (in Serbian), University of Belgrade, Građevinska knjiga, Beograd, Serbia, 1975.
- [5] **Chapman, S. J.**, Electric Machinery Fundamentals, 4th edition, McGraw Hill, Boston – Toronto, International Edition, 2005.
- [6] **Petrović, M.**, Električne mašine i postrojenja, (in Serbian), Naučna knjiga, Beograd, Serbia, 1988.
- [7] **Fitzgerald, A. E., C., Kingsley**, Electric Machinery, (translated in Serbian), Naučna knjiga, Belgrade, Yugoslavia, 1962.
- [8] *** Site of the UCT Company – UPCAST OY Company, Our legacy –Original UPCAST® -> First in upcasting, (accessed on 24. 07. 2020.)
<https://upcast.com/upcast-original-upcast-story/>
- [9] *** Tutorials in Power Electronics, Insulated Gate Bipolar Transistor, (accessed on 16. 07. 2020.) <https://www.electronics-tutorials.ws/power/insulated-gate-bipolar-transistor.html>
- [10] **Gallego Gomez, J. D.**, IGBT Half-Bridge Power Switching Analysis Based on a Semi-analytical Point of View, M. Sc. thesis, University of Antioquia, Medellin, Colombia, 2016. (accessed on 24. 07. 2020.)
- [11] *** <https://pdfs.semanticscholar.org/bc61/1256107b0009e1b0081bf9b4df1d704af934.pdf>
- [12] **Alciatore, D. G., M. B., Hystand**, Introduction to Mechatronics and Measurement Systems, 3rd edition, McGraw Hill, Boston – Toronto, International Edition, 2007.
- [13] **Veg, A., G., Šiniković, E., Veg, M., Regodić**, Mali rečnik mehatronike, (in Serbian), 3rd edition, Faculty of Mechanical Engineering, University of Belgrade, Belgrade, 2019.
- [14] *** Wikipedia article on V-Model, (accessed on 24. 07. 2020.)
<https://en.wikipedia.org/wiki/V-Model>
- [15] *** "V-Modell" site, (in German), (accessed on 24. 07. 2020.)
https://www.cio.bund.de/Web/DE/Architekturen-und-Standards/V-Modell-XT/vmodell_xt_node.html
- [16] *** Site with V-Modell Tutorials, (archived, in English), (accessed on 24. 07. 2020.)
<https://web.archive.org/web/20100129043254/http://v-modell.iabg.de/v-modell-xt-html-english/index.html#toc0>
- [17] **Papić, Lj., M., Šarenac**, Systems Reliability Management in Mechatronics, (in Serbian), The Research Center of Dependability and Quality Management DQM, Prijedor, Serbia, 2008.
- [18] **Matijević, M., G., Jakupović, J., Car**, Računarski podržano merenje i upravljanje, (in Serbian), 2nd edition, Faculty of Mechanical Engineering, University of Kragujevac, 2008.
- [19] *** Wikipedia article on Heat treating, (accessed on 28. 07. 2020.)
https://en.wikipedia.org/wiki/Heat_treating
- [20] *** Thermal Treatments (Heat-Treating), Education Resources of NDT Education Resource Center (NDT - Nondestructive testing), (accessed on 09. 07. 2020.) <https://www.nde-ed.org/EducationResources/CommunityCollege/Materials/Structure/thermal.htm#:~:text=Age%20Hardening%20is%20a%20relatively,then%20allowed%20to%20cool%20slowly.>

POVEĆANJE TOLERANCIJE GREŠKE ADC AD7799

INCREASING FAULT TOLERANCE OF ADC AD7799

Artem BASKO¹, Elena PONOMARYOVA^{*2}

¹ Department of Automation and Computer-Integrated Technologies,

Prydniprovsk State Academy of Civil Engineering and Architecture, Ukraine

² Department of Computer Science, Information Technology and Applied Mathematics,

Prydniprovsk State Academy of Civil Engineering and Architecture, Ukraine

Pri dizajniranju bilo kojeg automatskog sistema upravljanja procesima, za mnoge industrije nemoguće je isključiti upotrebu analogno-digitalnih pretvarača. Standardni 5V logički nivoi CMOS-a i TTL-a postupno se smanjuju na 3.3V logičke nivoe LVTTTL-a, a zatim na 2.5V i 1.8V logičke nivoe CMOS-a, kako bi se povećala brzina integriranih kola. U skladu s tim, zahtevi za takvim pokazateljima kao što su tačnost, brzina, greške u kvantizaciji i u većini slučajeva tolerancija grešaka u procesu pretvaranja signala su sve veći. Cilj rada je primeniti i u praksi rešiti dvosmislenost ADC signala tokom prenosa podataka s ADC-a na mikrokontroler kako bi se prilagodio stabilnom načinu rada, predlaže se korišćenje niskopropusnog filtra na bazi RC sklopa u digitalnom delu kola. Sastavljen je ispitni sto, a pomoću modelirajućeg okruženja MATLAB Simulink testiran je LPF filter. Pravi eksperiment na ispitnom stolu je takođe izveden. To pokazuje da je primena niskopropusnog RC filtra u digitalnom delu električnog kola efikasna metoda. Ovde je takođe opisano kako odabrati RC filter.

Ključne reči: stabilizacija signala, analogno-digitalni pretvarač, filtriranje signala, dinamičko merenje težine, automatizacija

Designing any automated or automatic process control system, for many industries, it is impossible to exclude the use of analog-to-digital converters. The standard 5V logical levels of CMOS and TTL gradually decrease to 3.3V of the logical level of LVTTTL, and then to 2.5V and 1.8V of logical levels of CMOS, to increase the speed of the integrated circuits. In accordance with this, the requirements for such indicators as accuracy, speed, quantization errors and, in most cases, fault tolerance in the process of signal conversion are increasing. The aim of the work is to apply on practice solve the ambiguity of the ADC signal during data transmission from the ADC to the microcontroller in order to tune to a stable mode of operation, it is proposed to use a low-pass filter based on the RC circuit to the digital part of the circuit. A test bench was assembled and using the MATLAB Simulink modelling environment, the LPF Filter was tested. The real experiment on test bench was made. That shows that the implementation of a low-pass RC filter to the digital part of the electrical circuit is an effective method. Here is also describes how to select an RC filter.

Key words: signal stabilization, analog-to-digital converter, signal filtering, dynamic weight measurement, automation.

1 Introduction

Nowadays, no one of the automation systems can be designed without using an analog-to-digital converter (ADC). Typically, control systems use an ADC with a resolution of 8 bits, 10 bits, 12 bits, 16 bits and rarely 24 bits, to convert an analog signal from various sensors. This provides the conversion of the analog signal to digital for the convenience of further signal processing.

In common, research works to improve signal stability is aimed at improving the signal of the analog part of the ADC and filtering the data already received from the ADC.

For example, an 8-bit pipelined ADC using preprocessing to divide the input signal range into sub-intervals and amplify the residual signal for further processing in the subsequent steps [1]. Or pipelined successive-approximation-register (SAR) ADC. That ADC shows very high resolution and

* Corresponding author, email: pricmech@ukr.net

even with low level of noise reducing, it also shows good energy efficiency and a high sampling rate [2-4].

Two-stage pipeline ADC architecture with a large first-stage resolution, enabled with the help of a SAR-based sub-ADC. Such kind of ADC achieves low-power, high-resolution and high-speed operation without calibration [5-6].

In that articles were discussed, the basics of analog low-pass filtering, frequency transformations for transforming analog low-pass filter into band-pass, band-stop, or high-pass analog filters are considered. Main applications for low-pass filters are channel-separation, A/D antialiasing and general signal processing [7-9].

Also, Sallen-Key active low pass filters based on passive components RC are used for many years, there are described applying it with active components such as amplifiers and passive components, low-pass SC filters based on the continuous-time version of the Sallen-Key low pass filter [10-11].

Moreover, there are a lot of studies of data filtering and processing. They are described a particular measurement situation, how best to reduce the noise while retaining as much of the signal as possible is important [12-16].

Decreasing of logic levels of microcircuits bring to the problem of signal instability arises while data transmitting from the ADC to the microcontroller. Furthermore, investigating ways to improve the stability of microcircuits, this research contributes to a further increasing of stability at even lower logical levels.

2 Analyze of the problem

In the practical application of microcircuits for various circuitry solutions, the problem of unstable operation often arises. Usually, engineers change a suitable chip to a more stable one, instead of improving the work of a suitable one.

This work presents an applied solution to the problem that occurs when transmitting data from the ADC to the microcontroller via the SPI interface.

Since the main issue is related to the instability of the signal during the data transfer between ADC and microcontroller, then let's look at an example of how to transfer data from the primary converter to the microcontroller. The channel of data transmitting is shown on Fig.1.

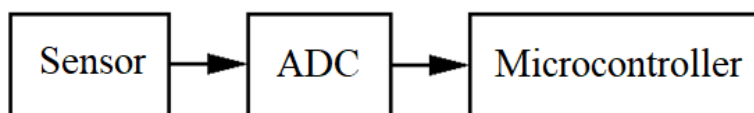


Fig. 1. The channel of transmitting data

The following communication channel is used in many automated or automatic control systems to obtain data from sensors of temperature, pressure, weight, speed, acceleration, etc. The problem of signal instability during transmission between the ADC and microcontroller. To solve such problem proposes method of signal filtering based on low-pass RC filter. It is simple and useful approach for such kind task.

To test the proposed method, a test bench was constructed. It is a scale for static weighing. An electrical schematic diagram of the test bench is shown in Fig.2.

As the primary transducer we will use the HBM PW6DC3 strain gauge weight sensor, it converts mechanical deformation of the body into an electrical signal.

The STM32 microcontroller, series F103C8T6, based on the ARM Cortex-M3 processor, was selected as the data collection, processing and control system.

According to the ADC problem encountered, AD7799-based ADC was used, it is a 24-bit sigma-delta ADC with low-noise instrumental amplifier and programmable gain. AD7799 uses the SPI interface, a sequential, full duplex synchronous data standard designed to provide simple and inexpensive high-speed connectivity to microcontrollers and peripherals. When the test bench was made and put it into operation, we will see the instability of data transmission. Instability of work is manifested in the noising of data transmission using SPI interface.

Looking for ways to solve this problem, it turned out that the AD 7799 ADC instability does occur not in a single case. Since there is a problem with this ADC, some engineers are usually used a hardware reboot mode to solve that problem at that time when the system crashes and data is not arrived.

But this is not a complete solution to the problem because it takes some time to restart, which means that digital data filtering algorithms cannot be used.

Initially, the circuit was investigated without a RC low-pass filter R7 and C22 which are shown in the electrical circuit of Fig.2.

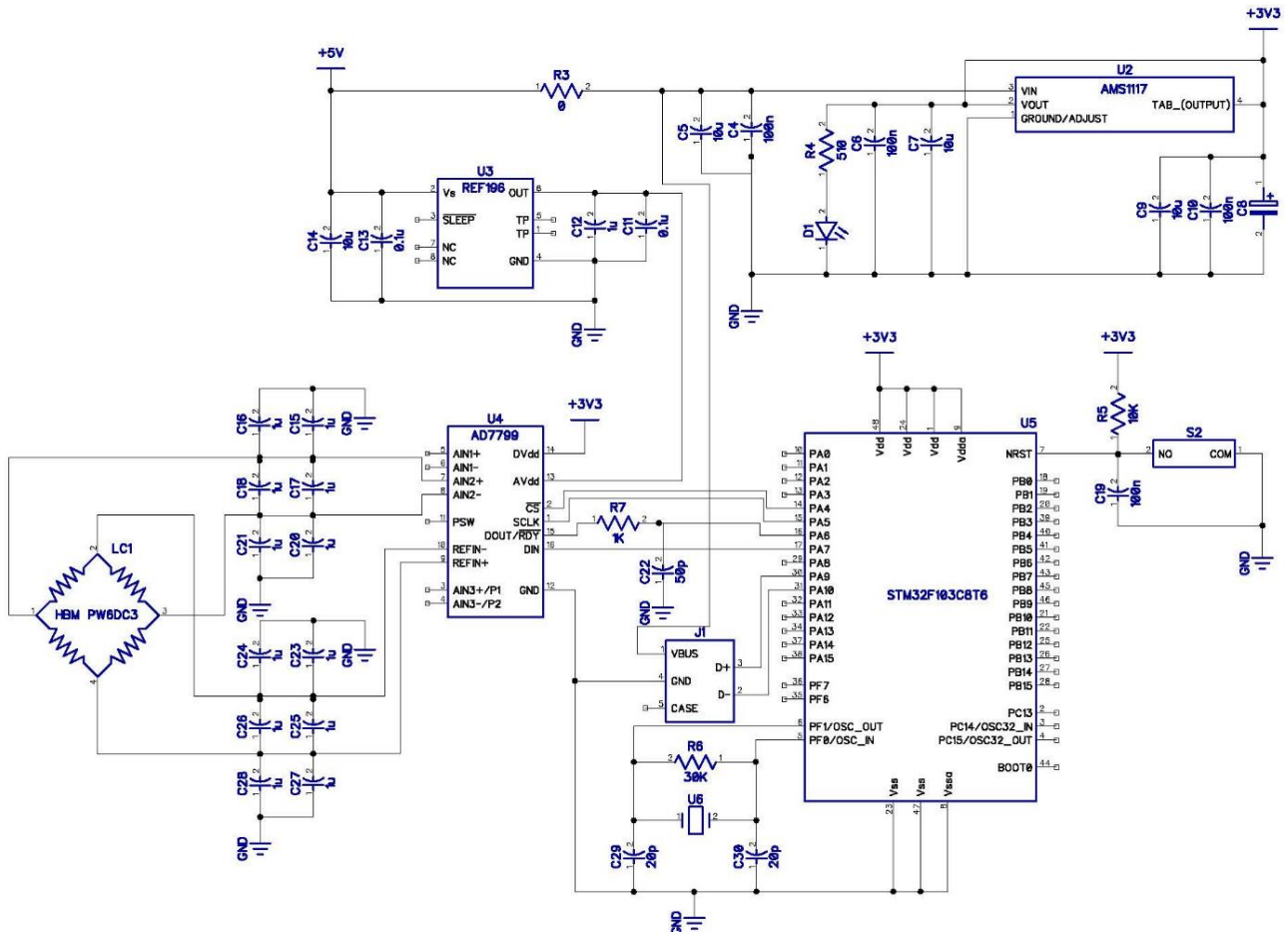


Fig. 2. Electrical schematic diagram of the test bench

An oscilloscope was used to investigate the forms of signals flowing during data exchange. The oscilloscope's probe was installed on the DOUT ADC, the diagram Fig. 3 is shown that the whole parcel is 32 bits. The first 8 bits duplicate the command that was submitted to the input DIN of the ADC from the microcontroller, it indicates from which ADC channel to receive data and what is the data request. Since the resolution of the ADC is 24 bits, the next 24 bits have an informative structure

Consider the upper form of the signal without the use of capacitor C22 and resistor R7, the Fig. 4 are showed the oscillations of the distorted data.

But it was clear that when studying the signal with the oscilloscope's probe, the ADC has begun work with more stability and the noise amplitude is in average 300 mV. It means without the oscilloscope's probe it will be more of a negative impact on data transmission and noise amplitude will be higher than 300 mV. So, we know that the capacity of the oscilloscope probe is about 15 pF and they are not enough to stabilize the data signal.

The ADC was launched at different update rates from 4.17 to 470 Hz, changing the FS0, FS1, FS2, FS3 registers of ADC AD7799. When the ADC update frequency changes, the microcircuit also works unstable, but at a lower frequency the time increases, but the operation failure is inevitable. The diagram of the dependence of the update rate on time to fault is shown in Fig.5.

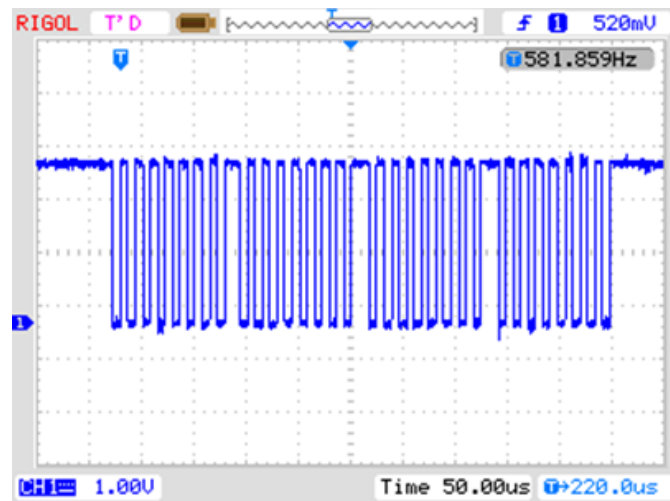


Fig. 3. Parcel from ADC on the pin DOUT ADC

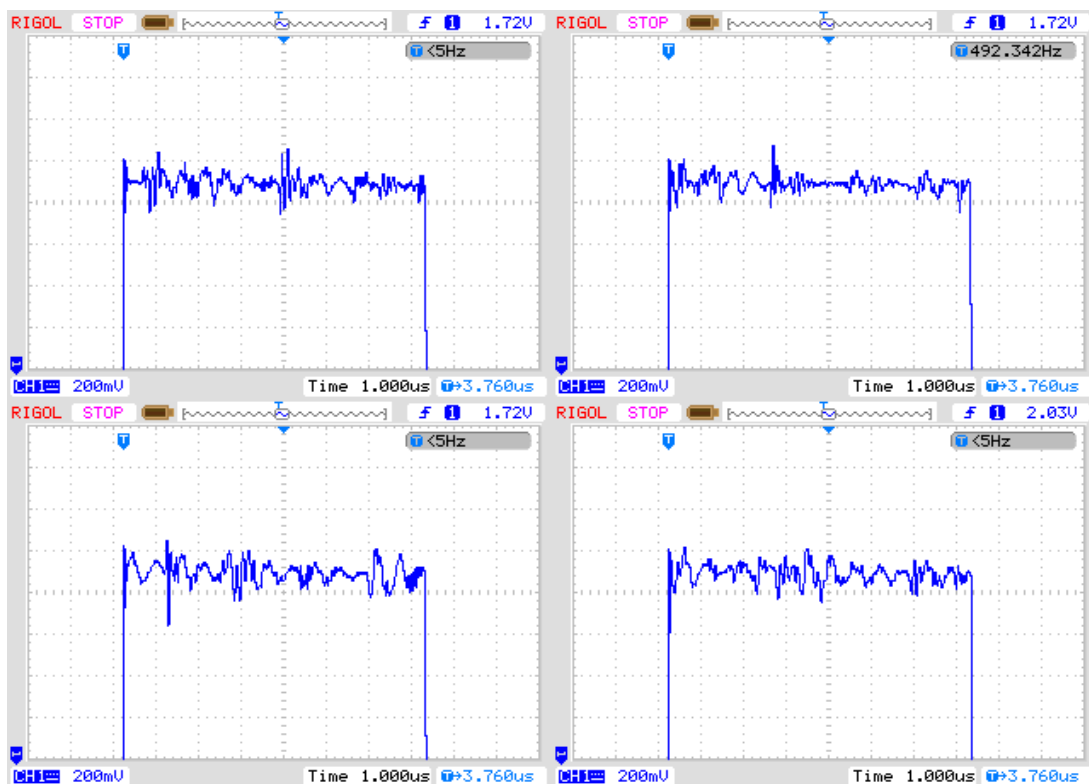


Fig. 4. Data signal without the use of an RC filter

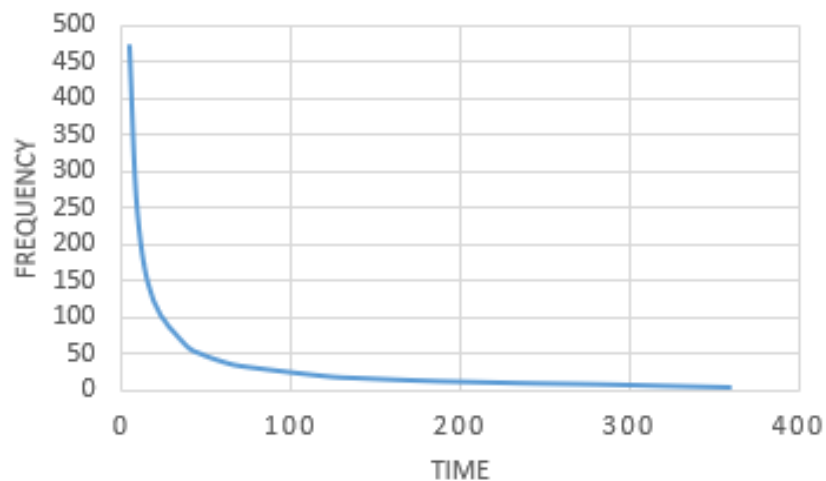


Fig. 5. Dependence of the update rate on time to fault

3 Modelling and testing of the proposed method

To stabilize the signal, it is necessary to select the correct combination of R and C electrical elements. In the general case, the output voltage of such an RC circuit is described by equation (1):

$$U_{out}(t) = U_{in}(t) + C \cdot e^{-\frac{t}{R \cdot C}} \quad (1)$$

Based on the theory of automatic control, this RC circuit is an aperiodic link (inertial link, aperiodic link of the first order). The following link is described by the differential equation (2):

$$T \frac{dy(t)}{dt} + y(t) = K \cdot x(t) \quad (2)$$

From theory of automation low pass continuous-time filter can also be described in terms of the Laplace transform. Their impulse response, in a way that lets all characteristics of the filter be easily analyzed. The low-pass filter of first-order can be described in Laplace notation as (3):

$$W(p) = \frac{K}{Tp+1} \quad (3)$$

In the equation of the transfer function (3), K is the gain, $T = R \cdot C$ is the time constant.

Earlier data were obtained using an oscilloscope in the wfm format, they were exported to the MATLAB environment for analysis and design. Using the MATLAB Simulink modeling environment, three models with different value of T were build, it is showed in Fig.6.

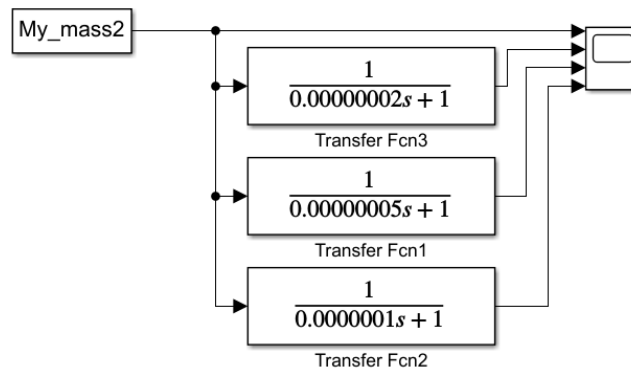


Fig. 6. Transfer function with different time constants T

Based on the data obtained in Fig.7, the graph 2 has more faster the slew rate than the graph 3, but has less stable signal.

The graph 4 has less faster the slew rate than graph 3, but has more stable signal. So, graph 3 has an optimal ratio of the slew rate to the reference voltage and a sufficiently stable signal.

For complex comparison RC filter must be implemented into test board and get new data signal. To rebuild existed board the nominals of R and C must be known. Resistor R7 is equal 1000 Ohm it is enough for flowing current between microcircuits. To calculate nominal of capacitor C22, need to use next an equation:

$$C = \frac{T}{R} = \frac{0.05 \cdot 10^{-6}}{1000} = 50 \cdot 10^{-12} \text{ F} = 50 \text{ pF}$$

Know the R and C we can also find the Pass Band, so the frequency range of cut-off point f_c is calculated by equation (4):

$$f_c = \frac{1}{2 \cdot \pi \cdot R \cdot C} \quad (4)$$

Using the equation (4) the cutoff frequency equals:

$$f_c = \frac{1}{2 \cdot 3.14 \cdot 1000 \cdot 50 \cdot 10^{-12}} = 3.18 \cdot 10^6 \text{ Hz}$$

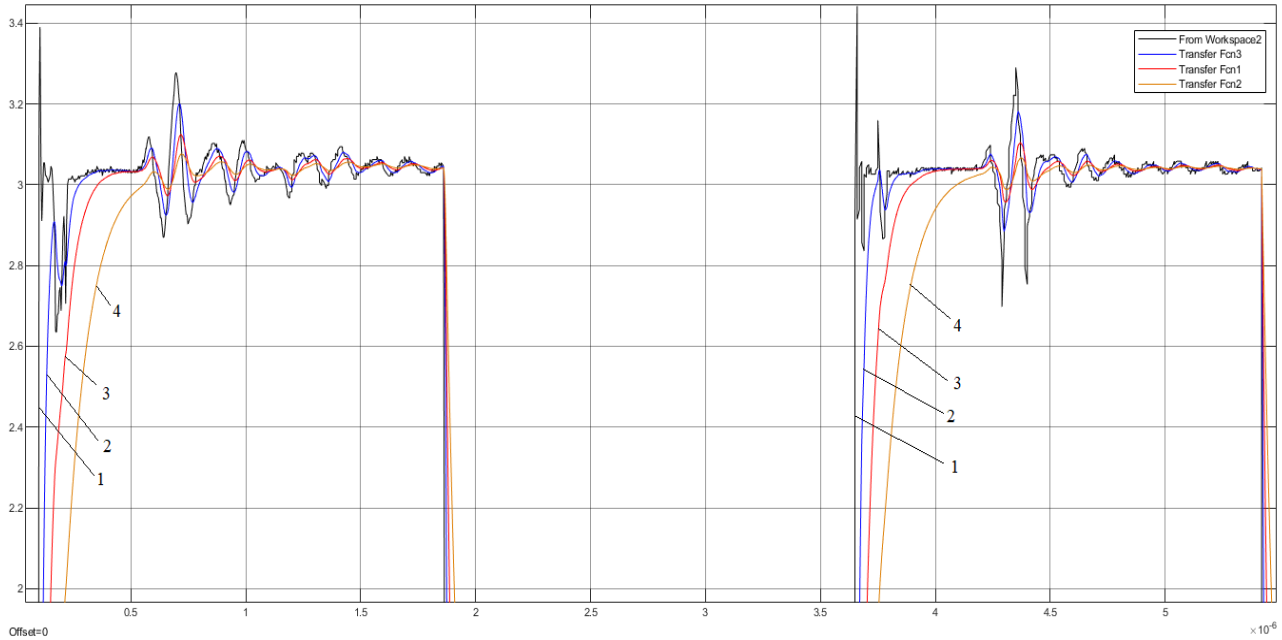


Fig. 7. Plots of transfer functions: 1 - original data from oscilloscope, 2 - transfer function with $T = 2 \cdot 10^{-8}$, 3 - transfer function with $T = 5 \cdot 10^{-8}$, 4 - transfer function with $T = 1 \cdot 10^{-7}$

Comparing the obtained Fig.8 using the RC filter and Fig.6 without it, we can conclude that the filter with the task of stabilizing the digital signal works quite well, and the signal became clearer, and the ADC stop disappeared, and therefore we can say that the implementation of the RC LPF filter is an effective solution.

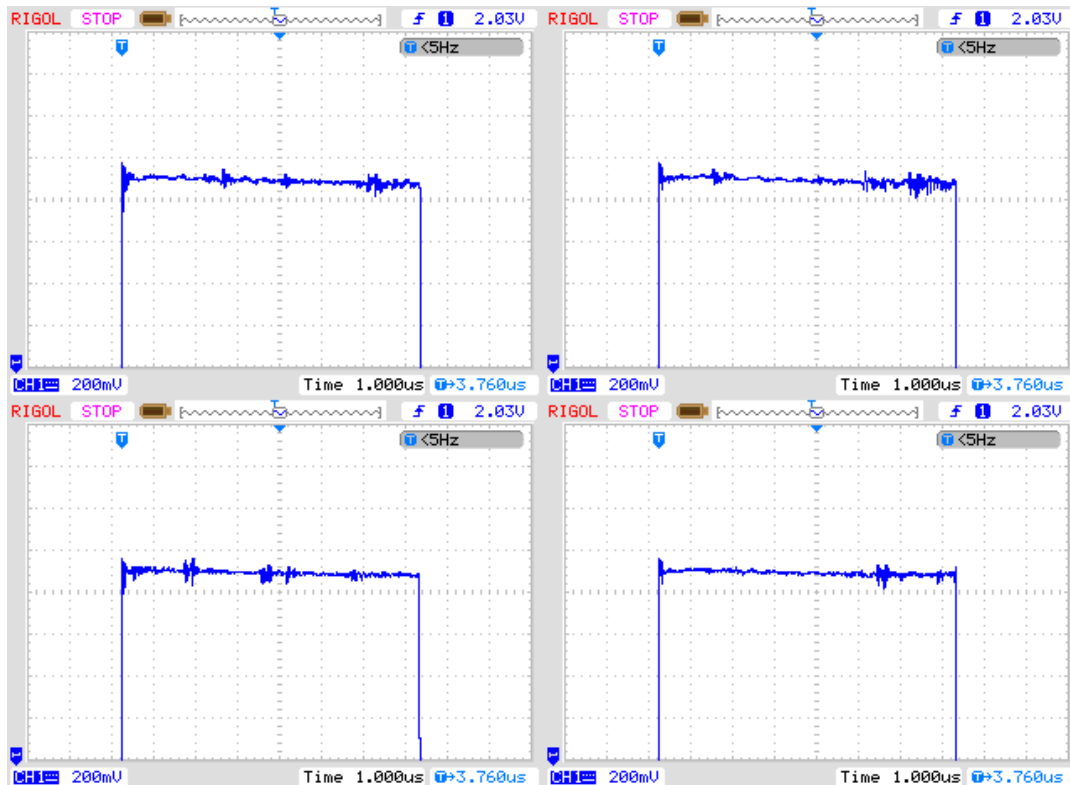


Fig. 8. RC is used for filter data signal

4 Conclusion

Complexity of devices are Increasing, so the volume and speed of information transfer between devices are exchanged has increased extremely. To improve performance digital part of ADC the known ways of solving this problem were analyzed and the own schematic solution of the problem was presented. The test bench was assembled and an experiment was conducted there is also was made computer modelling of LPF in MATLAB Simulink, using this approach amount of noise was reduced and stabilized the ADC.

Moreover, the proposed data filtering method can be applied not only to this AD7799 ADC model, but also to others will all depend on the frequency of data transmit, resistor nominal and the capacitor rating. The results presented can be used in radio engineering to design modern automatic and automated control systems of varying degrees of complexity.

The results of the study are planned to be used for the design of complex dynamic weighing systems, checkweighers in order to ensure high accuracy and quality of data during measurements.

5 References

- [1] **Brarua, A., M. Tausiff**, Code width built-in self-test circuit for 8-bit pipelined ADC, IEEE, (2011), pp. 287-291.
- [2] **Oh, S., K. Kim, H. Chae**, Bandpass $\Delta\Sigma$ ADC using pipelined SAR ADC, Electronics Letters, 56 (2020), 10, 480.
- [3] **Sarma, V., B.D. Sahoo**, Pipelined ADC based design of bandpass Delta Sigma-ADC, Electronics Letters, 49 (2013), 10, pp. 646-648.
- [4] **O'Hare, D., A. Scanlan, E. Thompson, B. Mullane**, Bandwidth Enhancement to Continuous-Time Input Pipeline ADCs, IEEE Transactions on Very Large Scale Integration, 26 (2017), 2, pp. 404-415.
- [5] **Lee, C., M.P. Flynn**, A SAR-assisted two-stage pipeline ADC, IEEE Journal of Solid-State Circuits, 46 (2011), 4, pp. 859-869.
- [6] **Fan, H., Y. Liu, Q. Feng**, A Reliable Bubble Sorting Calibration Method for SAR ADC, AEU-International Journal of Electronics and Communications, 122 (2020), p. 153.
- [7] **Thompson, M.**, Intuitive Analog Circuit Design, Newnes, New York, USA, 2014.
- [8] **Rao, K.**, Signals and Systems, Birkhauser, Cham, Switzerland, 2018.
- [9] **Molnar, G., M. Vucic**, Bernoulli Low-Pass Filters, Circuits and Systems II: Express Briefs, 9 (2014), 5, pp. 1-5.
- [10] **Soltan, A., A. Radwan, A.M. Soliman**, Fractional Order Sallen–Key and KHN Filters: Stability and Poles Allocation, Circuits Systems and Signal Processing, 34 (2014), 5, pp. 1461-1480.
- [11] **Serra, H., N. Paulino**, Design of Switched-Capacitor Filter Circuits using Low Gain Amplifiers, Springer, Cham, Switzerland, 2015.
- [12] **Suresh, R.D.**, Signals and Systems in Biomedical Engineering, Springer, Boston, Canada, 2013.
- [13] **Miura, G.**, Noise reduction, Nature Chemical Biology, 16 (2020), 2, p.106.
- [14] **Chen, W.**, The Regularized Low Pass Filter, Journal of Signal and Information Processing. 5 (2014). 1. pp. 14-16.
- [15] **Yu, F., J. Lu**, Symmetry in digital signal processing, Nanjing Li Gong Daxue Xuebao/Journal of Nanjing University of Science and Technology, 42 (2018), 5, pp. 615-621.
- [16] **Sengupta, S.**, Handbook for Digital Signal Processing Technometrics, Technometrics, 34 (2012), 4, p. 430.

MOGUĆNOST KORIŠĆENJA KOŠTICA VIŠNJE KAO BIOGORIVA ZA DOBIJANJE TOPLOTNE ENERGIJE

POSSIBILITY OF USING SOUR CHERRY PITS AS BIOFUEL FOR OBTAINING THERMAL ENERGY

Milorad PETROVIĆ¹, Milan JOVANOVIĆ¹, Zoran ŠTIRBANOVIC^{*2},
Jovica SOKOLOVIĆ², Vojka GARDIĆ³

¹ Šukom, Knjaževac, Knjaževac, Serbia

² University of Belgrade, Technical faculty in Bor, Bor, Serbia

³ Mining and Metallurgy Institute Bor, Bor, Serbia

<https://doi.org/10.24094/mkoiee.020.8.1.295>

Višnje se u Republici Srbiji uzgajaju na oko 14000 hektara i predstavljaju četvrtu voćnu vrstu po površini. Koštice koje ostaju nakon prerade višnje predstavljaju nus-proizvod koji opterećuje poslovanje prerađivača ovog voća. Količine koštica koje se godišnje proizvedu se procenjuju na oko 7000 tona. Ovo predstavlja dobar energetske potencijal imajući u vidu da je kalorična vrednost koštica višnje oko 22 MJ/kg suve materije. Dodatna pogodnost koštica višnje je u njihovim dimenzijama koje ih čine pogodnim za direktno korišćenje u kotlovima za pelet, bez ikakvog predtretmana. Jedan od kotlova u kome je moguće vršiti sagorevanje suvih koštica višnje u cilju dobijanja toplotne energije, je Šukoplam VENT, proizvođača kotlova Šukom iz Knjaževca. Ovaj kotao se po svojim karakteristikama odlikuje visokim stepenom korisnosti (do 94 %), kvalitetom materijala i izrade, mogućnošću upotrebe više vrsta biogoriva i njihovog kvalitetnog sagorevanja, na osnovu kojih je ispunio uslove za dobijanje Klase 5 (Ecodesing) vezano za emisije zagađujućih materija po najnovijim evropskim standardima.

Ključne reči: biomasa; koštice višnje; toplotna energija; kotao; Šukoplam VENT.

In the Republic of Serbia, sour cherries are grown on approximately 14,000 hectares and represent the fourth fruit species in terms of area. The pits that remain after the processing of sour cherries are a by-product that burdens the business of the processors of this fruit. The quantities of pits that are produced annually are estimated at around 7,000 tons. This represents a good energy potential, bearing in mind that the calorific value of sour cherry pits is around 22 MJ / kg of dry matter. An additional convenience of sour cherry pits is in their dimensions that make them suitable for direct use in pellet boilers, without any pre-treatment. One of the boilers in which it is possible to burn dried sour cherry pits in order to obtain thermal energy, is Šukoplam VENT, a manufacturer of boilers Šukom from Knjaževac. This boiler has good characteristics such as: high efficiency (up to 94%), quality of materials and workmanship, the possibility of using several types of biofuels and their quality combustion, based on which it met the requirements for Class 5 (Ecodesing) related to pollutant emissions by the latest European standards.

Key words: biomass; sour cherry pits; thermal energy; boiler; Šukoplam VENT.

1 Introduction

Energy production and consumption all over the world are continuously increasing. Traditional energy sources are limited so there are always demands for new alternative and renewable energy sources. Electrical energy production in the Republic of Serbia is mostly dependent on coal combustion (over 60%), some comes from hydro power and very little from renewable energy resources. Despite that it is being very little used, potentials in renewable energy resources, especially in biomass, in the Republic of Serbia are significant. According to the analysis done in 2016 by the

* Corresponding author, email: zstirbanovic@tfbor.bg.ac.rs

Department for strategic planning in energy sector in the Ministry of Mining and Energy of the Republic of Serbia, biomass potential in Serbia is estimated at 3.448 million toe and in the total potential of renewable energy participates with 61% [1]. The largest potential has wood biomass with 1.53 million toe and agricultural biomass with 1.67 million toe (including crop farming, cattle breeding, food growing, wine growing and primary fruit processing) [1]. There are also potentials of biodegradable municipal waste with estimated 205 thousand of toe and biodegradable waste, except municipal waste, (waste cooking oils and animal waste - slaughterhouse waste) with total amount of 0.043 million toe/per year [1].

While the use of wood biomass potential is relatively high (66.7%), agricultural biomass potential is used very little (about 2%) and the biodegradable municipal waste potential is not used at all [1]. It is very important to use agricultural biomass and biodegradable municipal waste instead of wood biomass because for the growth of a tree it takes years and agricultural biomass and biodegradable municipal waste are produced annually or daily.

2 Agricultural biomass in the Republic of Serbia

Serbia is an agricultural country with approximately 5 million ha of agricultural land, out of which 70% is arable [2]. Cereals (mainly maize and wheat) are grown on approximately 2 million ha, oilseeds on 300 thousand ha, fruits on 250 thousand ha, roots and tubers on 150 thousand ha, vegetables on 140 thousand ha, etc. [2].

The most of arable land in the Republic of Serbia is located in the northern province of Vojvodina, which is mostly known for crop production. In Figure 1 are shown arable lands in the Republic of Serbia. As can be seen most of arable lands are located in the north and smaller amounts in central, east and south, while in west there are very few.

Other areas of Serbia also have some potential in agriculture production, especially in fruit and wine production and processing, cattle breeding, etc. Figure 2 shows areas under orchards in Serbia.

As it can be seen from Figure 2, fruit production is mostly represented in western Serbia, central and some in the south also. Fruit cultures that are being grown the most are plums, apples, sour cherries, peaches, raspberries, etc.

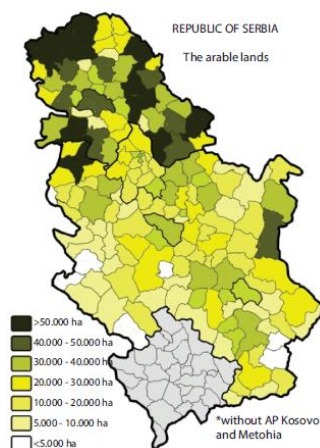


Figure 1 The arable lands on the territory of Serbia [3]

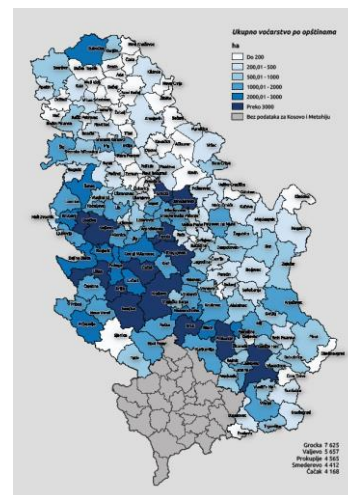


Figure 2 Areas under orchards in Serbia [4]

There are a lot of by-products from agricultural production such as harvest residues, fruit and vine cutting residues, manure, etc. that can be used as biomass for energy production. As it was said earlier, the Republic of Serbia has great potentials in agricultural biomass with 1.67 million toe. Figure 1 shows the structure of the real energy potential of agricultural biomass in Serbia.

From the graph shown in Figure 3 can be seen that 68% of all energy potential in agricultural biomass is from harvest residues, 11% manure, 9% each are cutting residues and biofuels, while 3% is from processing industry and biodegradable communal waste. It cannot be expected all of these

potentials to be used, especially harvest residues, because it is necessary to plow into ground some of amounts, but the others could be used.

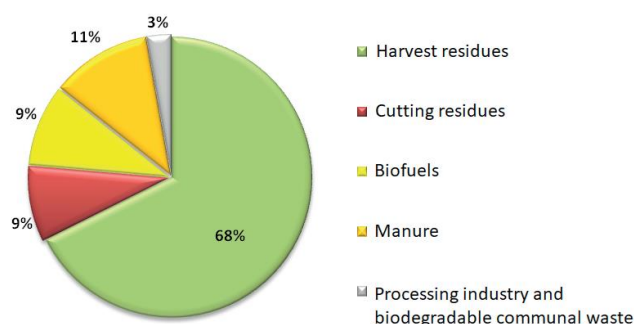


Figure 3 The structure of the real energy potential of agricultural biomass in Serbia [5]

3 Sour cherry pits as biofuel for thermal energy production

Sour cherries are grown on 13,990 ha in Serbia and represent the fourth fruit species in terms of area used for its growing [6]. Sour cherries are mainly grown in south, east and central parts of Serbia, and very little in the west and north. In Figure 4 are shown areas under sour cherry plantations in the Republic of Serbia.

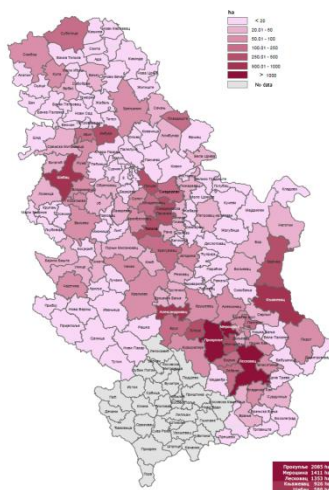


Figure 4 Areas under sour cherry plantations in Serbia [7]

Table 1 Sour cherry production statistics in period 2002-2006 [8]

	2002	2003	2004	2005	2006	Average
Average fruit yield (t)	48900	86200	112300	63900	80500	78360
Average fruit processing residues (t)	4401	7758	10107	5751	7245	7052,4

Perennial average production of sour cherries around 78000 tons (Table 1), on the basis of which Serbia is in fourth place in Europe by the production of this fruit. Most of the production of cherries is used primarily as frozen (with or without pits), canned, and a lot is related to the production of juices. The pits that remain after the processing of sour cherries are a by-product that burdens the business of the processors of this fruit. The quantities of pits that are produced annually are estimated at around 7,000 tons (Table 1). This represents a good energy potential, bearing in mind that the calorific value of sour cherry pits is 21,75 MJ / kg of dry matter (Table 2).

Table2 Calorific values for fruit processing residues [8]

Type of biomass	Calorific value (MJ / kg of dry matter)		Approximate analysis (Mass %)	
	Higher	Lower	Volatile	Ash
Sour cherry pits	21,75		84,20	1,00
Peach pits	20,82	19,60	79,12	1,03
Plum pits	21,14		58,30	0,10
Walnut shells	20,18	18,99	78,28	0,56

As it can be seen from Table 2, sour cherry pits have the highest calorific value of dry matter compared to peach pits, plum pits and walnut shells. On the other side, mass fraction of volatile is also highest in sour cherry pits and the ash content is the second highest after the peach pits.

An additional convenience of sour cherry pits is in their shape and size that make them suitable for direct use in pellet boilers, without any pre-treatment. One of the boilers in which it is possible to burn dried sour cherry pits in order to obtain thermal energy, is Šukoplam VENT, a manufacturer of boilers Šukom from Knjaževac. This boiler has good characteristics such as: high efficiency (up to 94%), quality of materials and workmanship, the possibility of using several types of biofuels and their quality combustion, based on which it met the requirements for Class 5 (Ecodesing) related to pollutant emissions by the latest European standards.



Figure 5 Šukoplam VENT boiler

Šukoplam VENT boilers are mainly used for wood pellet, but they can also be used for other kinds of biomass and coal too. They are made with fuel bunkers from 0,43 m³ up to 2,25 m³ in volume. The size of the boiler can also differ depending on a need. Technical characteristics of Šukoplam VENT boilers are given in Table 3.

Table3 Technical characteristics of Šukoplam VENT boilers

Boiler	Operating pressure	Measuring pressure	Temperature of exhausted gasses	Efficiency rate
Šukoplam Vent 100÷1000	3 bar	4,3 bar	max 180°C	up to 94,4%

4 Conclusion

The Republic of Serbia has great potential in agricultural biomass with 1.67 million toe, but it is not used enough. The most of electrical energy in Serbia (over 60%) is being generated by coal combustion. Coal is also often being used as a fuel for household heating, so the air in Serbia is much polluted especially in the winter season. Using renewable energy resources like biomass instead of coal can contribute to improving air quality and also preservation natural resources of coal.

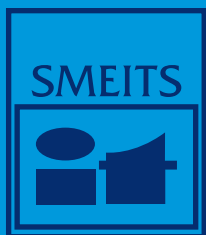
Residues from fruit processing such as plum pits, peach pits, sour cherry pits, walnut shells, etc. can be used for heating instead of wood or coal. Serbia has significant resources in fruit production which could be used. Sour cherry is fourth fruit specie in Serbia, in terms of area that it is being cultivated on. Average annual production of sour cherry in Serbia is approximately 80000 tons, and 7000 tons represents residue from processing industry. Sour cherry pits have good calorific value (21,75 MJ / kg of dry matter) and their shape and size are convenient for using in wood pellet boilers. Company Šukom from Knjaževac produces wood pellet boilers Šukoplam VENT, which is distinguished with high efficiency (up to 94%), quality of materials and workmanship and the possibility of using several types of biofuels and their quality combustion.

5 Acknowledgment

The research presented in this paper was done with the financial support of the Ministry of Education, Science and Technological Development of the Republic of Serbia, within the funding of the scientific research work at the University of Belgrade, Technical Faculty in Bor, according to the contract with registration number 451-03-68/2020-14/20013.

6 References

- [1] *** *Energy Sector Development Strategy of the Republic of Serbia for the period by 2025 with projections by 2030*, Republic of Serbia, Ministry of Mining and Energy, Department for strategic planning in energy sector, Belgrade, Serbia, 2016.
- [2] *** **ARCOTRASS - Consortium**, *Study on the State of Agriculture in Five Applicant Countries – Country Report: Serbia*, 2006.
- [3] **Dragović, Nj. M., M. D. Vuković, D. T. Riznić**, Potentials and prospects for implementation of renewable energy sources in Serbia, *Thermal science, Volume23*, (2019), issue 5B, pp. 2895-2907.
- [4] **Keserović, Z., N. Magazin, B. Milić, M. Dorić**, *Voćarstvo i vinogradarstvo*, Univerzitet u Novom Sadu, Poljoprivredni fakultet, Novi Sad, Srbija, 2016.
- [5] **Kovačević, V.**, *Status of Using Agricultural Biomass for Energy Purposes in Serbia*, UNDP Serbia, 2018.
- [6] *** <http://media.popispoljoprivrede.stat.rs/2014/Dokumenta/Radovi/03%20Vocarstvo%20Srbije%20%E2%80%93%20stanje%20i%20perspektive.pdf>
- [7] *** <http://media.popispoljoprivrede.stat.rs/2014/Dokumenta/Prezentacije/03%20Vocarstvo%20Srbije%20%E2%80%93%20stanje%20i%20perspektive.pdf>
- [8] **Đević, M., A. Dimitrijević, D. Blažin, S. Blažin**, Possibilities of using fruit processing residues as burning material, *Journal of Processing and Energy in Agriculture, Volume12*, (2008), issue 3, pp. 111-114.



8. Međunarodna konferencija o obnovljivim izvorima električne energije

Beograd, 16. oktobar 2020

8th International Conference on Renewable Electrical Power Sources

Belgrade, October 16, 2020